Università degli Studi di Ferrara

DOTTORATO DI RICERCA IN
'SCIENZE BIOMEDICHE E BIOTECNOLOGICHE'

CICLO XXX°

COORDINATORE Prof. Paolo Pinton

Novel trends in microRNA based theranostics

Settore Scientifico Disciplinare BIO/10

Dottoranda

Dott.ssa *Gasparello Jessica*

Tutore

Prof. *Gambari Roberto*

Co-tutore

Prof.ssa *Finotti Alessia*

Anni 2014/2017

L’importante non è quello che trovi alla fine di una corsa, l’importante è quello che provi mentre corri

Table of contents

Abstract

MiRNAs are a class of small non-coding RNA of about 19-23 nucleotides in length able to act as regulators of gene expression thanks to their ability to bind the 3'UTR which results in inhibition of translation or in mRNA degradation. Due to their short sequence, they can bind more than one transcript, so they may be involved in more than one biological pathway. Since their first identification in 1993, they have been associated to a long list of physiological or pathological conditions. The dysregulation of miRNA profile may be associated to several diseases, so therapies based on the restore of physiological miRNA levels may have huge impact on several pathologies, for this reason molecules able to both increase or decrease miRNA levels have been recently developed.

Through miRNAs levels regulation is possible to indirectly regulate their targets levels. This evidence was investigated in this thesis to reduce levels of BCL11A, one of the principal repressor of γ-globin gene. The following key results: a) miR-210 interaction with BCL11A coding region was demonstrated with SPR-based analysis, b) the increase of miR-210 intracellular levels leads to a decrease of BCL11A transcript and protein, encouraged us to consider the employment of miR-210 mimicking molecules as possible therapeutic approach to reduce BCL11A expression in the field of β-thalassemia treatment.

Modulation of miRNAs levels into cells can be achieve with different kinds of molecules and most of them generally require an appropriate vehicle. At this propose we investigated with encouraging results a calixarene-based structure compound called ML122, previously used for DNA delivery, to vehicle miRNA-based molecules and PNAs. a) High transfection efficiency, associated with b) evident biological effects obtained when both premiRNA molecules and PNAs are vehicled with ML122, allow us to consider ML122 as a possible alternative to commercial available transfection agents.

MiRNAs are present not only into cells but as demonstrated by Chim and colleagues they were found also in several body fluids, including plasma, in which have been demonstrated to be very stable. Several groups employed circulating miRNAs at diagnostic or prognostic propose opening a new important issue in the field of the non-invasive diagnostic techniques.

In the present thesis we employed the non-invasive diagnostic technique in two different fields. First, we considered circulating miRNA in colorectal cancer diagnosis and management. In this section, three important massages were obtained a) miRNA are normally released by cells, the release pattern is different in each cell line and often differs from the miRNA pattern into cells, b) a comparison between two different techniques, RTqPCR and ddPCR, demonstrates how the two techniques gave comparable results, even if ddPCR for technical issue is more suitable for miRNA quantification in plasma samples, c) analysis of the three selected miRNAs in CRC patients and healthy controls demonstrates how additional miRNAs (at 6 or 7 miRNAs) are needed to identify patterns associated to CRC patients.

The analysis of cmiRNAs was also, not applied to a health problem but to identify an illicit practice in sport such as autologous blood transfusion. The analysis of a limited number of samples using a high-throughput miRNA analysis method, i.e. microarray, allow us to identify two different list of miRNAs possible biomarkers for the detection of ABT: (a) a list of 8 miRNAs which modulation may be related to different oxygen availability immediately after the two key steps of ABT practice i.e. blood withdrawal and blood reinfusion. Moreover, a second list (b) was obtained considering all expressed miRNAs in our plasma samples. Despite the number of analysed samples is limited (6 ABT trained subjects and 3 control pools) preliminary encouraging data were obtained, which of course need to be confirmed increasing the samples size.

Abbreviations

7-ADD	7-aminoactinomycin D
µM	Micro Molar
αMEM	α-Minimal Essential Medium
AATK:	Apoptosis Associated Tyrosine Kinase
ABP	Athlete Biological Passport
ABT	Autologous Blood Transfusion
ADA	Adamantyl Acetic Acid
AGO	ArGOnaute
aM	Atto Molar
AMO	Anti MiRNA Oligonucleotide
AMPS	Ammonium PerSulfate
APC	Adenomatous Polyposis Coli
a-TAA	Tumor Auto Antibody
AuNP	Gold NanoParticle
AutoDG	Automated Droplet Generator
BCA	Bicinchoninic Acid
BCL11A	B-Cell Lymphoma/leukemia 11A
BFU-E	Burst Forming Unit-Erythroid
BMP3	Bone Morphogenetic Protein 3
BMT	Bone Marrow Transplantation
bp	Base Pair
BSA	Bovine Serum Albumin
CD	Crohn Disease
cDNA	Complementary DNA
cDNA	Circulating DNA
CDS	Coding Domain Sequence
CEA	Carcino Embryonic Antigen
cel	Caenorhabditis ELegans
cfDNA	Circulating Free DNA

cffDNA	Cell Free Fetal DNA
CFU-E	Colony Forming Unit-Erythroid
ChIP	CHromatin ImmunoPrecipitation
cLSPR	Collective Localised Surface Plasmon Resonance
CM	Conditioned Medium
cmiRNA	Circulating microRNA
CNB	Core Needle Biopsy
CNV	Copy Number Variation
COUP-TF2	Chiken Ovalbumin Upstream Promoter Trascription Factor interacting protein
CPP	Cell Penetrating Peptide
CRC	ColoRectal Cancer
csbDNA	Cell Surface Bound DNA
CT	Cycle Number
CT Scan	Computed Tomography Scan
CTC	Circulating Tumor Cell
ctDNA	Circulating Tumor DNA
CVS	Chorionic Villus Sampling
ddPCR	Droplet Digital PCR
DEHP	2-EthylHexyl Phthalate
DGCR8	DiGeorge syndrome Critical Chromosome Region 8
DMNT3b	DNA Methyltransferase 3 Beta
DMSO	Di Methyl SulfOxide
DNA	Deoxy Ribonucleic Acid
DNMT	DNA Methyl Transferase inhibitor
dNTP	Deoxynucleotide
DOPE	Di Oleoyl Phosphatidyl Ethanolamine
DPBS	Dulbecco's phosphate-buffered saline
dPCR	Digital PCR
DR	Direct Repeat
dsDNA	Double Strand DNA
DSN	Duplex Specific Nuclease

dsRBP	Double Strand RNA-Binding Protein
DTT	DiThioThreitol
ECL	ElectroChemiLuminescence
EDTA	Ethylene Diamine Tetraacetic Acid
EGFR	Epidermal Growth Factor Receptor
EKLF/KLF-1	Erythroid Kruppel-Like Factor
ELISA	Enzyme-Linked ImmunoSorbent Assay
EMT	Epithelial-Mesenchymal Transition
EPO	Erythropoietin
EPOR	Erythropoietin Receptor
ErPCs	Erythroid Precursor Cells
EV	Extracellular Vesicle
EXP-5	EXPortin 5
FACS	Fluorescence Activated Cell Sorting
FAP	Familial Adenomatous Polyposis
FBS	Fetal Bovine Serum
FDA	Food and Drug Administration
FIT	Fecal Immunochemical Test
FITC	Fluorescein Iso Thio Cyanate
fM	Femto Molar
FNAB	Fine Needle Aspiration Biopsy
FOBT	Fecal Occult Blood Testing
FOP	Friend Of Protein arginine methyltransferase
FRET	Foster Resonance Energy Transfer
FS	Flexible Sigmoidoscopy
FSC	Forward Scattered Light
GD2	Disialoganglioside
GEX	Gene Expression Analysis
gFOBT	Guaiac Fecal Occult Blood Testing
GYPA	Glycophorin A
GVHD	Graft Versus Host Disease

Hb	Haemoglobin
HDAC	Histone Deacetylase inhibitor
HDL	High Density Lipoprotein
HIF-1 α	Hypoxia Inducible Factor 1 α
hMLH1	MutL Homolog 1
HNPCC	Hereditary Non Polyposis Colorectal Cancer
HPCs	Hematopoietic Progenitor Cells
HPFH	Hereditary Persistence of Fetal Haemoglobin
HRE	Hypoxia Responsive Element
HRP	Horseradish Peroxidase
HS	Hypersensitive Site
hsa	Homo SApiens
Hsp90	Heat Shock Protein 90
HU	Hydroxyurea
IBD	Inflammatory Bowel Disease
IOC	International Olympic Committee
IVS	InterVening Sequence
KRAS	Kirsten Rat SARcoma
LDL	Low Density Lipoprotein
LNA	Locked Nucleic Acid
lncRNA	Long Non Coding RNA
LOD	Limit Of Detection
LOH	Loss Of Heterozygosity
LV	Lentiviral Vector
LYAR	human homologue of mouse Ly-1 Antibody Reactive clone
MCH	Mean Corpuscular Haemoglobin
MCV	Mean Corpuscular Volume
MgCl	Magnesium Chloride
miRISC	miRNA-Induced Silencing Complex
miRNA/miR	microRNA
mmu	Mus MUsculus

mRNA	Messenger RNA
MSTN	Myostatin
MTgAMO	Multiple-Target anti-MiRNA Oligonucleotide
MTH	Mithramycin
MVB	Multi Vesicular Body
ncRNA	Non Coding RNA
NDRG4	N-myc Downstream-Regulated Gene 4
NESPRI	Nanostructure Enhanced Surface Plasmon Resonance Imaging
NF-κB	Nuclear Factor Kappa-light-chain-enhancer of activated B cells
NGS	Next Generation Sequencing
NMD	Nonsense Mediated Decay
NPM1	Nucleophosmin 1
nSMase2	Sphingomyelinase 2
nt	NucleoTide
$p27^{Kip1}$	Cyclin-dependent kinase inhibitor 1B
p70	Ribosomal protein S6 kinase beta-1
PAP	Poly(A) Polymerase
Pasha	PAtner of droSHA
PAZ	Piwi/Argonaute Zwille
PCR	Polymerase Chain Reaction
PEG	PoliEtilenGlicol
PEI	Poly Ethylene Imine
PEPFSI	Plasmon Enhanced Fluorescence Spectroscopy Imaging
piRISC	piRNA Induced Silencing Complex
piRNA	PIwi-associated RNA
PIWI	P-element Induced WImpy testis
PLGA	Poly (Lactic-co-Glycolic Acid)
pM	Pico Molar
PNA	Peptide Nucleic Acid
PS	Phosphatidyl Serine
PSA	Prostate Specific Antigen

R_8	Poly Arginine Peptide
RanGTP	Ran Guanosine Tri-Phophate
RBC	Red Blood Cell
RED	Rare Event Detection
rHuEPO	Recombinant Human Erythropoietin
RIIIDs	RNAse III Domains
RLC	RISC Loading Complex
RNA	RiboNucleic Acid
RNApol	RNA Polymerase
RPMI	Roswell Park Memorial Institute
RT	Room Temperature
RTqPCR	Quantitative Reverse Transcription PCR
RV	Retroviral Vectors
RU	Resonance Unit
SA	StreptAvidin
SCD	Sickle Cell Disease
SCF	Stem Cell Factor
SCFAs	Short-Chain Fatty Acid
SD	ssDNA-dsDNA junction
SDS	Sodium Dodecyl Sulfate
shRNA	Short Hairpin-RNA
SMAD	Small Mother Against Decapentaplegic
snoRNA	Small NucleOlar RNA
SNP	Single Nucleotide Polymorphism
SPR	Surface Plasmon Resonance
SPRI	Surface Plasmon Resonance Imaging
SRY	Sex-determining Region Y
SSC	Side Scattered Light
ssRNA	Single Strand Ribonucleic Acid
STAT3	Signal Transducer and Activator of Transcription 3
TAE	Tris Acetic acid EDTA

Taq	Thermus AQuaticus
TC	Total Colonoscopy
TF	Transcription Factor
T_m	Melting Temperature
TMN	Tumor, Node, Metastasis
TNF-α	Tumor Necrosis Factor α
TRBP	Tar RNA-Binding Protein
trfR	Transferrin Receptor
tRNA	Transfer RNA
UC	Ulcerative Colitis
UNG	Uracil N-Glycosylase
UTR	UnTranslated Region
UV-Vis	Ultra-Violet Visible
VEGF	Vascular Endothelial Growth Factor
$VO2_{max}$	Maximal aerobic capacity
WADA	World Anti Doping Agency

Preface

The work that we are going to present in this thesis was possible thanks to the collaboration between professor Gambari research group and several others research groups which have a key role in this work.

The analysis of circulating miRNAs in CRC was performed as part of ULTRAsensitive PLAsmonic devices for early CAncer Diagnosis project, funded by the European Union's Horizon 2020 research and innovation programme. The ULTRAPLACAD principal aim is the development of a compact plasmonic-based device with an integrated microfluidic circuit and functionalized nanostructures for the detection of DNA, microRNA and tumor autoantibodies. The project is coordinated by Professor Giuseppe Spoto (Istituto Nazionale Biostrutture e Biosistemi, University of Catania), who for a long time have developed SPR-based techniques for detection and quantification of biological molecules. Moreover, our work would not has been possible without the collaboration with PhD Patrizio Giacomini and PhD Matteo Allegretti who are responsible for CRC patients recruitment.

Analysis of cmiRNAs in ABT trained athletes was performed in the context of MARATHON (novel Molecular biomARkers for detection of Autologous blood Transfusion in sport: fetal HemOglobin and microRNAs) project, founded by WADA (World Anti-Doping Agency). The projects was born from the collaboration with MD Fabio Manfredini team (Department of Biomedical and Surgical Specialties Sciences, Section of Sport Sciences, University of Ferrara), who for a long time has worked on assessment of physical performance in the sport and has studied factors and limiting or favouring athletic performance. The project realization was possible thanks to the precious help of Blood Transfusion Service (Ferrara Hospital), coordinated by MD Roberto Reverberi.

Moreover, ErPCs isolation and culture were perform thanks to kind collaboration of beta-thalassemia patients who have donated their precious blood, and to 'Day Hospital della Talassemia e delle Emoglobinopatie', (Ferrara Hospital) coordinated by MD Maria Rita Gamberini, who has collaborated for a long time with Professor Gambari. Moreover,

Professor Alessandra Romanelli (Department of Pharmacy, University of Naples 'Federico II', Napoli) and her research team, synthesized PNAs employed for fetal haemoglobin induction studies.

ML122 and its analogues were kindly donated by Professor Francesco Sansone research team, which for a long time has studied calix[n]arene scaffolds as cationic synthetic vectors for DNA delivery. Moreover, PNA employed for PNA delivery experiments were synthesized by Professor Roberto Corradini research team (Department of Chemistry, Parma University).

Introduction

Non Coding RNA

Non coding RNAs (ncRNAs) are a class of RNA molecules that are able to regulate gene expression at transcriptional or at post-transcriptional level. NcRNAs can be divided in two main groups: short or small ncRNA, that are generally, less than 30 nucleotides in length, and long ncRNAs (lncRNAs) that are characterized by a length of at least 200 nucleotides.

High-throughput sequencing and microarray analysis demonstrate that the alteration of ncRNA profile is the base for different types of diseases. Cancer is only an example of pathology in which ncRNAs dysregulation plays a key role. In particular, different works correlate ncRNA profile with neoplastic phenotype or disease progression suggesting ncRNAs not only, as biomarkers for diagnosis or prognosis but also, as targets for novel agents in cancer therapy [*Cowie et al., 2015*].

1.1 Long non coding RNA

LncRNA are a class of protein non-coding RNAs with a length greater than 200 nucleotides, which transcripts generally, reside in the introns of protein-coding genes. Currently, only a fraction of the thousands of mammalian lncRNA have been characterized. Increasing evidences suggest that they are involved in a broad spectrum of biological processes including cell proliferation, differentiation, apoptosis and stem cell self-renewal. Owing to their ability to bind DNA and RNA they are able to modulate protein activity [*Quinn et al., 2015*]. These regulatory RNAs are heterogeneous as regards characteristics, localization and modes of action. The subcellular localization of lncRNA is considered a good indicator of their mode of action [*Kung et al., 2013*]. LncRNA localized in the nucleus are involved in gene regulatory processes, including promoter-specific repression, activation of transcription or epigenetic gene regulation. Furthermore, several nuclear lncRNA were found to regulate the maintenance of nuclear architecture, particularly, they seem to regulate the abundance of nuclear structures called paraspeckles, that are involved in mRNAs retention [*Chen et al., 2009*]. On the contrary, lncRNAs localized in the cytoplasm seem to be involved in the post-transcriptional gene regulation processes like regulation of mRNA stability, regulation of miRNAs accessibility or translation pathways [*Yoon et al., 2013*]. Increasingly strong evidences have proposed lncRNA as molecules with a key role in

neoplastic disease; in fact, these RNA molecules can act as oncogenes or as tumor suppressor, depending on the signalling pathway in which they are involved. For example, HOTAIR, one of the most studied lncRNA, in colorectal cancer (CRC) seems to be related to tumor invasion and metastasis, indeed has been demonstrated that CRC patients with higher HOTAIR expression have higher recurrence rates and shorter overall survival compared with patients with lower HOTAIR expression [*Wu et al., 2014*].

1.2 Small non coding RNA

In the recent years, small non coding RNAs have emerged as key regulators of gene expression in different pathways and a growing number of small regulatory RNA classes have been discovered. MicroRNAs are still, the best-characterized class; however, other small RNA molecules have been investigated, such as piwi-associated RNAs (piRNAs) and small nucleolar RNAs (snoRNAs).

1.2.1 PiRNAs

PiRNAs (24-32 nucleotides in length) performed their main activity in the germline where they target and repress expression of transposable and repetitive elements to maintain genomic stability [*Siomi et al., 2011*]. They are processed from single-stranded RNA precursors that are transcribed from intergenic repetitive elements called piRNA clusters. Unlike miRNA, they are processed by a Dicer-independent mechanism. As the name suggest, piRNAs are associated with PIWI proteins, which are germline-specific members of AGO protein family. The association between piRNA and PIWI proteins forms the piRNA-induced silencing complex (piRISC) that recognizes and silences complementary targets RNA.

1.2.2 SnoRNAs

Small Nucleolar RNAs (snoRNAs) are well-conserved, abundant, short non-coding RNA molecules, 60-300 nucleotides in length. They are localized in the nucleolus into eukaryotic cells nucleus and are involved in the chemical modification of ribosomal RNA. The majority of snoRNAs are encoded in the introns of protein coding genes and are

transcribed simultaneously by RNA Polymerase II [*Sana et al., 2012*]. Despite, they are frequently used as reference genes in miRNA expression analysis, snoRNA are significantly modulated in several diseases, including cancer.

1.2.3 MicroRNA

MicroRNAs (miRNAs or miRs) are a family of small (19–25 nucleotides in length) non-coding RNAs that have a key role in the regulation of gene expression through the inhibition or the reduction of protein synthesis. They will be discussed in detail in the chapter 2.

MicroRNA

MicroRNA are non-coding small RNA molecules, found in both prokaryotes and eukaryotes, that are able to negatively regulate gene expression at post-transcriptional level by targeting mRNA. They were firstly introduced in 1993, when Lee [*Lee et al., 1993*] and Wightman [*Wightman et al., 1993*] independently reported that a small transcript: *lin-4* binds the 3' untranslated (UTR) region of the *C.Elegans* gene *lin-14,* negatively regulating *lin-14* protein expression. By this discovery several others miRs have been found, and at moment the known human mature miRNAs registered in miRBase are 2588 (miRBase.org, release 21, June 2014), and probably, will continue to increase.

2.1 Nomenclature of miRNA

The complete name of a miRNA can be divided into three parts: the first part, composed generally by three characters is referred to the species; *hsa* (Homo sapiens), *mmu* (Mus musculus) and *cel* (Caenorhabditis elegans) are only some examples. 'miR' is the second part and it is universal, followed by the third part, that is a number, specific for every miRNA sequence. At this general scheme can be added some others information for example:

- If two miRNAs with identical sequence are transcribed from different gene loci of the genome, they get a second number, after the identification number: for example miR-92-1 and miR-92-2.

- If two miRNAs differ only in one or two nucleotides, they get a character after the number: for example, miR-200a and miR-200b.

- If both strands of miRNA duplex maturate the less abundant is marked by a '*'

- If the miRNA precursor is cleaved close to 5' end the miRNA name is followed by -*5p*, instead if the cleavage is closer to the 3' end the miRNA name is followed by -*3p*.

2.2 microRNA Genes

MiRNA genes are distributed not randomly in human genome and have been found in all chromosome except in Y chromosome [*Ghorai et al., 2014*]. As regard miRNA genes location, it has been demonstrated that miRNA can be divided in two groups: intragenic miRNA and intergenic miRNA. Intergenic miRNAs are located between genes and their transcription is independent of coding gene, in fact they are generally transcribed by RNA polymerase III (RNApol III). Moreover, some studies reported that intergenic miRNAs are more evolutionary conserved than intragenic miRNA [*Schanen et al., 2011*]. Intragenic miRNAs are embedded within exon or introns of protein-coding genes, so are co-transcribed with their host genes by RNA polymerase II. Moreover, a small percentage of miRNAs have been found to be interspersed among repetitive elements and transcribed by RNApol III. MiRNA expression is regulated by transcription factors (TFs), enhancers and silencing elements and the regulation is development- and tissue-specific. The protooncogene c-MYC is only an example of transcription factor that is able to regulate miRNA expression [*O'Donnell et al., 2005*]. MiRNAs are generally located in cluster or miRNA families such as miR-200 family that presents two different clusters one in human chromosome 1, which expresses miR-200a, miR-200b and miR-429, and a second cluster located in human chromosome 12 which expresses miR-141 and miR-200c [*Korpal et al., 2008*]. MiRNA clusters generally include miRNAs with the same target site or with the same function.

2.3 miRNA Biogenesis

The first step of miRNA biogenesis takes place in the nucleus, where the transcription of miRNA gene locus by RNApol II or RNApol III generates a long primary RNA called pri-miRNA, that can contain more than one miRNA sequence. MiRNA precursor is several kilobases-long and presents a 7-methylguanosine cap in 5' position and a poly-adenyl tail in 3'. Pri-miRNA fold is into a hairpin, which contains a terminal loop, a stem (dsRNA) of about 33 bp and two flanking regions of single stranded RNA. This structure is processed by miRNA processor complex that is composed by Drosha and DGCR8 (DiGeorge syndrome critical Chromosome Region 8) also called Pasha (Partner of Drosha). Drosha is a member of class II ribonuclease III proteins and presents an amino-terminal proline-rich and serine-arginine- rich region responsible for the nuclear localization, a middle region that interacts with DGCR8, two RNase III domain (RIIIDs) that interact with each other to make

a dimer with catalytic activity, and a double stranded RNA-binding domain (dsRBD) [*Han et al., 2006*]. In the first step (substrate recognition) DGCR8 recognises the ssRNA-dsRNA junction (SD) and the 33 bp stem in the pri-miRNA followed by the interaction between Drosha and DGCR8 that activates the second step (catalytic reaction).

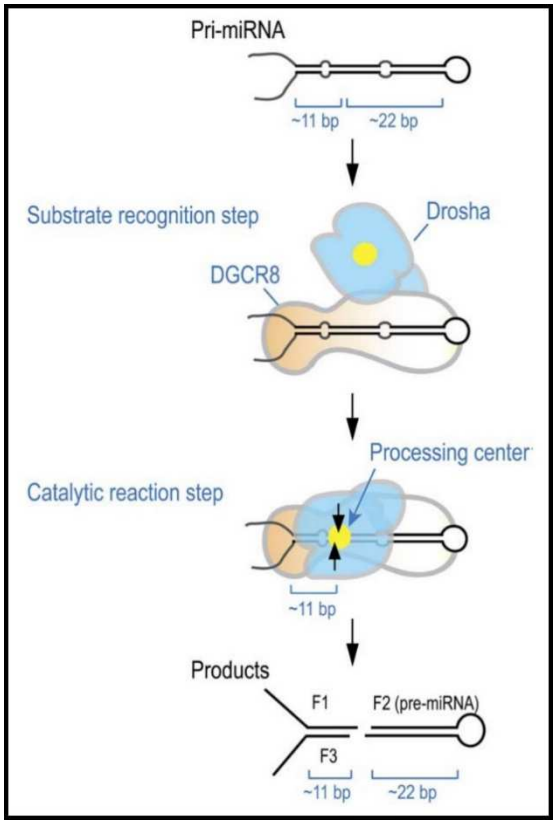

Figure 1: Pri-miRNA processing. DGCR8 recognises the ssRNA-dsRNA junction, then Drosha interacts with the substrate for catalysis. Picture taken from *Han et al., 2006.*

Drosha interacts with DGCR8 anchored stem in a region that is 11 bp from SD junction and cleaves the two strands generating a smaller hairpin-like miRNA precursor called pre-miRNA, containing 2 nucleotides 3' overhang. Exportin-5 receptor (EXP-5) associated with RanGTP (Ran Guanosine Tri-Phosphate) recognises the 2 nt overhang of the pre-miRNA and actively transports pre-miRNA from the nucleus to the cytoplasm [*Bartel, 2004*]. Once in the cytoplasm, pre-miRNA undergoes to two important modifications: 1) urilydation or less frequently adenylation, at 3'UTR and 2) methylation at 5'end. These modifications are very important because affect the pre-miRNA stability and allow an accurate cleavage in the following step [*Park et al., 2011*].

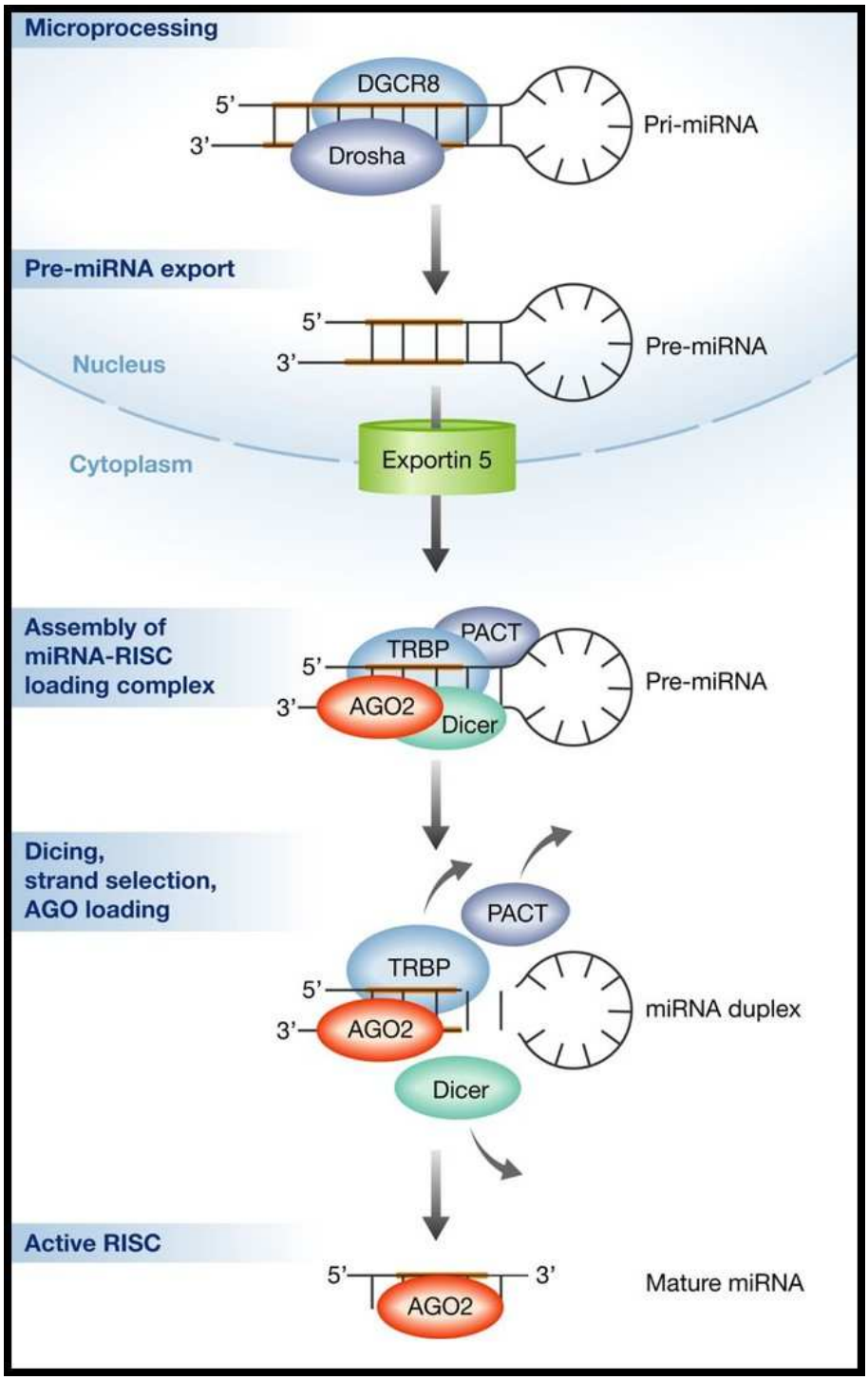

Figure 2: **Canonical pathways for miRNA maturation**. After transcription, the initial pri-miRNA transcript is processed by the Drosha/DGCR8 complex. The resultant intermediate precursor, pre-miRNA, is a 70-nt hairpin that is exported from the nucleus into the cytoplasm by Exportin 5. In the cytoplasm pre-miRNA is recognized by Dicer complex/miRNA-RISC-loading complex. Upon disassembly of the RISC-loading complex, AGO protein has a key role in strand selection. Picture taken from *Emde et al., 2014*.

A protein complex: RISC Loading Complex (RLC) binds to pre-miRNA to cleavage it. RLC is composed by three principal elements:

- *Dicer*: an endoribonuclease that takes part of RNase III-family and is essential for miRNAs maturation. Dicer presents several domains and between these, particularly important is PAZ (Piwi/Argonaute/Zwille) domain that has two pockets: the first one recognises and binds 2 nucleotides overhang at the 3' of the pre-miRNA. The second one, that is positively charged, binds the 5' terminal, negative charged phosphate group of the hairpin duplex [*Macrae et al., 2006*]. Moreover, essential for the pre-miRNA cleavage are the two catalytic RNase III domains.

- *Double-Stranded RNA-Binding Proteins* (dsRBPs) bind one of Dicer domain, generating a conformational rearrangement that results in Dicer activation. Moreover, as Wilson and colleagues described, these proteins, in particular TRBP (Tar RNA-Binding Protein) have an important role in strand selection [*Wilson et al., 2015*].

- *Argonaute-2* (AGO2) is a member of Argonaute family, which includes 8 different proteins, but between these only one, AGO-2 presents catalytic nuclease activity, while others one inhibit the translation, but the mechanism of action is at moment not clear [*Hock et al., 2008*].

After the cleavage by Dicer miRNA duplex is transported by Dicer to one of Argonaute proteins (AGO). The bind between miRNA duplex (5p strand-3p strand) and AGO is possible thanks to Hsp90 (Heat Shock Protein 90) that mediates a conformational change in AGO, allowing the bond [*Pare et al. 2009*]. AGO-2 binds at N-terminal PAZ domain the 3'end of the guide strand (5p strand) of the miRNA duplex, starting the duplex unwinding. Generally, the strand with the weaker bind at 5'end is chosen as guide strand, maybe because duplex opening is easier there. The other one (generally, 3p strand) is normally degraded, but there are several cases, in which is equally or even more important of 5p strand. The mature single strand, AGO proteins, and several others, not fully understood, proteins are part of a complex called miRISC (miRNA Induced Silencing Complex) that represents the functional unit of miRNA-mediated gene regulation.

2.4 miRNA Target Recognition

MiRNA associated with RISC in the miRISC complex is able to exert its function through the recognition of its complementary sequence in target mRNA. Nucleotides in miRNA sequence that are essential for the bond with the target mRNA, constitute the seed region. Seed region generally takes place from the 2nd and the 7th nucleotide on the 5'end of the mature miRNA and in most of cases recognises a complementary sequence in the 3'UTR of the target mRNA. However, is not uncommon that miRNAs can recognise target sequences also in 5'UTR and in highly conserved sequences of the coding domain sequence (CDS). If the role of miRNA targeting 3'UTR is well characterized, the regulatory functions of miRNAs targeting CDS or 5'UTR appear currently not completely clear [*Brummer et al., 2014*] and the issue is still much debated. Some authors argue that gene regulation is less effective when miRNA target sequence is located in the coding region [*Marin et al., 2013*] or in the 5'UTR [*Grimson et al., 2007*]. In fact, these authors postulate that in the CDS is possible that ribosomes displace RISC from the target site before RISC effects the translational repression. Others, as Hausser and colleagues, demonstrate that CDS and 3'UTR target sites have, not only similar sequence and structure proprieties, but also present similar efficiency in inducing translational repression of the mRNA; with an important difference: miRNAs targeting 3'UTR are more effective in inducing mRNA degradation [*Hausser et al., 2013*]. MiR-148 is only an example of miRNA that is able to down-regulate its target (the protein DMNT3b) through the bond with the complementary mRNA in the coding region [*Duursma et al., 2008*]. The seed sequence of miRNA can pair with target mRNA in different ways. The canonical way takes place when the seed region pairs with mRNA with 7 seed region nucleotides and

- the nucleotide opposite the 1st miRNA nucleotide is adenine (7mer-A1 site)

- the 8th nucleotide pairs with the opposite nucleotide (7mer-m8 site)

-in the first place is adenine and the 8th nucleotide pairs (8mer site).

To predict miRNA possible mRNA targets several methods are available, even if, generally the first step is a bioinformatics analysis through which is possible to predict miRNA targets *in silico*. This kind of analysis uses bioinformatical algorithms that allow to analyse three important parameters:

- Watson-Crick complementary between seed region of the miRNA and its target

- Evolutional conservation of the sequence through the species
- Thermodynamic proprieties of the target mRNA

For this propose several software are free available such as TargetScan (*www.TargetScan.com*), miRWalk (*www.umm.uni-heidelberg.de/apps/zmf/mirwalk*). After this first step the confirmation of *in silico* data must be performed.

2.5 miRNA detection techniques

The unique characteristics of miRNA, such as small size, low abundance and sequence similarity among family members make miRNA detection very complex. Because of the small miRNAs size, the GC content in miRNA sequences is very variable, leading to a wide range of melting temperature (T_m). Also, short primers are required for Polymerase Chain Reaction (PCR) leading to low oligonucleotide annealing temperature that causes the decrease of hybridization stringency and the consequent increase of cross-hybridization risk [*Pritchard et al, 2012*]. Furthermore, miRNAs represent only the 0.01% of total RNA [*Dong et al., 2013*], so bioanalysis devices must be able to differentiate very small amount of miRNA in the presence of total RNA. Another important characteristic to consider, is the extremely variable abundance of miRNAs, that can vary from a copy to 50.000 copies for a single cell [*Bartel, 2004*]. Currently a wide range of approaches have been explored for miRNA profiling. Besides traditional methods strategies as RTqPCR (Quantitative Reverse Transcription PCR), Northern Blot, microarray and RNA Seq, others strategies based, for example, on Surface Plasmon Resonance (SPR) are emerging. All of them require different sample input and present different Limit Of Detection (LOD) that is the lowest quantity of analyte that can be distinguished from the blank value. Moreover, some of these techniques present the ability to analyse multiple targets in the same run. It is important to underline that sample processing and RNA extraction have a substantial impact on the results of miRNA profiling.

2.5.1 Conventional Techniques

2.5.1.1 Quantitative Reverse Transcription Polymerase Chain Reaction

Actually is considered the gold-standard for miRNA detection, but it is used for single or small panel, miRNA detection. This technique is characterised by a wide dynamic

range, high sensitivity: few nanograms of total RNA are sufficient, high accuracy, low assay cost and can easily provide absolute miRNA quantification [*Baker, 2010*]. The technique relies on reverse transcription of miRNA to cDNA followed by quantitative real time polymerase chain reaction, monitoring the accumulation of reaction product.

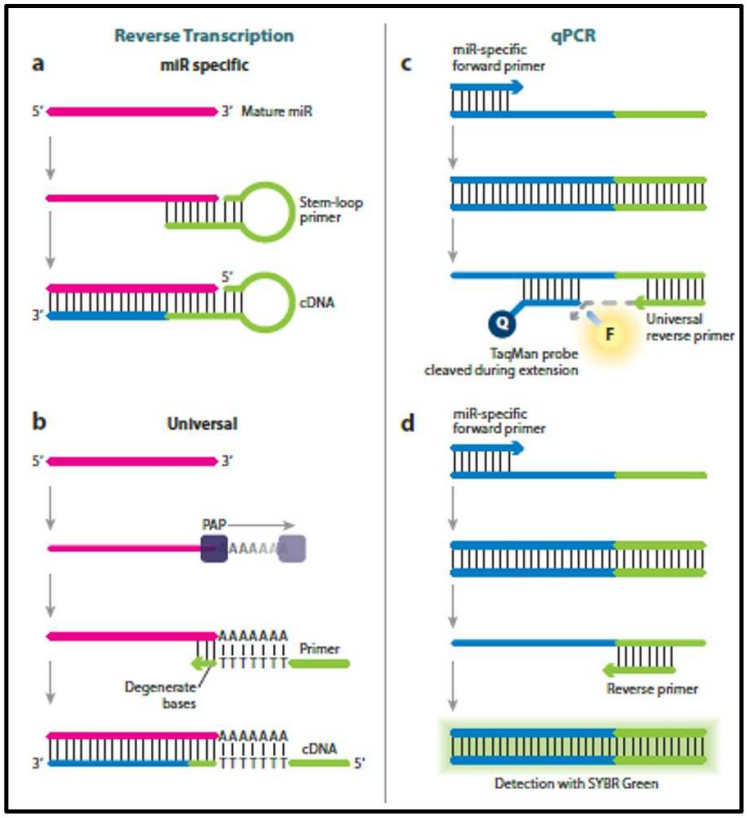

Figure 3: **PCR-based miRNA detection**. Panel a: miRNA specific reverse transcription using stem-loop primer followed by qPCR amplification using TaqMan probe (Panel c). Panel b universal miRNA reverse transcription and relative qPCR amplification using LNA primers and SYBR Green (Panel d). The Figure was taken from *Hunt et al., 2004*.

Two main strategies are used for priming the reverse transcription of miRNA to cDNA: the addition of a polyA tail at 3' of all miRNAs by *E.Coli* poly(A) polymerase (PAP), followed by reverse transcription using universal primers consisting on an oligo dT sequence. The PCR product formation is then quantified using a dsDNA-intercaling dye, such as SYBR Green [*Pritchard et al., 2012*]. Some researchers consider this method more suitable to detect miRNA from small amount of starting material (for example plasma sample). Another reverse transcription method is based on the use of stem loop primer: miRNA-specific primers that reversely transcribe only a particular miRNA. Stem loop primers are designed to contain 6-8 nucleotide overhang on the 3' end that is complementary to target miRNA.

After the hybridization between primer and the complementary miRNA the reverse transcription extends from miRNA 3' end. These kind of primers are able to differentiate between mature miRNA and pre- or pri-miRNA and present more specificity thanks to the optimization of T_m. Every stem loop primer can be recognized by a standard PCR primer, so the PCR amplification is performed using a universal reverse primer that binds to the conserved stem loop region of all RT products and a forward, miRNA-specific primer that recognizes the 3' and of the miRNA. To increase the specificity, the assay employs a TaqMan probe, that hybridizes in the region between the forward and reverse primer. In both SYBR Green and TaqMan detection method, the signal is measured as a function of cycle number (CT). In order to use RTqPCR approach for miRNA profiling are commercially available plates or cards that allows to analyse a small set of miRNA involved in a pathway of interest, that partially solve the problem of multiplex analysis. The main drawback of RTqPCR remains the complex primer design and the run to run variability in PCR amplification, that makes necessary the use of internal controls, as housekeeping genes [*Peltier et al., 2008*] or the spike-in of non-natural miRNA before RNA extraction step [*Sarkar et al., 2009*].

2.5.1.1.1 Digital PCR

The concept of digital PCR was first introduced by Sykes in 1992, when he proposed a PCR carried out in limiting dilution conditions, able to detect very rare targets [*Sykes et al., 1992*]. Digital PCR is employed to quantify nucleic acid in absolute way thanks to the partitioning of the analyte molecules into many replicate reactions at limiting dilution, resulting in one or zero molecules for partition [*Hindson et al., 2013*]. The partitioned sample is amplified by endpoint PCR and starting concentration of template is determined by Poisson statistical analysis of the number of positive (containing amplified target) and negative (no amplified target detected) partitions.

$$\boldsymbol{copies\ per\ droplet} = -\ln\left(1 - \frac{\boldsymbol{positive\ droplets}}{\boldsymbol{total\ counted\ droplets}}\right)$$

The major advantage of the dPCR compared to Real Time PCR is the possibility to obtain absolute quantification of the sample without external references. In the last years, several dPCR platforms were developed, with two different partition methods. Companies as

Fluidigm and Life Technologies divide the sample into chambers within specially designed chips or plates. On the other hand, Bio-Rad and RainDance divide reagents and sample into

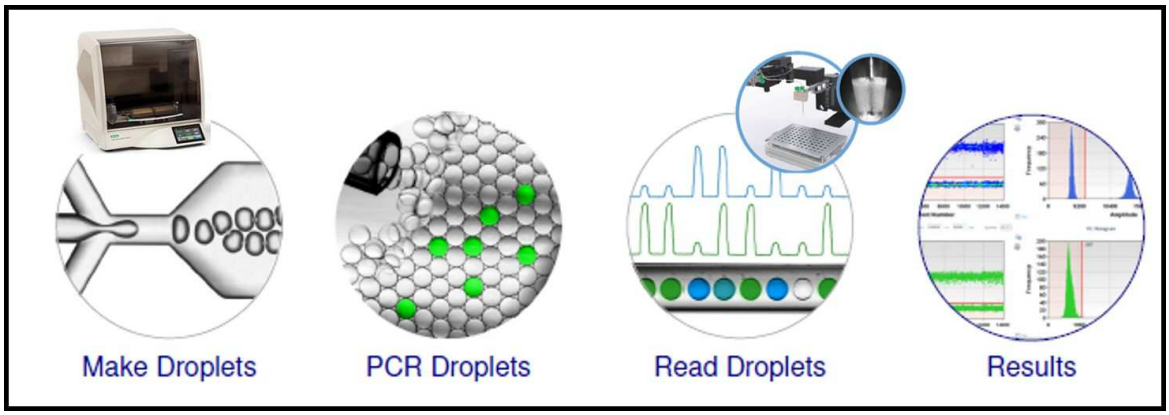

Figure 4: Droplet Digital PCR workflow. About 20.000 droplets are generated using Automated Droplets Generator (AutoDG), droplets are amplified using a common thermal cycler. Droplets are analysed for their fluorescence using QX200 droplets reader, applying Poisson law the number of starting copies/µL is calculated. Picture taken from *www.bio-rad.com.*

individual droplets, which are water-in-oil emulsion [*Baker, 2012*]. Bio-Rad platform divided the sample into about 20.000 nanoliters-sized, uniform droplets, and into each one the amplification reaction is performed. Droplets are then analysed for their fluorescence content and classified into positive or negative in order to apply Poisson law and quantify the target. Digital PCR presents several applications included Copy Number Variation detection (CNV assay), Rare Mutation Detection (RED Assay), Gene expression Analysis (GEX Assay), single-cell analysis, detection of pathogen through the research of viral or bacterial nucleic acids, and SNP genotyping. Digital PCR can be very useful in liquid biopsy in which target molecules are present at very low concentration. In this case is possible to quantify very diluted samples with high accuracy and without need of replicates. As well demonstrated by Miotto and colleagues, ddPCR has been successfully employed in miRNAs detection, in particularly way in miRNA sample extracted from plasma, in which miRNA content is very low (less than 1 copy/µL) [*Miotto et al., 2014*]. Moreover, the same assay employed in real time PCR can be used with minor changes in digital PCR technology.

2.5.1.2 MiRNA microarray

MiRNA microarray is well suited for parallel analysis of large numbers of miRNAs, but presents low sensitivity and requires an RNA input, in the order of micrograms. MiRNAs are tagged with fluorophore-labelled nucleotides using T4 RNA ligase, after the

dephosphorylation of the 5' end. MiRNAs detection is allowed by the hybridization of labelled miRNA with complementary 'capture' probes immobilized on a glass slide. The miRNA expression levels are provided by a two channel fluorescent imaging. It was demonstrated that T4 RNA ligase prefers some sequences to others, so it creates artefacts, especially in degraded samples [*Baker, 2010*].

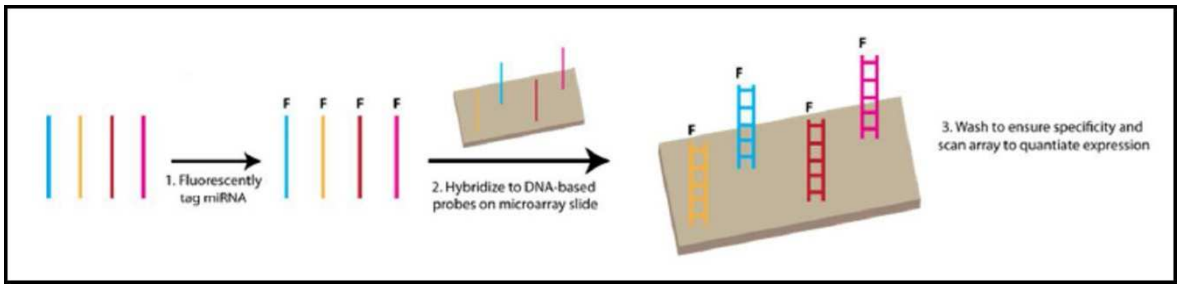

Figure 5: Typical microarray work-flow. In the first step miRNA are tagged with fluorophore-labelled oligonucleotide, than miRNA are recognised by complementary capture probes. Taken by *Graybill et al., 2015*.

In order to avoid these biases, different studies were performed to develop a labelled-free method for direct miRNAs detection. For example Lee and co-workers set-up a new direct miRNA detection method using short (about 10 nucleotides) LNA probes that not only reduce the cross-hybridization between miRNAs but also is able to detect attomolar miRNA concentration [*Lee et al. 2011*]. Generally, microRNA array is used to compare the relative abundance of a large numbers miRNAs between two or more groups (for example healthy versus disease status) and is considered a semi-quantitative method due to the absence of a calibration curve. Moreover, microarray is characterized by low specificity, for this reason, in most cases, microarray data need to be validated by other detection methods like RTqPCR or northern blot.

2.5.1.3 Northern Blotting

Northern Blotting is used to identify and quantify specific miRNA since 1993 [*Lee et al., 1993*]. The major limit is the high quantity of RNA required, generally in the range of micrograms and the low sensitivity (nM-pM). For this reason, this technique is not the first choice especially, for low abundance miRNA. Broadly, the technique includes a first electrophoretic step in which RNA is separated on the base of size, followed by the transfer to a positively charged nylon-membrane. MiRNA detection is achieved by hybridization with labelled oligonucleotide probes. Different probe-labelling techniques have been reported in the years: the most common is based on the incorporation of radio isotopes (^{32}P)

to the probe [*Valoczi et al., 2004*]. In order to obtain more safe technique and to reduce the time of exposure, several others labelling methods have been proposed such as Locked Nucleic Acid (LNA) probes and hapten-labeled probes coupled with enzymatic reaction methods [*Ramkissoon et al., 2006*].

2.5.1.4 RNASeq

This technique was made possible thanks to the advent of Next-Generation Sequencing (NGS). The method is based on the preparation of miRNA cDNA library from

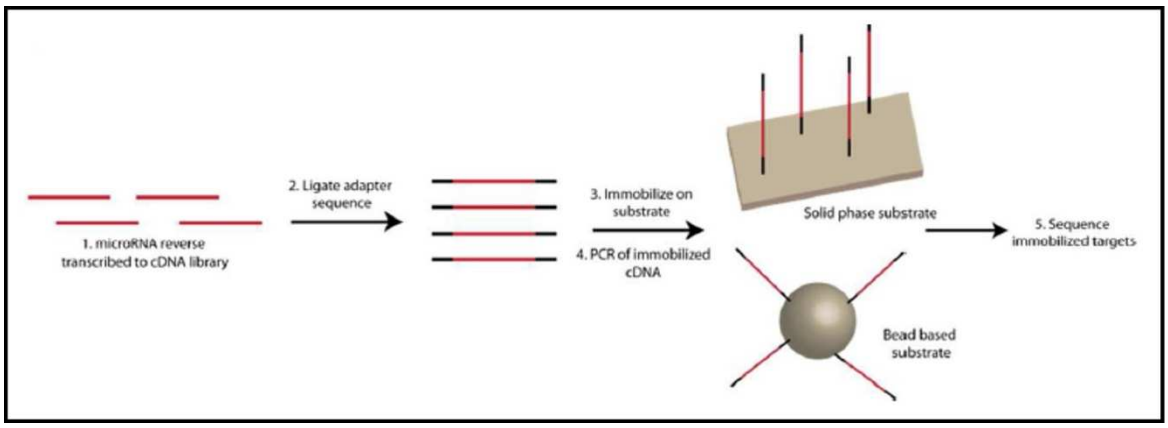

Figure 6: RNA sequencing analysis. MiRNAs are reverse transcribed into a cDNA library, cDNA are than immobilized into a solid substrate for data analysis. Taken by *Graybill et al., 2015.*

RNA of interest, followed by the parallel sequencing of millions of individual cDNA molecules in the library, in the same run [*Metzker, 2010*]. Data are analysed by a bioinformatic analysis that allowed to obtain a relative quantification of both known and new miRNAs. The estimation of the relative abundance of a miRNA is given from the ratio between the number of sequence reads for the miRNA of interest and the total reads in the sample [*Tian et al., 2010*]. The major advantages of this technique are the detection of both known and novel miRNA and the precise identification of miRNA sequence. One the other hand, NGS is expensive and requires computational infrastructure for data analysis.

2.5.2 Unconventional miRNA detection techniques

2.5.2.1 Biosensors methods

Biosensors are analytical devices that integrate biological sensing elements (probes, antibodies, enzyme) with a physical transducer (in most cases optical or electrochemical) whereby the interaction between the target and the recognition-molecule is translated into a measurable electrical signal [*Long et al., 2013*]. A large number of works were performed, in the last decade, regarding miRNA detection using biosensors, introducing new signal transducer, new type of capture sequences and new signal amplification strategies. However the most of works are characterized by low levels of multiplexing; in fact most of these, analyse only 2-3 miRNAs at a time. Between biosensors, the most promising for miRNA detection are electrochemical and optical devices.

2.5.2.2 Electrochemical Biosensors

Electrochemical sensors represent a great promise for multiplexed miRNA analysis. Different research team set-up electrochemical sensors with different characteristics, but generally the basic structure of the sensor is constituted by a electroactive hybridization indicator and a solid electrode with a immobilized short single stranded nucleotide probe [*Hamidi et al., 2013*]. The signal for detection is produced by the interaction between the immobilized probe (cationic species) and the complementary miRNA (anionic species) sequence. Generally, the detection is achieved through the measurement of redox signal or a change in capacitance. Various approaches are continuously investigated in order to improve the sensitivity of this kind of devices, that is generally in the range of attomolar or femtomolar [*Tosar et al., 2010*]. Yang and co-workers propose an electrochemical biosensor in which gold nanoparticles are used to enhance miRNA detection. They used a sandwich model, composed of two probes: AuNPs probe hybridized to the complementary target miRNA and a biotinylated capture probe. The hybridization complex is immobilized on a streptavidin-coated micro-plate surface. The signal of adsorbed AuNPs is enriched by silver and is recorded by a microplate reader. Authors declare a LOD of 10 fM miRNA starting from 2 nanograms of total RNA [*Yang et al, 2008*].

2.5.2.3 Optical Biosensors

Optical detection methods have recently become attractive for miRNA expression analysis because of their high sensitivity, dynamic range and multiplexing capabilities. Moreover, optical devices have been known to be less susceptible to interference from

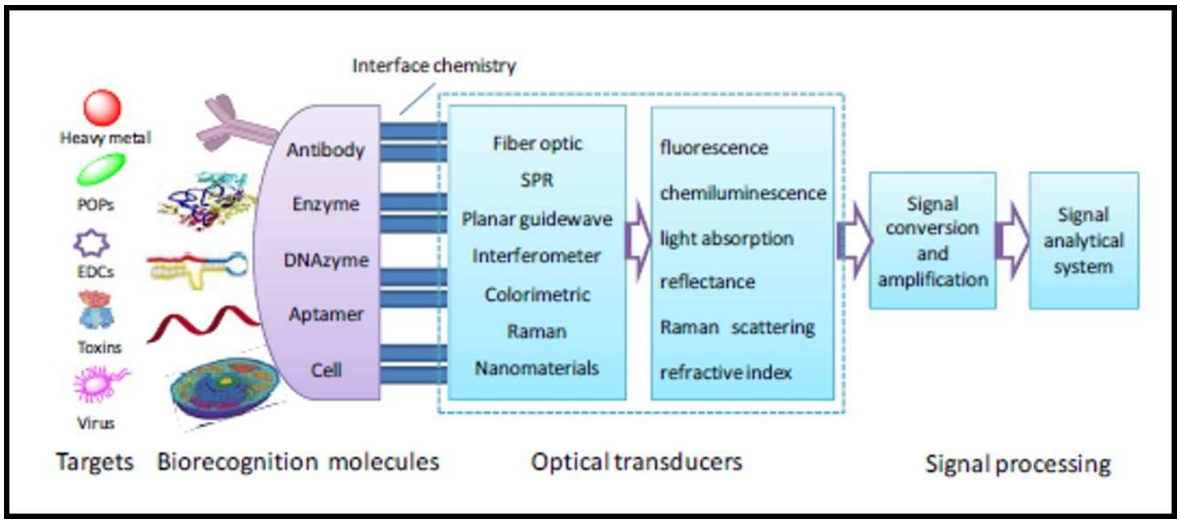

Figure 7: Optical biosensor. Optical biosensor is an analytical device that integrates a biological sensing element with a physical transducer, whereby the interaction between the target and the bio-recognition molecules is translated into a measurable electrical signal. Taken from *Long et al., 2013.*

matrix components than electrochemical devices and are ideally suited to direct miRNA detection with minimal purification requirements. A wide range of optical detection methods have explored, here are summarized some of the most interesting, considering LOD.

2.5.2.4 FRET approach

Foster Resonance Energy Transfer (FRET) is one of the most common methods to obtain a 'on/off' detection scheme in which the fluorescent signal is 'off' when no target is present and 'on' when target miRNA is present. A simple FRET approach was presented by Wu and co-workers, in this case a fluorescently tagged DNA capture probe was hybridized with a quencher. In the presence of the target, the quenching strand is displaced activating the fluorescent signal. Wu and colleagues obtain a LOD of 1fM and a dynamic range of 4 orders of magnitude, but also a high false positive rate [*Wu et al., 2014*]. The detection strategy developed by Wu is stoichiometric: a single miRNA molecule led to a single fluorophore being turn 'on'. In order to achieve better gain, was studied a technique in which a single miRNA can led to multiple fluorophore signatures using a Duplex-Specific Nuclease (DSN). The enzyme recognizes and cleaves the DNA:miRNA duplex that is employed to

detect miRNA, releasing the fluorophore to induce a detectable signal and at the same time after the cleavage, the miRNA is free to bind to another DNA capture probe to repeat the process [*Yin et al., 2012*]. In this way a single miRNA can bind thousands of capture probes increasing the signal levels (LOD 1 fM, range of 5 orders of magnitude).

2.5.2.5 ECL approach

Electrochemiluminescence (ECL) can be used to obtain an optical signal directly proportional to miRNA concentration in the sample. In this case the presence of the target causes a luminescent response in presence of ECL reporter molecule. The main advantage, compared to FRET, is the elimination of background fluorescence due to interfering species in solution. Using ECL approach a single miRNA was successfully detected in three different cell lines, obtaining a LOD of 100 pM and a dynamic range of 3 orders of magnitude [*Liu et al., 2014*].

2.5.2.6 Silicon photonic microring resonance approach

Recently Graybill and co-workers developed a new miRNA detection technique using a reverse transcription-enabled enzymatic signal enhancement strategy associated with silicon photonic microring resonators. This method not only avoid PCR amplification step but also, is able to analyse at least seven miRNAs per sample. When miRNAs bind the sensor surface, they generate a change in the refractive index and consequently a resonance shift, which is directly proportional to the number of molecules that are bound to the sensor surface. In order to enhance the target miRNA signal, Graybill propose a sandwich-based protocol that uses the reverse transcription to create a cDNA that is subsequently detected using horseradish peroxidise reaction. The reverse transcription is performed using stem loop primers. A biotinylated tag sequence of DNA, complementary to the universal stem loop region (in this way is possible to avoid the need of multiple tagging sequences) hybridize cDNA. The hybridization is performed at 72°C to allow the linearization of the stem loop sequence, that is now able to bind the DNA capture probes on the microring sensors. After the bond formation a streptavidin-HRP conjugate is flowed across the sensor surface and the reaction between HRP and a solution of 4-CN (4-chloro-1napthol) causes the formation of precipitates that shift the resonance wavelengths. The shift is measured in

Δ picometers and is directly proportional to the concentration of miRNA in the sample [*Graybill et al., 2016*].

2.5.2.7 SPR and SPRI approach

Surface Plasmon Resonance (SPR) is a label-free detection method emerged in the last two decades and used to study biomolecular interactions. SPR occurs when a photon of incident light hits a metal surface (generally made of gold). At a certain angle of incidence, a portion of the light energy couples through the metal coating with the electrons in the metal surface layer, which then move due to excitation. The movements of electron, called plasmon, propagate parallel to the metal surface [*Nguen et al., 2015*]. The SPR angle, at which resonance occurs, depends on the refractive index of the material near the metal surface, so when biomolecule attachment occurs there is a small change in the reflective index and the plasmon cannot be formed. The signal change is described using Resonance Units (RU). The principal obstacle in the development of SPR based biosensor for miRNA

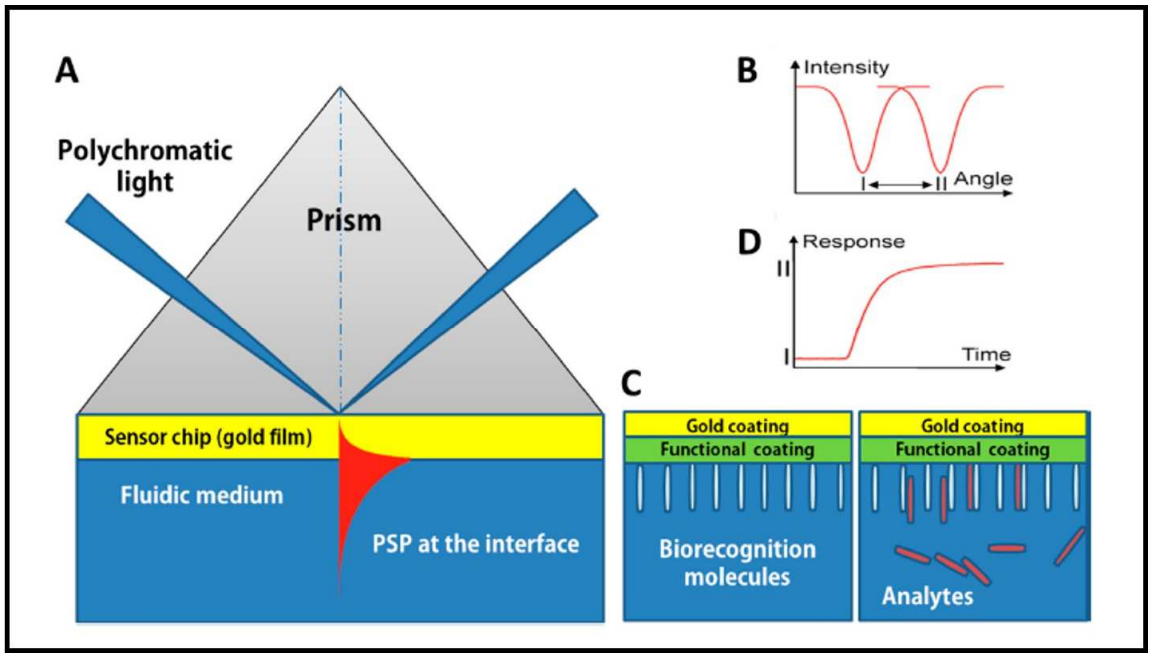

Figure 8: Surface Plasmon Resonance (SPR) biosensor. (A) in SPR a incident light is employed, (B) spectrum of reflected light before and after refractive index change, (C) analyte-biorecognition elements binding on SPR sensor surface, (D) refractive index changes caused by the molecular interactions.

detection is the small miRNA size. Due to their short size, miRNA hybridization doesn't cause a significant change in refractive index in the sensor surface, for this reason several strategies to improve the signal have been developed. Generally, the increase of the signal is obtained using a high mass recognition element that is able to bind the probe-miRNA duplex

[*Vaisocherova et al., 2015*]. Another important step can be achieved with SPRI, in which a multi-sample analysis can be performed using a biochip. The chip is prepared in an array format, in fact it contains several spots (in some case, more than four hundred), and in each spot a SPR reaction is performed. A broad-beam monochromatic polarized light from a laser diode, set at a specific wavelength, illuminates the chip and through a high resolution video CCD camera is possible to detect changes in all spots present in the chip, achieving information about molecular interaction in real time [*Scarano et al., 2010*].

2.6 Circulating miRNA

Recently it has been demonstrated that miRNAs are stably present in several body fluids such as blood, saliva, urine, milk and stools [*Chim et al., 2008; Weber et al., 2015*]. Moreover, extracellular miRNAs are very stable, even after long term storage of samples. The function of circulating miRNA (cmiRNA), at the moment, is not well established, some groups postulate that miRNAs are physiologically released by cells maybe as a 'mechanism of communication' both with cells that are in the immediate vicinity or with far sites and with others types of cells. Indeed, other groups sustain that cell-free miRNAs are only waste which enter into body fluids as consequence of cell death [*Turchinovich et al., 2012*]. Instead, no doubts are there about cmiRNAs involvement in disease, in fact, it is clear that the cmiRNA profile is very different between physiological and pathological condition. Due to their easy sampling and their good stability in body fluid, circulating miRNAs are considered between the best candidates as biomarkers for non invasive diagnosis techniques.

2.6.1 Circulating miRNA release

Cellular machinery involved in miRNAs packaging and release is not still well understood, all researchers have assumed that miRNAs must be packaged in some way to avoid nuclease degradation in body fluids. This assumption is supported by the evidence that if a synthetic miRNA is added into a body fluid, it is immediately degraded by RNase [*Turchinovich et al., 2011*]. Several mechanisms of cmiRNA protection have been proposed and all of them seem to be valid, but at moment it has not been identified a release mechanism that prevails on the others, maybe because the mechanism depends on several

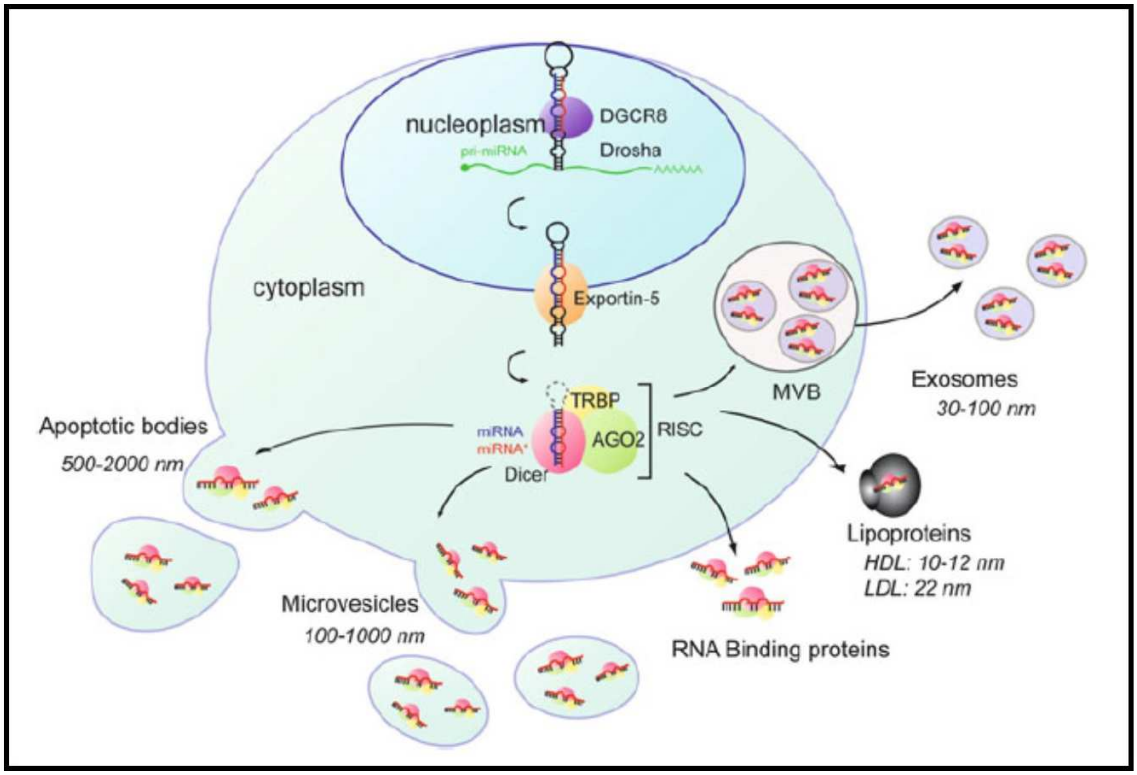

Figure 9: Possible miRNA export pathway. Multiple subclasses of miRNA carrier have been identified in serum, including three types of membrane-derived vesicles: exosomes, micro vesicles and apoptotic bodies. Additionally, lipoproteins such as high-density lipoproteins (HDL) can incorporate miRNA, and ribonucleoproteins such as AGO2 bind miRNAs. Taken from *Coenen-Stass et al., 2015.*

factors such as miRNA sequence, cell type, physiological or pathological condition and every mechanism has its specific biological role. Some proposed mechanisms require the inclusion of miRNA into lipid membranes as extracellular vesicles (EVs), exosomes or microvesicles, even if Wang and co-workers demonstrate that the large majority (about 90%) of miRNAs released from cells are vesicle-free and are frequently associated to ribonucleoproteins [*Wang et al., 2010*; *Wang et al., 2011*]. Subsequently, Turchinovich and colleagues clarify that vesicle-free miRNA are associated with AGO proteins [*Turchinovich et al., 2012*]. In addition, some miRNAs, as miR-126, were also identified into apoptotic bodies [*Zernecke et al., 2009*] or associated with high-density lipoprotein (HDL) [*Vickers et al., 2011*].

2.6.1.1 MiRNA vesicular carrier

Extracellular vesicles is a generic name to indicate all membranes that encapsulate particles and are released by cells. They can further be classified following different parameters such as size, biological function or biogenesis pathway. Referring to their

biogenesis, EVs can be classified into three types: exosomes, microvesicles and apoptotic bodies.

- *Exosomes*: are small lipid bilayer vesicles, about 30-120 nm in size, originated from in-budding of endosomal membranes, which in turn form multi-vesicular bodies (MVBs). MVBs contain intra-luminal vesicles, including exosomes, which are released in the extracellular environment after the fusion between MVBs and cell membrane [*Diana et al., 2017*]. Exosomes contain lipids, proteins, more of these involved in their biogenesis, and RNAs. Baglio and co-workers reported that in exosomes not only miRNA are present, but also tRNA, but its function is at the moment unknown [*Baglio et al., 2015*].

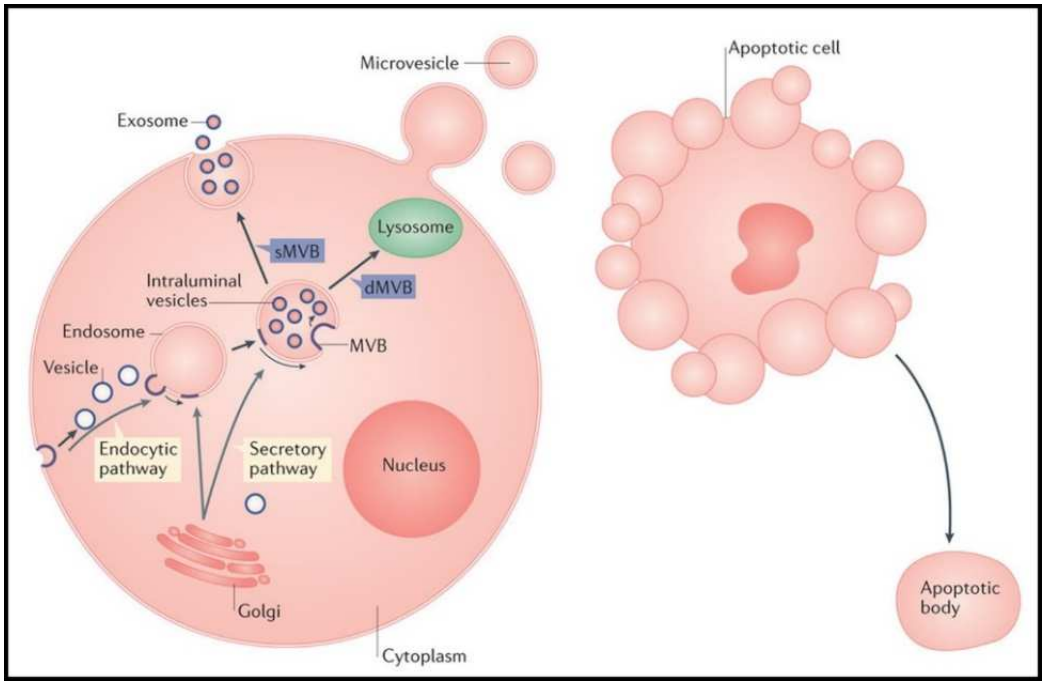

Figure 10. MiRNA vesicular carriers. MiRNAs can be included into exosomes, micro vesicles and into apoptotic bodies.

- *Microvesicles*: are formed directly from cellular membrane outward budding and fission and then released into extracellular space [*Chari et al., 2010*]. They have a size generally up to 1000 nm. The function of microvesicles depends on the cargo they carry, that, in turn, is dependent on the cell type from which they originate. In microvesicles were found proteins, included transmembrane proteins as integrins or surface receptors, and both coding and non coding RNAs.

- *Apoptotic bodies*: are formed during the process of programmed cell death, also in this case they are originated by cellular membrane, but they differ from microvesicles for their size which can reach 2 µm and also for their high content of exposed phosphatidylserine and fragmented DNA.

MiRNAs export through EVs is positively regulated by the protein sphingomyelinase (nSMase2) which is involved in EVs biogenesis. Several studies demonstrate that nSMase2 inhibition reduces miRNAs export in vesicles [*Trajkovic et al., 2008*], but it is not the only one, others proteins as ALIX or ESCRT present similar effects [*Raiborg et al., 2009*]. Studies demonstrate that miRNA profile into EVs is dependent to miRNA post-transcriptional modifications; for example 3'end uridylated miRNAs are more frequently secreted into EVs than 3'end adenylated, that are retained into cells [*Koppers-Lalic et al., 2014*]. Several others motifs, called EXOmotifs were found to be very frequent in EVs released miRNAs, as the sequence GGAG [*Villarroya-Beltri et al., 2013*]. At the moment the knowledge about EVs internalization by cells is very limited, a variety of endocytic pathways have been described, due to the EVs heterogeneity is very probable that EVs internalization is mediated by multiple uptake mechanisms, depending on protein and glycoprotein composition of the EVs and target cells surface [*Tian et al., 2013*].

2.6.1.2 miRNA non vesicular carrier

Three independent research groups, using different methods for miRNAs separation, conclude that the large majority of miRNAs are not associated in vesicles, despite this, they result protected against RNase [*Wang at al., 2010; Arroyo et al., 2011; Turchinovich et al., 2011*]. They conclude that miRNAs are in some way protected by degradation, and hypothesize that they form complexes with proteins. Non vesicular miRNA carriers include two kind of proteins: lipoproteins and ribonucleoproteins.

- *Lipoproteins*: lipoproteins form a mono lipid layer with a hydrophobic core, in which can be contained water-insoluble molecules, that result in lipoprotein particle of about 8-12 nm in size. HDL lipoproteins are the principal lipoprotein able to vehicle miRNAs, but some studies reveal that also LDL proteins carry miRNAs even if much lesser than HDL [*Vickers*

et al., 2011]. Between miRNAs, for example miR-223 was identified as one of the most abundant in HDL complexes [*Wagner et al., 2013*].

- *Ribonucleoproteins:* several proteins have been shown to carry miRNAs, the most abundant is nucleophosmin 1 (NPM1) a 33 kDa protein that was shown by Wang and colleagues to stabilising synthetic miRNAs in presence of RNase A [*Wang at al., 2010*]. Other proteins as AGO1 and AGO2 were shown to be associated with miRNAs.

2.6.2 Circulating miRNA as clinical biomarkers

All studies demonstrate a correlation between a specific miRNAs profile and human pathologies, suggesting miRNAs as a new class of biomarkers. As biomarkers miRNAs present several advantages including stability, specificity for certain physiological or pathological condition and the possibility to be accessible with non-invasive methods. Of course, there are still several pitfalls to solve as the standardization of sample preparation, quality control of samples and data normalization. MiRNA biomarkers can be divided into two classes: miRNAs originating from tissue or cell injured which have not active role in disease process but are considered only as signal of injury. For example, miR-133, miR-208 and miR-499 are miRNAs well expressed in heart muscle, and a high release of these miRNAs in blood has been shown after cardiac infarct [*Corsten et al., 2010*]. Instead, miRNAs that are considered to have an active role in disease process are part of the second class. For example, miR-126 have been shown to be altered in diabetes 2, and its alteration was shown before disease manifestation, suggesting that miR-126 can be involved in disease process [*Zampetaki et al., 2010*].

2.7 miRNA and cancer

A large number of evidences demonstrate that miRNAs and more generally, ncRNAs have functional roles in both physiological and pathological processes, regulating the expression of their target genes. In the recent years miRNAs were demonstrated to play a crucial role in cancer, in particular way, they are involved in cancer initiation and development, in the metastasis formation and also in the drug resistance. In addition, miRNAs can be considered as biomarkers for cancer diagnosis and prognosis [*Cho et al., 2010*]. MiRNAs expression profile differs, not only from normal and tumor tissues, but most

importantly differs from tumor types and cellular differentiation status. One of the first demonstration of the correlation between cancer and miRs, was presented by Calin and colleagues in 2002 [*Calin et al., 2002*], when they demonstrated the correlation between miR-15a and miR-16-1 down-regulation and chronic lymphocytic leukaemia. Depending on their function, miRNAs can be divided into two groups: tumor-suppressors miR and onco-miRNAs [*Cho et al., 2007*]. Tumor suppressor miRNAs enhance genes involved in apoptosis, tumor suppression and decrease genes with oncogenic activity, while onco-miRs enhance proliferation, angiogenesis and invasion reducing tumor suppressor mRNA.

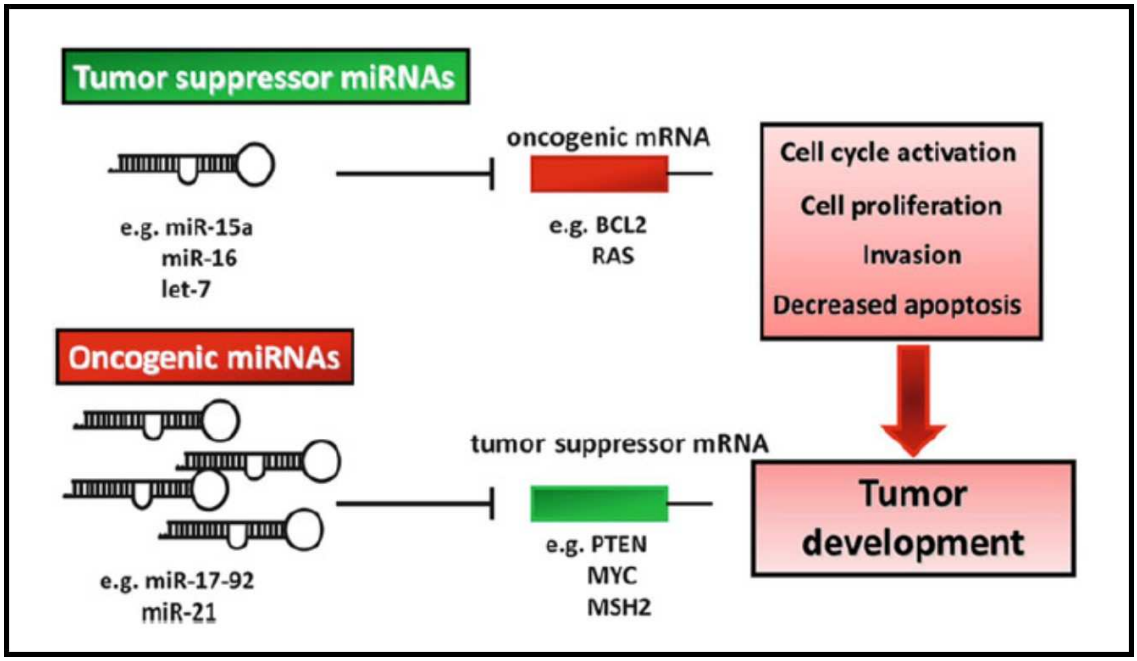

Figure 11: Onco-miRNA e tumor suppressor miRNA in tumorigenesis. Taken from *Nagy et al., 2015.*

This classification is not so definitive; in fact, in some cases the same miRNA can have tumor suppressor function in a tissue while in another one presents oncogenic function. Is the case, for example, of miR-24: its over-expression reduces cell proliferation and invasion in CRC [*Cao et al., 2014*], while in hepatocellular carcinoma its inhibition reduces tumor proliferation. The number of cancer-related miRNAs is extremely high, and is certainly going to increase, in the next years, thanks to the introduction of more sensitive technology and new miRNAs discovery.

2.8 Therapies targeting miRNA

Recently, miRNAs and the protein machinery involved in their biogenesis and activity have become targets for new therapeutic approach in several diseases. MiRNA regulation represents a very attractive field of application in the last years and this is confirmed by the high number of published patents. In fact, as Christopher and co-workers review the annual number of US and European published patents applications and issued patents related to miRNAs is close to 500 [*Christopher et al., 2016*]. The number of miRNA-based therapeutic molecules that are in clinical trials is very limited and is summarized in the following Table.

Target miR	Disease	Chemistry	Effect	Stage
miR-122	HCV infection	Anti-miR	Reduction in viral plasma RNA levels	Phase II a
miR-10b	Glioblastoma	Anti-miR	Blocks cell cycle and induces cell death	Preclinical
miR-221	HCC	Anti-miR	Delayed tumor progression	Preclinical
miR-21	Renal fibrosis	Anti-miR	Reduced expression of extracellular matrix proteins	Preclinical
miR-33	Atherosclerosis	Anti-miR	Regulation of cholesterol homeostasis	Completed
miR-34	Liver cancer	Mimic	Reduction of oncogene expression	Phase I
miR-155	Haematological malignancies	Anti-miR	Reduced aberrant cell proliferation	Completed
miR-92	Peripheral artery disease	Anti-miR	Improved functional recovery of damaged tissue	Preclinical
miR-15	Myocardial infarction	Anti-miR	Reduces heart muscle cell death	Preclinical

Table 1: MiRNA-based molecules in therapy. Taken from *Christopher at al., 2016.*

This new therapeutic approach can have two possible goals: the inhibition or the restore of miRNA activity, depending on miRNA function.

2.8.1 MiRNA replacement therapy

This kind of therapeutic approach is based on the use of molecules that are able to restore physiological levels of miRNA and is particularly useful for example to increase levels of tumor suppressor miRNAs. The use of miRNA mimics presents several advantages: one of the most important is that these molecules present the same sequence of the endogenous miRNA, so they are expected to target the same mRNA, and non-specific off target effects are expected [*Bader et al., 2010*]. Moreover, every miRNA presents several targets, so using a single molecule is possible to influence several pathways. On the other hand, the delivery of miRNA mimic is not cell-specific and the accumulation of exogenous miRNA in not-affected cells may influence physiological cellular functions. At the moment, no significative data are available, about miRNA mimics toxicity in *in vivo* models. One of the most studied way to replace physiological miRNA levels is the use of expression vectors carrying miRNA sequence. For example, miR-26a levels were restored in hepatocellular carcinoma cells using an adenoviral vector [*Kota et al., 2009*]. In other cases, synthetic miRNA mimic are delivered into cells. As Wiggins and colleagues propose the delivery of a synthetic miR-34a mimic is able to restore miR-34a levels and consequently inhibits lung tumor growth in mouse models [*Wiggins et al., 2010*]. In some disease, as in cancer, was observed a global miRNA down-regulation, in this case the use of a single miRNA mimic molecule is not sufficient, and a therapy that is able to restore the global 'miRNAome' may be required [*Esteller, 2011*]. At this propose a molecule called enoxacin was studied for its ability to promote miRNAs processing. Enoxacin has been tested both in cancer cell lines and in *in vivo* models where was shown that it is able to restore the physiological miRNAs expression pattern, with no effects in normal cells [*Melo et al., 2011*].

2.8.2 MiRNA inhibition strategies

MiRNA inhibition strategy involves the use of molecules with sequences complementary to the endogenous miRNA in order to inhibit miRNA function. Several types of molecules are able to perform this function and each of them presents different chemical modifications in order to enhance miRNA affinity. Some of these molecules act trapping endogenous miRNA in a configuration that can not be processed by RISC, in other case can be use molecules that induce miRNAs degradation.

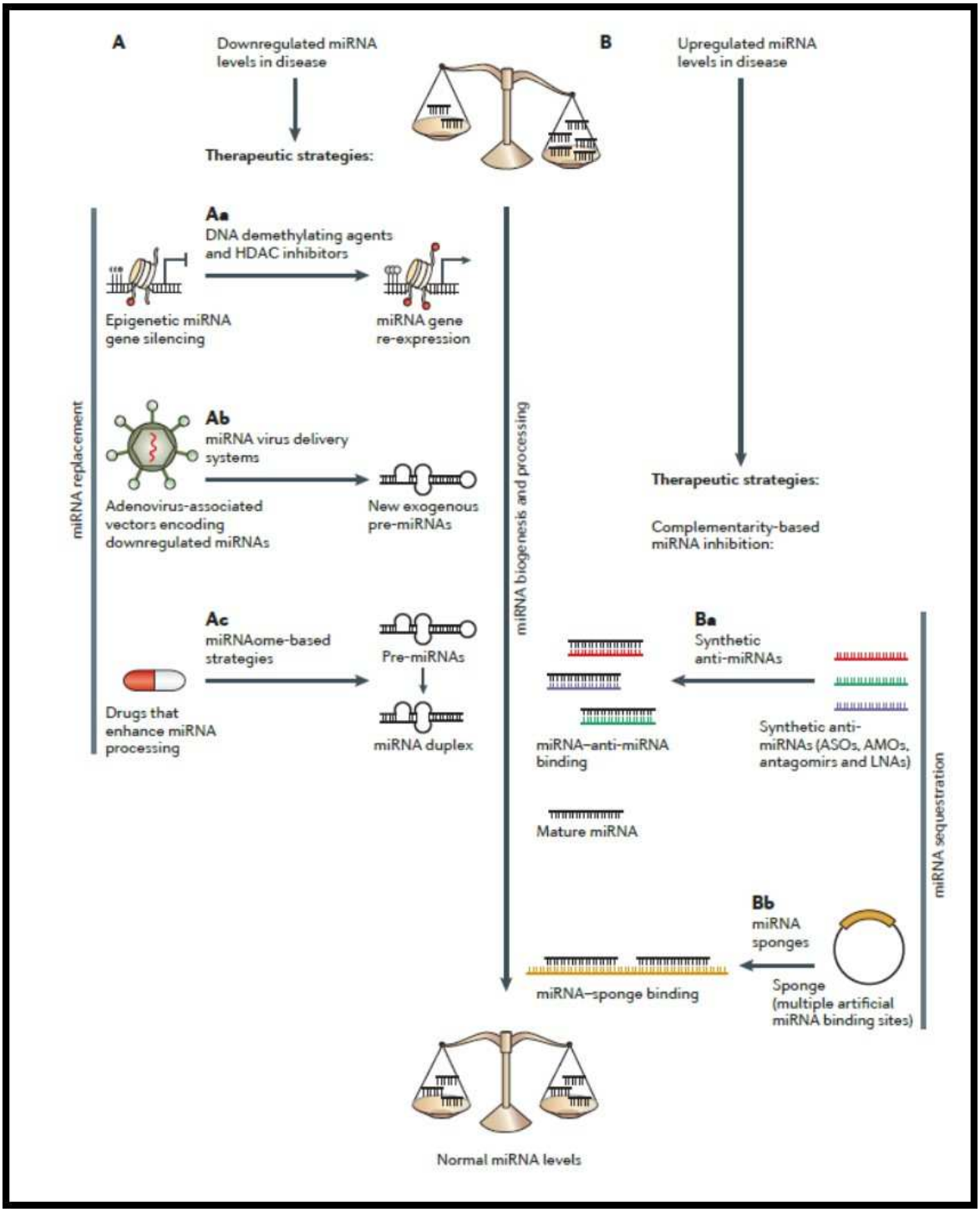

<u>Figure 12</u>: MiRNAs targeting therapeutic approach. Two types of approach are possible: miRNA expression reduction and miRNA content increase, depending on miRNA function**.**

2.8.2.1 Anti-miRNA Oligonucleotides (AMOs)

The therapeutically inhibition of miRNAs function is based on the use of Anti-MiRNA Oligonucleotides (AMOs) a heterogeneous class of molecules that present a sequence complementary to their target, miRNA. The most important features of these kind of molecules are the specificity and the high binding affinity with RNA. The bond between miRNA and the complementary AMO results in miRNA function inactivation as miRNA is

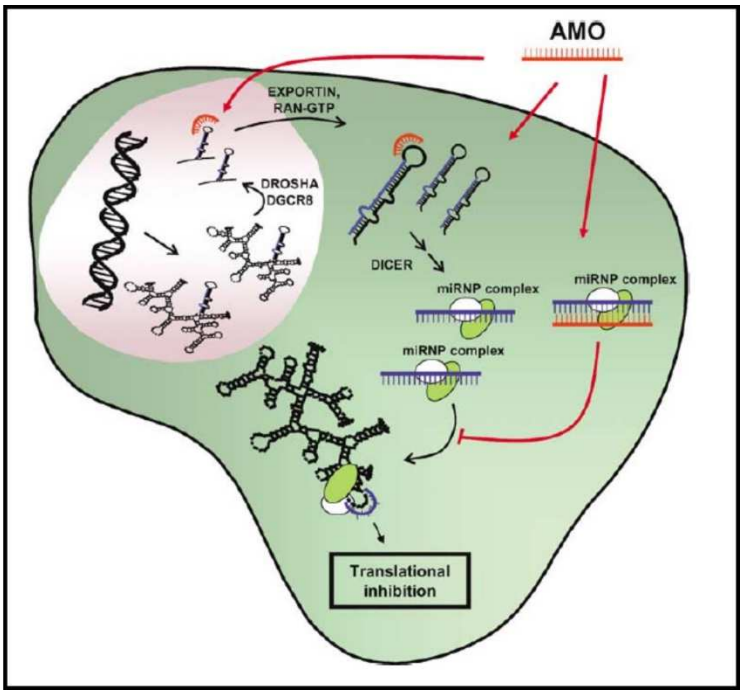

Figure 13: AMO strategy. Reduction in miRNA content can be obtained using anti-miRNA oligonucleotides (AMOs).

no longer able to bind its natural target. In the last years several modifications were performed in order to obtain increasing specificity for miRNA. One of the most successful modification leads to the design of Locked Nucleic Acids AMOs. Locked Nucleic Acids (LNA) are RNA analogs in which the ribose ring is 'locked' by a methylene bridge, connecting the 2'-O atom and the 4'-C atom. They contain the common nucleobases that appear in DNA and RNA and are able to form base pairs according to Watson-Crick base pairing law. LNAs modification leads to a thermodynamically stronger duplex formation and the bound between the LNA AMOs and miRNA results in inhibition of miRNA function [*Weiler et al., 2006*]. Levels of miR-155 were significative decrease in mouse models of B-cell Lymphoma, using a 8mer complementary LNA [*Zhang et al., 2015*]. In the most of cases silencing a single miRNA is not sufficient, for this reason, recently several researchers try to produce a Multiple-Target anti-MiRNA Oligonucleotide (MTgAMO) that is able to

inhibit at same time, several miRNA, using a single molecule [*Lu et al., 2009*]. Lu and co-workers synthesize an MTgAMO that is able to target at same time three onco-miRNAs: miR-21, miR-155 and miR-17-5p that are over-expressed in several types of tumor.

2.8.2.2 MiRNA sponges

MiRNA sponges are vectors containing multiple artificial miRNA binding sites, under the control of strong promoters [*Esteller, 2011*]. In this way, after the transfection, this vector is able to express high quantities of target multiple transcripts, which will be bind by the miRNAs, preventing the association between the miRNA and its natural target. The major advantage is that this kind of molecule is able to block a whole family of related miRNAs. For example, Ma and colleagues used this strategy to recruit miR-9, involved in the reduction of E-cadherin protein production that results in tumor metastasis [*Ma et al., 2010*].

2.8.2.3 Peptide Nucleic Acids (PNA)

Peptide Nucleic Acids (PNA) are synthetic oligonucleotide that are able to bind with high specificity and affinity for target DNA or RNA molecules. A more detailed discussion about PNA will be present in the following chapter.

2.9 MiRNA delivery

One of the major obstacles in the miRNAs based therapy is the delivery of miRNA or miRNA-targeting molecules. Several problems have been encountered in miRNA delivery as poor *in vivo* stability, inappropriate biodistribution, disruption and saturation of endogenous RNA machinery [*Zhang et al., 2013*]. Elaboration of miRNA delivery systems is essential for clinical application of miRNA-based therapy, in fact delivery systems not only allow cells internalization of the molecules, but also stabilize miRNAs and prevent their degradation. Even if viral vectors are at the moment the most efficient vehicles, safety concerns limit their employment and focus the attention of researchers to non-viral approaches. Between non-viral strategies, lipid-based delivery is probably the most used and consists in a mixture of cationic lipids and helper lipids (for example polyethylene glycol:

PEG or 1,2- dioleoylphosphatidylethanolamine: DOPE). Positive charges of cationic lipids interact electrostatically with negative charged nucleic acids to form lipoplexes that are internalized by cells through endosomal pathway [*Piao et al., 2012*]. Liposomes are routinely used in laboratory practice to perform miRNA or siRNA transfection. Lipofectamine ® (Invitrogen) or Siport ® (Ambion) are only two common examples. Despite a big optimization have been reached as regard loading capacity and delivery efficiency, the major limit is still the toxicity. Several examples of miRNA *in vivo* delivery using lipoplexes have been reported. Wu and colleagues employed lipoplexes to deliver miR-29a both *in vitro* and *in vivo* (murine xenografts) models of lung cancer, reaching an increase of miR-29a content of about five fold. To reduce toxicity and have a more biocompatible system, exosomes have been proposed as miRNAs vehicles. In term of composition exosomes are similar to liposomes, both in fact present bilayered phospholipids but are cells themselves to produce them. Exosomes are small membrane vesicles, in which endogenous miRNAs are physiologically encapsulated to prevent their degradation in body fluids. Generally, miRNAs are introduced into exosomes through electroporation of mature exosomes. Ohno research group isolated exosomes from HEK293 cells and introduced into them synthetic miR-let-7 that has been delivered in epidermal growth factor receptor (EGFR)-expressing breast cancer cells [*Ohno et al., 2013*]. More importantly Alvarez-Erviti and co-workers demonstrate that exosomes functionalization with neuron-specific RVG peptide are able to cross the blood-brain barrier in mouse models opening a new field for the miRNA-based treatment of brain diseases [*Alvarez-Erviti et al., 2011*]. Other kinds of vehicle are borrowed by DNA delivery as the polymer polyethylene imine (PEI) a positive charged molecule that interact with anionic polysaccharides on cell membranes. Moreover, studies demonstrate that PEI facilitates miRNAs release from endosomes thanks to their disruption due to an influx of hydrogen ions and water into endosomes [*Boussif et al., 1995*]. Interestingly, PEI functionalized with RVG peptide transports through the blood-brain barrier miR-124a, even if, unfortunately no functional effects were found [*Hwang et al., 2011*]. Likewise, PolyLactic-co-Glycolic Acids (PLGA) a family of water insoluble polymers have been employed mostly for antagomiR molecules transfection because of their ability to protect nucleic acids from degradation and their high loading capacity. Even these carriers give good results in *in vivo* models in which have been transfected a PNA against miR-155 [*Babar et al., 2012*]. Often miRNAs can be complexed with nanoparticles. Materials it constitutes nanoparticles are very heterogeneous but all are monodispersed particle size and present optical proprieties. Two well-known examples are silica

nanoparticles and gold nanoparticles [*Crew et al., 2012*]. As regard silica nanoparticles miRNA-based molecules are entrapped into the nanoparticles in a non-covalently way and then are released following the hydrolysis of the matrix. Nanoparticles are functionalised with receptor-targeting ligand that is essential for the interaction with cells surface and internalization. GD2 (disialoganglioside) has been employed as receptor-targeting ligand for the delivery of miR-34a into neuroblastoma cells [*Tivnan et al., 2012*]. For both, even if the transfection has been shown to be efficient, several doubts relative to their toxicity and clearance are still present.

Liquid Biopsy

Biopsy is a medical procedure in which a sample of cells or tissue is extracted and analysed in order to determine the presence of a disease and to guide the subsequent therapeutic approach. Biopsy techniques are very different and generally depend on disease site.

3.1 Traditional Biopsy Technique

Tumor biopsy is an essential tool for cancer diagnosis, prognosis and prediction of response to the treatment. There are four principal biopsy methods: surgical biopsy, needle biopsy, endoscopic or laparoscopic biopsy, and sentinel lymph biopsy. In surgical biopsy we can distinguish two major cases: excisional biopsy, in which the entire tumor is removed or incisional biopsy where only a small part of the tumor is removed. Surgical biopsy is the procedure that provide the greatest amount of tumor tissue, but is, also, most invasive technique, costly, frequently can lead to clinical complications [*Overman et al., 2013*] and obviously is not well-accepted by the patient. Needle biopsies include Fine Needle Aspiration Biopsy (FNAB) and Core Needle Biopsy (CNB). Both FNAB and CNB are less invasive and safer than surgical biopsy because the tissue collection is performed through a needle. In FNAB a very thin needle (23-25 gauche) is employed, but in this case the collected cells do not preserve their initial structure, while CNB is performed using slightly larger needle, that allows to collect cells in their natural state. Both techniques provide small tumor sample, which is not totally representative, because is only a small area of a single tumor and the heterogeneity of tumor tissue is not well established [*Jamal-Hanjani et al., 2015*]. In either FNAB or CNB, the needle can be guided by imaging test such as ultrasound or CT scan. Endoscopic biopsies are performed using an endoscope a thin, flexible and lighted tube, with a video camera on the end that can take pieces of tissue. Sentinel node biopsy is a common way to evaluate if the cancer has spread to lymph nodes [*ww.cancer.org*]. Traditional biopsy present several limits: the greatest limit is that sampling of a single area of the tumor does not reveal all present mutations, moreover, cancer can readily mutate, so would be useful monitoring the tumor at frequent intervals to evaluate treatment response or changing in tumor features and it is not possible with these invasive methods. Another important point to consider is that generally, biopsy samples are formalin-fixed and paraffin-

embedded for preservation, but this techniques can alter DNA and RNA making difficult routine analysis such as RTqPCR.

3.2 Liquid Biopsy

It is now well known that the heterogeneous cells within the tumor constantly, release into body fluid a large number of biomolecules, as DNA, RNA, proteins, peptides and metabolites, that can be free, protein- or lipid-bound or contained in extracellular-vesicles. These molecules, called biomarkers, can be used as diagnostic or prognostic tools, or as tools to evaluate the response to the therapy. Liquid biopsy proposes the analysis of circulating biomarkers as an alternative to traditional tissue biopsy, reducing the invasively and offering a representative sample of the entire tumor. Moreover, this technique is simpler and well-tolerated by the patient.

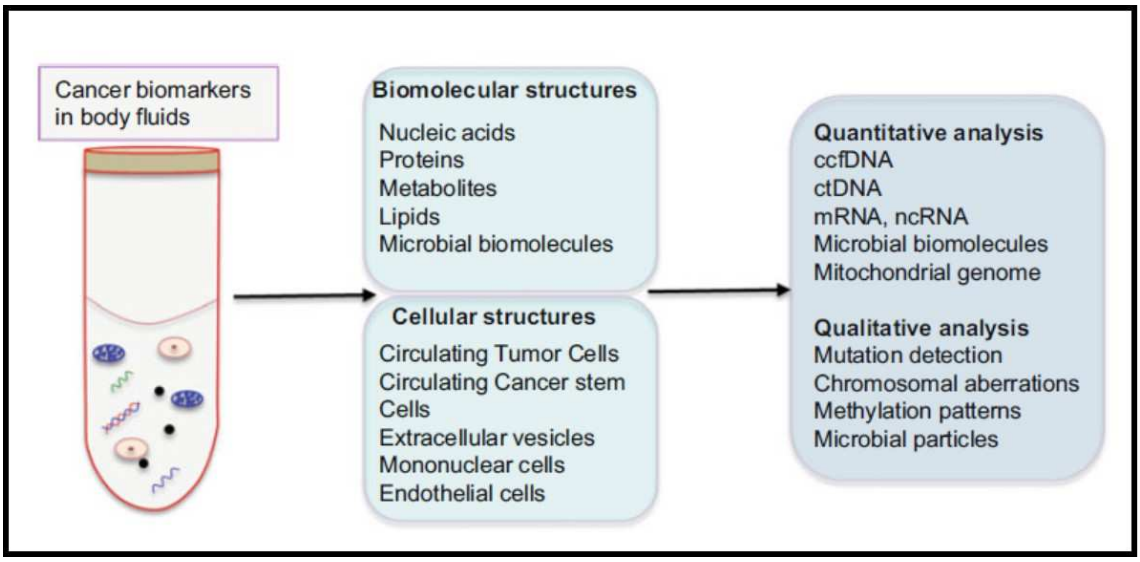

Figure 14: Liquid biopsy. Body fluids are a source of several types of biomarkers that can be detected and measured qualitatively and quantitatively. Taken from *Dakubo, 2016.*

3.2.1 Body Fluids

Body fluids are fluid normally produced by physiological body functions, as blood or cerebrospinal fluids or waste products, as urine. Moreover, the list of body fluids includes: saliva, sweat, tears, broncho-alveolar fluids, seminal fluids and several others, but fluids commonly assayed for systemic conditions are generally, blood, urine and saliva. The main concerns of body fluid analyses is the low copy number of target and possible biomarkers

degradation due, for example, to nuclease. For this reason sample collection and management is a key step to avoid pre-analytical variables that can lead to diagnostic inaccuracies. Despite in the world there are millions of biospecimens, stored in biobanks, there is not yet standardized protocol for collection, process and storage of bio-sample to maintain biomarkers integrity.

3.2.1.1 Plasma

Blood is the most investigated body fluid for disease biomarkers, probably because all cells in the body and all tissue biomarkers are represented in this fluid. Blood is a fluid connective tissue, which primarily function is the distribution of nutrients and oxygen to cells and the removal of waste material and carbon dioxide (CO_2) from cells. It is composed by cells (erythrocytes, leukocytes and platelets) and by an extracellular matrix called plasma. Plasma is composed for the 90% by water in which are dissolve proteins, electrolytes nutrients, hormones, enzymes and dissolved gases. Plasma is obtained by blood centrifugation; in fact, after the centrifugation blood gives three different layers: the top layer is plasma, the middle thin layer is composed by leukocytes and platelets and the lower one contains erythrocytes. Because of the absence of cells, plasma is an optimal sample for the investigation of cell-free biomarkers. Following standard protocols to obtain plasma, blood is collected by venipuncture or by phlebotomy, in EDTA (ethylenediaminetetraacetic acid) tube and processed within an hour after the collection. There are several protocols for plasma isolation, usually plasma is obtained by a first low-speed centrifugation followed by higher-speed spin to remove remaining blood cells without lysis [*Chiu et al., 2001*]. Plasma is, then, frozen at -80°C for further analysis.

3.2.2 Liquid biopsy in cancer management

3.2.2.1 Cancer Biomarkers

The National Institute of Health defines a biomarker as a ‘characteristic that is objectively measured and evaluated as indicator of normal biologic process, pathogenic process or pharmacologic response to therapeutic intervention [*Biomarkers definitions working group, 2001*]. Cancer biomarkers have a wide range of applications: they can be used for familiar risk assessment, screening of target population before the disease

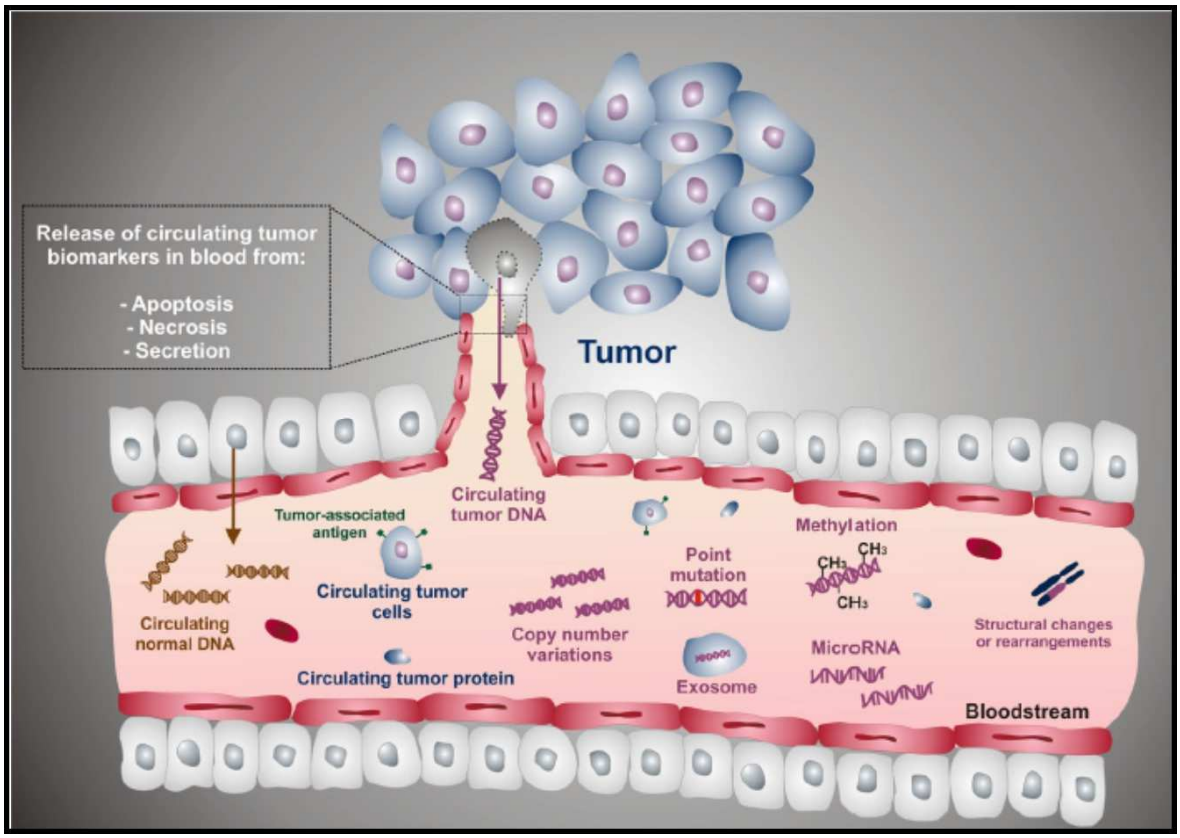

Figure 15: Tumor-linked molecular markers. Cancer cells release tumor markers in blood through various physiological events as apoptosis, secretion and necrosis. Taken from *Bellassai et al., 2016.*

occurrence, early cancer detection, differential diagnosis, prognosis, selection of patient for specific target therapy or monitoring for therapy response. An ideal cancer biomarker should accurately predict what is intended for and should have some minimal features like: be present at early stage of the disease, high sensitivity and specificity, be easily measurable with no-invasive methods and be cost-effective. Cancer biomarkers can be classified in several ways, one of the most useful is the classification based on their clinic and research application:

- *Risk assessment*: these kind of biomarkers change in the early development of cancer, for this reason are used as alarm of impending cancer development. Alterations in body fluids of these biomarkers indicate higher risk of cancer-onset for this reason are used as screening tools in high-risk population. KRAS mutations for colorectal cancer [*Arrington et al., 2012*] and BRCA for breast and/or ovarian cancer are only two examples [*Katapodi et al., 2011*].

- *Early detection and diagnosis*: these biomarkers provide evidence of the likelihood of disease in asymptomatic individuals at risk of a particular disease. These

biomarkers are generally investigated in screening programs and positive outcomes are more deeply investigated with more invasive procedure. In some cases these kind of biomarkers are used even in symptomatic patients, associated with other investigational procedures in the establishment of the disease.

- *Prognosis*: prognosis biomarkers, thus are able to predict, at time of the diagnosis, the progression of the cancer. Obviously, this is a very helpful tool for physicians to establish the protocol for tumor management.

- *Therapy prediction*: they predict the likelihood of a cancer patient responding to a particular therapeutic agent.

- *Recurrence monitoring*: they indicate the return to disease state.

3.2.2.2 Mechanism of biomarkers release in body fluid

Several mechanisms explain how biomarkers can enter in the circulation, for example dead cancer cells or circulating tumor cells can release a large amount of molecules that can be used for genomic, transcriptomic, proteomic and metabolomic analyses. Moreover, cells can actively secrete in body fluids proteins, nucleic acid and metabolites. Mechanisms of biomolecules release include: death by necrosis or apoptosis of cancer cells in tissues or circulation, active and spontaneous release of metabolites or proteins by cells, release by tumor-derived microvesicles (as exosomes), tumor angiogenesis and in some cases surgical procedures may release biomolecules into circulation, but generally their levels return to normal values in short time.

3.2.2.3 Current Tumor Markers in Clinical Practice

Traditional tumor markers generally consist of secreted proteins, for example PSA, used in prostate cancer screening [*Filella et al., 2016*], cell-surface expressed molecules as HER2 that is a routine prognostic and predictive factor in breast cancer [*Mirabelli et al., 2013*], hormones (for example Calcitonin), enzymes, receptors and oncofetal antigens as

CEA. The measurement of serum tumor markers levels is an economic and non-invasive assay, frequently requested by oncologists in order to obtain information about the presence of disease, but also to have information about disease evolution. Despite their wide use in clinical practice, the debate about their real usefulness is still opened. The major limit of these markers is their low specificity, in fact they can be expressed also, in several physiologic conditions or in others non-cancerous pathologic states. Moreover, most of these are not specific for a single cancer type; for example, the CarcinoEmbryonic Antigen (CEA) levels in serum were demonstrated to be modulated in several tumor types as colorectal cancer [*Nollau et al., 1997*], endometrial cancer [*Bamberger et al., 1998*], breast cancer [*Riethdorf et al., 1997*] and prostate cancer [*Hsieh et al., 1995*]. Thus, cancer markers are now used mostly to evaluate surgical or pharmacological treatment response, in fact markers usually increase with the disease progression and decrease with the remission of the pathology [*Sharma, 2009*]. In the Table 2 are reported some of the most requested serum tumor markers [*Sturgeon et al., 2009*].

Tumor Marker	**Relevant Cancer**
α-fetoprotein	Hepatocellular carcinoma (Ertle et al., 2013) Testicular tumor (Milose et al., 2012)
Calcitonin	Medullary thyroid carcinoma (Frangu, 2007)
Cancer Antigen 125 (CA125)	Ovarian cancer (Osman et al., 2008)
Cancer Antigen 15-3 (CA15-3)	Breast Cancer (Duffy et al., 2000)
Cancer Antigen 19-9 (CA19-9)	Pancreatic cancer (Ballehaninna et al. 2011)
CarcinoEmbryonic Antigen (CEA)	Colorectal cancer (Ballesta et al., 1995)
Human Chorionic Gonadothropin (HCG)	Testicular cancer (Leman et al., 2010)
Paraproteins (M protein, Bence Jones protein)	Multiple myeloma (Cook et al., 2007)
Prostate Specific Antigen (PSA)	Prostate cancer (Oesterling, 1991)
Thyreoglobulin	Thyroid cancer (Kim et al., 2010)

Table 2: Current cancer biomarker in clinical practice.

3.2.2.4 Novel biomarkers for cancer detection

Alongside the traditional tumor markers, others possible markers have been proposed in the recent years as Circulating Tumor DNA (ctDNA), Circulating Tumor Cells (CTC) and Circulating miRNA (cmiRNA).

3.2.2.4.1 Circulating tumor DNA

The presence of circulating nucleic acids in plasma was firstly described by Mandel in 1948 [*Mandel et al., 1948*] however, their potential role in cancer detection was proposed only some decades after by Leon and co-workers, that not only associated the increase of circulating DNA (cDNA) with cancer, but also proposed a radioimmunoassay for cDNA quantification [*Leon et al., 1977*]. Circulating DNA was found both in healthy individuals and in cancer patients, in fact even healthy cells, physiologically, release cDNA as a result of cells turnover process. Quantification data of cDNA in both healthy subject and patients with different types of cancer demonstrate a significant difference in serum cDNA content between the two groups: a mean of 13 ng/mL of cDNA was found in healthy subject, while in cancer patients the mean is 180 ng/mL [*Jahr et al., 2001*]. Moreover, several studies demonstrate the correlation between Circulating Tumor DNA (ctDNA) content in serum/plasma and the tumor stage: as Shao and colleagues showed in their work ctDNA content is significantly higher in stage III and VI, compared with patient in the early stages [*Shao et al., 2015*]. Despite, data about the size of DNA fragment in circulation are very variable, probably due to extraction technique and sensibility of detection methods, most authors agree that the distribution of DNA fragments could have a diagnostic significance. The unbound ctDNA is only a small percent of total ctDNA, in fact it circulates in blood in different forms: bound to others proteins (for example lipoproteins), attached to erythrocytes or white blood cells surface: defined csbDNA [*Bryzgunova et al., 2015*], or as nucleosomal DNA. Nucleosomes, complexes of DNA and histone proteins, are released during cell death process: when a cell die the internal endonucleases (for example caspases) cleave chromatin, at linker regions, generating mono- (180 bp size) or oligo-nucleosomes which enter in blood circulation [*Holdenrieder et al., 2008*]. The release of ctDNA in bloodstream is not yet completely clear, but several mechanisms have been proposed to explain ctDNA release:

- Death of cells by apoptosis or necrosis: generally, apoptosis is a physiological process of cells turnover and represents the typical mechanism of cDNA release in

healthy subjects, while, in cancer, DNA is released mostly by necrosis. Macrophages scavenge the apoptotic or necrotic cells and release cell content, included DNA, into bloodstream. Generally, apoptotic process release cDNA as nucleosomes, so cDNA size is 180 bp or multiples of this size in case of oligonucleosomes. While ctDNA fragments, that are originate from necrotic process, are longer than 10.000 bp [*Jahr et al., 2001*].

- Breakdown of micrometastatic cancer cells: circulating disseminated tumor cells can undergo to lysis, in these cases, they release their content, including nucleic acids, into circulation.
- Active or spontaneous release of DNA by cells, typical both of healthy and cancer cells.

Despite the use of ctDNA in oncology is still in the early stages, it seems to have a great potential in cancer risk assessment, diagnosis, prognosis, cancer management and in monitoring therapy efficacy. Furthermore, a comparative study of cancer genes mutations between tumor tissue and plasma sample demonstrates the 76% of concordance between the two types of sample, suggesting that plasma can be tested as an alternative to metastatic biopsies [*Rothé et al., 2014*]. CtDNA analysis allow a qualitative detection of cancer specific alteration as epigenetic modification (as DNA methylation or hystone modification) or genetic modification (mutations, SNPs). In analysis of circulating DNA is important to consider that ctDNA amount is influenced by various issues. First, the difference between plasma and serum, in fact in serum ctDNA content is higher (about 20-fold) than plasma [*Lee et al., 2001*]. The author suggests that most cDNA in serum samples is generated by the lysis of the residual white blood cells, making serum a worse source for tumor specific DNA analysis because of the possible presence of wild-type DNA that can decrease the sensitivity of detection of ctDNA. Another important feature to consider is cDNA degradation, usually DNases contained in blood are not active against protein-bound DNA, and however ctDNA is removed by bloodstream through physiological clearance mechanism. As shown in mouse models, liver is the primary uptake site and obviously, the uptake rate is related to DNA size [*Emlen et al., 1984*]. Determination of ctDNA half-life is quite complex due to the possible presence of occult metastases or residual disease after resection. More informations are present about the mean half-life of circulating fetal DNA, that is about 16 minutes and 2 hours post-partum circulating fetal DNA is completely removed from bloodstream. The situation should be the same for ctDNA [*Lo et al., 1999*].

3.2.2.4.2 Colon Cancer-specific Gene Mutations

Several types of DNA alterations have been detected in ctDNA of CRC patients, with variable frequency, including mutations of oncogenes and tumor suppressors genes, DNA microsatellite instability, Loss Of Heterozygosity (LOH), hypermethylation of gene promoters and mutations of mithocondrial DNA [*Gold et al., 2015*]. Several studies correlate the detection of KRAS, APA and P53 mutant DNA in CRC patients with diagnosis, prognosis and response to the therapy [*Hsieh et al., 2005*]. The overall detection rate of KRAS mutation in serum or plasma of CRC patients ranges from 25% to 30%, moreover this mutation has been detected not only in the more advanced stages, where it reaches the highest levels, but also in the early stages and in premalignant disease [*Kopreski et al., 2000*]. The same works demonstrate, also, how the presence of KRAS mutations can be associated with higher risk of recurrence. Even the rate of APC and P53 mutations have been shown to be significant in CRC patients and where respectively in 45% [*Lecomte et al. 2002*] and 40% of cases [*Lecomte et al., 2010*].

3.2.2.4.3 Circulating Tumor Cells (CTCs)

Circulating Tumor Cells (CTCs) are metastatic cells detached from primary tumor and released into vascular or lymphatic circulation to colonize other tissues [*Maheswaran et al., 2010*]. Their formation is correlated to the metastatic cascade, and their number is directly proportional to primary tumor size. Just only a little percentage (0.01%) of released CTCs are able to colonize other tissue forming metastatic deposits. Several mechanisms interfere with CTCs activity as physical forces of blood flow, which can destroy cells, or antitumor immunity able to recognise and destroy these cells. Even if, has been demonstrated in several tumours as CRC, that the presence of specific membrane receptor, and CD47 is an example, avoids the recognition of CTCs by dendritic cells and macrophages [*Steinert et al., 2014; Lu et al., 2015*]. Analysis of CTCs provides important information by a diagnostic and prognostic point of view, for this reason CTCs need to be separated from blood cells. Taking advantage from physical differences between CTCs, that normally have epithelial origin, and blood cells, several physical property-based separation approaches including gradient centrifugation, filtration, and use of microelectrochemical systems can be applied [*Vona et al., 2000*]. Moreover, more complex methods, based on the use of immunomagnetic bead, able to identify surface marker specific for epithelial cells have been developed

[*Nagrath et al., 2007*]. An isolation system based on this mechanism: CELLSEARCH® (Veridex) have already been approved by FDA, and is routinely used for automated CTCs isolation from metastatic breast, colorectal and prostate cancer patients [*www.roswellpark.org/pathology/laboratory-medicine/circulating-tumor-cells*]. Although

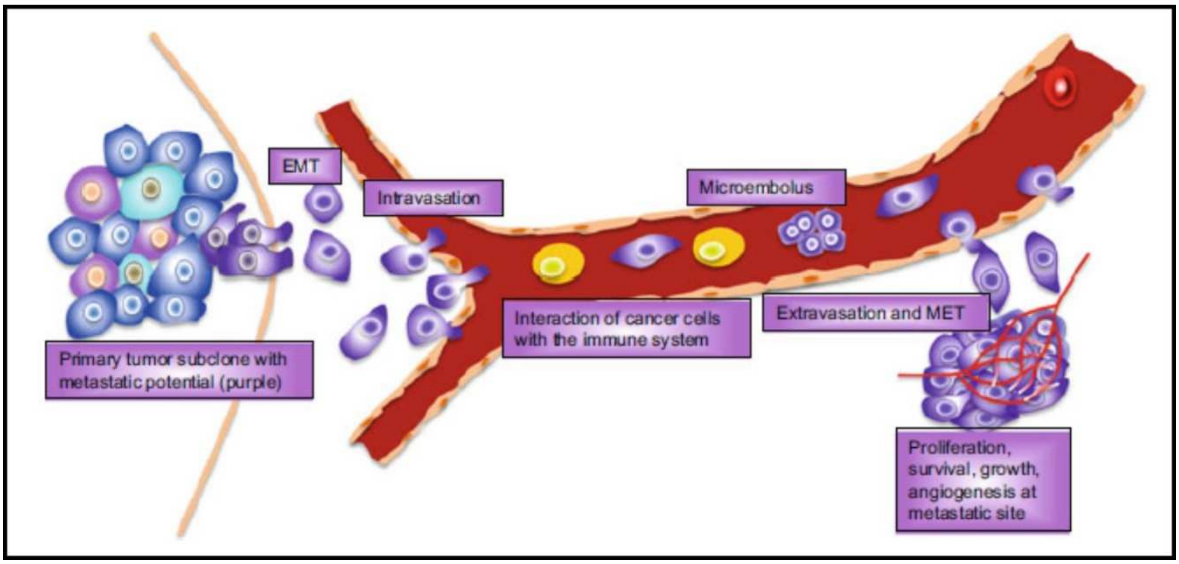

Figure 16: The metastatic cascade. Cells released from primary tumor are transported by blood flow and can colonize others tissues forming metastatic deposits. Taken from *Dakubo, 2016*

CTCs analysis is not suitable for early cancer diagnosis, in these case ctDNA or cmiRNA are more efficiently, they can be employed as prognostic markers. In fact, in some cases, CTCs characterization has shown to be even superior to conventional imaging and other clinical metrics of treatment response prediction. Moreover, molecular characterization of CTCs is very useful to identify therapeutic targets as well as can reveal possible tumor evolution that can lead to therapy resistance. Indeed, several comparative studies between primary tumor and CTCs demonstrate that CTCs have different genetic features compared to primary tumor. For example KRAS mutation status may differ between primary tumor and CTCs from the same tumor and the presence of KRAS mutant CTCs, explaining treatment failures with anti-EGFR drugs in CRC patients whose primary tumor have wild-type KRAS [*Kalikaki et al., 2014; Kondo et al., 2017*].

3.2.2.4.4 Circulating miRNA

miRNAs have been demonstrated to be present not only into cells, but also in body fluids, where they are very stable. CmiRNA have already be discussed in detail in chapter 2.

3.2.3 ULTRAPLACAD project

ULTRAPLACAD (ULTRAsensitive PLAsmonic devices for early CAncer Diagnosis) is a project funded by the European Union's Horizon 2020 research and innovation programme. The aim of the project is the development of a compact plasmonic-based device with an integrated microfluidic circuit and functionalized nanostructures for the detection of DNA, microRNAs and tumor autoantibodies (a-TAAs) [*http://ultraplacad.eu/*]. The device will be used for cancer early diagnosis and prognosis and for patient's follow-up. All analysis will be performed in plasma samples isolated from

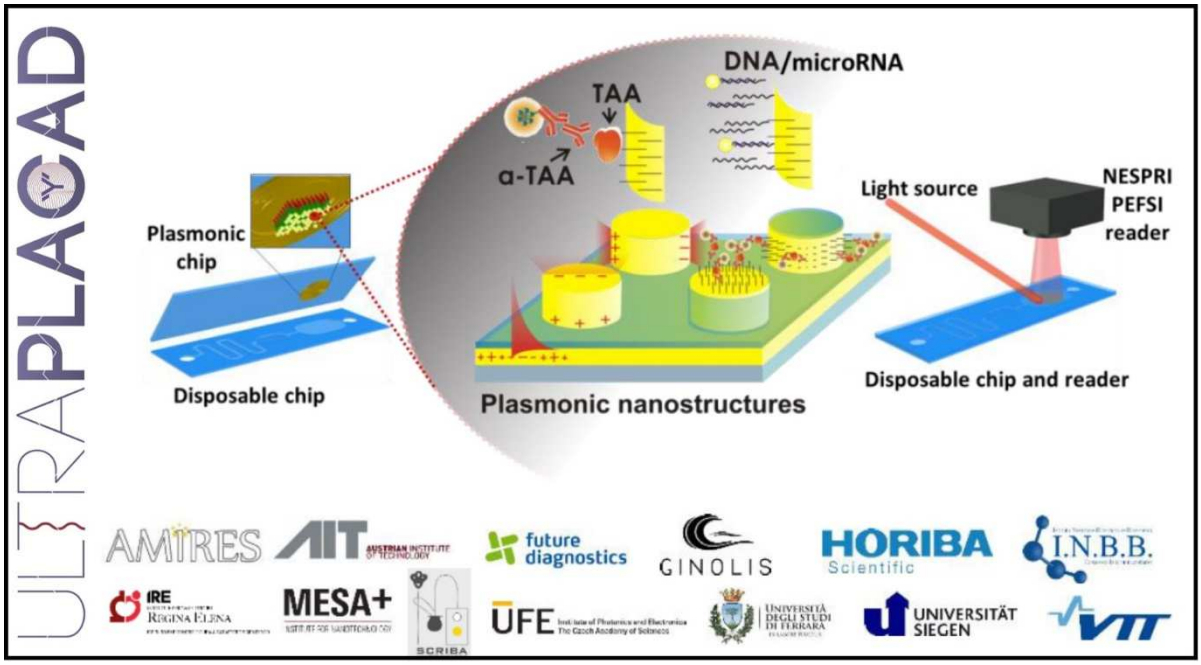

Figure 17: Concept figure of ULTRAPLACAD disposable plasmonic chip. Disposable chip is able to detect at same time ctDNA, miRNAs (using NESPRI) and tumor auto-antibodies (using PEPFSI).

peripheral blood reducing significantly, the invasiveness of the technique. Moreover, at the moment the platform proposed by ULTRAPLACAD project is the only one system that allow a comprehensive analysis of DNA, microRNAs and tumor autoantibodies at same time, using the same device. The project will be set-up employing samples from colorectal cancer patients, but identifying the appropriate biomarkers, is applicable to almost all cancer types.

The project has four important goals:

- Rapid times of analysis: thanks to the employment of PCR free techniques is possible to perform the analysis within one hour.
- Performed a multiparametric analysis, which includes three different cancer biomarkers, thanks to the application of two complementary modalities of ultrasensitive biomarkers detection.
- Reaching attomolar (10^{-18}M) limit of detection for all the three types of biomarkers, in order to detect cancer even at very early stage.
- Set-up disposable chip easy to used and cost-effective (price lower than 500 euros)

As previously said biomarkers detection using ULTRAPLACAD device does not require PCR amplification target, and is based on NESPRI (Nanostructures-Enhanced Surface Plasmon Resonance Imaging) for nucleic acids or miRNAs and PEFSI (Plasmon-Enhanced Fluorescence Spectroscopy Imaging) for tumor antibodies. Both techniques take advantage of metallic nanostructures, that increase significantly sensitivity and so allow to detect biomolecules at very low levels (aMolar). Metallic nanostructures are diffractively coupled and every sensor is composed by arrays of diffractively coupled metallic nanostructures, arranged following a refractive index symmetrical geometry. This kind of structure is used to evaluate the analyte binding using collective localized surface plasmons (cLSPs).

3.2.3.1 NESPRI for nucleic acids detection

As previously described in 'MiRNA detection methods' chapter, SPRI is very useful tool for real time SPR based analysis of interaction. Respect to SPR sensors based on spectroscopy of surface plasmons SPRI present worse resolution and smaller operating range. To improve SPRI efficiency two important improvements have been introduced: the substitution of monochromatic light with polarization contrast, achieving larger operating range and better resolution, thanks to the improvement of signal to noise ratio [*Piliarik et al., 2010*]. The second important improvement was the introduction of plasmonic nanoparticles: gold nanorods that functionalize the sensor surface to further improve device performance [*Kwon et al., 2012*]. This new technique, called NESPRI (Nanostructures-Enhanced Surface Plasmon Resonance Imaging), was already employed with success by D'Agata and colleagues for PCR-free detection of single-point mutation in genomic DNA [*D'Agata et al., 2011*], and will be applied, with minor changes, for detection of KRAS

mutations and for the detection of three miRNAs: miR-221-3p, miR-222-3p and miR-141-3p which have been demonstrated to be modulated in CRC.

3.2.4 Liquid biopsy in prenatal genetic diagnosis

Liquid biopsy can have multiple field of application and cancer diagnosis and management is only one of these. In the recent times, liquid biopsy was used as very useful tool in non-invasive prenatal diagnosis of genetic conditions. As for cancer, traditional biopsy techniques, that in this case are amniocentesis or chorionic villus sampling (CVS), are very invasive and the risk of procedural related miscarriage is reported at about at 1%. Several studies demonstrate that DNA release from the fetus: Cell Free Fetal DNA (cffDNA) is detectable in maternal blood starting from the first week of pregnancy [*Guibert et al., 2003*]. CffDNA represents only the 3-6% of total amount of Circulating Free DNA (cfDNA), unfortunately is still impossible isolate pure fetal DNA, for this reason prenatal diagnosis using cffDNA is limited to the detection of genetic sequence that are not present in maternal cfDNA [*Lun et al., 2008*]. One of the first application of cffDNA in prenatal diagnosis is fetal sexing, based on the research of specific targets expressed only in Y chromosome in maternal blood. One of the most used target is SRY, its presence in maternal blood suggests that the fetus is male, while no SRY amplification indicates that the fetus is female [*Hyett et al., 2005*]. Analysis is performed at 7th week of gestation or later and presents an accuracy of 95% [*Bustamante-Aragones et al., 2008*]. After these first important evidences, cffDNA have been used to detect several autosomal recessive disorders in the cases where the mutated allele is inherited by the father or maternal and paternal alleles present two different mutations. For example, Breveglieri and colleagues demonstrate that analysing cffDNA is possible to detect paternal-inherited β-thalassemia mutations starting from the 9th week of gestation with very good accuracy [*Breveglieri et al., 2017*].

Peptide Nucleic Acids (PNA)

Peptide Nucleic Acids (PNA) are synthetic oligonucleotides that are able to bind with high specificity and affinity target DNA or RNA molecules. In PNA the typical sugar-phosphate back-bone of nucleic acids is replaced by a synthetic peptide backbone: 2-aminoetyl glycine and the nucleobases are linked to the backbone with a methyl carbonyl linker [*Gaglione et al., 2011*].

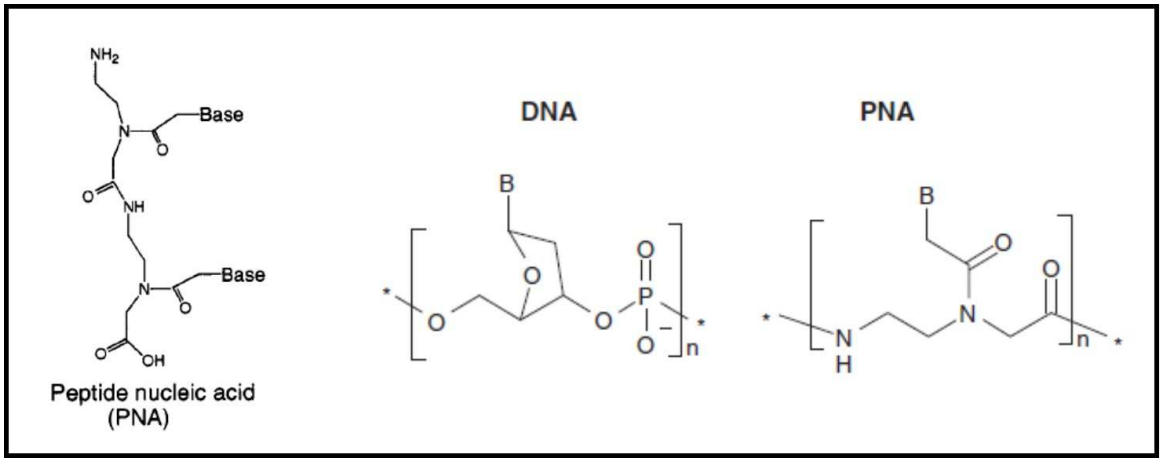

Figure 18: PNA structure. The sugar-phosphate back-bone typical of nucleic acids is replaced by a synthetic peptide back-bone.

This chemical change removes completely the charge (negative charge) that is typical of nucleic acids and makes these molecules biologically and chemically stable. Despite their radical change in structure respect to nucleic acids, they are able to hybridize with DNA or RNA following Watson-Crick rules and the hybrid complex is thermodynamically stable. Not less important, PNAs present high resistance to both DNase and protease [*Dean, 2000*]. Thanks to their features, PNAs are employed in several application fields as potential therapeutic molecules to modulate gene expression [*Nielsen, 2010*] or as diagnostic probes, for the detection of mutations and SNPs, in biosensors such as BIAcore [*Itonaga et al., 2016*].

4.1 PNA as probes for molecular diagnosis

Thanks to their high affinity for nucleic acids, in the last years, PNAs have been employed for several types of molecular analysis. For example, have been employed for the identification of bacterial or viral nucleic acids causing disease. Another, even more

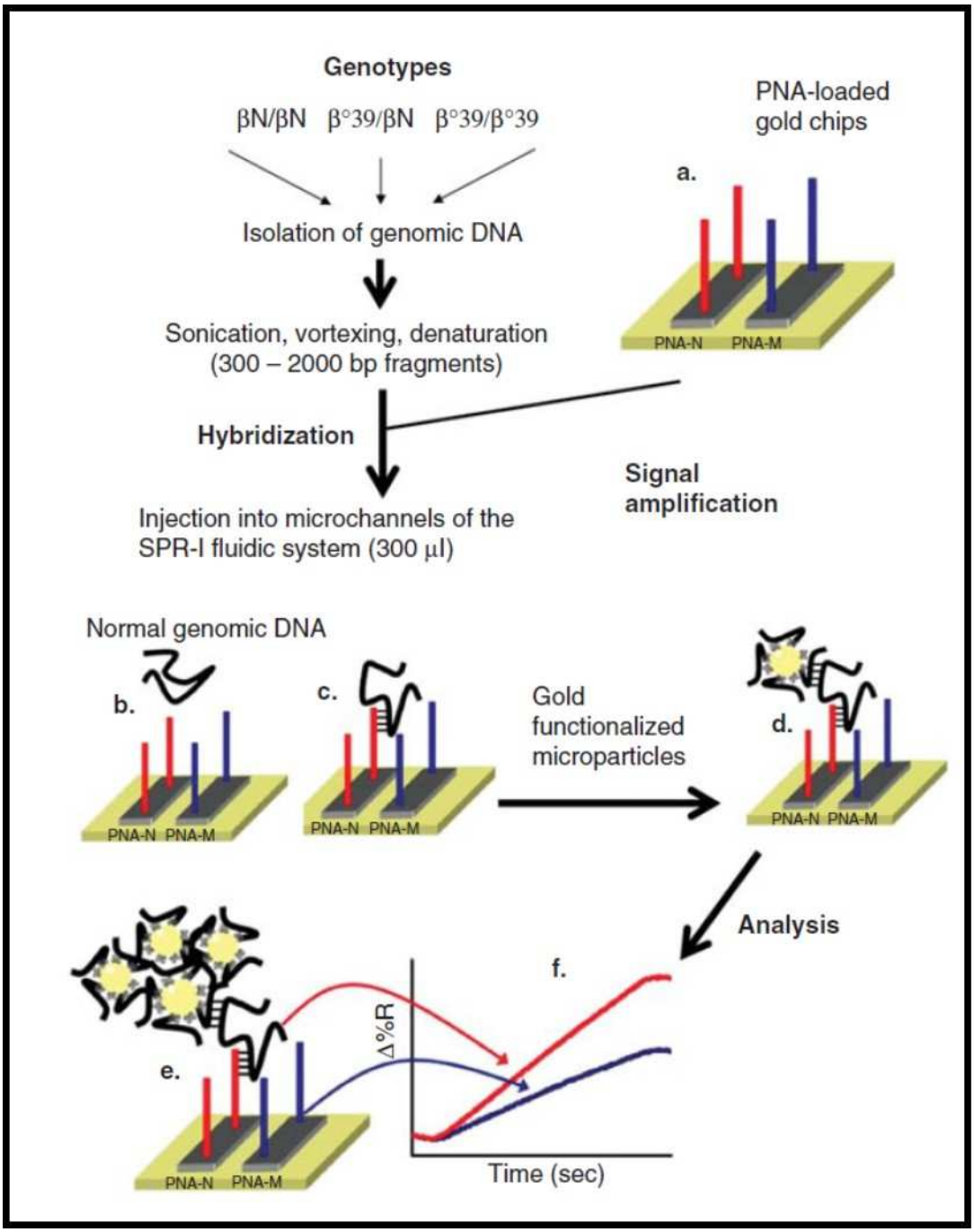

Figure 19: PNA employed in SPR technology for β-thalassemia mutations detection. PNA probes loaded in a gold-chip, recognise normal (PNA-N) or mutated (PNA-M) human β-globin gene. Taken from *Gambari, 2014.*

important application, is the use of PNA as probes for the detection of mutations, even in the case of single nucleotide mutation. For example, Feriotto and colleagues employed PNA probes associated with SPR to identify the W1282X point mutation in cystic fibrosis. The employment of PNAs as molecular probes represents one of the most valid alternative to the PCR methods for mutations detection. D'Agata and co-workers are able to detect β-thalassemia mutation starting from attomolar concentration of not amplified genomic DNA

using PNA probes applied to nanoparticle enhanced imaging SPR strategy [*D'Agata et al. 2011*].

4.2 PNA as therapeutic molecules

For their affinity for RNA, that is even higher than the affinity for DNA [*Gambari, 2014*], PNAs have been proposed as tools for miRNA levels regulation. Even if PNAs are synthesized to bind miRNAs, the end point of PNA against miRNA strategy is targeting miRNA-regulated genes. Several works demonstrate that PNAs through miRNA repression are able to restore levels of endogenous, target of the miRNA, mRNA. For example, Brognara and colleagues to increase levels of p27-kip1 protein, that is one of miR-221 targets, employed a PNA against miR-221 with good results [*Brognara et al., 2012*]. Interestingly, miRNAs can be inhibited not only at mature state, but also during their biogenesis. Avitabile and colleagues, synthesize a PNA perfect complementary to the sense strand of the pre-miRNA. Starting from the evidence that bases belonging to the stem are not perfectly complementary, they hypothesized that the mismatched duplex of the pre-miRNA could be easily opened by PNA oligomers, perfectly complementary to the sense strand of the pre-miRNA [*Avitabile et al., 2012*]. Data confirmed their hypothesis, providing an additional strategy for miRNA inhibition. MiRNAs are not the only biological molecules that can be targeted by PNAs, these kind of molecules, in fact have been also used to block mRNA transcription from DNA. In this case PNA binds gene promoter forming a triple-helix structure that inhibits transcription. An example was proposed by Tonelli and co-workers, which developed an antigene PNA that inhibits NMYC gene transcription in neuroblastoma cell lines [*Tonelli et al., 2005*]. Using the same mechanism of action PNAs can be used also to target Transcription Factors (TFs). Two possible effects can be achieved: PNA can bind TF, preventing the interaction between TF and gene promoter, this results in the reduction of gene expression [*Vikers, 1996*]. On the contrary, also PNAs, that are able to interact with gene promoter mimicking the function of true TFs, have been described [*Møllegaard et al., 1994*].

4.3 PNA cellular delivery

To realize PNAs therapeutic potential, an efficient intracellular delivery method is required. Generally, these molecules present low cellular uptake and eukaryotic cells have

been shown to be almost impermeable to micromolar concentration of naked PNA, for this reason several transfection protocols have been set up.

4.3.1 Cellular delivery of unmodified PNAs

At the beginning, a series of techniques that not require PNA sequence modification have been evaluated to internalize PNAs in cells. Between these techniques is included microinjection which was probably the first method used for PNA cellular internalization, but it is very laborious and applicable only in small scale experiment set-ups [*Koppelhus et., 2002*]. After the transfection about 50% of target inhibition was achieved reaching the estimated concentration of 1 μM of PNA within cells [*Hanvey et al., 1992*]. A more feasible transfection method respect to microinjection is electroporation, which have been employed in several studies with good results. These methods, that can be define 'physical' methods, present the advantage to be efficient and selective, but are also harmful for cells and above all are not applicable *in vivo*. Another effective strategy for PNA delivery is co-transfection. In this case PNA is hybridized with a partially complementary DNA oligomers and the resulting PNA-DNA complex is than, conveyed into cells using cationic lipids [*Hamilton et al., 1999*]. Others researchers pre-treated cells with streptolisyn-O to permeabilize cells for PNA up-take but using fluorescent labelled PNA have demonstrated that a large amount of PNA was located in cytoplasm, while only a little percentage was internalized in the nucleus [*Farugi et al., 1998*]. Others methods that do not require PNA modification are the internalization of PNA in cationic liposomes [*Borgatti et al., 2002*], microsphere [*Chiarantini et al., 2006*] or more recently, nanoparticles [*Fang et al., 2009*], but in these case is important to consider the toxicity of the vehicles, especially in primary cells.

4.3.2 Cellular delivery of modified PNAs

In these case cell permeability is obtained modifying directly the PNA molecule itself. At this propose, several modifications have been attempted during the years, with different results. Several research groups proposed the conjugation of PNA with lipophilic moiety such as Adamantyl Acetic Acid (Ada) [*Ljungstrom et al., 1999*] or triphenylphosphonium cation [*Muratovska et al., 2001*] but in both cases transfection efficiency is closely related to cell type and specific PNA sequence. In other cases PNAs

were conjugated with short peptides named Cell Penetrating Peptide (CPP) and able to transport molecules such as oligonucleotides across cellular membrane, without involving membrane receptors. The mode of action of CPPs is still unclear. Penetratin (RQIKIYFQNRRMKWKK) a 16 residues peptide, was the first small peptide used at this propose and allow a diffuse PNA distribution both in cytoplasm and nucleus [*Simmons et al.,1997*]. CPPs are normally classified into two main groups, depending on the way they interact with PNA. Some CPP are covalently bounded to PNA, such as polyarginine peptide (R_8) sequence. In another cases, peptides can form non-covalent complex with PNA. Generally, are employed short amphipathic peptide carriers consisting of a hydrophilic (polar) domain and a hydrophobic (non-polar) domain, as Pep-1. The mode of action of CPPs is still unclear. All data confirm that an important role is played by positive charges in the peptide sequence, which interact with phospholipids in the cellular membrane. Some authors hypothesize that PNAs are internalised with an endocytosis-like mechanism and transferred in the cytoplasm trapped into vesicles [*Richard et al., 2003*]. Another possibility is that CPPs interacts with negatively charged phospholipids, inducing the formation of an inverted micelle inside the lipid bilayer [*Derossi et al., 1996*]. Maybe, these mechanisms could also, occur simultaneously [*Drin et al., 2003*]. Often, is particularly important to vehicle PNAs only in specific cells to avoid adverse side-effects, for these reason PNAs functionalized with peptide sequence that is bounded only by specific cell surface receptors have been developed [*Basu et al., 1997*].

Calix[n]arenes

Calix[n]arenes are a class of macrocycle oligomers, which have a hydrophobic cavity that can contain small molecules or ions making these molecules ideal as drug carrier. They are obtained by a reaction of hydroxyl alkylation between phenol and formaldehyde in the presence of strong acid or base as catalyst [*David, 1989*]. They can be modified in two

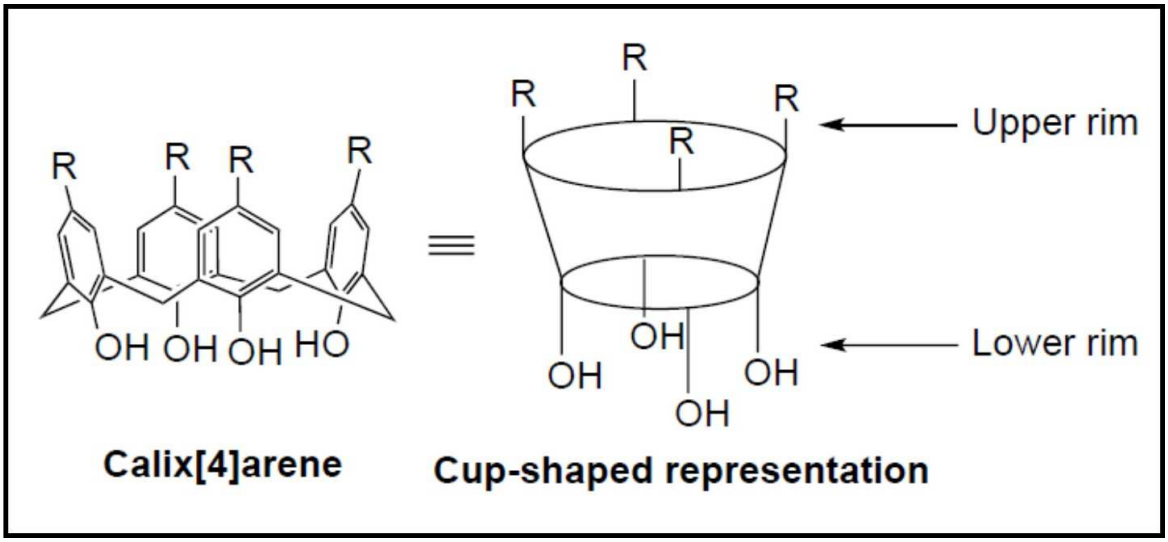

Figure 20: Calix[4]arene cup-shaped representation. Taken from *Yousaf et al., 2015*

different places: in the phenolic hydroxyl groups, that are located in the lower rim of calix[n]arene structure, or at p-positions of the phenol molecule. Calix[n]arenes present several applications in pharmacological field as drugs and, also, as drugs carriers. The field of application includes antibacterial, antiviral, antifungal and anticancer activity. Some of the possible modification and relative activities as drugs, are reported in the Table 3.

5.1 Calix[n]arenes as drug carriers

Because of their cup-shape calix[n]arenes can accommodate several compound forming complexes though no-covalent bonds as Van Der Waal's interactions, and hydrogen bonds [*Brown et al., 2012*]. Calix[n]arenes are used, for example, for the transport of Imatinib an anticancer drug used for its tyrosine kinase III inhibition activity. The investigation about the interaction between calix[n]arene and imatinib, performed by Galindo-Murillo and colleagues demonstrates that calix[n]arene cavity size in association with the proprieties of

Modification	Activity	Mechanism of action	Reference
		Calix[4]arenes	
Methylenebisphosphonic acid groups	Anti-obesity Anti-diabetic	Inhibition of protein Tyrosine Phosphatase 1B	Trush et al., 2013
Platinum II	Anti-cancer	Growth inhibition	Nasuhi et al., 2014
Glyco-conjugation	Anti-cancer	Reduction in tumor growth	Hulíková et al., 2010
Phosphonic acid residues	Anti-cancer	Inhibition of phosphatase	Cherenok et al., 2012
Hydroxymethylphosphonic acids	Anti-cancer	Inhibition of glutathione S transferase	Cherenok et al., 2006
Thymine/adenine 2'deoxynucleotide	Anti-cancer Anti-bacterial	Inhibition of DNA replication	Consoli et al., 2007
p-sulfonated	Anti-cancer	Prevention of angiogenesis	Dings et al., 2006
Tetra-amines on the lower rim and tert-butyl at upper rim	Anti-cancer	Inhibition of angiogenesis	Dings et al., 2013
Tn antigen glycomimetic units	Anti-cancer	Immune system stimulator against cancer	Viola et al., 2010
Platinum	Anti-cancer	inhibit tumor growth	Galindo-Murillo et al., 2014
Polyethylene glycol	Anti-cancer	photodynamic therapy	Piette et al., 2003
		Calix[6]arenes	
Polycationic modification	Anti-cancer	inhibits growth	Dings et al., 2013
Imidazole	Anti-cancer	Upregulates tumor suppressor gene, p53 gene	Kamada et al., 2010
p-sulfonated	Anti-cancer	Photodynamic therapy	Gutsche et al., 1985
		Calix[8]arenes	
Glycoxylation	Anti-cancer	Prevent tumor migration and proliferation	Geraci et al., 2013
TLR2 ligands	Anti-cancer	Stimulate B lymphocytes for antibody production	Brown et al., 2012

Table 3: Therapeutic application of calixarenes. Taken from *Yousaf et al., 2015*

functional groups are essential for the stability of the complex [*Galindo-Murillo et al., 2014*]. An essential point to consider is the mechanism behind drugs are released from calix[n]arene. All studies demonstrate that pH, play a key role in the drugs release, particularly, the release increase significantly at non physiological pH value. This is extremely important because while in physiological condition tissues have a pH of about 7.4, in cancer condition a decrease of pH values was shown (from 5.7 to 7.8) so calix[n]arenes can be very useful for controlled delivery of anticancer drugs [*Lee et al., 2007*] in order to reduce problems due to the non-selectivity of chemotherapies.

5.2 Calixarenes for DNA delivery

Cup-shape of calix[n]arenes is useful not only for drugs delivery but also for DNA delivery, in fact several researches, the pioneers in this field were Aoyama and Ungaro, demonstrate that thanks to their cup-shape calix[n]arenes make complexes with DNA.

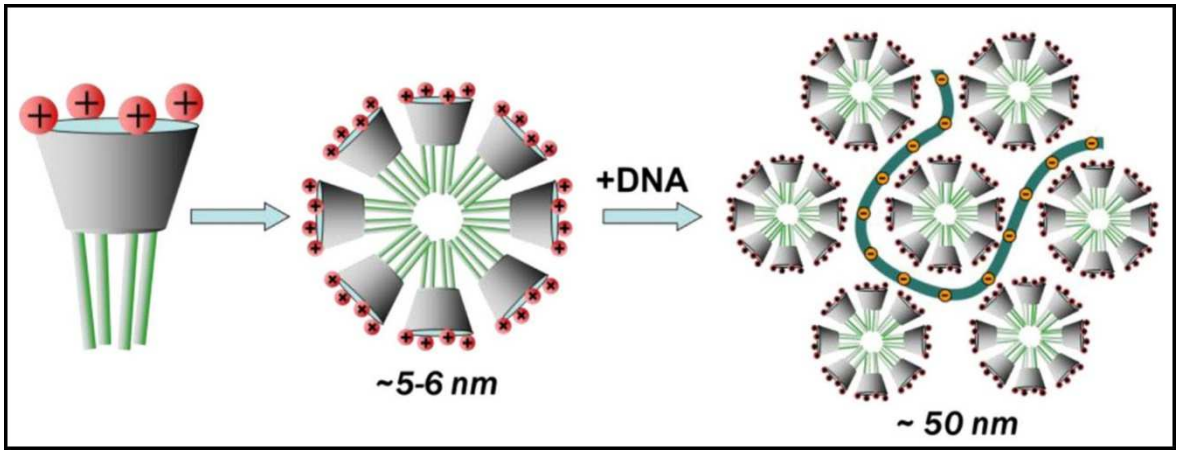

Figure 21: Model of DNA complexation with calix[n]arenes. Calix[n]arenes initially form micelles, who themselves form more complex structure complexing DNA. Taken from *Rodik et al., 2014.*

It has been shown that calix[n]arenes, and in particular, calix[n]arenes with amphiphilic structure complex DNA with a two steps mechanism. In the first step, calix[n]arenes are assembled into micellar building blocks (about 6 nm in diameter) which in turn form small virus-sized DNA nanoparticles (50 nm diameter) with high transfection efficiency and low toxicity [*Rodik et al., 2014*].

5.3 ML122

In the last years, Ungaro and co-worker synthetized several calix[n]arene-based molecules in order to identify the best DNA carrier. Very promising results were obtained by a molecule with calix[4]arene scaffold in which at the upper rim is functionalized with four single units of arginine covalently attached to the p-position of the aromatic units, while the low rim is composed by hexyl chains which allow cell penetration even in absence of helper lipids as DOPE [*Bagnacani et al., 2013*]. The molecule so drawn presents a polar region corresponding to the upper rim and an apolar region at lower rim. Due to the presence

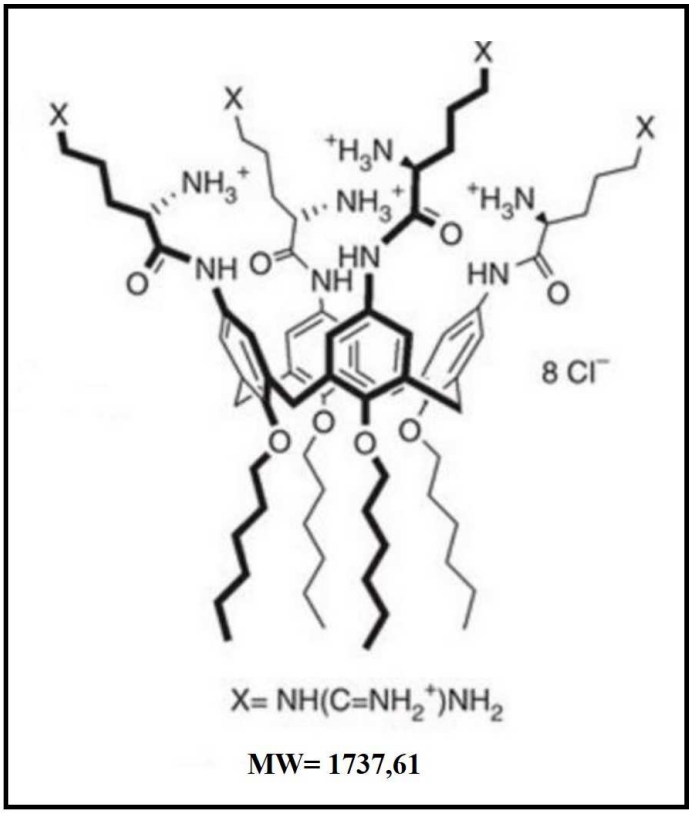

Figure 22: ML122 structure.

of aliphatic chains at lower rim, ML122 presents low solubility in water and tends to form aggregates. Solubility can be improved adding little amount of ethanol or dimethylsulfoxide (DMSO). ML122 was tested for its transfection efficiency in human rhabdomyosarcoma (RD-4) cells, notoriously very difficult to be transfected. Transfection efficiency of ML122 is very good, even better than reagent routinely used for DNA delivery, in fact ML122 at 10 μM concentration, is able to transfect 75% of cells, while Lipofectamine LTX used according to the manufacturer's instructions, transfects only 35% of cells. Moreover, toxicity of ML122 is comparable with commercial available transfection agents.

CRC

Colorectal cancer (CRC) is the second most commonly diagnosed cancer and the second leading cause of cancer death in Europe, with an incidence of 43600 new cases between 2007 and 2008 [*Ferlay et al., 2010*]. The majority of cases, about 90%, occur in subjects over 50 years old [*Imperiale, 2012*] and generally, are preceded by slow progressive premalignant lesions, as adenomatous polyps, that can be removed leading to cancer prevention.

6.1 CRC premalignant lesions

The first step of CRC carcinogenesis is the development of neoplastic polyps in the colonic mucosa. From a histologic point of view, polyps can be divided into two groups: hyperplastic polyps and adenomatous polyps, these two groups present different features and different malignant potential. In cells composing adenomatous polyps significant changes in nucleus shape are described: hyperchromatism, cigar-shaped and palisade pattern are the main features. The presence of adenomatous polyps is closely related to CRC development and several studies demonstrate the correlation between Familial Adenomatous Polyposis (FAP) and colorectal cancer [*Stryker et al., 1987*]. Patients who present FAP develop hundreds of adenomatous polyps throughout the colon starting from the puberty and if they are not submitted to colectomy inevitably develop CRC [*Bussey et al., 1975*]. FAP is an inherited condition due to an autosomal dominant mutation of the APC tumour suppressor gene located on the chromosome 5. APC protein, through β-catenin protein interaction, regulate cell proliferation [*Robbins et al., 2002*]. The second type of polyps are hyperplastic polyps, in these case an increase of glandular cells was shown, but not significant changes in nucleus shape are observed. In these case no correlation with CRC was observed, excluding serrated adenoma. Serrated adenoma generally, arises into hyperplastic polyp, but differs from it for the abnormal proliferation of crypt epithelium and for nuclear atypia. Serrated adenoma does not present APC mutation, but several others mutations such as BRAF mutation or extensive DNA methylation were detected [*Chulmska et al., 2006*].

6.2 Molecular genetics of CRC

Most of CRC are sporadic, but a significant proportion, about 5-6% has a genetic background [*Marra et al., 1995*]. For this reason, colorectal cancers are classified into two main groups.

- *Hereditary Non Polyposis Colorectal Cancer (HNPCC)*

Hereditary Non Polyposis Colorectal Cancer (HNPCC), also known as Lynch syndrome is an autosomal dominant disease characterized by the early onset of CRC in more than two generations in the family, but in this case the CRC development is not associated with FAP [*Robbins et al., 2002*] and more in general very few colonic polyps are present. Cancer is more frequently localised in the proximal colon and generally, is diagnosed in the early 40 years. HNPCC present sample characteristic features as lymphocytic infiltration, mucinous character and poor differentiation. Moreover, Lynch syndrome patients tend to develop tumor extra-colon sites as endometrium, ovary, stomach, urinary tract and pancreas. By a molecular point of view, the 90% of HNPCCs are characterized by mutations in hMLH1 and hMLH2 genes, which regulate the DNA mismatch repair system [*Lynch et al., 2003*]. The consequence of these mutations is a defective DNA mismatch repair system resulting acquisition of multiple mutations especially in the microsatellite sequences, in which are contained growth-regulatory genes [*Duval et al., 2002*].

- *Sporadic colorectal cancer*

Non-hereditary CRC, one of the most common cancer in the world, is due to a step-wise progression from normal colonic epithelium to a malignant growth caused by the accumulation of molecular anomalies [*Kinzler et al., 1996*]. In particular, anomalies regard oncogenes, that are activated, and tumor suppressor genes, that result inactivated [*Fearon et al., 1990*]. As shown by Vogelstein and colleagues, in colorectal cancer several chromosomal segments are deleted, and every cancer presents its unique pattern of deletions [*Vogelstein et al., 1988*]. Several tumor tissues are characterized by Loss Of Heterozygosity (LOH), and some chromosomal loci are more prone to this event than others. Alleles that are frequently deleted in CRC are located in position 17p (75% of CRC present these deletion) where is located the tumor suppressor gene p53. In many cases, the other p53 allele may be mutated, resulting in a complete loss of p53. P53 has a key role in regulating cell

cycle, in fact in case of injury cell cycle is arrested by p53 protein to allow DNA repair if it is possible or in other cases, when the damage is irreversible, p53 induces cellular apoptosis. So is clear that the loss of p53 results in the uncontrolled replication of possible genetic errors [*Jack et al., 2009*]. Another position that is frequently deleted (50% of CRC cases) is the position 5q where is located APC gene. APC inhibits cell proliferation and promotes apoptosis by degradations of β-catenin protein [*Oving et al., 2002*]. Consequently, mutations in APC gene result in increased cell proliferation and reduced apoptosis. The most common site for LOH in colorectal cancer is 18q (deleted in 70% of CRC) where are located genes coding for proteins SMAD-2 and SMAD-4. In addition, in 50% of cases the mutation of the oncogene KRAS was reported. KRAS protein function is the transmission of extracellular growth signal to the nucleus. Mutations in KRAS, that commonly occur at codon 12, 13 and 61, lead to a continuous growth signal and consequently to un-controlled cellular growth.

6.3 CRC and inflammation

Already in the early nineteenth century was demonstrated that cancer is often linked to inflammatory conditions, in some cases inflammatory conditions are present before a malignant change occurs, on other neoplastic disease, the oncogenic change induces the inflammation. In both cases the inflammatory condition promotes not only the development of the tumor, but also the angiogenesis and the metastasis formation. Inflammatory Bowel Diseases (IBD), autoimmune disorders that include Crohn's Disease (CD) and ulcerative colitis (UC), are well-known to be associated with cancer. In patients suffering these diseases the relative risk for developing CRC is about 5.6 (CD patients) and 30 (UC patients) times higher in comparison to the general population [*Goel et al., 2015*]. Inflammatory response aims to eliminate pathogens and restore homeostasis, this process involves a big number of molecular mediators and needs to be finely regulate in order to avoid tissue injury. The dysregulation of the inflammatory response can lead to chronic inflammation and a pro-tumorigenic environment, which may cause malignant transformation [*Shetter et al., 2010*]. Several inflammatory mediators are closely related to molecules involved in CRC signalling pathways. For example, cytokines and chemokines, the responsible of immune cell activation in the inflammatory pathway, when the process is deregulated, participate in oncogenesis, sustaining cell proliferation, survival, invasion and metastasis. The transmission of inflammatory stimuli to the nucleus, performed by cytokines, leads to the activation of several transcription factors that are involved not only in the inflammation

pathway. As described in the work of Ben-Neriah, the transcription factor NF-kB, activated by the cytokine TNF-α (Tumor Necrosis Factor-α) is, not only, the responsible of the of immune cells activation, but also regulate the expression of genes involved in cell proliferation (c-Myc), in anti-apoptotic response (Bcl-2) and the regulation of adhesion molecules (ICAM) [*Ben-Neriah et al., 2011*]. Another cytokine: IL-6 is able to activate the protein STAT3. Both STAT3 and NF-kB act in a synergic manner and interfere with the synthesis of the tumor suppressor p53.

6.4 CRC histology

Colon cancers are classified in well differentiated, moderately differentiated and poor differentiated depending on the grade of preservation of the glandular architecture and cytologic features. Poor differentiated condition is normally associated with a high number of genetic mutations, some of these still unknown, and results in poor prognosis [*Hassan et al., 2005*]. Several CRC are characterized by an important accumulation of mucin in the intracellular regions with the consequent nucleus displacement at the periphery. This type of colon cancer is defined mucinous and due to the aggressiveness are associated with poor prognosis [*Kang et al., 2005*].

6.5 CRC stages

Colorectal cancer starts with a local invasion that can reach contiguous organs by lymphatic or vascular way. When cancer is confined to mucosa without penetration of the muscularis mucosa is defined carcinoma *in situ* or high-grade dysplasia. This kind of cancer is not able to produce metastases because it does not reach lymphatic and vascular channels that are in the muscularis mucosa. Invasive CRCs were originally classified following Duke's classification. According to Duke's classification CRCs were staging from A to D: stage A cancer are characterized by penetration in submucosa, in stage B1 tumor penetration reaches muscularis propria, while in B2 stage muscularis serosa is reached. CRCs that are classified as C grade are characterized by regional lymph nodes metastases, while stage D CRC presents distant metastases [*Fisher et al., 1989*]. Recently, Duke's classification has been replaced by Tumor, Node, Metastasis classification (TNM), that considers the mural depth of primary tumor (T), the presence of local lymph nodes (N) and the presence of distant

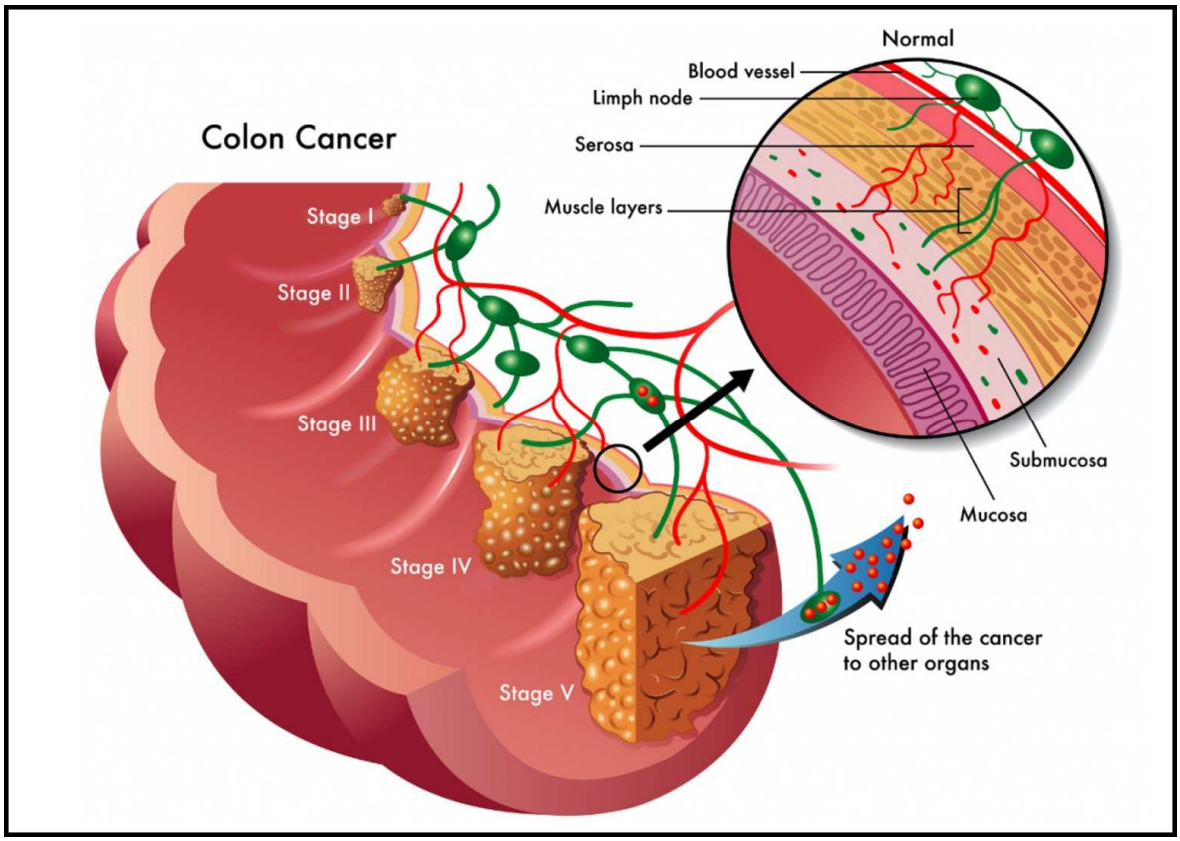

Figure 23: CRC stages. According to TNM classification four different stages are possible, depending of primary tumor infiltration, lymph nodes involvement and presence of metastasis.

metastases (M). According to this new classification: stage I in the TNM classification corresponds to Duke's A and B1 stages, stage II corresponds to Duke's B2 lesion, stage III is associated at Duke's stage C, while stage IV corresponds to Duke's D lesions [*Greene et al., 2004*]. As the TNM stage increases, the five-years overall survival declines dramatically, starting from percentage al 90% in case of stage I and reaching percentage inferior to 10% in grade IV patients. Most common sites of CRC metastases are regional lymph nodes and liver. Colorectal cancer metastasizes early in the liver because of venous drainage of the colon via portal system. Other metastases sites are lungs, peritoneum and pelvis.

6.6 Epithelial-Mesenchymal Transition (EMT)

While for the treatment of primary tumor, the surgical resection, sometimes associated with adjuvant therapy, can be used with success, metastatic disease is currently incurable, because of its system nature and the resistance of disseminated tumor cells to the

Primary Tumor (T)	
T_x	Primary tumor cannot be assessed
T_{is}	Carcinoma in situ
T_1	Tumor invades submucosa
T_2	Tumor invades muscularis propria
T_3	Tumor invades through muscularis propria into subserosa
T_4	Tumor invades others organs or structures or perforates visceral peritoneum
Regional lymph nodes (N)	
N_x	Regional lymph nodes cannot be assessed
N_0	No regional lymph nodes metastases
N_1	Metastases in one to three regional lymph nodes
N_2	Metastases in four or more regional lymph nodes
Distant metastases (M)	
M_x	Presence or absence of distant metastases ca not be determined
M_0	No distant metastases detected
M_1	Distant metastases detected

Table 4: TNM cancer classification.

therapeutic agents. For this reason about the 90% of mortality from cancer is due to metastases [*Steeg et al., 2006*]. Epithelial to mesenchymal transition is a cellular trans-differentiation program typical of the embryogenic developmental stages, this process is aberrantly co-opted by epithelial tumor cells to increase their migratory and invasive abilities. EMT is involved in the intravasation of the primary tumor cells into the bloodstream, that is one of the first stage of the invasion-metastasis cascade. Generally circulating tumor cells disseminated from primary tumor present mesenchymal characteristics that allow the survival within the bloodstream and consequently the seeding to distant organs. Cells undergone to EMT display increased resistance to apoptosis, reduced proliferation rate and also higher resistance to chemotherapeutic drugs and radiations. For this reason, the presence of cells transitioned into mesenchymal state is associated with tumor recurrence after the treatment and decrease of patient survival. Several intracellular pathways are able to activate EMT, including TGF-β, Wnt and various grown factors that are also involved in the control of EMT during embryonic development. Furthermore, extracellular conditions as hypoxia or inflammation have been shown to induce EMT [*Thiery et al., 2009*].

6.7 CRC Symptoms

If symptoms are common in the late CRC, when prognosis is already poor, no symptoms are, generally, reported in the early stages. Symptoms depend on cancer location, size and on the presence of metastases. More frequently, left colon cancer causes partial or total intestinal obstruction because left colonic lumen is generally narrower than right side. Moreover, distal cancer can be associated by rectal bleeding, while in proximal cancer blood becomes mixed with stools or degraded by colonic transit. Most common symptoms associated with CRC are abdominal pain, change in bowel habits, melena, weakness and involuntary loss of weight [*Oving et al., 1991*].

6.8 CRC treatment

Treatment of CRC is essentially based on the stage of the cancer, when is possible surgical resection is the first choice, but in the later stages surgical resection is not applicable

or needs to be associated with others therapeutic approaches. Several types of molecules have been proposed in the last years.

-*Fluorouracil*: is the first choice in the chemical treatment of CRC. It acts through the inhibition of thymidylate synthetase, an enzyme involved in nucleotides synthesis [*Sobrero et al., 2000*] and is normally administrated with leucovorin a folate that is considered to stabilize the interaction between fluorouracil and thymidylate synthetase enzyme. Between metastatic patients treated with the combined treatment fluorouracil and leucovorin about 20% present a reduction of 50% in tumor size and the medial survival is increased from 6 months to about one year [*Piedbois et al., 1998*]. The most common side effects of this treatment are neutropenia and stomatitis.

- Irinotecan: is a semi-synthetic derivate of camptothecin, a natural alkaloid. It acts inhibiting topoisomerase I enzyme, that regulates DNA replication, resulting in DNA fragmentation and programmed cell death [*Garcia-Carbonero et al., 2002*]. Principal side effects includes: diarrhea, myelosuppresion and alopecia [*Rougier et al., 2008*].

-Oxaliplatin: is a diaminocyclohexane platinum compound that leads to impaired DNA replication and cellular apoptosis [*Raymond et al., 1998*]. Oxaliplatin used as single drug presents very limited efficacy, for this reason is, generally, used in combined therapy with fluorouracil and leucovorin, in a mixed compound called FOLFOX that is able to increase disease-free survival and overall survival [*Giacchetti et al., 2000*].

-Bevacizumab: is a humanized monoclonal antibody against VEGF normally used in combination with chemotherapy [*Hurwitz et al., 2005*]. Bevacizumab inhibits the Vascular Endothelial Growth Factor (VEGF) involved in neo-angiogenesis formation during malignant proliferation. Generally, it is well tolerated even if rarely serious side effects were observed as bowel perforation (risk of 1-2%), serious bleeding (risk of 2-3%) and arterial embolic events (risk of 2-3%) [*Glusker et al., 2006*].

-Cetuximab: is an antibody direct against the extracellular domain of Epidermal Growth Factor Receptor (EGFR), a transmembrane glycoprotein, which interacts with pathways involved in cellular growth, proliferation and programmed cell death [*Baselga et al., 2002*]. Cetuximab has been tested in patients whose disease had progressed with standard therapy

based on fluorouracil and oxaliplatin, with improvements in overall survival [*Jonker et a., 2007*].

Despite, the improvements in pharmacological treatment of CRC, patients who receive all of these available therapies can expect a median overall survival of about two years [*Brian et al., 2008*].

6.9 CRC detection

Early detection of CRC has a key role in prevention and treatment of CRC, unfortunately current CRC screening methods are still inadequate because of their low sensitivity and specificity, their high cost and low compliance due to their high invasivity. Screening is the process of looking for cancer in people who have no symptoms of the disease. Generally, population is divided into two different categories: average risk and high risk and each category is targeted with a different screening program. High risk category includes subjects with family history of CRC, personal history of polyps or affected by IBD: these cases are generally screening directly with a total colonoscopy (TC). The second class: average risk, includes over 50 years old subjects without CRC history, no polyps or IBD, these cases are screened by less-invasive methods. In the recent years, several studies try to set-up less-invasive methods based on available biological samples such as urine, serum or plasma, stool or breath for CRC detection [*Di Lena et al., 2013*].

6.9.1 CRC detection: Traditional screening methods

Clinically validated screening strategies includes Fecal Occult Blood Testing (FOBT), Total Colonoscopy (TC), Flexible Sigmoidoscopy (FS), and radiographic imaging as double contrast barium enema. European guidelines recommend annual screening with FOBT. Between non-invasive screening, FOBT is the most used method, because it is safe and acceptable by patients, however it has poor sensitive and specificity for CRC diagnosis, in fact FOBT screen reduces the risk associated with CRC-related mortality only by 16-25% [*Mandel et al., 1993*]. Actually two types of FOBTs are used in clinical practice: guaiac FOBT (gFOBT) which works by detecting peroxidise-like activity of the heme molecule. The major limit of this method is that this test is not automated and its interpretation is not

objective [*Imperiale, 2012*]. There is also a more recent method: FIT which uses antibodies, against globin, to detect human blood in stools, in this case the test is automated and objective. There are several studies that compare the two methods, generally, FIT seems to have greater sensitivity, but slightly lower specificity. There are also methods based on the research of circulating proteins, that are conventional cancer biomarkers, such as CEA (Carcino-Embryonic Antigen) or CA19-9. These biomarkers permit early detection, but this approach has a limited specificity [*Toiyama et al., 2014*].

6.9.2 CRC detection: New approaches for CRC screening

In the last years researchers are looking for more effective screening test based on genomic (genetic or epigenetic alterations), transcriptomic (mRNA) proteomic (cancer related antigens or mutated proteins) metabolomic (organic metabolites) techniques [*Di Lena et al., 2013*]. Between biological samples, stools are one of the most investigated and several studies were performed in order to identify fecal DNA hyper-methylation. In particularly way, researchers proposed the analysis of a fecal DNA mutations panel, such as the first stool-based colorectal cancer screening test (Cologuard®), approved in 2014 [*www.esmo.org*]. Cologuard® is able to detect the presence of both haemoglobin (using ELISA technology) and DNA mutations. The panel of DNA alterations analysed in this test includes: the analyses of aberrant gene promoter region methylation: NDRG4 (N-Myc Downstream-Regulated Gene 4) and BMP3 (Bone Morphogenetic Protein 3) that have been shown to be hypermethylated in CRC, and the analyses of point mutations in KRAS gene: in particularly the test is able to identify 7 mutations in exon 2 of KRAS, that represent the 98% of KRAS mutations. Test, also uses β-actin as reference gene for the quantification of total human DNA amount [*Kadiyska et al., 2015*]. Others molecular screening strategies are based on fecal mRNA amplification using RT-qPCR [*Ahmed et al., 2014*], or on mRNA markers in blood. From a proteomic point of view, some antigens like urokinase-type plasminogen or small intestinal mucin antigen were proposed as potential biomarkers, but actually, none of these have demonstrate an acceptable reliability in clinical testing. With the exception of Cologuard®, none of these methods has been independently validated.

6.9.2.1 Non-coding RNAs as biomarkers for CRC diagnosis

In the last 10 years, hundreds of studies proposing non-coding RNA as biomarkers in CRC have been published. In particularly, the most frequently studied subclass of non-coding RNA are miRNA. In addition, for miRNAs based screening, stools represent a good

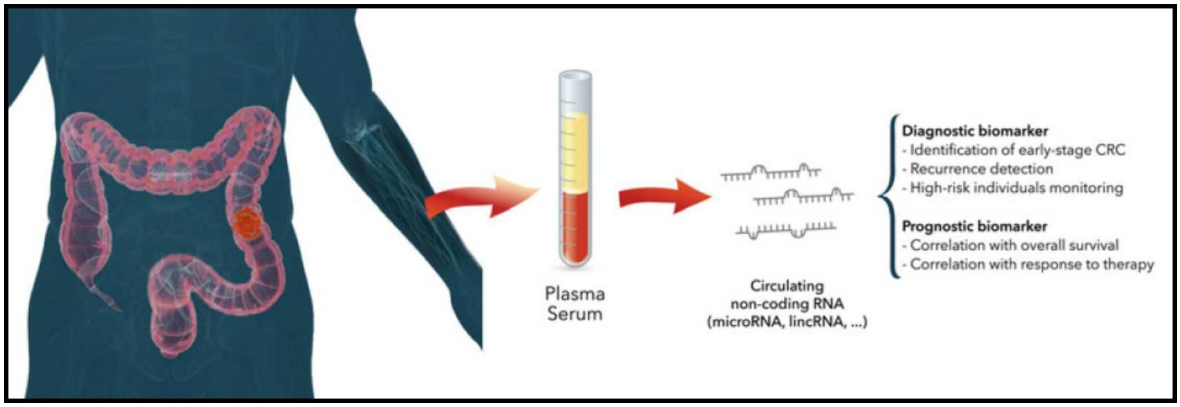

Figure 24: Non coding RNA as colorectal cancer biomarkers. Taken from *Ferracin et al., 2016.*

biological sample, in fact colonocytes are replaced every 3 or 4 days and continuously shed into the fecal stream, and the release rate is higher in the case of neoplastic cells. Moreover, a high number of miRNAs are released from the tumor directly in the intestinal lumen and these miRNAs have been shown to be extremely stable [*Ragusa et al., 2015*]. The first study reporting stool miRNAs as biomarkers in CRC was performed in 2009, by Ahmed an colleagues [*Ahmed et al., 2009*], in this case authors analysed miRNAs expression in colonocytes isolated from stools and identified a panel of 7 up-regulated miRNAs and a second one, composed by 7 down-regulated miRNAs in CRC patients. Other researchers focused their attention on cell-free miRNAs in stool, leading to identify miR-21 and miR-106a as up-regulated miRNAs in stools of CRC patients [*Link et al., 2010*]. Very interesting is miR-221 that is not only increased in tumor tissue and in plasma, but also in stool samples of stages I-IV CRC patients [*Yau et al., 2014*]. Recently, was also considered the combined miRNAs expression analysis in both stool and blood sample. The combined approach demonstrates more specificity and higher sensitivity and allows to identify two miRNAs that are up-regulated in both biological samples: miR-223 and miR-92a [*Chang et al., 2016*]. Although miRNAs analyses in stool seems to be promising, the major limitation is the standardization of the procedure, in fact stools are more prone to daily changes than plasma or serum samples.

miRNA	Sample	Change	Reference
miR-17-3p	Plasma	Up-regulated	*Ng et al., 2009*
miR-92	Plasma	Up-regulated	*Ng et al., 2009*
miR-92a miR-29a	Plasma	Up-regulated Up-regulated	*Huang et al., 2010*
miR-221	Plasma	Up-regulated	*Pu et al., 2010*
miR-601 miR-760	Plasma	Down-regulated Down-regulated	*Wang et al., 2012*
miR-409-3p miR-7 miR-93	Plasma	Up-regulated Down-regulated Down-regulated	*Wang et al., 2015*
miR-21	Serum	Up-regulated	*Toiyama et al., 2013*
miR-21 miR-92a	Serum	Up-regulated Up-regulated	*Liu et al., 2013*
miR-21 let-7g miR-31 miR-92a miR-181b miR-203	Serum	Up-regulated Up-regulated Down-regulated Down-regulated Down-regulated Down-regulated	*Wang et al., 2014*
miR-155	Serum	Up-regulated	*Lv et al., 2015*
miR-223 miR-92a	Plasma	Up-regulated Up-regulated	*Chang et al., 2016*
miR-145 miR-106a miR-17-3p	Serum	Down-regulated Up-regulated Up-regulated	*Li et al., 2015*
miR-106a	Plasma	Up-regulated	*Chen et al., 2015*
miR-20a	Plasma	Up-regulated	*Chen et al., 2015*

Table 5: Circulating miRNAs modulated in CRC patients.

6.9.2.2 Circulating miRNAs as diagnostic biomarkers in CRC

After the discovery of miRNAs in blood plasma by Lawrie and co-workers [*Lawrie et al., 2008*] a great number of studies was performed in order to evaluate circulating miRNAs expression in a wide range of diseases, considering miRNAs as a tool for cell to cell communication within the tumor or between tumor and host cells. The first miRNA

expression profiling study in CRC patients was performed by Ng and colleagues who evaluate miRNA expression alterations in tissue and plasma samples from CRC patients and identify two miRNAs: miR-92a and miR-17-3p which are up-regulated in CRC patients [*Ng et al., 2009*]. After this first study tens of studies have been performed, some of the most interesting results are summarized by Ferracin and co-workers and reported in Table 6 [*Ferracin et al., 2016*]. Considering the heterogeneity in CRC carcinomas is clear that the identification of a single miRNA is not sufficiently adequately, for this reason several articles propose panels of miRNAs to increase the accuracy of the analysis [*Kannan et al., 2013*].

6.9.2.3 Circulating miRNAs as prognostic biomarkers in CRC

The first work demonstrating the association between miRNA expression and CRC prognosis was performed by Xi and co-workers [*Xi et al., 2006*]. In his work, Xi demonstrated that CRC patients with higher miR-200c-3p levels had shorter survival time compared with patients with lower expression. Several others studies demonstrate that miRNAs levels in plasma or serum are good markers for cancer prognosis prediction. Also miR-221 was proposed as prognosis biomarker, in fact, not only high levels of miR-221 are associated with poor overall survival, but in addition was demonstrated a strong correlation between high levels of miR-221 in plasma and p53 expression, that candidates miR-221 as both diagnostic and prognostic biomarker [*Pu et al., 2010*]. If miR-221 can be detected even in the first stages, miR-141-3p expression is significantly increased in the IV stage, and its high levels are associated with poor survival [*Cheng et al., 2011*]. Several others miRNAs are associated with lymph node infiltration (miR-183-5p), metastasis formation (miR-29a-3p) and short disease-free or overall survival (miR-155-5p and miR-17-3p).

Plasma		Serum	
miRNA	**Reference**	**miRNA**	**Reference**
miR-15b-5p	*Giraldez et al., 2013*	Let-7 g-5p	*Wang et al., 2014*
miR-17-5p	*Kanaan et al., 2013*	miR-21-5p	*Wang et al., 2014*
miR-17-3p	*Ng et al., 2009*	miR-23a-3p	*Young et al., 2013*
miR-18a-5p	*Giraldez et al., 2013*	miR-31-5p	*Wang et al., 2014*
miR- 19a-3p	*Giraldez et al., 2013*	miR-92a-3p	*Wang et al., 2014*
miR- 19b-3p	*Giraldez et al., 2013*	miR-181b-5p	*Wang et al., 2014*
miR- 20a-5p	*Luo et al., 2013*	miR-193a-3p	*Young et al., 2013*
miR- 21-5p	*Luo et al., 2013*	miR-203a	*Wang et al., 2014*
miR- 29a-3p	*Giraldez et al., 2013*	miR-338-5p	*Young et al., 2013*
miR- 92a-3p	*Ng et al., 2009*		
miR- 106b-5p	*Luo et al., 2013*		
miR- 133a-3p	*Luo et al., 2013*		
miR- 142-3p	*Kanaan et al., 2013*		
miR- 143-3p	*Luo et al., 2013*		
miR- 145-5p	*Luo et al., 2013*		
miR- 195-5p	*Kanaan et al., 2013*		
miR- 331-3p	*Kanaan et al., 2013*		
miR- 335-5p	*Giraldez et al., 2013*		
miR-378a-3p	*Zanutto et al., 2014*		
miR-532-5p	*Kanaan et al., 2013*		
miR-532-3p	*Kanaan et al., 2013*		
miR-652-3p	*Kanaan et al., 2013*		
miR-601	*Wang et al., 2012*		
miR-760	*Wang et al., 2012*		

Table 6: Circulating miRNA as diagnostic biomarkers in CRC. *Taken from Ferracin et al., 2016.*

miRNA	Modulation	Effect	Reference
		Plasma sample	
miR-221-3p	Increase	Shorter survival and reduced p53 expression in CRC.	*Pu et al., 2010*
miR-141-3p	Increase	Advanced stage and shorter survival	*Cheng et al., 2011*
miR-183-5p	Increase	Shorter disease-free survival and overall survival.	*Yuan et al., 2015*
		Lymph-node metastases, distant metastases	
miR-182-5p	Increase	Decrease after surgical tumor removal	*Perilli et al., 2014*
miR-378a-5p	Increase	Decrease after surgical tumor removal	*Zanutto et al., 2014*
miR-24-3p	Decrease	Increase after surgical tumor removal.	*Fang et al., 2015*
miR-320a	Decrease	Increase after surgical tumor removal	*Fang et al., 2015*
miR-423-5p	Decrease	Increase after surgical tumor removal	*Fang et al., 2015*
		Serum sample	
miR-372-3p	Increase	Shorter overall survival	Yu et al., 2016
miR-592	Increase	Correlation with distant metastases.	*Liu et al., 2015*
miR-106a-5p	Increase	Shorter overall survival.	*Li et al., 2015*
miR-29a-3p	Increase	Early detection of CRC with liver metastases.	*Wang et al., 2012*
miR-199a-3p	Increase	Correlation with deep wall invasion.	*Nonaka et al., 2014*
miR-200c-3p	Increase	Lymph node metastases, tumor recurrence, distant metastasis.	*Toiyama et al., 2014*
miR-155-5p	Increase	Shorter progression-free and overall survival.	*Lv et al., 2015*
miR-17-3p	Increase	Shorter progression-free and overall survival.	*Li et al., 2015*
miR-19a-3p	Increase	Lymph node metastases, liver metastases.	*Matsumura et al., 2015*
miR-92a-3p	Increase	Shorter survival.	*Liu et al., 2013*
miR-21-5p	Increase	Tumor size, metastases, poor survival.	*Toiyama et al., 2013*
miR-21-5p	Decrease	High local recurrence and increased mortality.	*Menendez et al., 2013*
miR-145-5p	Decrease	Increase after surgical tumor removal.	*Li et al., 2015*
miR-218-5p	Decrease	Increase after surgical tumor removal.	*Yu et al., 2013*
miR-148a-3p	Decrease	Early relapse after tumor resection.	*Tsai et al., 2013*

Continue from page 70

miRNA	Modulation	Effect	Reference
		Serum sample	
miR-20a-5p miR-130 miR-145-5p miR-216a-5p miR-372-3p		Chemosensitivity prediction.	*Zhang et al., 2014*
miR-19a	Increase	Resistance to therapy.	*Chen et al., 2013*

Table 7: MiRNAs prognostic biomarkers in CRC. Taken from *Ferracin et al., 2016.*

Blood doping

Blood doping is the illegal use of techniques and or substances to increase red cells mass, that results in an increase of oxygen transport to muscles and consequently an increase of athletic performance [*www.wada-ama.org*]. Doping includes several types of practice as blood transfusions, administration of drugs stimulating erythropoiesis, administration of blood substitutes, employment of altitude facilities and innovative gene therapies. First evidences that the increase of haemoglobin (Hb) increases also the volume of transported oxygen and consequently the athlete's performances, were shown by Ekblom and colleagues [*Ekblom et al., 1972*]. In his study Ekblom, not only correlates Hb level with the maximal aerobic capacity (VO2max), but also demonstrates that the effects are equally present in subjects with either high or low basal haemoglobin levels.

7.1 Gene doping

Gene therapy is the new field in doping strategies and is based on the introduction of a specific gene in the athlete cells through the use of viral vectors. The most relevant targets are gene which naturally occurring mutations as Myostatin gene (MSTN) or Erythropoietin Receptor EPOR [*Juvonen et al., 1991*]. Recently, was developed an adenovirus vector containing EPO gene, under the control of O2-dependent hypoxia response element (Repoxigen). The vector was developed for the treatment of chronic anaemia and has been tested in mouse models, even if tests were stopped before the beginning of clinical trials in human because of the lack of safety [*Binley et al., 2002*]. These kinds of doping strategies are at moment undetectable, even if both World Anti Doping Agency (WADA) and International Olympic Committee (IOC) included gene doping in the list of prohibited substances and methods.

7.2 Erythropoietin

Erythropoiesis is a part of the more complex haematopoietic pathway: the responsible for the production of mature cells composing blood and lymphoid organs [*Koury et al., 2002*]. Even if the haematopoietic pathway is continuously active, for the normal turn

over of hematopoietic cells, when an abnormal loss of erythrocytes takes place, the production of erythrocytes markedly increases. The production of erythrocytes takes place in bone marrow, where are present stem cells that proliferate and differentiate in order to produce blood cells component. Briefly, the erythropoiesis starts from Burst Forming Unit-Erythroid (BFU-E): the most undifferentiated stage of erythroid progenitors. The result of BFU-E differentiation is the formation of Colony Forming Unit- Erythroid (CFU-E), which descendants are erythroid precursor cells, that include proerythroblasts, basophilic erythroblasts, polychromatophilic erythroblasts and orthochromatic erythroblasts. This last, do not divide but, enucleate forming reticulocyte. Erythropoiesis pathway is regulated by Erythropoietin (EPO) a glycoprotein hormone produced in cortical interstitial cells of the kidney. The absence of oxygen in tissues, also called hypoxia condition, is sensed by intracellular molecules that interact with enhancer elements of EPO gene promoter, inducing EPO gene transcription, that is, then, released in plasma [*Ebert et al., 1999*]. EPO is carried by blood flow in bone marrow where recognises and binds specific cell surface receptors in CFU-E and pro-erythroblasts cells increasing their ability to survive and reach the reticulocyte stage [*McMullin et al., 1999*]. In doping practice, EPO is used to stimulate red blood cells production and consequently the oxygen-carrying capacity. On the contrary, due to the increase of erythrocytes percentage, blood becomes thicker resulting in risk of heart failure, for this reason, the International Olympic Committee banned EPO in 1990. The detection of recombinant human EPO (rHuEPO) can be performed using two different methods. The first one is based on the detection of indirect blood markers such as haemoglobin concentration in erythrocytes (MCH: Mean Corpuscular Haemoglobin) and Mean Corpuscular Volume (MCV) [*Casoni et al., 1993*]. The major advantage of this technique is the possibility to detect rHuEPO administrated more than a week before that is not possible for direct methods. In fact, with direct methods is possible to identify only administration of rHuEPO performed less than 3 days before. Direct methods take advantage from the slightly differences between endogenous and recombinant EPO [*Rush et al., 1995*]. Indeed, the two forms present a different glycosylation pattern that result in different charge status, thanks to this difference is possible to separate endogenous EPO from recombinant one [*Wide et al., 1995*]. Recently, studies demonstrate that several drugs which are able to induce endogenous EPO synthesis can be used as alternative to rHuEPO, even only a little part of these drugs have been tested in human. For example, prolyl-hydroxylase inhibitor, in phase 1 clinic trial was shown to increase EPO synthesis [*Bernhardt et al., 2010*].

7.3 Blood transfusion

Blood transfusion is an old practice originally developed for the treatment of subjects that present severe anaemia. In some cases, especially in the cases in which a surgical practice is expected, is possible to proceed with a pre-operative collection of blood, that is re-infused in the post-surgical stages. The major advantage of autologous blood transfusion is the reduction of risks due to exposure to allogenic-blood such as red-cells allo-immunization, onset of transfusion-trasmitted diseases and in general can prevent transfusion related-reactions [*Lawrence et al., 1998*]. Starting from 1970s blood transfusions were improperly used to improve the performance in sport. As for the therapeutic practice, even in doping practice two kind of blood transfusions are possible: homologous blood transfusion: the athlete receives the blood from an external donor and autologous blood transfusion: the blood donor and the recipient are the same person.

7.3.1 Homologous blood transfusion

Homologous blood transfusions are not common in doping practice, partly due to the greater side effects that this practice presents, but, most of all, because are very easy to detect. Modern practice, as erythrocytes phenotyping through FACS analysis or erythrocytes genotyping by DNA sequencing, allow to easy detect the blood transfusion. Detection of homologous blood transfusion is based on the evidence that membrane of RBCs expresses several blood group antigens, which are genetically determined and consequently unique for each subject. So using specific fluorescence-labelled antibody is possible, using FACS analysis, to discriminate donor RBCs from receiver one [*Nelson et al., 2002*]. Using this technique is possible to identify also small population, less than 5%, of exogenous RBCs with high sensitivity. Moreover, is possible to detect the illicit practice, for a long period, in fact in an athlete, generally red blood cells remain in circulation for about 60-90 days [*Nelson et al., 2003*]. An alternative method, is the screening of RBCs antigens through the analysis of genomic DNA and the associated Single Nucleotide Polymorphisms (SNPs). This kind of analysis allow to distinguish receiver cells from donor cells using a PCR related technique. The assay is fast and cheap, but presents all the issues associated to a PCR reaction, such as the possible amplification of contaminations [*Flegel et al., 1998*].

7.3.2 Autologous blood transfusion (ABT)

First cases of Autologous Blood Transfusion (ABT) date back to 70s, that due to high number of athletes, which have employed ABT to enhance their performances, was called

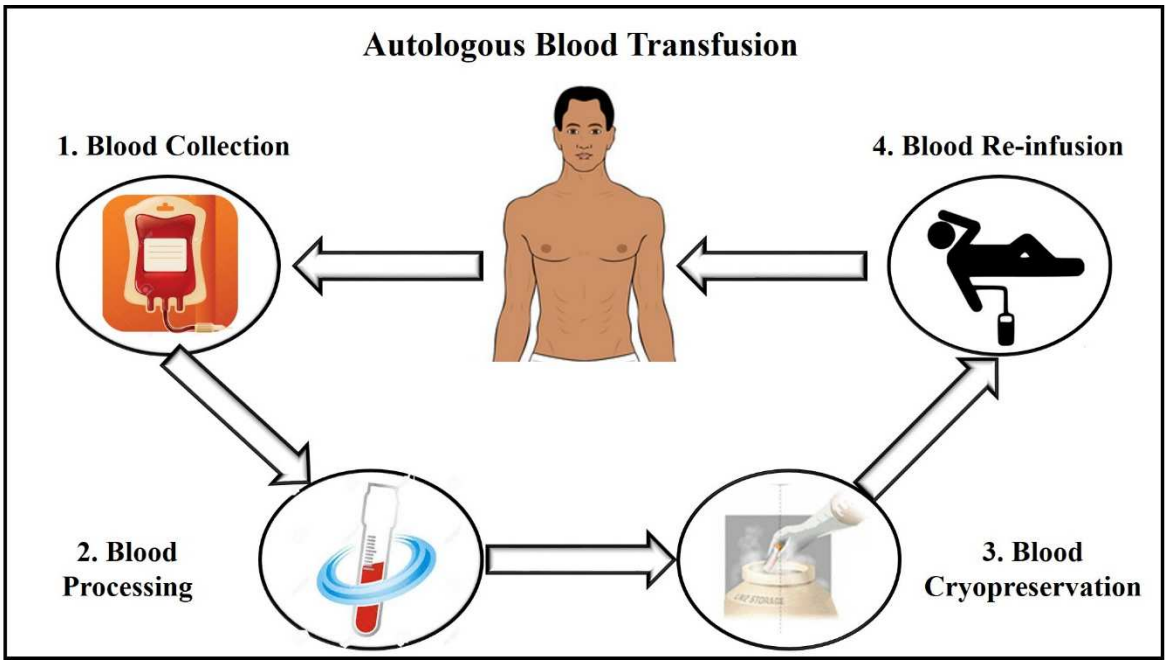

Figure 25: Autologous Blood Transfusion (ABT) work-flow. Blood is collected from the athlete, processed, to reduce volume and stored at +4°C or -80°C. Blood is than re-funded in the athlete immediately before the performance.

'the transfusion era'. In the next decennium, EPO replaces, almost completely, ABT thanks to its easier administration. The development of new and more sensitive tests to detect EPO administration, induces athletes to go back to autologous blood transfusion [*Waddington et al., 2008*]. The traditional procedure for ABT consist in withdrawal of one to four units of blood several weeks before the competition, in order to restore physiological levels of Red Blood Cells (RBCs). Each unit is composed of about 450 mL of blood and is immediately centrifuged to concentrate RBCs in a final volume of 225 mL. Samples are stored at -80°C or at +4°C, until some day before the competition. Generally, reinfusion is performed from one to seven days before the competition [*Leigh-Smith et al., 2004*]. In most of cases blood is conserved at -80°C, in fact this technique offers two main advantages: the blood can be stored for longer time, while +4°C stored blood must be reinfused within 40 days from withdrawal, new techniques for blood cryopreservation at -80°C allow to store sample for more than ten years [*Chang et al., 2017*]. Moreover, some studies demonstrate that +4°C storage results in decreased activity of several enzymes involved in energy metabolism [*Lolla et al., 2017*]. On the other hand, cryopreservation at -80°C is more complex, in fact

to protect cells by freeze the addition of cryopreserving compounds is required. Several molecules were studied at this propose, and probably the most extensively studied is glycerol. Even if glycerol presents very low or no toxic effects, its high intracellular concentration makes necessary to remove it after thawing to avoid osmotic cell lysis [*Lovelock, 1953*]. Several techniques can be employed to remove glycerol as dialysis, Cohn fractionation, serial centrifugation or reversible agglomeration, but all of them are damaging for red blood cells [*Meryman et al., 1977*] and with no differences between methods, about 15% of cells are haemolysed, during the process.

7.3.3 Detection of ABT

Even if ABT is forbidden by WADA since several years, at the moment no detection methods for ABT are available. Several indirect methods have been proposed, and all of them are based on the identification of significant deviations from the individual physiological haematological profile. Several physiological adjustment of hematopoietic response were detected immediately after blood withdrawal, including [*Smith et al., 1996*]:

- Increase (about 4 fold) of serum erythropoietin levels within 1 day from blood withdrawal

- Increase (about 2 fold) of RBCs count in the seven days following blood withdrawal

- Reduction (decrease of 15%) of haemoglobin content for two weeks

- Change in iron metabolism: decrease of serum levels of ferritin associated with increase (until 60%) of soluble transferrin receptor levels, until 14 days after blood withdrawal.

- Increase of hypochromic reticulocytes starting from the first day after the withdrawal and reaching the maximum increase at the 9th day after the practice.

At the same way, even blood reinfusion modifies athlete blood profile, in this case the major changes are [*Damsgaard et al., 2006*]:

- Increase of reticulocytes count, starting from the first day after re-infusion, and reaching the maximum increase of 55%. Their levels then, decline progressively from the 7th to the 21th day after the reinfusion.

- Increase of haemoglobin concentration until 14% compared to pre-infusion levels

- Decrease (in some cases the decrease reaches 50%) of EPO production within 24 hours from the reinfusion.

- Increase (until 68%) of ferritin concentration

All these changes offer only an indirect proof of blood manipulation, and may be affected by several other events, such as pathologies or changes in life style.

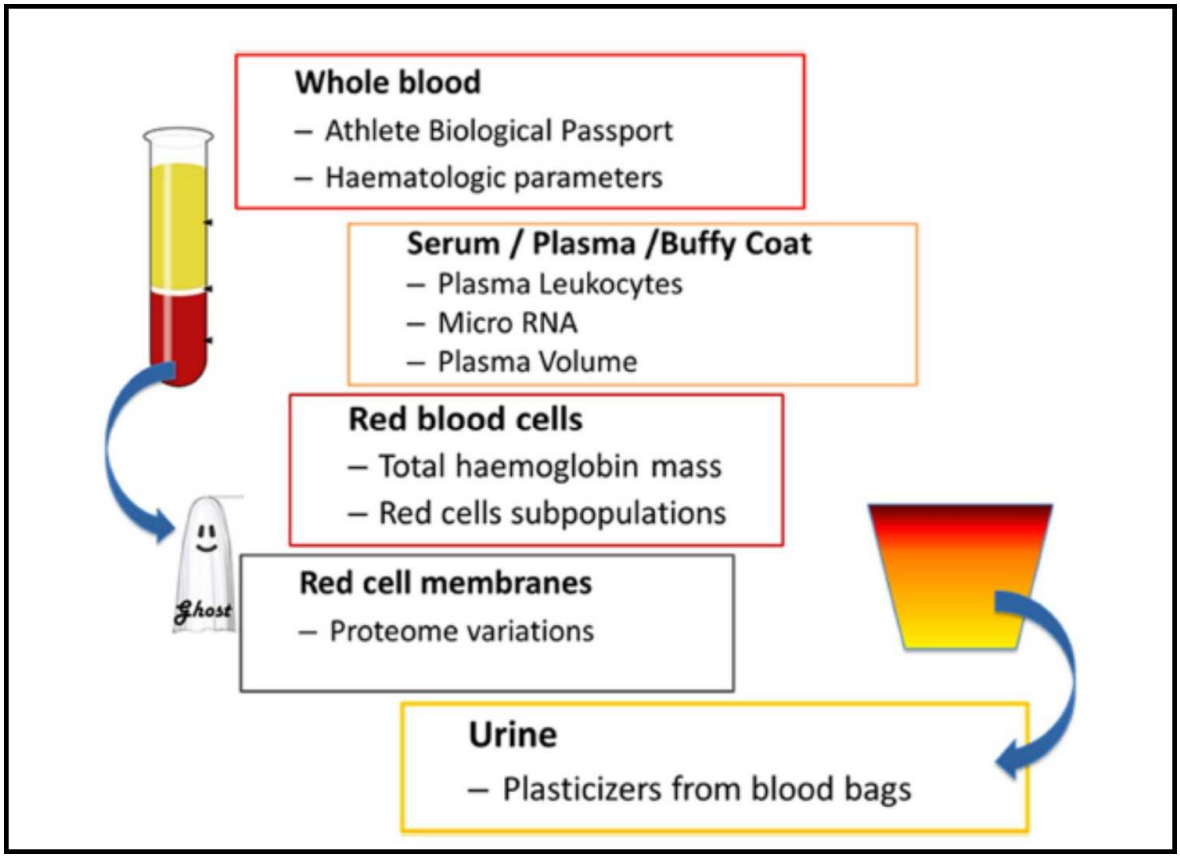

Figure 26: Possible biological matrices and methodologies for ABT detection. Taken from *Segura et al., 2014.*

Between proposed tests for ABT detection, an example is the analysis of plastic residues that may be contained in some blood bags [*Solymos et al., 2011*]. Solymos and colleagues demonstrate that in the urines of athletes undergo to ABT, increased levels of 2-ethylhexyl phthalate (DEHP) metabolites are present. DEHP derives from materials composing blood bags and is released into the stored blood, but such event involved only some bags. Another possible method is based on the evidence that red blood cells reinfusion causes gene expression alteration in white blood cells. Pottgiesser and colleagues analyse the transcriptional response in T-lymphocytes after ABT and identify more than 700 genes altered after blood reinfusion. In particularly, apoptosis-associated tyrosine kinase (AATK) transcript expression is upregulated 72-96 hours after the blood reinfusion [*Pottgiesser et*

al., 2009]. However, is important to underline that the expression of this gene can be altered in several others cases as in infection or haemolysis. Furthermore, also iron metabolism was investigated as possible ABT marker. In particular, hepcidin a 25 amino acids hepatic peptide regulating iron absorption was found significantly increased (from 4 to 7 fold) 12-24 hours after blood reinfusion [*Leuenberger et al., 2016*]. Hepcitin can be easy detected in serum or plasma, using liquid chromatography, but even in this case ABT can be detect only immediately after reinfusion.

7.3.3.1 Athlete Biological Passport

Athlete Biological Passport (ABP) seems the best currently available tool for detection of ABT, even if, with this method is not possible to establish at 100% that an athlete has practiced doping. In fact, ABP is an indirect evidence of blood manipulation that underlines only anomalies in athlete's blood profile through a longitudinal comparison of data. ABP was firstly proposed by Cazzola in 2000 [*Cazzola et al., 2000*]. He proposed to monitor a personalised panel of biomarkers indicative of doping, in order to detect several types of doping practices. As regard blood doping, parameters as red blood cells count or haemoglobin concentration or haematocrit are considered using a software system. Repeated evaluation over a period of time, of several parameters were performed in order to design a haematological profile that is supposed to be stable in time. Generally, at least five sequential determinations during the time, were performed in order to define a subject-specific reference range. Values exceeding this range may be due to illegal practice. In the first step the analysis is performed using a software that is able to identify abnormal blood profiles, that are then submitted to an experts committee. Experts evaluate each case, and eventually open the disciplinary procedure. Morkerberg and colleagues apply ABP protocol in a controlled autologous blood transfusion study, with disappointed results, ABP protocol demonstrate a sensitivity rate lower than 20% [*Morkerberg et al., 2011*]. In fact, several parameters can affect results, such as altitude, sample manipulation and type of instruments used to perform the analysis. Some of these drawbacks can be solved standardizing protocols, for others solutions are at moment not available.

7.3.3.2 microRNA as ABT biomarkers

Recently Leuenberger and colleagues analysed the expression profile of a panel of miRNAs in plasma isolated from athletes which underwent to ABT. Volunteers donate a bag of blood (about 500 mL), blood was processed and store at +4°C, then after 42 days blood

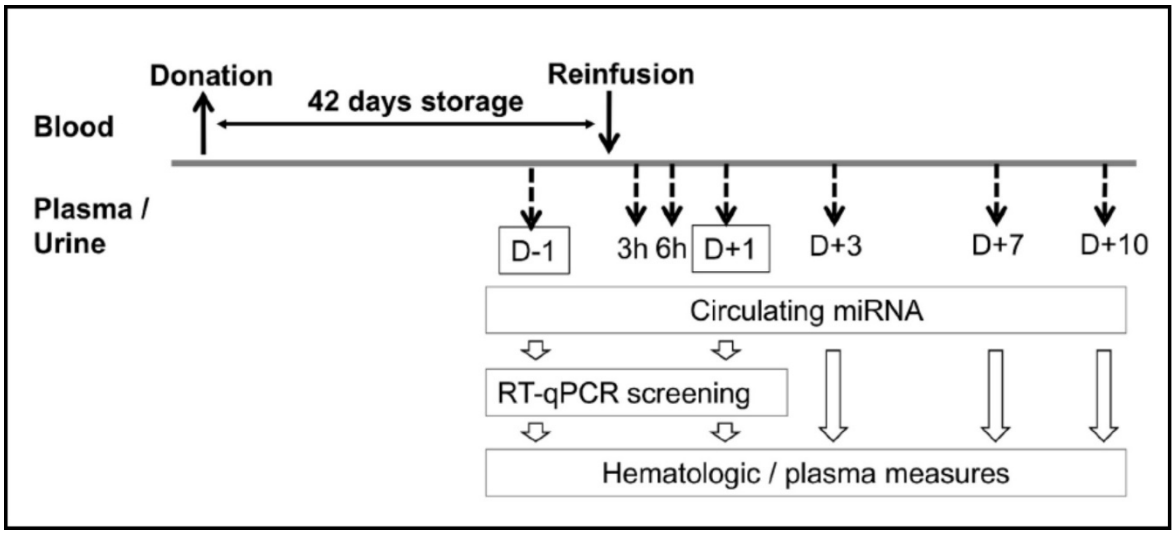

Figure 27: Study design performed by Leuenberger and colleagues. Samples were taken at different time points after blood reinfusion. For the control group, no samples were collected at 3 (3 h) and 6 hours (6 h). Taken from *Leuenberger et al., 2013.*

was reinfused. MiRNAs levels were verified at different times points, as indicated in Figure, and data were compared to miRNAs levels present at the day before the reinfusion. All data were compared to a control group, that do not undergo to ABT. Ten miRNAs were identified as possible biomarkers of ABT (Table 8) and between these miR-26a, miR-30c and miR-30b were selected as the best candidates. Even in this case best results were obtained in time points immediately after blood transfusion (from 3 to 24 hours after reinfusion) while no significative changes in miRNA expression were shown at longer time points. Moreover, Donati and co-workers analysed a panel of eight selected miRNAs, in blood samples taken from athletes. Samples were collected and miRNAs content was analysed at three different time points: at moment of collection, after 15 days-storage and after 30 days-storage. The expression of miR-144 and miR-923 was founded to change consistently during the blood storage, demonstrating that storage methods can affected significantly circulating miRNA data [*Donati et al., 2015*].

Modulated MiRNA	Reference
let-7d-5p	*Leuenberger et al., 2013*
let-7d-5p	*Leuenberger et al., 2013*
let-7g-5p	*Leuenberger et al., 2013*
miR-103a-3p	*Leuenberger et al., 2013*
miR-142-3p	*Leuenberger et al., 2013*
miR-144-3p	*Donati et al., 2015*
mir-150-5p	*Donati et al., 2015*
miR-196a-5p	*Donati et al., 2015*
miR-197-3p	*Donati et al., 2015*
miR-26a-5p	*Leuenberger et al., 2013*
miR-26b-5p	*Leuenberger et al., 2013*
miR-30b-5p	*Leuenberger et al., 2013* and *Donati et al., 2015*
miR-30c-5p	*Leuenberger et al., 2013*
miR-339-5p	*Leuenberger et al., 2013*
miR-451a	*Donati et al., 2015*
miR-923	*Donati et al., 2015*
miR-96-5p	*Donati et al., 2015*

Table 8: Principal miRNAs founded to be modulated in ABT.

Beta thalassemia

Beta thalassemia (β-thalassemia) is an autosomal recessive genetic disease, caused by mutations within or near the beta (β) globin gene. Mutations generally, result in absence of synthesis of β-globin chains (β^0-thalassemia) or in reduced synthesis: called β^+-thalassemia [*Olivieri, 1999*]. β-thalassemias can be classified in different ways, by a genotypic point of view is possible to identify three genotypes:

-heterozygosity: with a wild type allele, while the second one carries the mutated β-globin gene. These subjects, called microcitemic, are able to transmit the mutated allele to their offspring. The offspring of two microcitemic subjects with the same mutation have the 25% of probability to be wild type for the mutation, 50% to be heterozygotes as their parents and 25% to be homozygotes for the mutation.

-heterozygosity for two different β-globin gene mutations, in this case the severity of the disease depends on the type of mutations.

-homozygosity for the same mutation, generally, it is the most severe condition and is called thalassemia major or Cooley's disease, from the surname of the doctor who first described the disease. Even in this case the severity of disease depends on mutations type, in fact several mutations result in reduction of β-globin production, others led to the complete lack of β-globin chains production.

Subjects affected by β-thalassemia, present different phenotypes:

- silent β-thalassemia: their haematological parameters do not present anomalies and only a slight imbalance in the *in vitro* chain synthesis can be observed [*Gonzalez-Redondo et al., 1989*]. These subjects, generally present a heterozygote genotype [*Moi et al., 2004*].

- β-thalassemia trait (microcitemic subject): they present a mild anaemia, decreased haemoglobin (Hb) levels, reduction in Mean Corpuscular Volume (MCV) and in Mean Corpuscular Haemoglobin (MCH). These individuals are generally, heterozygous for a β-globin gene mutation, and the severity of disease is related to mutation type.

- β-thalassemia intermedia: in some cases, patients present a reduced disease severity thanks to the inheritance of mild β-thalassemia mutations, that allow the production of good quantity of β-globin chains. In other case, despite the subject presents the complete absence of β-globin chains, is able to compensate this absence, with high production of β-like globin,

like gamma (γ) globins. On the contrary, in some cases, heterozygous patients present unusually severe β-thalassemia disease, due to the co-inheritance of β-globin gene mutation and extra alfa (α) globin gene [*Danjou et al., 2011*].

- β-thalassemia major: is the most severe form of β-thalassemia, characterized by very low or absent production of β-globin chains. Generally, is typical of homozygosity for the same β^0 mutation or heterozygosity for a β^0 and a β^+ mutation. Patients present a severe anaemia and need regular blood transfusions to survive [*Danjou et al., 2011*].

8.1 Beta globin cluster

β-globin gene cluster is located in the short arm of chromosome 11 and contains inside five β-like genes, arranged in order of expression during development [*Efstratiadis et al., 1980*]. Upstream of the globin genes there is the Locus Region Control (LCR), that is the major regulatory element of the β-cluster and contains four erythroid-specific hypersensitive sites (HS), present at all stages of erythroid development. Cluster beta is composed by the embryonic gene ε, that is expressed until the 8th week of gestation, by the fetal 'block' composed by the two genes $^{A}\gamma$ and $^{G}\gamma$ which codify for two similar globin chains that differ only for an amino acid located in the position 136. The two gamma genes are

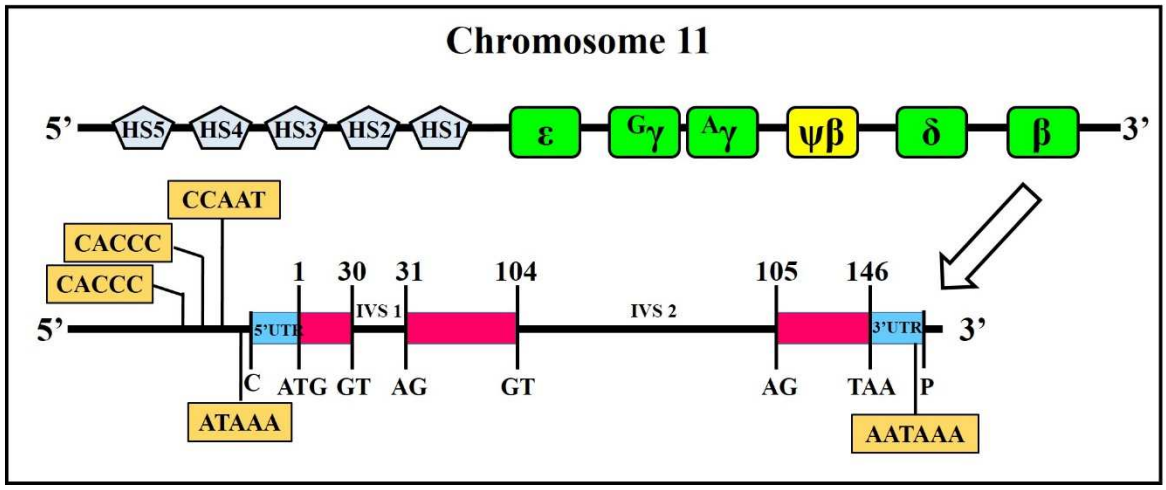

Figure 28: Cluster β and β-globin gene sequence.

active starting from the 8th week of gestation, until the 3rd month after the birth, when fetal block is silenced and replaced by the adult block. Adult block is composed by two genes: δ and β producing similar globin chains that differ only for ten amino acids [*Efstratiadis et al., 1980*]. The genomic sequence of β gene is composed by three exons, interrupted by two

introns (IVS). Exons 1 and 3 encode for the non-heme region of β-chains, while exon 2 codifies for the region involved in heme binding [*Joy et al., 2000*]. β-globin genes are fine regulated during the development, initially, in the embryonic period three types of haemoglobin are produced: Gower I, Portland and Gower II, composed as indicated in Table 9. Subsequently, embryonic gene is gradually silenced and replaced by gamma genes, codifing for γ-globin chains that constitute fetal haemoglobin, which is gradually replaced by adult haemoglobin after birth [*Cao et al., 2002*].

α-like chain	**No α-like chain**	**Hb composition**	**Hb name**	**Stage of production**
ζ	ε	ζ2ε2	Gower 1	First 8 weeks of gestation
α	ε	α2ε2	Gower 2	First 8 weeks of gestation
ζ	γ	ζ2γ2	Haemoglobin Portland	First weeks of gestation and hydrops foetalis due to homozygous α-thalassaemia
α	γ	α2γ2	Fetal Haemoglobin (HbF)	From 6th week of gestation to the first month after birth
α	β	α2β2	Adult Haemoglobin (HbA)	Dominant haemoglobin in normal adult
α	δ	α2δ2	Adult Haemoglobin 2 (HbA2)	About 3% of total haemoglobin in normal adult

Table 9: Principal haemoglobin produced during development.

Mutations involving β-globin gene are very heterogeneous, in fact, more than two hundred mutations causing β-thalassemia have been characterized. The majority of these mutations involves only a single nucleotide and in particular are characterized by single nucleotide substitution, deletion or insertion leading to frameshift, while rarely disease is due to the complete gene deletion [*Cao et al., 2010*]. Point mutations, causing β-thalassemia can be divided into free principal groups:

- Mutations leading to defective beta-gene transcription: in most of cases they involved β-globin gene promoter. Three functionally important sequences are involved: CACCC, CCAAT and ATAA boxes. Normally mutations within promoter sequence reduce but not completely inhibit β-globin production so lead to mild thalassemia phenotypes. Studies

demonstrate that these kind of mutations causes a decrease in β-globin mRNA production between 10 and 25% [*Treisman et al., 1983*].

- Mutations affecting messenger RNA (mRNA) maturation: different types of mutations can interfere with primary mRNA processing. For example, mutations that alter normal splicing sites, which can occur both within exon or intron. When the mutation is located in the exon, results in the creation of new splicing sites, that are preferred to the normal splice sites, leading to the production of abnormal protein. While mutations located in introns can disrupt the normal splice junction formed by the dinucleotides GT and AG, resulting in the repression of splicing process and consequently to a β°-thalassemia phenotype. The mutation IVS1-110 (G->A), that is frequent in Mediterranean population, is an example of mutation affecting splicing process, in fact the replacement of guanine with an adenine results in the formation of an alternative splice site, which is preferred in the 80-90% of the transcripts, resulting in a severe β°-thalassemia [*Busslinger et al., 1981*]. In other cases, mutations involve the polyadenylation signal sequence (AATAAA) and result in very unstable mRNA. In fact, due to the presence of the mutation, the polyadenylation takes place beyond the normal polyadenylation site, resulting to a longer transcript, even 900 bp longer than the normal one, that is not stable [*Orkin et al., 1985*].

- Mutations resulting in abnormal mRNA translation: about half of β-thalassemia cases are due to the introduction of premature stop codon, that can be caused both by a single point mutation or by insertion or deletion of a nucleotide leading to a change in the reading frame. One of the best characterized and more common mutation occurs at the codon 39 and is due to the substitution of a cytosine with a thymine (CAG->TAG) [*Humphries et al., 1984*]. Genes carrying this mutation are normally transcribed, but the produced RNA seems to be unstable, probably because of the Nonsense Mediated Decay (NMD) quality-control mechanism [*Isken et al., 2007*].

8.2 Physiopathology of β-thalassemia

The reduced or absent synthesis of β-globin chains in β-thalassemia results in a excess of un-matched α-globin chains that are not able to form tetramers, so precipitate into erythroid precursors in bone marrow, leading to their premature death and to ineffective erythropoiesis [*Galanello et al., 2010*].

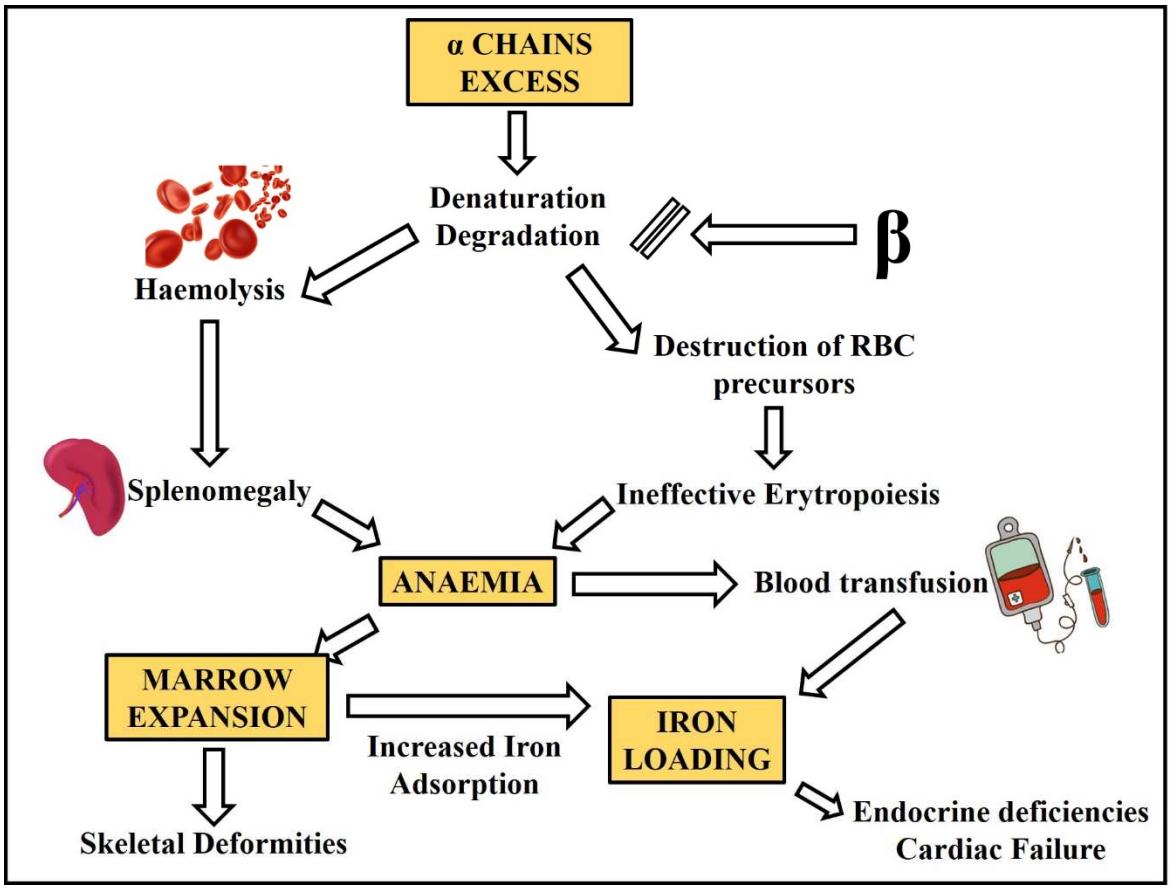

Figure 29: Physiopathology of β-thalassemia.

This results in a severe reduction of mature red blood cells that are able to reach blood stream. Moreover, cells that are able to enter into the general circulation are generally, damage, with low elasticity and smaller, so once in the spleen they are degraded resulting in increased bilirubin and more importantly, in increased activity of spleen that leads to one of the principal features of β-thalassemia patients: splenomegaly [*Galanello et al., 2010*]. The most important manifestation of β-thalassemia is anaemia, due to the lack of β-globin chains and the consequent reduction or absence of adult haemoglobin (HbA). Direct consequence of anaemia are increase of erythropoiesis that results in expansion of bone marrow and consequently skeletal deformities and iron overload (also known as hemocromatosis) due to blood transfusions and to the increased gastrointestinal iron absorption. Iron stores are located especially in heart and in the endocrine organs, liver and spleen. Iron excess is extremely toxic and causes irreversible organic damages as cirrhosis, diabetes, hypogonadism and heart disease [*Leecharoenkiat et al., 2016*]. In particularly cardiac diseases are one of the most frequent causes of death in β-thalassemia patients.

8.3 Management of β-thalassemia

Therapies for the treatment of β-thalassemia can be divided into two main groups: definitive therapies and maintenance therapy.

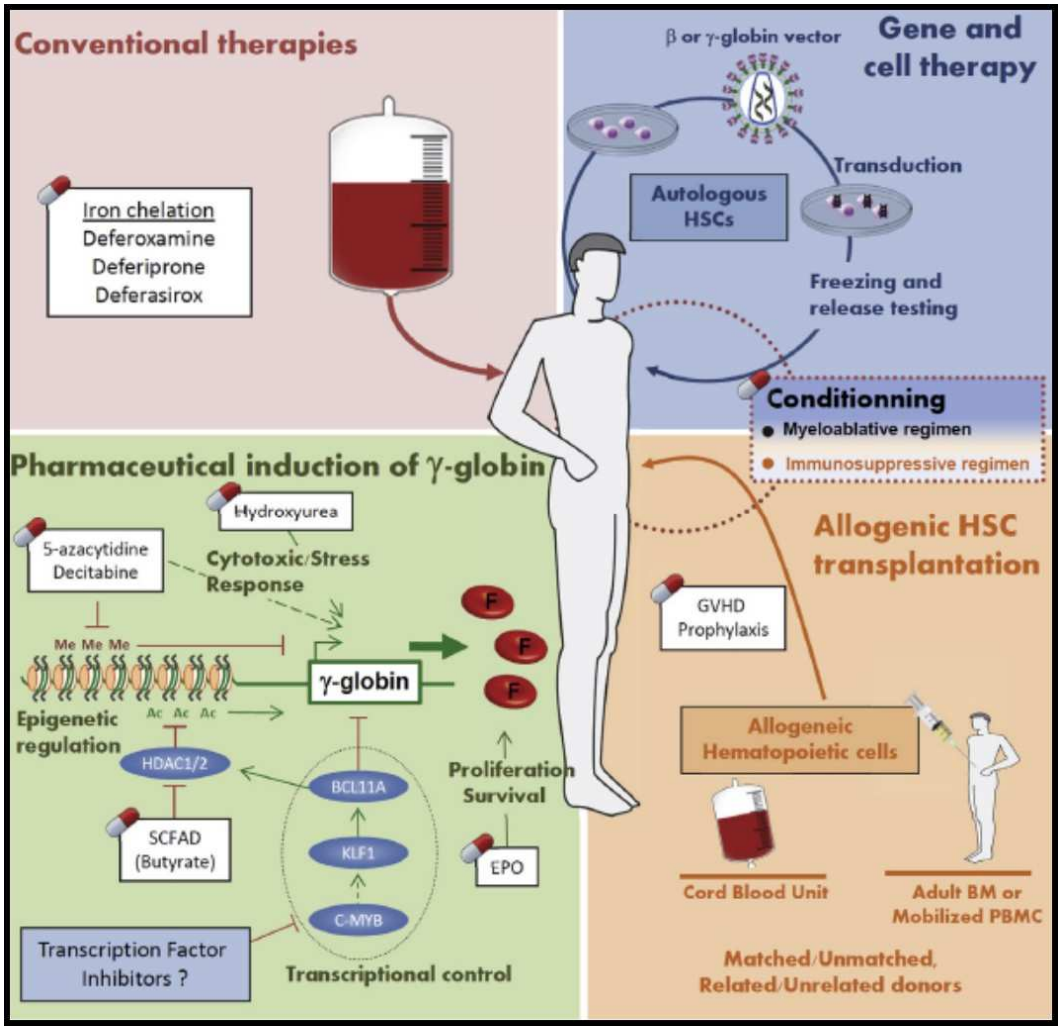

Figure 30: Principal therapeutic approach for β-thalassemia.

Definitive therapies goal is to completely resolve the disease and two main therapeutic approach are considered:

-*Bone Marrow Transplantation* (BMT): the essential pre-requisite to apply this approach is the availability of a compatible donor. Only after the identification of a possible donor, the patient is subjected to ablation of the hematopoietic and immune systems by the combined treatment with busulfan (hematopoietic system inhibitor) and cyclophosphamide (immune system inhibitor) [*Lucarelli et al., 2012*]. The patient is than transplanted by the infusion of bone marrow cells into a peripheral vein. Main complications are reject of the transplant or

a disease named Graft Versus Host Disease (GVHD) that is due to the immune response of donor lymphocytes against the recipient lymphoid tissue. GVHD can affect several organs with different degrees, but the most frequently affected are skin, gastrointestinal tract, and liver and in some cases can be lethal. Frequently, even if BMT is successful, iron chelation therapy is anyway necessary to reduce iron overload generated in the period before the transplant [*Lucarelli et al., 2002*]. To reduce GVHD is also, possible to replace bone marrow transplantation with umbilical cord blood cells transplantation, even if this technique is not yet widely used for the treatment of β-thalassemia [*Hall et al., 2004*].

-*Gene therapy*: β-globin gene transfer into hematopoietic stem cells is a widely studied method to treat β-thalassemia. The main advantage derives from the use of patient own cells, so no compatible donors are required resulting in reduction of immunological complications associated with bone marrow transplantation. Gene therapy strategy has four principal goal: a) the transfer of a single gene in specific hematopoietic stem cells, b) the endogenous expression of the transgene at high levels, c) the maintenance of that expression over time and d) the use of not pathogenic vectors. Most of methods currently available do not satisfy

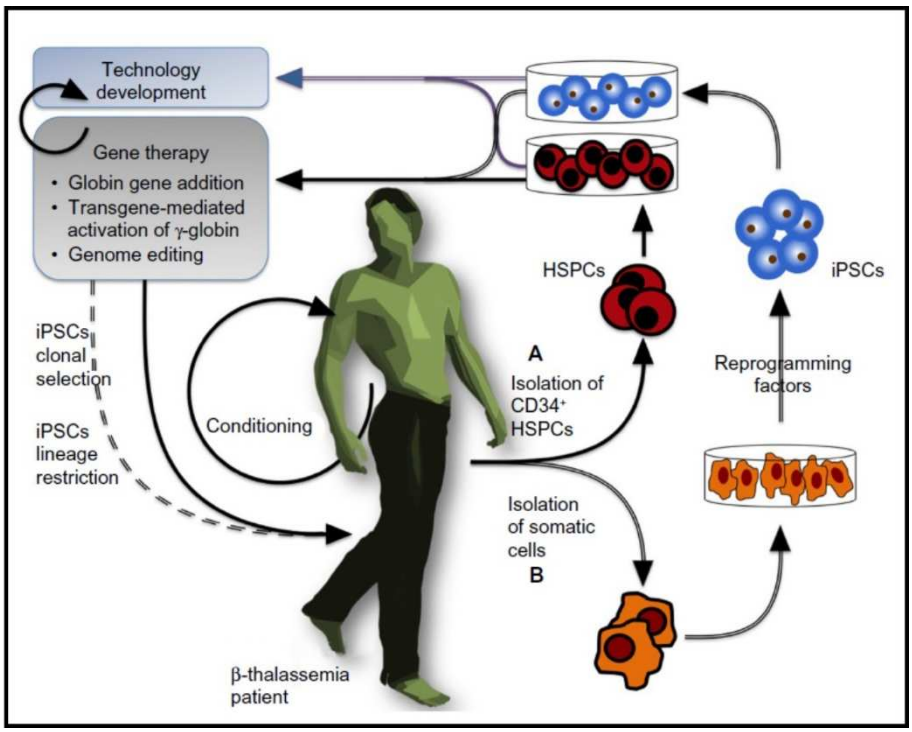

Figure 31: Schematic work-flow of gene therapy. Taken from *Finotti et al., 2015*

all the four features. Even if the concept of gene therapy for β-thalassemia was introduced several years ago, the first promising results were obtained only in the last years [*Kolata et*

al., 1980]. One of the major issue was the identification of the regulatory sequences required to obtain high expression of the transferred gene. In this field, the identification of the LCR sequence upstream the globin genes, has played a crucial rule in the design of strong expressed β-globin vectors [*Talbot et al., 1989*]. Another important step was made thanks to the replace of retroviral vectors (RVs) by the more safety lentiviral vectors (LVs). LVs are not only safer, but also are able to transfer longer sequences than RVs and furthermore, are able to transduce no-dividing cells [*Naldini et al., 1996*]. Despite this several issues are still unsolved, for example was well demonstrated that LVs [*Bushman et al., 2005*], including β-globin-LVs [*Imren et al., 2004*] generally, integrate into active genes, changing their expression. At moment several in vivo transfection in mouse model were performed, and also some clinical trials are in progress, but the major limit is still the low number of transduced stem cell, which is between 10 and 20%. Some of the most promising vectors in clinical trial are summarize in Table 10.

Vector	Hb levels post-transplant	Transfusion independent	Reference
HPV569	Subject 1: 8-9 g/dl Subject 2:	Yes No	*Cavazzana-Calvo et al., 2010*
HGB-205	Subject 1: 10.2 g/dl Subject 2: 13.4 g/dl	Yes Yes	*Cavazzana et al., 2014*
HGB-204	Subject 1+2: 8.6 and 9.6 g/dl Subject 3-5: data not available	Yes Data not available	*Thompson et al., 2014*
TNS9.3.55	Subject 1-3: not declared	Not declared	*Boulad et al., 2014*

Table 10: Principal clinical trials using lentiviral vectors carrying β-globin gene.

Maintenance therapies: the recommended therapeutic protocol to treat β-thalassemia is normally based on blood transfusions, to fight anaemia, and iron chelation therapy in order to reduce iron tissue accumulation.

- *Blood transfusions*: principal goals of blood transfusion are the reduction of anaemic state and consequently the suppression of erythropoiesis and the reduction of gastrointestinal iron adsorption. Generally, β-thalassemia patients are subjected to blood transfusion when their Hb levels are below 7 g/dl for more than two weeks [*Galanello et al., 2010*]. Frequency of transfusions depends on the severity of the disease, but are normally performed every two-three weeks, and the amount of transfused RBCs is about 15-20 ml/kg/day, infused at a maximum rate of 5 ml/kg/hour, to avoid a fast increase in blood volume. Before the

transfusion RBCs are deprived of leukocytes to avoid feverish reactions. Thanks to the new diagnostic techniques, that allow the early detection of the pathology, blood transfusions in patients with severe β-thalassemia, are started from the second half of the first year of life. Although blood transfusions are necessary for β-thalassemia patients, they present several risks: one of the major is the risk of infections, as hepatitis B or C, due to infected blood. Moreover, continuous blood transfusions increase significantly the assumption of iron, which is added to the increase of gastrointestinal adsorption due to the anaemic state, leading to the large formation of deposits.

- *Iron chelation therapy* is necessary in all β-thalassemia patients that require regular transfusions and generally is initiated prophylactically, before the onset of symptoms due to iron overload [*Olivieri et al., 2013*]. One of the first agents used for iron-chelation was deferoxamine (Desferal), a hexadentate chelator, able to bind iron at 1:1 molar ratio, rendering it inactive. The resulting complex is then excreted through urines and stools. Deferoxamine is poor absorbed orally, for this reason it must be administered by prolonged parenteral infusion, normally by subcutaneous way, using a portable pump, for about 8 hours a day, every day [*Propper et al., 1977*]. The complex method of administration associated with side effects limits the acceptability. Recently others iron chelation molecules were introduced in therapy, between these, Deferasirox (Exjade), a tri-dentate iron chelator, that is administrated once a day orally. Deferasirox chelates iron stored in hepatocytes, forming a complex that is excreted by bile. Another oral-administered, iron-chelator molecule is Deferiprone (Ferriprox), which is a bidentate chelator that binds to iron in a 3:1 ratio [*Olivieri et al., 2013*]. While deferoxamine is able to remove only bound or unbound iron in plasma or bile, both Deferasirox and Deferiprone are able to enter into cells and remove intra cellular iron deposits, for this reason a combined therapy has been proposed [*Roberts et al., 2007*].

-*Fetal haemoglobin induction*: it was demonstrated that high level of fetal haemoglobin reduces the severity of β-thalassemia and ameliorates the symptomatology, for this reason several molecules that are able to increase HbF levels were studied. Fetal haemoglobin inducers can be divided into two main classes: natural compound and epigenetic modifiers, which in turn can be classified in several classis depending on their mechanism of action. Between natural compound particularly interesting is Mithramycin, a DNA binding drug, isolated from Streptomyces, that was shown to induce γ-globin mRNA accumulation and HbF production in erythroid precursors isolated from β-thalassemia patients [*Fibach et al.,*

2003]. Several others molecules were investigated with promising results and some of the most promising are summarized in the Table 11.

Molecule	Biological Effect	Reference
Bergaptene	Erythroid differentiation of K562 cells	Lampronti et al., 2003
Angelicin	HbF production	Lampronti et al., 2003
Rapamycin	HbF production	Mischiati et al., 2004
Resveratrol	HbF production	Rodrigue et al., 2001
Mitramycin	HbF production	Bianchi et al., 1999
YiSui ShengXue Granule	Erythroid differentiation of K562 cells and HbF production	Zhang et al., 2008
Cucurbitacn D	HbF production and Erythroid differentiation of K562cells	Liu et al., 2010
Terminalia catappa distilled water active fraction (TCDWF)	Erythropoiesis, cell proliferation, and transcription	Aimola et al., 2014

Table 11: Principal natural fetal haemoglobin inducers.

Class	Mechanism of action	Compounds
Cytotoxic agents	Increase erythroid re-generation	Vinblastin Busulfan, Cytosine arabinoside Hydroxyurea.
Short-chain fatty acids (SCFAs)	Enhance both fetal and total hemoglobin levels	Sodium phenylbutyrate Arginine butyrate
DNA methyl transferase (DNMT) inhibitors	Inhibit CpG methylation in the promoter of γ-globin gene	5-azacytidine Decitabine adenosine-2 3-dialdehyde (Adox)
Histone Deacetylase (HDAC) inhibitors	Inhibit Histone deacetylation in γ-globin gene	Trichostatin Apicidin Scriptaid

Table 12: Principal synthetic fetal haemoglobin inducers divided for classes.

Between epigenetic modifiers, particularly important is Hydroxyurea (HU) a cytotoxic agent that was shown to increase HbF expression. Normally used for the treatment of Sickle Cell Disease (SDC), in some cases can be administrated also in β-thalassemia patients, even if

modest responses have been observed and it is not able to prevent blood transfusions. Others epigenetic modifiers are present in the Table 12.

8.4 Hereditary Persistence of Fetal Haemoglobin

Hereditary Persistence of Fetal Haemoglobin (HPFH) is a state in which the haemoglobin pattern typical of the fetal stage continues into adult life. In other words, even if subjects with HPFH are adult they continue to produce fetal haemoglobin, with no apparent clinical effects. HPFH becomes clinically relevant when it is inherited together with β-thalassemia, because in the case γ-globin chains partially replace the absence of β-globin chains, ameliorating symptomatology. HPFH is generally, the result of single point mutations not only in the γ-globin gene promoter. In fact, three major loci were identified as able to influence HbF levels: a) the C→T single nucleotide polymorphism at position −158 of the $^{G}\gamma$-gene, creating a restriction site for the enzyme XmnI [*Gilman et al., 1985*]; b) a polymorphism in the long arm of chromosome 6 (6q23) located in a non-coding region between genes HBS1L and MYB [*Creary et al., 2006*]; and c) the polymorphism located into the intron 2 of B-cell lymphoma/leukemia 11A (BCL11A) gene, which encode for a zinc finger transcription factor [*Sankaran et al., 2008*].

8.5 Molecular control of γ-globin gene expression

The switch from fetal haemoglobin to adult haemoglobin is regulated by several transcription factors, generally, acting as multi-protein complexes. Probably one of the widely studied is the transcription factor BCL11A.

BCL11A (B-cell lymphoma/leukemia 11A) is a multi-zinc finger transcription factor, which recently was suggested to have a key role in γ-globin gene silencing [*Xua et al., 2013*]. The key role played by BCL11A was demonstrated by studies based on the use of lentiviral short hairpinRNA (shRNA)-mediated knock-down of BCL11A. Studies demonstrate that at 97% of BCL11A knock-down corresponds an increase of γ-globin expression of about 6.5 fold [Sankaran et al., 2008]. Resulting from alternative splicing processes, at least four BCL11A isoforms were characterized: eXtra-Long isoform (XL), transcript is 5.9kb long and the resulting protein 125 kD in weight; Long isoform (L), transcript 3.8 kb and protein 100 kD

in weight; Short isoform (S), mRNA 2.4 kb in long and protein 35 kD in weight, while eXtra-Short (XS), transcript 1.5 kb in long and protein 25 kD in weight [Liu et al., 2006].

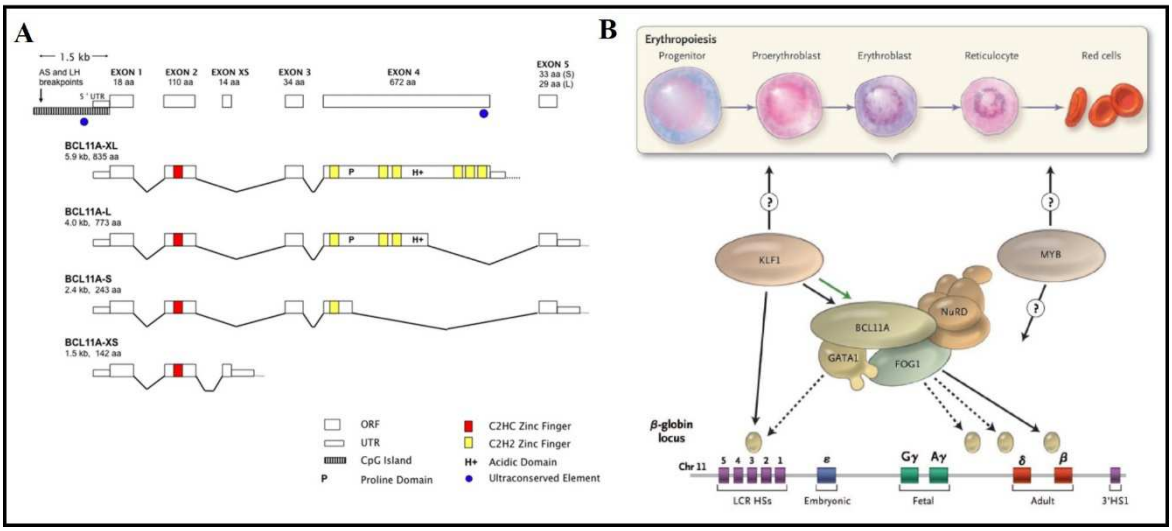

Figure 32: BCL11A principal isoforms and mechanism of action. (A) BCL11A presents four well characterized isoforms: XL, L, S, XS. Taken from *Liu et al., 2016.* **(B)** Molecular regulation of 'to fetal from adult haemoglobin switch', in which BCL11A play a key role. Taken from *Sankaran et al., 2011.*

Exons 1 and 2 are common to all isoforms, while a portion of exon 4 is common to XL, L and S isoforms. The different portions of exon 4 leads to a variable number of C2H2 zinc fingers at the N-terminus between isoforms. In primary adult erythroid cells, major BCL11A isoforms are L and XL, starting from this evidence Sankaran and colleagues performed several studies and concluded that BCL11A is developmentally regulated and the longer isoforms are typical of the adult stage, and probably the major responsible for γ-globin gene repression [*Sankaran et al., 2008*]. As suggested by chromatin immunoprecipitation (ChIP) analysis, BCL11A is able to bind both LCR at the third hypersensitive site (HS3) and also, an intergenic region between ^{A}γ-globin gene and the δ-globin gene, which is commonly deleted in subjects presenting HPFH [*Sankaran et al., 2008*]. The activity of BCL11A is the result of the interaction with several other transcription factors, such as SOX6 [*Xua et al., 2013*].

KLF-1, also called EKLF (Erythroid Kruppel-Like Factor) is a zinc finger-containing, erythroid-specific transcription factor binding a conserved DNA sequence (CACCC) present in several erythroid-specific promoters, included β-globin gene promoter [*Feng et al., 1994*]. A study performed by Borg and colleagues demonstrates the correlation between HPFH phenotype and a nonsense mutation in KLF-1 gene, which ablates the complete zinc finger domain and therefore abrogates DNA binding of the mutant protein [*Borg et al., 2008*]. In

addition, KLF-1 was shown to bind also BCL11A gene promoter, activating its expression. So, KLF-1 is able to regulate fetal to adult haemoglobin switch acting through two different mechanisms and acting both in β-globin gene and BCL11A promoters.

HBSL1-MYB DNA Region: the intergenic region between HBSL1 and MYB contains three hypersensitive sites that show features of active chromatin only in erythroid cells [*Wahlberg et al., 2009*]. If MYB is strictly related to erythroid development, HBSL1 is considered an house keeping gene due to its stable expression in all tissues. Both genes were shown to be down-regulated in subjects presenting HPFH, but while MYB over-expression was shown to inhibit γ-globin gene, probably in indirect way through the activation of LMO2 and KLF-1, no effects were shown in case of HBSL1 over-expression [*Bianchi E et al., 2010*].

SOX6: is able to interact with BCL11A to bind γ-globin gene promoter, though a mechanism that probably involves chromatin looping [*Xu et al., 2010*]. Studies demonstrate that SOX6 alone is able to inhibit only in a little percentage HbF expression.

TR2/TR4 Direct Repeat (DR) erythroid-definitive complex: is a heterodimer composed by the two nuclear receptor TR2 and TR4. The dimer is able to bind DRs both in ε-globin gene promoter and γ-globin gene promoter [*Omori et al., 2005*]. As demonstrate by Collins and colleagues a point mutation in the γ-globin gene promoter, associated with HPFH, involved DR element, inhibiting the heterodimer bond [*Collins et al., 1985*].

COUP-TFII: was demonstrated to bind γ-globin gene promoter in DR sequence [*Filipe et al., 1999*] and four different HPFH mutations in the γ-globin gene promoter were shown to reduce COUP-TFII binding.

FOP (Friend Of Protein arginine methyltransferase) is a target of the protein arginine methyltransferase 1 (PRMT1) which interacts with chromatin [*Van Dijk e al., 2010*]. Studies correlate FOP knock-down with the increase of γ-globin expression, also associated with the reduction of SOX6 expression, while no effects were shown in BCL11A expression. This allows to speculate that FOP is able to increase γ-globin expression through SOX6 down-regulation.

NF-E4: is considered an activator of γ-globin transcription, by the interaction with the ubiquitous transcription factor CP2. The interaction between NF-E4 and CP2 results in the recruitment of p45 NF-E2 and RNA polymerase II to the promoter [*Zhou et al., 2004*].

GATA-1: is a zinc finger transcription factor, playing a key role in erythroid differentiation, that is able to bind LCR and β-globin gene promoter through the interaction with several other co-factors. For example, was demonstrated that GATA-1 is able to form a complex with two others co-factors: FOG-1 and Mi2, which binds γ-globin gene promoter, leading to its silence [*Harju-Baker et al., 2008*].

STAT3 (Signal Transducers and Activators of Transcription 3): is a transcription factor that was shown to bind γ-globin gene 5'UTR, inhibiting γ-globin gene expression [*Foley et al., 2002*]. Interestingly, other studies demonstrate that another transcription factor: GATA-1 binds the same target region of STAT3, with opposite effects; in fact the interaction between GATA-1 and γ-globin gene results in increased expression of fetal haemoglobin. The two TFs was proposed to interact each other, through the formation of a bond between N-terminal GATA-1 zinc finger and the DNA-binding domain of STAT3. The result of this interaction is the reduction of the transcriptional effects that each single transcription factor exerts on γ-globin gene [*Yao et al., 2009*].

LYAR (human homologue of mouse Ly-1 antibody reactive clone): is a nuclear zinc-finger transcription factor that is able to directly bind a DNA motif (GGTTAT) in the 5'UTR of the γ-globin gene silencing it [*Ju et al., 2014*].

8.6 Strategies for BCL11A down-regulation

As previously said, BCL11A has a key role in γ-globin gene repression, for this reason several strategies in order to reduce BCL11A expression have been developed. For example, Pule and colleagues recently demonstrate that a molecule that was longer studied for γ-globin chains induction: Hydroxyurea is able to act directly in BCL11A expression leading to its significative down-regulation. Moreover, HU was shown also, to reduce the expression of KLF-1 transcription factor, which in turn is one of the major activator of BCL11A gene [*Pule et al., 2016*]. Others authors such as Vikas and co-workers used a more specific method based on the use of siRNA against BCL11A obtaining significative but not sharp decrease of BCL11A mRNA and protein, even if the chosen cellular model is questionable [*Vikas et al., 2013*]. In fact, authors chose K562 cell line to perform their experiments, despite is commonly known that BCL11A, especially the longer isoforms, is expressed at very low levels in this cellular model [*Finotti et al., 2015*]. In some cases, also miRNAs were used to regulate expression of specific mRNA, Lulli and colleagues employed

this technique to BCL11A; they identified a miRNA: miR-486-3p, which expression is strongly increased during erythroid differentiation. Studying possible target of miR-486-3p they identify a miR-486-3p binding site in the 3'UTR sequence of BCL11A mRNA. In particularly, the target sequence of the miRNA is specific only for the longer isoform of the transcription factor [*Lulli et al., 2013*]. Interestingly, the indirect effects of miR-486-3p can be appreciate also in γ-globin gene expression, in fact the treatment of the selected cellular model: CD34+ Hematopoietic Progenitor Cells (HPCs), with miRNA mimic molecule results in an increase of γ-globin expression.

8.7 MiR-210 and erythroid differentiation

MiR-210 has been studied for a long time for its implication in several diseases. Several studies correlate miR-210 with an hypoxic state, which was demonstrated to induce the expression of miR-210 [*Camps et al., 2008*]. In particular the over-expression of miR-210 under hypoxic condition is induced by the transcription factor HIF-1α, able to bind hypoxia-responsive element (HRE) located on the miR-210 promoter [*Huang et al. 2009*]. Probably due to its role in hypoxic pathway, miR-210 was found to be modulated in several solid tumours and its levels generally, correlate with a negative clinical outcome [*Mircea et al., 2009*]. The number of already validated targets of miR-210 is very high and probably it is expected to grow up [*http://mirtarbase.mbc.nctu.edu.tw/*]. In a work performed by Bianchi and colleagues miR-210 was related with erythroid differentiation, in fact authors demonstrate that the cells treatment with mithramycin (MTH) a well-known fetal haemoglobin inducer, result in increase of miR-210 expression [*Bianchi N et al., 2009*] even if at moment is not clear what is the actual target of miR-210 in this pathway.

Aim of the thesis

MiRNAs are a class of small non-coding RNA of about 19-23 nucleotides in length. They were firstly described in 1993 by two different researchers, independently, Lee [*Lee et al., 1993*] and Wightman [*Wightman et al., 1993*]. Until the first identification, the number of known miRNAs continues to grow, and at the moment, more 2500 miRNAs have been identified [*http://www.mirbase.org/*].

Most of the studies are in strong agreement in defining miRNAs as key players in regulation of gene expression, thanks to their ability to bind the 3'UTR or less frequently 5'UTR or coding region of target mRNA. The interaction between miRNAs and target mRNAs results in inhibition of translation or, depending on the interaction type, in mRNA degradation. In most cases, due to its short sequence, a miRNA can bind more than one transcript, and this means that a miRNA is able to be involved in more than one biological pathway. In fact, miRNAs have been associated to a long list of physiological or pathological conditions.

For these reasons the research field on miRNAs has become very crowded by a continuously increasing number of publications about the key role of miRNAs and about their modulation. Thanks to their ability to regulate target mRNA levels, miRNAs have been proposed as possible therapeutic tools. In fact, using molecules mimicking miRNA function efficient reduction of the expression of a gene responsible for the pathology can be reached.

On the contrary, it was show that some miRNAs are overexpressed in pathological condition, causing the reduction of their target mRNAs. OncomiRNAs are only an example of miRNAs that are overexpressed in pathological condition, in this case, in cancer. Several types of molecules able to reduce miRNAs levels, such as peptide nucleic acids (PNAs) or miRNA sponges, have been developed and proposed as therapeutical tools. In this respect several molecules have been already employed in clinical trials, such as antimiR-155, which is currently tested for the treatment of haematological malignancies.

On the other hand, in 2008 Chim and colleagues demonstrated the presence of miRNAs also in plasma, opening a new important field of research aimed at determining the importance of miRNAs as diagnosis tools. In fact, starting from this first work, several others authors demonstrated that miRNAs are present not only in plasma but also in others body fluids such as serum, saliva, urine or cerebrospinal fluid. The high stability of miRNAs in body fluids associated with the possibility to obtain samples with no invasive

procedures makes miRNAs very useful diagnostic reagents. However, despite a large number of works, which demonstrate the correlation between the disease presence and change in circulating miRNAs profile, at moment circulating miRNAs are not yet approved as diagnostic biomarkers.

In this thesis, we consider miRNAs from different point of view, in order to demonstrate their high flexibility in research practice.

Our first aim was to demonstrate how miRNAs released in body fluids, in particular plasma, may be useful tools in indicating the presence of a pathological condition, in our case colorectal cancer (CRC). Moreover we have considered the role of changes in plasma miRNA profile occurring in other alterations of physiological condition, in our case the change in oxygen availability after autologous blood transfusion (ABT) in sport.

Our first aim was, therefore, to identify a set of miRNA with modulated levels in plasma, in the presence of CRC (as example of pathology) and ABT (as example of a practice requiring efficient detection procedures). Furthermore, we compared different available miRNAs detection techniques, such as RTqPCR, ddPCR or microarray, and we tried to identify principal pitfalls of this relative new research field.

In the second part of the thesis, we wanted to validate possible application of miRNAs for therapeutic purposes, on the basis of miRNAs ability to bind target mRNA affecting complex regulatory pathways. In our case we wanted to verify whether miR-210-3p is able to bind the transcription factor BCL11A. In this case the employment of miRNA mimicking molecules (increasing miR-210-3p intracellular levels and thereby able to reduce the transcription factor levels) was considered to reach alterations of gene expression of possible clinical application. Our aim was to verify whether miR-210-3p levels may be a useful tool for the treatment of β-thalassemia.

In the third part of the thesis, we considered the important issue of the delivery of molecules altering miRNA activity. In this context we characterized a new possible delivery system useful for miRNA-based molecules delivery. Specifically, our purpose was to demonstrate that a calix[n]arene-structure molecule (called ML122), previously employed for delivery of plasmid DNA, may be useful for the delivery of not only miRNA-based molecules (such as antimiRNA or premiRNA molecules), but also of miRNA-targeting PNAs.

Materials and Methods

1. Blood and blood derived samples collection and management

1.1 Blood withdrawal

450 mL of total blood were collected from each athlete that underwent to ABT, according to international standard methods of transfusion medicine. Briefly, venous blood was collected from an antecubital vein and then was either refrigerated or cryopreserved. As regard +4°C stored blood, packed RBCs and plasma were isolated, and the RBCs were stored at +4°C in a storage solution composed of saline, adenine, glucose and mannitol. At same way, packed RBCs were conserved at -80°C using cryopreserving compounds. All samples were stored for 35 days and then reinfused in athletes. All procedures of blood withdrawal, storage and reinfusion were performed by qualified personnel at the Blood Transfusion Service of Ferrara, Arcispedale Sant'Anna.

1.2 Blood samples collection for plasma isolation

Blood collection represents a key step, for circulating miRNAs analysis for this reason starting from blood collection all steps need to be standardized. In fact, several studies demonstrate that variables in phlebotomy step can cause the lysis of erythrocytes or others blood cells that can affect the final miRNAs quantification. Generally, erythrocytes lysis, which results in haemoglobin release, can alter final miRNAs concentration in plasma and as reported by some authors can also inhibit RTqPCR analysis [*Moldovan et al., 2014*]. Samples which for some reason appeared hemolysed were not considered for analysis. All whole blood samples were collected in 6 mL tubes containing EDTA (K2 ethylenediaminetetraacetic acid) [Vacutainer K_2 EDTA tubes, BD Biosciences, San Jose, CA, USA] as anticoagulant. No others anticoagulant were employed, in fact several studies demonstrate that both lithium-heparin and sodium-citrate can affected later applications [*Al Soud et al., 2001*]. In fact, while heparin was shown to inhibit reverse transcriptase enzyme, sodium citrate interferes with PCR amplification [*Willems et al., 1993*]. Venous blood samples were collected from an antecubital vein and after the collection, tube was gently inverted from 8 to 10 times to mix blood with EDTA, which reaches the final concentration of 1,8 mg for mL of blood. Samples were processed within an hour according to the protocol established by the project, in order to isolate plasma. As it will be explained, two different

protocols were employed for plasma isolation, depending on the project. This is not surprising, in fact analysing literature about circulating miRNAs, very different protocols were employed and each protocol presents advantages and disadvantages. Independently by the employed protocol, all plasma samples, are divided into single use aliquots, in order to avoid freeze-thaw cycles, and stored at -80°C until the moment of the use.

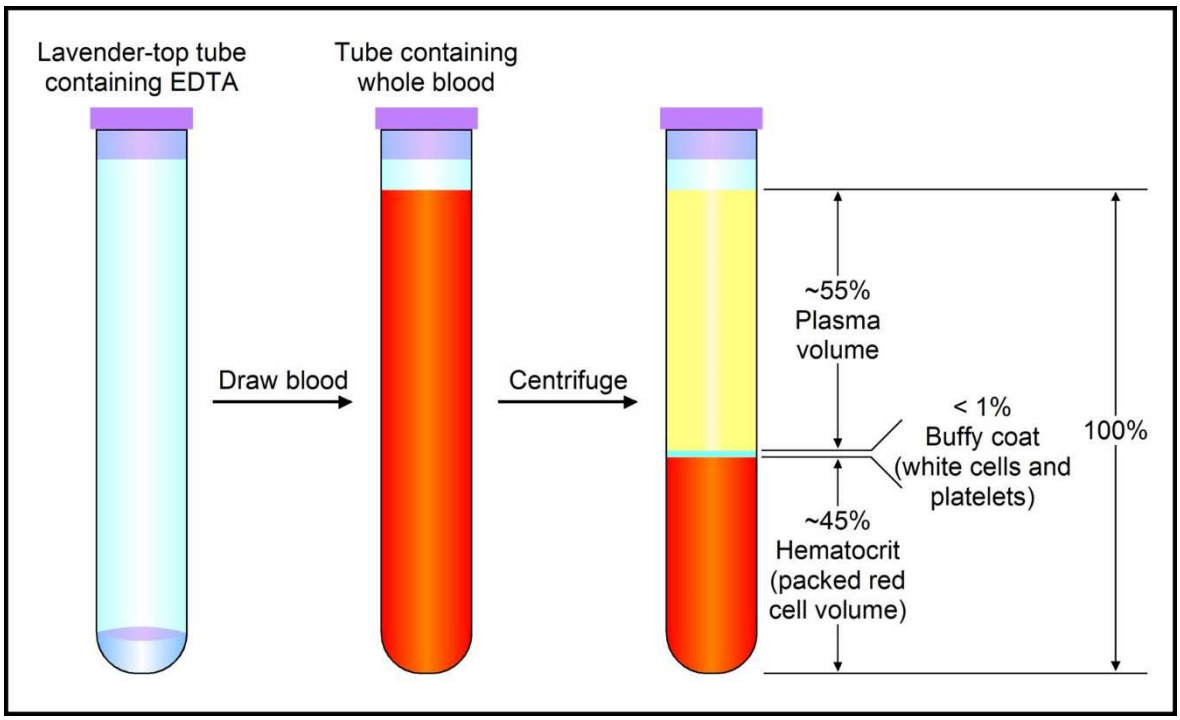

Figure 33. Plasma isolation protocol. Tube containing EDTA as anticoagulant were employed, tube were inverted 8-10 times to mix EDTA with blood. Blood was processed within 1 hour after the collection. After centrifugation three phases can be distinguished: the upper phase containing plasma, a thin white phase containing white cells and platelets and a lower phase containing red blood cells. Taken from *www.physiology lab.com*

1.2.1 Plasma isolation from blood collected from athletes which underwent to ABT

Whole blood samples were collected at different time points established by the study from both control athletes (12 subjects) and transfused athletes (12 subjects). All samples were collected before performing others procedures such as blood withdrawal, blood reinfusion or physical test. Before starting plasma isolation, tubes containing collected blood were mixed for 5 minutes with a rotator, samples were then transferred in 15 mL polypropylene tube and centrifuged at 1200g for 10 minutes at 4°C without brake in order to avoid the interphase disruption. Three different phases can be recognized after centrifugation the upper yellow phase constituted by plasma, a middle white phase, called buffy coat, which contains platelets and leukocytes and the lower red phase composed by red blood cells. The upper phase was collected, transferred into a clean tube and centrifuged

twice. The first time at 2400g for 20 minutes at 4°C and then the collected plasma was centrifuged again, at 1500g for 10 minutes at 4°C to completely remove platelets and others precipitates. Collected plasma was then divided into small aliquots and stored. The study was approved by the Ethics Committee of Ferrara (approval number: 06/2014).

1.2.2 Plasma isolation from blood collected from CRC patients and relative healthy controls

Blood was collected from CRC patients at the moment of diagnosis, before any surgical or pharmacological treatment. Collected blood was mixed in a rotator for 5 minutes before starting isolation. Blood was centrifuged at 2000g for 20 minutes at 4°C without brake. Resulting plasma was collected and transferred in new clean tube and centrifuged again at 16000g for 10 minutes at 4°C. Obtained plasma samples were stored at -80°C in single used aliquots.

1.2.3 Plasma isolation from mouse xenografts

Whole blood was taken at the sacrifice, from mouse xenografts. Briefly, isolated blood was collected in BD Vacutainer K3EDTA tubes, [BD Biosciences, San Jose, CA, USA], and processed within an hour. Whole blood was centrifuged at 2000g for 20 min at 4°C. Plasma was recovered and further centrifuged at 16000g for 10 min at 4°C to remove all cell debris. Isolated plasma was divided into small aliquots and stored at -80°C until RNA extraction.

1.3 Spiked plasma sample preparation

As previously explained, the presence of RNAses enzyme causes the immediate degradation of naked miRNAs, so in order to create plasma samples spiked with a known concentration of mature miRNA, plasma was previously treated with a ribonuclease inhibitor [RNAse inhibitor, Applied Biosystems, ThermoFischer Scientific, Waltham, Massachusetts, USA] a 50 kDa recombinant enzyme which is able to inhibit the activity of RNAses present in plasma. A suitable volume of RNase Inhibitor 20U/µL was added to plasma sample in order to achieve the final concentration of 0,4 U/µL, and the sample was incubated for 10 minutes at room temperature. After the incubation a suitable volume of synthetic mature

miRNA (IDT, Integrated DNA Technology, Coralville, Iowa, USA) was added to each sample in order to obtained the final concentrations in plasma of respectively: 100 fM, 10 fM, 1 fM and 0,1 fM. An aliquot of prepared spiked samples was analysed to quantify miRNA content using ddPCR, while a second aliquot was sent to I.N.B.B in order to analysed samples with NESPRI based device. Both aliquots were conserved at -80°C until the analysis.

2. RNA samples preparation

2.1 RNA extraction from plasma

RNA extraction represents a key point, which can affect substantially miRNAs yield and consequently miRNAs quantification data. If for miRNAs isolation from cells and tissue generally, the optimal method is based on the classical phenol-chloroform extraction, more complex is the RNA extraction from body fluids. Main pitfalls are the generation of large volumes of aqueous phase and the high content of proteins, which need to be denatured and removed. MiRNAs isolation techniques from plasma can be essentially divided into two main groups: techniques based on phenol-chloroform extraction, or column-based miRNA recovery methods. As regard the first case, a solution of phenol and guanidinium thyocianate is used to denature proteins carrying miRNAs, and others proteins, such as RNAse enzyme, and to confer long-term stability at the obtained samples. Denaturation step is followed by phase separation using chloroform and the consequently RNA precipitation using isopropyl alcohol. This method is, of course, easy to apply and allows to process several samples at same time, for this reason it is widely employed for miRNAs isolation despite a recent study demonstrates that when the phenol-chloroform method is employed a loss of small RNA molecules with low GC content, such as miR-141, can occur [*Kim et al., 2012*]. At the same time, several kits based on the use of columns for miRNAs isolation are available. Essentially, two kinds of columns can be employed: columns containing a glass-fibre filter such as miRVana PARIS or a silica-based column system. MiRVana PARIS kit is based in phenol-chloroform extraction followed by sequential filtrations using incremental concentrations of ethanol, and allows the collection of an enriched fraction of RNA molecules below 200 nucleotides. Similarly, miRNeasy Serum/Plasma kit is also based on phenol-chloroform extraction, but in this case the recovered material is absorbed in a silica-

based filter, which is then washed with ethanol solutions. This two kits represent only two of the most employed kit for miRNA isolation, in fact based on the same methods, several companies developed similar kit with variable recovery yield, which were compared in several studies [*Page et al., 2013*].

2.1.1 RNA extraction from plasma using phenol-chloroform method

Total RNA, including miRNAs, was extracted from 800 µL of plasma isolated from six athletes which underwent to ABT (3 athletes reinfused with +4° stored blood and 3 athletes transfused with cryopreserved autologous blood) and from three pool of control subjects. Each pool was obtained mixing equal volumes of plasma from three control subjects. The extraction was performed according to the manufacturer's instruction. Briefly, plasma samples were thawed at room temperature for 10 minutes, then 2,4 mL of TRIzol LS Reagent [Invitrogen, Thermo Fisher Scientific, Waltham, Massachussetts, USA] were added to plasma maintaining the ratio TRIzol LS:plasma 3:1. The sample was homogenized pipetting up and down several times and incubated 5 minutes at room temperature. After the incubation 400 amoles of cel-miR-39-3p [miRVana, Thermo Fisher Scientific, Waltham, Massachussetts, USA], as exogenous control, were spiked and 600 µL of nuclease free chloroform [Sigma-Aldrich, Saint Louis, Missouri, USA] were added. Samples were shaken vigorously for 15 seconds and incubated at room temperature for 5 minutes. After the centrifugation, performed at 12000g for 15 minutes at 4°C, three phases were separated: a lower organic phase, a white interphase and an upper colourless phase containing RNA. The upper aqueous phase, was collected and transferred in a new clean tube. 1,6 mL of nuclease free isopropanol [Sigma-Aldrich, Saint Louis, Missouri, USA] were added to the aqueous phase, the mixture was shaken vigorously, 4 µL of 5 mg/mL glycogen [Ambion, Thermo Fisher Scientific, Waltham, Massachussetts, USA] were added and the sample was incubated at room temperature for 10 minutes. After the incubation, samples were centrifuged at 12000g for 10 minutes at 4°C. Supernatant was removed and the RNA pellet was washed with 3,2 mL of 75% ethanol [Carlo Erba, Milano, Italy]. Samples were centrifuged at 7500g for 5 minutes at 4°C, ethanol was removed and RNA pellet was air-dried for 5 minutes and re-suspended with 20 µL of nuclease free water [Sigma-Aldrich, Saint Louis, Missouri, USA]. Obtained RNA was stored at -80°C.

2.1.2 RNA extraction from plasma using silica columns

Plasma samples from CRC patients and healthy donors were extracted using miRNeasy Serum Plasma Kit [Qiagen, Hilden, Germany] according to the manufacturer's protocol with some minor changes. 150 µL of plasma were lysed with 5 volumes (750 µL) of Qiazol Lysis Reagent, which contains a solution of phenol and cyanoguanidine. The mixture plasma-QIAzol was vigorously shaken and incubated at room temperature for 5 minutes. At the end of the incubation 400 amoles of synthetic mature Cel-miR-39-3p [miRVana, Thermo Fisher Scientific, Waltham, Massachussetts, USA] were spiked into the mixture as exogenous control to evaluate extraction efficiency. 150 µL of nuclease free chloroform [Sigma-Aldrich, Saint Louis, Missouri, USA] was added to each sample, the mixture was shaken vigorously for 15 seconds and then incubated at room temperature for 3 minutes. Samples were centrifuged at 4°C for 15 minutes at 12000g in order to separate three phases: the lower organic phase, a white interphase and an upper aqueous phase, which contains RNA. The upper phase was collected avoid touching interphase or organic phases, and transferred to a new clean tube. The collected aqueous phase was measured and 1,5 volumes of 100% nuclease free ethanol [Carlo Erba, Milano, Italy] was added. 700 µL of solution were added for each time to miRNeasy MinElute Spin Column, columns were centrifuged at 8000g for 30 seconds at room temperature and the flow-through was discarded. This step was repeated until all the volume of the mixture was added to the

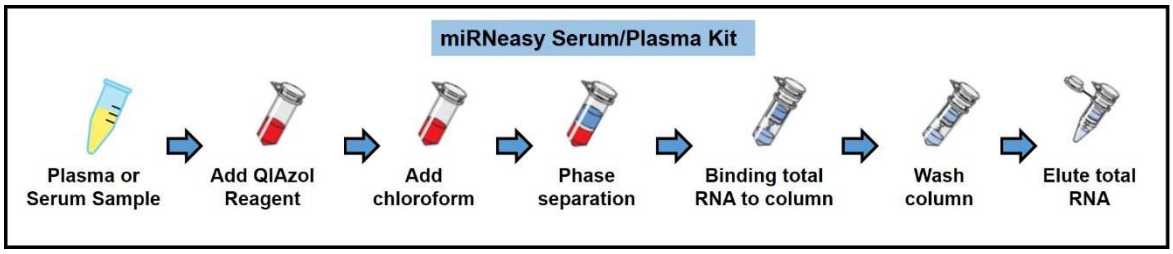

Figure 34. RNA isolation from plasma using miRNAeasy Serum/Plasma Kit work-flow. RNA is extracted from plasma using QIAzol Reagent and chloroform, the resulting aqueous phase is added to a silica column. Column is washed with buffers containing different ethanol concentration and then RNA was eluted in an opportune nuclease free water volume.

column.

Columns were washed with two solutions, purchased from the kit: RWT Buffer and RPE Buffer. Firstly, 700 µL of RWT Buffer were added to the columns, which was centrifuged

at 8000g for 30 seconds at RT and the flow-through was discarded. In the second step, 500 µL of RPE buffer were added to the column, the columns were centrifuged at 8000g for 30 seconds at RT and the flow-through was discarded. Columns were washed with 80% ethanol, centrifuged at 8000g for 2 minutes at RT. Flow-through was discarded, and collection tube was replaced with a new collection tube. Columns with open lid, were centrifuged at 12000 rpm for 5 minutes to dry completely the filter. Collection tube was discarded and column was placed in a new collection tube. 18 µL of nuclease free water were placed in the centre of the column, without touching walls. After an incubation of 10 minutes at room temperature, columns were centrifuged at 14000g for 1 minute at room temperature. Collected RNA was stored at -80°C for further applications.

2.2 RNA extraction from cell-culture supernatants

RNA extraction from cell-culture supernatants was performed as indicated in Turchinovich et al., 2011 with some minor variations. A combination of phenol-chloroform and columns based extraction was employed. 400 µL of supernatants, isolated from 72 hours cell-culture were lysed with 1,2 mL of TRIzol LS Reagent [Invitrogen, Thermo Fisher Scientific, Waltham, Massachussetts, USA], and incubated for 5 minutes at room temperature. At the end of the incubation respectively a) 400 amoles of synthetic, mature Cel-miR-39-3p [miRVana, Thermo Fisher Scientific, Waltham, Massachussetts, USA] and b) 12 µg of nuclease free glycogen [Ambion, Thermo Fisher Scientific, Waltham, Massachussetts, USA], were added. 320 µL of nuclease free chloroform [Sigma-Aldrich, Saint Louis, Missouri, USA] were added, the mixture was vigorously shaken, incubated for 5 min at room temperature and then centrifuged at 14000g for 20 min at 4°C. After phase separation, the aqueous phase, containing RNA, was collected and transferred in a new tube. RNA was purified from the collected aqueous phase using miRNeasy Serum Plasma columns [Qiagen, Hilden, Germany] as explained in detail in ‘RNA extraction from plasma using silica columns’ chapter. RNA was eluted using 18 µL of nuclease-free water [Sigma-Aldrich, Saint Louis, Missouri, USA] and stored at -80°C.

2.3 RNA extraction from cells

In order to isolate total RNA cells were isolated by centrifugation at 1200 rpm for 10 minutes at 4°C, washed twice in 1 mL of DPBS 1X [Gibco, Thermo Fischer Scientific,

Waltham, Massachussetts, USA] and lysed with Tri-Reagent [Sigma-Aldrich, Saint Louis, Missouri, USA], using the ratio 1 mL of Tri-Reagent for $1x10^6$ cells. After 5 minutes incubation with Tri-Reagent, 200 µL of nuclease free chloroform [Sigma-Aldrich, Saint Louis, Missouri, USA] for each mL of Tri-Reagent were added, the mixture was shaken vigorously and incubated at RT for 3 minutes. Samples were centrifuged at 12000 rpm for 10 minutes in order to obtain phase separation. The aqueous, upper phase was collected and transferred to a new collection tube, and 500 µL of nuclease free isopropanol [Sigma-Aldrich, Saint Louis, Missouri, USA] were added for 1 mL of starting Tri-Reagent. The mixture was incubated at room temperature for 10 minutes and then centrifuged at 12000 rpm for 15 minutes to precipitate RNA. Supernatant was removed and RNA was washed with 1 mL of cold 75% ethanol. After 5 minutes centrifugation at 12000 rpm at 4°C, ethanol was aspirated and RNA pellet was air-dried and resuspended in a suitable nuclease free water volume. Obtained RNA was stored at -80°C for further applications.

2.4 RNA extraction from tumour tissue

Total RNA was isolated from fresh-frozen tumour tissue, obtained by xenograft mice at the sacrifice. Fresh-frozen tumor tissue, about 20 mg, each one, were thawed at room temperature for 5 minutes and homogenized with IKA T10 Basic Ultraturrax [IKA Werke GmbH & Co. KG, Staufen, Germany] in 1 mL of Tri-Reagent [Sigma-Aldrich, Saint Louis, Missouri, USA] at maximum speed for 1 minute. Samples were incubated at room temperature for 5 minutes and 200 µl of chloroform [Sigma-Aldrich, Saint Louis, Missouri, USA] were added. Phase separation was obtained centrifuging at 12000 rpm for 10 minutes at 4°C and upper aqueous phase was collected and transferred in a new clean tube. 500 µL of nuclease free isopropanol were added to each sample, and the mixture was incubated at RT for 10 minutes. In order to obtain RNA pellet precipitation, samples were centrifuged at 12000 rpm for 15 minutes at 4°C, and supernatant was carefully removed. RNA pellet was washed with cold 75% ethanol, followed by the centrifugation at 12000 rpm for 5 minutes. Ethanol was removed and pellets were air-dried and resuspended in 100 µL of nuclease free water.

2.5 RNA quantification

If RNA isolated from plasma sample is almost unquantifiable, RNA isolated from cell samples or tissues have been quantified using a UV-Vis, microvolume spectrophotometer [DeNovix, Wilmington, Delaware, USA]. 1 µL of starting RNA sample was added directly in the optical sensor. The instrument is able to measure the absorbance from 220 to 350 nm. Considering that 1 OD at 260 corresponds to 40 µg/mL of ssRNA, to calculate RNA sample concentration the absorbance value at 260 nm was multiplied by 40, the conversion factor for RNA samples. Moreover, in order to evaluate the possible presence of contaminations, three others wavelength values were considered. We considered the ratio between the absorbance value at 260 nm and at 280 nm, which indicates the presence of protein contamination. Generally, the ratio must be higher than 1,8; lower values indicate the presence of proteins contamination. In fact, proteins which contains amino acids with aromatic rings adsorbed at 280 nm. Another important value to considered is the absorbance at 230 nm, generally different compound adsorbed at this wavelength, including salts, carbohydrates, urea, EDTA, peptides, glycerol used for RNA precipitation or guanidine thiocyanate. Even in this case ratio between absorbance value at 230 nm and at 260 nm may be higher than 1,5 and close to 1,8. Moreover, phenol, normally used for RNA extraction can contaminate RNA samples. Phenol adsorbed at 270 nm, and samples which do not contain phenol present a ratio 260/270 higher than 1,2.

2.6 RNA quality control

The most common way to verify RNA quality and integrity is to perform an agarose gel, RNA check. Generally, for RNA analysis an agarose gel at 0,8 % is prepared dissolving agarose powder [Sigma-Aldrich, Saint Louis, Missouri, USA] in an appropriate volume of TAE 1X buffer (40 mM Tris-Acetate, 1 mM EDTA, pH 8) and boiling until agarose is completely dissolved. Solution is cooled and 0,5 µg/mL ethidium bromide [Sigma-Aldrich, Saint Louis, Missouri, USA] was added. Gel was done solidify for about 30 minutes in a base plate with 0,75 mm combs and then immersed into 1X TAE buffer. A solution containing 500 ng of RNA sample and 1 µL of loading buffer, composed by 0.25% Orange G [NEB, New England BioLabs, Ipswich, Massachusetts, USA], 50% glycerol in TE buffer, was prepared, reaching the final volume of 10 µL with nuclease free water. Samples were loaded and migration was performed for 30 minutes at 80 Volts. RNA, which is negative charged, migrates toward the anode in the presence of electric current. RNA was visualised

using ChemiDoc MP System [Bio-Rad, Hercules, California, USA] and images were elaborated using Image Lab software [Bio-Rad, Hercules, California, USA]. Mammalian total RNA presents two intensive band, which correspond to 28s and 18s ribosomal RNA

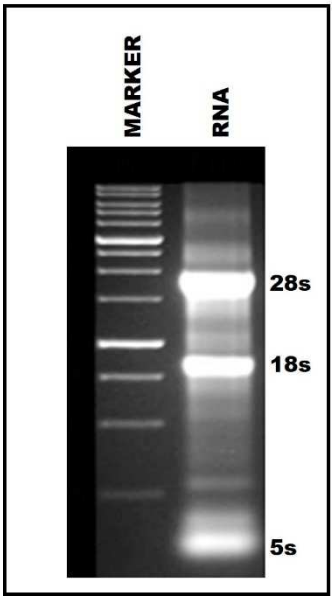

Figure 34. Example of RNA sample in agarose gel. Three bands can be distinguished, an upper band, which is most intense and corresponds to 28s ribosomal subunit of RNA, a middle band which correspond to 18s subunit and a lower weak band that relative to 5s ribosomal subunit.

and a weaker band which corresponds to 5s ribosomal RNA. Generally, 28s and 18s bands are present with the ratio 2:1. Furthermore, electrophoretic analysis of RNA can give information about the presence of possible DNA contamination in the sample; in this case, a further band at high molecular weight can be detected at UV analysis.

3. MiRNA detection methods

As previously described in the chapter 'miRNA detection' several techniques have been developed in the recent years to detect and quantify miRNAs. In this thesis we employed two methods: PCR-based methods and microarray method, both methods present advantages and disadvantages. The choice depends on several factors, including number of analysed miRNAs, samples type and type of final output.

3.1 PCR-based techniques

PCR-based techniques are considered the gold standard for miRNAs detection, the low quantity of starting material required, the dynamic range and the relative low costs make

this technique the first choice for miRNA analysis. The major limit is the low number of miRNAs, which can be analysed starting from single sample, despite in the recent years several microfluidic platforms able to profile small or medium panels of miRNAs and based on PCR, have been developed.

3.1.1 Reverse transcription

All PCR based techniques before the amplification require an additional step, in which extracted target miRNAs are reverse transcribed to a cDNA, which is then amplified by PCR. This step is called reverse transcription and at the moment two different reverse transcription methods are available. The first one, is able to generate a universal cDNA, in which all miRNAs contained in the starting sample are reverse transcribed. The enzyme poly(A) polymerase (PAP) catalyses the addition of a poly A tail at the 3' of all miRNAs and then a universal primer containing an oligo dT sequence is employed as starter for reverse transcriptase enzyme. This reverse transcription method is considered very useful when small amount of starting RNA are available, in fact starting from the same reverse transcription reaction, several miRNAs can be analysed. The major disadvantage is associated to the specificity; in fact, this method is considered less specific than method based on the use of miRNA specific primers. In this case, each reverse transcription reaction is performed using a stem loop primer, containing 6-8 nucleotide overhang on the 3' end, which is complementary to target miRNA. In this case only a miRNA can be reverse transcribed for each reaction mix, but this method is considered more specific and also, able to discriminate between mature miRNA and miRNA precursors, such as pre-miRNAs and pri-miRNAs.

3.1.1.1 MiRNA reverse transcription using universal primer

RNA extracted from plasma and isolated from control group and athletes which underwent to ABT was reverse transcribed using miRCURY LNA Universal RT microRNA PCR [Exiqon, Qiagen, Vedbaek, Denmark], which is probably the most used reverse transcription kit based on the use of universal primers. 3 µL of extracted RNA were reverse transcribed in a final volume of 10 µL. The reaction mix contains 3 µL of RNA, 2 µL of 5X Reaction Buffer, 1µL of enzyme mix (10X) and the final volume of 10 µL was reached using nuclease free water purchased from the kit. The reverse transcription reaction was incubated

at 42°C for 60 minutes and then at 95° C for 5 minutes to inactivate the enzyme activity. Obtained cDNA was stored at -80°C until the moment of use.

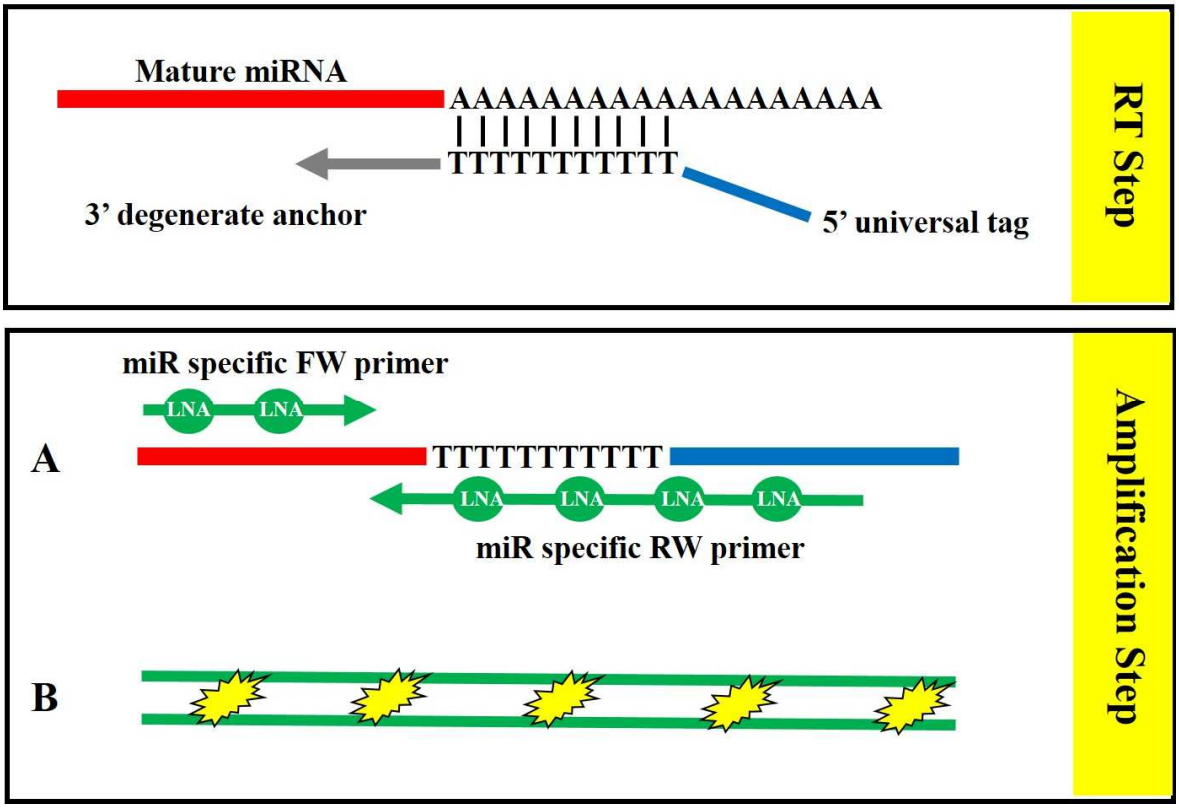

Figure 36. Reverse transcription and amplification using universal primer. A poly (A) was added at the 3' end of mature miRNA. A universal primer containing a oligo dT sequence is employed as starter for reverse transcriptase enzyme. Amplification reaction is performed using a couple of miRNA-specific RNA primers and a DNA binding dye.

3.1.1.2 MiRNA reverse transcription using a specific primer

MiRNAs isolated from plasma of CRC patients and healthy donors, miRNAs analysed in CRC cells or culture medium, miRNAs analysed in plasma or tissues isolated from xenografted mouse, miRNAs analysed in ErPCs after the MTH treatment and miRNAs quantified after the transfection with ML122 or commercial agents were reverse transcribed using TaqMan MicroRNA Reverse Transcription Kit [Applied Biosystems, Thermo Fisher Scientific, Waltham, Massachussetts, USA]. Reverse transcription was performed starting from a) 3 µL of eluted RNA, when RNA isolated from plasma samples was employed or b) 300 ng of total RNA when RNA isolated from cultured cells or tissue was employed. In order to reverse transcribe more than one miRNA for single reverse transcription reaction

we optimized a reverse transcription protocol in which in a single reverse transcription reaction we reverse transcribed three miRNAs. Is important to underline that before to reverse transcribe more than one miRNA for each reaction, miRNA sequence was analysed, in order to avoid the contemporary reverse transcription of miRNAs with similar sequence,

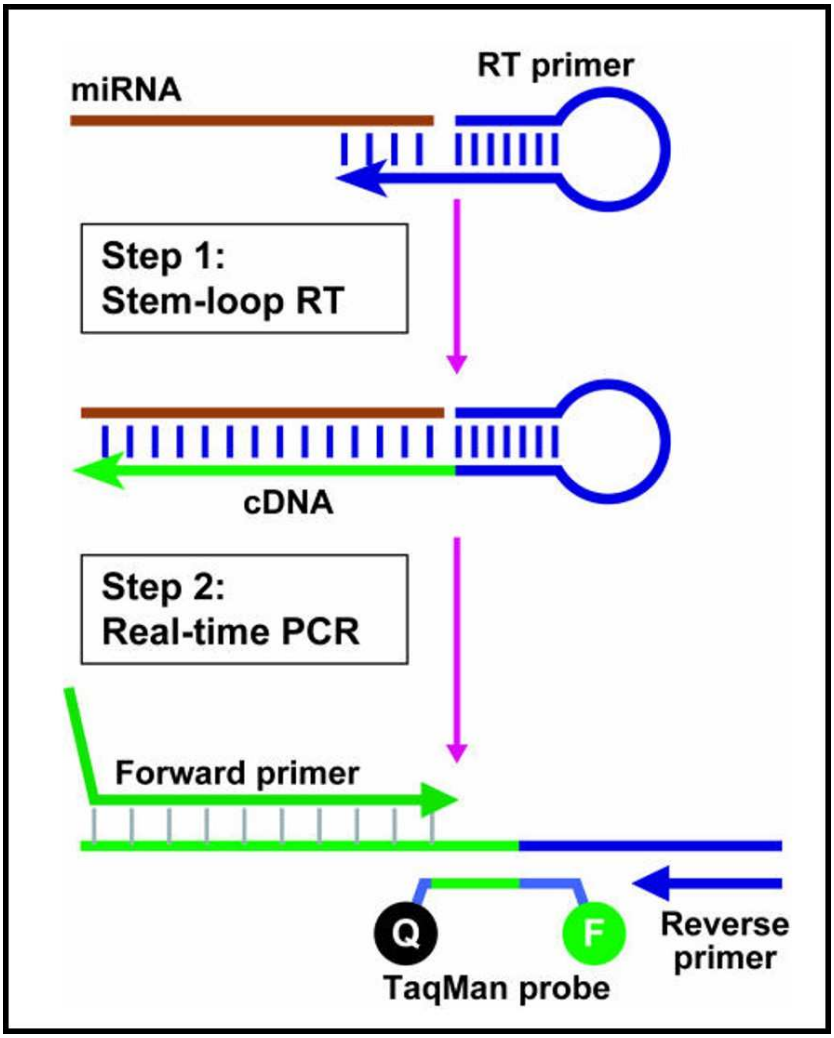

Figure 37. MiRNA reverse transcription using specific primer. A specific stem loop primer, containing 6-8 nucleotide overhang on the 3' end, is employed to perform reverse transcription. A couple of primers is employed to performed RTqPCR. While forward primer is specific for each miRNA, reverse primer is universal for reverse transcription products.

especially at the 3' end. For RNA samples obtained from plasma a) the reverse transcription reaction was performed in a final volume of 20 µL, while for samples obtained for cells or tissues the final volume of 30 µL was reached. In both cases a) and b) a mix of three primers at final concentration of 25 nM was prepared and RNA was added. The mixture was incubated at 16°C for 30 minutes in order to allow primers annealing. Then a reverse transcription mix, composed by dNTP's (with dTTP) final concentration of 1 mM, 5 U/µL of MultiScribe Reverse transcriptase, 1X Reverse Transcription Buffer, 0,25 U/µL of RNase

Inhibitor, was prepared and added to samples. The reverse transcription reaction was incubated at 42°C for 30 minutes, followed by a step at 98°C for 5 minutes to inactivate the enzyme. The obtained cDNA was stored at -80°C until the moment of the use.

3.1.2 RTqPCR using miRNA TaqMan probes

MiRNA assays based on TaqMan probes are composed by a couple of primers: the forward primer is specific for every miRNA and binds the 3'end of the miRNA sequence, while reverse primer is the same for each assay and binds a sequence present in the stem loop region of the reverse transcription primer. Moreover, the specificity of the assay is further increased by the employment of a TaqMan probe which binds the region between the forward and reverse primer. RTqPCR reaction was performed starting from 3 µL of obtained cDNA, which were mixed with RTqPCR reaction mix composed by TaqMan Universal PCR Master Mix, no AmpErase UNG 2X [Applied Biosystems, Thermo Fischer Scientific, Waltham, Massachussetts, USA] and 20X miRNA assay (assay name and code are indicated in the Table 13), in a final volume of 25 µL.

miRNA	**Assay ID**
Hsa-miR-124-3p	001182
Hsa-miR-141-3p	000463
Hsa-miR-210-3p	000512
Hsa-miR-221-3p	000524
Hsa-miR-222-3p	002276
Hsa-let-7c	000379
Hsa-snRNAU6	001973
Cel-miR-39-3p	000200

Table 13. MiRNA assays employed in the thesis.

Each amplification reaction was performed in duplicate. The following amplification programme was employed: 95°C for 10 minutes to activate Taq polymerase enzyme, 95°C for 15 seconds to denature cDNA double-strand structure followed by a step at 60°C for 1

minute to allow primers and probe annealing. The last two steps were repeated for 50 cycles, and at the end of each cycle fluorescence was measured. All RTqPCR analysis were performed using CFX96 instrument [Bio-Rad, Hercules, California, USA], while for data elaboration and analysis Bio-Rad CFX Manager Software [Bio-Rad, Hercules, California, USA] was employed. For relative expression analysis, fold change analysis was performed using Livak method [*Livak et al., 2011*] ($2^{\wedge-\Delta\Delta CT}$). All data were normalised using as references miR-let-7c and snRNAU6. While for miRNA absolute quantification in cells, supernatants, tumour tissue and plasma, a standard curve was employed. For each miRNA (miR-141-3p, miR-221-3p and miR-222-3p) a standard curve was created using a synthetic mature miRNA [IDT, Integrated DNA Technology, Coralville, Iowa, USA] at different concentrations from 60 amoles to 0,018 amoles. Absolute concentration of samples has been extrapolated from standard curve using Microsoft Excel. Mature miRNAs employed for standard curve creation and relative sequences are reported in the Table 14.

miRNA	**Sequence**	**Length**
Hsa-miR-141-3p	UAACACUGUCUGGUAAAGAUGG	22 bp
Hsa-miR-221-3p	AGCUACAUUGUCUGCUGGGUUUC	23 bp
Hsa-miR-222-3p	AGCUACAUCUGGCUACUGGGU	21 bp

Table 14. Mature miRNA employed for miRNA absolute quantification.

3.1.3 Droplet Digital PCR

Droplet digital PCR is a relatively new PCR technology, which is able quantify nucleic acid in absolute way thanks to the partitioning of the analyte molecules into many replicate reactions at limiting dilution. The main advantage of this technique is the possibility to achieve the absolute quantification of the sample without the employment of standard curve. We employed this technique for the absolute quantification of miRNAs levels, in different types of biological samples. As for RTqPCR, also ddPCR can be performed using TaqMan probes, labelled with FAM or HEX fluorophores or with DNA-binding molecules, such as EvaGreen.

3.1.3.1 ddPCR miRNA analysis using EvaGreen

EvaGreen is a green fluorescent DNA-binding dye, which in the recent years was employed for several applications including qPCR. Low PCR inhibition, high sensibility and stability, low or absent toxicity, are only some features that make this dye very useful for nucleic acids quantification [*Mao et al., 2007*]. A final volume of 20 µL of ddPCR reaction was prepared according to the manufacturer's protocol. Reaction mix was prepared adding Supermix for EvaGreen 2X [Bio-Rad, Hercules, California, USA], 20X MicroRNA LNA ™ PCR primer set (employed primers set and their ID are reported in the Table 15) [Exiqon, Qiagen, Vedbaek, Denmark] and 9 µL of 1:50 diluted cDNA. The mixture was loaded in suitable 96-wells plate [Eppendorf, Hamburg, Germany] and droplets were automatically generated using Automated droplets generator (AutoDG) [Bio-Rad, Hercules, California, USA], thanks to the employment of specific cartridges [DG32 Automated Droplet Generator Cartridges, Bio-Rad, Hercules, California, USA] which contain a microfluidic system able to generate nanoliter-volume droplets. Number of generated droplets generally, varies from 12.000 and 20.000 droplets for each reaction well. Only samples in which the number of generated droplets is higher than 10.000 have been taken in consideration and analysed. Generated emulsion was automatically transferred into a new 96-well PCR plate, which was sealed with an aluminium foil using PX1 PCR plate sealer [Bio-Rad, Hercules, California, USA]. Generated emulsion was then amplified using the following amplification programme: 95°C for 5 minutes to activate Taq-polymerase enzyme, 95°C for 30 seconds in order to denature double-strand DNA structure and 58°C for 1 minute to allow LNA primers annealing. Steps two and three were repeated for 40 cycles and ramp rate was set slower than 1.6°C/sec, in order to heat homogeneously the emulsion and to avoid droplets disruption. Others two steps were added: 4°C for 5 minutes to stabilized the emulsion, followed by a step at 90°C for 5 minutes to inactivate polymerase enzyme activity. Amplified droplets were analysed for the fluorescent content using QX200 Droplet Digital PCR system. Considering the number of positive (fluorescent) droplets respect to total generated droplets and applying Poisson Law, the absolute concentration of target miRNA was calculated. Data analysis was performed using QuantaSoft software, version 1.7.4 [Bio-Rad, Hercules, California, USA], which allows to determine sample absolute concentration.

miRNA	Assay ID
Hsa-miR-425-3p	204038
Hsa-miR-486-3p	339306
Cel-miR-39-3p	203952

Table 15. LNA based probe employed for miRNA quantification using ddPCR.

3.1.3.2 ddPCR miRNA analysis using TaqMan probes

TaqMan probes are generally, employed in RTqPCR for their high specificity and sensitivity, the same features are maintained also in ddPCR, where generally, the same miRNA assays employed in RTqPCR can be employed with some minor changes. Protocol for miRNA analysis using ddPCR is similar to that just described for EvaGreen chemistry, with some minor changes regarding sample dilution and amplification programme. An appropriate volume of cDNA was added to the ddPCR reaction mix. Starting input of cDNA generally, depends on types of biological sample and on miRNA expression levels, a) for cDNA obtained from cells or tissue samples starting cDNA was diluted 1:100 and 1,3 µL of diluted cDNA were loaded in ddPCR plate, while for supernatants and plasma samples derived from mouse models 1,3 µL of undiluted cDNA were employed. A further cDNA volume was employed for human plasma samples obtained from healthy donors or CRC patients. In this case 1,3 µL of undiluted cDNA were used for both miR-221-3p and miR-222-3p amplification, while when the very low expressed miR-141-3p, was analysed, 10 µL of undiluted cDNA were employed. cDNA was added to a ddPCR mix composed by ddPCR Supermix for probes (no dUTP) 2X [Bio-Rad, Hercules, California, USA], miRNA assay 20X [Applied Biosystems, Thermo Fischer Scientific, Waltham, Massachusetts, USA] and water until the final volume of 20 µL. The mixture was partitioned in thousands of droplets using AutoDG [Automated Droplets generator Bio-Rad, Hercules, California, USA] and the obtained water in oil emulsion was amplified using the following thermal cycler conditions: 95°C for 10 minutes to activate Taq polymerase enzyme, 40 cycles of 95°C for 15 seconds to denature cDNA double-strand structure and 60°C for 1 minute (ramp rate 2.5°C/sec) to allow primers annealing and elongation step, and a final step of 98°C for 10 minutes to inactivate the enzyme. Each droplet was investigated for its fluorescent content at the end of amplification programme, using QX200 Droplet Reader [Bio-Rad, Hercules, California,

USA], and data were analysed using QuantaSoft version 1.7.4 [Bio-Rad, Hercules, California, USA].

3.2 Microarray analysis

If PCR based method is the gold standard when a limited list of miRNAs needs to be analysed, when high number of miRNAs must be analysed microarray analysis is generally, more suitable. If fact, using the most recent miRNA array panels all miRNAs at moment registered in miRBase can be analysed. We employed this technique to identify miRNAs as possible markers for detection of ABT. In fact, in this case, we were not only interested in analysing a short list of selected miRNAs, but we needed to analyse all known miRNAs to verify their expression in our samples and to identify miRNAs which expression was modulated after ABT. At this porpoise, microarray miRNA detection technique seemed us the most suitable technique. 39 RNA samples were analysed for microRNA microarray profiling. All analysis were performed starting from 8 µL of each RNA sample extracted from ABT underwent athletes or control subjects. The global microRNAs profiling was performed using the Agilent Human microRNA microarray v.21.0 [Agilent Technologies, Palo Alto, CA, USA]. Labelled RNA was hybridized according to the manufacturer's procedure. This chip, consisting of 60-mer DNA probes, contains 15000 features, which represent 2549 microRNAs, sourced from miRBase database (Release 21). MiRNA labelling and hybridization were performed in accordance to manufacturer's indications. Microarray results were analysed using the GeneSpring GX 13 software [Agilent Technologies, Palo Alto, CA, USA]. Data transformation was applied to set all negative raw values at 1.0, followed by a quantile normalization. A filter on low gene expression was used to keep only the probes expressed in at least one sample. Differentially expressed miRNAs were selected by using fold-change analysis. All fold changes were calculated respect to the T1 (-40) time point which was taken as control. Both up-regulated and down-regulated miRNAs were considered at three different time points: T3 (-25), T6 (+3) and T8 (+15). Only miRNAs which at one of the previously indicated time points presented an absolute fold change upper than 1.5 were taken in consideration. Microarray analysis was performed by Microarray facility, LTTA (Laboratorio per le Tecnologie delle Terapie Avanzate), Ferrara University.

4. Cellular and animal models

4.1 Colorectal cancer cell lines

As model of CRC we employed three different cell lines kindly provided by PhD Patrizio Giacomini (IRE, Istituto Regina Elena, Roma, Italy). The human adenocarcinoma cell line HT-29, which are able to form a monolayer with tight junctions between cells and a typical apical brush border. Cells were isolated from a primary tumor of a 44 years old

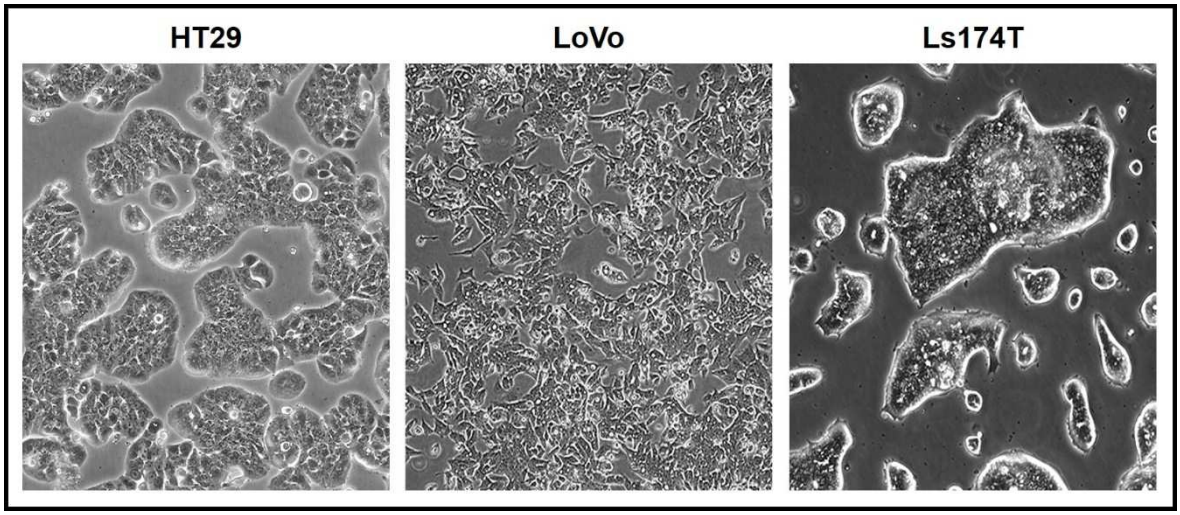

Figure 38. CRC cell lines. Three different CRC cell lines were employed as models: HT29, LoVo and Ls174T.

Caucasian female presenting Dukes'C primary tumor. HT-29 cell line presents the characteristics of mature intestinal cells, such as enterocytes or mucus producing cells [*Fogh et al., 1975*]. The epithelial cells LoVo that were isolated in 1971 from a fragment of a metastatic tumor nodule in the left supraclavicular region of a 56-year-old Caucasian male patient with a histologically proven diagnosis of Dukes' type C, grade IV, colorectal adenocarcinoma [*Drewinko et al., 1976*]. While Ls174T cells are epithelial cells isolated from a 58-year-old Caucasian female patient with a Dukes' type B, colorectal adenocarcinoma [*Tom et al., 1976*]. All three cell lines grown in adhesion and are cultured in RPMI 1640 with L-Glutammine [EuroClone, Pero, Milano, Italy], supplemented with penicillin 100 U/mL and streptomycin 100 mg/mL [Pen-Strep, Sigma-Aldrich, Saint Louis, Missouri, USA] and 10% fetal bovine serum [FBS, Biowest, Nuaillé, France] at 37°C in humidified atmosphere of 5% CO_2. Cells were refreshed twice a week, to obtain the detachment, cells are washed with DPBS 1X [Gibco, Thermo Fischer Scientific, Waltham, Massachusetts, USA], and treated with trypsin (0,05% trypsin and 0,02% EDTA) [Sigma-Aldrich, Saint Louis, Missouri, USA]. Cultures were tested for mycoplasma infection using

Cell line	KRAS	BRAF	PIK3CA	TP53
HT-29	/	V600E	P449T	R273H
LoVo	G13D; A14V	/		/
Ls174T	G12D	/	H1047R	/

Table 16. Principal genetic features of CRC employed cells. Taken from Ahamed et al., 2013**.**

Myco Alert Mycoplasma Detection Kit [Lonza, Basel, Switzerland] according to the manufacturer's protocol. For miRNA profile in cells and supernatants cells were cultured for 72 hours to confluence. Collected supernatants were centrifuged twice, firstly at 2000 g for 20 minutes, and then the collected supernatant was centrifuged again at 16000 g for 10 minutes, and immediately stored at -80°C in order to reproduce the same protocol used for plasma isolation.

4.2 Xenograft models

Xenotransplanted tumours were established by inoculating $5x10^6$ cells of HT-29, LoVo and LS174T human colorectal cancer cell lines in the flank of 4-month old Nu/CD1 mice [Charles River, Wilmington, Massachusetts, USA]. Tumours (two separate cohorts of three mice for each cell line) were allowed to grow to 0,5 cm^3 in size, and were taken at sacrifice along with blood. Animal studies were performed according to Directive 2010/63/EU and Italian Decree Law 26/2014. They were approved by the EU Research Executive Agency (REA), the Intramural Regina Elena Board for Animal Welfare, and the Italian Ministry of Health (prot n. 700-2015-PR, dated July 17, 2015). Xenograft models preparation was performed by PhD Elisa Tremante at IRE.

4.3 K562 cell line

Human leukaemia K562 cells *[Lozzio et al, 1975*] were cultured in Roswell Park Memorial Institute 1640 medium with 2mM L-Glutammine [RPMI-1640, EuroClone, Pero, Milano, Italy] supplemented with 10% fetal bovine serum [FBS, Biowest, Nuaillé, France],

100 units/mL penicillin and 100 mg/mL streptomycin [Pen-Strep, Sigma-Aldrich, Saint Louis, Missouri, USA]. Cells grown in suspension and are refreshed three times a week with a dilution 1:10 in new fresh medium. Cell cultures were tested routinely for mycoplasma infection using Myco Alert Mycoplasma Detection Kit [Lonza, Basel, Switzerland] according to the manufacturer's protocol. As it is possible to see in literature K562 are a very suitable model for study of compounds with erythroid differentiation activity.

4.4 K562 BCL11A clones

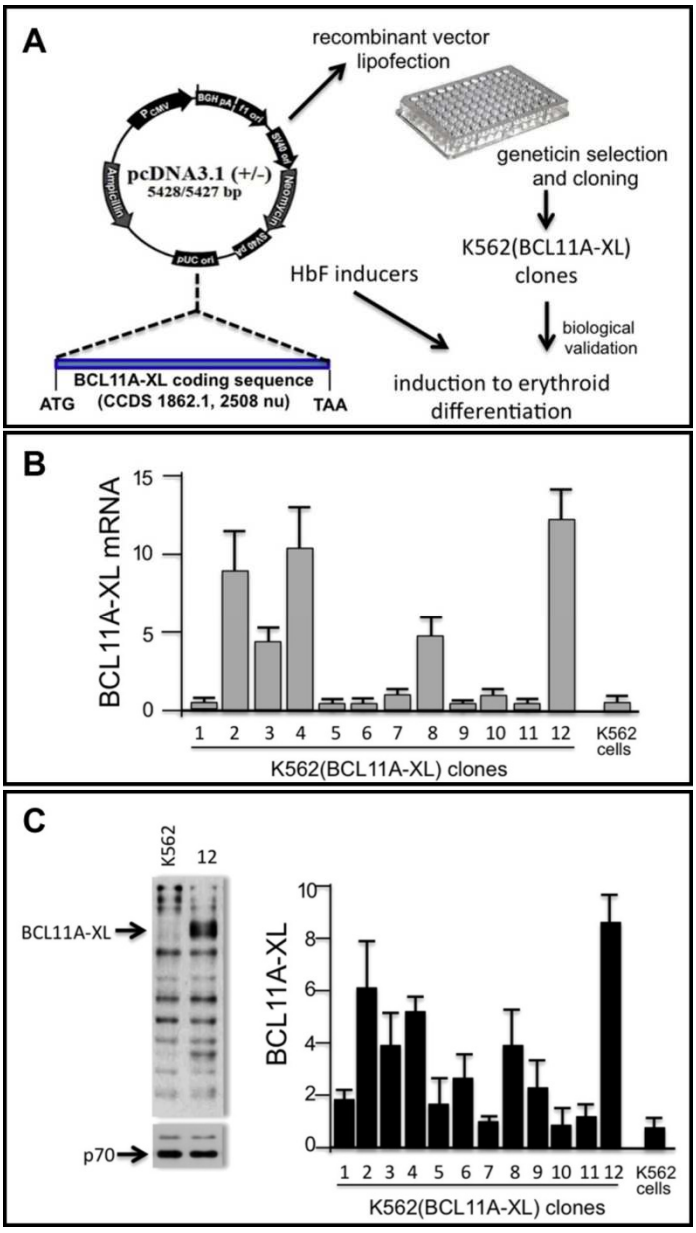

Figure 39. K562-BCL11A-XL clones characterization. Panel A, K562 cells were transfected with a vector containing BCL11A sequence and selected in G418. Clones were then characterized as regard mRNA expression (Panel B) and BCL11A protein expression (Panel C).

Despite K562 cells are well kwon models for identification and study of compound able to induce erythroid differentiation, they express at very low levels the transcription factor BCL11A-XL, which is one of the principal repressor of gamma globin gene expression. As well explained in Finotti et al., [*Finotti et al., 2015*] K562-BCL11A-XL clones were created to verify the activity of compounds, which are able to act directly in BCL11A expression. Briefly, K562 cells were transfected with pCDNA3.1-BCL11A-XL vector, cloned and positive cells were selected by limiting dilutions in the presence of geneticin [G418, Sigma-Aldrich, Saint Louis, Missouri, USA]. Twelve clones, expressing different levels of BCL11A transcript and protein were produced. All 12 clones were characterized for BCL11A transcript expression (RTqPCR) and protein production (western blot analysis). For data exposed in this thesis we employed K562-BCL11A-XL clone #12, which expresses at higher levels both BCL11A mRNA and protein. K562-BCL11A-XL clones are cultured in conditions very similar of K562 cells. A medium composed by RPMI-1640 with 2mM L-Glutammine [EuroClone, Pero, Milano, Italy], supplemented with penicillin 100 U/mL and streptomycin 100 mg/mL [Pen-Strep, Sigma-Aldrich, Saint Louis, Missouri, USA], 10% fetal bovine serum [FBS, Biowest, Nuaillé, France] and G418, final concentration 0,4 mg/mL [Sigma-Aldrich, Saint Louis, Missouri, USA] is employed. Cells are maintained at 37°C in humidified atmosphere of 5% CO2.

4.5 Erythroid Precursors Cells culture

ErPCs isolation from peripheral blood is carried out in two phases liquid medium, as well described by Fibach and colleagues [*Fibach et al., 2005*]. Generally, 18 mL of blood are collected, in tube containing lithium-heparin as anticoagulant [BD Vacutainer Heparin Blood Collection Tubes, BD Biosciences, San Jose, CA, USA], from β-thalassemia patients, before blood transfusion. Blood is diluted with DPBS 1X [Gibco, Thermo Fischer Scientific, Waltham, Massachussetts, USA] to the final volume of 40 mL and is stratified and centrifuged for density gradient on Lympholyte-H [NycogradeTM polysucrose 400 and sodium diatrizoate, Celbio, Milano, Italy]. Lympholyte-H creates a gradient of dextran and other substances to facilitate the separation of corpuscular parts of the blood. Centrifugation is performed at 2000g for 25 minutes at room temperature, without brake in order to avoid phase separation perturbation. After the centrifugation four separated layers can be distinguished, from top to bottom: a) plasma, b) a whitish ring containing lymphocytes, fibroblasts, macrophages and erythroid precursors, c) a cloudy part containing Lympholyte

with not separated cells and d) a red fund formed by red blood cells. The whitish ring is taken off, and washed three times with 1X DPBS. After each wash, to remove DPBS 1X, sample was centrifuged at 1200 rpm for 8 minutes at room temperature. At the end of washes, collected cells were resuspended in phase I medium, composed by: αMEM medium [α-minimal essential medium, Sigma-Aldrich, Saint Louis, Missouri, USA], 10% FBS [Biowest, Nuaillé, France], 10% conditioned medium (CM), obtained from cell cultures of bladder cancer which are rich in haematopoietic growth factors, 1 µg/mL cyclosporine A [Sigma-Aldrich, Saint Louis, Missouri, USA]. Culture was maintained at 37°C in humidified atmosphere of 5% CO2/air, for seven days. After 7 days of culture in phase I medium, not adherent cells were recovered, washed three times with DPBS 1X and resuspended with fresh medium of phase II, composed by α-MEM; 30% FBS; 10% deionized bovine serum albumin [BSA, Sigma-Aldrich, Saint Louis, Missouri, USA], 10 µM β-mercaptoethanol [Sigma-Aldrich, Saint Louis, Missouri, USA], 1 µM dexamethasone [Sigma-Aldrich, Saint Louis, Missouri, USA], 2 mM L-Glutamine [Sigma-Aldrich, Saint Louis, Missouri, USA], 1 U/mL human erythropoietin [EPO, Tebu-bio, Magenta, Milano, Italy], 10 ng/ml Stem Cell Factor [SCF, Gibco, Thermo Fischer Scientific, Waltham, Massachussetts, USA]. Cells were maintained in phase II medium for 7 days, before the treatment, which is performed in phase II medium. Before the treatment cells were counted using Z2 Coulter Counter [Beckman Coulter, Brea, California, USA]. The use of human material was approved by the ethics committee of the Ferrara District, Document No. 06/2013, approved on 20 June 2013. All peripheral blood samples were obtained after receiving written informed consent from patients or their legal representatives.

4.6 U251 cell line

U251 cell line was isolated more than 40 years ago from a male patient with astrocytoma [*Westermark et al., 1973*]. They are adherent cells, which are grown in RPMI-1640 with 2mM L-Glutammine, supplemented with penicillin 100 U/mL and streptomycin 100 mg/mL [Pen-Strep, Sigma-Aldrich, Saint Louis, Missouri, USA] and 10% fetal bovine serum [FBS, Biowest, Nuaillé, France] at 37°C in humidified atmosphere of 5% CO2. Cells were refreshed twice a week, with 1:5 dilution. To obtain cells detachment, cells are washed with DPBS 1X [Gibco, Thermo Fischer Scientific, Waltham, Massachusetts, USA], and treated with trypsin (0,05% trypsin and 0,02% EDTA) [Sigma-Aldrich, Saint Louis, Missouri, USA]. Cultures were tested routinely for mycoplasma infection using Myco Alert

Mycoplasma Detection Kit [Lonza, Basel, Switzerland] according to the manufacturer's protocol.

5. Employed compound and biological molecules

5.1 Mithramycin

Mithramycin (MTH) (cat n° M6891) was purchased from Sigma- Aldrich [Sigma-Aldrich, Saint Louis, Missouri, USA], as well described by Bianchi et colleagues [*Bianchi et al., 1999*] is a powerful inducer of erythroid differentiation in K562 cells and in erythroid precursors cells. MTH powder was resuspended, in sterile condition, in a solution of culture grade-water [Sigma-Aldrich, Saint Louis, Missouri, USA] and methanol (ratio 1:1) at stock concentration of 10 mM. Stocks are conserved at -20°C, protected from the light, because MTH is photo-sensible. At moment of the use, stock solution is diluted in culture grade-water, in order to obtain a solution at 10 µM concentration. Generally, both K562 and ErPCs are treated with MTH at final concentration of 20 or 30 nM. At the moment of treatment cells are counted and seeded at starting concentration of $5x10^4$ cells/mL in the case of K562 cells or their relative clones or $1x10^6$ cells for mL, in the case of ErPcs. Treatment effects were generally evaluated after 5 days of treatment.

5.2 PremiRNA and antimiRNA and mature miRNA molecules

PremiRNA and antimiRNA molecules were purchased from Ambion [Ambion, ThermoFischer Scientific, Waltham, Massachusetts, USA], while mature miRNAs were synthesized by IDT [Integrated DNA Technology, Coralville, Iowa, USA]. PremiRNA and antimiRNA molecules were resuspended at stock concentration of 100 µM in nuclease free water (provided with premiRNA or antimiRNA) and conserved at -80°C until the use. While, mature miRNAs were resuspended with nuclease free water [Sigma-Aldrich, Saint Louis, Missouri, USA] at stock concentration of 1 mM and maintained at -80°C until the moment of use.

Target miRNA	Catalog Number and ID
PremiR-210-3p	Cat. AM17100, ID PM10516
AntimiR-210-3p	Cat. AM17000, ID AM10516
AntimiR-221-3p	Cat. AM17000, ID AM10337
PremiR-124-3p	Cat. AM17100, ID PM10691
PremiR Negative Control	Cat. AM17010

Table 17. Employed premiRNA and AntimiRNA molecules.

MiRNA name	Sequence	Molecular Weight	Base pair
miR-210-3p	CUGUGCGUGUGACAGCGGCUGA	7089,3	22 bp
miR-221-3p	AGCUACAUUGUCUGCUGGGUUUC	7278,3	23 bp

Table 18. Employed mature miRNAs.

5.3 Peptide Nucleic Acids (PNA)

Peptide nucleic acids (PNA) employed for data presented in the thesis are synthetized from two different research groups.

5.3.1 PNA against miR-210 binding sequence in BCL11A coding region

PNA against miR-210 binding sequence, employed to reduce BCL11A transcription factor levels were kindly provided by Professor Alessandra Romanelli research group (Department of Pharmacy, University of Naples 'Federico II', Napoli, Italy). PNAs were resuspended in sterile water at final concentration of 500 µM and stored at -20°C until the moment of use. According to our previously experience with PNAs, for preliminary tests, we employed PNAs final concentration of 2, 4 and 8 µM. For short term treatment (48 hours) K562-BCL11A-XL clones were seeded at starting concentration of $1x10^5$ cells/mL, while for long term, MTH combined treatment, considering MTH toxicity, cells were seeded at concentration of $5x10^4$ cells/mL. ErPCs were seeded at concentration of $1x10^6$ cells/mL immediately before the treatment with PNAs. Both PNAs present a polyarginine peptide (R8) sequence that allows PNA cells internalization.

PNA	Sequence
PNA miR210-3p_like	H2N-ctgtgcgtgtgacagcggctgaRRRRRRRR-CONH2
PNA antiBCL11A miR210-3p_site	H-ctgtgcgtgttgcaagagaaaacRRRRRRRR-NH2

Table 19. Employed miRNAs targeting BCL11A sequence.

5.3.2 PNA against miR-221-3p

PNAs against miR-221-3p were purchased from Professor Roberto Corradini and co-workers (Department of Chemistry, University of Parma, Italy). All PNAs were resuspended in culture grade-water and employed at final concentration of 2 μM, as previously performed by Brognara and colleagues [*Brognara et al., 2014*]. Transfection procedure for PNAs without R8 peptide sequence is reported in the chapter transfection with ML122 and analogues.

PNA name	Sequence	Features
PNA F1	H-AAACCCAGCAGACAATGT-NH_2	PNA against miR-221 without R8 polypeptide.
PNA F2	Fl-AEEA-AAACCCAGCAGACAATGT-NH_2	PNA against miR-221 without R8 polypeptide and labelled with fluorescent molecule
PNA F3	H-RRRRRRRR-AAACCCAGCAGACAATGT-NH_2	PNA against miR-221 with R8 polypeptide.
PNA F4	Fl-AEEA-RRRRRRRR-AAACCCAGCAGACAATGT-NH_2	PNA against miR-221 with R8 polypeptide and fluorescence labelled.

Table 20. Employed PNA for transfection experiments. 5(6) carbossifluorescein was employed as fluorescent molecules, while AEEA (2-(2 aminoetoxy) etoxyacetyl) was employed as spacer.

5.4 ML122 and ML122 analogues

ML122 and ML122 analogues were synthesized and purchased from Professor Francesco Sansone (Department of Chemistry, University of Parma, Italy). Compounds synthesis protocol is well described by Bagnacani and colleagues [*Bagnacani et al., 2013*]. ML122 and analogues were resuspended in solution of water:ethanol [Sigma-Aldrich, Saint

Louis, Missouri, USA]:DMSO [dimethyl-sulfoxide, Sigma-Aldrich, Saint Louis, Missouri, USA] (2:2:1) in sterile condition, in order to reach the stock concentration of 400 µM and stored at -20°C until the moment of use.

6. Transfection procedures

Different transfection agents were employed to perform miRNA-based molecules transfection and each transfection agent require specific transfection condition, which are summarized in the following chapters.

6.1 Transfection using Lipofectamine RNAiMAX

Lipofectamine RNAiMAX [Invitrogen, ThermoFischer Scientific, Waltham, Massachusetts, USA] is a commercial available transfection agent composed by cationic-lipids and indicated for transfection of miRNA and siRNA molecules. Two different mixes of 50 µL, each one, were prepared. The first mix was composed by Lipofectamine RNAiMAX diluted in Opti-MEM I Reduced Serum medium [Gibco, ThermoFischer Scientific, Waltham, Massachusetts, USA] while the second was prepared diluting premiRNA or antimiRNA molecule in Opti-MEM I Reduced Serum medium [Gibco, ThermoFischer Scientific, Waltham, Massachusetts, USA]. Two mixtures were matched together and incubated at room temperature for 5 minutes, in order to allow the complexation between biological molecules and cationic lipids. The resulting 100 µL transfection mixture was transferred to cells.

6.2 Transfection using Lipofectamine LTX with Plus Reagent

Lipofectamine LTX is a lipid-based transfection agent suitable for plasmid transfection. Even in this case two separate mixes were prepared: the first one was composed by Lipofectamine LTX [Invitrogen, ThermoFischer Scientific, Waltham, Massachusetts, USA] diluted in Opti-MEM I Reduced Serum medium [Gibco, ThermoFischer Scientific, Waltham, Massachusetts, USA], while in the second, premiRNA or antimiRNA molecule, and an optimised volume of Plus Reagent and Opti-MEM I Reduced Serum medium were added to the final volume of 50 µL. The second mixture, containing premiRNA molecule and Plus Reagent was incubated at room temperature for 5 minutes, and at the end of

incubation, the first mix, containing Lipofectamine LTX diluted in OptiMEM medium was added. The resulting final mixture was incubated at room temperature for 30 minutes, in order to allow complexation between nucleic acids and liposomes, and transferred to cells.

6.3 Transfection using siPORT NeoFX

siPORT NeoFX is a lipid-based transfection agent, used for siRNA and miRNA transfection. siPORT NeoFX [Ambion, ThermoFischer Scientific, Waltham, Massachusetts, USA] was diluted at final volume of 25 µL in Opti-MEM I Reduced Serum medium [Gibco, ThermoFischer Scientific, Waltham, Massachusetts, USA], at same way, also premiRNA molecules where diluted at final volume of 25 µL. Two mixtures have been matched, the resulting final mixture have been incubated 10 minutes at room temperature and finally, transferred to cells.

6.4 Transfection using ML122 or analogues

Two different protocols were employed to transfect miRNA-based molecules or PNA with ML122. Firstly, a protocol very similar to that proposed for DNA transfection in Bagnacani et al. [*Bagnacani et al., 2013*] was employed. This protocol, which was called short term transfection protocol, is not very suitable for *in vivo* treatment, in fact, contemplate the removal of transfection mixture after 5 hours contact with cells. A second protocol has been developed by our research group, and in this case lower concentration of transfection agent was employed, but the transfection mixture was maintained in contact with cells, until the end of treatment. This second protocol, in our opinion, is more suitable for *in vivo* treatment, where the removal of transfection mixture is not possible. This second protocol was called continuous contact protocol.

6.4.1 Short term transfection protocol

In short term transfection protocol, a mixture containing RPMI-1640 medium [EuroClone, Pero, Milano, Italy], ML122 or analogues at 10 µM final concentration, and the biological molecule which needs to be transferred into cells (mature miRNA, PremiRNA, AntimiRNA or PNA) was prepared and incubated for 20 minutes at room temperature, without serum, to allow the complexation between transfection agent and biological

molecules. After the incubation at 450 µL of transfection mixture, were added 50 µL of FBS [Biowest, Nuaillé, France]. Cell culture medium was removed and replaced with the transfection mixture, which was maintained in contact with cells for 5 hours in a humidified atmosphere of 5% CO_2/air at 37°C. At the end of 5 hours incubation, transfection mixture was removed, cells were washed with DPBS 1X [Gibco, ThermoFischer Scientific, Waltham, Massachusetts, USA] and new fresh medium was added.

6.4.2 Continuous contact protocol

In the continuous contact protocol, a mixture containing RPMI-1640 medium [EuroClone, Pero, Milano, Italy], ML122 or analogues at 2,5 µM final concentration, and the biological molecule which needs to be transferred into cells (PremiRNA, AntimiRNA or PNA) was prepared and incubated for 20 minutes at room temperature, without serum, to allow the complexation between transfection agent and biological molecules. After the incubation at 450 µL of transfection mixture, were added 50 µL of FBS [Biowest, Nuaillé, France]. Cell culture medium was removed and replaced with the transfection mixture, which was maintained in contact with cells until the end of the treatment. Cells were maintained in a humidified atmosphere of 5% CO_2/air at 37°C for all the treatment time.

7. mRNA expression analysis

mRNA expression was analysed using Reverse Transcription quantitative Polymerase Chain Reaction (RTqPCR). Briefly, RNA obtained after RNA extraction was reverse transcribed to a complementary DNA (cDNA) using a MMLV (Moloney Murine Leukemia Virus) reverse transcriptase enzyme and oligonucleotides with random sequences (random examers) as reverse transcription primers. The obtained cDNA was then used as template for RTqPCR.

7.1 mRNA Reverse transcription reaction

Reverse transcription reaction was performed using TaqMan Reverse Transcription Reagents [Applied Biosystems, ThermoFischer Scientific, Waltham, Massachusetts, USA]. A mixture containing 300 ng of total RNA and nuclease free water [Sigma-Aldrich, Saint Louis, Missouri, USA] was heated at 60°C for 5 minutes to disrupt RNA secondary structure.

After the incubation, sample was put immediately on ice and RNAse inhibitor enzyme was added at final concentration of 0,4 U/µL. Moreover, reverse transcriptase enzyme to synthesize cDNA requires the presence of primers able to bind mRNA template. At this purpose, we have chosen short sequences composed by six nucleotides called random examers, which can potentially anneal to all RNA sequences present in the sample and can also recognise sequence in degraded RNA. Random examers were added to the reverse transcription reaction mix at final concentration of 2,5 µM, and the mixture was incubated 10 minutes at 20°C to allow primers annealing. At the end of primer annealing step, others reagents necessary for reverse transcription reaction were added, including: dNTPs at final concentration of 2 mM, MgCl (magnesium chloride) 5,5 mM, RT Buffer 1X and MultiScribe Reverse Transcriptase 1,25 U/µL. The mixture was incubated at 42°C for 30 minutes to allow mRNA reverse transcription, followed by a step at 98°C for 5 minutes to inactivate reverse transcriptase enzyme. Obtained cDNA was stored at -80°C until RTqPCR was performed.

7.2 mRNA quantification using RTqPCR

Quantification of mRNA using RTqPCR can be obtained using different fluorescent labelling techniques. To quantify our transcripts, we employed the two most common techniques: TaqMan probes and Sybr Green.

7.2.1 RTqPCR using TaqMan probes

Each TaqMan probe-based assay is composed by a couple of primers specific for the target of interest, a primer forward (FW), a primer reverse (RW) and a probe, which is a oligonucleotide containing at the 5' end a fluorescent reporter at the 5' end, and a quencher in 3' end. Probe binds a sequence in the region between primer FW and primer RW. When the probe sequence is intact, the fluorescence of the reporter is quenched due to its proximity to the quencher. During the annealing and extension step of the amplification reaction, the probe hybridizes to the target, but the exonuclease activity of DNA polymerase enzyme cleaves the reporter. In this way, reporter is separated by the quencher and its fluorescence is no more quenched. This result in an emission of fluorescence that is directly proportional to the amount of amplified product in reaction well. In real time PCR, emission of fluorescence is measured at the end of each cycle and values are collected in a graphical

representation called amplification curve. All RT-PCR assay employed in this thesis are reported in Table 21. Briefly a PCR reaction mix composed by 1µL of cDNA, 1,25µL of 20X TaqMan assay for the transcript of the interest, 12,5 µL of TaqMan Universal PCR Master Mix 2X [Applied Biosystems, ThermoFischer Scientific, Waltham, Massachusetts, USA], and nuclease free water [Sigma-Aldrich, Saint Louis, Missouri, USA] at final volume of 25 µL was prepared. Each sample was prepared and loaded in duplicate. Amplification programme consists of an initial step at 50°C for 2 minutes, in which AmpErase UNG enzyme acts degrading all possible PCR contamination containing dUTP, followed by a step at 95°C for 10 minutes to activate DNA polymerase enzyme, and 45 cycles in which sample is heated at 95°C for 15 seconds to denature double-strand structure, followed by a step at 60°C for 1 minute in which primers annealing and extension phase occurred. At the end of each cycle, fluorescence is measured. Amplification programme was performed using CFX96 [Bio-Rad, Hercules, California, USA] and data analysis was performed using Bio-Rad CFX Manager Software [Bio-Rad, Hercules, California, USA]. Relative expression was calculated and fold change analysis was performed using Livak method [Livak et al., 2011] (2^-ΔΔCT). All data were normalised for their starting cDNA content using as reference RPL13A and 18s.

Target Name	**Company**	**Assay ID**
B-Cell lymphoma/leukemia 11A (BCL11A)[a]	Applied Biosystems	Hs00256254_m1
B-Cell lymphoma/leukemia 11A (BCL11A)[b]	Applied Biosystems	Hs00250581_s1
γ-globin	IDT	Custom assay
TP53	IDT	Hs.PT58.123122
Caspase 3	IDT	Hs.PT56a.24277143
Ribosomal protein L13a (RPL13A)	Applied Biosystems	Hs03043885_g1
18S ribosomal RNA	Applied Biosystems	4310893E

Table 21. Employed TaqMan assay.

7.2.2 RTqPCR using Sybr Green

Sybr Green is a DNA-binding dye, able to bind non-specifically all double strand sequences. Unbounded Syber Green present low background fluorescence, but when it binds double-strand sequences its fluorescence increases of about 1000 fold. So, in this case emitted fluorescence is directly proportional to the amount of double strand product and

consequently to the quantity of amplified target. Syber Green can be used with any couple of unlabelled primers. RTqPCR reaction mix is composed by 1µL of cDNA, 4 µL of each primer (50 ng/µL), 12,5 µL of iTaq Universal SYBR Green Supermix 2X [Bio-Rad, Hercules, California, USA] and nuclease free water [Sigma-Aldrich, Saint Louis, Missouri, USA] at final volume of 25 µL. Each sample was prepared and loaded in duplicate. The following amplification programme was performed: 3 minutes at 95°C to activate DNA polymerase enzyme, 40 cycles of 95°C for 15 seconds to denature double strand structure, 58°C for 30 seconds to allow primers annealing followed by 30 seconds at 72°C for the extension phase. At the end of the amplification, a melting curve from 55°C to 95°C with 0,5°C/sec increment was performed to verify the presence of non-specific products, as primer dimers. Amplification programme was performed using CFX96 [Bio-Rad, Hercules, California, USA] and data analysis was performed using Bio-Rad CFX Manager Software [Bio-Rad, Hercules, California, USA]. Relative expression was calculated and fold change analysis was performed using Livak method [Livak et al., 2011] (2^-ΔΔCT). All data were normalised for their starting cDNA content using as reference RPL13A and 18s.

Target	Primer FW sequence	Primer RW sequence
Interleukin 6 (IL_6)	5'-AGGAGACTTGCCTGGTGAAA-3'	5'-CAGGGGTGGTTTATTGCATCT-3'
Ribosomal protein L13a (RPL13A)	5'-ACGCTGTGAAGGCATCAACATT-3'	5'-GCTGTCACTGCCTGGTACTTCC-3'
18S ribosomal RNA subunit	5'-CGAACGTCTGCCCTATCAACTTT-3'	5'-GCTGTCACTGCCTGGTACTTCC-3'

Table 22. Primers employed for Sybr Green RTqPCR.

8. Benzidine staining assay

Haemoglobin containing cells were detected by specific reaction with a benzidine/hydrogen peroxide solution containing 0,2% benzidine dihydrochloride [Sigma-Aldrich, Saint Louis, Missouri, USA] in 5 M glacial acetic acid [Sigma-Aldrich, Saint Louis, Missouri, USA], activated, immediately before the use with 10% (v/v) of a solution 30% H_2O_2 [Sigma-Aldrich, Saint Louis, Missouri, USA]. 5µL of culture medium containing cells were added to 5 µL of benzidine-H_2O_2 solution, cells were observed at microscope and

$$H_2O_2 + \text{Chromogen} \xrightarrow[\text{Peroxidase Activity}]{\text{Haemoglobin}} H_2O + \underset{\text{(Blue color)}}{\text{Oxidized Chromogen}}$$

benzidine reactive cells, which were blue coloured, were counted. Data are expressed as benzidine positive cells (blue cells) respect to total number of cells (blue and colourless cells). Test is based on the peroxidase activity of heme group contained in haemoglobin. In fact the peroxidase activity of heme group caused H_2O_2 reduction and at same time the chromogen (benzidine) oxidation resulting in blue colour as indicated in the reaction proposed at page 142.

9. SPR-based Analysis

All procedures were performed at 25°C and at a 5 µL/min flow rate, by using the Biacore™ X100 analytical system [GE Healthcare, Chicago, Illinois, USA] and HBS-EP+ (0,01 M HEPES, 0,15 M NaCl, 3 mM EDTA and 0,05% v/v Surfactant P20, pH 7,4) as running buffer as previously described. In order to obtain an efficient capture of 5'-biotinylated oligonucleotide mimicking the miR-210 binding site of BCL11A mRNA onto the sensor chip, the well documented streptavidin-biotin interaction was employed. To this aim, the sensor chip SA, precoated with streptavidin, was used. After pre-treatment with three 10 µL pulses with 50 mM NaOH-1 M NaCl, an injection of 10 ng/µL biotinylated oligonucleotide carrying sequences mimicking the miR-210 binding site of the BCL11A mRNA [IDT Integrated DNA Technologies, Coralville, IA, USA] was performed, followed by a wash with 50 mM NaOH. Hybridization to the immobilized oligonucleotide was performed by a 20 µL injection of 2,3 µM microRNA (miR-210-3p, miR-221-3p, miR-222-3p) [IDT Integrated DNA Technologies, Coralville, IA, USA], followed by a wash with 15 µL HBS-EP+ buffer and a regeneration of the sensor chip with a 5 µL pulse of 50 mM NaOH. The BiacoreTM X100 Control Software and BiacoreTM X100 Evaluation Software, version 2.0.1 [GE Healthcare, Chicago, Illinois, USA] were used for operation and data analysis, respectively. Suitable blank control injections with running buffer were performed, and the

Name	Sequence 5'- 3'	Accession No.	Location
BCL11A	biot-GTT TCT CTT GCA ACA CGC ACA G	NM_022893.3	789-798
DNA aBCL11A	CTG TGC GTG TTG CAA GAG AAA C	NM_022893.3	789-798
RNA aBCL11A	CUG UGC GUG UUG CAA GAG AAA C	NM_022893.3	789-798
miR-210	CUG UGC GUG UGA CAG CGG CUG A	MIMAT0000267	-
miR-221	AGC UAC AUU GUC UGC UGG GUU UC	MIMAT0000278	-
miR-222	AGC UAC AUC UGG CUA CUG GGU	MIMAT0000279	-

Table 23. Oligonucleotides sequences used in Biospecific Interaction Analysis

resulting sensorgrams were subtracted from the experimental sensorgrams. All Biacore experiments were performed under the supervision and with the precious help of PhD Giulia Breveglieri (Life Science and Biotechnology Department, University of Ferrara).

10. Western Blot analysis

10.1 Protein extracts preparation

Protein extracts analyzed by western blotting analysis were prepared using commercial RIPA buffer according to manufacturer's instruction. Briefly, cells were washed with cold DPBS 1X [Gibco, Thermo Fischer Scientific, Waltham, Massachussetts, USA] and centrifuged at 1200 rpm for 10 minutes at 4°C. Obtained pellet was suspended and lysed using RIPA Lysis and Extraction Buffer [Thermo Scientific, Thermo Fischer Scientific, Waltham, Massachussetts, USA], maintaining the ratio 1 mL of RIPA Lysis and Extraction Buffer for $1x10^6$ cells. Samples were incubated 20 minutes of ice, and then centrifuged at 14000 g for 15 minutes at 4°C, to remove cell debris. Supernatant, containing protein extracts was collected and stored at -80°C until the moment of western blot analysis.

10.2 Protein extracts quantification

Obtained protein extracts were quantified using Pierce BCA Protein Assay Kit [Thermo Scientific, Thermo Fischer Scientific, Waltham, Massachussetts, USA], according to the manufacturer's instruction. BCA Protein Assay is a colorimetric assay based on the reduction of Cu^{2+} to Cu^{1+} by proteins in an alkaline medium. According to Biuret reaction, copper reduction is caused by four amino acid residues: cysteine, cystine, tyrosine, and tryptophan normally present in proteins. Reduced copper forms complexes, composed by a Cu^{+} chelated with two molecules of bicinchoninic acid (BCA). Complexes, which are purple-colored, adsorbed at 562 nm and absorbance values are directly proportional to proteins concentration. Protein extracts concentration is calculated by a standard curve created using known concentration of albumin protein. Standard curve was created adding incremental amount (from 1,25 µg to 40 µg) of albumin starting from an albumin solution which stock concentration is 2 mg/ml. Two µL of protein extracts were quantified for each sample. Both standard curve samples and unknown samples were added to 1 mL of working solution composed by Reagent A (bicinchoninic acid 0,1M) and Reagent B (Cupric sulfate 4%) in ratio 50:1. Samples were incubated at 60°C for 30 minutes to enhance reaction, and

the absorbance at 562 nm was read using SmartSpec Plus Spectrophotometer [Bio-Rad, Hercules, California, USA].

10.3 Western blotting

A mixture composed by 20 µg of protein total extracts, 1/3 of the final volume of 3X Reducing SDS Loading Buffer [Cell Signaling Technology, Leiden, Netherlands], and 1/30 of 1,25 M dithiothreitol (DTT) [Cell Signaling Technology, Leiden, Netherlands] was prepared. In order to destroy protein secondary structure, samples were denatured for 5 minutes at 98°C and then put immediately on ice until they were loaded on SDS–polyacrylamide gel. Running gel was composed by acrylamide 7% [40% Acrylamide/Bis Solution, Bio-Rad, Hercules, California, USA], Tris-HCl pH 8.8, final concentration 375 mM, SDS (Sodium Dodecyl Sulfate) 0,1%, Temed [Bio-Rad, Hercules, California, USA] and AMPS (Ammonium persulfate) 0,625 ng/µL, while stacking gel was prepared with 4% acrylamide [40% Acrylamide/Bis Solution, Bio-Rad, Hercules, California, USA], Tris-HCl pH 6.8, final concentration 125 mM, SDS (Sodium Dodecyl Sulfate) 0,1%, Temed [Bio-Rad, Hercules, California, USA] and AMPS (Ammonium persulfate) 1,3 ng/µL. Before stacking gel polymerization, 1 mm wells combs were added to form wells. Samples and 10 µL of Precision Plus Protein WesternC Standards (size range: 10–250 kDa) [Bio-Rad, Hercules, California, USA] as marker to determine molecular weight, were loaded. Migration was performed at 200V for 45 minutes using Tris–glycine buffer (25 mM Tris, 192 mM glycine, 0,1% SDS) [Bio-Rad, Hercules, California, USA] in order to separate proteins, according to their molecular weight. Separated proteins were transferred into a 0,2 µm nitrocellulose membrane [Thermo Scientific, Thermo Fischer Scientific, Waltham, Massachussetts, USA] using Trans-Blot Electrophoretic Transfer Cell [Bio-Rad, Hercules, California, USA]. The electrophoretic transfer was performed at 360 mA, over night, at 4°C, using CAPS Buffer (10 mM 3-(cyclohexylamino)-1-propanesulfonic acid, 10% methanol pH 11). The day after, protein transfer was verified using Ponceu S solution, then membrane was decoloured washing three times with TBS-T 1X (Tris-buffered saline, 0,1% Tween 20). Obtained membrane was incubated in blocking Buffer (5% non-fat dry milk in TBST-1X) for 1 hour, to prevent the nonspecific binding of the antibodies. After the incubation membrane was washed three times with TBS-T 1X and probed with BCL11A primary rabbit monoclonal antibody (1:10.000) [Cat. Ab191402, AbCam, Cambridge, UK] in a solution of 5% BSA (Bovine Serum Albumin). The day after membrane was washed three times with

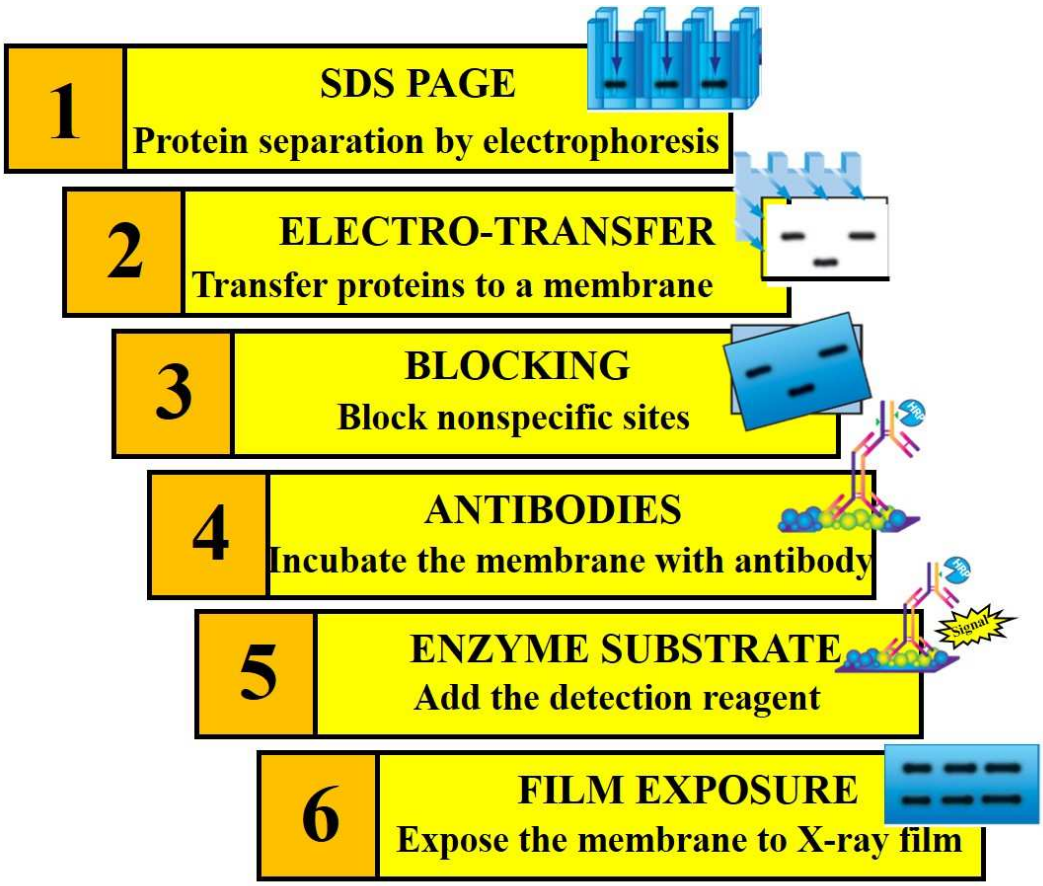

Figure 40. Principal steps of western blotting analysis. Protein extracts were loaded into a SDS polyacrylamide page and separated according to their molecular weight, proteins are transferred in a nitrocellulose membrane, which was probed firstly with a primary antibody and then with an appropriate secondary HRP conjugated antibody. Membrane was treated with a HRP substrate and exposed to X-Ray film.

TBS-T 1X and incubated for an hour with an appropriate HRP-conjugated secondary antibody (1:2000) [Goat Anti-Rabbit Igg HRP conjugated Cat. 7074P3, Cell Signaling Technology, Leiden, Netherlands] and Precision Protein StrepTactin-HRP conjugate (1:10000) [Bio-Rad, Hercules, California, USA], used to detect protein marker. Membrane was washed three times with TBS-T 1X and incubated 5 minutes, protected from the light with the substrate that allow luminescence emission: Phototope-HRP Western Blot Detection System [Cell Signaling Technology, Leiden, Netherlands]. HRP (Horseradish peroxidase) enzyme conjugated at the secondary antibody catalyses the oxidation of luminol, contained in the detection solution, that results in emission of light which is captured in ECL film [GE Healthcare, Little Chalfont, UK] and is directly proportional to the amount of target protein in samples. The same membrane was stripped, to remove the previously bounded antibody, using Restore Western Blot Stripping Buffer [Thermo Scientific, Thermo Fischer Scientific, Waltham, Massachussetts, USA]. Membrane was incubated 1 hour with 30 mL of Stripping Buffer and then, washed three times with TBS-T 1X. After a 1 hour incubation with blocking buffer and three washings with TBS-T 1X, membrane was re-probed with the

primary antibody against p70S6K [Catalog No. 2708, Cell Signaling, Leiden, Netherlands], used as normalization control. Films obtained with both antibodies BCL11A and p70, were analysed using ChemiDoc MP System [Bio-Rad, Hercules, California, USA] and Image Lab software [Bio-Rad, Hercules, California, USA]. The ratio between BCL11A band intensity and p70 band intensity was calculated for each sample.

11. Elisa Analysis

Elisa (Enzyme-Linked Immunosorbent Assay) is an assay designed to detect and quantify proteins or peptides. For our analysis we employed a sandwich direct Elisa method. In this case antigen capture is made possible thanks to the employment of a capture antibody which has been attached to the plate. Detection of antigen is possible thanks to the employment of a primary HRP- conjugated antibody, which binds the antigen and at same time interacts to the substrate to produce a measureable signal.

11.1 Protein extracts preparation

ErPCs were washed twice with cold DPBS X [Gibco, Thermo Fischer Scientific, Waltham, Massachussetts, USA] and centrifuged at 1200 rpm for 10 minutes at 4°C to obtain cellular pellet which was resuspended using cold water to lyse cells using the ratio 1 µL of water for $5x10^5$ cells. Samples were frozen in dry ice for 5 minutes and then thaw at room temperature. Freeze and thaw cycles were repeated for 5 times, then samples were centrifuged at 14000g for 10 minutes to remove cell debris. Supernatants, containing protein extracts, were collected and stored at -80°C.

11.2 Gamma globin quantification using Elisa assay

Analysis of gamma globin protein content was performed using Human Hemoglobin Gamma 1 (HBγ1) ELISA Kit [MyBioSource, San Diego, California, USA]. Elisa analysis was performed according to manufacturer's instruction. Protein extracts were diluted 1:50 in apposite sample diluent, purchased by the kit, and loaded in pre-coated wells. At same way, also samples with a known concentration of gamma haemoglobin were loaded to create a standard curve. 100 µL of HRP-conjugate reagent were loaded to each well, and plate was incubated at 37°C for 1 hour. At the end of incubation plate was manually washed four times with Wash Solution 1X. 50 µL of chromogen solution A and 50 µL of chromogen solution

B were added to each well and plate was incubated at 37°C for 15 minutes, protected from the light. 50 µL of Stop Solution was added to each well and absorbance at 450 nm was read using Sunrise plate reader [Tecan, Männedorf, Switzerland] and data were analysed using Xflour4 software [Tecan, Männedorf, Switzerland].

12. FACS analysis

FACS analysis is a particularly useful tool, that allow to obtain several information about the morphology and the fluorescence emitted by cells. Cells pass through a narrow channel one by one and are illuminated by a light. A series of sensors detect the types of light that is refracted or emitted from the cells and the optical data are transformed in electrical data and finally in a picture. In particular, three different parameters are considered: FSC (Forward scattered light) which is typically used to identify particle size, SSC (Side scattered light) used to obtain information about granularity and complexity of cells and fluorescent light emitted after excitation by a compatible wavelength laser. Fluorescence can derive from different sources: fluorescent molecules internalised by cells, or fluorescence-tagged antibodies that have been used to label a specific target in the cell.

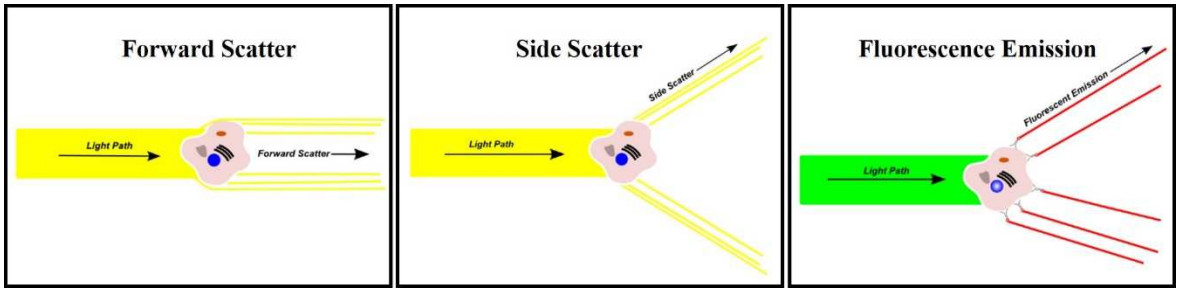

Figure 41. Principal parameters considered in FACS analysis. FSC gives information about cell size, SSC gives information about cell complexity. Fluorescence can derive from different sources, fluorescent molecules internalization, or by the use of fluorescent labelled antibody able to bind proteins expressed in cell's surface.

12.1 FACS analysis using fluorescent antibody

The erythroid differentiation status of ErPCs transfected with premiR-210 was investigated studying Transferrin Receptor (trfR) and Glycophorin A (GYPA) expression by FACS analysis. Cells were washed twice with DPBS 1X [Gibco, Thermo Fischer Scientific, Waltham, Massachussetts, USA], centrifuged at 1200 rpm for 8 minutes to remove supernatant and cellular pellet was resuspended with 50 µL of DPBS 1X [Gibco, Thermo Fischer Scientific, Waltham, Massachussetts, USA] additioned with 1% FBS [Biowest,

Nuaillé, France]. Two labelled antibodies were added: anti-human CD71 FITC-conjugated antibody [Miltenyi Biotec, Bergisch Gladbach, Germany] and anti-human CD235a (Glycophorin A) antibody PE-conjugated [Miltenyi Biotec, Bergisch Gladbach, Germany]. According to the manufacturer's protocol 10 µL of each antibody were added and cells were incubated on ice for 30 minutes. Cells were washed twice DPBS 1X [Gibco, Thermo Fischer Scientific, Waltham, Massachussetts, USA], resuspended in 200 µL of DPBS 1X [Gibco, Thermo Fischer Scientific, Waltham, Massachussetts, USA] and analysed using BD FACS Canto II [BD, Becton Dickinson, Franklin Lakes, New Jersey, USA]. Data analysis was performed using BD FACSDIVA software [BD, Becton Dickinson, Franklin Lakes, New Jersey, USA].

12.2 FACS analysis for fluorescent molecules internalization

Up-take of fluorescent PNAs or miRNAs was evaluated using FACS analysis. Cells were collected, washed twice with DPBS 1X [Gibco, Thermo Fischer Scientific, Waltham, Massachussetts, USA], cells were pelleted at 1200 rpm for 8 minutes at room temperature and supernatant was discarded. Cellular pellets were resuspended in 150 µL of DPBS 1X [Gibco, Thermo Fischer Scientific, Waltham, Massachussetts, USA] and analysed by FACS analysis for FITC (Fluorescein IsoThioCyanate) fluorescence. For each sample 30.000 events were acquired using FACScan or FACS Canto II [BD, Becton Dickinson, Franklin Lakes, New Jersey, USA] and data analysis was performed using CellQuest Pro or BD FACSDIVA software [BD, Becton Dickinson, Franklin Lakes, New Jersey, USA].

13. Cell imaging acquisition using BioStation®

Cell internalization of fluorescent molecules was evaluated using BioStation IM [Nikon, Minato, Tokyo, Japan] a system that allow to monitor cells, maintaining them in their physiological condition. Thanks to the employment of cell incubator and a monitoring system is possible to evaluate cellular features as morphology or cell growth for long time laps. Three different magnifications can be employed x20, x40 and x80. Cells were seeded in a suitable BioStation plate and treated with the opportune fluorescent molecules. Until image recording, cells were pre-treated with Hoesct 33342 dye [Thermo Scientific, Thermo Fischer Scientific, Waltham, Massachussetts, USA], which is able to stain DNA and consequently allow to identify nucleus position into cells. Briefly, medium was removed,

cells were washed with DPBS 1X [Gibco, Thermo Fischer Scientific, Waltham, Massachussetts, USA] and incubated with a solution containing culture medium and Hoesct 33342 [Thermo Scientific, Thermo Fischer Scientific, Waltham, Massachussetts, USA] at final concentration of 1 µg/mL. Cells were incubated at 37°C for 20 minutes, protected from the light. Staining solution was removed, cells were washed twice with DPBS 1X [Gibco, Thermo Fischer Scientific, Waltham, Massachussetts, USA] and fresh medium was added. Cells images were taken for 24 hours using DAPI filter (461 nm) to visualize nuclei and 530 nm filter to visualise FITC conjugate molecules.

14. Cell viability Assay

Cell viability after the transfection with calixarene-based molecules was evaluated with Muse Count & Viability Kit [Millipore, Billerica, Massachusetts, USA], using Muse Cell Analyser [Millipore, Billerica, Massachusetts, USA]. Test allow to discriminate between alive and dead cells on the base of their membrane permeability to two DNA binding dyes. The first dye is used to discriminate viable cells, which do not stain, from non-viable cells, which are stained. Instead, the second reagent stains all cells with a nucleus, in order to distinguish cells from debris. To perform analysis, 50 µL of suspension cells were added to 225 µL of Muse Count & Viability Reagent, the solution was incubated at room temperature for 5 minutes, protected from the light and then $1x10^3$ events were analysed using Muse Cell Analyser [Millipore, Billerica, Massachusetts, USA].

15. Evaluation of apoptotic rate

The possibility that calixarene-based delivery molecules may induce apoptosis in cells, was investigated using Muse Annexin V & Dead Cell Kit. One of the first steps of apoptosis pathway is the externalization of phosphatidylserine (PS) to the cell surface. The assay is based on the use of two different reagents: annexin V, which binds PS and 7-AAD (7-aminoactinomycin D) a fluorescent DNA intercalator. In this way is possible to identify four different populations: cells negative to both reagents (live cells), cells positive to annexin V, but negative to 7-AAD (early apoptotic cells), cells negative to annexin V and positive to 7-ADD (cellular debris) and cells positive to both reagents (late apoptotic cells). 50 µL of suspension cells were added to 50 µL of Muse Annexin V & Dead Cell reagent, sample was gently mixed and incubated at room temperature, protected from the light for 15

minutes. Samples were analysed using Muse Cell Analyser [Millipore, Billerica, Massachusetts, USA].

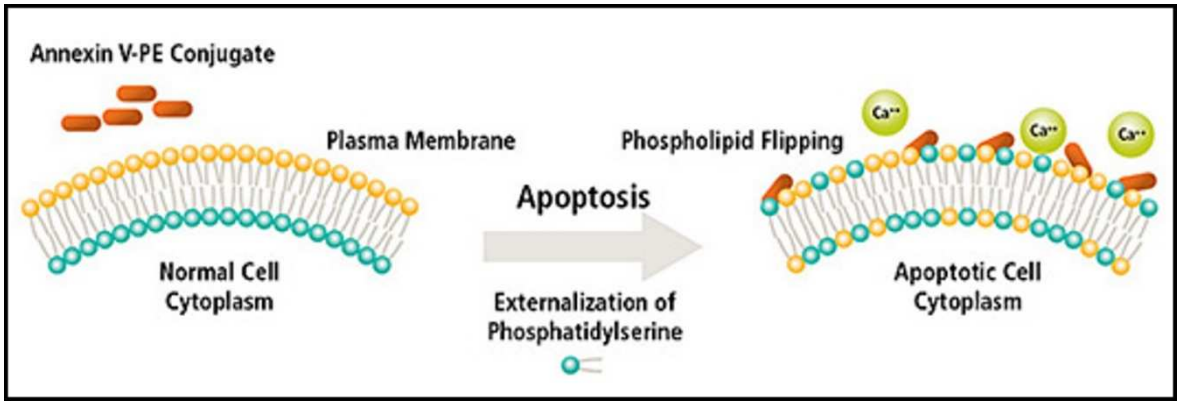

Figure 42. Annexin V in apoptosis signal. Phosphatidylserine (PS) is normally located on the cytoplasmic face of the plasma membrane. During apoptosis PS translocates to the outer leaflet of the plasma membrane. PS is bound by fluorochrome-labeled Annexin V in presence of calcium.

16. Bioplex analysis

Cytokines release in supernatants after transfection with calixarene-based molecules was evaluated considering U251 cell line. Cytokines quantification was performed using Bio-Plex cytokine assay [Bio-Rad, Hercules, California, USA] according to the manufacturer's instruction. In our experiments, we used the premixed multiplex beads of the Bio-Plex human cytokine Human 27-Plex Panel [Cat. 171-A11127, Bio-Rad, Hercules, California, USA], which included twenty-seven cytokines (IL-1b; IL-1ras, IL-2, IL-4, Il-5, IL-6, IL-7, IL-8, IL-9, IL-10, IL-10, IL-12 (P70), IL-13, IL-15, IL-17, Basic FGF, Eotaxin, G-CSF, GM-CSF, IFN-γ, IP-10, MCP-1, IP -1 (MCAF), MIP-1α, MIP-1β, PDGF-BB, RANTES, TNF-α, VEGF). Briefly, 50 µL of cytokine standards or samples (supernatants from transfected cells) were incubated with 50 µL of anti-cytokine conjugated beads in 96-well filter plates for 30 minutes at room temperature with shaking. Plates were then washed by vacuum filtration three times with 100 µL of Bio-Plex wash buffer, 25 µL of diluted detection antibody was added, and plates were incubated for 30 minutes at room temperature with shaking. After three filter washes, 50 µL of streptavidinphycoerythrin was added, and the plates were incubated for 10 minutes at room temperature with shaking. Finally, plates were washed by vacuum filtration three times, beads were suspended in Bio-Plex assay buffer, and samples were analysed on Bio-Rad 96 plate reader using the Bio-Plex suspension array system and Bio-Plex manager software [Bio-Rad, Hercules, California, USA]. Bio-

plex analysis was performed by PhD Giulia Montagner (Department of Life Science and Biotechnology, University of Ferrara).

17. Bioinformatics tools for miRNA analysis

MiRNA putative target identification was performed using TargetScan [*http://www.targetscan.org/vert_71/*] and miRWalk 2.0 [*http://zmf.umm.uni-heidelberg.de/apps/zmf/mirwalk2/*], while already validated miRNAs target were identified using miRTarBase [*http://mirtarbase.mbc.nctu.edu.tw/]*. Valuation of sequence homology between miRNAs of different species was performed using miRNAminer [*http://groups.csail.mit.edu/pag/mirnaminer/*]. While interaction between miR-210 and BCL11A coding region was evaluated using RNAfold web server [*http://rna.tbi.univie.ac.at/cgi-bin/RNAWebSuite/RNAfold.cgi*].

18. Graphic tools

Heat maps presented in results section were elaborated using the free online available tool [*http://www2.heatmapper.ca/expression/*], while Venn Diagram representation were created using an on-line tool [*http://bioinformatics.psb.ugent.be/webtools/Venn/]*

19. Statistics

Results are expressed as mean ± standard error of the mean (SEM). Comparisons between groups were made by using moderate paired Student's t test. Statistical significance was defined as $p<0.01$ highly significant (**) and $p<0.05$ significant (*).

Results

I. MicroRNA for non-invasive diagnosis: liquid biopsy on colon carcinoma model systems and colorectal cancer (CRC) patients

In order to verify whether miRNA patterns might be useful for diagnostic purposes in the field of non-invasive diagnostics of cancer, we have analysed miRNAs in colon carcinoma (CRC) model systems and CRC patients. The final objective was to validate a non-invasive approach for diagnosis/prognosis of CRC, starting from plasma-based liquid biopsy. This activity was conducted under the Horizon-2020 ULTRAPLACAD project.

1. Production of samples for the set-up of plasmonic-based device applied to miRNAs analysis

Within the ULTRAPLACAD project, the major goal of our research group was the determination of miRNAs content in biological samples using conventional miRNA detection techniques, such as RTqPCR or ddPCR. The same samples are expected to be in the future analysed, at same time, by I.N.B.B. (Istituto Nazionale Biostrutture e Biosistemi) unit, in order to compare PCR-based techniques with NESPRI based method. Samples have been characterized for three different miRNAs: miR-141-3p, miR-221-3p and miR-222-3p which, have been shown to be modulated in plasma of CRC patients, as already pointed out in the chapter "cmiRNA as diagnostic tools in CRC".

1.1 Protocol Set-up

While the final ULTRAPLACAD devices will be able to detect biomarkers directly from plasma, PCR-based techniques used for validation of miRNA as biomarkers for tumour detection, require a preliminary step, in which miRNAs are extracted from the plasma matrix, and then reverse transcribed in order to obtain a cDNA to be considered as the starting sample for the PCR methods. It is well documented that the employed method for miRNA extraction can significantly influence the final miRNA concentration [*McAlexander et al., 2013*]. On the basis of data available in literature and focusing on miRNA extraction from plasma, we have chosen miRNeasy Serum/Plasma Kit (Qiagen), that requires small amount of starting sample and according to several authors, allows a good sample recovery.

Before starting samples preparation, we have set-up extraction condition and evaluated the reproducibility of the method.

1.1.1 Exogenous Control Set-up

The amount of RNA recovered from plasma is very limited, and generally are small RNA, so samples, in most of cases, can not be quantified. At same time it is very important

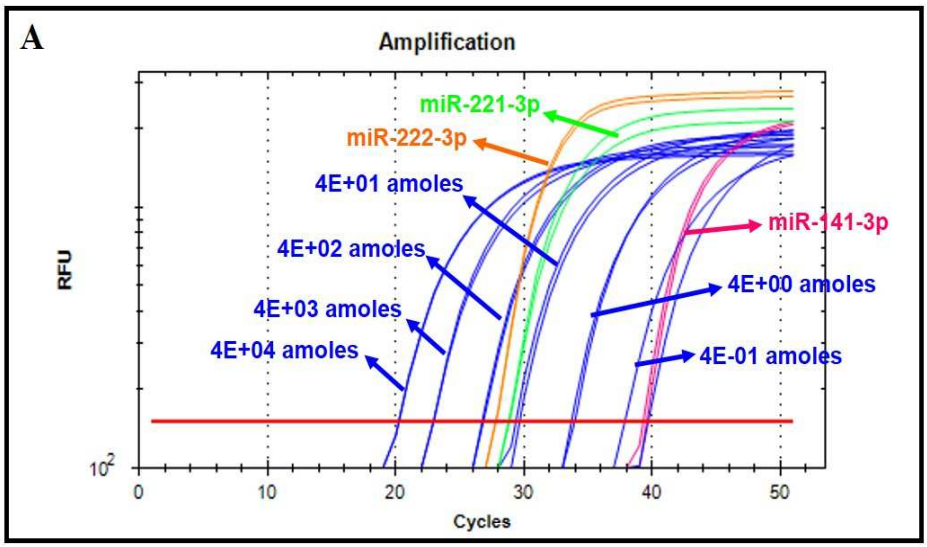

B

Cel-miR-39 Amount	CT value
4E+04 amoles	20,27 ± *0,16*
4E+03 amoles	24,67 ± *0,15*
4E+02 amoles	28,13 ± *0,21*
4E+01 amoles	30,41 ± *0,06*
4E+00 amoles	34,62 ± *0,16*
4E-01 amoles	39,38 ± *1,50*

C

miRNA	Mean CT value
miR-141-3p	40,05 ± *0,96*
miR-221-3p	29,01 ± *0,42*
miR-222-3p	28,36 ± *0,46*

Figure 1. Exogenous control Set-up. Panel A amplification curves obtained by RTqPCR analysis, blue curves are obtained by the analysis of cel-miR-39 in samples spiked with incremental amount of synthetic miRNA, while, pink, green and yellow curves are relative to respectively miR-141, miR-221 and miR-222. In Panel B are reported CT values for each sample spiked with different amount of cel-miR-39, while the mean CT values of the three investigated miRNAs are reported in Panel C.

to verify the efficiency of the extraction method, in particular in our case. Therefore, in order to verify if RNA recovery is similar between samples, we spiked into each sample, immediately after the phenol-lysis, a synthetic miRNA (cel-miR-39), which is not present in human plasma. In order to identify the most suitable amount of cel-miR-39 to add into

plasma, we extracted six plasma samples and we added at each one incremental concentration of mature cel-miR-39: starting from 0,4 amoles to 40.000 amoles. After the extraction, we reverse transcribed RNA and performed RTqPCR analysis to quantify cel-miR-39 content (**Figure 1**). As expected, CT values are inversely proportional to the amount of spiked cel-miR-39 (**Panel B**). At same time we also considered the mean CT values of three miRNAs that are relevant for diagnosis/prognosis of CRC, i.e. miR-141-3p, miR-221-3p and miR-222-3p. As indicated in Panel C, while miR-221 and miR-222 are expressed at medium-high levels (CTs: 28-29), miR-141 is expressed at very low levels. In order to have a cel-miR-39 expression similar to our selected miRNA, we chose 400 amoles amount of cel-miR-39, which was considered as the standard amount of spiked control miRNA, in all the following experiments.

1.1.2 Yield Determination

Assuming that both the reverse transcription step and the PCR step are 100% efficient, the most important bias in miRNA detection using PCR-based methods is represented by the extraction step. Moreover, in our case we have to compare data from two different matrices: plasma, that is used in ULTRAPLACAD device, and extracted RNA, used for PCR-based methods. Therefore, in order to compare data obtained by PCR quantification with data obtained by NESPRI analysis, we have firstly evaluated the mean recovery starting from known amounts of microRNA. The same amount of cel-miR-39 was added to three plasma samples, obtained from the same pool of healthy donors, after the lysis with phenol. Also in this case mature synthetic cel-miR-39 was chosen, because it is not expressed in human plasma. Samples were extracted following the miRNeasy Serum/Plasma Kit extraction protocol and the amount of cel-miR-39 in RNA samples was quantified using ddPCR. Cel-miR-39 copies/µL for each reaction well, reported in **Panel C** of **Figure 2**, were employed to calculate the final number of miRNA copies contained in the recovered RNA, considering the volumes of sample used to performed reverse transcription and ddPCR. As indicated in **Panel A**, the ratio (R) between the starting amount of cel-miR-39 added to the plasma (black rhombus: $2{,}26*10^{10}$) and the number of miRNA copies recovered in the RNA (white boxes) was calculated. The experiment was conducted in triplicate in order to calculate a mean loss of sample to the miRNA extraction step. As indicated in the Figure, the ratio is from 585 to 1028, with a mean ratio value of 803, indicating that the starting

sample is normally 800 times more concentrated than the recovered sample, and the loss is in the order of about 10^3.

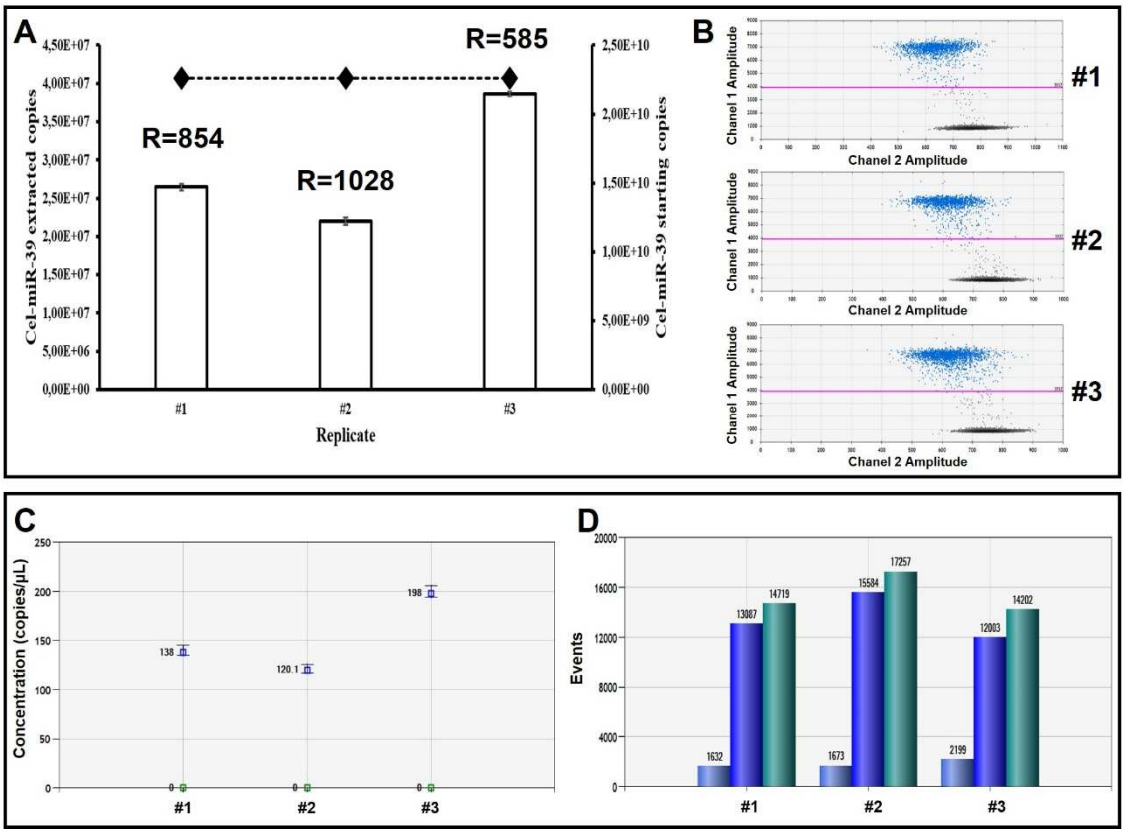

Figure 2. Yield Determination. In the **Panel A**, the ratio (R) between the added and the recovered amount of cel-miR-39 was calculated. In **Panels B, C** and **D** ddPCR plots were proposed: in box B, 2D plots were shown: blue points represent positive droplets, while black points represent droplets which do not contain template. Box C shows concentration of cel-miR-39 for each replicate, expresses as copies/µL for each reaction well, while in the box D the total number of generated droplet (positive or negative) is shown in green box, while negative droplets and positive droplets are represented respectively by blue boxes and light blue boxes.

1.1.3 Comparison between different batches of the same kit

Since samples were analysed at different times, in order to exclude that possible differences between samples were due to different batches of the same kit, we purchased during the year three different batches of the kit and we extracted the same starting sample, a pool of plasma obtained from a healthy donor, using the three different batches, as described in the left part of the **Figure 3**. The content of miR-141, miR-221 and cel-miR-39 was then quantified using ddPCR. MiRNAs concentration expressed as copies/µL for each reaction well was reported in the concentration plots in right part of Figure 3. As indicated in the Figure, miR-141 concentration is in the range of 10,7-9,7; while for miR-221 value are between 3 and 4,1; in both cases standard deviation between sample is very limited. In

the case of cel-miR-39 the value range is between 173 and 268, slightly more respect to the others miRNAs but compatible with physiological differences between samples.

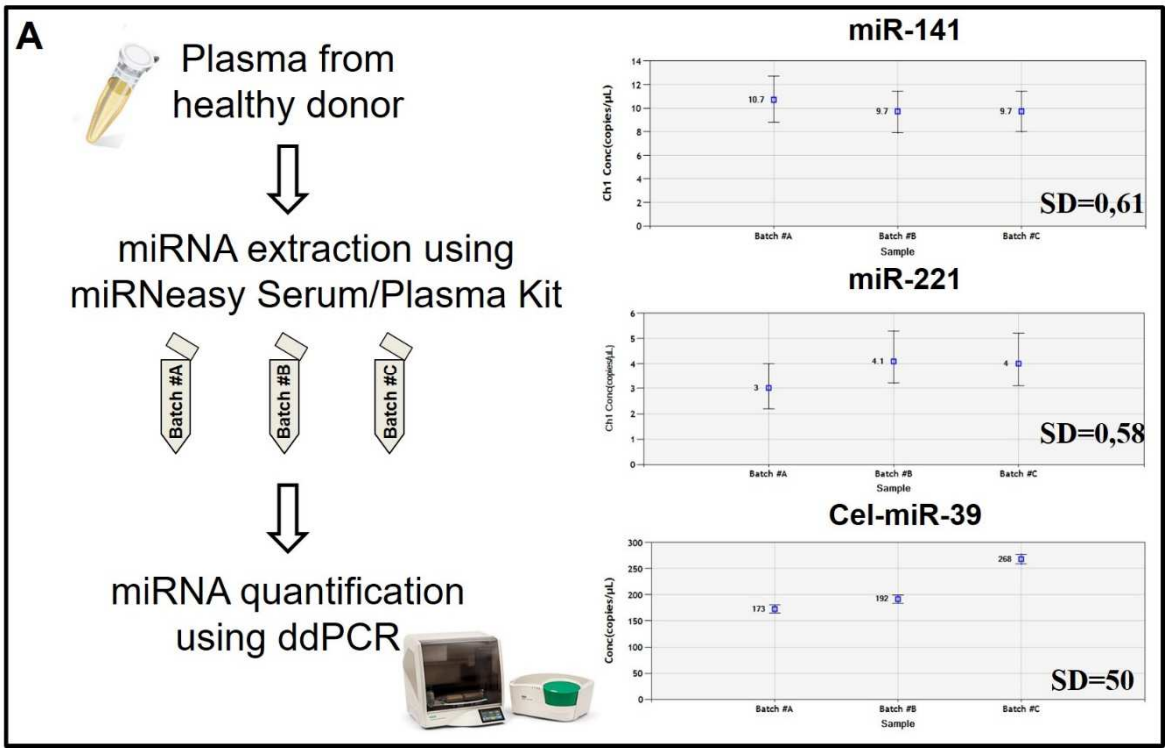

Figure 3. Comparison between different batches of the same kit. Left side of the Figure, description of the experiment work-flow: three aliquots of the same plasma sample obtained from a pool of healthy donors were extracted using three different batches of the same extraction kit purchased at different time points. The extracted RNA was reverse transcribed and analysed using ddPCR. Concentration of analysed miRNAs for each batches are reported in the right part of the Figure. All concentrations are reported as copies/µL for each reaction well.

1.1.4 Plasma Isolation Protocol

Despite liquid biopsy is becoming increasingly important in diagnostic practice and probably will replace, in due time, traditional biopsy techniques, the lack of validated protocols for plasma or in general biological fluids isolation and storage appears to be a major issue. In recent years hundreds of studies were published about biomarkers analysis in plasma samples, and no agreement has been reached concerning the different protocols proposed. In this respect, it is important to underline that the isolation protocol can deeply affect the final data and it is not surprising to find different results in the case of a sample isolated from the same donor and processed with different protocols. In order to evaluate how much the isolation protocol of plasma can affect the final miRNA concentration we isolated plasma samples from healthy donors with three different protocols and then analysed miRNAs content. Three different protocols were performed starting from the same

blood aliquot and isolation was performed at same time, in order to reduce, as much as possible, differences between starting blood samples. Three different protocols were chosen according to the methods indicated in the literature. In the first protocol called 'Protocol A', blood was centrifuged at 1200g for 10 minutes at 4°C without brake to avoid the alteration of interphase. In protocol B the first step is identical to the protocol A, but in this case the collected plasma is centrifuged again at 2400g for 20 minutes at 4°C. While protocol C provides a first centrifugation step at 2000g for 20 minutes at 4°C without brake, followed by a second centrifugation at 16000g for 10 minutes. Sample collected with different protocols were extracted: three sample for each protocol were extracted, and miRNA content was analysed. In the **Figure 4**, miR-221 concentration was reported for the three different protocols. Mean miR-221 value for protocol B is about 7, very similar to the mean value found using protocol C (mean value 7,3), while about ten-fold difference was detected in protocol A (mean value 77,8). In order to avoid biases due to extraction procedure, all samples were also analysed for cel-miR-39 content and no significant differences were found (data not shown).

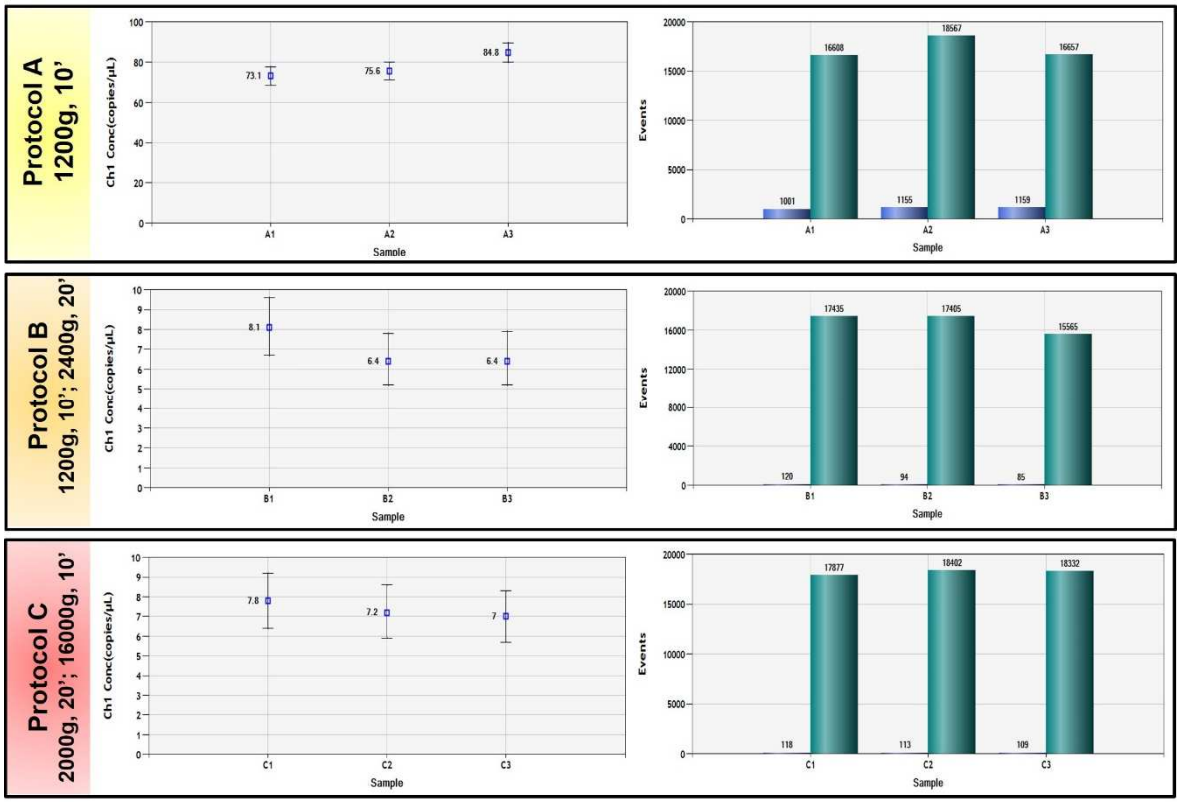

Figure 4. Plasma Isolation Protocol. Left part of the Figure: concentration (copies/µL) of miR-221 was evaluated in three different replicates. Concentration plot obtained by ddPCR analysis was reported. In the right part of the Figure, generated droplets analysis for each replicate was shown: green boxes indicate the number of total generated droplets, while blue boxes are relative to positive droplets.

1.1.5. MiRNA stability in plasma sample

Several works reported good stability of miRNAs in plasma. In our case, especially for the device validation step in the ULTRAPLACAD project, is important to verify if frozen sample are stable during the time [*Balzano et al., 2015*]. For this reason we analysed the same sample at two different time points (time zero and six month later) in order to evaluate the reproducibility of the data obtained and related to the miRNA concentration. Is important to underline that two different aliquots of the same plasma sample were analysed in order to avoid freeze-thaw cycles. In **Figure 5** a representative example is reported. MiR-221 concentration was detected in CRC patient plasma at time zero (T1) and after six month of storage at -80°C (T2). Only minor differences were detected when these two time points were compared: 78,8 versus 61,7 copies/µL per well. Also in this case cel-miR-39 was used to verify the efficiency of extraction and no significative differences were detected.

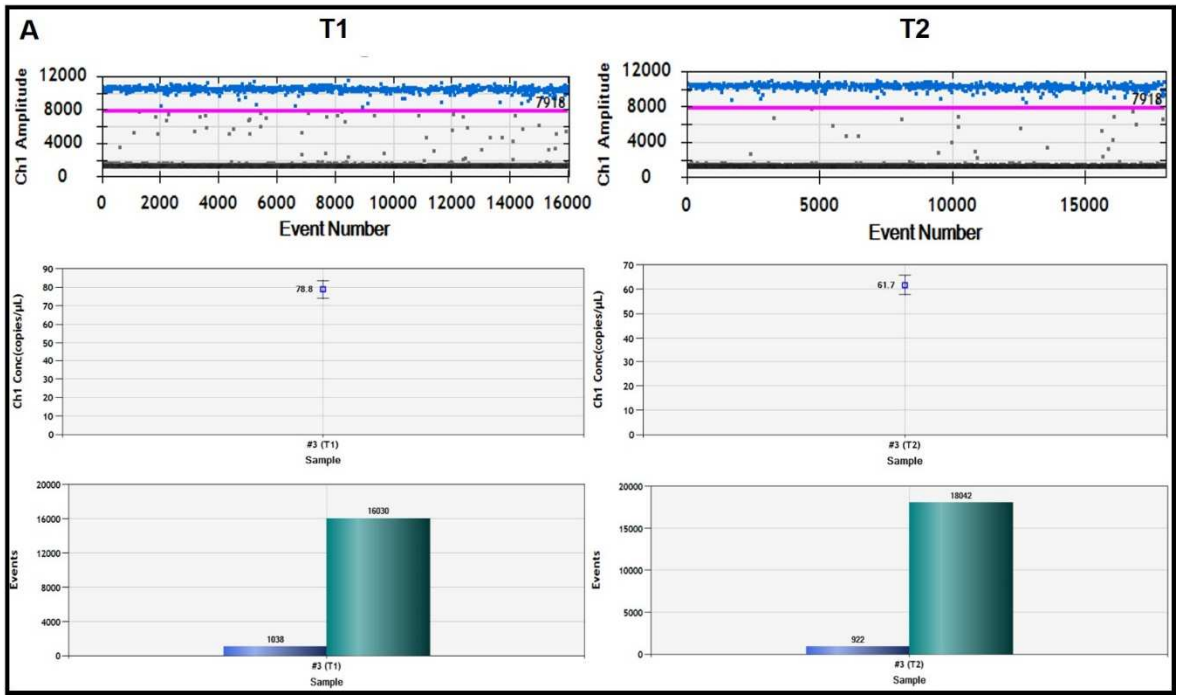

Figure 5. MiRNA stability in plasma sample. Left part of the Figure, miR-221 content in the sample at time zero: 1D plot (upper part): blue points indicates positive droplets while black points represent negative droplets, concentration plot (middle part) and droplets plot (lower part): green box represents total analysed droplets, while blue box is relative to positive droplets. In the same way, data about miR-221 concentration in 6 month-stored samples were reported.

2. Model validation

As described in 'miRNA release' chapter, miRNAs are physiologically released by cells, including tumor cells, probably as a mechanism of 'communication'. In the presence

of a cancer, the miRNAs release might results higher, probably due to the increased number of cells that undergo to apoptosis or necrosis process. In order to study the mechanism of miRNAs release two different models were employed, based on three different CRC cell lines: HT-29 cells derived from colorectal adenocarcinoma (KRAS wt), LoVo cells (Dukes' type C, grade IV) harbouring KRAS G13D mutation and LS174T cells (Dukes' type B) which present KRAS G12D mutation.

2.1 Experiment work-flow

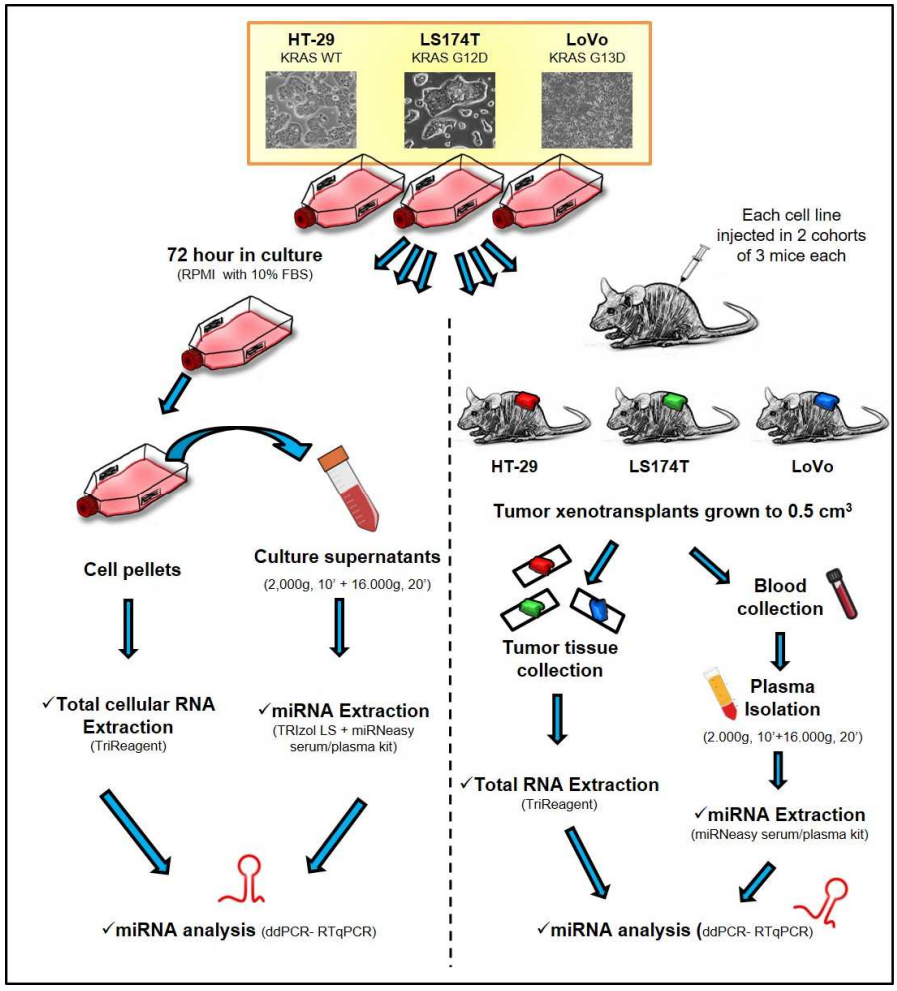

Figure 6. Experiment work-flow. To validate the release model three different cell lines were employed: HT-29, LS174T and LoVo, that were characterized for their miRNA content and moreover their ability to release extracellular miRNA was evaluated, analysing miRNAs content in conditioned medium, after three days of culture (left part of the Figure). In parallel to have a more complex model, each cell line was injected in three mice. Tumor was grown at the size of 0.5 cm^3 and tumor tissues and blood were taken at sacrifice.

The three cell lines were characterized for their miRNAs content, moreover the same miRNAs were also investigated in the relative supernatants. As indicated in **Figure 6**, cells

were cultured in their traditional culture medium composed by RPMI supplemented with FBS 10% for 72 hours. After 72 hours, when cells reach the 90-95% of confluence, cells were detached and lysed in order to extract total RNA using the phenol-chloroform method. At same time, the relative supernatants were collected, using the same protocol employed for isolation of all plasma samples (2000g, 20 min at 4°C; 16000g, 10 min at 4°C), and RNA was extracted as indicated in Turchinovich et al., 2011 and detailed described in the chapter 'Materials and methods'. In both types of samples (cells and supernatants), miR-141, miR-221 and miR-222 content were analysed using both ddPCR and RTqPCR. At the same time the three cell lines were grown as xenotransplants at the size of 0,5 cm^3 in 4-month old Nu/CD1 mice in order to obtain an *in vivo* model mimicking liquid biopsies. Three mice for each cell line were employed and two independent experiments were performed. Tumor tissues and blood were taken at sacrifice. Plasma was isolated from blood using the same protocol employed for supernatants isolation in order to reproduce the same analytical condition. Plasma RNA extraction was performed using miRNeasy Serum/Plasma Kit, while tissue samples were homogenized and RNA was extracted using phenol-chloroform method. Even in this case miRNAs content, in plasma and tissue samples, was evaluated using both absolute RTqPCR and ddPCR.

2.2 FBS influence evaluation

Since the cell lines employed for the analysis were grown in conditioned medium composed by RPMI and 10% FBS, the relative supernatants might contain, although to a limited extent, bovine miRNAs. In this respect we have to bear in mind that the miRNA sequences are very conserved through evolution. For these reason, before performing experiments aimed at detection and quantification of human miRNAs secreted by the HT-29, LoVo and LS174T cells, we wanted to evaluate the possible background signal derived from the presence of FBS-related miRNAs. First of all, using miRNAminer [*groups.csail.mit.edu/pag/mirnaminer*] a bioinformatic tool that allow to analyse homologies between miRNAs of different species, we verified if human and bovine miR-141, miR-221 and miR-222 have the same sequence. As indicated in **Panel A** of **Figure 7**, unfortunately, *Homo sapiens* and *Bos taurus* miRNAs are perfectly homologous. For this reason, samples containing only RPMI and FBS at 10% were analysed to quantify the percentage of miRNA coming from FBS. MiRNAs content in RPMI+FBS 10% samples was compared to other sample using both ddPCR (**Panel B**) and RTqPCR (**Panel C**). As

indicated in panel C there are at least four CTs in difference between cell-supernatants and conditioned medium samples. Therefore, FBS-related miRNAs do not affect our analysis of miRNAs released by the employed tumor cells.

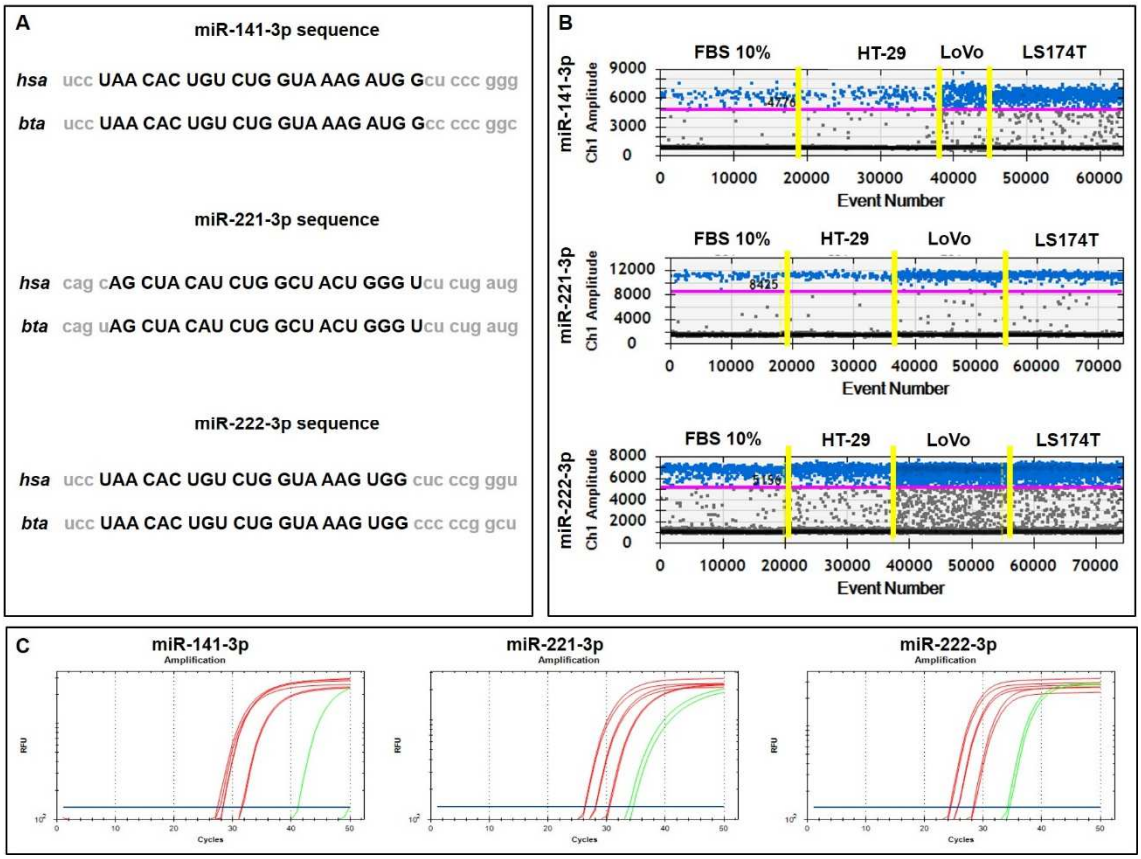

Figure 7. FBS influence evaluation. Panel A, sequence homology between *Homo sapiens* (hsa) and *Bos Taurus* (bta) miRNAs. Analysis was performed using miRNAminer software. **Panel B** and **C**, miRNAs content difference between RPMI+FBS 10% sample and cell-supernatants samples, analysis was performed using both ddPCR (B) and RTqPCR (C). In panel B 1D plot, taken from ddPCR analysis, is reported: blue points are relative to droplets in which amplification occurs, while black points represent droplet in which no target was detected.

2.3 MiRNAs content comparison between cells and supernatants

To evaluate miRNAs release profile, we analysed miRNAs content both in cells and in their relative supernatants. Due to the different protocols employed for miRNAs reverse transcription and ddPCR in the two different kinds of sample, we reported all data to the miRNAs concentration in RNA sample, expressed as copies/µL in RNA. Δ release was calculated making the ratio between the miRNA concentration in cell sample and in supernatants sample. As indicated in the **Panel A** of the **Figure 8**, the three cell lines present,

as expected, different miRNA profiles (black circles). For example, LoVo cells present the lowest concentration of miR-141, between the three cell lines, but, on the contrary, they

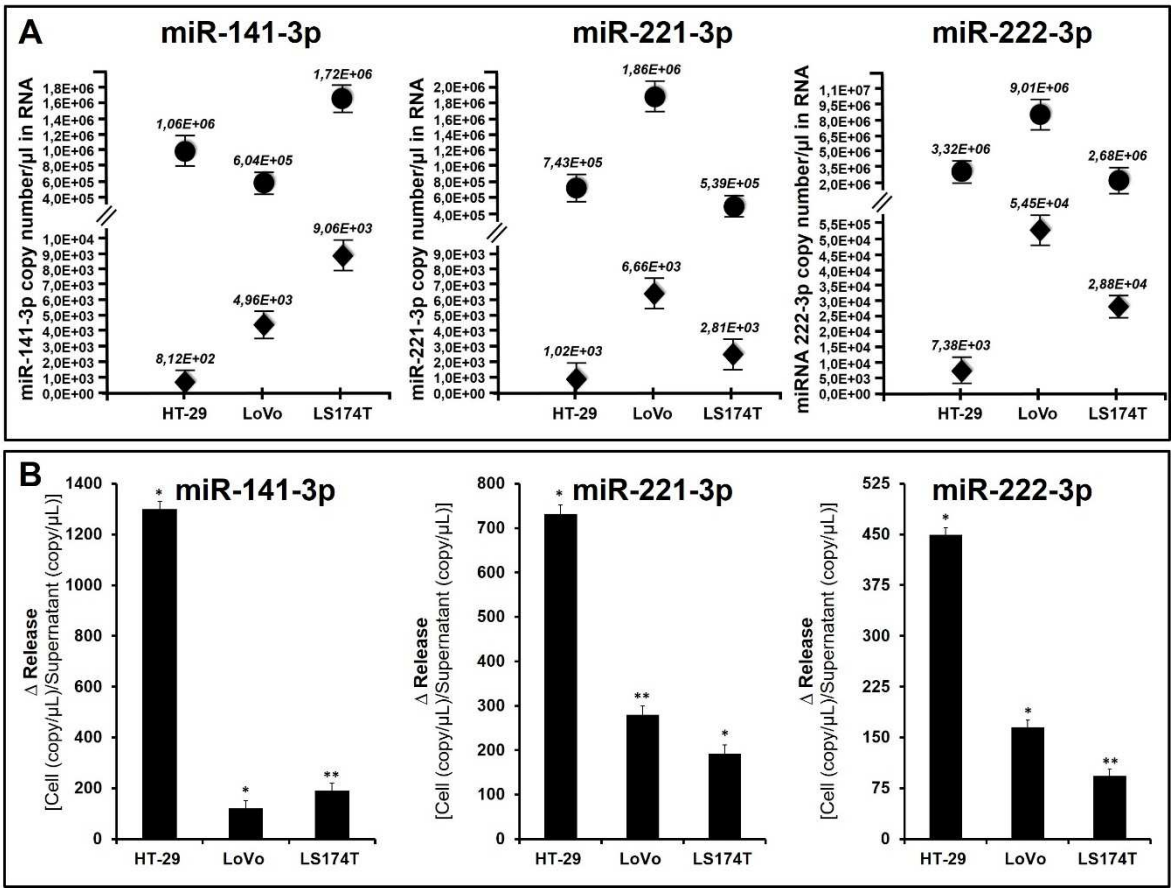

Figure 8. MiRNAs content comparison between cells and supernatants using ddPCR. Panel A: miRNAs concentration was determined in both cells (black circles) and supernatants (black rhombus) using ddPCR. Concentration is expressed as copies/µL in RNA samples. **Panel B**: the ratio (Δ release) between miRs concentration in cells and in supernatants was calculated. Standard deviation was calculated considering three independent experiments.

express at highest levels miR-221 and miR-222. Moreover, if miR-221 and miR-222 present the same trend between the three cell lines, although with different concentration values, miR-141 profile is completely reverse. Between miRNAs, miR-222 is expressed at highest levels, while miR-221 and miR-141 present more similar values. Furthermore, supernatants miRNA profile (black rhombus) does not always reflect cellular profile. In fact, despite the fact that miR-221 and miR-222 profiles in supernatant generally reflect the cellular trend, a very different trend was observed for miR-141, which, despite being expressed at low levels by LoVo cells, is well-released in supernatants. The ratio between miRNA content in cells and in their relative supernatants was calculated (**Panel B**), indicating that HT-29 cells present higher release efficiency for all the three analysed miRNAs, followed by LoVo and LS174T cells, exhibiting a miRNAs release ability remarkably less efficient than HT-29 cells. In this case analysis was performed employing the ddPCR technique and plots indicate

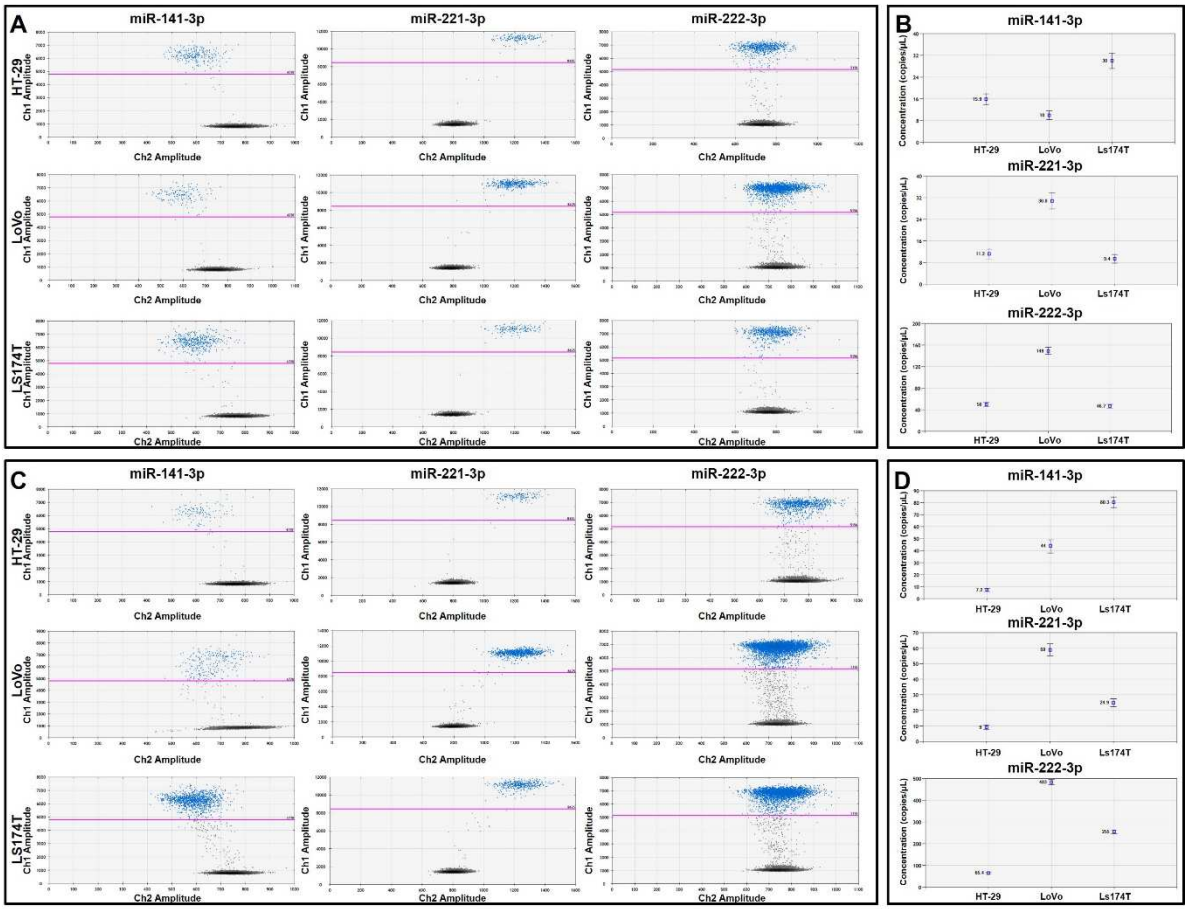

Figure 9. MiRNAs content comparison between cells and supernatants, ddPCR plots. Plots obtained by ddPCR analysis have been reported, **Panel A**: 2D plots relative to cells samples for each miRNAs. Blue points represent positive droplets, while black points are relative to negative droplets. Panel B: concentration plot, the concentration as copies/µL in each reaction well is reported. Plot are obtain starting from a cDNA sample that was diluted 1:100, for technical issues explained in chapter materials and methods. The same plots were reported for supernatants samples (**Panels C** and **D**) in this case no dilutions of ddPCR template were performed.

the concentration in copies/µL for each reaction (**Figure 8**). It is important to underline that cDNAs obtained from cellular samples (panel A and B), were diluted 1:100 for analysis in ddPCR, while no dilution was performed in case of cDNA derived from supernatants samples (panel C and D). At same time samples were analysed using RTqPCR (**Figure 10**). In this case, unlike ddPCR, in order to achieve an absolute miRNA concentration value, a standard curve was required. As shown in the upper part of the Figure 10, a standard curve for each investigated miRNA was performed, using a synthetic mature miRNA purchase from IDT. Even if miRNA profile in the three cell lines is the same with both techniques, differences in the order of 10^1 were shown in the concentration values of both types of sample. The difference in copy number obtained using two different techniques does not surprise us, considering that in creation of standard curve with mature synthetic miRNA same little biases in dilution procedure may be introduced, and this can affect final miRNA quantification in samples.

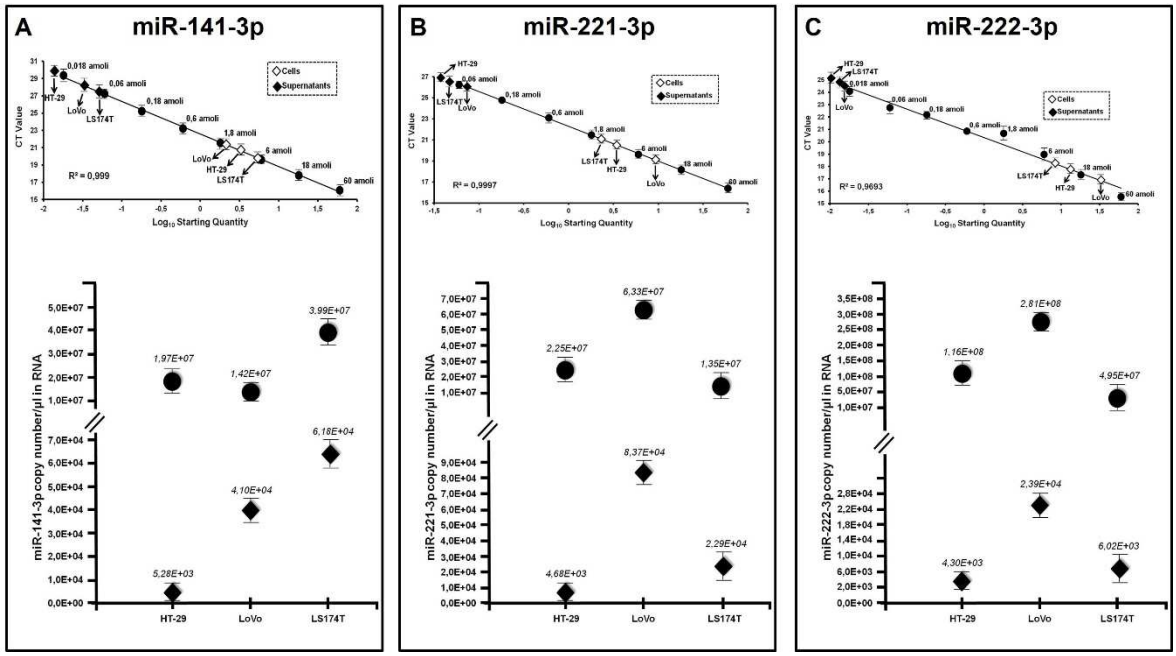

Figure 10. MiRNAs content comparison between cells and supernatants using RTqPCR. For each miRNA a standard curve, employing known amounts of synthetic mature miRNA, was performed (upper part of each panel). Using the standard curve the absolute miRNA concentration for each samples was extrapolated (lower part of each panel). Standard deviation was calculated considering three independent experiments.

2.4 MiRNA quantification in the *in vivo* experimental model system constituted by xenografted mice

MicroRNA content was also evaluated in plasma and tissue samples obtained from the *in vivo* models. Also in this case miRNA content was determined using both RTqPCR and ddPCR, in order to compare the results obtained using the different techniques. As regard ddPCR analysis (**Figure 11**) absolute concentration of the three selected miRNAs was determined and expressed as copies/µL in RNA samples, in order to avoid biases due to the different sample-processing protocols. MiRNAs concentrations are reported in **Panel A** of Figure 11, HT-29 cell line presents the highest concentration for all the three miRNAs, and also in this case miR-222 presents the higher concentration in all the three cellular lines in both plasma and tissue samples. Considering only miRNA levels in plasma samples HT-29 xenograft presents the highest of all the three miRNAs, indicating that this tumor cell line has an high ability to share miRNAs in blood stream, at least for what concerns the three analysed miRNAs. Is also important to underline that miRNA release in blood stream depends not only by its tissue concentration, but also on several others factors including posttranscriptional miRNA modification. For this reason we also considered Δ release profile. The analysis of Δ release values (**Panel B** of Figure 11), the HT-29 cell line shows

the higher ratio between tissue content and plasma content, followed by LS174T, exhibiting good release capacity, although lower than HT-29 (especially for miR-221 and miR-222). Analysing Δ release values, miR-141 presents the higher ratio, while very low release ratio was found for miR-222, with a difference that is in the order of 10^2. Analysis plots are presented in **Figure 12**.

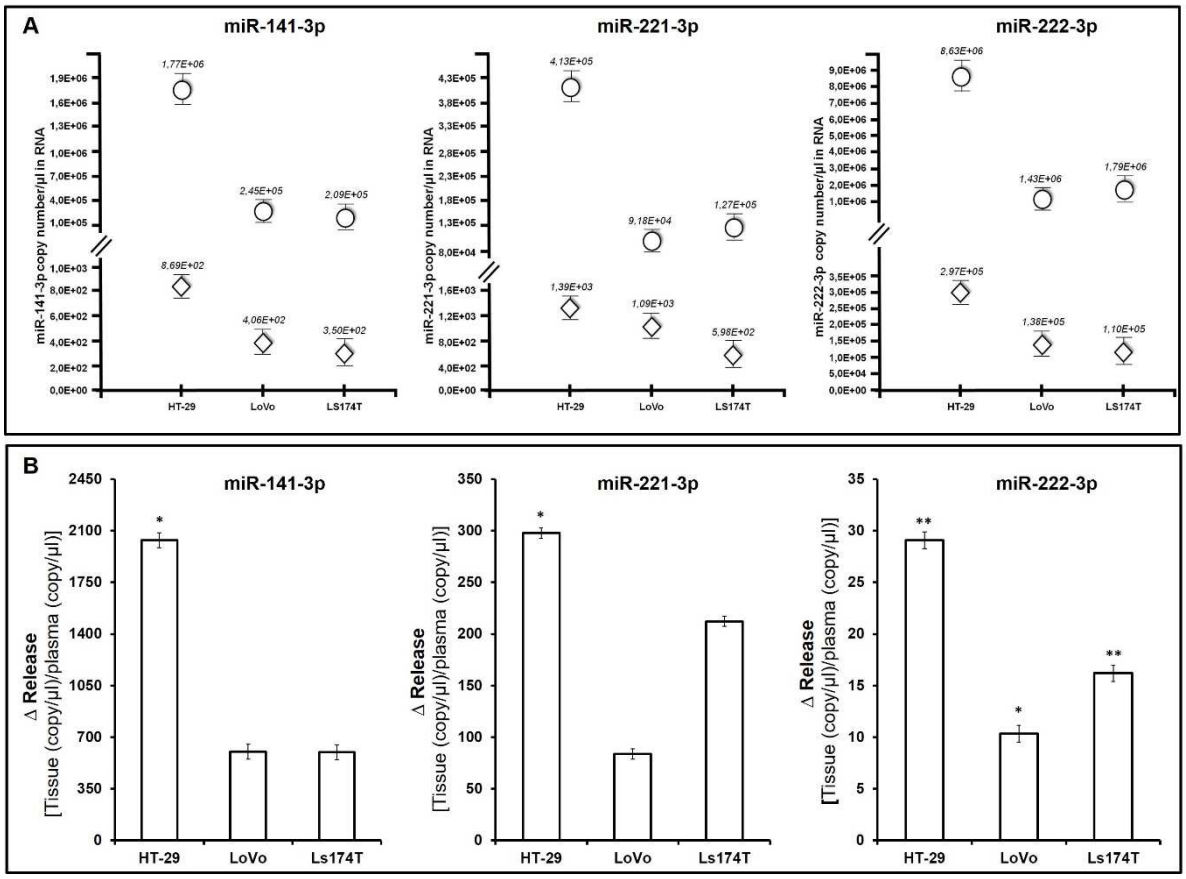

Figure 11. MiRNA quantification in *in vivo* model. Panel A, miRNAs concentration in both tissue (white circles) and plasma (white rhombus) samples, data are expressed as copies/µL in RNA. The ratio between copies of miRNA in tissue and in plasma (Δ release) was shown in panel B. Three independent experiments were performed.

In conducting these experiments, cDNA samples from tissues (**Panel A** and **B**) were diluted 1:100 before ddPCR analysis for technical issues (more detailed information are reported in the chapter 'Materials and methods'), while no dilution was perform for plasma samples. At same time, samples were also analysed by RTqPCR. Three standard curves, one for each miRNAs, were made using known amount of synthetic mature miRNA (upper part of **Figure 13**) and concentration data were calculated (lower part of the Figure 13). MiRNA profiles present some slight differences in the trend between two methods, that are more appreciable

in plasma samples, with respect to tissue samples. As in cells and supernatants analysis, concentration difference is in the order of 10^1. Moreover, miRNA expression levels in mice plasma was compared with that of no xenografted (healthy) control mice. Data were expressed both as copy number change (data obtained by ddPCR), showed in **Panel A**, and as fold change (data obtained by RTqPCR analysis), showed in **Panel B**, and are reported in **Figure 14**. No significant differences were found when the two different miRNAs detection techniques were compared.

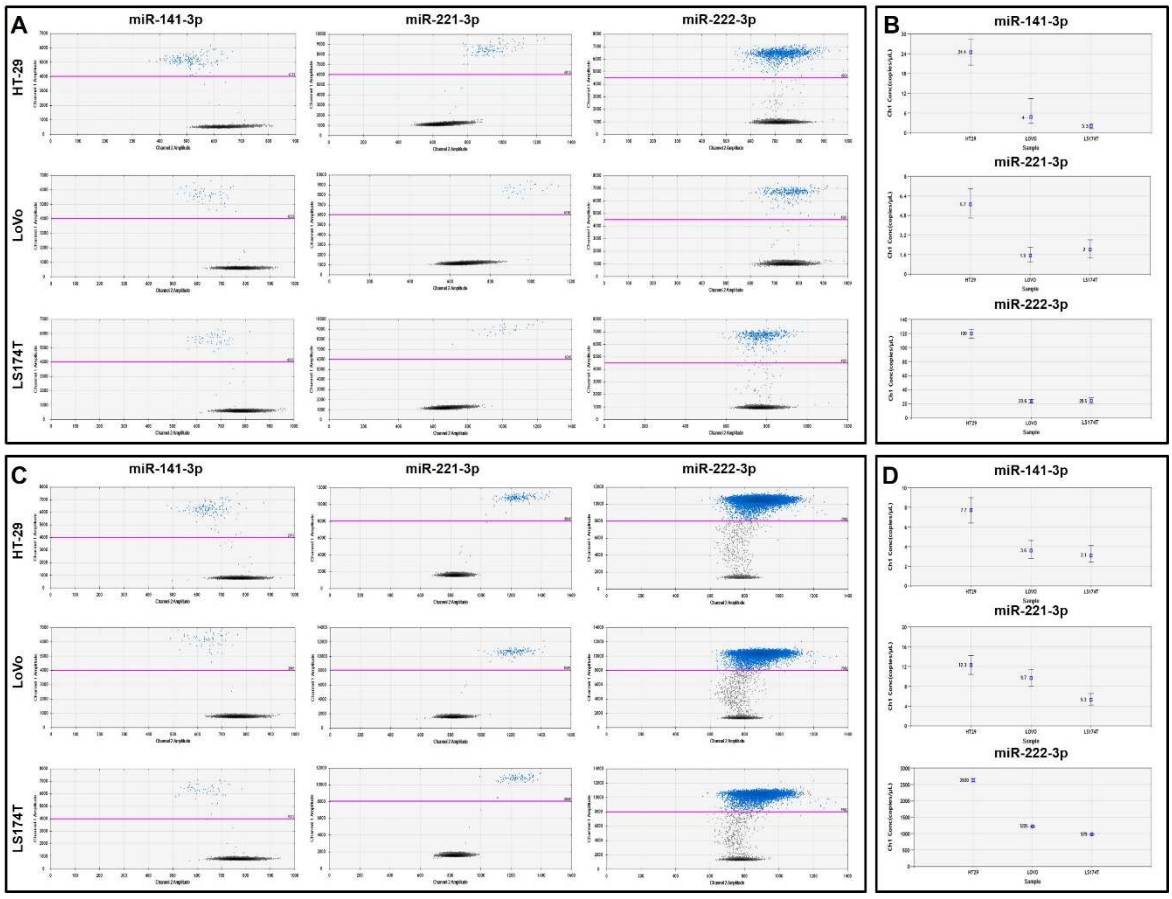

Figure 12. MiRNA quantification in *in vivo* model, ddPCR plots. 2D plots (**Panels A** and **C**) and concentration plot (**Panel B** and **D**) were shown both for tissue samples (panels A and B) and for plasma samples (panels B and D). 2D plots represent droplets in which amplification takes place (blue points) and droplets in which no amplification occurs (black points). Instead, in concentration plots, miRNA concentration for each reaction well (copies/µL) is expressed.

According with the data previously shown, in the HT-29 xenografted mice a significant increase of all the three miRNAs was found, being particularly sharp in the case of miR-222 and miR-141. In contrast, the increase is less evident, although significant, in the case of miR-221, which as described in the Figure 11 is also the less expressed in the tumour tissues. No significant variations in miRNAs expression were, on the contrary, detected when

LS174T cells were xenografted in nude mice. Finally, in LoVo xenografted mice the most significant change involved miR-221 that is also the miRNA expressed at lower levels in the tissues (see Figure 11).

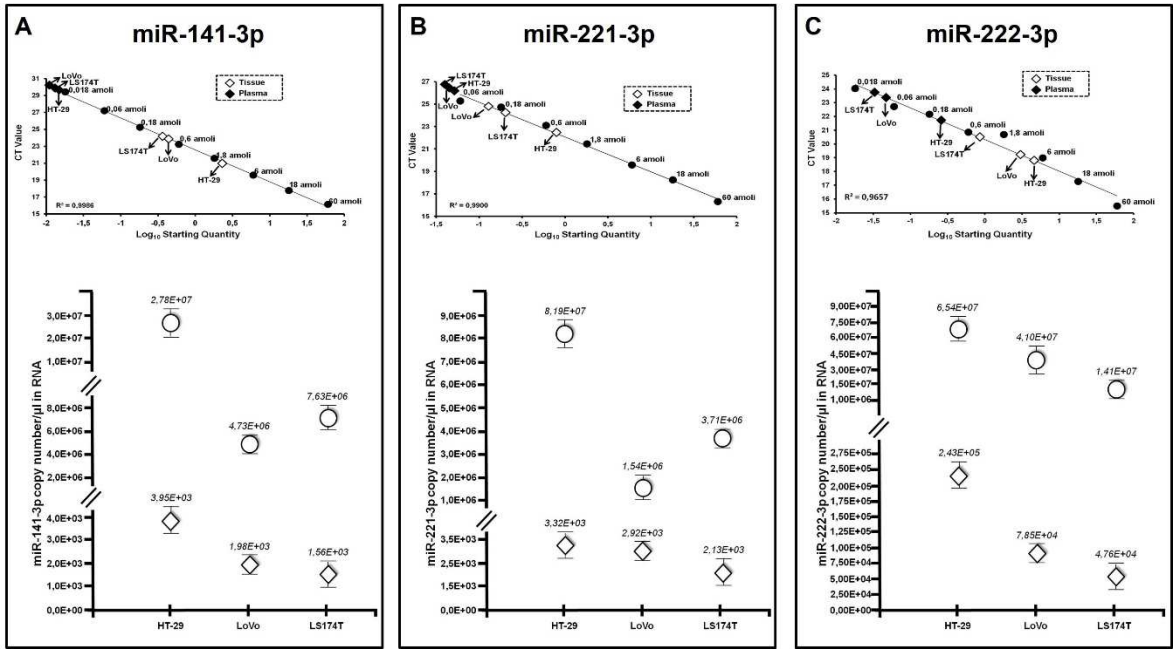

Figure 13. MiRNA quantification in *in vivo* model by RTqPCR. Known amounts of synthetic mature miRNA were employed to create standard curves, one for each investigated miRNA, through which miRNAs content in each sample is calculated (upper part of each panel). The extrapolated miRNAs concentration in tissues (white circles) and in plasma (white rhombus) was shown in the lower part of the Figure.

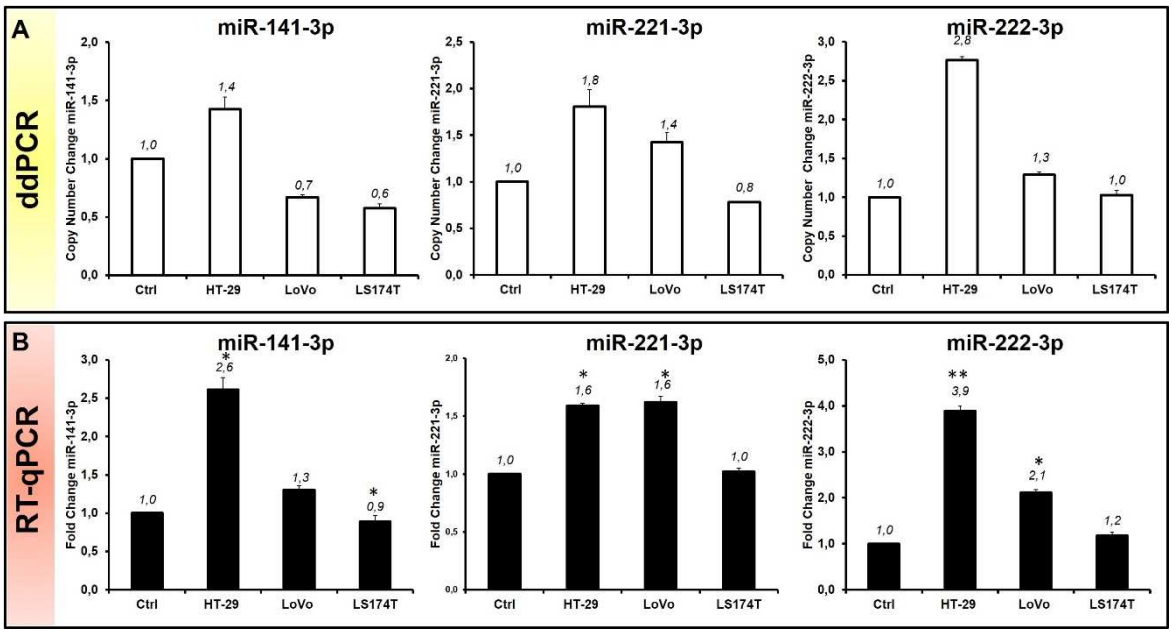

Figure 14. Fold change in xenografted mice. Panel A, copy number change has been calculated as the ratio between miRNAs copies in xenografted mice and copies in control (ctrl) mice. Copy number data were obtained by ddPCR. In panel B, RTqPCR data were proposed, fold change was calculated with $2^{-(-\Delta\Delta CT)}$ method. Three independent experiments were performed.

3. Spike-in preparation

The preliminary set-up of the ULTRAPLACAD-device has required high amounts of plasma with a known amount of at least one of the selected miRNAs in order to verify reliability of data and to solve problems relative to the plasma matrix and sample injection. The employment of "real" CRC plasma samples, at least in the first step of the device set up was not the first choice (the biological material from patients is low and very precious), so the preparation of spiking was considered the most suitable method to perform paired analysis with ddPCR and ULTRAPLACAD device. As previously underlined one of the most innovative features of ULTRAPLACAD device is the possibility to analyse directly plasma samples, in which biomarkers are diluted. On the contrary, ddPCR or RTqPCR require at least two additional steps: analytes extraction from plasma (RNA or DNA depending on the biomarker type and specific project) and reverse transcription (only in the case of microRNA) that of course, can introduce variability to be carefully considered. In order to perform paired analysis, it is important to know the miRNAs concentration into the starting samples, in this case plasma, and considering that different amount of plasma was employed in the two methods. Therefore, miRNA concentration was reported as copies of miRNA for µL of plasma. The detailed protocol to calculate final miRNA concentration was reported in the chapter 'Materials and methods'.

3.1 Spike-in set up

MiRNA are very stable in body fluids. For this reason they are employed as biomarkers. However, their stability is strictly dependent to the mechanism of miRNAs release. In fact miRNAs are usually contained within extracellular vesicles, or in other cases, are associated with several types of proteins which prevent miRNA degradation due to RNAses activity. Completely different is the situation if a 'nude' mature miRNA is added into plasma. As somewhere reported, when a 'nude' miRNA is added into plasma, it is quickly degraded by RNAse, [*Turchinovich et al., 2011*]. The same situation occurred in our case (**Figure 15**). Starting from the same plasma sample, obtained by a pool of healthy donors, increasing concentrations (from $4*10^1$ to $4*10^4$ amoles) of mature miRNA were added to plasma immediately before the sample lysis (**Panel A**) or after the lysis with phenol (**Panel B**). As indicated by the amplification curves reported in panel A, no differences were shown in the spiked samples with respect to no spiked sample (light green curve), indicating that only physiologically-present miRNA is detectable and then the added "free" miRNA

molecules are degraded. On the contrary, if the spiking is performed after the sample lysis with phenol, and consequently, also the RNAses lysis, an increase, directly proportional to

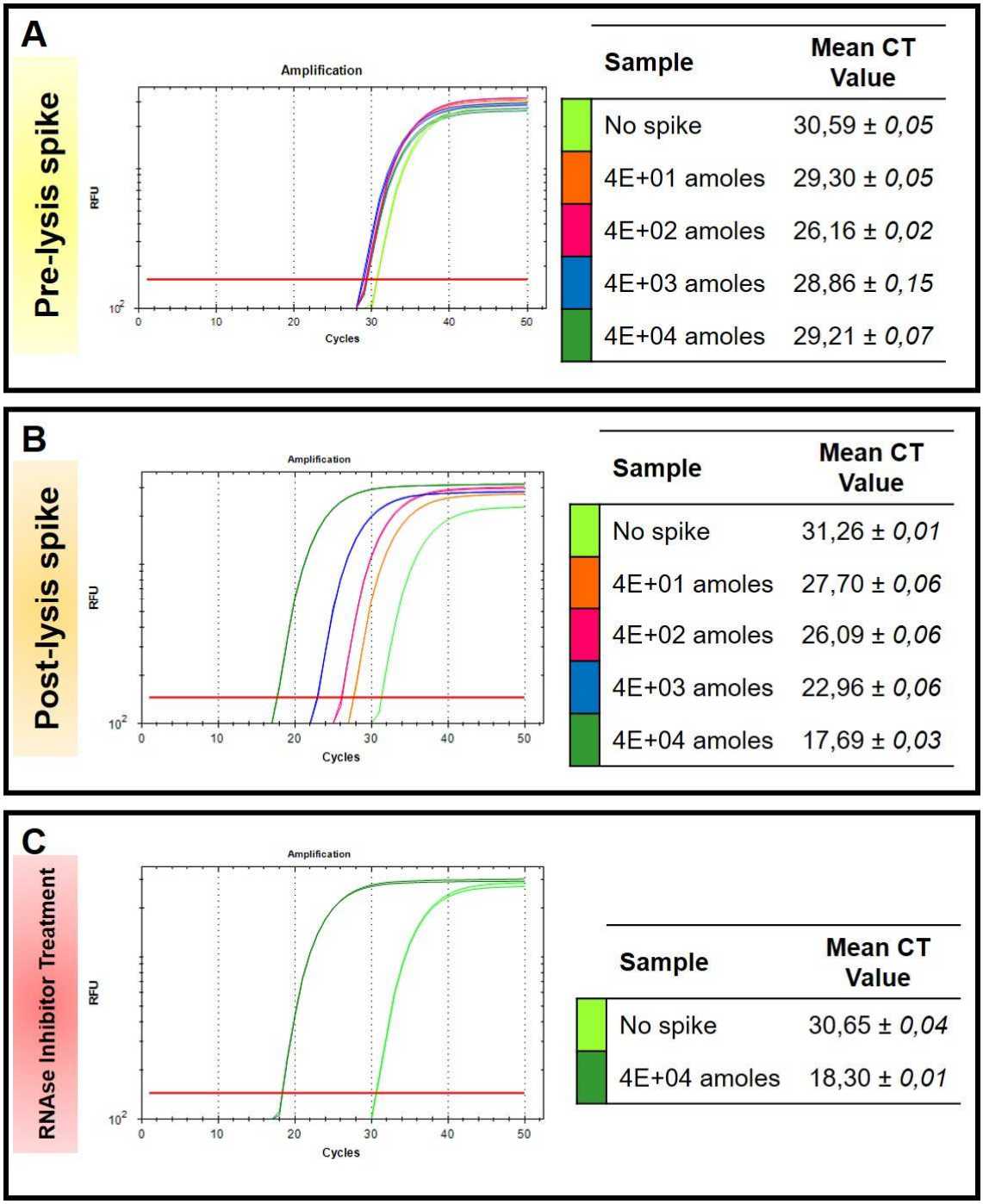

Figure 15. Spike-in set up. Two different spiking protocols where tried: a mature synthetic miRNA was add in plasma sample immediately before the sample lysis (Panel A), in parallel miRNA was also spiked in the plasma sample after the sample lysis (Panel B). The amplification curves obtained by RTqPCR where shown for both protocols. A plasma pre-treatment with RNAse Inhibitor was tried to avoid mature miR degradation (Panel C). Spiked samples (orange, pink, blue, green curves) where compared with no spiked sample (light green curve). Representative curves of three independent experiments were reported.

the added amount of miRNA was shown. At same time another strategy to avoid miRNA degradation was tested. In this experiment plasma samples were firstly, treated with RNAse

inhibitor enzyme, and then miRNA was spiked before the lysis. As shown in Panel C, the increase of miRNA content is well evident after comparison with the "no spiked sample" and at same time miR-221 CT values are comparable with the CTs obtained with the same amount of miRNA, spiked after the lysis (CT value of 18,30 versus 17,69).

3.2 Spike-in preparation

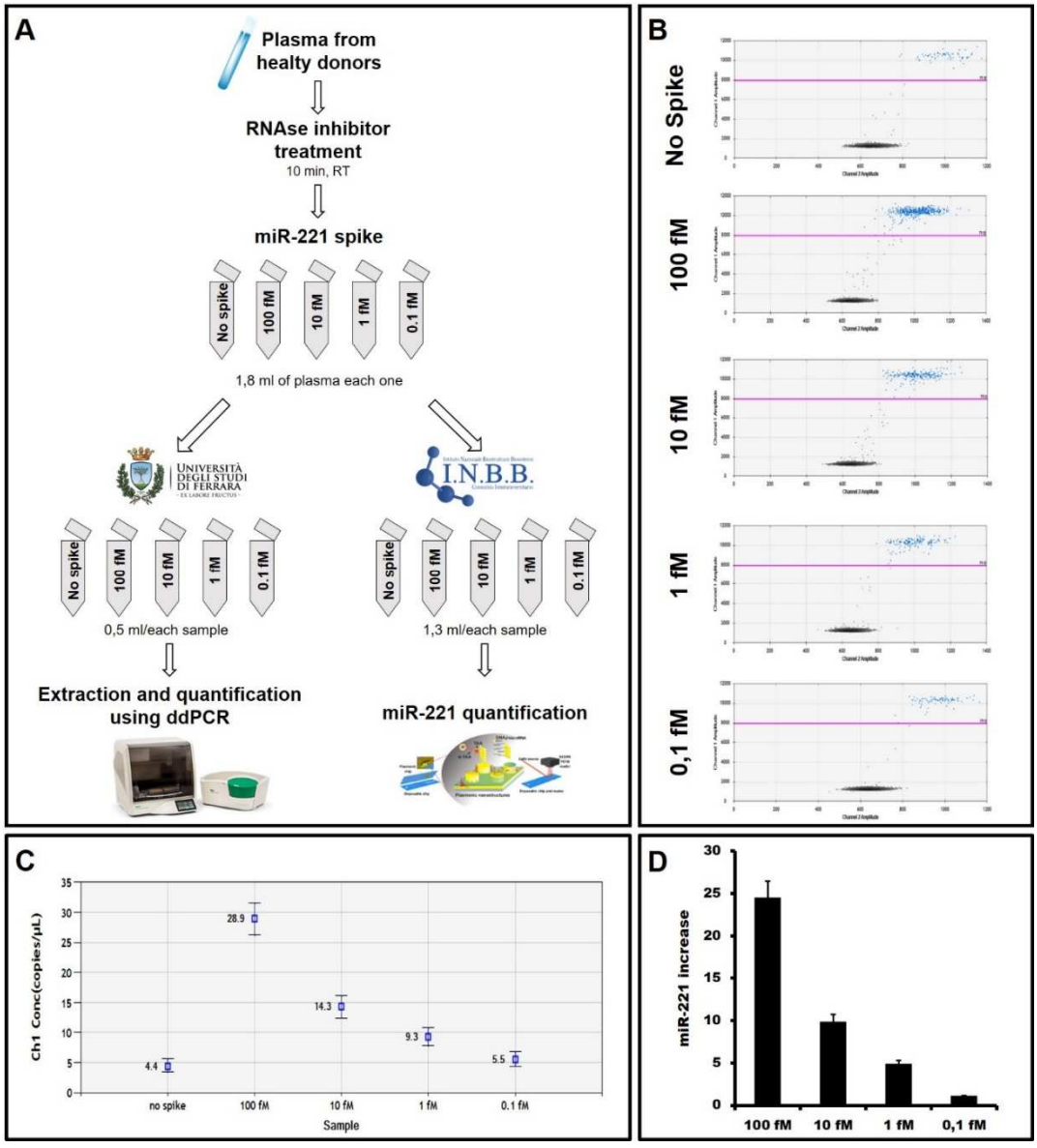

Figure 16. Spike-in preparation. **Panel A** work-flow of the spike-in preparation: plasma obtained by a pool of healthy donors was pre-treated with RNAse Inhibitor enzyme, and then different amounts of mature synthetic miRNA were added. An aliquot of plasma was analysed by ddPCR, while a second one was analysed by ULTRAPLACAD device. **Panel B** 2D plot obtained by the ddPCR analysis of the different samples were proposed. Positive droplets are represented by blue points, while black points, with low amplitude values are relative to negative droplets. Sample concentration in ddPCR reaction well is indicated in the concentration plot shown in the panel C, while in the panel D the ratio between copies of miRNA in the spiked sample and copies in the no-spiked sample is calculated.

After setting-up the method, high amount of spike-in were prepared, in order to perform a paired analysis by both ddPCR and ULTRAPLACAD device. Starting plasma samples were obtained by a pool of healthy donors, and were pre-treated with the RNAse inhibitor enzyme to avoid spiked-miRNA degradation. After the RNAse treatment different amounts of synthetic mature miRNA were added to each sample in order to obtain a final concentration

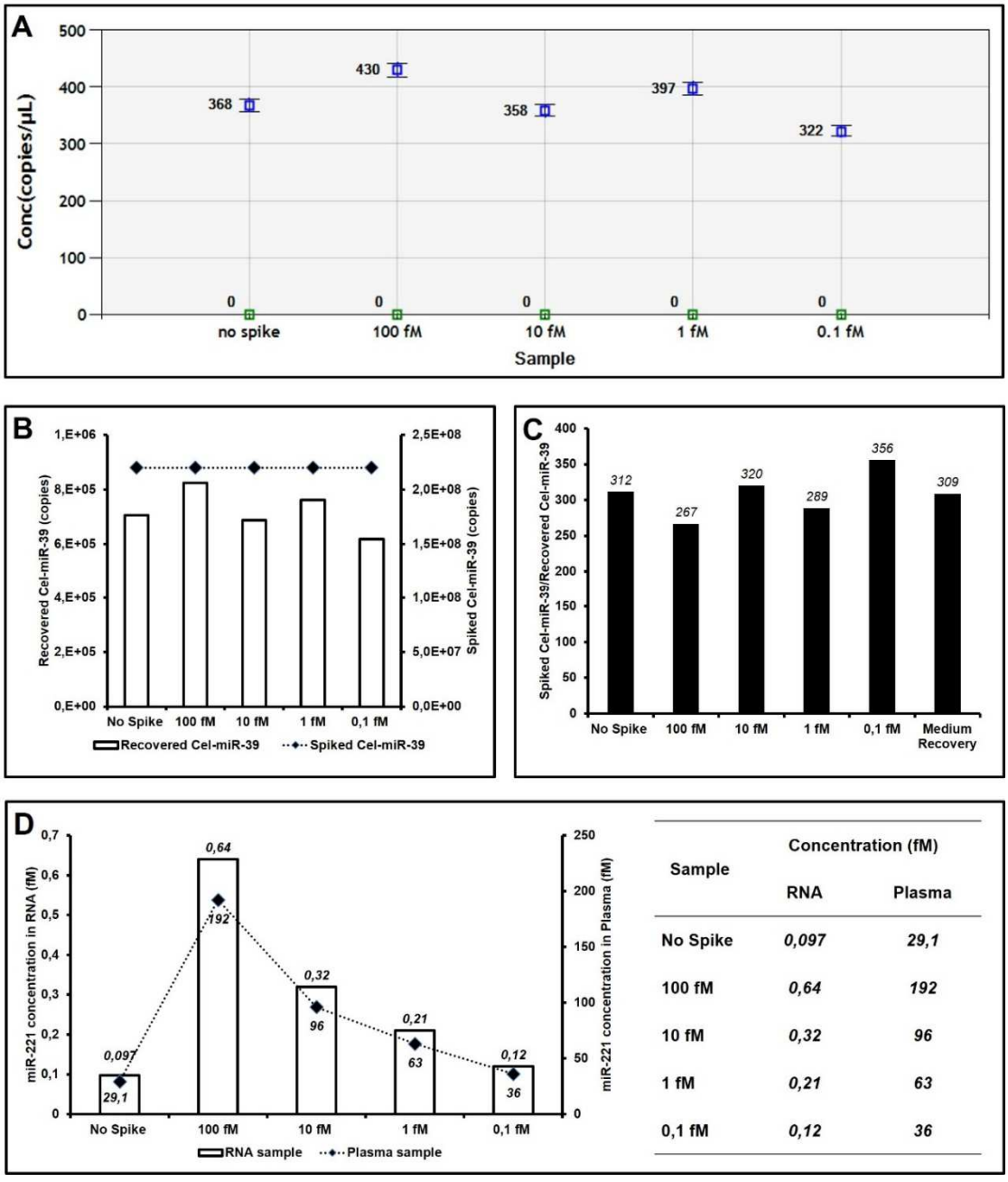

Sample	Concentration (fM)	
	RNA	Plasma
No Spike	*0,097*	*29,1*
100 fM	*0,64*	*192*
10 fM	*0,32*	*96*
1 fM	*0,21*	*63*
0,1 fM	*0,12*	*36*

Figure 17. Determination of miRNA concentration in starting plasma sample. Panel A: cel-miR-39 concentration (copies/µL) in each reaction well was reported. Panel B: starting from concentration plot in panel A the final number of copies in RNA sample was calculated (black boxes) while initial spiked copies are represent by black rhombus. The ratio between total cel-miR-39 copies in RNA samples and starting spiked copies of cel-miR-39 was calculated. Panel D, the real miR-221 concentration (fMolar) in RNA samples (white boxes) and the estimated miRNA concentration (black rhombus) in plasma samples was calculated.

in

the plasma in the range 0,1 fM-100 fM. Also a no spiked sample was prepared to analyse the physiological amount of miR, present in the starting sample of plasma, considering that the three selected miRNA are normally expressed, also in heathy subjects, even at different levels. Spiked plasma was divided as follows: 1,3 mL of sample was sent to INBB in order to perform analysis with ULTRAPLACAD devices, while 0,5 mL were employed in our laboratory to perform a triplicate extraction of the sample and quantify miRNA content by ddPCR. The work-flow of the experiment is described in the panel A of the **Figure 16**. MiRNA increase was found directly proportional to the amount of spiked miRNA, and miRNA concentration values were reported in concentration plot showed in the panel C. The ratio between the spiked sample copy/µL and the no-spiked miRNA concentration, expressed also in this case as copy/µL, was calculated (**Panel D**). As shown in concentration plot (**Panel C**), miR-221 content in control sample (no-spiked) is low but still detectable by ddPCR, while spiked points are directly proportional to the amount of spiked miR-221, until 0,1 fM in which the increase is very limited. A graphical representation of the different concentration of miRNA between samples was reported in **Panel B**. As previously said, we need to express data as miRNA concentration (copies/µL) in plasma samples. So to bring back data to plasma samples, was essential in this case, to known how much sample was lost during the extraction phase. So for each sample the yield was calculated making the ratio between the starting amount of spiked cel-miR-39, and copies recovered in the RNA sample (Figure 17). As reported in the panel C, on average, the real amount of miRNA in plasma sample is 306 times more concentrated respect to the calculated due to the loss of sample in extraction phase. The real concentration of miRNA in RNA sample and the estimated concentration in plasma samples are shown in the table and in the plot presented in panel D.

4. Plasma from CRC patients analysis

The final goal of this part of the thesis was the analysis of plasma samples in order to verify the efficiency of ULTRAPLACAD device. Even in this case data obtained by NESPRI analysis are compared with selected miRNAs concentration determined by ddPCR. For this reason, 32 samples of plasma collected from CRC patients were analysed and characterized for their miR-141, miR-221 and miR-222 content (**Table 1**). Moreover, 8 healthy subjects and a pool composed by plasma from six healthy donors, different from the 8 individually considered, were analysed, in order to establish a 'physiological' miRNAs pattern (**Table 2**). Data were reported as a) miRNA copy/µL for each reaction well (first

column), b) miRNA concentration in RNA samples (expressed as copies/µL) and finally, c) estimated concentration in plasma starting sample (third column), calculated considering the

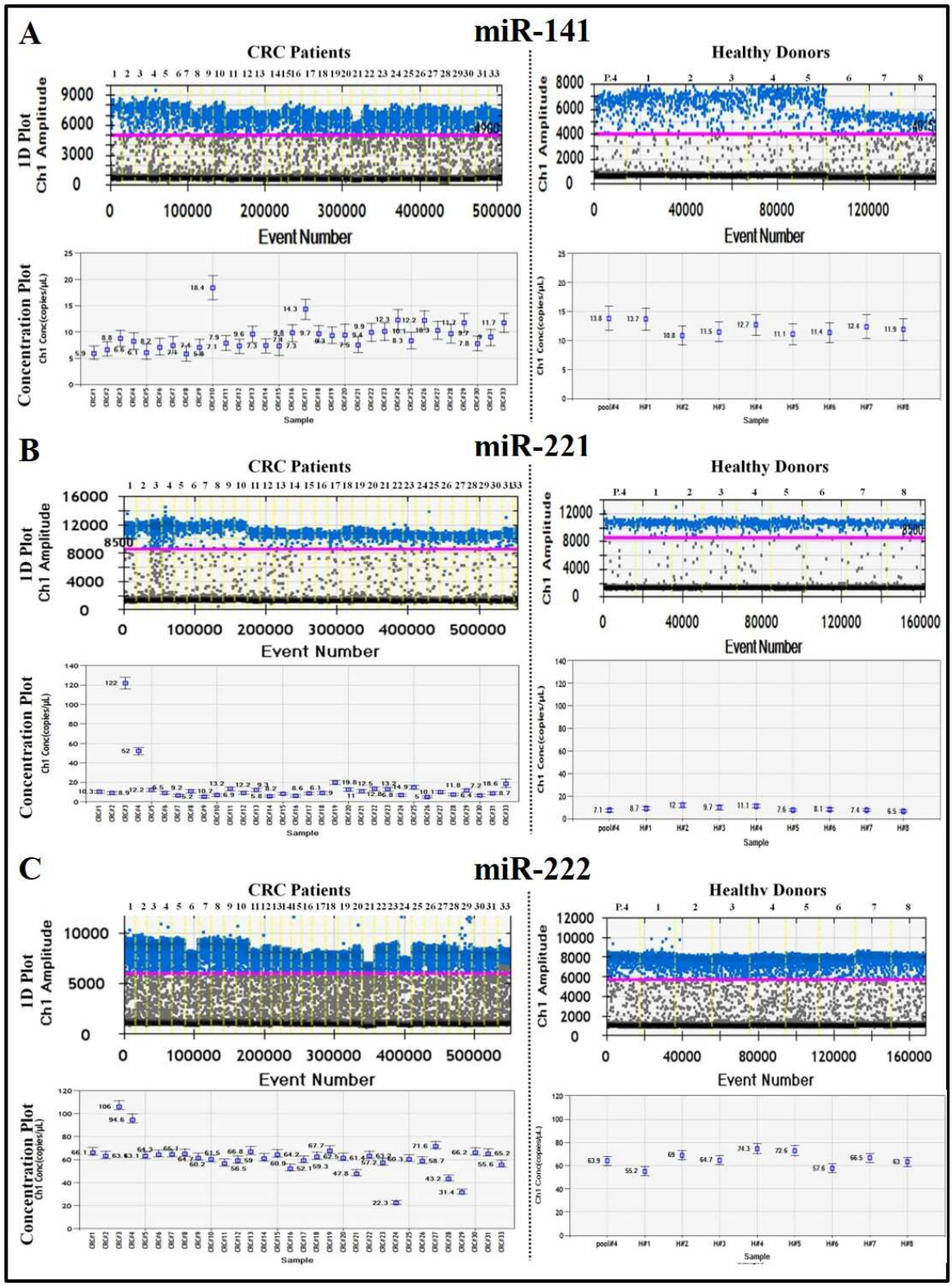

Figure 18. ddPCR plot from CRC and healthy donor plasma samples. Left part of the Figure 1D plot and concentration plot obtained for the 32 CRC samples, for each selected miRNA. Right part of the Figure 1D plot and concentration plot obtained for the 8 individually analysed healthy donor and the pooled sample of healthy donors. 1D plot ranks droplets into two different group: droplets in which amplification takes place (blue points) and droplets in which target amplification have occurred (black points), while in concentration plot, concentration of each sample expressed as copy/µL for each reaction well is shown.

	Hsa-miR-141-3p				Hsa-miR-221-3p				Hsa-miR-222-3p			
	Copy/µL per well	Copy/µL in RNA	Estimated Copy/µL in plasma		Copy/µL per well	Copy/µL in RNA	Estimated Copy/µL in plasma		Copy/µL per well	Copy/µL in RNA	Estimated Copy/µL in plasma	
CRC#1	5,90E+00	8,65E+01	3,67E+04	*SD ± 7,04E+03*	1,03E+01	1,16E+03	4,93E+05	*SD ± 9,45E+04*	6,61E+01	7,46E+03	3,16E+06	*SD ± 6,06E+05*
CRC#2	6,60E+00	9,68E+01	4,10E+04	*SD ± 7,87E+03*	8,90E+00	1,00E+03	4,26E+05	*SD ± 8,17E+04*	6,31E+01	7,12E+03	3,02E+06	*SD ± 5,79E+05*
CRC#3	8,80E+00	1,29E+02	5,47E+04	*SD ± 1,05E+04*	1,22E+02	1,38E+04	5,84E+06	*SD ± 1,12E+06*	1,06E+02	1,20E+04	5,07E+06	*SD ± 9,72E+05*
CRC#4	8,20E+00	1,20E+02	5,10E+04	*SD ± 9,78E+03*	5,20E+01	5,87E+03	2,49E+06	*SD ± 4,77E+05*	9,50E+01	1,07E+04	4,54E+06	*SD ± 8,72E+05*
CRC#5	7,70E+00	1,13E+02	4,79E+04	*SD ± 9,18E+03*	1,22E+01	1,38E+03	5,84E+05	*SD ± 1,12E+05*	6,31E+01	7,12E+03	3,02E+06	*SD ± 5,79E+05*
CRC#6	7,10E+00	1,04E+02	4,42E+04	*SD ± 8,47E+03*	9,20E+00	1,04E+03	4,40E+05	*SD ± 8,44E+04*	6,43E+01	7,25E+03	3,08E+06	*SD ± 5,90E+05*
CRC#7	7,40E+00	1,09E+02	4,60E+04	*SD ± 8,83E+03*	6,50E+00	7,33E+02	3,11E+05	*SD ± 5,96E+04*	6,47E+01	7,30E+03	3,09E+06	*SD ± 5,94E+05*
CRC#8	5,80E+00	8,51E+01	3,61E+04	*SD ± 6,92E+03*	1,07E+01	1,21E+03	5,12E+05	*SD ± 9,82E+04*	6,51E+01	7,34E+03	3,11E+06	*SD ± 5,97E+05*
CRC#9	7,10E+00	1,04E+02	4,42E+04	*SD ± 8,47E+03*	5,20E+00	5,87E+02	2,49E+05	*SD ± 4,77E+04*	6,15E+01	6,94E+03	2,94E+06	*SD ± 5,64E+05*
CRC#10	1,84E+01	2,70E+02	1,14E+05	*SD ± 2,19E+04*	6,90E+00	7,78E+02	3,30E+05	*SD ± 6,33E+04*	6,02E+01	6,79E+03	2,88E+06	*SD ± 5,52E+05*
CRC#11	7,90E+00	1,16E+02	4,91E+04	*SD ± 9,42E+03*	1,32E+01	1,49E+03	6,31E+05	*SD ± 1,21E+05*	5,65E+01	6,37E+03	2,70E+06	*SD ± 5,18E+05*
CRC#12	7,30E+00	1,07E+02	4,54E+04	*SD ± 8,71E+03*	9,30E+00	1,05E+03	4,45E+05	*SD ± 8,53E+04*	5,90E+01	6,66E+03	2,82E+06	*SD ± 5,41E+05*
CRC#13	9,60E+00	1,41E+02	5,97E+04	*SD ± 1,14E+04*	1,22E+01	1,38E+03	5,84E+05	*SD ± 1,12E+05*	6,68E+01	7,54E+03	3,20E+06	*SD ± 6,13E+05*
CRC#14	7,40E+00	1,09E+02	4,60E+04	*SD ± 8,83E+03*	5,80E+00	6,54E+02	2,77E+05	*SD ± 5,32E+04*	6,09E+01	6,87E+03	2,91E+06	*SD ± 5,59E+05*
CRC#15	7,30E+00	1,07E+02	4,54E+04	*SD ± 8,71E+03*	8,20E+00	9,25E+02	3,92E+05	*SD ± 7,52E+04*	6,43E+01	7,25E+03	3,08E+06	*SD ± 5,90E+05*
CRC#16	9,80E+00	1,44E+02	6,09E+04	*SD ± 1,17E+04*	6,10E+00	6,88E+02	2,92E+05	*SD ± 5,60E+04*	5,21E+01	5,88E+03	2,49E+06	*SD ± 4,78E+05*
CRC#17	1,43E+01	2,10E+02	8,89E+04	*SD ± 1,71E+04*	8,60E+00	9,70E+02	4,11E+05	*SD ± 7,89E+04*	5,93E+01	6,69E+03	2,84E+06	*SD ± 5,44E+05*
CRC#18	9,70E+00	1,42E+02	6,03E+04	*SD ± 1,16E+04*	9,00E+00	1,02E+03	4,31E+05	*SD ± 8,26E+04*	6,25E+01	7,05E+03	2,99E+06	*SD ± 5,73E+05*
CRC#19	9,30E+00	1,36E+02	5,78E+04	*SD ± 1,11E+04*	1,98E+01	2,23E+03	9,47E+05	*SD ± 1,82E+05*	6,78E+01	7,65E+03	3,24E+06	*SD ± 6,22E+05*
CRC#20	9,40E+00	1,38E+02	5,85E+04	*SD ± 1,12E+04*	1,25E+01	1,41E+03	5,98E+05	*SD ± 1,15E+05*	6,15E+01	6,94E+03	2,94E+06	*SD ± 5,64E+05*
CRC#21	7,50E+00	1,10E+02	4,66E+04	*SD ± 8,94E+03*	1,10E+01	1,24E+03	5,26E+05	*SD ± 1,01E+05*	4,78E+01	5,39E+03	2,29E+06	*SD ± 4,39E+05*
CRC#22	9,90E+00	1,45E+02	6,16E+04	*SD ± 1,18E+04*	1,32E+01	1,49E+03	6,31E+05	*SD ± 1,21E+05*	6,32E+01	7,13E+03	3,02E+06	*SD ± 5,80E+05*
CRC#23	1,01E+01	1,48E+02	6,28E+04	*SD ± 1,20E+04*	1,28E+01	1,44E+03	6,12E+05	*SD ± 1,17E+05*	5,72E+01	6,45E+03	2,74E+06	*SD ± 5,25E+05*
CRC#24	1,23E+01	1,80E+02	7,65E+04	*SD ± 1,47E+04*	6,80E+00	7,67E+02	3,25E+05	*SD ± 6,24E+04*	2,23E+01	2,52E+03	1,07E+06	*SD ± 2,05E+05*
CRC#25	8,30E+00	1,22E+02	5,16E+04	*SD ± 9,90E+03*	1,49E+01	1,68E+03	7,13E+05	*SD ± 1,37E+05*	6,03E+01	6,80E+03	2,88E+06	*SD ± 5,53E+05*
CRC#26	1,22E+01	1,79E+02	7,59E+04	*SD ± 1,46E+04*	5,00E+00	5,64E+02	2,39E+05	*SD ± 4,59E+04*	5,87E+01	6,62E+03	2,81E+06	*SD ± 5,39E+05*
CRC#27	1,03E+01	1,51E+02	6,41E+04	*SD ± 1,23E+04*	1,01E+01	1,14E+03	4,83E+05	*SD ± 9,27E+04*	7,16E+01	8,08E+03	3,43E+06	*SD ± 6,57E+05*
CRC#28	9,70E+00	1,42E+02	6,03E+04	*SD ± 1,16E+04*	7,20E+00	8,12E+02	3,44E+05	*SD ± 6,61E+04*	4,32E+01	4,87E+03	2,07E+06	*SD ± 3,96E+05*
CRC#29	1,17E+01	1,72E+02	7,28E+04	*SD ± 1,40E+04*	1,18E+01	1,33E+03	5,64E+05	*SD ± 1,08E+05*	3,14E+01	3,54E+03	1,50E+06	*SD ± 2,88E+05*
CRC#30	7,80E+00	1,14E+02	4,85E+04	*SD ± 9,30E+03*	6,40E+00	7,22E+02	3,06E+05	*SD ± 5,87E+04*	6,62E+01	7,47E+03	3,17E+06	*SD ± 6,07E+05*
CRC#31	9,00E+00	1,32E+02	5,60E+04	*SD ± 1,07E+04*	8,70E+00	9,82E+02	4,16E+05	*SD ± 7,98E+04*	6,54E+01	7,38E+03	3,13E+06	*SD ± 6,00E+05*
CRC#33	1,17E+01	1,72E+02	7,28E+04	*SD ± 1,40E+04*	1,86E+01	2,10E+03	8,90E+05	*SD ± 1,71E+05*	5,56E+01	6,27E+03	2,66E+06	*SD ± 5,10E+05*

Table 1. Determination of miR-141, miR-221 and miR-222 concentration in plasma from CRC patients. The concentration of the three selected miRNAs was calculated for each sample. Data are relative to each reaction well (first column), to miRNAs concentration in RNA sample (second column) and to miRNAs concentration in plasma samples (third column). As regard miRNA concentration in plasma samples, the amount of present miRNA was estimated. In fact, the possible loss of sample due to extraction method, was considered and calculated, evaluating the average loss of spike cel-miR-39. All data are expressed as copies/µL.

	Hsa-miR-141-3p				Hsa-miR-221-3p				Hsa-miR-222-3p			
	Copy/µL per well	Copy/µL in RNA	Estimated Copy/µL in plasma		Copy/µL per well	Copy/µL in RNA	Estimated Copy/µL in plasma		Copy/µL per well	Copy/µL in RNA	Estimated Copy/µL in plasma	
Pool#4	1,27E+01	1,86E+02	7,90E+04	*SD ± 1,51E+04*	6,50E+00	7,33E+02	3,11E+05	*SD ± 5,96E+04*	5,94E+01	6,70E+03	2,84E+06	*SD ± 5,45E+05*
H #1	1,27E+01	1,86E+02	7,90E+04	*SD ± 1,51E+04*	8,40E+00	9,48E+02	4,02E+05	*SD ± 7,71E+04*	4,96E+01	5,60E+03	2,37E+06	*SD ± 4,55E+05*
H #2	9,70E+00	1,42E+02	6,03E+04	*SD ± 1,16E+04*	1,13E+01	1,27E+03	5,41E+05	*SD ± 1,04E+05*	6,30E+01	7,11E+03	3,01E+06	*SD ± 5,78E+05*
H #3	1,01E+01	1,48E+02	6,28E+04	*SD ± 1,20E+04*	9,00E+00	1,02E+03	4,31E+05	*SD ± 8,26E+04*	5,89E+01	6,65E+03	2,82E+06	*SD ± 5,40E+05*
H #4	1,12E+01	1,64E+02	6,96E+04	*SD ± 1,34E+04*	1,03E+01	1,16E+03	4,93E+05	*SD ± 9,45E+04*	6,85E+01	7,73E+03	3,28E+06	*SD ± 6,28E+05*
H #5	9,70E+00	1,42E+02	6,03E+04	*SD ± 1,16E+04*	7,40E+00	8,35E+02	3,54E+05	*SD ± 6,79E+04*	6,70E+01	7,56E+03	3,21E+06	*SD ± 6,15E+05*
H #6	8,70E+00	1,28E+02	5,41E+04	*SD ± 1,04E+04*	7,70E+00	8,69E+02	3,68E+05	*SD ± 7,06E+04*	5,26E+01	5,93E+03	2,52E+06	*SD ± 4,83E+05*
H #7	9,10E+00	1,33E+02	5,66E+04	*SD ± 1,09E+04*	6,90E+00	7,78E+02	3,30E+05	*SD ± 6,33E+04*	6,14E+01	6,93E+03	2,94E+06	*SD ± 5,63E+05*
H #8	8,20E+00	1,20E+02	5,10E+04	*SD ± 9,78E+03*	6,10E+00	6,88E+02	2,92E+05	*SD ± 5,60E+04*	5,84E+01	6,59E+03	2,79E+06	*SD ± 5,36E+05*
Healthy Average			6,36E+04				3,91E+05				2,86E+06	

Table 2. Determination of miR-141, miR-221 and miR-222 concentration in plasma from healthy donor. The concentration of the three selected miRNAs was calculated for 8 individually analysed healthy donors, and for a pool sample obtained by pooling plasma from 6 different healthy subjects, different from the 8 individually analysed subjects. Data are relative to each reaction well (first column), to miRNAs concentration in RNA sample (second column) and to miRNAs concentration in plasma samples (third column). As regard miRNA concentration in plasma samples, the amount of present miRNA was estimated. In fact, the possible loss of sample due to extraction method was considered and calculated, evaluating the average loss of spike cel-miR-39. All data are expressed as copies/µL.

average recovery of cel-miR-39, in order to compare data with ULTRAPLACAD device. As demonstrated in the tables miR-141 is the less expressed in plasma sample, and the difference is in the order of 10^1 compared with miR-221, while is even greater (10^2), if the comparison is performed between miR-141 and miR-222, which is the most expressed miRNA in the plasma both of CRC patients and healthy donor. Is important to underline, that, even if we have employed a high sensitive technique as ddPCR, to obtain significative miR-141 concentration in the reaction well, the employment of a higher amount of cDNA was necessary. DdPCR plots obtained for all the 32 CRC samples (left part of the **Figure 18**) and for the 8 healthy samples and the pool of healthy donor (right part of the Figure 18) were reported in Figure 18. Comparing miRNAs concentration between healthy subjects and CRC patients, only seven CRC patients present a clear difference in miRNA concentration for at least one of the three analysed miRNAs. Is so clear that, despite the several literature available works propose the three selected miRNAs as good CRC markers, considering the high interpersonal variability, analyse only three miRNAs is not enough and further investigations to identify miRNAs modulated in all CRC patients are required.

5. Conclusions and take-home messages

The conclusions of this part of the thesis are related to two major fields of investigation: (a) the analysis of microRNAs in plasma from colon cancer (CRC) patients and (b) the analysis of miRNAs in plasma isolated from experimental mice xenotransplanted with colon cancer tumor cell lines. The important methodological objective related to threshold sensitivity and comparison between RT-qPCR and RT-ddPCR has been assessed.

A. Set-up of spiking experiments: human donor plasma spiked with microRNAs, extraction of miRNAs and identification of miRNA levels and recovery by quantitative PCR. We spiked specific miRNAs (miR-141, miR-221 and miR-222) in such a way that the resulting plasma contains miRNA concentrations ranging from 40 attomoles to 40 fmoles. These samples were tested for miRNA content using the Biorad CFX 96 Touch RT-qPCR system.

B. First experiments of ddPCR on RNA extracted from donor plasma and from plasma spiked with different quantities of microRNAs. We performed set-up experiments in order to define the protocol for ddPCR amplification and quantitation of endogenous and spiked

microRNA in healthy human plasma samples. We have confirmed the ddPCR limit of detection ranking in the attomolar range.

C. MiR-141, miR-221 and miR-222 quantification in plasma from donors and from CRC patients. Using plasma obtained from 32 CRC patients, we performed set-up experiments in order to define the protocol for ddPCR amplification and quantitation of endogenous a microRNA in CRC patients and healthy human plasma samples. MiR-221 and miR-222 are always detectable using our protocol but miR-141 content is very low (almost undetectable) in plasma of all patients analysed.

D. Establishment of the biological mini-bank. The mini-bank is constituted by biological material to be shared with other ULTRAPLACAD project members, including miRNAs extracted from cell lines, plasmas, spiked plasmas and RNA samples both from CRC patients and healthy donors.

E. Analysis of miRNAs in mouse plasma from mice xenotransplanted with validated cells. Circulating miRNA levels did show variability among experiments, cell lines and specific miRNAs but they were invariably detected, often at higher levels, in mice carrying xenografts as compared to untreated, tumor-free mice ("healthy controls"). The results show that miRNA can be detected in the blood of mice using the protocols employed by the ULTRAPLACAD consortium.

F. Analysis of miRNAs in supernatants of CRC cells used for the production of xenotransplanted mice. MiRNAs (miR-141, miR-221 and miR-222) were assessed in cell culture supernatants. Results indicate that specific miRNAs were always detected but the microRNA pattern released by the cells is slightly different from the miRNA patter present within the cells.

G. Analysis of miRNAs in mouse plasma from mice xenotransplanted with validated cells comparing RT-qPCR and ddPCR. The results show that miRNA can be detected in the blood of mice and moreover, the two analytical approaches (RTqPCR and ddPCR) gave comparable results.

The following general conclusions might be considered.

Degradation of spiked material was detected in plasma. A solution was proposed and validated: use of RNase inhibitor to be added to the plasma samples before spiking. In

addition, the methods for plasma preparation and miRNA extraction are key steps for miRNA detection and comparison.

MiRNAs in plasma from CRC patients. This key issue might require in the future to focus, in fact, in addition to miR-141, miR-221 and miR-222 also to others (less than 6-7) miRNA sequences are needed to identify patterns associated to CRC patients. MiR-141 content is very low in plasma of patients. Collecting plasma from patients with colon cancer in an advanced stadium (for example grade IV cancer) will allow a final conclusion on this issue.

Xenografted mice. Mice xenografted with tumor cell lines have been generated and validated as a very useful model system for miRNA evaluation using alternative technologies.

II. MicroRNA for non invasive monitoring: miRNAs as possible biomarkers for the detection of autologous blood transfusions

In this part of the PhD Thesis the analysis of miRNAs was not applied to a health problem (as in the case of miRNA-based liquid biopsy of CRC), but to a very important issue that involves a large field of human society, i.e. the identification of frauds in sport. We focused here on the miRNA-based detection of autologous blood transfusion in sports.

Autologous blood transfusion (ABT) is an illicit practice used by several athletes to improve their performances. Despite this practice was introduced more than forty years ago, at the moment not definitive tests have been developed to detect ABT in sports. In fact, in the last few years several possible markers for direct or indirect detection of ABT have been proposed, but none of these was shown to be sufficiently reliable. As previously stated in the Introduction section and in part I of the Results, miRNAs have been proposed as possible biomarkers in several diseases. Accordingly, few unconclusive reports are available in the literature suggesting that these molecules may be employed to detect a change in physiological condition as in the case of ABT. First preliminary studies were already performed by Leuenberger and colleagues demonstrating that a panel of miRNAs are modulated after blood reinfusion. The main goal of our project is the identification of miRNAs that can be potentially employed as biomarkers for the detection of ABT as illicit practice in sport.

2.1 Study design

In order to verify possible miRNAs expression changes during the ABT procedure, 24 healthy athletes were enrolled and were randomized into two groups: transfusion (T) and control (C). Subjects of both groups presented similar anthropometric characteristics as age (25 ± 3 years for T group and 23 ± 2 years for control group), height, weight and body mass, similar training hours and similar performance-related parameters (**Table 3**). Moreover, only no smoker subjects were included in the study and for the whole duration of the study athletes were asked to avoid also occasional smoking. For both groups blood was collected following the schedule indicated in the **Figure 19**: T1 (-40): blood was collected 40 days before the

blood reinfusion: at this point no intervention was performed in athletes, so this time point is indicative of the 'basal' conditions of each subjects.

	Transfusion (n = 12)	Control (n = 12)
Antropometric		
Age (years)	25 ± 3	23 ± 2
Heigth (m)	1.79 ± 0.07	1.77 ± 0.05
Weigth (kg)	79 ± 11	70 ± 6
Body mass index (kgm^{-2})	24.6 ± 3.4	22.3 ± 2.2
Sport discipline		
Training hours/week	8 ± 3	7 ± 3
Sport vintage (years)	15 ± 5	13 ± 7
Performance		
Anaerobic threshold (ml/kg/min)	39.2 ± 8.3	40.6 ± 6.5
VO_2max (ml/kg/min)	56.7 ± 9.2	59.1 ± 6.1
Total running time (s)	846 ± 234	905 ± 86

Table 3. Anthropometric characteristics of recruited athletes. In the table were reported the principal anthropometric characteristics of the athletes that have taken part to the study.

At this time point a physical test to verify athletes performances was performed. Blood withdrawal was performed at T2 (-35): 35 days before blood reinfusion. 450 ml of whole blood were collected from each subject part of transfusion (T) group. Collected blood was stored at +4°C (6 subjects) or cryopreserved at -80°C after appropriate treatment (6 subjects). In respect to the control group, only 18 mL of blood needed for plasma isolation were collected. It is important to underline that also for transfusion group, 18 ml of blood were collected for plasma isolation at T2 (-35) and in this case, the collection was performed before blood withdrawal. 25 days and 15 days before blood reinfusion, respectively: T3 (-25) and T4 (-15) another aliquot (18 mL) of blood was collected both by T and C groups, to verify possible effects of blood withdrawal in miRNA expression. At T5 (0) T group athletes underwent to ABT while no interventions were performed in control group. 18 mL of blood were collected from both T and C group to isolate plasma, in the case of T group blood for plasma isolation was collected before blood reinfusion. As regard +4°C refrigerated blood it was heated at 37°C and then reinfused, while cryopreserved blood was carefully treated to eliminate cryopreserving compound before reinfusion. Others aliquots of whole blood were taken from both groups 3, 6, 15 and 35 days after the reinfusion corresponding respectively at T6 (+3), T7 (+6), T8 (+15) and T9 (+35) time points. At T3 (-25) and T8 (+15), blood

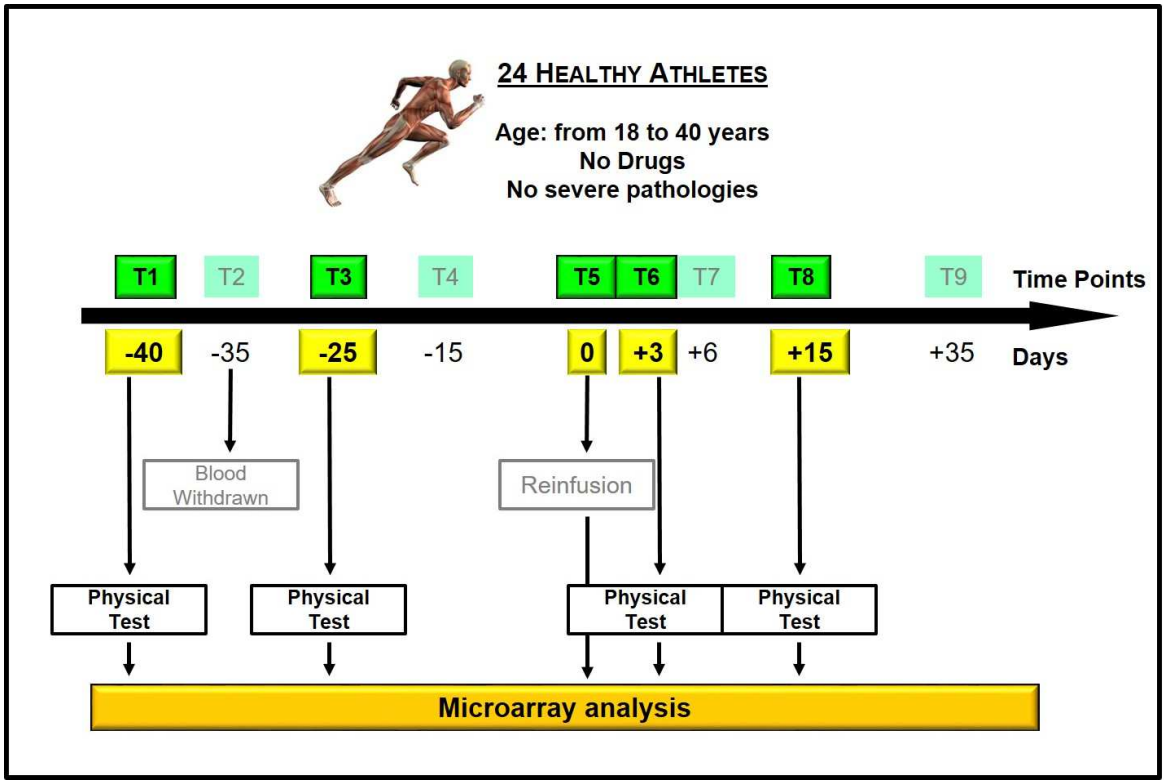

Figure 19. Study design. 24 healthy athletes were enrolled and divided randomly into two groups: T, transfused (12 subjects) which underwent to blood withdrawal and reinfusion and C control (12 subjects) in which no intervention was performed. Whole blood was collected at 9 time points. At each time point, 18 ml of whole blood were collected and processed within an hour to isolate plasma. In four key time points a physical test was performed to evaluate athlete's performances and the effects of blood manipulations. Plasma isolated from five time points (T1, T3, T5, T6 and T8), was analysed for miRNAs expression by microarray analysis.

collection was also, associated to a physical test to evaluate possible changes in performances. Five key time points were selected to perform microarray analysis in a limited number of subjects: 3 pools of healthy donors, each one composed by plasma isolated from 3 subjects and 6 samples collected by athletes that underwent to ABT and more in detail: 3 athletes reinfused with blood stored at +4°C and 3 athletes reinfused with cryopreserved blood.

2.2 Plasma biobank preparation

The first step of the study was the preparation of a biobank composed by plasma aliquots isolated from each subjects at time points previously described. About 18 mL of whole blood were collected from each subject at each time point and were processed within an hour after the collection. The same plasma isolation protocol was employed for each sample and 800 µl aliquots of plasma were prepared for each subject. As indicated in **Table 4**, more than 2000 aliquots of plasma were produced. Our biobank includes an average of

118 aliquots of plasma for each time point as regard control group and more than 1000 aliquots considering all the 12 control subjects for the nine time points. The same number of aliquots was reached with transfusion group, in this case about 500 plasma aliquots have been obtained by athletes that were reinfused with blood conserved at +4°C and a similar number was reached for athletes reinfused with cryopreserved blood.

WADA-UNIFE ABT plasma Biobank									
source	Time points								
	T1 (-40)	T2 (-35)	T3 (-25)	T4 (-15)	T5 (0)	T6 (+3)	T7 (+6)	T8 (+15)	T9 (+35)
Control untrained athletes									
01C	8	10	10	10	10	10	10	10	9
03C	9	9	10	10	10	10	10	10	10
05C	10	10	11	10	10	10	10	10	10
07C	10	10	10	10	9	10	10	10	10
09C	10	10	10	10	11	10	10	10	10
11C	11	10	9	10	10	10	10	10	10
13C	9	10	10	5	10	10	9	10	10
15C	10	10	10	10	10	10	10	10	10
17C	10	10	10	10	11	9	10	10	9
19C	10	10	9	10	10	10	10	10	10
21C	8	10	9	9	10	10	10	10	10
23C	11	10	10	10	10	10	10	10	9
12 athletes	**116**	**119**	**114**	**121**	**121**	**119**	**119**	**120**	**117**
ABT-trained athletes (blood storage 4°C)									
02T	7	10	9	10	9	8	9	7	10
04T	10	10	10	10	10	10	10	10	10
20T	10	11	10	10	9	9	10	9	10
22T	10	10	10	10	10	10	10	8	10
24T	10	11	8	10	9	7	10	9	10
26T	10	10	10	10	10	11	10	10	10
6 athletes	**57**	**62**	**57**	**60**	**57**	**55**	**59**	**53**	**60**
ABT-trained athletes (blood storage -80°C)									
06T	10	10	11	10	10	10	10	10	10
08T	10	11	10	10	11	10	10	9	10
10T	10	10	10	11	10	10	10	10	10
12T	9	11	10	10	9	8	10	10	9
14T	9	10	8	10	9	8	10	7	10
16T	9	9	9	10	9	9	10	8	10
6 athletes	**57**	**61**	**58**	**61**	**58**	**55**	**60**	**54**	**59**

Table 4. Plasma Biobank. More than 2000 aliquots of plasma are prepared from whole blood and collected from control (C) and transfused (T) subjects. All plasma samples were prepared following the same protocol: 1200g for 10 minutes, followed by a second centrifugation of collected plasma at 2400g for 20 minutes. All plasma samples were stored at -80°C.

2.3 Analysis of miRNAs related to HbF and erythroid differentiation

Three control-pooled samples, each one composed by three subjects who did not undergo to blood withdrawal and reinfusion and six samples obtained from subjects who underwent reinfusion were analysed through microarray technology. With respect to T group five key time points were considered: T1 (-40), T3 (-25), T5 (0), T6 (+3) and T8 (+15), while for C group only three points were considered T3 (-25), T6 (-25) and T8 (+15), considering that in these subjects no blood manipulation was performed, and therefore all miRNAs changes were due to 'physiological' variation. A first analysis was conducted considering a limited list of miRNAs. In fact, we started from the hypothesis that the two key phases of ABT: blood withdrawal and reinfusion produce a change in oxygen availability, and consequently several parameters associated to oxygen levels can be affected. Several studies correlate hypoxic state with both the increase of fetal haemoglobin production and the erythropoiesis induction [*Haase et al., 2013; Risso et al., 2012*]. For this reason, we focused our attention on miRNAs that were shown in literature to be correlated with erythroid differentiation and/or fetal haemoglobin production.

2.3.1 List of miRNAs potentially candidates for ABT detection

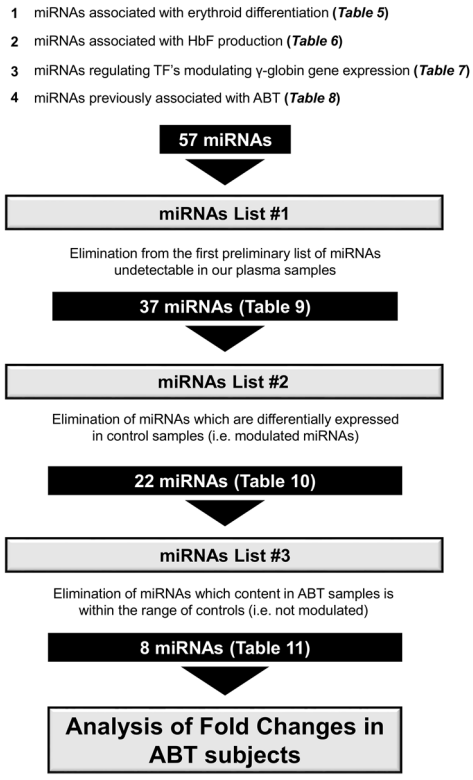

Figure 20. Work-flow for miRNAs list selection. Considering different parameters (Table 3-6) 57 miRNAs were selected. Considering different parameters, a final list (Table 9) of 12 miRNAs was identified.

As previously stated, the first analysis for the identification of possible miRNAs associated with ABT as doping practice was performed considering a limited list of miRNAs. The list has been drawn up considering several parameters that are summarized in the work-flow presented in the **Figure 20**. First of all, starting from data available in literature, and using miRTarBase [*http://mirtarbase.mbc.nctu.edu.tw/*] a software that allow to identify all the miRNA targets already validated, we prepared four miRNAs lists. The first

microRNA	Reference
miR-107	*Ruan et al., Mol Med Rep, 2015*
miR-125a-3p	*Ganan-Gomez et al., PlosOne, 2014*
miR-126-3p	*Huang et al., Blood, 2011*
miR-144-3p	*Pase et al., Blood, 2009*
miR-146b-5p	*Zhai et al., J BioChem, 2014*
miR-150-5p	*Sun et al., Oncotarget, 2015*
miR-155-5p	*O'Connell et al., J Exp Med, 2008*
miR-191-3p	*Zhang et al., Genes Dev, 2011*
miR-199b-5p	*Li et al., Mol cells, 2014*
miR-210-3p	*Bianchi et al., BMB Reports, 2009*
miR-218-5p	*Li et al., In J Mol Sci, 2016*
miR-221-3p	*Gabbianelli et al., Haematologica, 2010*
miR-222-3p	*Gabbianelli et al., Haematologica, 2010*
miR-223-3p	*Felli et al, Haematologica, 2009*
miR-23a	*Zhu et al., Nucleic Acids Research, 2013*
miR-24-3p	*Wang et al., Nucleic Acids Research, 2014*
miR-27a-3p	*Wang et al., Nucleic Acids Research, 2014*
miR-320a	*Mittal et al., Int l J of bioch cell biology, 2013*
miR-376a	*Wang et al., Cell Res, 2011*
miR-451	*Kouhkan et al., Iran J Basoc Med, 2013*
miR-451a	*Pase et al., Blood, 2009*
miR-486-5p	*Wang et al., Blood, 2015*
miR-6087	*Yoo et al., Stem Cells Dev, 2012*
miR-92a -3p	*Li et al., Blood, 2010*
miR-99a-5p	*Emmrich et al., Genes Dev, 2014*

Table 5. MiRNAs associated to erythroid differentiation. In the table are listed miRNAs that was shown to be modulated in erythroid differentiation both in cellular models and in plasma samples.

list (**Table 5**) includes all miRNAs that, at the moment of the analysis, were shown to be associated to erythroid differentiation (26 miRNAs have been identified). The second list includes miRNAs which are shown to regulate gamma globin gene expression or are shown to be modulated during the fetal to adult haemoglobin switch (**Table 6**).

microRNA	Reference
Let-7 family	*Noh et al., J Transl Med, 2009*
miR-144-3p	*Fu et al., Blood, 2009*
miR-151-3p	*Pule, Clin Transl Med, 2016*
miR-26b-5p	*Alijani et al., Avicenna J Med Biotechnol, 2014*
miR-96-5p	*Azzouzi et al., PlosOne, 2011*

Table 6. MiRNAs involved in gamma globin expression. In the table were included miRNAs that were shown to regulate directly gamma globin mRNA expression or were shown to be involved in the switch from fetal to adult haemoglobin.

Moreover, starting from the evidence that γ-globin gene silencing is regulated by several transcription factors, including BCL11A [*Xua et al., 2013*], KLF-1 [*Borg et al., 2008*], Oct-1 [*Xu et al., 2009*], MYB [*Wahlberg et al., 2009*], SOX6 [*Xu et al., 2010*] and STAT3 [*Foley et al., 2002*], we also considered all miRNAs that are able to target mRNA, coding for these transcription factors (**Table 7**).

microRNA	Target	Reference
miR-30a-5p	*BCL11A*	*Jiang et al., Mol Cancer, 2013*
miR-486-3p		*Lulli et al., PlosOne, 2013*
miR-34a	*KLF-1*	*Ward et al., Exp Biol Med, 2016*
miR-15a-5p	*MYB*	*Sankaran et al., Protl Natl Acc Sci USA, 2011*
miR-150-5p		*Xiao et al., Cell, 2007*
miR-16-5p		*Sankaran et al., Protl Natl Acc Sci USA, 2011*
miR-34a-5p		*Navarro et al., Blood, 2009*
miR-1185-1-3p	*Oct-1*	*Xiao et al., Oncol Lett, 2014*
miR-1467		*Xiao et al., Oncol Lett, 2014*
miR-3919		*Xiao et al., Oncol Lett, 2014*
miR-449a		*Liu et al., Oncotarget, 2016*
miR-4493		*Xiao et al., Oncol Lett, 2014*
miR-155-5p	*SOX6*	*Xie et al., Cancer, 2012*
miR-16-5p		*Zhu et al, Cell Physiol Biochem, 2014*
miR-208a-3p		*Ding et al., Nat Genet, 2015*
miR-208b		*Kim et al., Anim Genet, 2015*
miR-499		*Kim et al., Anim Genet, 2015*
miR-766-3p		*Li et al., Onco Targets Ther, 2015*
miR-34a	*STAT3*	*Ward et al., Exp Biol Med, 2016*

Table 7. MiRNAs targeting TFs involved in gamma globin expression. In this table are considered all miRNAs that were shown to target mRNA of transcription factors involved in gamma globin gene regulation.

In addition, two independent research group proposed two different lists of miRNAs as possible candidates as biomarkers for ABT detection, that we considered in our analysis (**Table 8**).

microRNA	Reference
let-7b-5p	*Leuenberger et al., PloSOne, 2013*
let-7d-5p	*Leuenberger et al., PloSOne, 2013*
let-7g-5p	*Leuenberger et al., PloSOne, 2013*
miR-103a-3p	*Leuenberger et al., PloSOne, 2013*
miR-142-3p	*Leuenberger et al., PloSOne, 2013*
miR-144-3p	*Donati et al., 2015*
mir-150-5p	*Donati et al., 2015*
miR-196a-5p	*Donati et al., 2015*
miR-197-3p	*Donati et al., 2015*
miR-26a-5p	*Leuenberger et al., PloSOne, 2013*
miR-26b-5p	*Leuenberger et al., PloSOne, 2013*
miR-30b-5p	*Leuenberger et al., PloSOne, 2013*
miR-30b-5p	*Donati et al., 2015*
miR-30c-5p	*Leuenberger et al., PloSOne, 2013*
miR-339-5p	*Leuenberger et al., PloSOne, 2013*
miR-451a	*Donati et al., 2015*
miR-923	*Donati et al., 2015*
miR-96-5p	*Donati et al., 2015*

Table 8. MiRNAs previously associated with ABT. In the table were reported miRNAs that in previously studies were proposed as ABT markers.

MiRNAs of the four lists were analysed in order to identify miRNAs common to all lists. As depicted in the Venn diagram proposed in the **Figure 21**, 25 miRNAs result to be involved in erythroid differentiation, while 13 miRNAs have been shown to regulate fetal haemoglobin production, 19 are able to target mRNA of transcription factors involving in γ-globin gene silencing and 18 were previously shown to be in some way related with autologous blood transfusion. One miRNA, miR-144-3p appears in three of the four lists, in fact, results to be involved in erythroid differentiation, is involved in fetal haemoglobin

expression and moreover, was shown to be related with ABT. Five miRNAs were found to be common to at least two of the four presented lists. MiR-150-5p and miR-155-5p result to be involved in erythroid differentiation and at same time are able to target the transcription factors, respectively MYB and SOX6. Instead, miR-451a results to be involved in erythroid differentiation and at same time it was shown to be modulated when ABT occurred. MiR-96-5p and miR-26b-5p are involved in fetal haemoglobin production and at same time miR-26a-5p was shown by Leuenberger and colleagues to be upregulated in athletes, which underwent to ABT. While miR-96-5p was found to be modulated during the blood storage by Donati and colleagues.

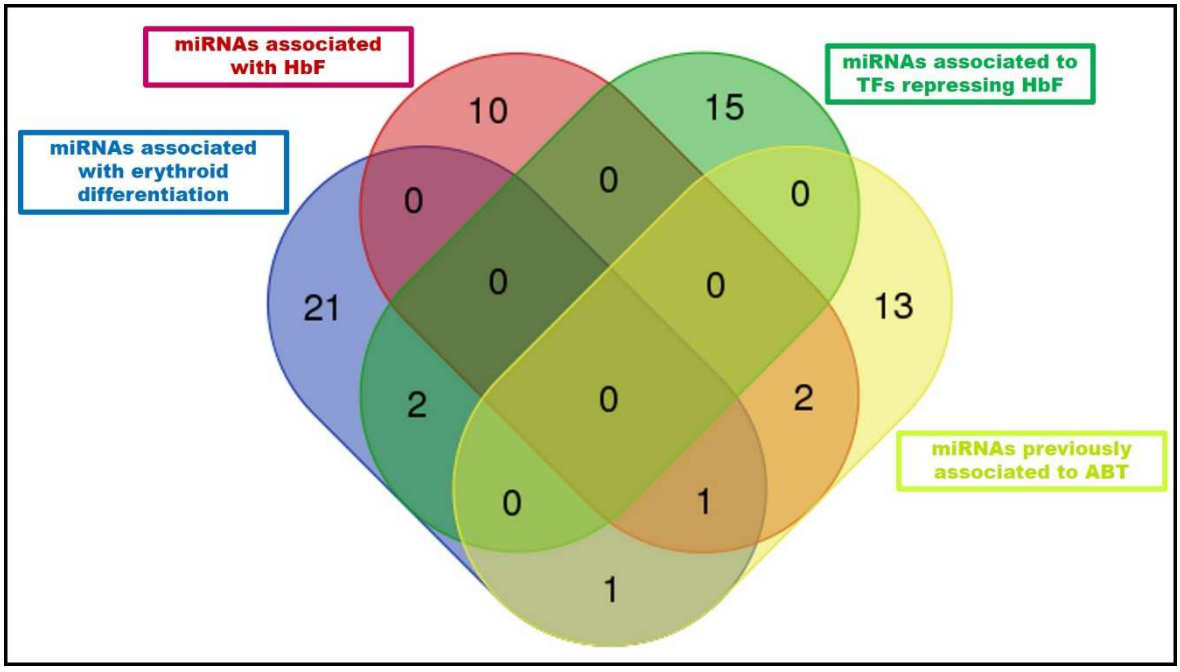

Figure 21. Venn diagram of the four miRNA lists. MiRNA contained in the previously presented miRNAs lists were considered. 25 miRNAs result to be associated to erythroid differentiation (blue circle), 13 miRNAs result to be related with HbF expression (pink circle), 19 miRNAs were found in literature to modulate the expression of TFs involved in gamma globin gene expression (green circle) and 14 miRNAs were previously found to be associated with ABT (yellow circle).

2.3.2 Identification of target miRNAs possibly modulated following ABT.

We obtained a final list composed by 57 miRs but not all miRNAs are detectable in our plasma sample, so, for example, miR-96-5p, miR-99a-5p, miR-146a-5p and several others, were excluded from the initial list. A new list including 37 miRNAs (**Table 9**) was obtained and further investigated to remove miRNAs which were differentially expressed at different time points in control samples. All miRNAs which presented a fold change higher than 3 between different time points of the same pool were considered intrinsically unstable

MicroRNA	Characteristics
let-7a-5p	miRNA associated with fetal hemoglobin
let-7b-5p	miRNA associated with fetal hemoglobin
let-7d-5p	miRNA associated with fetal hemoglobin
let-7e-5p	miRNA associated with fetal hemoglobin
let-7g-5p	miRNA associated with fetal hemoglobin
miR-103a-3p	miRNA associated with erythroid differentiation/hemopoiesis
miR-107	miRNA associated with erythroid differentiation/hemopoiesis
miR-1185-1-3p	miRNA regulating transcriptional repressors
miR-125a-3p	miRNA associated with erythroid differentiation/hemopoiesis
miR-126-3p	miRNA associated with erythroid differentiation/hemopoiesis
miR-142-3p	miRNA associated with erythroid differentiation/hemopoiesis
miR-144-3p	miRNA associated with fetal hemoglobin
miR-150-5p	miRNA associated with erythroid differentiation/hemopoiesis
miR-151a-3p	miRNA associated with fetal hemoglobin
miR-155-5p	miRNA associated with erythroid differentiation/hemopoiesis
miR-15a-3p	miRNA regulating transcriptional repressors
miR-16-5p	miRNA associated with erythroid differentiation/hemopoiesis
miR-191-3p	miRNA associated with erythroid differentiation/hemopoiesis
miR-197-3p	miRNA associated with erythroid differentiation/hemopoiesis
miR-210-3p	miRNA associated with erythroid differentiation/hemopoiesis
miR-221-3p	miRNA associated with erythroid differentiation/hemopoiesis
miR-223-3p	miRNA associated with erythroid differentiation/hemopoiesis
miR-23a	miRNA associated with erythroid differentiation/hemopoiesis
miR-24-3p	miRNA associated with erythroid differentiation/hemopoiesis
miR-26a-5p	miRNA associated with erythroid differentiation/hemopoiesis
miR-26b-5p	miRNA associated with fetal hemoglobin
miR-27a-3p	miRNA associated with erythroid differentiation/hemopoiesis
miR-30a-5p	miRNA regulating transcriptional repressors
miR-30b-5p	miRNA associated with erythroid differentiation/hemopoiesis
miR-320a	miRNA associated with erythroid differentiation/hemopoiesis
miR-34a-5p	miRNA regulating transcriptional repressors
miR-451a	miRNA associated with erythroid differentiation/hemopoiesis
miR-486-3p	miRNA regulating transcriptional repressors
miR-486-5p	miRNA associated with erythroid differentiation/hemopoiesis
miR-6087	miRNA associated with erythroid differentiation/hemopoiesis
miR-766-3p	miRNA regulating transcriptional repressors
miR-92a-3p	miRNA associated with erythroid differentiation/hemopoiesis

Table 9. **MiRNA list #1.** The first list was obtained considering all miRNAs reported in tables 3-6 and eliminating all miRNAs that are not expressed in our plasma samples or are expressed only in some samples. 37 miRNAs were identified.

and therefore were excluded. Following this criterion, 15 miRNAs were excluded and a new list composed by 22 miRNAs was obtained (**Table 10**).

miRNA	Features	Reference
let-7a-5p	miRNA associated with fetal haemoglobin	*Noh et al., J Transl Med, 2009*
let-7d-5p	miRNA associated with fetal haemoglobin	*Noh et al., J Transl Med, 2009*
let-7e-5p	miRNA associated with fetal haemoglobin	*Noh et al., J Transl Med, 2009*
let-7g-5p	miRNA associated with fetal haemoglobin	*Noh et al., J Transl Med, 2009*
miR-126-3p	miRNA associated with erythroid differentiation	*Huang et al., Blood, 2011*
miR-142-3p	miRNA previously associated with ABT	*Leuenberger et al., PloSOne, 2013*
miR-144-3p	miRNA associated with fetal haemoglobin	*Fu et al., Blood, 2009*
	miRNA previously associated with ABT	*Donati et al., 2015*
miR-150-5p	miRNA associated with fetal haemoglobin	*Pule, Clin Transl Med, 2016*
miR-191-3p	miRNA associated with erythroid differentiation	*Zhang et al., Genes Dev, 2011*
miR-197-3p	miRNA previously associated with ABT	*Donati et al., 2015*
miR-210-3p	miRNA associated with erythroid differentiation	*Bianchi et al., BMB Reports, 2009*
miR-320a	miRNA associated with erythroid differentiation	*Mittal et al., Int l J of bioch cell biology, 2013*
miR-486-3p	miRNA regulating transcriptional repressors	*Lulli et al., PlosOne, 2013*
miR-486-5p	miRNA associated with erythroid differentiation	*Wang et al., Blood, 2015*
miR-766-3p	miRNA regulating transcriptional repressors	*Li et al., Onco Targets Ther, 2015*
miR-92a -3p	miRNA associated with erythroid differentiation	*Li et al., Blood, 2010*

Table 10. MiRNA List #2. From the 37 miRNAs list were removed all miRNAs which were modulated at different time points in control subjects and a list of 22 miRNAs was obtained.

Moreover, all miRNAs which expression in ABT trained subjects was within the range of control samples values were excluded. In this way a final miRNAs list composed by 8 miRNAs was obtained (**Table 11**).

miRNA	Features	Reference
let-7a-5p	miRNA associated with fetal hemoglobin	*Noh et al., J Transl Med, 2009*
miR-126-3p	miRNA associated with erythroid differentiation	*Huang et al., Blood, 2011*
miR-144-3p	miRNA associated with fetal hemoglobin	*Fu et al., Blood, 2009*
miR-191-3p	miRNA associated with erythroid differentiation	*Zhang et al., Genes Dev, 2011*
miR-197-3p	miRNA associated with erythroid differentiation	*Donati et al., 2015*
miR-486-3p	miRNA regulating transcriptional repressors	*Lulli et al., PlosOne, 2013*
miR-486-5p	miRNA associated with erythroid differentiation	*Wang et al., Blood, 2015*
miR-92a-3p	miRNA associated with erythroid differentiation	*Li et al., Blood, 2010*

Table 11. MiRNAs list #3. From the previously list were excluded all miRNAs which expression was not modulated in ABT trained subjects respect to controls. Finally, 8 miRNAs were considered, and their expression was analysed in 6 ABT subjects.

The expression of the 8 selected miRNAs in ABT samples was analysed and data are reported in the heat map proposed in the **Figure 22**. For all the 8 miRNAs the fold change at T3 (-25), T6 (+3) and T8 (+15) was calculated respect to the respective T0 (-40) sample for each subject and data are reported in the **Table 12**. All fold changes are calculated as $2^{\wedge(T6(or\ T8\ or\ T3)-T1)}$. As reported in the Table 12, all T group subjects, excluded 16T, overexpressed, after the reinfusion at least one miRNA, part of the proposed list.

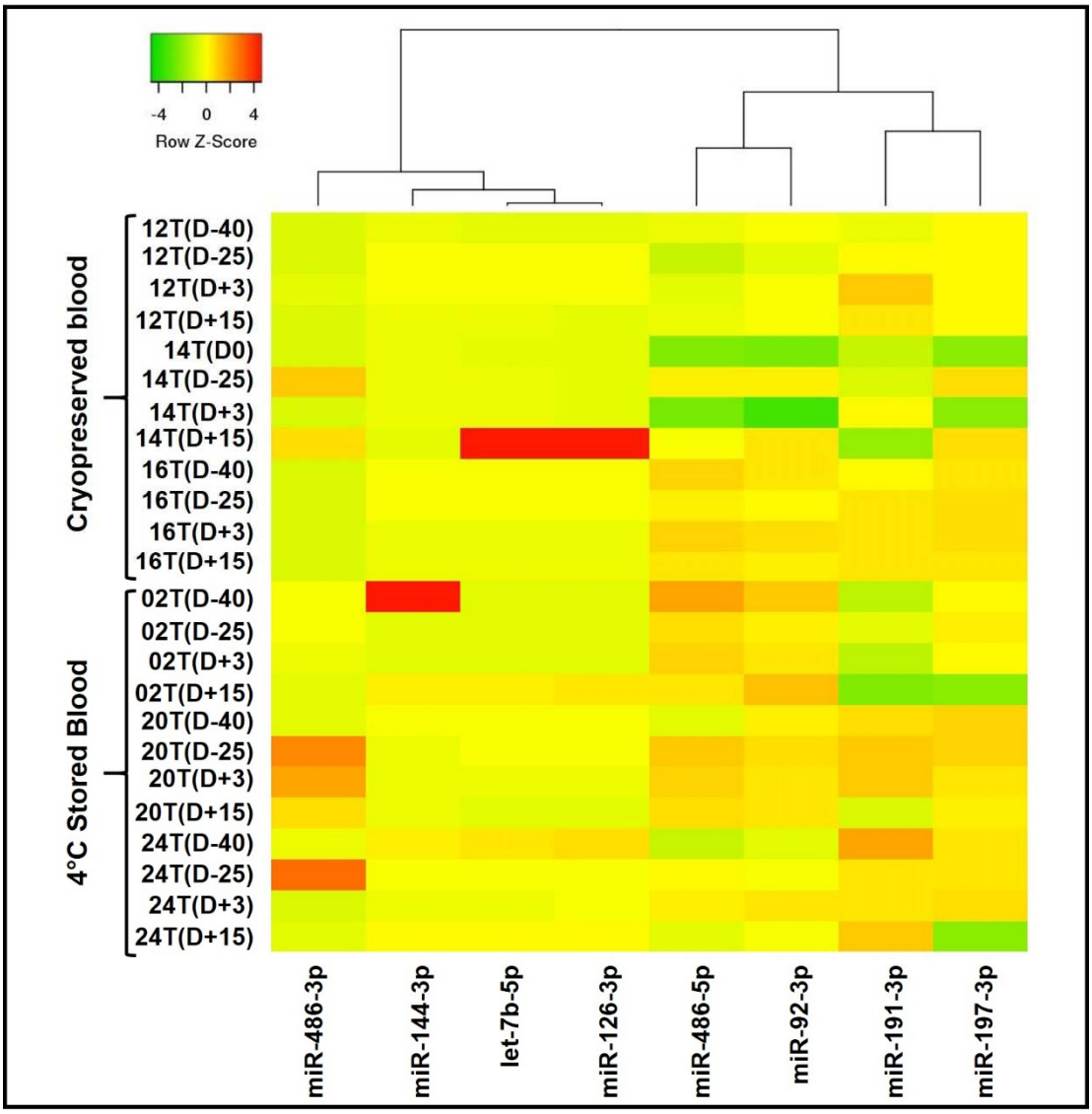

Figure 22. **Erythroid miRNAs expression in ABT athletes**. Expression of 12 selected miRNAs was verify through microarray analysis in 6 athletes: 3 were reinfused with cryopreserved blood (12T,14T and 16T), while the others three were reinfused with +4°C conserved blood.

Three subjects, two reinfused with +4°C stored blood (20T and 24T) and one reinfused with -80°C stored blood (14T) overexpressed the same miRNA, miR-486-3p. The same subjects presented also an alteration in miR-191-3p expression. It should be considered that the number of modulated miRNAs depends on the subject. For instance, some subjects (such as 14T) overexpressed at least 7 of 8 listed miRNAs after the reinfusion, while in others only one miRNA (12T) or no miRNAs were found to be overexpressed (16T) following ABT. A first conclusion is therefore that a great heterogeneity does exist in response to ABT practice when the analysis is limited to a short list of candidate miRNAs.

A

miRNA name	Control group						miRNA features
	Pool 1		Pool 2		Pool 3		
	D+3	D+15	D+3	D+15	D+3	D+15	
hsa-let-7a-5p	1,0	1,0	1,0	1,0	1,0	1,1	miRNA associated with fetal hemoglobin
hsa-miR-126-3p	1,0	1,0	2,7	1,4	1,0	1,1	miRNA associated with erythroid differentiation/hemopoiesis
hsa-miR-144-3p	1,0	1,0	1,0	1,0	1,0	1,1	miRNA associated with fetal hemoglobin
hsa-miR-191-3p	2,2	2,4	2,1	2,4	1,1	2,6	miRNA associated with erythroid differentiation/hemopoiesis
hsa-miR-197-3p	2,2	1,3	1,2	1,3	2,9	2,7	miRNA associated with erythroid differentiation/hemopoiesis
hsa-miR-486-3p	1,0	2,7	1,3	1,7	1,0	1,1	miRNA regulating transcriptional repressors
hsa-miR-486-5p	1,3	1,3	1,4	1,6	1,1	2,4	miRNA associated with erythroid differentiation/hemopoiesis
hsa-miR-92a-3p	1,7	1,7	1,3	1,4	1,6	2,3	miRNA associated with erythroid differentiation/hemopoiesis

B

miRNA name	Cryopreserved (-80°C) Blood									miRNA features
	12T			14T			16T			
	D-25	D+3	D+15	D-25	D+3	D+15	D-25	D+3	D+15	
hsa-let-7a-5p	1,1	1,1	1,0	1,0	1,0	4,3	1,0	1,0	1,0	miRNA associated with fetal hemoglobin
hsa-miR-126-3p	1,1	1,1	1,0	1,0	1,0	3,1	1,0	1,0	1,0	miRNA associated with erythroid differentiation/hemopoiesis
hsa-miR-144-3p	1,1	1,1	1,0	1,0	1,0	1,0	1,0	1,0	1,0	miRNA associated with fetal hemoglobin
hsa-miR-191-3p	1,6	4,9	2,5	1,6	3,7	4,0	1,8	1,8	1,8	miRNA associated with erythroid differentiation/hemopoiesis
hsa-miR-197-3p	1,0	1,2	1,0	231,6	1,0	231,6	1,2	1,4	1,1	miRNA associated with erythroid differentiation/hemopoiesis
hsa-miR-486-3p	1,1	1,1	1,0	4,1	1,0	3,0	1,0	1,0	1,0	miRNA regulating transcriptional repressors
hsa-miR-486-5p	1,8	1,1	1,0	9,5	1,1	7,5	1,8	1,1	1,4	miRNA associated with erythroid differentiation/hemopoiesis
hsa-miR-92a-3p	1,8	1,0	1,1	126,9	4,3	151,4	1,9	1,1	1,3	miRNA associated with erythroid differentiation/hemopoiesis

C

miRNA name	4°C Stored Blood									miRNA features
	02T			20T			24T			
	D-25	D+3	D+15	D-25	D+3	D+15	D-25	D+3	D+15	
hsa-let-7a-5p	1,0	1,0	1,3	1,0	1,1	1,1	1,2	1,2	1,1	miRNA associated with fetal hemoglobin
hsa-miR-126-3p	1,0	1,0	1,3	1,0	1,1	1,1	1,2	1,2	1,1	miRNA associated with erythroid differentiation/hemopoiesis
hsa-miR-144-3p	6,0	6,0	4,8	1,0	1,1	1,1	1,2	1,2	1,1	miRNA associated with fetal hemoglobin
hsa-miR-191-3p	2,2	1,0	4,5	1,6	1,6	6,0	5,3	6,7	2,6	miRNA associated with erythroid differentiation/hemopoiesis
hsa-miR-197-3p	1,4	1,1	61,3	1,0	1,6	2,4	1,0	1,4	129,9	miRNA associated with erythroid differentiation/hemopoiesis
hsa-miR-486-3p	1,0	1,1	1,2	11,6	6,6	2,6	14,7	1,2	1,1	miRNA regulating transcriptional repressors
hsa-miR-486-5p	2,5	1,9	3,1	3,7	3,0	2,5	2,6	3,1	1,7	miRNA associated with erythroid differentiation/hemopoiesis
hsa-miR-92a-3p	3,0	2,6	1,3	2,3	1,6	1,5	1,9	3,9	1,8	miRNA associated with erythroid differentiation/hemopoiesis

Table 12. Erythroid miRNAs which expression changes in ABT athletes. Change of the 8 miRNAs expression was calculated in the 6 ABT subjects. Fold change at time points T3, T6 and T8 was calculated respect to T1 of each subjects. Fold change was calculated as $2^{\wedge(T6-T1)}$, miRNAs which fold change is higher than 3 are indicated by black box.

2.3.3 MiR-486-3p evaluation.

Among the 8 miRNAs identified by microarray analysis we focused our attention on miR-486-3p. In the **Figure 23,** miR-486-3p trend in the 6 ABT trained subjects was reported, on the basis of obtained microarray data. As shown in Figure 23, three subjects (20T, 24T, 20T and 14T) presented a significant increase of miR-486-3p expression after blood withdrawal.

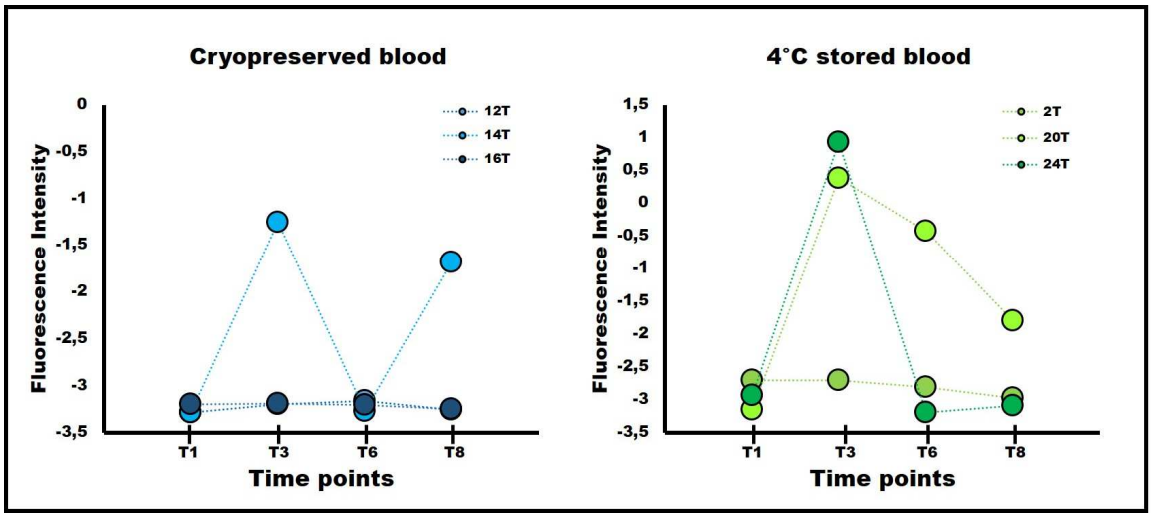

Figure 23. MiR-486-3p content in ABT subjects. MiR-486-3p fluorescence intensity value obtained by microarray analysis of the three athletes that underwent to ABT with cryopreserved blood (blue circles), or 4°C stored blood (green circles) at four different time points T1 (-40), T3 (-15) T6 (+3) and T8 (+15).

Due to the absence of a calibration curve, several authors define microarray as a semi-quantitative miRNA detection method. Therefore, to have quantitative data and to confirm the data obtained by microarray analysis, we verified miR-486-3p trend also using ddPCR. In **Figure 24** a representative plot of miR-486-3p quantification by ddPCR is reported.

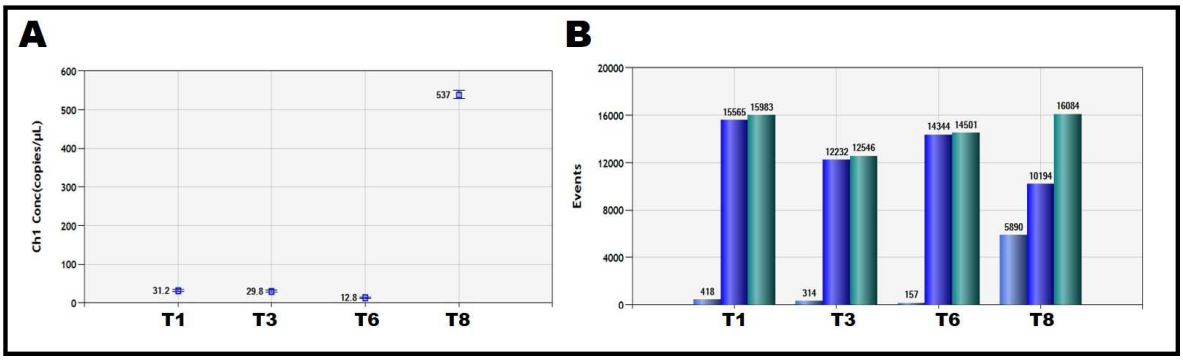

Figure 24. MiR-486-3p quantification using ddPCR. Representative results obtained on miR-486-3p quantification in the plasma obtained from the athlete 14T, who underwent to ABT. Panel A: concentration of miR-486-3p, reported as copies/µl for each reaction well. Panel B, event plot was presented and positive (light blue boxes), negative (blue boxes) and total droplets (green boxes) are reported.

2.4 Total miRNA analysis

As previously stated, the number of miRNAs present in miRBase continues to increase year after year and several miRNAs were recently introduced and characterized, even if for a large number of them their target mRNAs and the relative regulated networks are still unknown. For this reason, in the second part of the analysis, taking advantage from microarray data, we considered all miRNAs expressed in our samples. The analysis was performed using a chip that is able to detect 2549 miRs, corresponding to the last release of miRBase (Release 21). Of all 2549 miRs, 703 were detected in at least one plasma sample (**Figure 25**).

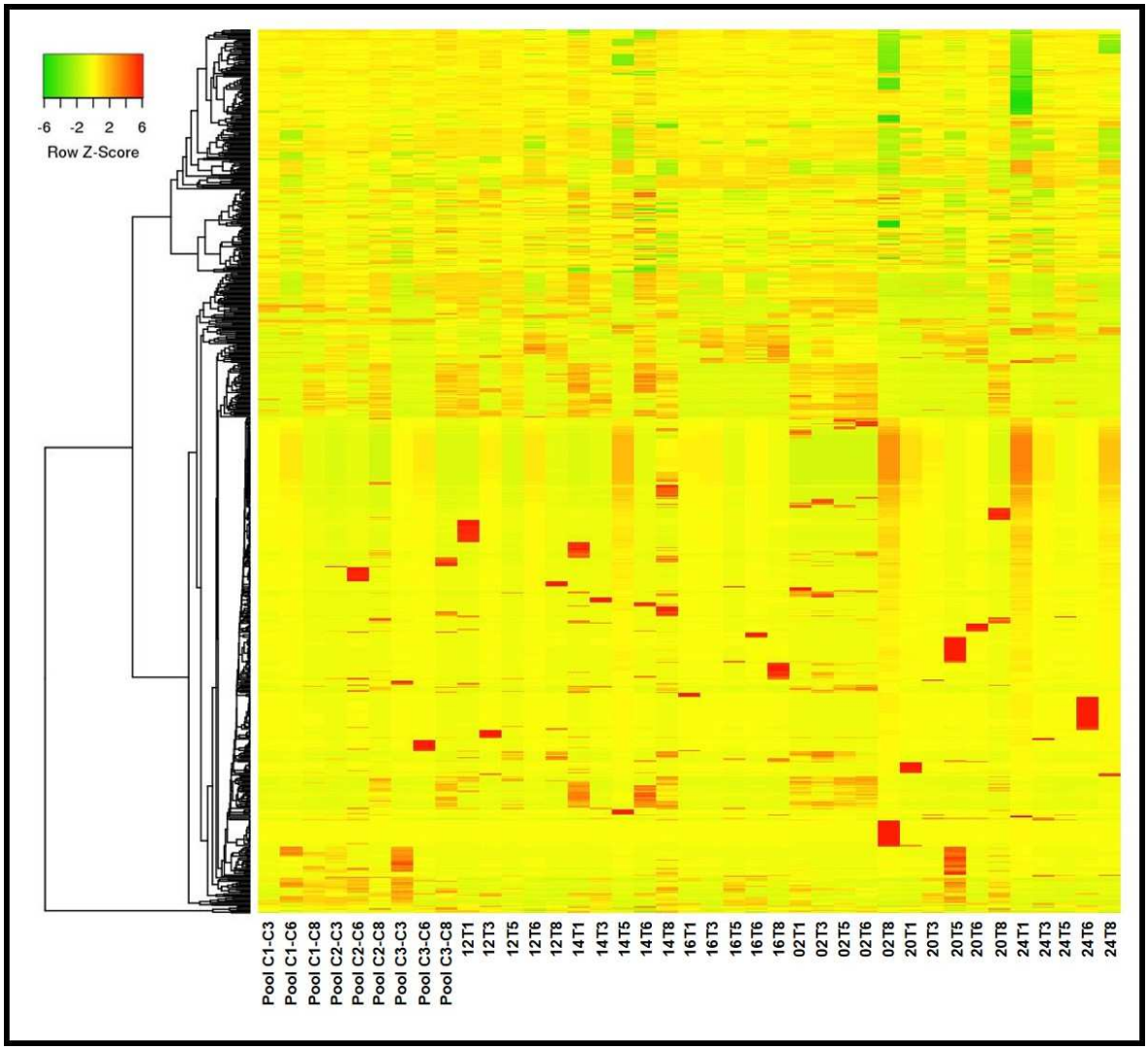

Figure 25. Expression of all 703 miRNA detected in plasma in all analysed samples. Of all 2549, known miRNAs, 703 were detected in at least one of total 39 samples analysed by microarray technology.

Differentially expressed miRNAs were selected using a fold change analysis and T1 (-40) of each subject was employed as control. In particular, three time points have been

investigated: a) T3 (-25) compared to T1 (-40) to identify miRs modulated following blood withdrawal, b) T6 (+3) compared to T1 (-40) to found miRNAs which expression changes in days immediately after the blood reinfusion and c) T8 (+15) compared to T1 (-40) to select miRNAs which maybe modulated at long term, after reinfusion. Both miRNAs that are up-regulated and miRs that are down-regulated were considered. Athletes reinfused with cryopreserved blood (12T, 14T and 16T) were considered separately with respect to athletes who underwent reinfusion with +4°C stored blood (02T, 20T and 24T). In our analysis we considered only miRNAs that present a fold increase or decrease higher than 1.5.

2.4.1 Evaluation of modulated miRNAs at T6 (+3)

As first point of our analysis, we considered all miRNAs which were modulated in the days immediately following blood reinfusion. Only miRNAs displaying an expression change higher than 1.5 were considered. Moreover, three different pools of plasma collected from C group athletes were analysed in order to exclude all miRNAs displaying 'physiological' expression change also in the control samples. Each pool was composed by plasma obtained from three different C group athletes, and three different key time points were considered for controls: T1 (-40), T6 (+3) and T8(+15).

2.4.1.1 Up-regulated miRNAs in athletes that underwent to reinfusion with cryopreserved blood.

Athletes that underwent ABT with cryopreserved blood were considered separately with respect to subjects transfused with +4°C stored blood. This was due in consideration of the expected difference in the response in relation to the different blood storage. The different treatment before the reinfusion may in fact bring to a different profile of modulated miRNAs. Among the six subjects that were transfused with cryopreserved blood, three were analysed by microarray: 12T, 14T and 16T. As depicted in the Venn diagram shown in **Figure 26**, while for 12T and 16T subjects a similar number of upregulated miRNAs was detected, a significant higher number of miRNAs were found to be up-regulated in 14T subject. Therefore, we have considered only miRNAs modulated in all the three subjects (24 miRNAs were found to be up-regulated in all the three athletes). The complete list of the 24 up-regulated miRNAs is reported in Figure 26.

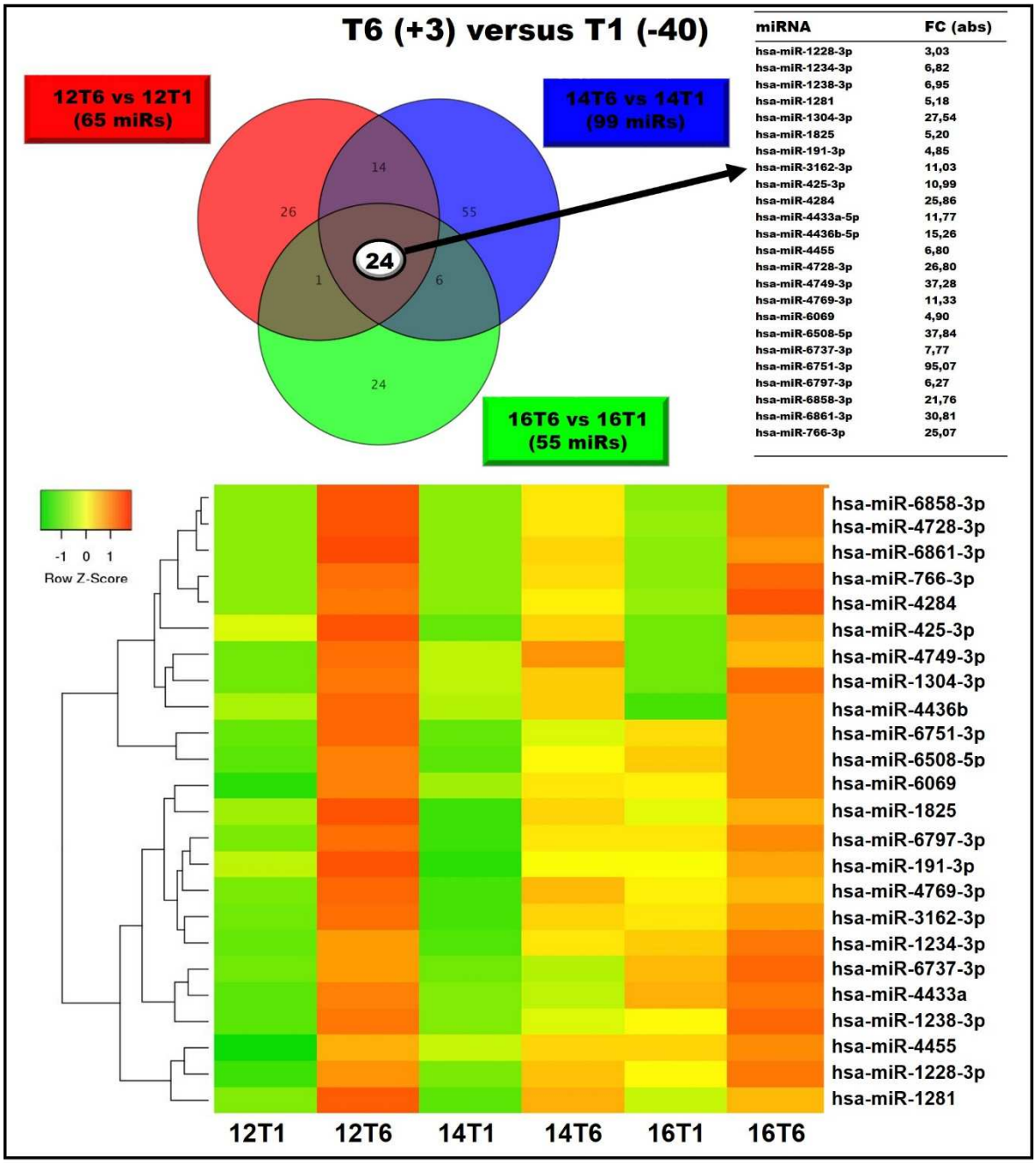

Figure 26. Up-regulated miRNAs in athletes transfused with cryopreserved blood. The number of up-regulated miRNAs in three different subjects, which underwent to ABT was reported in the Venn diagram, respectively red circle up-regulated miRNAs in 12T subject, blue circle: up-regulated miRNAs in 14T athlete, and green circle up-regulated miRNAs in 16T subject. In the intersection of three circles, the number of miRNAs up-regulated in all the three athletes is reported. The list of 24 miRNAs up-regulated in all the three athletes and their respective mean fold change are reported. A heat map summarizing the expression values of the 24 up-regulated miRNAs is reported in the lower part of the figure.

2.4.1.2 Down-regulated miRNAs in athletes that underwent to reinfusion with cryopreserved blood.

Using a similar strategy, we have also considered miRNAs which were found to be down-regulated in reinfused patients. As indicated in **Figure 27**, the number of down-

regulated miRNAs is sharp different between three subject, in fact while in 12T athlete (red circle) 172 miRNAs were found to be down-regulated a lower number of down-regulated

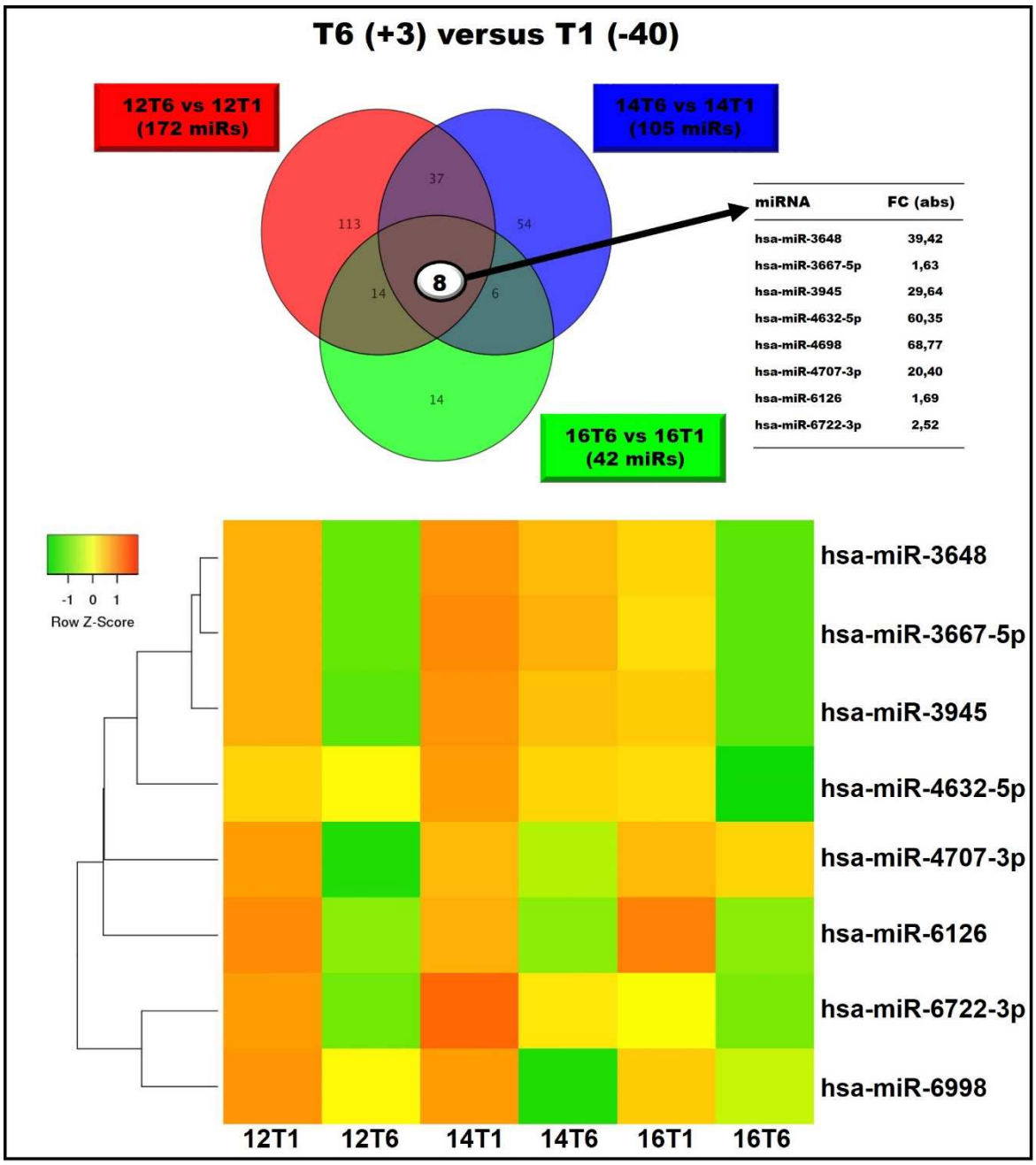

Figure 27. Down-regulated miRNAs in athletes reinfused with cryopreserved blood. 172 miRNAs were found to be down-regulated in 12T athlete (red circle), 105 in 14T athlete and 42 in 16T athlete. 8 miRNAs were found to be downregulated in all three athletes. The heat map relative to the 8 common downregulated miRNAs is reported in the lower part of the figure.

miRNAs was found in the 14T subject sample (blue circle), in which 105 miRNAs were identified, and in the 16T athlete sample, in which only 42 down-regulated miRNAs were found. Among these down-regulated miRNAs, 8 were found to be in common to the three

athletes. As summarized in the Table reporting the mean fold change, some of these miRNAs (such as miR-4698 and miR4632-5p) were found to be deeply modulated.

2.4.1.3 Up-regulated miRNAs in athletes who underwent reinfusion with +4°C stored blood.

Another group of athletes was transfused with blood, which, after the withdrawal, was conserved at +4°C, until the moment of the reinfusion (**Figure 28**). In fact,

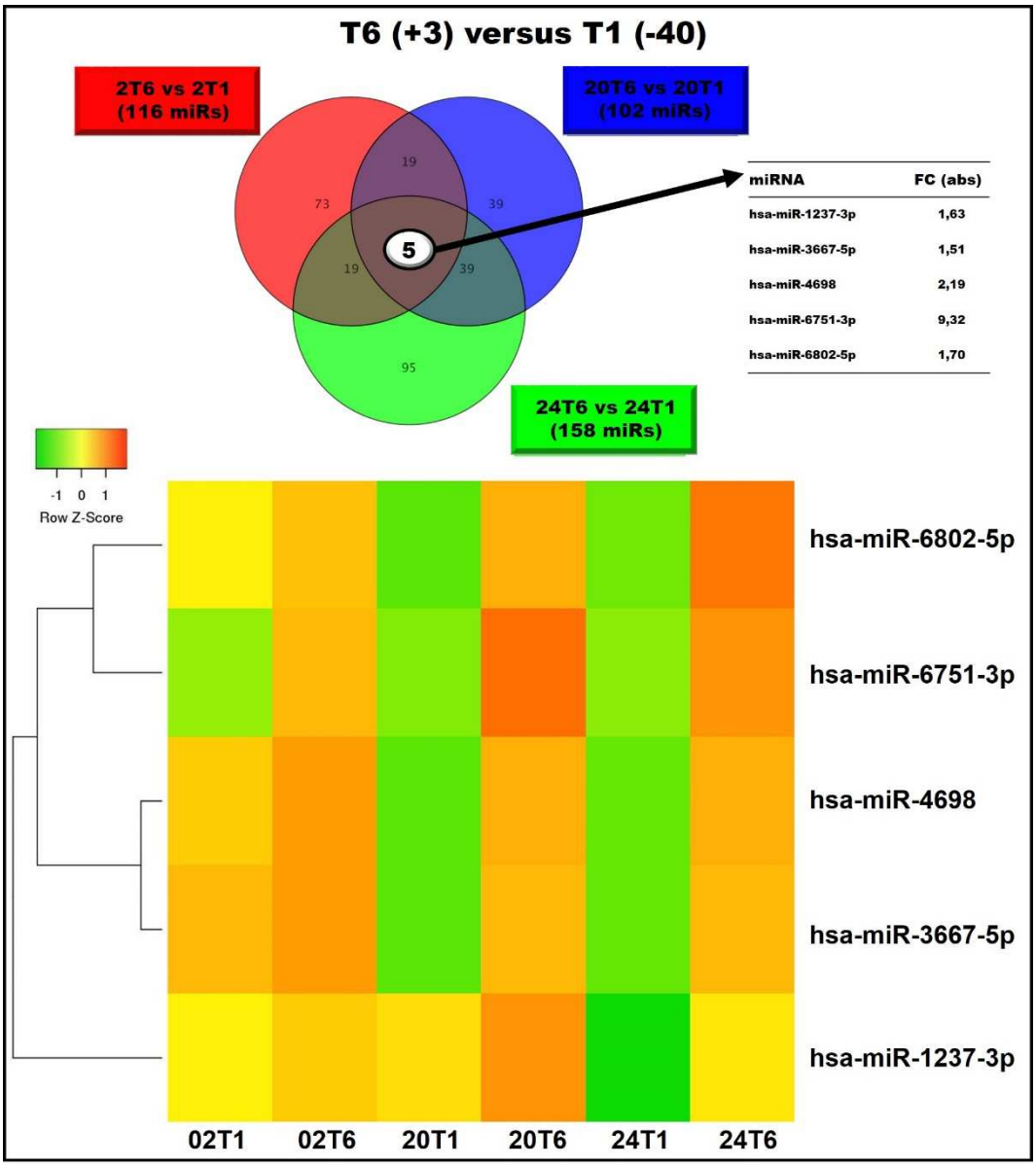

Figure 28. Up-regulated miRNAs in athletes that underwent to reinfusion with +4°C stored blood. In the upper part of the figure, Venn diagram, reporting the 5 miRNAs up-regulated in all the three athletes transfused with +4°C stored blood was reported. 116 miRNAs were found to be up regulated in 2T subject, 102 miRNAs were reported as up-regulated miRNAs in 20T subject while 158 miRNAs were identified as up-regulated in 24T athlete. The heat map in the lower part of the Figure reported the expression of the 5 common up-regulated miRNAs at two time points T1 (-40) and T6 (+3) in athletes 02T, 20T and 24T.

while +4°C blood is only pre-heated at 37°C before reinfusion, cryopreserved blood is pre-treated before being transfused, in order to remove cryopreserving compound added to avoid red blood cells damage. For this reason at least in the preliminary step, the two different kind of samples were considered individually. With respect to athletes transfused with blood stored at +4°C, five miRNAs were found to be up-regulated in all the three samples (02T, 20T and 24T). This is a significantly lower number when compared to that found in plasma samples from subjects reinfused with cryopreserved blood (Figure 27). Moreover, as shown in the Table, the fold change values were considerably lower with respect to the values found for cryopreserved blood-transfused subjects. In this case the highest fold change was registered for miR-6751-3p, while for the others four miRNAs fold change values between 1.5 and 2.2 were detected. Interestingly, no miRNAs were found to be down regulated in all the three athletes that were transfused with +4°C stored blood.

2.4.1.4 Up-regulated miRNAs in athletes who underwent reinfusion with both +4°C stored blood or cryopreserved blood

To verify the possible presence of common miRNAs we considered at same time miRNAs that (a) were up-regulated in at least two athletes who were transfused with +4°C stored blood and that (b) were up-regulated in two subjects reinfused with cryopreserved blood (**Figure 29**). With respect to the second group (cryopreserved blood) 45 miRNAs were identified, while 82 miRNAs are up-regulated in at least 2 of the three subjects who were transfused with +4°C conserved blood. By the intersection of the two lists 20 miRNAs were found to be in common when the two groups were considered. Their expression at the two time points (T1 and T6) is reported in the heat map shown in the lower part of Figure 29. Among the 20 miRNAs identified, particularly interesting were miR-1237-5p, miR-6751-3p and miR-425-3p, which as shown in heat map, are modulated at T6 (+3) in almost all samples.

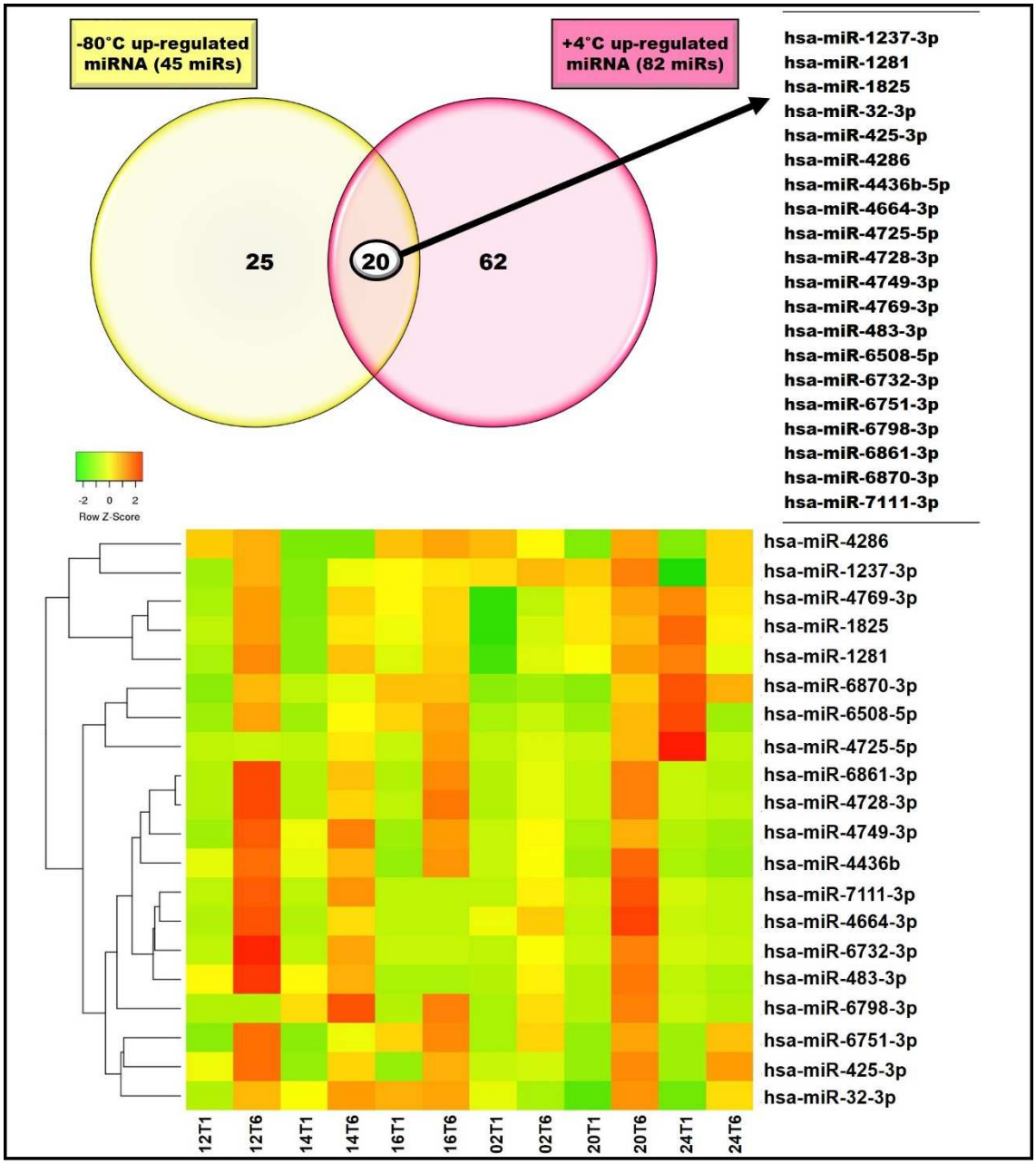

Figure 29. Up-regulated miRNAs in athletes that underwent to reinfusion with both +4°C stored blood or cryopreserved blood. Upper part of the figure: yellow circle: list of 45 up-regulated miRNAs in at least two athletes which underwent to ABT with cryopreserved blood, pink circle: list of the 82 up-regulated miRNAs in at least two subjects transfused with blood conserved at +4°C. 20 miRNAs were found to be modulated in at least 2 athletes transfused with cryopreserved blood and in two transfused with +4°C stored blood. MiRNAs expression levels in all six athletes were reported in the heat map in the lower art of the figure.

2.4.1.5 MiR-425-3p evaluation

MiR-425-3p is one of the miRNA modulated in all 6 subject, with no distinction between cryopreserved blood and +4°C stored blood (Figure 29). As shown in the **Figure 30**, the trend of miR-425-3p in the plasma samples from the six subjects was analysed more

in detail and, as evident, in 5 of the 6 subjects (with the exception of subject 2T) a clear increase of miR-425-3p content was detected at T6 (+3).

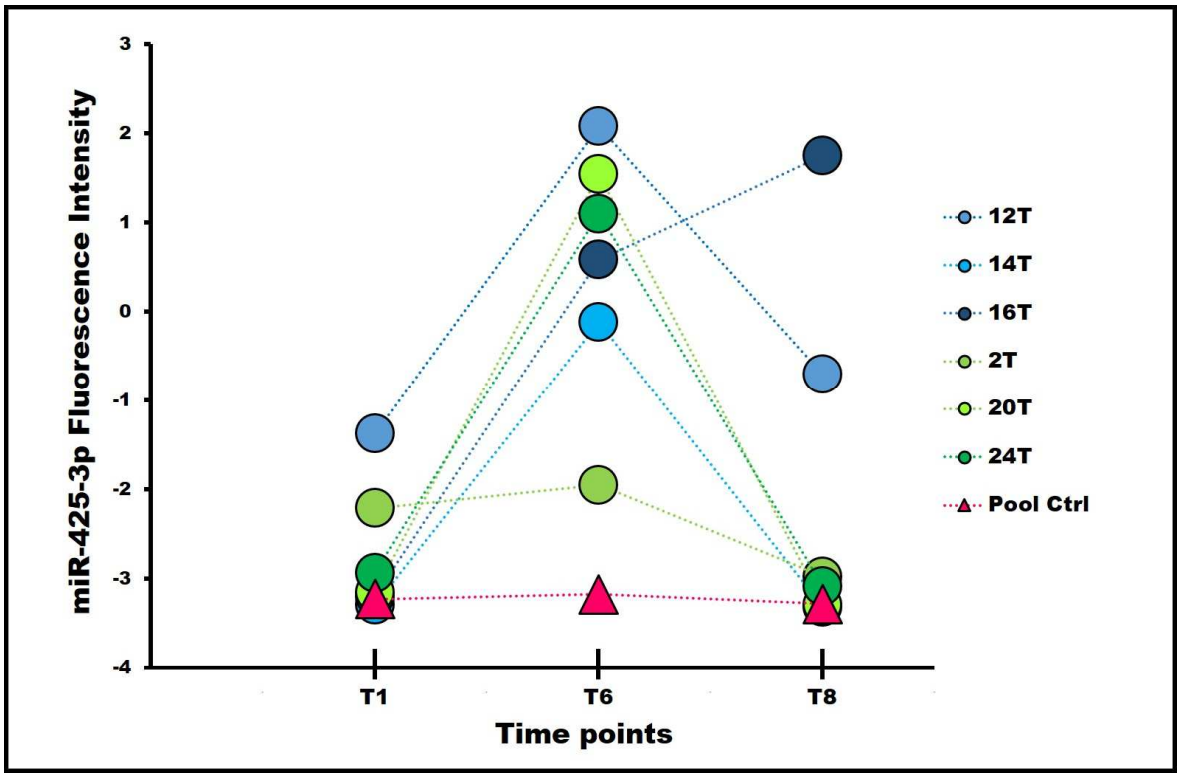

Figure 30. **MiR-425-3p content in ABT athletes and in control subjects.** MiR-425-3p content detected by microarray analysis was reported both for subjects transfused with cryopreserved blood (green circles) and for athletes reinfused with blood stored at +4°C (blue circles). At same time, miR-425-3p levels in a pool composed by plasma collected from three subjects part of control group, were reported (pink triangles).

However, in most of the cases (with the exception of subjects 16T) the miR-425-3p levels were again found at the starting levels fifteen days after the reinfusion. Interestingly in the 16T athlete at T8 (+15) a further increase of miRNA was found. At the same time a representative control sample was analysed (pink triangles). The shown control sample was obtained by pooling plasma collected from three different athletes that were part of control group. In this case no differences in miR-425-3p content were shown at T6 (+3) and T8 (+15) with respect to T1 (-40) time point.

The found miR-425-3p trend was also confirmed by another miRNA detection technique (ddPCR). In fact, considering that miRNAs content in plasma samples is generally low, ddPCR was employed that allowed us to quantify diluted samples, without the requirement of endogenous reference miRNAs.

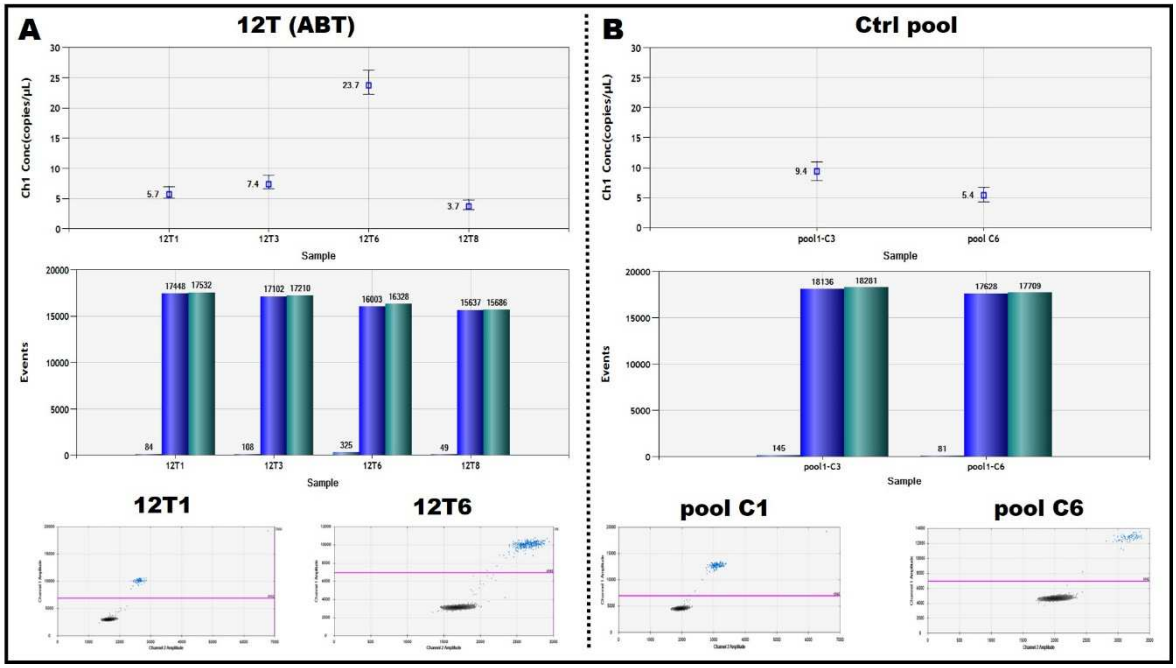

Figure 31. MiR-425-3p quantification using ddPCR. MiR-425-3p trend was also verified using another miRNA detection technique: ddPCR. MiRNA concentration, expressed as copies of miRNA for µL in each reaction well, was reported in the concentration plot, in the upper part of the figure, while number of droplets generated from each sample is reported in the event plot in the middle part of the figure: green boxes (total generated droplets), blue boxes (negative droplets), light blue boxes (positive droplets). 2D plots for the two key samples: T1 (-40) and T6 (+3) were reported in the lower part of the figure.

As shown in **Figure 31** four time points T1 (-40), T3 (-25), T6 (+3) and T8 (+15) were considered. In ddPCR the additional T3 (-25) was analysed in ordered to verify possible miR-425-3p changes due also to blood withdrawal. While at T1 (-40) and T3 (-25) miRNA concentration is almost stable, a sharp increase is registered at T6 (+3), followed by the decrease of miR-425-3p levels at T8 (+15), which came back to the starting levels. At same time, a pool of control subjects was analysed at two key time points: T1 (-40) and T6 (+3) and no significant changes between the two time points were detected. Therefore, the two analytical technologies gave similar results further validating the microarray data.

2.4.2 Evaluation of modulated miRNAs at T8 (+15)

As previously stated, at least another research group in the recent years investigated miRNAs as potential ABT biomarkers. In this case, the analysis was performed in the hours immediately following blood reinfusion; therefore, only miRNAs modulated in the short period were identified. By contrast, our study was designed to evaluate miRNAs profile not only immediately after blood reinfusion, but also in the medium-long period after ABT.

Therefore, it was possible to investigate, using the microarray method, also miRNAs variations 15 days after blood reinfusion: T8 (+15). Even in this case miRNAs expression at T8 (+15) was compared to starting miRNAs levels at T1 (-40) and the fold changes were calculated. Only miRNAs exhibiting a fold change higher than 1.5 were considered.

2.4.2.1 Up-regulated miRNAs at T8 (+15)

In the first stage of the analysis, T group subjects were as usual divided into two groups: subjects reinfused with cryopreserved blood (12T, 14T and 16T) and subjects transfused with autologous blood conserved at +4°C, and the two groups were considered individually. As shown in **Figure 32**, considering the three athletes reinfused with cryopreserved blood (Panel A), 6 miRs were found to be up-regulated in all three subjects, even if with different intensity (see in the relative heat map). In fact, while in 16T a major miRNAs increase was found, the increase in 14T subject was more moderate especially for miR-4515 and miR-3151-3p. Comparing the list of modulated miRNAs in subjects transfused with autologous cryopreserved blood, no analogies were found with athletes who underwent reinfusion with +4°C stored blood. Five miRNAs were found to be modulated in all the three subjects reinfused with blood stored at +4°C. It is important to underline that the number of modulated miRNAs for each athlete is generally lower in the subjects transfused with blood stored at +4°C, with respect to samples from subjects transfused with cryopreserved blood.

However, the possibility that same miRNAs can be modulated regardless of blood storage method was considered, and we therefore searched for miRNAs which were found to be modulated in at least two of three subjects for each group. Eight miRNAs, indicated in the panel C of the Figure were found to be modulated at same time in athletes transfused with autologous cryopreserved blood and in athletes reinfused with +4°C stored blood. The major changes were detected for 16T, 02T and 12T athletes, while no significant changes were detected in 20T athlete, in which some of the selected miRNAs, as miR-4284 and miR-1237-3p seem to be down-regulated with respect to the control.

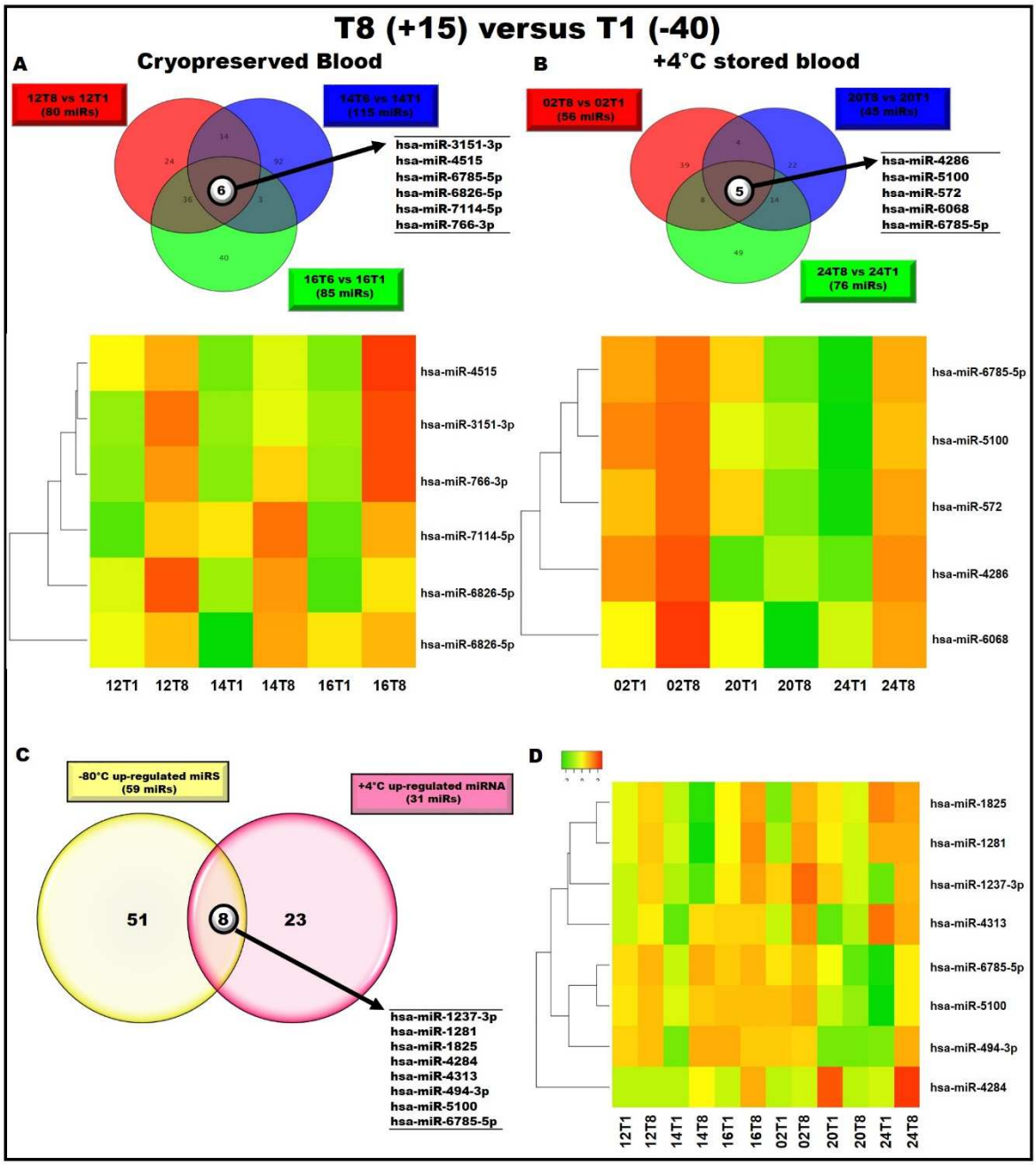

Figure 32. Up-regulated miRNAs at T8 (+15). Up regulated miRNAs in athletes which underwent to ABT with cryopreserved blood were considered in panel A, and the relative modulation intensity was report in the heat map. Plasma obtained from three athletes: 12T (red circle), 14T (blue circle) and 16T (green circle) was analysed. At same way in panel B, 02T (red circle), 20T (blue circle) and 24T (green circle) were considered, and 5 miRNAs were found to be commonly up-regulated. In both cases fold change was calculated respect to T1 (-40) sample. Panel C miRNAs modulated in at least 2 of the three subjects reinfused with +4°C stored blood and in 2 of the three subjects transfused with cryopreserved blood, were analysed. A list of 8 miRNAs was found and the relative heat map was proposed in panel D.

2.4.2.2 Down-regulated miRNAs at T8 (+15)

In addition to up-regulated miRNAs, miRNAs exhibiting reduced expression in the medium-long period of time after blood reinfusion were considered. In this case, 15 miRNAs were found to be down-regulated 15 days after cryopreserved blood reinfusion in all the three athletes.

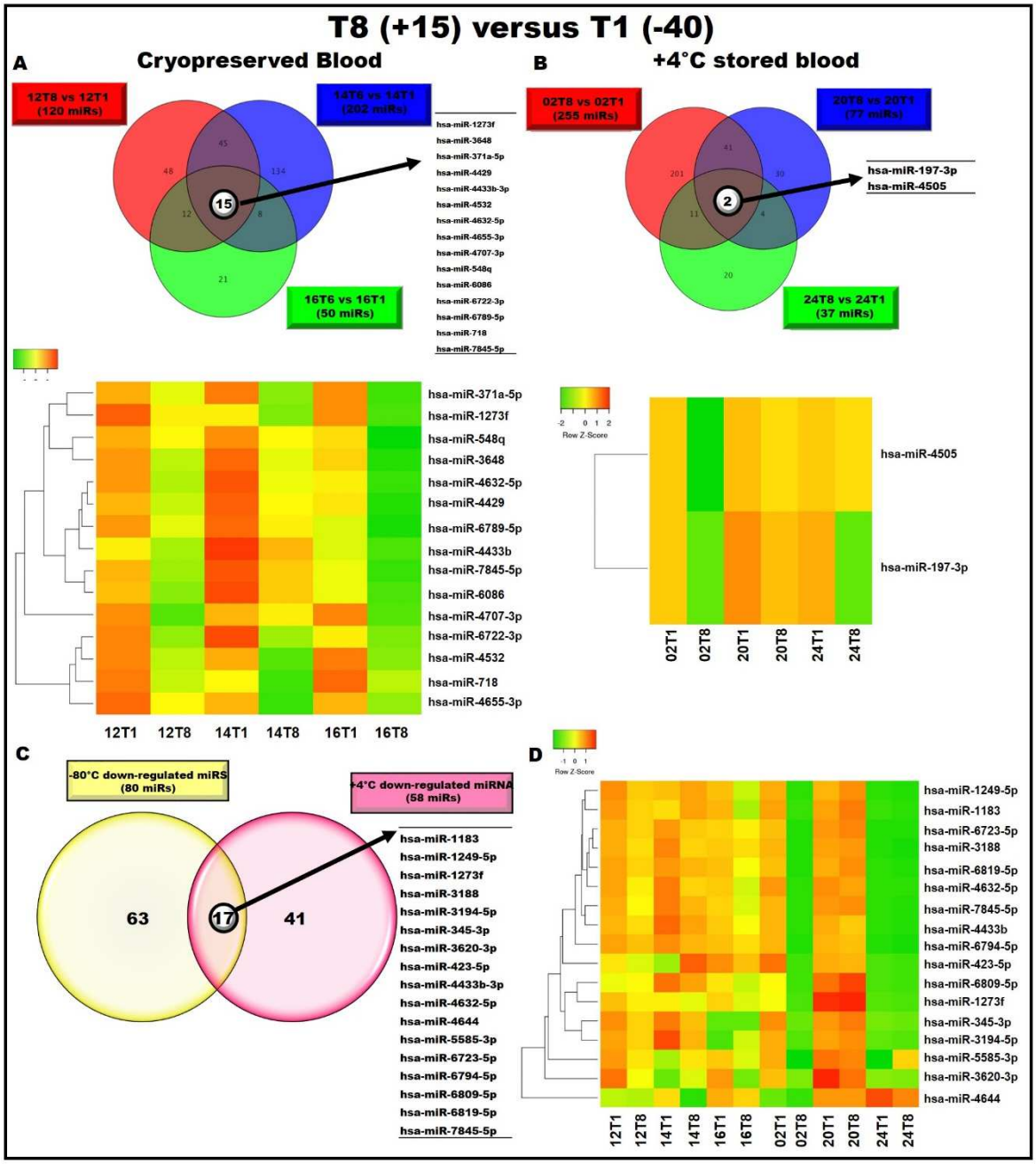

Figure 33. Down-regulated miRNAs at T8 (+15). Panel A, 15 miRNAs were found to be down-regulated in all three subjects transfused with autologous blood cryopreserved at -80°C. The relative miRNAs expression change at two time points: T1 (-40) and T8 (+15) was reported in the heat map in the middle part of the figure. At same way the list of modulated miRNAs is reported also for subjects that underwent to ABT with +4°C conserved blood. In Panel C a list of miRNAs modulated at same time in at least two subjects that underwent to ABT with cryopreserved blood and two subjected reinfused with +4°C stored blood is reported, with the relative heat map for selected miRNAs (Panel D).

Following this analysis, very different numbers of miRNAs were found to be modulated in the three subjects. In fact, while in the 14T athlete, more than 200 miRNAs were found to be altered after blood reinfusion, only 50 miRNAs were identified in the 16T subject. Surprisingly, none of the found miRNAs was common to the T6 (+3) list. With respect to athletes who underwent ABT with +4°C stored blood (**Figure 33**, Panel B) only two miRNAs (miR-197-3p and miR-4505) were found to be down-regulated in all the three subjects. We also considered miRNAs modulated in at least two of the three athletes for each different conservation method, and we identified 17 miRNAs, exhibiting the expression intensity reported in the heat map in panel D of Figure 33. As it is possible to see, major miRNAs content changes were detected in 02T, 12T and 14T subjects, while no significant changes were shown especially for 24T subject, who however presented already very low levels of the investigated miRNAs at the starting point T1 (-40).

2.4.3 Evaluation of modulated miRNAs at T3 (-25)

Until now, we considered only the possibility that miRNAs profile change may be due to blood reinfusion, but is important to underline that also blood withdrawal can change physiological condition inducing modifications in miRNAs profile; so, we evaluated miRNAs profile at T3, 10 days after blood withdrawal. In this case, usual classification of ABT trained athletes into two groups (+4°C stored blood and cryopreserved blood), was not performed, in fact after blood withdrawal no differences between two groups are expected.

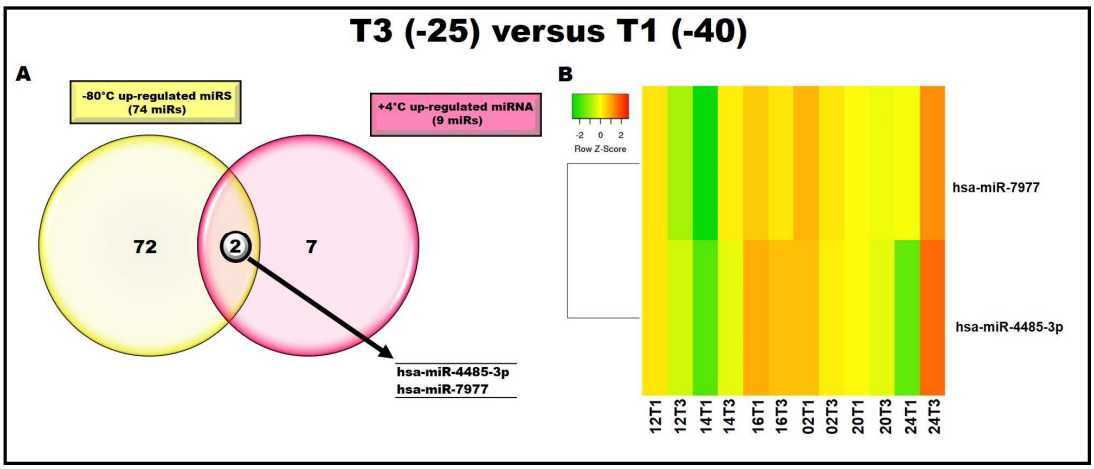

Figure 34. Modulated miRNAs at T3 (-25). Panel A, two miRNAs were found to be up regulated in at least four of six ABT trained athletes, independently by the blood storage method. Panel B, the relative heat map was presented, indicating miRNA expression.

For this reason, we considered miRNAs modulated in at least four of six total ABT trained athletes. As it is possible to see in **Figure 34** only two miRNAs: miR-4485-3p and miR-7977 were found to be up-regulated in at least 4 subjects: two athletes reinfused with +4°stored blood and two reinfused with cryopreserved blood. While no common down-regulated miRNAs were found.

2.5 List of miRNAs possible ABT biomarkers

In conclusion, considering all up and down-regulated miRNAs common to both athletes reinfused with +4°C stored blood and athletes transfused with cryopreserved autologous blood, we identify a final list composed by 17 miRNAs, possible candidates as autologous blood transfusion markers (**Table 13**). The list is composed, by the five most

MiRNA name	Mean FC	Regulation	Time point
miR-1183	12,0	down	T8(+15)
miR-423-5p	13,1	down	T8(+15)
miR-4284	13,6	up	T8(+15)
miR-4286	20,1	up	T6(+3)
miR-4313	10,5	up	T8(+15)
miR-4436b-5p	17,3	up	T6(+3)
miR-4485-3p	195,6	up	T3(-25)
miR-4632-5p	11,2	down	T8(+15)
miR-4725-5p	25,9	up	T6(+3)
miR-494-3p	113,1	up	T8(+15)
miR-5100	23,3	up	T8(+15)
miR-5585-3p	23,5	down	T8(+15)
miR-6751-3p	27,4	up	T6(+3)
miR-6785-5p	37,7	up	T8(+15)
miR-6794-5p	12,2	down	T8(+15)
miR-6508-5p	45,4	up	T6(+3)
miR-7977	55,9	up	T3(-25)

Table 13. List of possible miRNAs markers of ABT. A list of 17 miRNAs was identified, considering three key time points T3 (-25), T6 (+3) and T8 (+15) and both blood storage methods.

modulated miRNAs, when more than five miRNAs were found to be modulated in both transfused groups. All the three time points, T3 (-25), T6 (+3) and T8 (+15), were considered, in order to evaluate both miRNAs modulated following blood withdrawn and miRNAs for which modulation is associated to blood reinfusion. At same time, both up and down regulated miRNAs were considered. The final list includes: two modulated miRNAs at T3 (-25), all upregulated, five modulated miRNAs at T6 (+3), all upregulated, and ten miRNAs modulated at T8 (+15), including five upregulated miRNAs and five downregulated miRNAs.

III. MicroRNAs-based therapeutics: Identification of miR-210 as possible miRNA targeting the gamma globin gene repressor BCL11A

As previously discussed, the reactivation of fetal haemoglobin is one of the most promising therapeutic strategies for the treatment of β-thalassemia. This therapeutic approach is based on the evidence that β-thalassemia patients with HPFH generally, present less severe symptomatology, due to the partial replacement of lacking beta globin chains with gamma globin chains. For this reason, several studies in the recent years were addressed to find strategies to reactivate gamma globin chains production. The mechanism of γ-globin gene silencing was deeply studied and BCL11A was found to have a key role in regulating this mechanism. Starting from the consideration that miRNAs are able to target a large variety of mRNAs, we searched for miRNAs that are able to target directly BCL11A mRNA, in order to reduce its expression and consequently increase gamma globin gene expression.

3.1 Background data

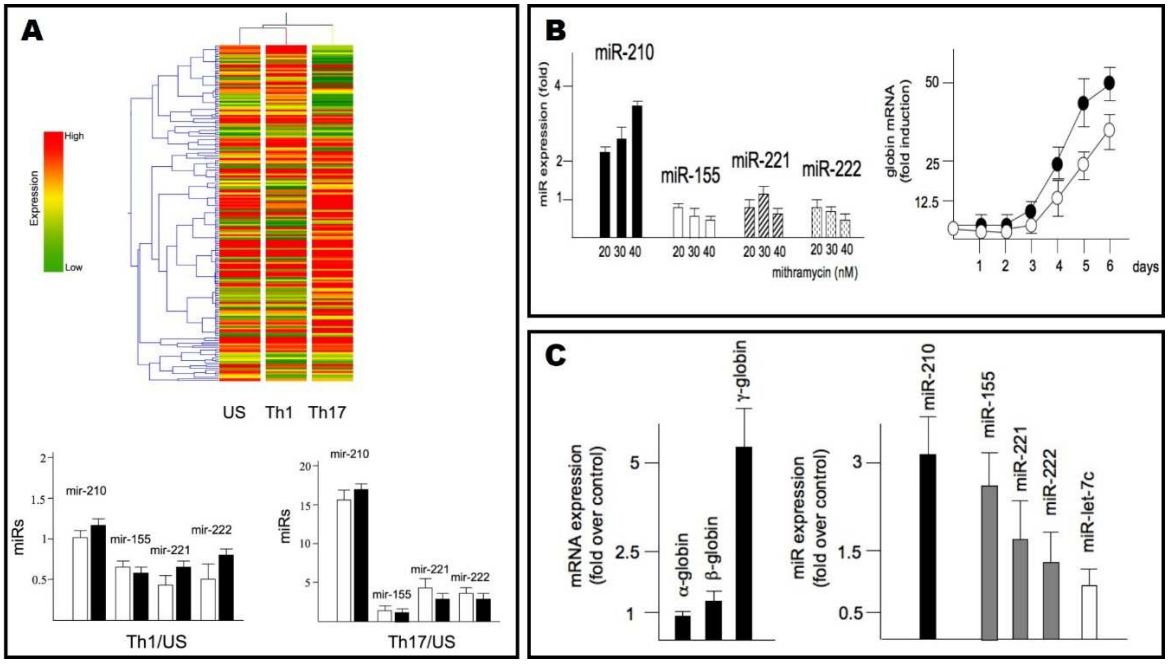

Figure 35. **Background data.** Panel A microarray analysis was performed in a healthy donor (left line), in a β-thalassemia patient with low levels of fetal haemoglobin (middle line: Th1) and in a patient with HPFH phenotype (right line: Th17). MiR-210 was found to be differentially expressed, between samples. Data were also confirmed by RTqPCR analysis, in this case miR-210 expression in β-thalassemia patients was compared with miRNA levels in healthy donors. Panel B: miR-210 expression was evaluated in K562 cells in which gamma globin production was induced using MTH. At same way miR-210 expression was evaluate in ErPCs isolated from β-thalassemia patients. All data and pictures were taken from Bianchi N et al. 2009.

Our approach was largely based on a work published by Bianchi and colleagues [*Bianchi N et al., 2009*], demonstrating that miR-210-3p is more expressed in erythroid precursors cells

isolated from β-thalassemia patients producing high levels of HbF compared to patients with low HbF production and healthy donors (**Figure 35**, Panel A). Moreover, miR-210-3p levels were analysed in both erythroid precursors cells and K562 cells, in which the production of fetal haemoglobin was induced using one of the most powerful fetal haemoglobin inducers mithramycin (MTH). Also in this case miR-210-3p was shown to be up-regulated, when gamma globin production was induced. Furthermore, the miR-210 increase was proportional to the concentration of the HbF inducer (Panel B and C). Starting from these evidences we searched for miR-210-3p possible mRNA targets.

3.2 Evaluation of miR-210 expression in induced ErPcs

Starting from what previously shown by Bianchi and colleagues, we evaluated miR-210 expression after HbF induction with MTH in a panel of 18 erythroid precursors (ErPCs) samples, isolated both from healthy donors (9 subjects) and β-thalassemia patients (9 subjects). After the isolation ErPCs were treated with 30 nM MTH for 5 days. At the end of the treatment, RNA was extracted, and gamma globin mRNA expression was evaluated in order to verify whether the activation of HbF-related expression occurred. All samples were then verified for miR-210-3p expression and their relative expression was reported in the **Figure 36**. As it is evident, miR-210-3p was overexpressed after treatment with MTH in

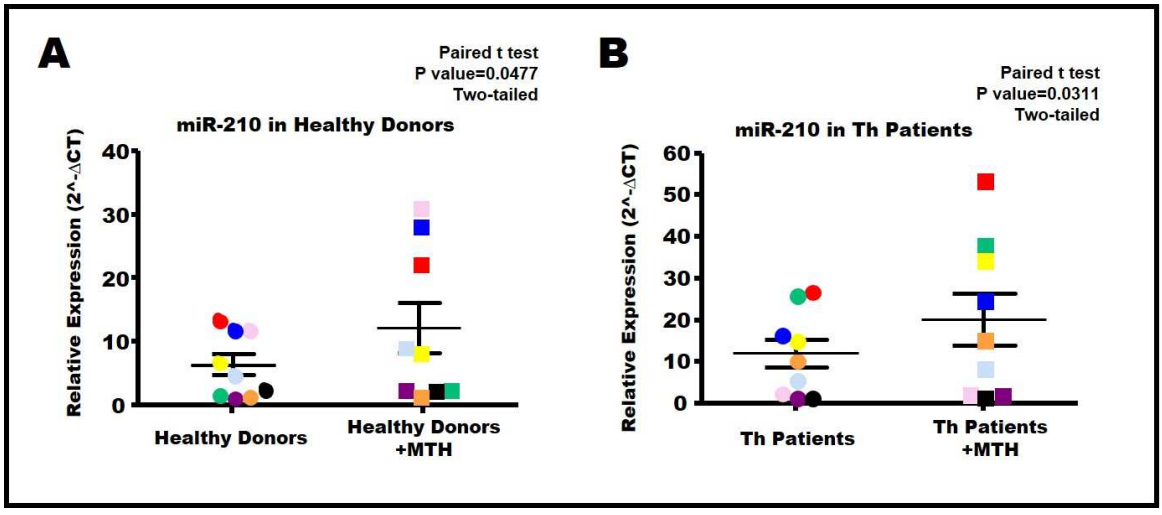

Figure 36. **MiR-210 expression in induced ErPCs.** Erythroid precursors cells isolated both from healthy subjects (panel A) and β-thalassemia patients (panel B), were treated with MTH in order to induce gamma globin expression. MiR-210-3p expression, in induced samples, was compared with miR-210-3p levels in untreated samples and the relative expression was calculated. Nine subjects for each group (healthy donors and β-thalassemia patients) were considered.

ErPCs from both healthy donors and β-thalassemia patients, with only minor differences. Moreover, as expected, each subject sample started from different miR-210-3p levels and

some differences can be observed between the mean miR-210-3p expression in untreated samples from healthy donors and β-thalassemia patients.

3.3 Identification of miR-210 binding site in BCL11A mRNA

Considering that all data obtained sustain the concept that miR-210 was deeply involved in HbF production, we searched for possible miR-210 targets within the BCL11A mRNA sequence. Analysis was performed with different on-line available softwares for miRNAs putative target identification. For our analysis we found particularly useful miRWalk 2.0 [*http://zmf.umm.uni-heidelberg.de/apps/zmf/mirwalk/*], which, when compared with other software is able to identify not only miRNAs that probably bind 3'UTR of their target mRNA, both also miRNAs targeting 5'UTR and the coding region. This software was particularly useful, because allowed us to identify a possible miR-210 binding

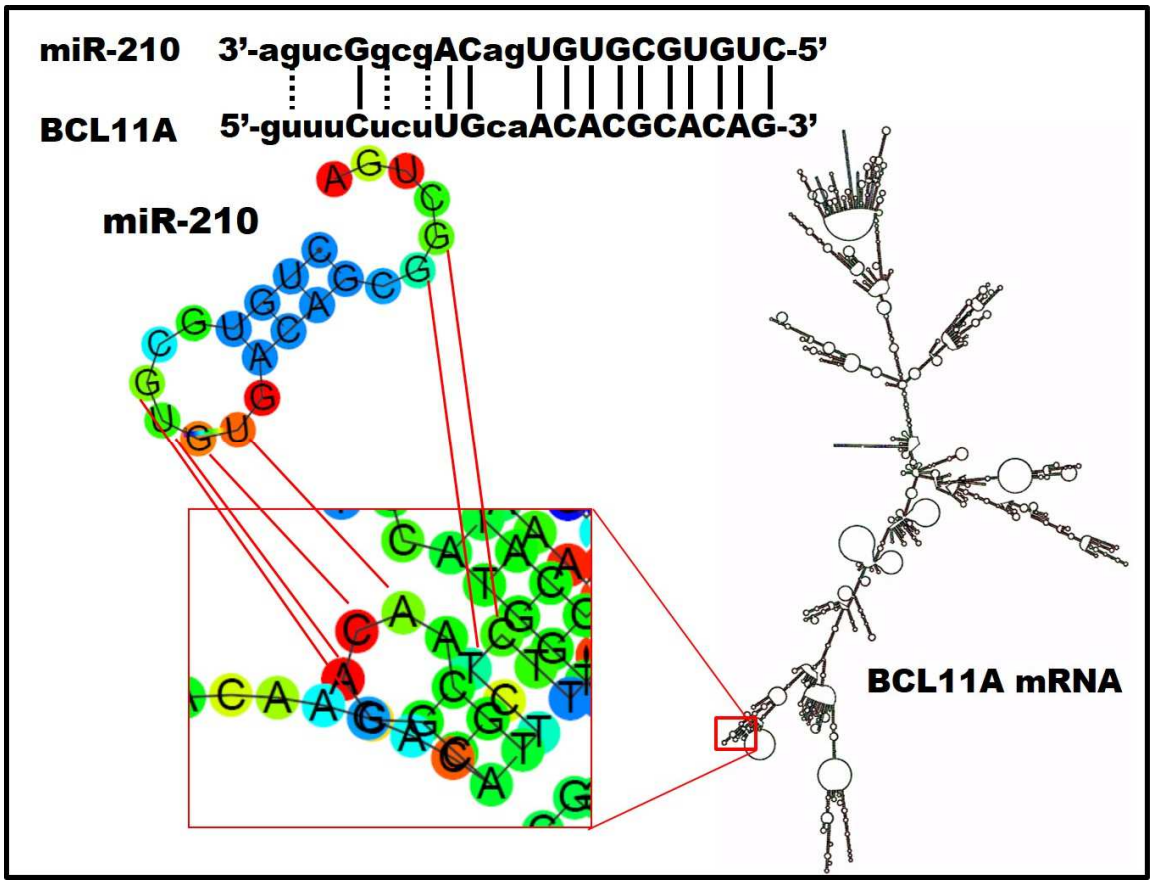

Figure 37. **Identification of miR-210 binding site in BCL11A mRNA**. A bioinformatics analysis was performed to identify the interaction between BCL11A mRNA sequence and mature miR-210 sequence. The combined used of miRWalk 2.0 and RNAfold, allow us to identify a binding site located at nucleotides 789-798 in the coding region of BCL11A mRNA.

site in the coding region of BCL11A mRNA located at nucleotides 789-798. As indicated in **Figure 37**, the homology involved thirteen C-G or U-A and three G-U base pairing. The

extent of complementary between human BCL11A mRNA sequence (NM_022893) and mature miR-210 was analysed using RNAfold [*http://rna.tbi.univie.ac.at/cgi-bin/RNAfold.cgi*] and a complementary of 72.7% between the two sequences was calculated. Moreover, the binding site is located at nucleotides 789-798, as previously predicted by miRWalk, with a predicted length of ten nucleotides and a p-value of 0.0024. The interaction takes place in the coding region and exhibits partial single stranded secondary structure interaction.

3.4 Analysis of putative miR-210 binding site

Despite the fact that the sequence of BCL11A mRNA presents some minor variations among species, the BCL11A mRNA sequences concerning the miR-210 binding site are highly conserved through molecular evolution. As reported in **Figure 38**, six different

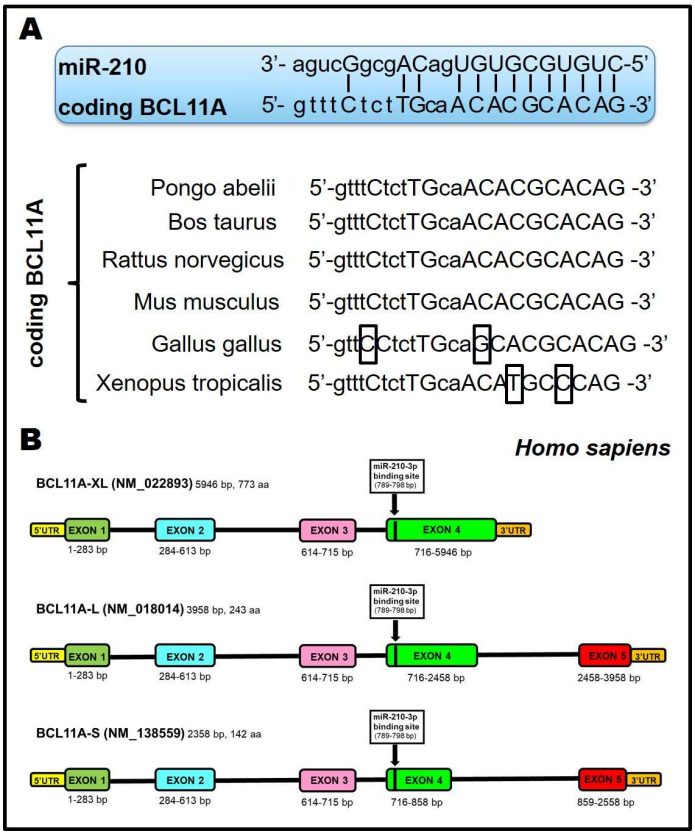

Figure 39. Analysis of putative miR-210 binding site. Panel A putative miR-210 binding site was evaluate in six different species: orangutan (*Pongo abelli*, XM_002812009.2, nucleotides 709-718), bovine (*Bos Taurus*, NM_001076121.1, nucleotides 787-796), mouse (*Mus musculus*, NM_016707.3, nucleotides 896-905), rat (*Rattus norvegicus*, NM_001191683.1, nucleotides 803-812), red junglefowl (*Gallus gallus*, NM_001031031.1, nucleotides 812-821) and frog (*Xenopus tropicalis*, NM_001079189.1, nucleotides 592-601). Panel B location of miR-210 binding site within the different BCL11A isoforms. The three principal BCL11A isoforms have been considered: XL, L, S.

species were considered and in four of them (*Pongo abelli*, *Bos taurus*, *Rattus norvegicus* and *Mus musculus*) the sequence was found perfectly homologous, while two nucleotides

differences were found in *Gallus gallus* and *Xenopus tropicalis*. Moreover, as well explained in Liu et al., 2006, BCL11A presents several isoforms, the principal and best characterized being isoforms XL, L and S. While exons from 1 to 3 are common to all the isoforms, major differences involved exon 4, which presents different length between isoforms and exon 5 which is present only in isoforms L and S. MiR-210-3p binding site in located in the exon 4. Interestingly the sequence bound by miR-210-3p is present in all the three principal isoforms.

3.5 Evaluation of miR-210 interaction with BCL11A mRNA using Biacore analysis

As reported in Witkos et al, [*Witkos et al., 2011*] the functional interaction between miRNA and its respective target 3'UTR sequence is usually confirmed and validated by luciferase based reporter assay. While this kind of assay is very useful when miRNA binds

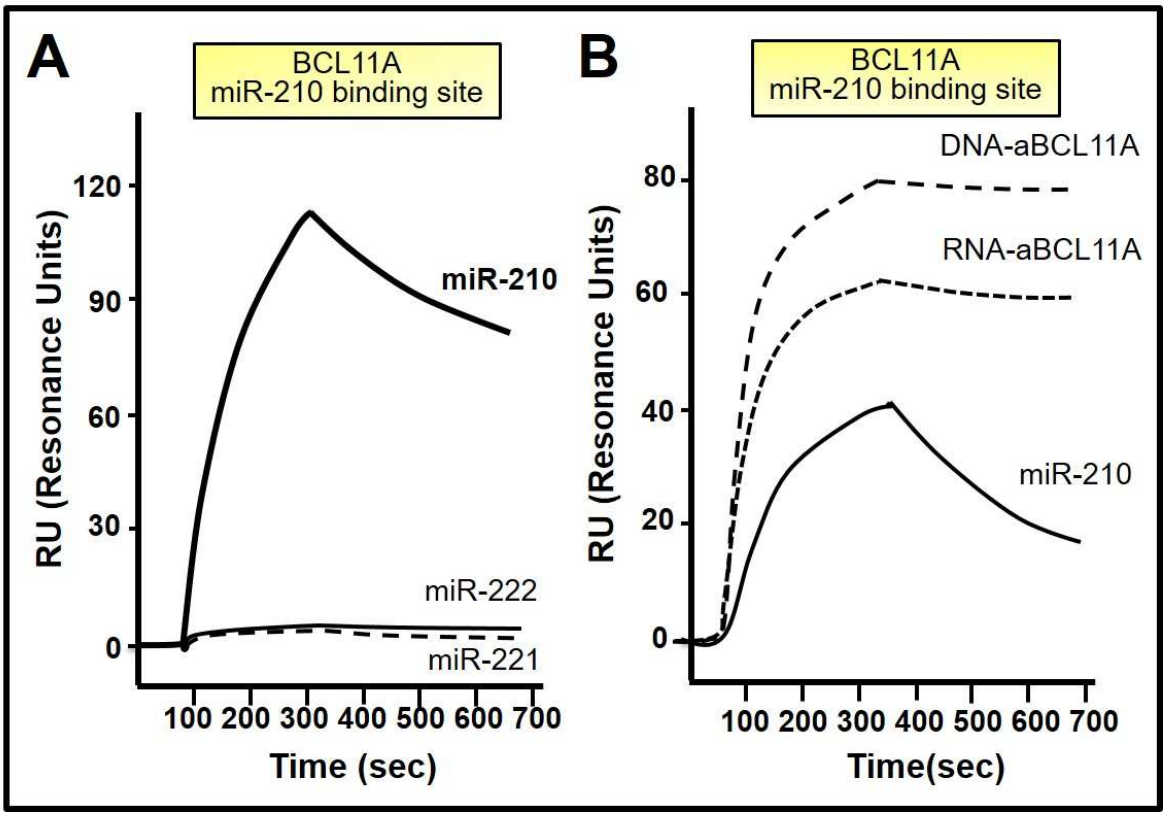

Figure 39. Evaluation of miR-210 interaction with BCL11A mRNA using SPR-based technology. Panel A, the interaction between a sequence containing miR-210 binding site, immobilized in the sensor chip and three different synthetic mature miRNAs (miR-210, miR-221, miR-222) was analysed. Panel B: the interaction between a sequence containing miR-210 binding site, immobilized in the sensor chip and the synthetic mature miR-210 (black continuous line) or a perfectly complementary RNA or DNA sequence (dotted lines) was analysed.

the 3'UTR of the target mRNA, it is not suitable when miRNA binds a sequence located within the coding region of the target mRNA, as in our case. For this reason, in order to

validate the binding between BCL11A mRNA and miR-210-3p an SPR-based method was employed, using the Biacore X100 biosensor. As reported in panel A of **Figure 39**, a biotinylated oligonucleotide mimicking the miR-210 binding site sequence of BCL11A mRNA was immobilized in the SA sensor chip, and three different synthetic mature miRNAs: miR-210-3p, miR-221-3p and miR-222-3p were injected and the obtained sensorgrams are reported. As it is possible to see in the Figure when miR-210 is injected a significative increase of RU values was obtained, indicating the formation of a molecular complex between the injected miRNA and the target sequence immobilized on the sensor chip. On the contrary, no changes in RU values were shown, when two unrelated miRNAs, used as negative control were injected. At same time as further control, the synthetic DNA or RNA sequence fully complementary to the immobilized sequence were injected. When miR-210 is injected a high difference between RUres value and RUfin value is detected, indicating that the generated complex is not fully stable, while, as expected, when fully complementary DNA or RNA are used, no differences were found between RUres and RUfin, indicating that the formed hybrid is completely stable.

3.6 PremiR-210 transfection in clones overexpressing BCL11A, effects in mRNA levels

As explained in the "Materials and methods" chapter, K562 cells, which are normally employed for fetal haemoglobin induction studies, are not useful in our case, because they express only low levels of BCL11A. For this reason, our research group developed K562 cell clones which are able to express high levels of BCL11A mRNA and protein, as described in Finotti et al. [*Finotti et al., 2015*]. Cells were treated with increasing concentrations (from 30 to 270 nM) of premiR-210, in order to increase miRNA levels present within the cells and verify their effects on BCL11A mRNA and in gamma globin mRNA expression. All reported data are expressed with respect to the results obtained using a premiR negative control, i.e. a premiR with a sequence completely unrelated to miR-210. At same time also untransfected cells were considered, to verify possible differences with premiR negative control. As it is possible to see in **Figure 40**, no significant differences were seen when untreated sample or sample treated for 48 hours with premiR negative control were compared. On the contrary, when premiR-210 was employed a significant decrease of BCL11A mRNA content was detected. Moreover, the effects of premiR-210 seem to be dependent on the employed concentration. Similarly, gamma globin mRNA content was quantified using RTqPCR. The results obtained are shown in Figure 41, and demonstrate

that the BCL11A mRNA decrease is associated with an increase in gamma globin mRNA content (very low when 30 nM of premiR-210 was employed, but much higher when increasing concentrations of premiR-210 were used).

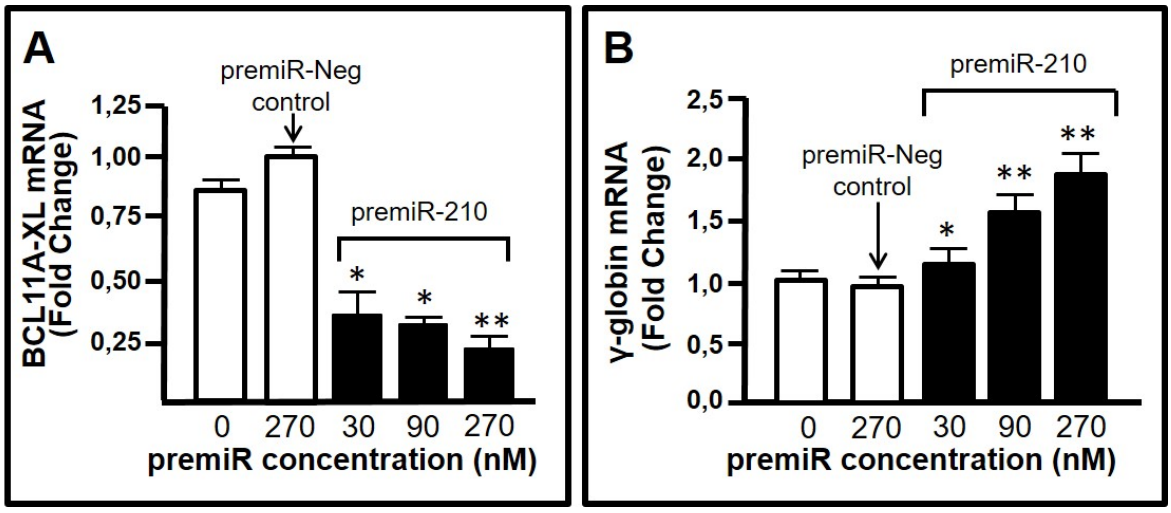

Figure 40. **PremiR-210 transfection in clones overexpressing BCL11A, effects in mRNA levels.** Panel A three different concentrations of premiR-210 were employed: 30, 90 and 270 nM, relative expression was calculated respect to the sample treated with premiR negative control. At same time an untreated sample was considered. Panel B, in the same samples, gamma globin mRNA expression was quantified respect to premiR negative control treated sample. For premiR negative control only the highest concentration (270 nM) was considered. Reported data are obtained by the average of three independent experiments.

3.7 PremiR-210 transfection in clones overexpressing BCL11A, effects on protein expression

There is a general agreement on the fact that miRNAs targeting the 3'UTR sequences of mRNAs are more effective in inducing mRNA degradation. By contrast, for miRNAs targeting the coding region, generally is more probable to see effects only in protein production. In order to verify effect of premiR-210 on its putative target, a western blot analysis was performed, and BCL11A protein content was verified. In **Figure 41** (Panel A) a representative western blotting analysis of the protein BCL11A is reported. Only one concentration of premiR (200 nM) was employed, and three different control samples are included, i.e. an untreated sample, a sample treated with only the premiRNA vehicle (Lipofectamine) and a sample treated with premiR negative control. In this case 72 hours treatment was performed. For both premiR-210-3p and premiR negative control the same concentration was employed. While no differences in protein content were shown between the three control samples, a significant decrease in protein content was detected when premiR-210-3p was transfected in K562 BCL11A clones. The same membranes were also

re-probed with and antibody against p70 protein used as reference protein to verify that all samples contained the same starting protein extracts content. The ratio between the intensity of BCL11A protein and the intensity of p70 protein was calculated and data are reported in panel B. As evident, again no significant differences are appreciable between the three different controls, while an about 40% decrease in protein content was detected when premiR-210 was employed.

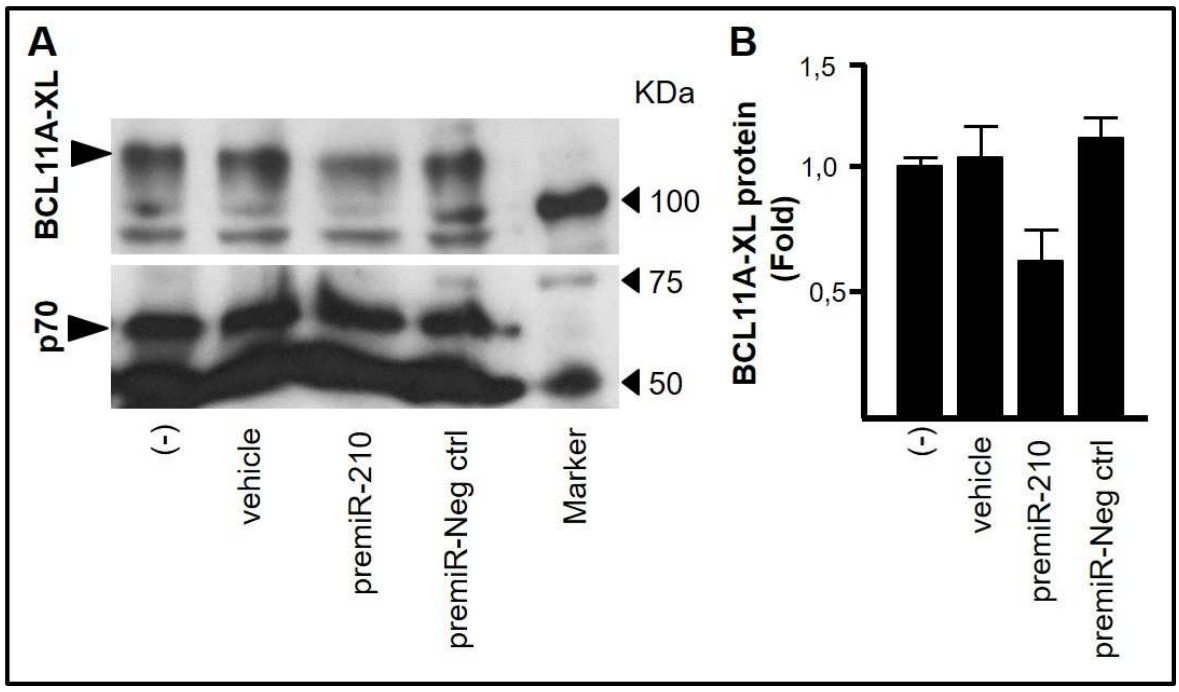

Figure 41. **PremiR-210 transfection in clones overexpressing BCL11A, effects on protein expression.** Panel A: representative western blotting analysis of BCL11A protein. Upper line BCL11A band intensity in the four samples is reported. As it is possible to see BCL11A protein has a molecular weight of about 125 kDa. In the lower line, band intensity of p70 protein, used as reference protein, is reported. Both BCL11A and p70 were detected in the same membranes, which were firstly probed with antibody against BCL11A and then stripped and re-probed with an antibody against p70 protein. Samples are analysed 72 hours after the transfection.

3.8 PremiR-210 transfection to ErPCs: effects on the transcript

PremiR-210 effects were also verified in a more suitable cellular model: erythroid precursors cells isolated from beta-thalassemia patients. At the end of the two weeks purification and expansion protocol (see methods section), ErPCs were transfected with premiR-210-3p or premiR negative control at the final concentration of 200 nM. RNA was collected 72 hours after the transfection and BCL11A and gamma globin mRNA content was quantified using RTqPCR, as indicated in **Figure 42**. Relative expression was calculated with respect to sample transfected with the premiR negative control. No major differences were found between untreated sample and sample transfected with premiR negative control

when BCL11A and gamma globin content were determined. When premiR-210 transfected samples were considered, a decrease of about 40% in BCL11A mRNA content was detected associated with a weak but significant increase in gamma globin mRNA expression.

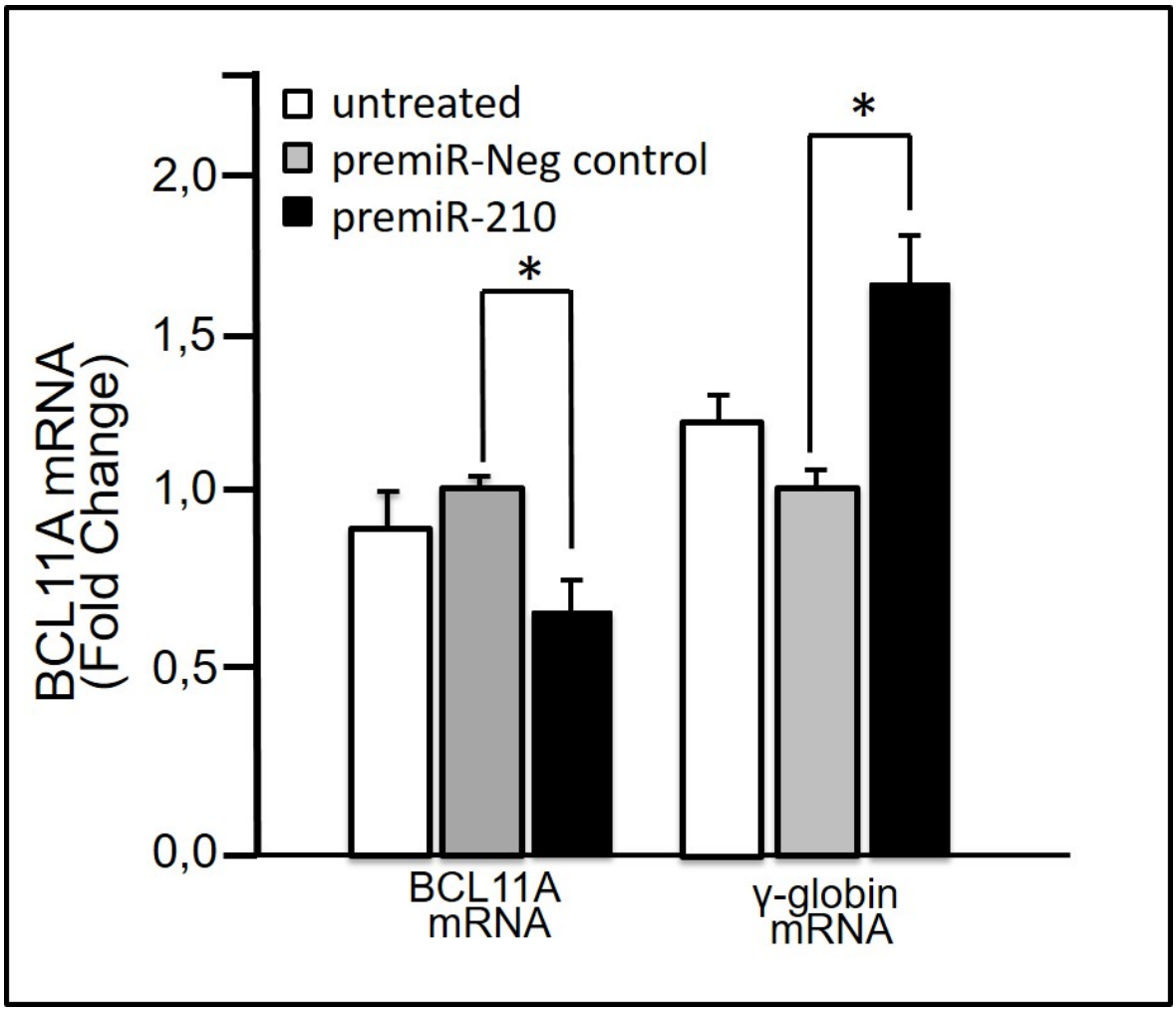

Figure 42. **PremiR-210 transfection in ErPCs, effects on transcript**. ErPCs were transfected with 200 nM of premiR-210 or premiR negative control. 72 hours after the transfection RNA was isolated and BCL11A and gamma globin mRNA was quantified using RTqPCR. Fold changes have been calculated respect to sample treated with premiR negative control. Five different beta-thalassemia patients were recruited to performed analysis. Data are expressed as the average of three independent experiments.

3.9 PremiR-210 transfection in ErPCs, effects on gamma globin protein expression

Since transcript data demonstrated an increase in gamma globin mRNA content after the transfection with premiR-210, we further investigated miR-210 effects on gamma globin protein production, quantifying gamma globin protein content, through Elisa analysis, 72 hours after the transfection with premiRNA. As reported in **Figure 43**, about two-fold increase in gamma globin protein production was detected when ErPCs transfected with premiR-210 were considered. In order to verify whether the effects of the transfection with

premiR-210 are restricted to BCL11A and γ-globin gene expression, additional erythroid associated markers, such as CD71 and Glycophorin A, were studied in transfected ErPCs. As reported in the Panel B of the Figure 43, no differences were detected when premiR-210 is transfected in erythroid precursors cells.

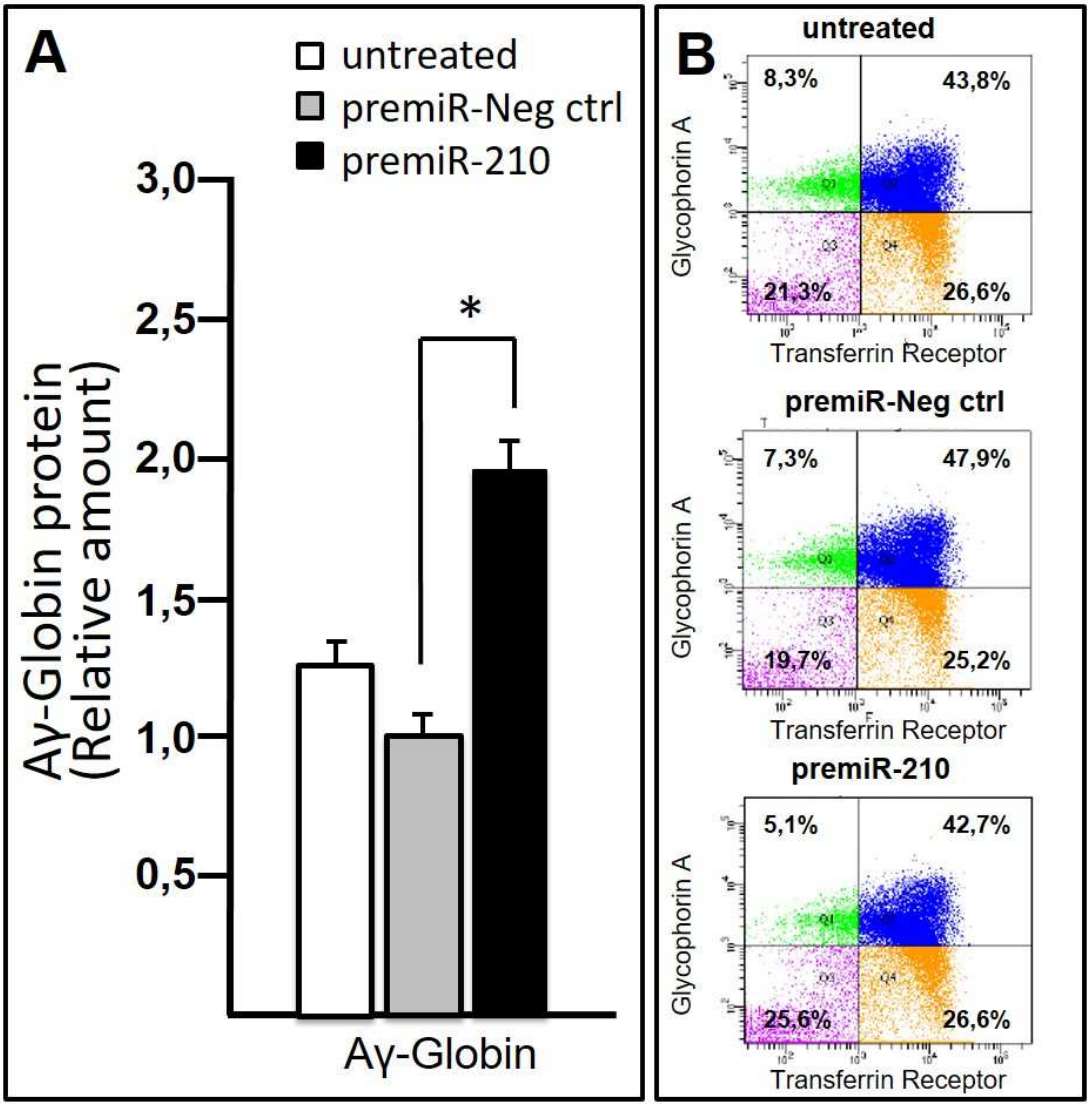

Figure 43. PremiR-210 transfection in ErPCs, effects on gamma globin protein expression. Panel A: A-gamma globin protein was quantified using Elisa analysis and the relative amount of protein was calculated respect to sample treated with premiR negative control. Data are relative to 72 hours transfection with 200 nM of premiR-210 or premiR negative control. Panel B: effects of premiR-210 transfection in two erythroid associated markers: CD71, transferrin receptor, (Y-axis) and GPA: Glycophorin A (X-axis) were verified in ErPCs after the transfection with premiR-210. Representative plots of FACS analysis with fluorescent labelled antibodies were reported.

3.10 PNAs targeting miR-210 binding site in BCL11A

As previously described, peptide nucleic acids (PNAs) are very useful to regulate miRNAs and gene expression. One of the major advantages in using PNAs is related to their high resistance to both DNAse and RNAse. For this reason, starting from the data reported

in 3.4-3.7 sections and demonstrating miR-210 mediated modulation of BCL11A expression through a binding to a specific coding sequence of the BCL11A mRNA, we designed, in collaboration with Prof Romanelli's research group, two different PNAs, both able to bind BCL11A in the same sequence bound by miR-210. In this case, obtained PNAs acts as antisense molecules, binding BCL11A mRNA and leading to its inhibition. The first PNA (PNA miR210-3p_like), exhibit the same miR-210 sequence; the second one is constituted by a sequence fully complementary to the miR-210 binding site in the coding region of BCL11A mRNA.

3.10.1 Treatment of clones over-expressing BCL11A with PNAs binding miR-210 target sequence

Also in this case, K562-BCL11A clones were very useful for a preliminary validation of the biological effects of the employed PNAs. Three different PNAs concentrations (2, 4 and 8 µM) were tested and BCL11A mRNA content quantified 48 hours after the treatment.

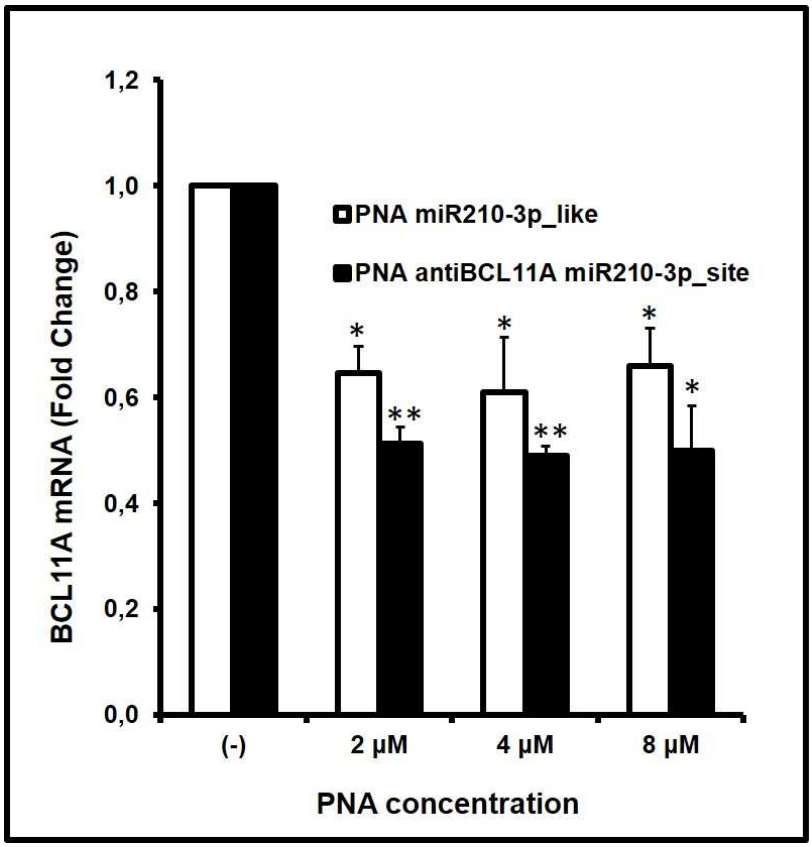

Figure 44. Treatment of clones overexpressing BCL11A with PNAs binding miR-210 target sequence. Two different PNAs were tested: PNA miR210-3p_like (white boxes) and PNA antiBCL11A miR210-3p_site (black boxes). Three different concentrations: 2, 4 and 8 µM of PNA were used to treat K562 clones overexpressing BCL11A. 48 hours after the treatment RNA was extracted and BCL11A mRNA expression was evaluate respect to untreated control. All data were normalised using RPL13A as house keeping gene. Reported data are the average of three independent experiments.

As shown in **Figure 44**, both PNAs are able to down-regulate BCL11A mRNA expression even if with some differences. In fact, as expected, the PNA fully complementary to miR-210 binding site is able to reduce BCL11A mRNA (50% of reduction) with higher efficiency when compared with the PNA miR210-3p_like (reduction not exceeding 35-40%). While no differences were founded considering the three different concentrations for both PNAs.

3.10.2 Combined treatment of BCL11A clones with PNA and MTH

In the same cellular model, PNAs were used in association with one of the best fetal haemoglobin inducers (mithramycin, MTH), in order to evaluate possible combined effects. Considering that MTH needs at least 96 or 120 hours to induce the production of HbF, we treated for 5 days K562 clones with 2 μM PNA concentration, selected after the first

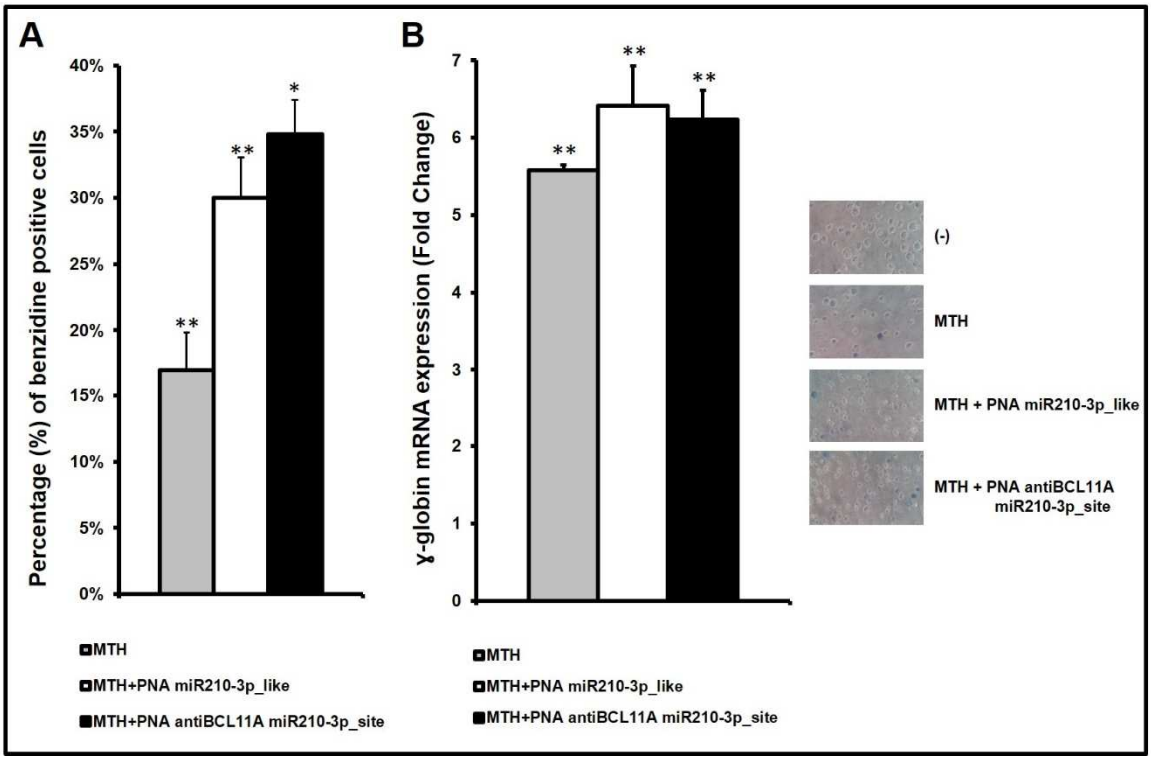

Figure 45. **Combined treatment of BCL11A clones with PNA and MTH.** Clones overexpressing BCL11A were treated with both MTH and PNA miR210-3p_like (white box) or PNA antiBCL11A miR-210-3p_site (black box). Panel A percentage of benzidine positive cells was reported and relative picture are shown in the right part of the Figure. Panel B: gamma globin mRNA expression was shown; data are expressed as fold change respect to the untreated sample. Fold change was reported for MTH treated sample (grey box), MTH + PNA miR210-3p_like (white box) and MTH + PNA antiBCL11A miR210-3p_site (black box).

preliminary analysis (see Figure 44), and with 20 nM MTH. At 5th day, the percentage of benzidine positive cells was calculated and reported in panel A of **Figure 45**. As it is evident in the Figure 45, when MTH is used in association with PNAs an increase in percentage of benzidine positive cells of 13% and 17% for PNA miR210-3p_like and for PNA

antiBCL11A miR210-3p_site was detected, respectively. Pictures relative to cells positive to benzidine staining are reported in the right part of the Figure. Moreover, the effects of combined treatment were verified also by analysing gamma globin mRNA expression. As reported in the panel B, mithramycin used alone is able to generate a sharp increase of gamma globin mRNA, moreover, if MTH is used in association with a PNA an increase of about one fold is detected, with no major differences between the two PNAs.

3.10.3 Treatment of ErPCs with PNAs binding miR-210 target sequence

The same PNAs were also tested on ErPCs isolated from beta-thalassemia patients. On the basis of the data obtained treating clones overexpressing BCL11A, only 2 µM PNA

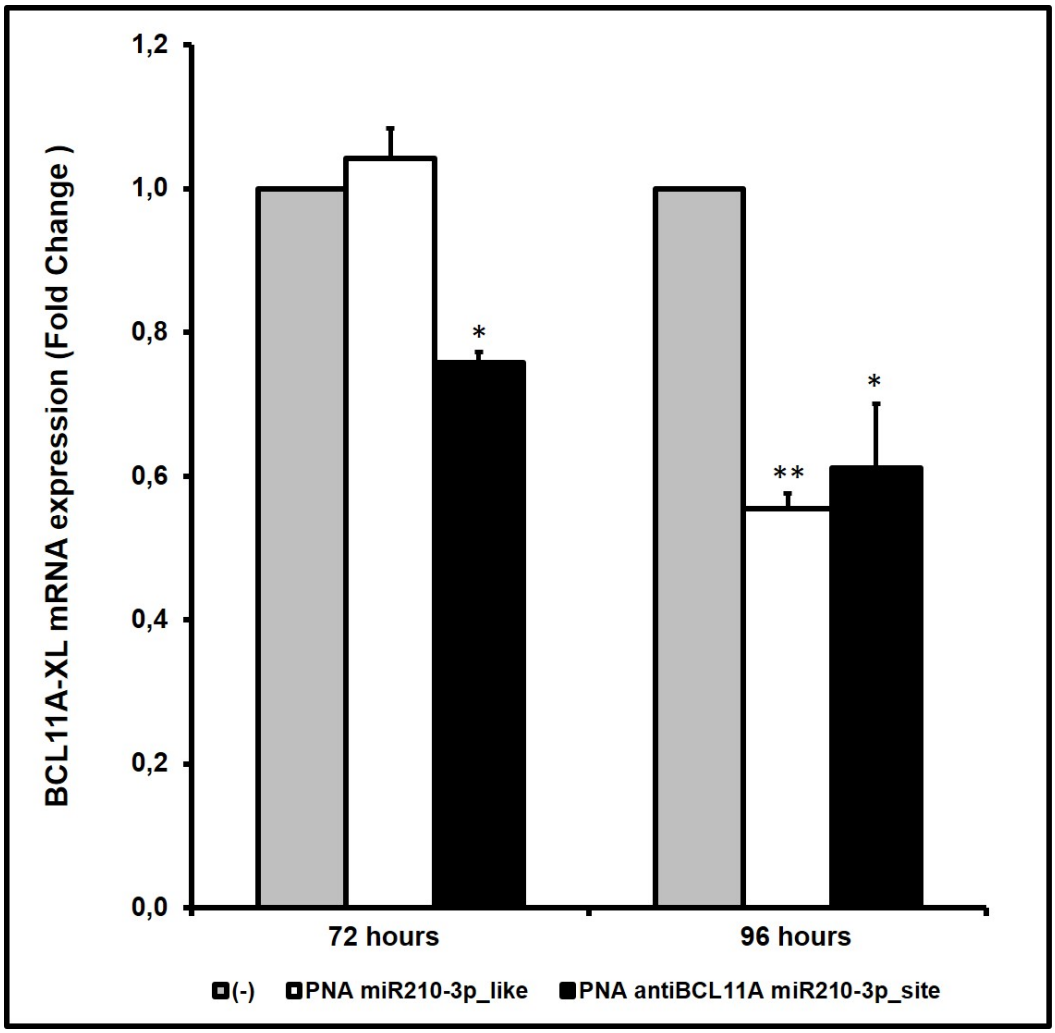

Figure 46. Treatment of ErPCs with PNAs binding miR-210 target sequence. ErPCs were treated for 72 and 96 hours with 2 µM concentration of both PNAs: PNA miR210-3p_like (white boxes) and PNA antiBCL11A miR210-3p_site (black box). BCL11A mRNA relative expression was calculated respect to untreated control. Presented data are obtained by the average of three independent experiments.

concentration was used to treat ErPCs. Cells were treated with PNA miR210-3p_like or PNA antiBCL11A miR210-3p_site for 72 or 96 hours. As shown in **Figure 46**, after 72 hours treatment no effects in BCL11A mRNA were detected, while a weak reduction of about 20% was detected when PNA antiBCL11A miR210-3p_site was employed. More significant effects were instead seen when ErPCs were treated for 96 hours. In this case, an average decrease of 35-40% was reported, with no high differences between the two PNAs.

3.11 General conclusions and take-home messages

The results of this part of the thesis should be considered in the context of novel therapeutic options leading to fetal hemoglobin (HbF) induction in β-thalassemia. There is a general agreement on the fact that the validation of new approaches for reactivation of γ-globin genes are required to develop novel options in the therapy of β-thalassemia. In this respect, of great interest is the recent finding that the transcriptional regulation of γ-globin gene expression is under the negative control of several transcriptional repressors, including MYB, BCL11A, KLF-1, KLF-2, Sp1, LYAR. These evidences allow the identification of specific targets for the development of possible strategies to reactivate γ-globin gene expression (as consequently HbF production) by targeting repressors of γ-globin gene transcription. Among possible alternatives the use of microRNA-based approaches can be proposed. In fact, the involvement of miRNAs in the control of transcriptional repressors of the human γ-globin genes has been firmly demonstrated. Examples are miR-15a and miR-16-1 (targeting MYB mRNA), miR-486-3p (targeting BCL11A mRNA), miR-23a (targeting KLF-2) and miR-27a (targeting Sp1).

In the present part of the thesis we have described a coding sequence of BCL11A mRNA as possible target of miR-210. The following results sustain this hypothesis: (a) interactions between miR-210 and the miR-210 BCL11A mRNA site were demonstrated by SPR-based biomolecular interaction analysis (BIA) (see Figure 39); (b) the miR-210 site of BCL11A-XL is conserved through molecular evolution, possibly indicating that these sequences play a key biological function (see Figure 38); (c) forced expression of miR-210 leads to decrease of BCL11A mRNA and increase of γ-globin mRNA content in erythroid cells, including erythroid precursors isolated from β-thalassemia patients (see Figures 40 and 42). However, the effects of the transfection with pre-miR-210 are restricted to BCL11A and γ-globin gene expression, and no changes of the other erythroid markers CD71 and GPA were detectable suggesting that the treatment with pre-miR-210 is not sufficient to induce

the activation of erythroid differentiation and, therefore, should be combined with other inducers of erythroid differentiation in order to fully induce HbF accumulation. Interestingly a decrease of BCL11A expression was found in ErPCs from β-thalassemia patients treated with HU and MTH together with the expected increase of γ-globin mRNA content, further supporting the role of this transcriptional regulator and its modifiers.

While most of validated miRNA/mRNA interactions involve the 3'-UTR of the target mRNAs, functional interactions between microRNAs and coding sequences of target genes have been reported in several studies. Our study suggests that, in addition to the already reported binding of miR-486-3p to the 3'UTR sequence of the BCL11A mRNA, the coding mRNA sequence of BCL11A can be targeted by miR-210 (see the scheme reported in Figure 48). In the experimental approaches described, upregulation of γ-globin gene expression can be achieved by different miRNA-based approaches, including the use of

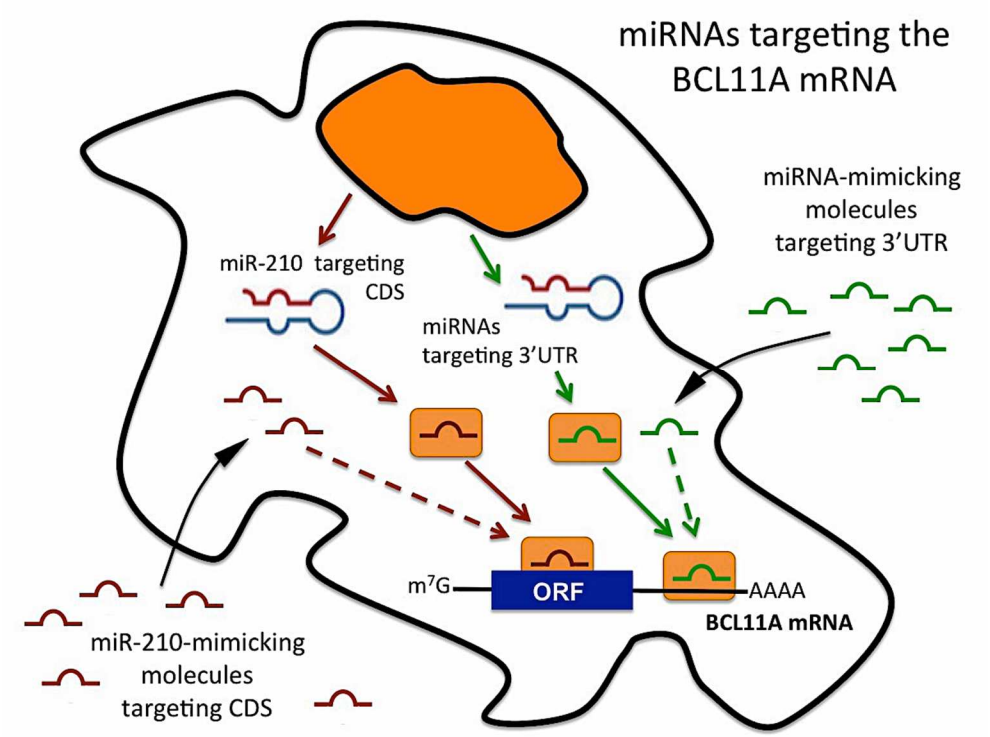

Figure 47. Possible miRNA mimicking approach. Scheme outlining the possible miRNA mimicking approach for targeting the 3'UTR and the coding sequence (CDS) of the BCL11A mRNA using miRNA mimicking molecules. Down-regulation of BCL11A gene expression will lead to up-regulation of γ-globin mRNA, as reported in Figure 40.

premiRNA targeting the 3'UTR region of the BCL11A mRNA, or the use of premiR-210, possibly targeting the coding region. Both strategies, that might involve different miRNA which, at least in theory, can be combined in a "multi-miRNAs therapeutic approach" might lead to BCL11A down-regulation and induction of γ-globin gene expression, in consideration of the γ-globin genes repressor function of BCL11A.

In addition to the theoretical point of view, these data are of interest, in our mind, from the applied point of view, since might indicate a novel strategy to inhibit BCL11A by mimicking miR-210 functions. This is of interest, since inhibition of BCL11A is a recognized strategy for HbF induction for treatment of β-thalassemia, as suggested by several papers and patent applications. Further controls, including studies on the effects of miRNAs unable to target the BCL11A mRNA and analysis of the effects of miR-210 on BCL11A mRNA carrying a mutated and not functional miR-210 binding site should be considered for deeper validation. Moreover, a most extensive analysis on overall gene expression patterns should be considered, especially in consideration of the fact that this BCL11A site covers the nucleotide region 789-798, which is common to all the BCL11A isoforms (see Figure 39). Finally, it should be considered that this strategy might also be applied in combination with other approaches using miRNA mimics targeting the 3'UTR of BCL11A mRNA, as well as other transcriptional repressors of the γ-globin genes, or chemical HbF inducers.

A second conclusion of data reported in this section is that BCL11A inhibition can be reached using PNAs targeting the miR-210 binding sites. The PNA-BCL11A mRNA recognition is greatly facilitated by the evolutionary conserved miR-210 binding sites (Figure 39) which makes these regions prone to molecular interactions with biomolecules (in our case not only miR-210, but also PNAs binding miR-210 target sequence). When PNAs binding miR-210 target sequence are used the effects on BCL11A is simply an antisense effects leading to BCL11A inhibition.

As final conclusion, while the targeting of BCL11A mRNA (for instance with PNAs mimicking miR-210) and/or BCL11A regulators (i.e. premiR-210 molecules) might lead to a sharp inhibition of the γ-globin gene repressor BCL11A this approach should be combined with the effects of other HbF inducers (eventually used at sub-optimal concentrations) for best HbF inducing activity.

IV. MicroRNA therapeutics: Delivery of miRNAs and miRNA-targeting PNAs using Calixarenes

MiRNA-based therapy is one of the emerging fields of investigation in recent years, and, as described in the 'miRNA therapy' chapter, several types of therapeutic approaches have been proposed to target miRNAs. One of major issues encountered in miRNA-based therapy is the miRNAs/premiRNAs delivery. It should be underlined that miRNA-carrying vehicles not only are essential to transfer miRNA-based molecules into target cells, but also have a key role in avoid degradation of this kind of molecules. Moreover, also the delivery of antagomiRNAs is a key step to obtain an efficient miRNA-therapeutic approach. A large number of vehicles were tested both *in vitro* and *in vivo*, but most of them present several issues such as inappropriate biodistribution, disruption and saturation of endogenous RNA machinery and high toxicity [*Zhang et al., 2013*]. Starting from the experience of Professor Sansone and co-workers, who studied for a long time calixarene-based molecules for DNA delivery, we tried to use these molecules to deliver miRNA mimic molecules [*Bagnacani et al., 2013*]. The calixarene-based molecule ML122 was chosen as first molecule to investigate, starting from the evidence that this molecule, among a panel of calixarene-based molecules, showed the highest ability to deliver DNA. Moreover, we also employed calixarene-based molecules to delivery PNAs. PNAs, that are employed to target several kind of biological molecules, including miRNAs or mRNA, are stable molecules, but exhibit low cellular uptake. Therefore, they require an efficient delivery system to finalize their therapeutic potential.

4.1 Delivery of miRNA mimicking molecules using ML122

In order to increase miRNA levels into cells, miRNA mimicking molecules are used. These molecules exhibit usually the same sequence of the endogenous premiRNA to be mimicked in its biological functions. They are internalised and processed by the miRNA processing machinery mimicking the same function of physiological miRNAs. In the laboratory practice, one of the most useful methods to carry synthetic premiRNA molecules into cells, is the use of cationic liposomes able to interact with negative charges, present in the premiRNA structure, forming a complex that is internalised by cells. Lipofectamine ®

(Invitrogen) or Siport ® (Ambion) are only two examples of reagents commonly used at this purpose. Generally, these reagents present high toxicity, and a very variable transfection efficiency depending on the employed. In these studies we used as a model system cell growing attached to the flask (such as the human glioma U251 cells), and cell growing in suspension (such as the human leukemia K562 cell line).

4.1.1 Mature miRNA transfection using ML122

To evaluate the transfection ability of ML122 we firstly employed a synthetic mature miRNA conjugated with a fluorescent molecule (fluorescein), that allows to verify miRNA internalization using rapid methods as fluorescence microscopy and FACS analysis. As shown in **Figure 48**, the adherent U251 cell line was transfected with the fluorescent mature miR-210, using ML122 at final concentration of 10 µM. For this preliminary experiment the same ML122 concentration, previously used by Bagnacani and colleagues for DNA transfection was chosen [*Bagnacani et al., 2014*]. Cells, transfected with two different

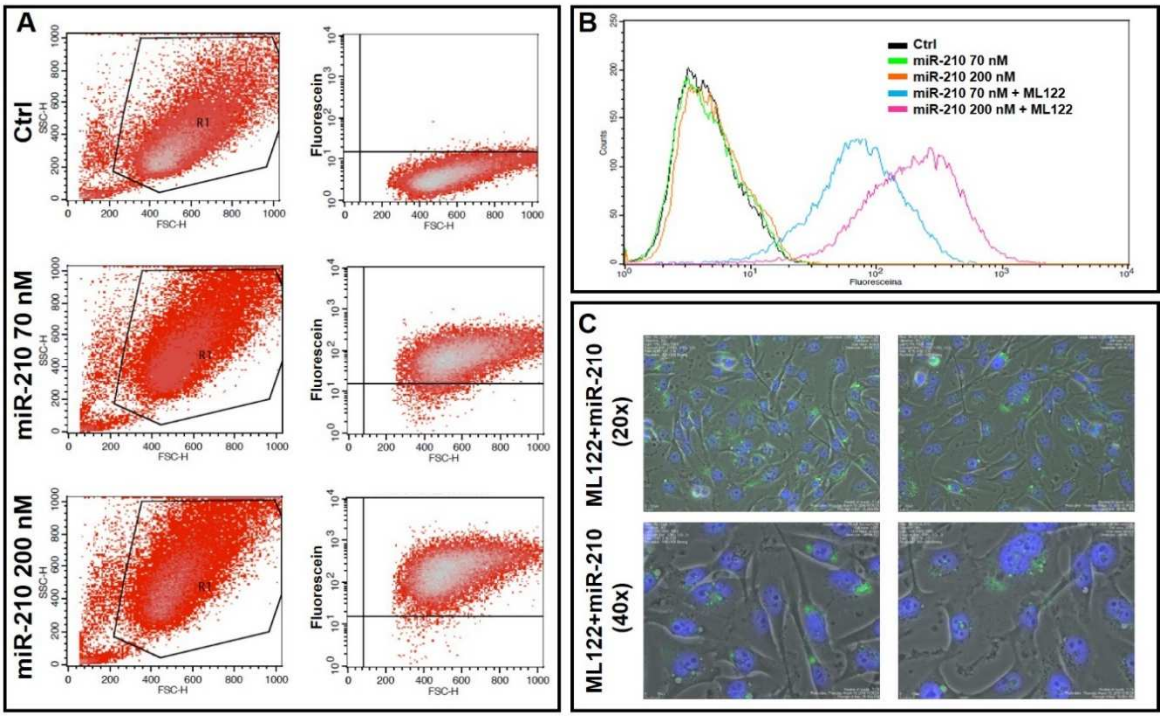

Figure 48. Fluorescent mature miRNA transfection with ML122. Panel A: three representative samples are reported: no transfected cells (Ctrl) and cells transfected with two different concentrations of miR-210 and ML122. In the left part of panel A forward and side scatter plot for each samples are reported, while in the right part of the panel fluorescence (FITC) plot are reported. Overlay of all analysed data are shown in Panel B. Five different samples are considered: Ctrl (black curve), cells transfected with no ML122 and 70 nM of miR-210 (green curve), miR-210 200 nM without ML122 (orange curve), cells transfected with 70 nM of miR-210 and ML122 10 µM as vehicle (light blue curve) and transfected cells with 200 nM of miR-210 and ML122 10 µM (pink curve). Two representative pictures obtained by fluorescence microscopy observation were reported in Panel C. Both 20x image (upper part of the panel) and 40x image (lower part of the panel) are reported.

concentrations of miR-210 (70 nM and 200 nM) were firstly analysed by FACS (**Panel A** and **B**) and fluorescence variation with respect to the control cells was reported. As indicated in panel B, when miR-210 was added with no vehicle, no variation of fluorescence is detected, while the transfection of miR-210 with ML122 leads to a shift in fluorescence directly proportional to the miR-210 concentration. Moreover, pictures obtained by a fluorescence microscopy system, and reported in **Panel C**, were done using in this case only the lower concentration (70 nM) of miR-210.

Data obtained by fluorescence analysis were then confirmed by the quantification of intracellular levels of miRNAs after the transfection using RTqPCR (**Figure 49**). Two different cells lines were employed, the adherent U251 cell line and the in suspension

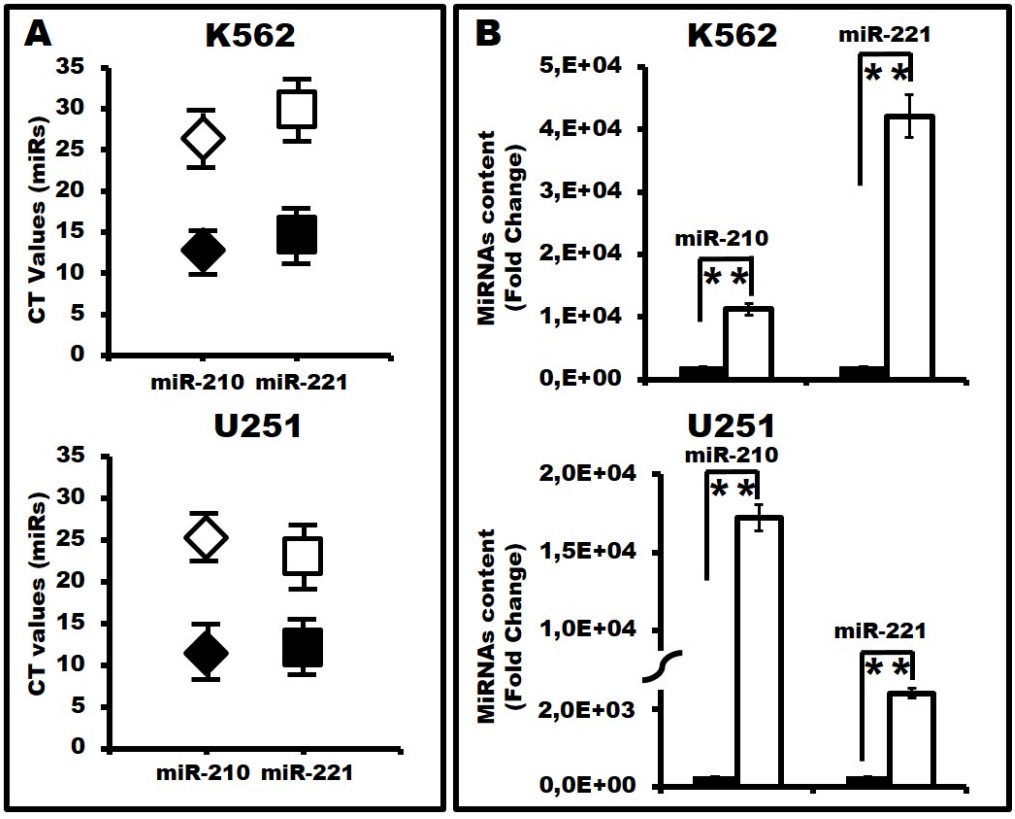

Figure 49. Mature miRNAs transfection with ML122. Two different cell lines: K562 and U251 were employed. Cells were characterized for their starting miR-210 (white rhombus) and miR-221 (white square) levels, comparing CT values. Moreover, measured CT values after transfection were reported: black rhombus (miR-210) and black square (miR-221). Fold change in transfected cells (white boxes) respect control samples (black boxes) was calculated. To calculate fold change and CT values, three independent experiments were performed, and the mean value was reported.

growing K562 cell line, which is known to be difficult to transfect. Moreover, an additional mature miRNA (miR-221) was transfected, to exclude sequence-selective interactions to ML122. As reported in **Panel A**, starting CT values before transfection were determined for

both miR-210 and miR-221 miRNAs and for both cell lines. While miR-210 seems to have similar CTs values in the two cells lines, miR-221 is more expressed in the U251 cell line with respect to K562 cells. MiRNAs content in transfected cells was compared with not transfected samples (**Panel B**). For both miRNAs and in both cell lines a significant increase of miRNAs levels after the transfection was detected, but interestingly, while similar levels of miR-210 were reached in both cell lines after the transfection of mature miR-210, marked difference in fold increase was detected when the two cell lines were transfected with the mature miR-221.

4.1.2 PremiRNA transfection using ML122

In the usual laboratory practice, in order to increase miRNA levels, generally premiRNA molecules are preferred to mature miRNA, for functional issues. In fact, premiRNAs are processed by the cellular miRNA processing machinery. For this reason, after the first promising data shown in Figure 49, we tried to transfect also a premiRNA molecule using ML122, as transfection reagent (**Figure 50**, **Panel A** and **C**). The positive data obtained with mature miR-210 (Figure 49) suggested to use premiR-210. Both cell lines were transfected with two different concentrations of premiRNA, normally used with commercial available transfection reagents (see data miR-210/BCL11A), and ML122 at final concentration of 10 μM. The increase of miR-210 intracellular concentration with respect to the not transfected sample was calculated using RTqPCR and let-7c and snRNA U6 as reference endogenous controls. In both cell lines levels of miR-210 were significantly increased 24 hours after the transfection, even if with some important differences. In fact, in the K562 the fold change seems to be directly proportional to transfected premiRNA concentration (panel A), while in the U251 cell line, no marked increase in fold change was detected between the lower and higher premiRNA concentration (Panel C), suggesting the amount of transfected premiRNA should be verified for each target cell line. Moreover, a comparative analysis was performed between ML122 and a limited panel of commonly used commercial available transfection agents. For the comparative analysis ML122 was used at its usual concentration (final concentration 10 μM, see materials and methods for the transfection procedure), while transfection with commercial available reagents was performed according to the manufacturer's protocols. At same premiR-210 concentration, ML122 demonstrates a miR-210 fold increase that is at least 10 times higher than the most efficient commercially available transfection agent (**Panels B** and **D** of **Figure 50**).

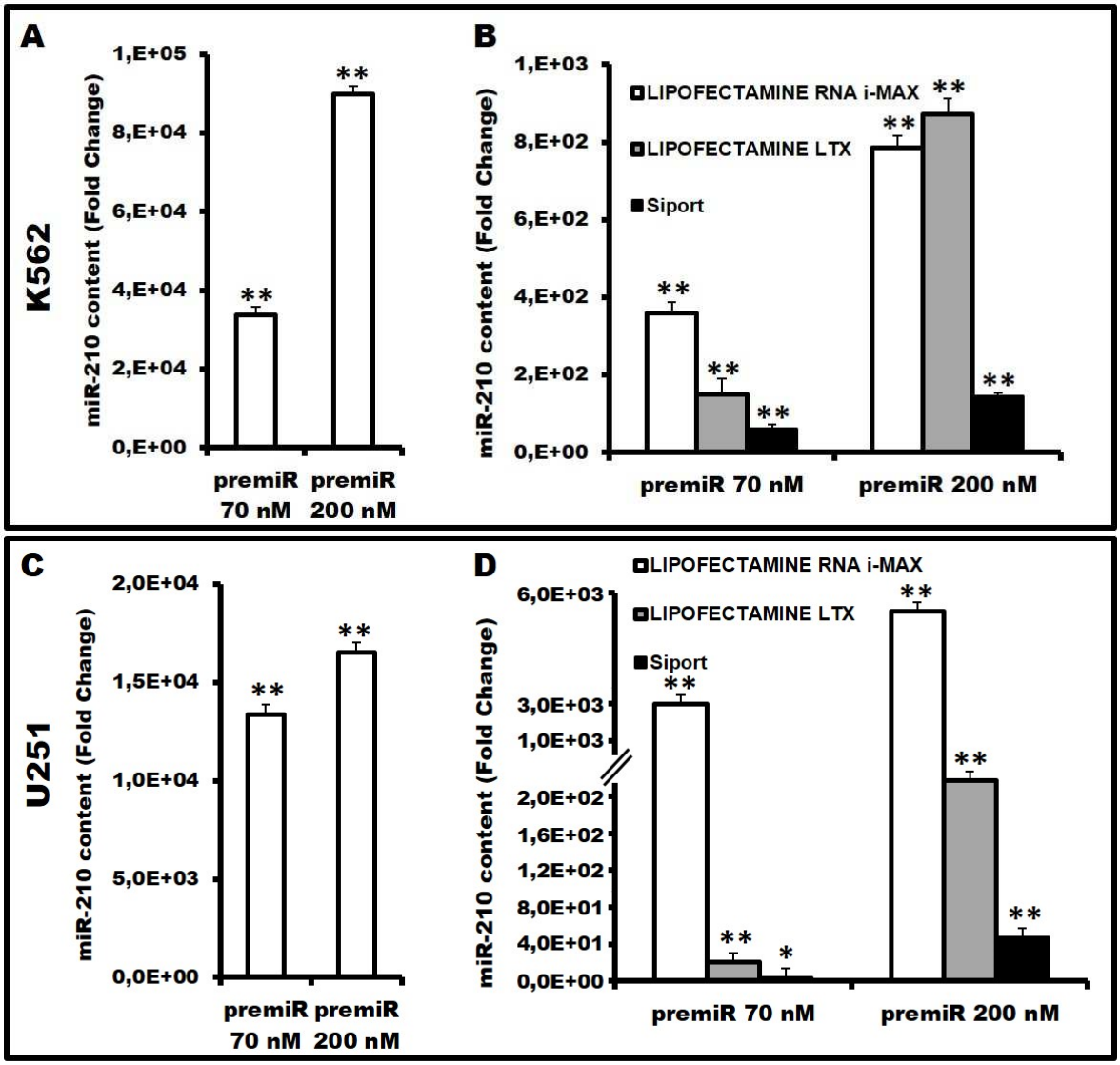

Figure 50. PremiRNA transfection using ML122. **Panel A** and **C**: Two different concentration (70 and 200 nM) of premiR-210 were transfected in both cell lines: K562 (upper part of the Figure) and U251 (lower part of the figure) and miR-210 fold change was determined 24 hours after premiRNA transfection using RTqPCR. **Panel B** and **C:** three commercial available transfection agents: Lipofectamine RNA IMAX (white boxes), Lipofectamine LTX (grey boxes) and Siport (black boxes) were compared with ML122. All data were expressed as miR-210 fold change in transfected samples respect to untransfected samples. The average values of three independent experiments were reported in Figure.

4.1.3 PremiRNA transfection with ML122: experimental set-up of the optimal parameters

All the experiment until now presented were performed using ML122 concentration previously used to perform DNA transfection and premiRNA concentrations that were normally used with commercial available vehicles. In the following experiments we tried to set-up optimal transfection conditions, when ML122 was used as vehicle and premiR was used as molecule to be carried. First of all, we tried to set up the optimal premiRNA

concentration, using the same ML122 10 µM concentration for each point. Increasing concentrations ranging from 5 to 200 nM of premiR-210 were tested in both cell lines. Also in this case the fold change with respect to the control was used to compare different premiRNA concentrations (**Figure 51**, **Panel A** and **C**). The two cell lines presented a different response. In U251 glioblastoma cells the fold change increase was found to be directly proportional to transfected premiRNA concentration; in the case of erythroleukemic K562 cells, no major differences were shown in the range 15-35 nM of premiR, while a significative difference was shown for the higher and the lower premiRNA concentrations.

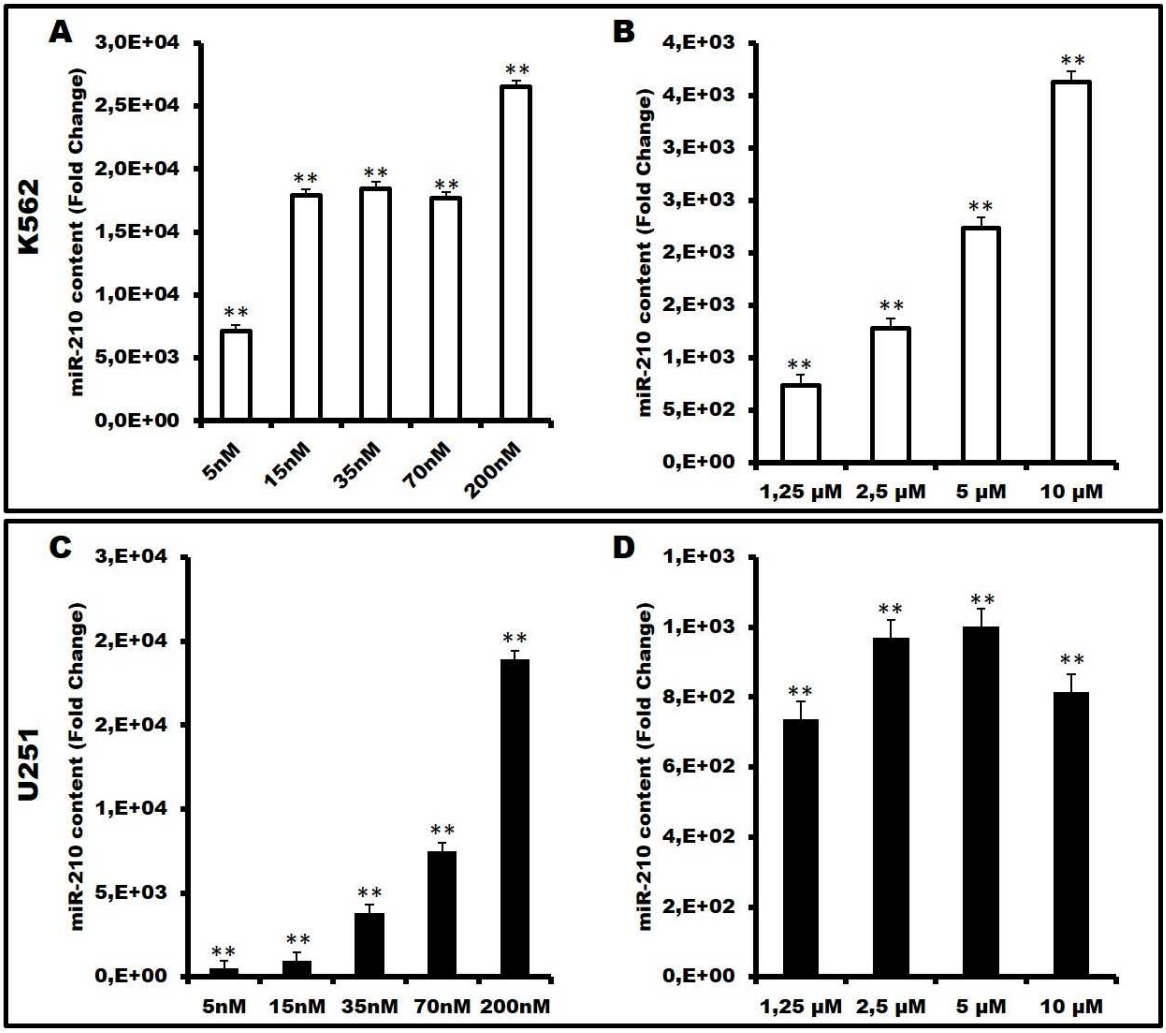

Figure 51. PremiRNA transfection with ML122 condition set-up. The optimal transfection protocol was set up for both K562 cells (white boxes) and U251 cells (black boxes). In histograms miR-210 fold change in transfected cells respect to control was calculated 24 hours after the transfection. In **Panel A** and **C** incremental final concentration of premiR-210 (from 5 to 200 nM) were tested using for each point the same ML122 concentration (10 µM), while in **Panels B** and **D** four different concentration of ML122 (1,25; 2,5; 5 and 10 µM) were tested using for each point the same premiR-210 concentration (35 nM). All data are presented as the average of three independent experiments ± SD.

Once established the optimal premiRNA concentration, also ML122 concentration was investigated. Starting from the 10 µM as the optimal concentration for DNA transfection and

considering the high difference in molecular weight and length between DNA and premiRNA, we tried to reduce the amount of employed ML122. Four different decreasing ML122 concentrations were investigated (from 10 µM to 1.25 µM) and fold changes with respect to control were compared (**Panels B** and **D** of **Figure 51**). In K562 fold change increase is directly proportional to ML122 concentration, while no correlation between ML122 concentration and miR-210 fold change was found in U251 cells.

4.1.4 PremiRNA transfection with ML122: optimal contact time with target cells

In all the previously performed experiments, transfection was performed using the protocol indicated in the work of Bagnacani and co-workers [*Bagnacani et al.,2014*], described in detail in the chapter 'Materials and methods'. Briefly, a mix containing culture medium, without FBS, ML122 and the molecule that needs to be carried is prepared and after 20 minutes of incubation at room temperature is transferred to the cells. After 5 hours contact, the mixture is removed and replaced with fresh culture medium. This protocol does not present particular problems when experiments are carried out using *in vitro* models, but

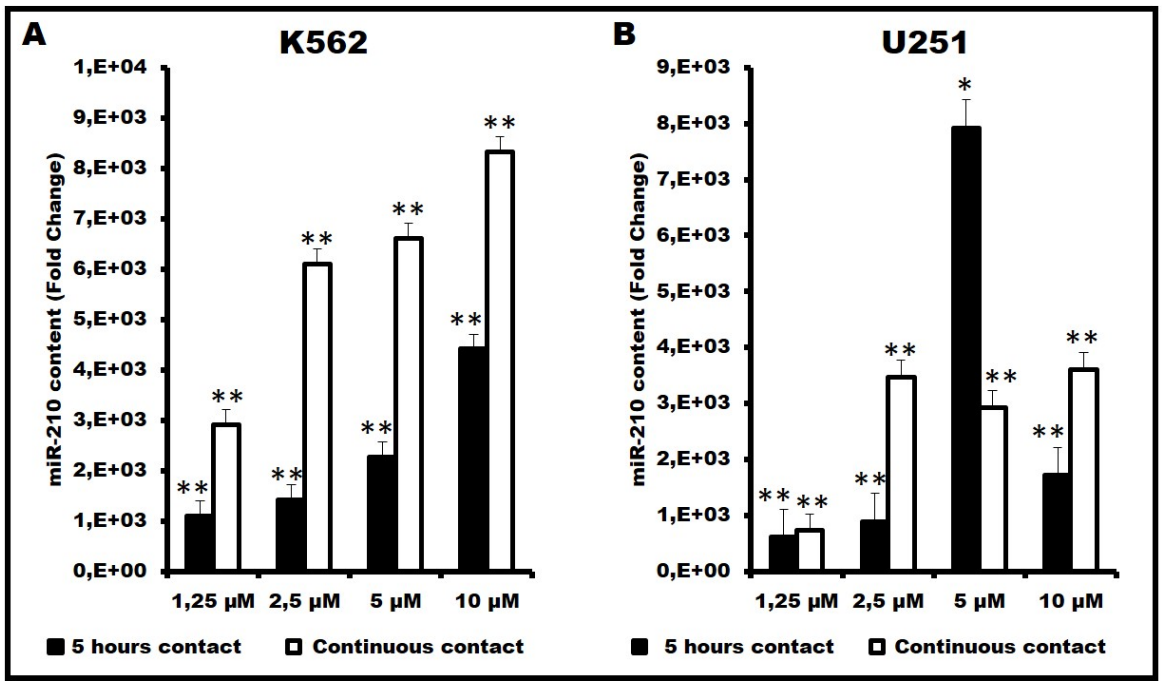

Figure 52. PremiRNA transfection with ML122 protocol set-up. Two different transfection protocols were tested. In the first protocol mix ML122-premiRNA maintained in contact with cells for five hours and then was removed and replaced with new fresh medium (black boxes). In the second case ML122-premiR-210 mix was maintained in contact with cells for all the treatment time (white boxes). Two protocols were tested in both cell lines: K562 cells (**Panel A**) and U251 (**Panel B**). Experiment was performed in triplicate and the average values ± standard deviation was reported.

clearly is not feasible in *in vivo* experiments and/or in designing experiments to be applied for long-term treatments. It should be underlined that of course our final goal is the

application of calixarene-based vehicle on *ex vivo* and *in vivo* models in order to mimic therapeutic interventions. For this reason, we also evaluated the possibility to maintain the transfection mix in contact with cells for the entire period of the treatment time (**Figure 52**). Starting from the hypothesises that in the case of a continuous contact less amount of ML122 might be required, we tested four different concentration of ML122, starting from 1.25 to 10 µM and we compared miR-210 increase obtained after 5 hours cells-mix contact with data obtained with continuous contact (24 hours). Also in this case transfection efficiency was evaluated as increase of miRNA levels in transfected cells with respect to not transfected cells 24 hours after the transfection. In both K562 (**Panel A**) and U251 (**Panel B**) cell lines 2.5 µM of ML122 maintained in contact with the cells for 24 hours was able to determine a miR-210 fold change equal or even better than 10 µM ML122 maintained in contact with cells for only 5 hours.

4.1.5 Transfection of antimiRNA molecules with ML122

In miRNA-based therapy not only miRNA mimicking molecules, but also antagomiRNA molecules require a delivery system. AntagomiRNAs are key molecules that are usually used to reduce miRNA levels inducing the expression of the miRNA regulated mRNAs.

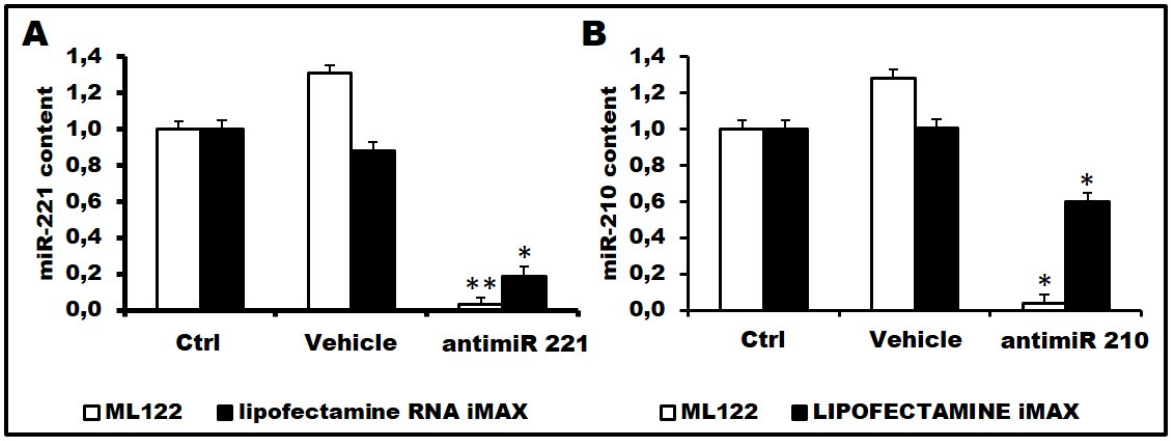

Figure 53. AntimiRNA molecules transfection with ML122. Two different antagomiRNA molecules were transfected using ML122 (white boxes): antimiR-221 transfected in U251 cells (**Panel A**) and antimiR-210 transfected in K562 cell line (**Panel B**). Moreover, ML122 transfection efficiency was compared with Lipofectamine RNA iMAX (black boxes), used according to the manufacturer's instructions. MiR-221 and miR-210 fold change in transfected samples respect control samples was calculated, and the mean value of three independent experiments was reported in the boxes.

Usually commercial available delivery systems are able to deliver both premiRNA and antagomiRNA molecules, using similar transfection condition. Starting from this consideration, we verified the ability of ML122 carrying antagomiRNA molecules to target

cells, in both cell lines (**Figure 53**). We tested two different antagomiRNA molecules, antimiR-210 which was transfected into K562 cells, and antimiR-221, which was transfected to U251 cells lines, considering the fact that these cells express miR-221 at very high levels. Moreover, a comparison between ML122 (white boxes) and one of the most efficient commercial available transfection agent was performed (black boxes). Similar miRNA level decreases were shown for both antimiR-210 and antimiR-221 delivered with ML122. Moreover, miRNA decrease seems to be greater when ML122 was used as transfection agent in respect to the commercial one.

4.1.6 Transfection of PremiRNA and antimiRNA molecules with ML122 to primary cells

All the previously shown experiments were performed using immortalised cell lines. To further investigate ML122 transfection efficiency, we also employed as primary cell model the erythroid precursors isolated from peripheral blood (ErPCs), which also are

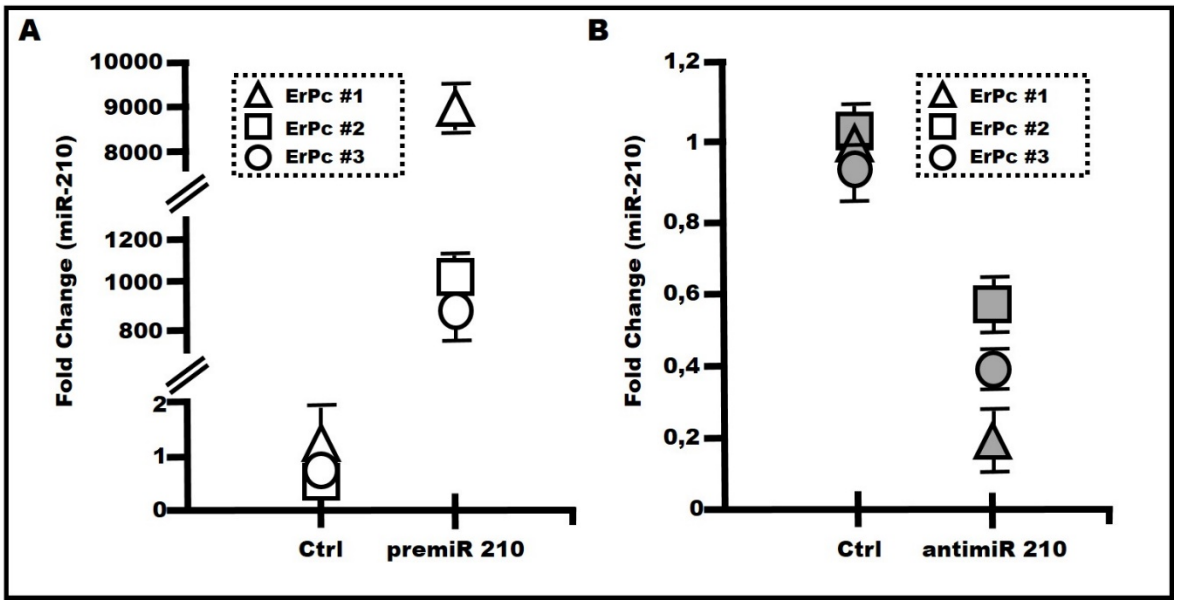

Figure 54. PremiRNA and antimiRNA molecules transfection with ML122 in ErPCs. ErPCs isolated from three different donors were transfected with both premiR-210 (**Panel A**) and antimiR-210 (**Panel B**), using ML122 as vehicle. MiR-210 content in samples was determined using RTqPCR and miR-210's expression change of miR-210 was calculated using $2^{-\Delta\Delta CT}$ method. The average of three independent experiments was reported.

generally poorly transfected (**Figure 54**). The employment of ErPCs allowed us to verify the behaviour of ML122 in a more 'physiological' model. Transfection was performed according to the 'standard' protocol, 10 μM of ML122 and 5 hours mix contact, using both premiR-210 (**Panel A**) and antagomiR-210 (**Panel B**). MiR-210 intracellular levels in ErPCs

isolated from three different donors, were quantified using RTqPCR, miR-210 fold change was calculated with respect to the control sample (no transfected sample) and snRNA U6 was employed as internal reference. In the experiment shown in Figure 54 the increase of miR-210 was clearly associated with the ML122 mediated transfection with the premiR210; on the contrary efficient transfection of the antimiR-210 caused a sharp decrease of miR-210 content.

4.1.7 Biological effects

MiRNAs are intensely studied for their ability to modulate target mRNA. Therefore, the alteration of miRNA content (either increase or reduction) should be further analysed with respect to the miRNA-mediated biological alterations. Therefore, it was important to verify if miRNA modulation is able to modify the expression of its target mRNA, representing this issue, the real goal of miRNA based therapy. Accordingly, it was essential for us to verify whether premiRNA or antimiRNA molecules carried by ML122 were able to mediate the expected final biological effects.

In the case of premiR-210 delivery, we started with what we have previously demonstrated in the section III of results. Briefly miR-210 is able to target BCL11A, which is well known as one of the most important γ-globin gene transcriptional repressors. For this

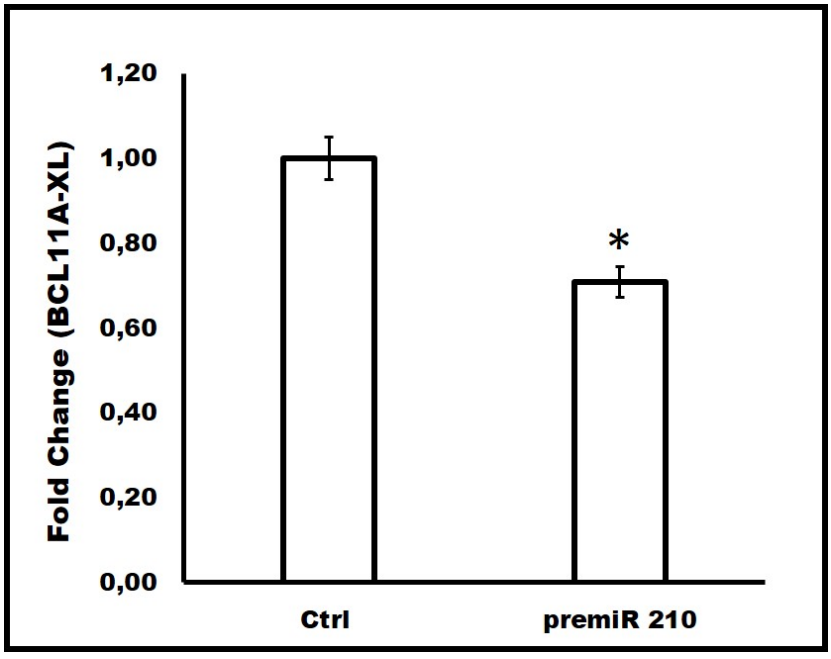

Figure 55. Biological effect of premiR-210 in ErPcs. Erythroid precursors isolated from three different donors were transfected with premiR-210 (final concentration of 200 nM) and ML122 (final concentration 10 μM). 48 hours after the transfection RNA was extracted and BCL11A-XL expression was analysed using RTqPCR.

reason, we transfected ErPCs cells, the most suited cellular model for this kind of experiment, with premiR-210 using ML122 (**Figure 55**). As previously done for premiR-210 transfection using Lipofectamine RNA iMAX, we employed only one concentration of premiR-210 (200 nM), that was shown to be the most effective in this cellular model. BCL11A-XL mRNA expression was analysed using RTqPCR 48 hours after the transfection, and fold change respect to the control sample was calculated. The results obtained confirm BCL11A-XL down-regulation after ML122 mediated premiR-210 delivery.

A second proof-of-principle concerning the biological activity of ML122 delivered antimiRNA was investigated using the glioma U251 cellular system. As demonstrated in several studies, miR-221-3p is involved in the apoptotic pathway and its down regulation causes a sharp increase of apoptosis in several cell lines [*Brognara et al., 2015*]. Accordingly, if antimiR-221 delivered by ML122 is able to decrease miR-221 levels in cells, an increase of apoptotic cells should be detected. U251 cells were transfected with antimiR-221 at final concentration of 70 nM, using ML122 2.5 µM. The mixture ML122-antimiR-221 was maintained in contact with the cells for 72 hours and then the percentage of apoptotic cells was determined (**Figure 56**) using the annexin V assay. As it clearly evident in panel A of Figure 56, the cell population, on the base of the fluorescence levels, is divided

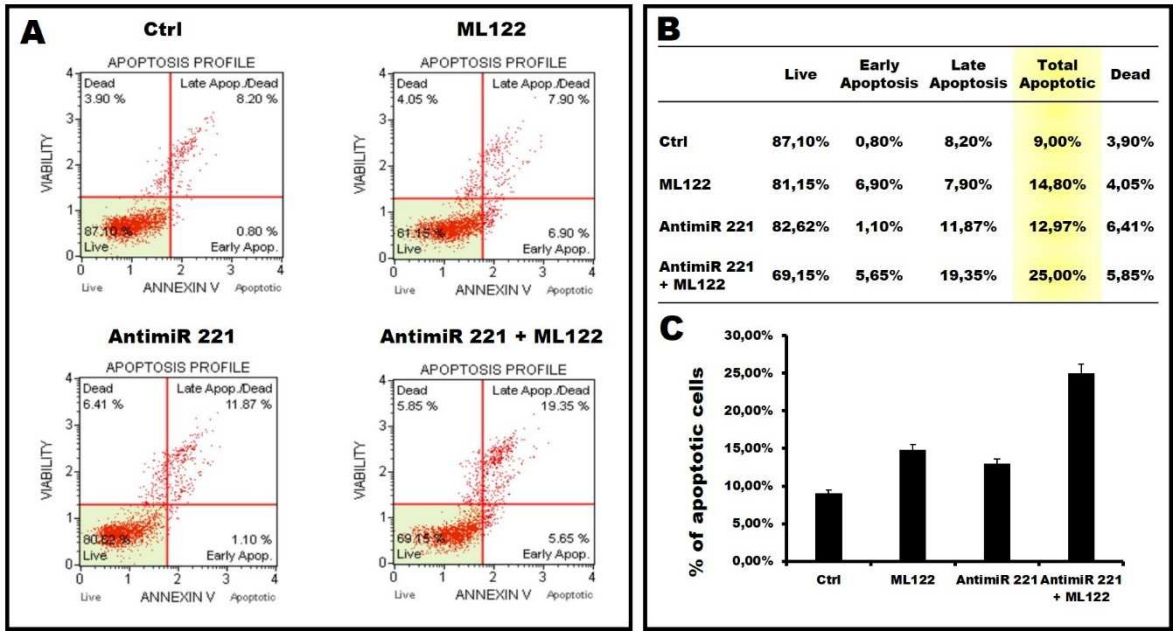

Figure 56. Biological effect of antimiR-221 in U251 cell line. Panel A representative apoptosis profile plots, cellular population is divided into live cells (low-left), early apoptotic cells (low-right), late apoptotic cells (up-right) and dead cells (up-left). In **Panel B** are reported data relative to the showed plots. The histogram in panel C the average percentage of total apoptotic cells is reported.

into four groups: live cells, early apoptotic cells, late apoptotic cells and dead cells. Mean values for each samples are reported in the Table depicted in the **Panel B of Figure 56**, while the percentage of apoptotic cells in each samples is reported in the histogram of **Panel C**. When cells are transfected with antimiR-221-3p delivered by ML122 a significant increase of the percentage of apoptotic cells was detected. Also, when only ML122 was employed, an increase of apoptotic cells was noticed, but lower than the value observed for ML122-delivered antimiR-221. Interestingly the apoptotic profile observed is significantly different between sample treated with only ML122 and cells treated with antimiR-221 transfected with ML122. In fact, while the percentage of early apoptotic cells in the two samples are very similar, a marked difference was found in the case of late apoptotic cells. Percentage of late apoptotic cells in the ML122 sample is much lower than the percentage found in U251 cells treated with ML122 delivered antimiR-221.

4.2 PNA delivery using ML122

Peptide nucleic acids are among the most interesting compounds able to modify gene expression. While PNAs stability and ability to bind with high affinity their target makes them very useful tools, one of the important issue of PNAs usage is represented by their delivery. In fact, very low or no up-take was demonstrated by PNA administered to the cells without a suitable delivery system. Is important to underline that PNAs are not charged molecules, so if for miRNA-based molecules was easy to hypothesize that the interaction miRNA-calixarene takes place between negative charges in miRNA structure and positive charges present in the upper rim of ML122, explain how PNA-calixarene interaction takes place is much more complex. We speculate that PNA internalization mediated by ML122 is possible thanks to ML122 cup-shape, which may contain PNA molecules. Starting from data obtained for miRNA-based molecule we investigated the possibility of ML122 to deliver PNA molecules.

4.2.1 Cellular up-take of fluorescent PNA delivered by ML122

For a preliminary analysis we employed a fluorescence-labelled PNA with no chemical modification added to improve cellular uptake (PNA F2). We also employed a second fluorescent PNA, with the same sequence of PNA F2, in which a polyarginine peptide (R8) was added to improve cellular up-take. Is important to underline that in our

experience, the PNA functionalization with the polyarginine peptide represents one of the most successful methods to improve PNA cellular uptake. As for miRNA-based molecules, for preliminary data we started from the 'standard' transfection condition reported by

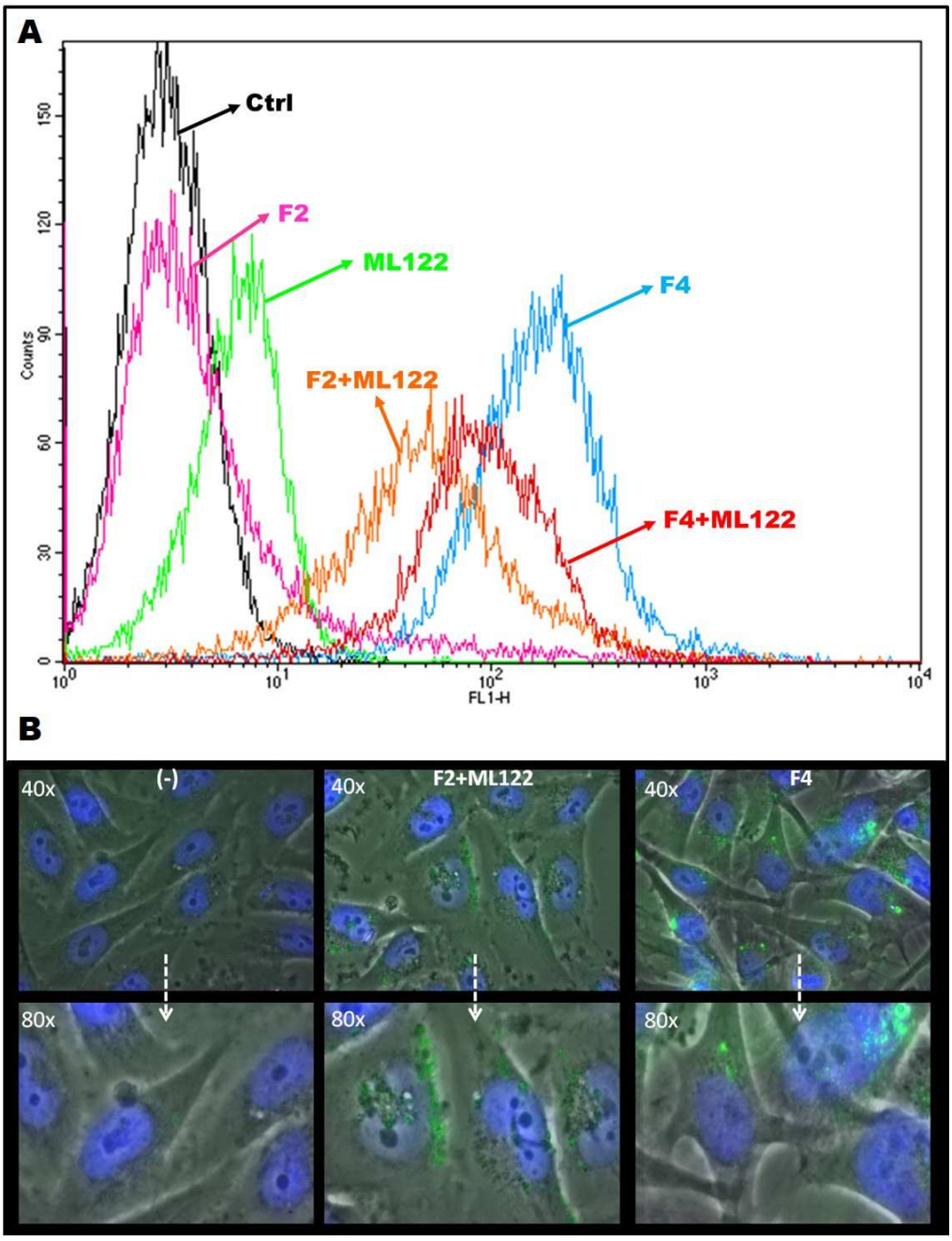

Figure 57. Cellular up-take of fluorescent PNA delivered by ML122. Panel A, 24 hours after the transfection cells were analysed for their fluorescence by FACS analysis. The fluorescence of the following sample was analysed: control (black curve), naked PNA F2 (pink), cells treated with only ML122 (green), naked PNA F2 transfected with ML122 (orange), R8 PNA F4 (light blue) and finally, PNA F4 delivered with ML122 (red). Fluorescence was also analysed using fluorescence microscopy system. Representative 40x and 80x pictures were reported (Panel B).

Bagnacani and colleagues in their experiments for DNA delivery. Accordingly, a transfection mix constituted by ML122 at final concentration of 10 µM, PNA at concentration of 2 µM and culture medium, was prepared. The mix was maintained in

contact with cells for 5 hours and then removed and replaced with fresh medium (**Figure 57**). Both PNAs (PNA with R8 and naked PNA) were used at final concentration of 2 µM, in agreement with previously published studies [*Brognara et al., 2015*]. 24 hours after the transfection, the cells (in the representative experiment U251 cells) were detached and analysed for fluorescence content by FACS (**Panel A**). No differences were found when the naked PNA F2 was used without vehicle, while an increase in percentage of fluorescence positive cells was detected when PNA F2 was associated with ML122. Fluorescence shift is, anyway lower than the shift reported when PNA F4 (carrying the R8 delivery peptide) is used. Moreover, when R8 functionalized PNA is delivered with ML122, no improvement in transfection efficiency was shown. FACS analysis data were also confirmed by direct cell observation with fluorescent microscopy (**Panel B** of **Figure 57**).

4.2.2 Biological effects of PNA delivered by ML122

According to what shown for miRNA-based molecules, also for PNAs transfection conditions were investigated, and, finally, a 2.5 µM ML122 concentration, and the

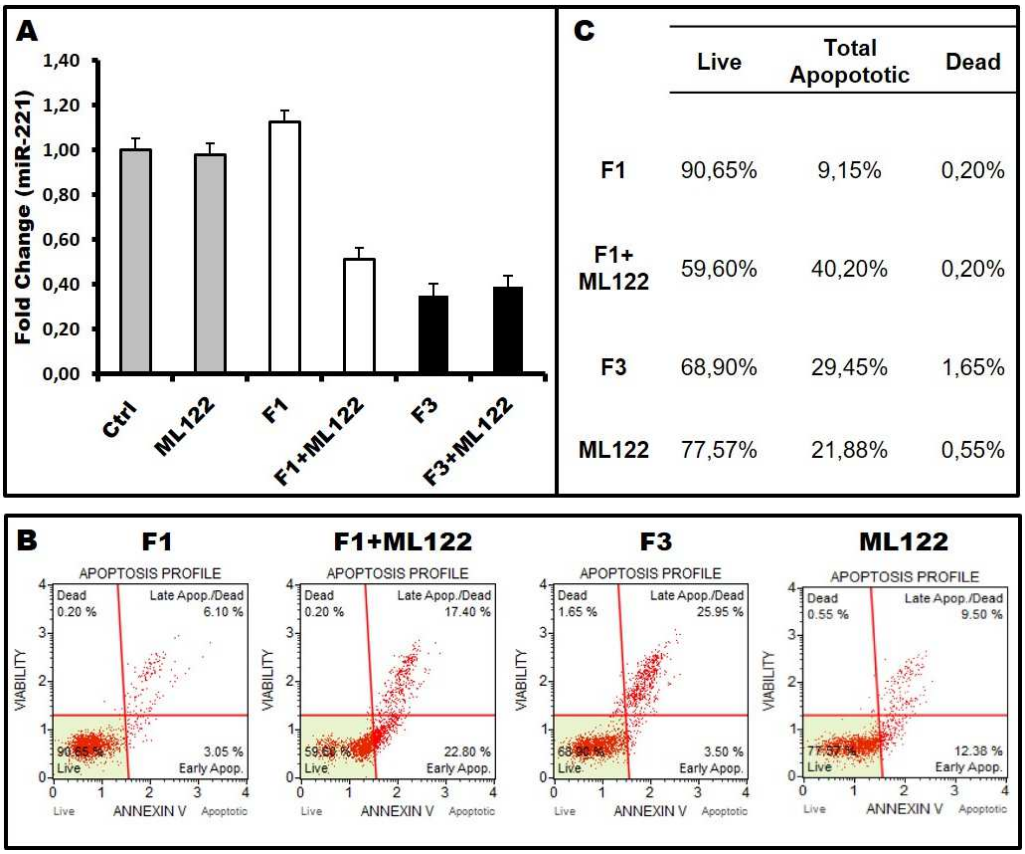

Figure 58. **Biological effects of PNA delivered by ML122. Panel A** miR-221 relative expression was determined in U251 cell line 48 hours after the transfection by RTqPCR. **Panel B** and **C** annexin V assay was performed in U251 cells, transfected for 72 hours with PNA F2 delivered with ML122 or with PNA F4 used as positive control. Representative apoptotic plots are reported in panel B, while a summary table of percentage of total apoptotic cells for each sample is reported in panel C.

continuous contact between cells and mix, was individuated as the optimal protocol for PNA delivery. In order to verify whether PNAs delivered with ML122 are able to exert a biological effect, U251 cells were transfected according to the protocol previously described (**Figure 58**). After 48 hours RNA was extracted to quantify miR-221 (**Panel A**). In fact, PNA F1 presents a sequence perfectly complementary to miR-221; therefore, the first evidence of a PNA effect should be a sharp decrease of the miR-221 specific hybridization signal in U251 cells treated with ML122 carrying the anti-miR-221 PNA. As indicated in the panel A of Figure 58 miR-221 in transfected sample was compared with untransfected control and fold change was determined. Both PNA F3 (carrying the R8 delivery peptide) and PNA F1 (lacking the R8 peptide) delivered by ML122 are able to decrease miR-221 hybridization signals in the cells, with slight differences. On the contrary, no significant difference in fold decrease was shown when PNA F3 was added to ML122 as vehicle. In order to verify whether the decrease of miR-221 is associated with biological effects, pro-apoptotic activity of ML122 delivered anti-miR-221 F1 PNA was assessed as described in chapter 'Materials and methods' and apoptosis was analysed after 72 hours treatment by the Annexin V assay. The most significant plots are reported in the **Panel B** of **Figure 58**, while the percentage of apoptotic cells relative to the shown plots are reported in **Panel C**. As evident from the Table depicted in panel C of Figure 58, ML122 treatment by itself is able to induce apoptosis to some extent (20% of apoptotic cells). Considering the apoptotic rate due to the presence of ML122, the net percentage of total apoptotic cells obtained with PNA F1 transfected with ML122 is about 20%; this value is lower than that obtained with PNA F3, but still significant.

4.3 Screening of others ML122 analogs

Sansone and co-workers synthesized starting from ML122 structure several other calixarene-based structures. Several chemical modifications were introduced to increase calixarene vehicles affinity for PNAs and to better understand the mechanism of PNAs complexation. Five new calixarene-based molecules were rapid screened using FACS analysis. Taking advantage from knowledge obtained by the ML122 investigation, the new molecules were employed at final concentration of 2.5 μM and the mix calixarene-PNA F2 was maintained in contact with cells until FACS analysis, that was performed 24 hours after the transfection (**Figure 59**). PNA F2 and the R8 polyarginine conjugated PNA F4 were used as negative (PNA F2) and positive (PNA F4) transfection controls. As indicated in

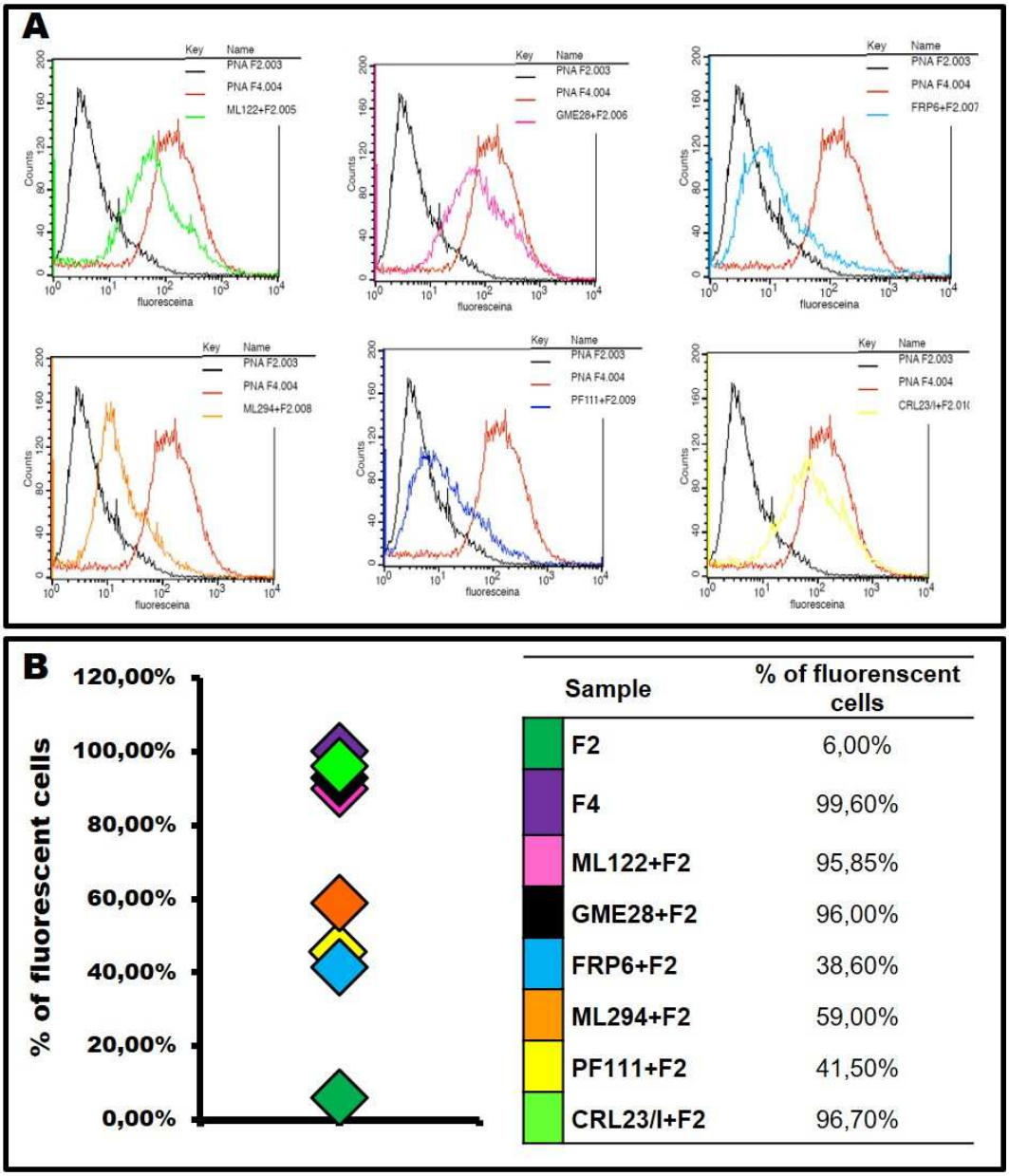

Figure 59. Screening of others ML122 analogs, FACS analysis. Panel A representative FACS overlay plot for each calixarene based molecule was reported. In each overlay plot the fluorescence intensity (x axis) is reported in function of the number of cells (y axis). Transfection efficiency data are summarized in the **Panel B**. Naked PNA F2 (dark green rhombus), PNA F4 functionalised with polyarginine peptide (purple rhombus) and PNA F2 delivered with ML122 have been used as controls. Five new calixarene based molecules were considered: GME28 (black rhombus), FRP6 (light blue rhombus), ML294 (orange rhombus) and PF111 (yellow rhombus). The mean percentage of fluorescent cells are reported in table in the right part of the panel B.

Figure 59 the new molecules can be clustered into two main groups: a fist group including GME28 and CRL23/I molecules that present transfection efficiency very similar to ML122 and PNA F4 (percentage of fluorescent cells higher than 90%), while the second group composed by PF111, ML294 and FRP6 present percentage of fluorescent cell (35-60%) significantly lower than the first group, despite the percentage of fluorescent cells is anyway higher than the naked PNA.

The compounds that demonstrated to have transfection efficiency similar to ML122 were further analysed with a microscopy fluorescence system to confirm PNA internalization. As indicated in the **Figure 60** CRL23/I and GME28, were selected after the first preliminary

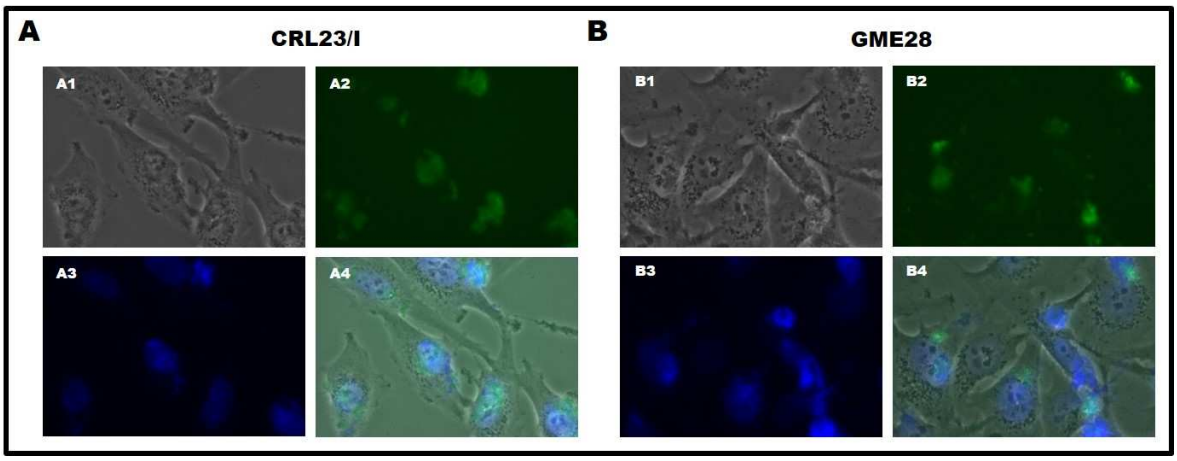

Figure 60. **Screening of others ML122 analogs fluorescent microscopy analysis**. CRL23/I (A) and GME28 (B) were observed at fluorescent microscopy to verify PNA internalization. 40x representative picture were proposed. Figures A1 and B1 live cell image, picture B1 and B2 FITC filter image, A3 and B3 DAPI filter image, A4 and A4 marge of both FITC and DAPI filters.

FACS analysis. Before the observation the cells were pre-treated with Hoechst to identify the nucleus position. The results obtained formally demonstrate internalization of the PNAs delivered by the ML122 analogues, fully in agreement with the FACS analysis reported in Figure 59.

4.4 PremiRNA and PNA co-transfection with ML122

Combined therapy is a promising therapeutical approach based on the simultaneous action of the employed drugs/molecules against several targets. Targeting more than one biological pathway at same time can increase the response to therapeutic treatment and moreover, in several case, it is expected to be possible to reduce the therapeutic concentration of the employed molecules (and therefore their side effects). Usually, in this case two different delivery systems are required, one for PNA and a second specific for premiRNA or antagomiRNA molecule. On the basis of the results described in section 4.1 and 4.2, we have investigated the ability of ML122 to transfect at same time both a PNA and a premiRNA molecules. To verify this, we employed a PNA against miR-221-3p and a premiRNA mimicking miR-124-3p effects. The reason for this choice is that both treatments with premiR-124-3p and with PNA against miR-221-3p are pro-apoptotic. As well

demonstrated by several works in literature miR-221 is able to target several pro-apoptotic genes, among which: PUMA [*Zhang et al., 2010*], p27kip1 [*Lu et al., 2011*], PTEN and TIMP3 [*Garofalo et al., 2009*]. Therefore, by reducing miR-221 expression it is at least in theory possible to increase apoptosis. At same time, miR-124 targets the transcript that codifies for MGMT protein, an enzyme which is able to regulate the response to alkylating chemotherapy in patients affected by glioblastoma [*Khalil et al., 2016*] and to induce apoptosis. Accordingly to previously obtained data U251 cells were transfected with ML122 at final concentration of 2.5 μM, both PNA F2 and premiR-124 were added to the transfection mix, in association with cell medium. Transfection mix was incubated for 20 minutes and then transferred to cells. The mix was maintained in contact to cells for all the treatment time (48 hours). Cells were detached and analysed by FACS analysis to verify PNA up-take (**Figure 14, Panel A**). As demonstrated in panel A, very similar fluorescence values are obtained when PNA F2 is used individually or in association with premiR-124. Moreover, also cells transfected with PNA F4 were analysed, as usual, and considered as a positive control, with no significant difference with respect to the sample in which PNA F2

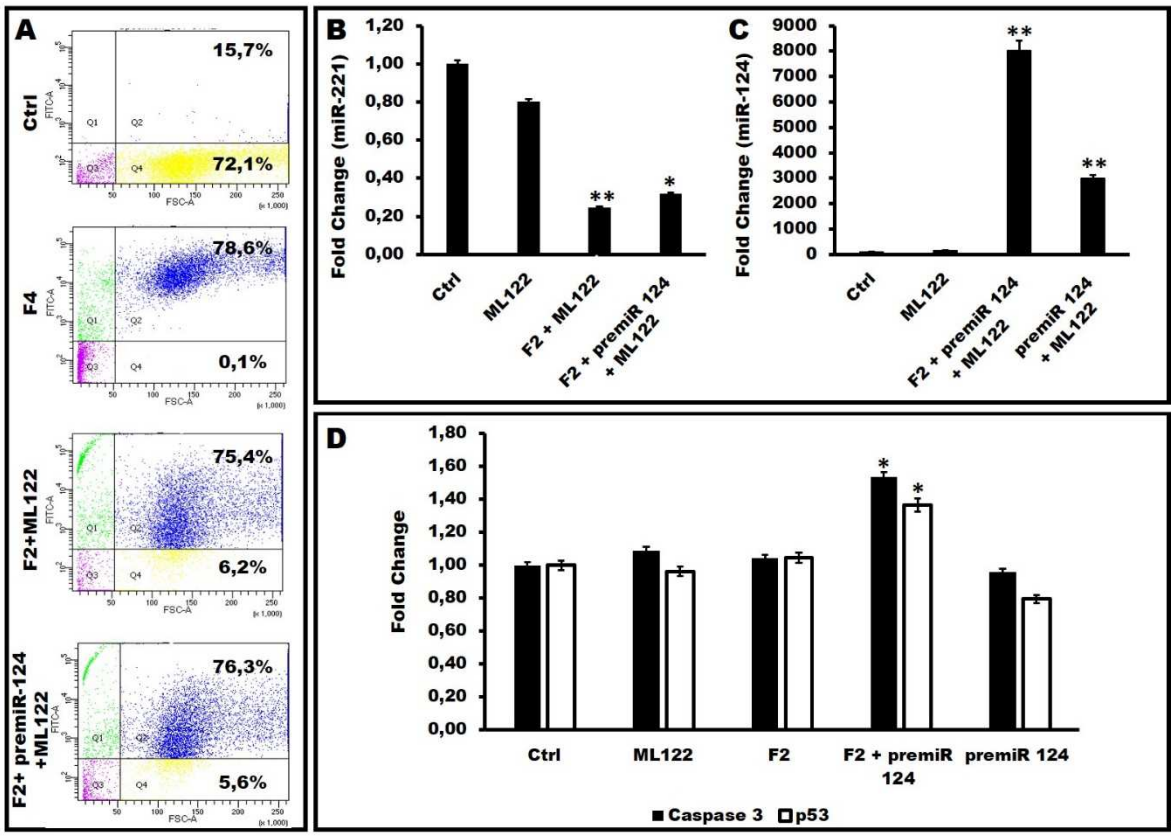

Figure 61. PremiRNA and PNA co-transfection with ML122. Panel A: FACS analysis in U251 transfected with the fluorescent PNA F2. Blue points (up-right) represent fluorescent cells, while yellow points are relative to no fluorescent cells (down-right). **Panel B** and **C**: miR-221 (panel B) and miR-124 (panel C) content, 48 hours after the transfection were calculated. Data are reported as fold increase respect to control sample. **Panel D**: two genes involved in apoptotic pathway are considered: caspase 3 (black boxes) and p53 (white boxes), even in this case fold change respect to the control sample is considered.

was delivered by ML122. At same time RNA was extracted and miR-124 (**Panel B**) and miR-221 (**Panel C**) content was analysed by RTqPCR. The fold change in transfected cells with respect to control cells was calculated for both miR-221 and miR-124. Interestingly the miR-124 content increases dramatically in cells transfected with ML122 carrying premiR-124-3p and the antimiR-221. At the same time sharp decrease of miR-221 was observed. Finally, the effect of transfection was verified considering two key mRNA for the apoptotic pathway: caspase 3 and p53 (**Panel D**). Figure 61 demonstrates that increase of caspase-3 and p53 mRNA was found only in cells transfected with ML122 carrying PNA F2 and premiR-124.

4.5 Toxicity and inflammatory profile of calixarene

One of the major issue associated with the use of commercial available vehicles is the high toxicity of these compounds. For this reason ML122 and its two analogs, CRL23/I and GME28, were investigated to evaluate cells alteration when they are used to transfect molecules. Considering that the optimal protocol for *in vivo* treatment is continuous contact protocol, only this protocol was investigated for determining the apoptosis and inflammatory profile.

4.5.1 Viability assay

Through several available viability assays it is possible to detect the % of live cells, in a sample. All the three molecules were tested, ML122 in both U251 and K562 cell lines, GME28 and CRL23/I, only in the most sensible U251 cell line. To this purpose, the same protocol used for transfection experiments was employed and a transfection mix, without the molecule that need to be transfected was prepared. Viability profile was determined at three different time points: 24, 48 and 72 hours after the transfection and three different calixarene-based molecules concentrations were tested (1.25, 2.5 and 10 μM). All the compounds, administered at the three concentration reported, were maintained in contact with the cells for all the treatment time (**Figure 62**). 24 hours after the transfection no differences in percentage of total live cells were found when the two lower concentration (1.25 and 2.5 μM) of ML122 was used, while only a slight decrease of live cells percentage was detected with 10 μM ML122. When the others two calixarene-based molecules were considered, they present at lower concentration a viability profile comparable with that found with

ML122, but when the highest concentration of vehicle was taken into consideration a marked decrease of live cells was found, that reaches values lower than 50% when the GME28

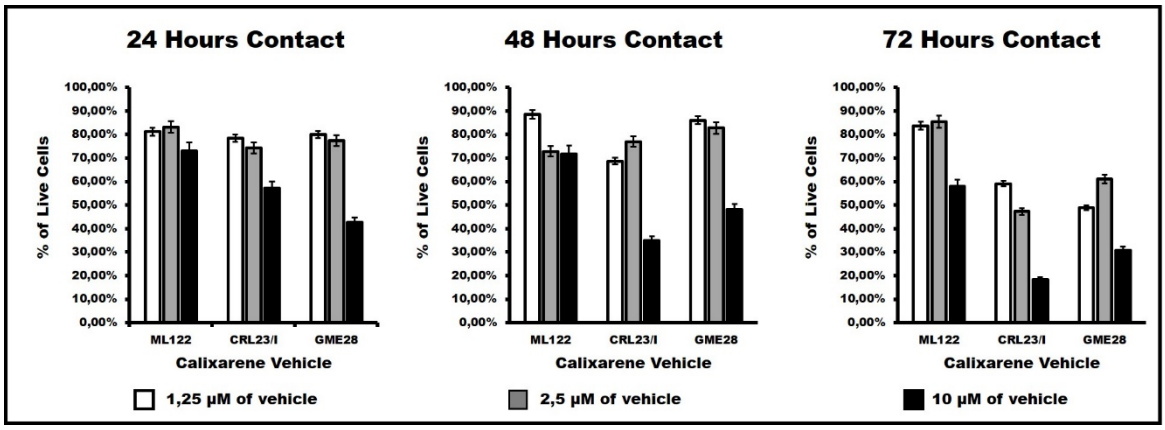

Figure 62. Viability profile in U251 cells. Viability profile in U251 cells was reported for three calixarene compounds: ML122, CRL23/I and GME28, at three different time points: 24, 48 and 72 hours after the transfection. Three different concentrations were investigated: 1,25 µM (white boxes) 2,5 µM (grey boxes) and 10 µM (black boxes) of vehicle.

compound was considered. The same deep difference between ML122 and the two analogs was maintained 48 after the transfection. 72 hours after the transfection, a significant reduction of live cells was found when the highest (10 µM) concentration of ML122 was employed. This reduction is much lower in any case when comparison is performed with GME28 or CRL23/I. In fact at highest vehicle concentration only a little percentage of cells are still alive in the experiment performed with these ML122 analogs: about 20% for CRL23/I and 30% for GME28. Moreover, the percentage of live cells in the samples transfected with the two lowest concentrations (1.25 and 2.5 µM) of GME28 and CRL23/I is comparable to what is obtained when the highest concentration of ML122 is used. The profile obtained when ML122 is used in K562 cells is similar to U251 cells transfected with ML122 as reported in **Figure 63a**. Detailed viability profiles are presented in the next pages, where viability plots are proposed for all the three compound (ML122, GME28 and CRL23/I) in U251 cell line and for ML122 only in K562 cells.

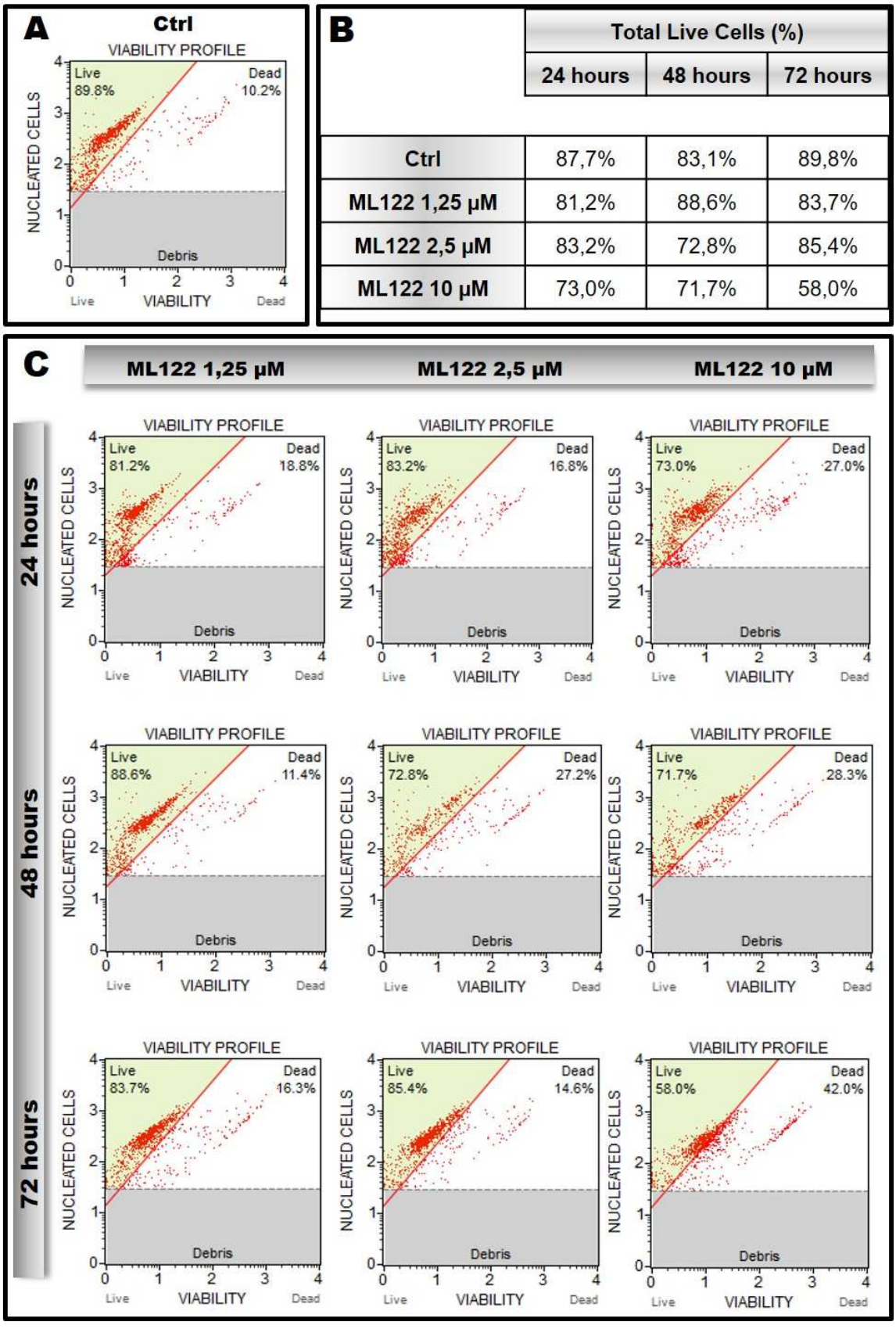

Figure 63a. Detailed viability profile in K562 cells with ML122.

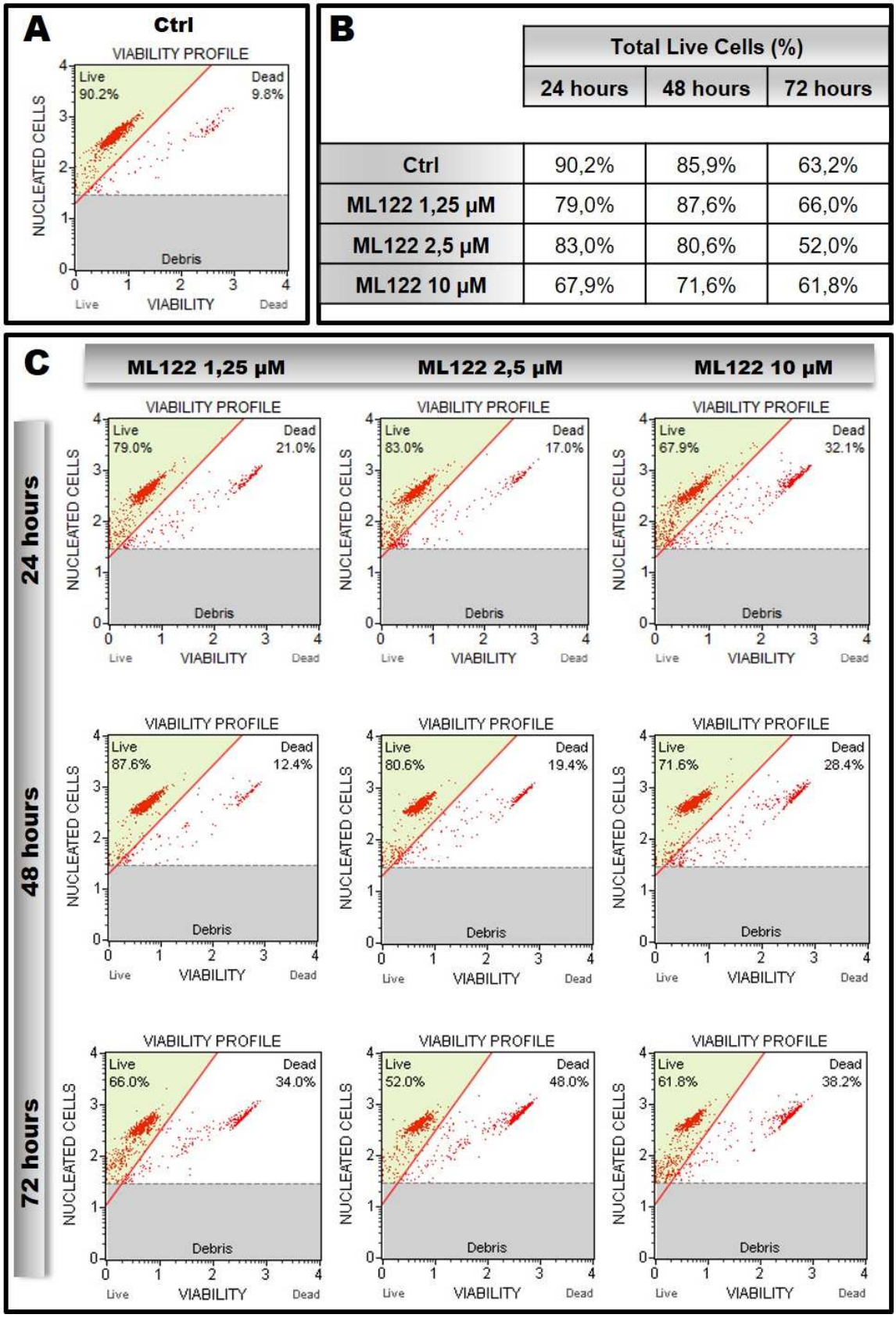

Figure 63b. Detailed viability profile in K562 cells with ML122.

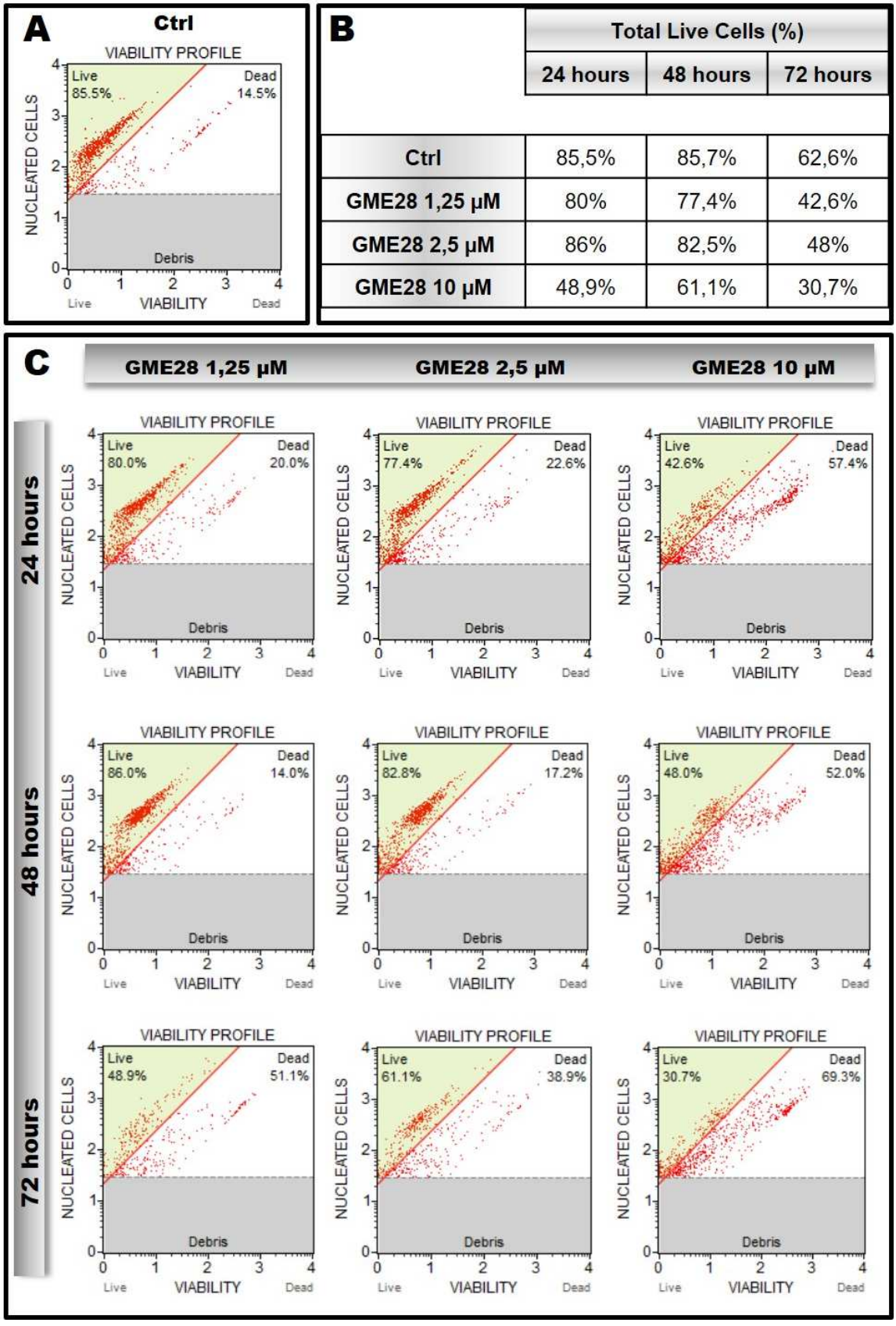

Figure 63c. Detailed viability profile in U251 cells with GME28.

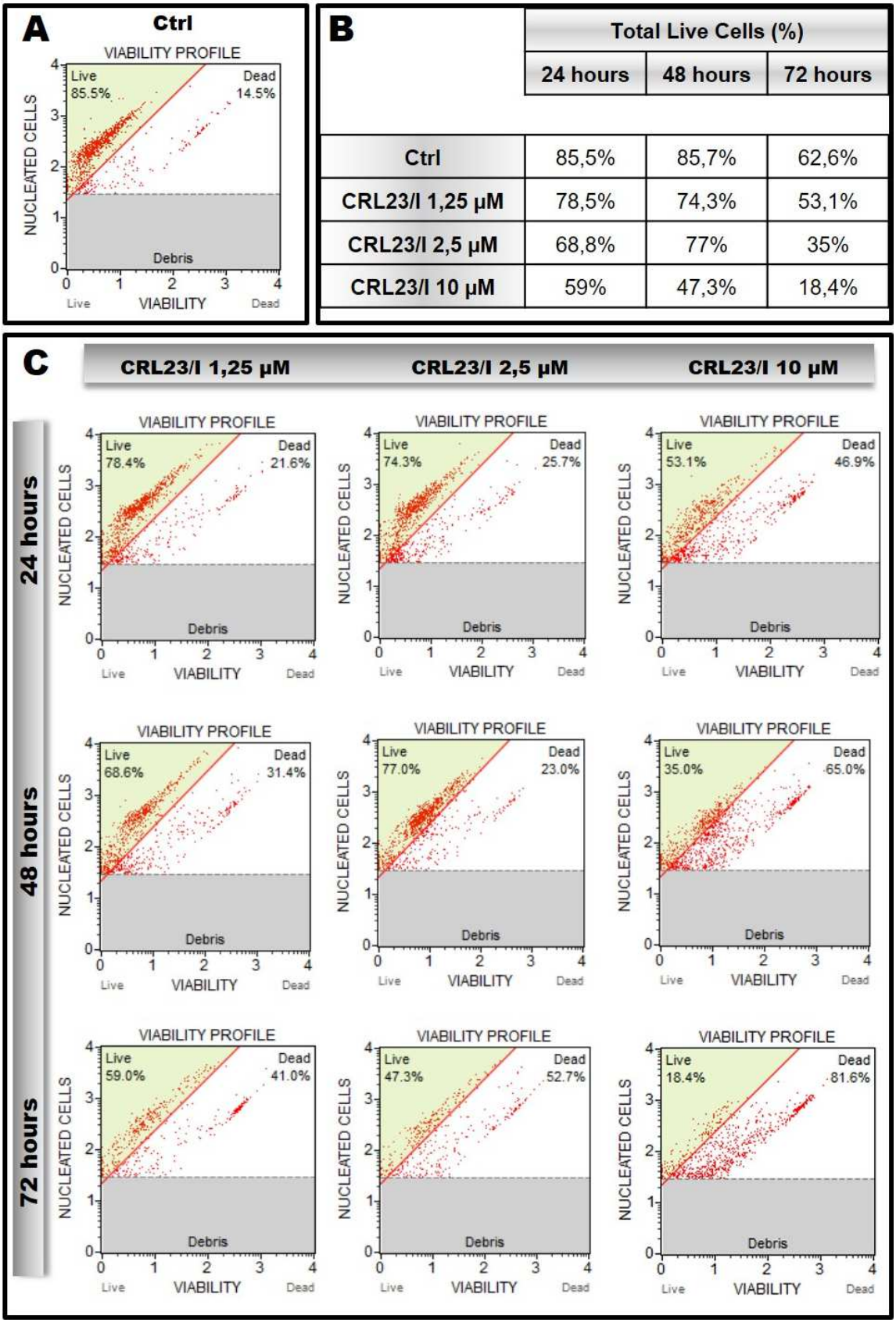

Figure 63d. Detailed viability profile in U251 cells with CRL23/I.

4.5.2 Apoptosis assay

ML122 and analogs were also tested for their pro-apoptotic effects. In fact, it is particularly important that vehicles does not create apoptotic stimuli in transfected cells. As previously done for vitality assay cells were treated with different concentrations of calixarene-based vehicles (1.25, 2.5 and 10 µM) which was maintained for all the treatment time (from 24 to 72 hours). Cells were then analysed through Annexin V assay. Percentages of total apoptotic cells for each calixarene-based molecule, are reported in **Figure 64**. In the histogram on the left of the Figure the percentages of apoptotic cells are reported after 24 hours of contact with the vehicles. While ML122 and GME28 exhibited low apoptotic profile at 1.25 µM, high levels of apoptotic cells were detected when CRL23/I was used, even at the lowest concentration of vehicle. This conclusion was the same when 2.5 µM concentration was considered: ML122 and GME exhibited similar apoptotic profile, despite percentage of apoptotic cells was significantly increased with respect to 1.25 µM. Instead a high increase of percentage of apoptotic cell was found when 2.5 µM CRL23/I was employed. In fact, in this case the percentage of apoptotic cells reached the 50%, a value even higher than that reached with the highest concentration of ML122. Interestingly, there are also differences between the three compounds with respect to the kinetics. In fact while

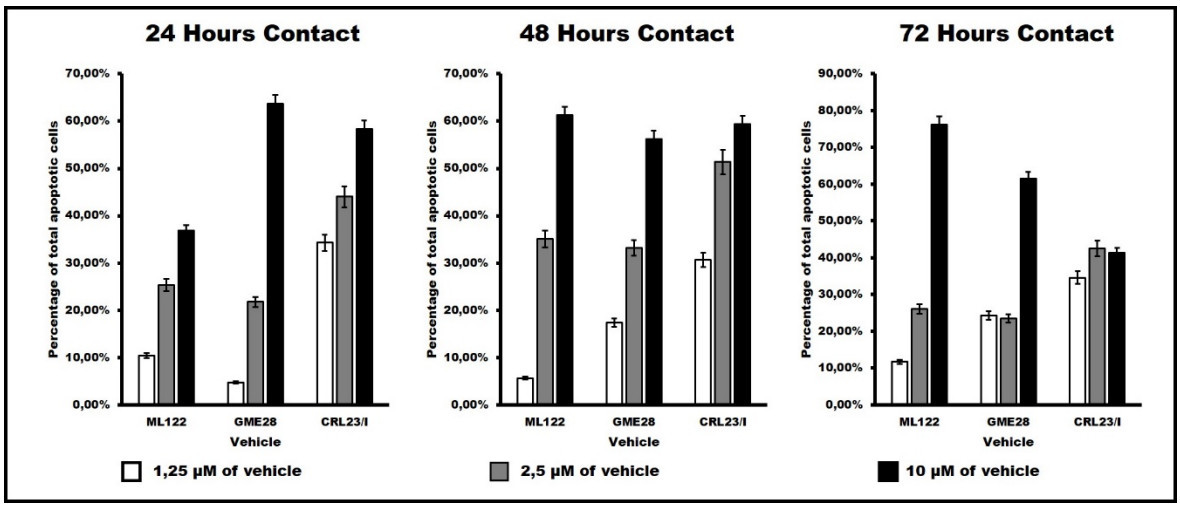

Figure 64. Apoptotic profile in U251 cells transfected with calixarene-based vehicles. Apoptosis profile was investigated for three different vehicle concentration: 1,25 µM (white boxes), 2,5 µM (grey boxes) and 10 µM (black boxes). Apoptosis profile was evaluated at three different time points 24, 48 and 72 hours and percentage of total apoptotic cells is reported.

for ML122 and GME28 the maximum toxicity levels were reached at 48 hours after the treatment, in the case of CRL23/I high apoptosis levels were found immediately after the transfection (24 hours after the transfection), while at later time points (48 and 72 hours after the transfection) the percentage of apoptotic cells decreased reaching the lowest levels 72

hours after the transfection. The same situation was found when 2.5 μM concentrations were used for all the three compound: highest apoptosis levels were detected 48 hours after the transfection, while a decrease in the percentage of apoptotic cells was reported 72 hours after the transfection. Detailed apoptosis plots are reported in the following pages. These data are compatible with a selection of U251 resistant to pro-apoptotic effects.

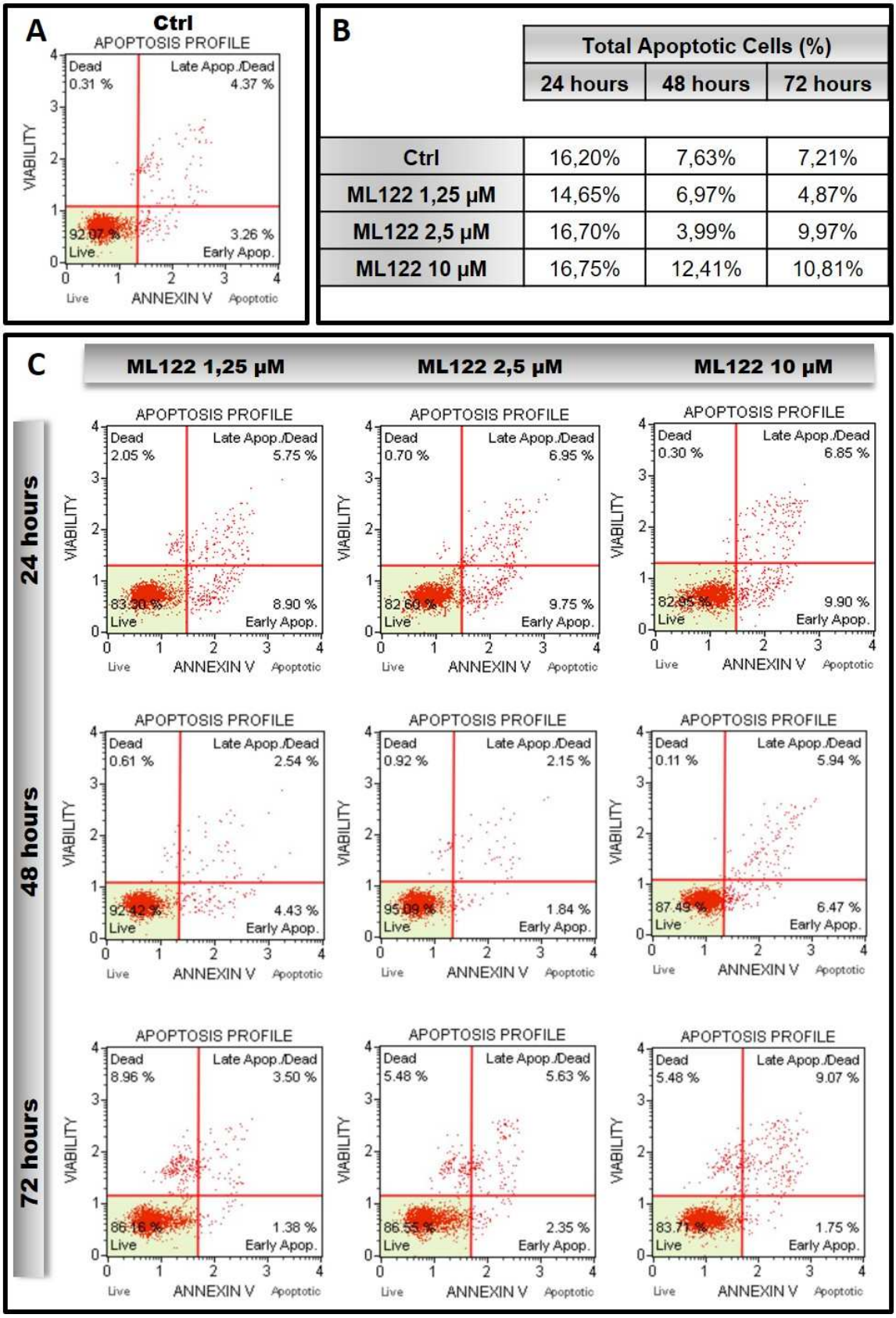

Figure 65a. Detailed apoptosis profile in K562 cells transfected with ML122.

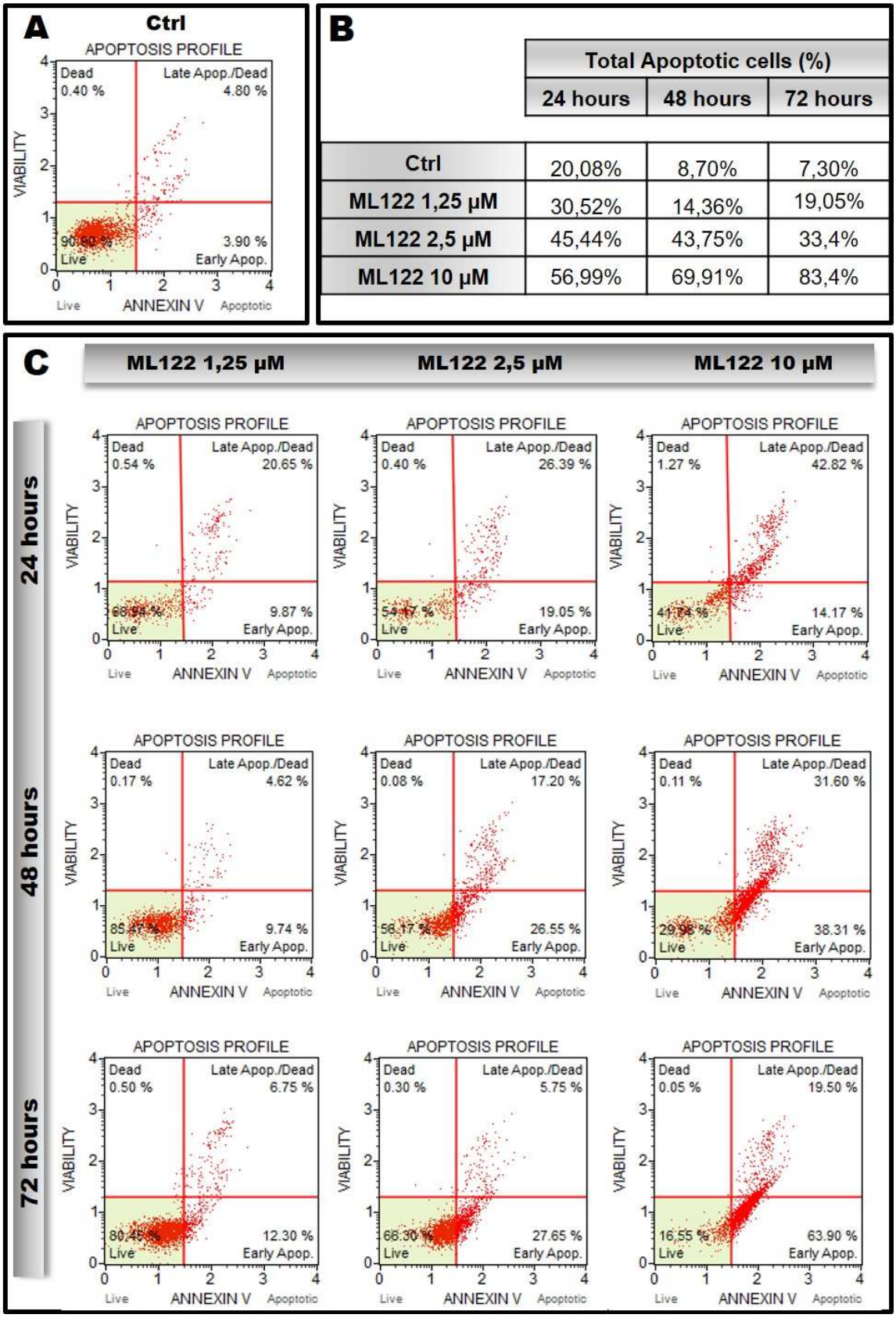

Figure 65b. Detailed apoptosis profile in U251 cells with ML122.

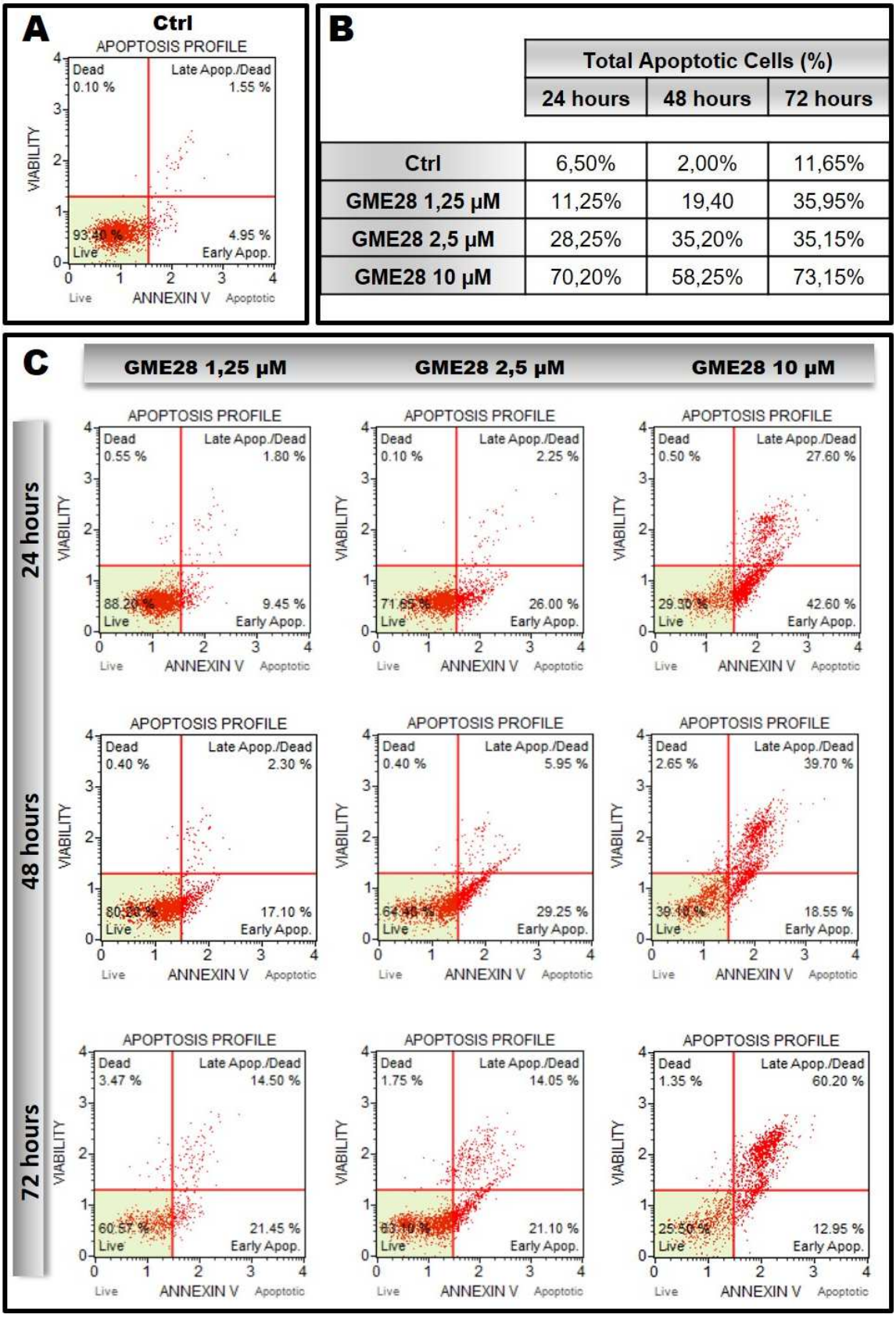

Figure 65c. Detailed apoptosis profile in U251cells transfected with GME28

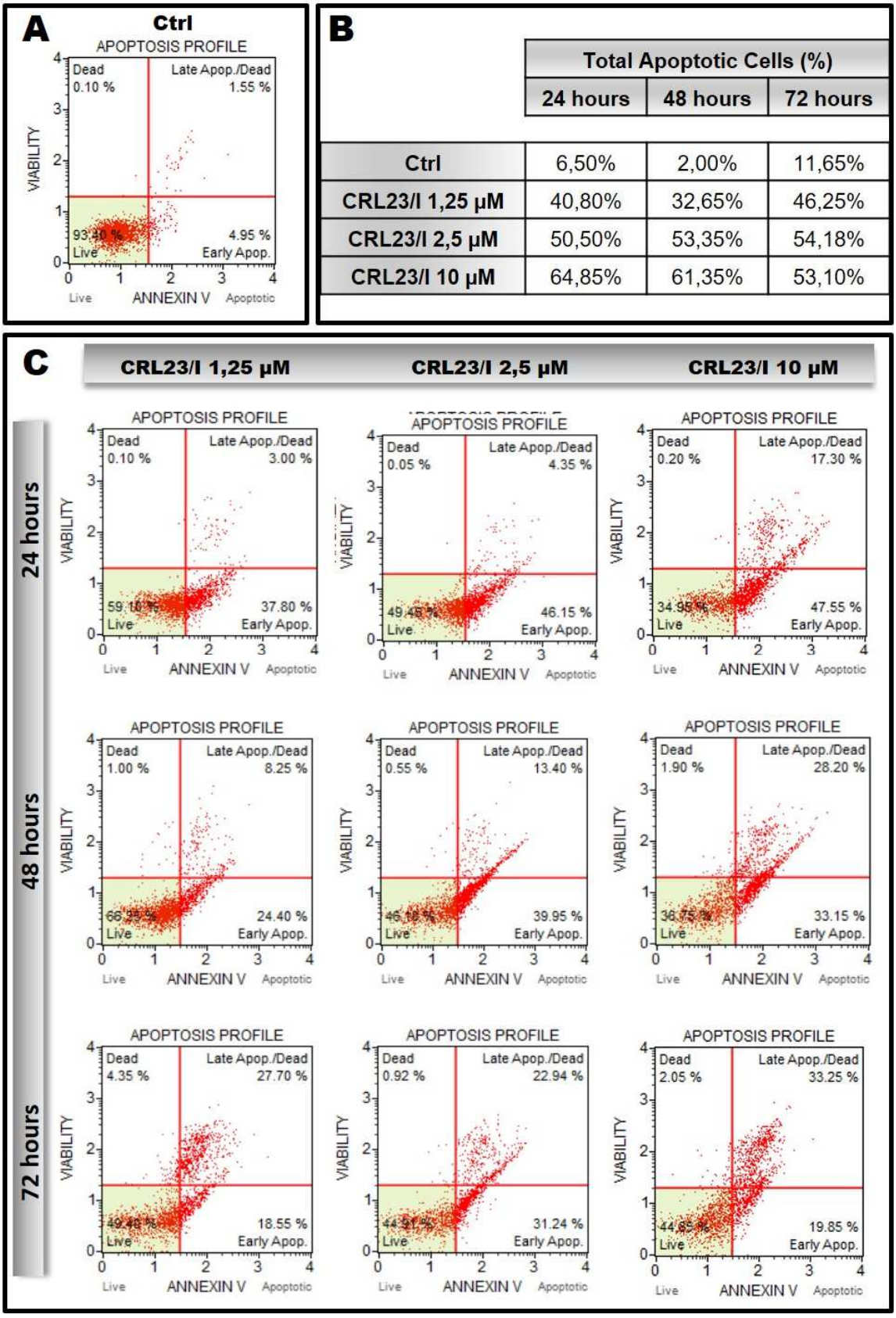

Figure 65d. Detailed apoptosis profile in U251cells transfected with CRL23/I.

4.6 Inflammatory profile evaluation

Another important issue to consider is whether cell culturing with calixarenes generates pro-inflammatory response. Preliminarily, the IL-6 mRNA expression was evaluated by RTqPCR as reported in **Figure 66**. In panel A and B U251 cells were treated with (**Panel A**) commercial available transfection agents, as indicated, or (**Panel B**) with increasing concentrations of ML122. In both cases cells were maintained in contact with the vehicle for 48 hours, and then RNA was extracted and IL-6 mRNA fold change respect to the control was calculated. In addition, also GME28 and CRL23/I were analysed at two different concentrations (2.5 and 5 µM) and compared with ML122 with respect to

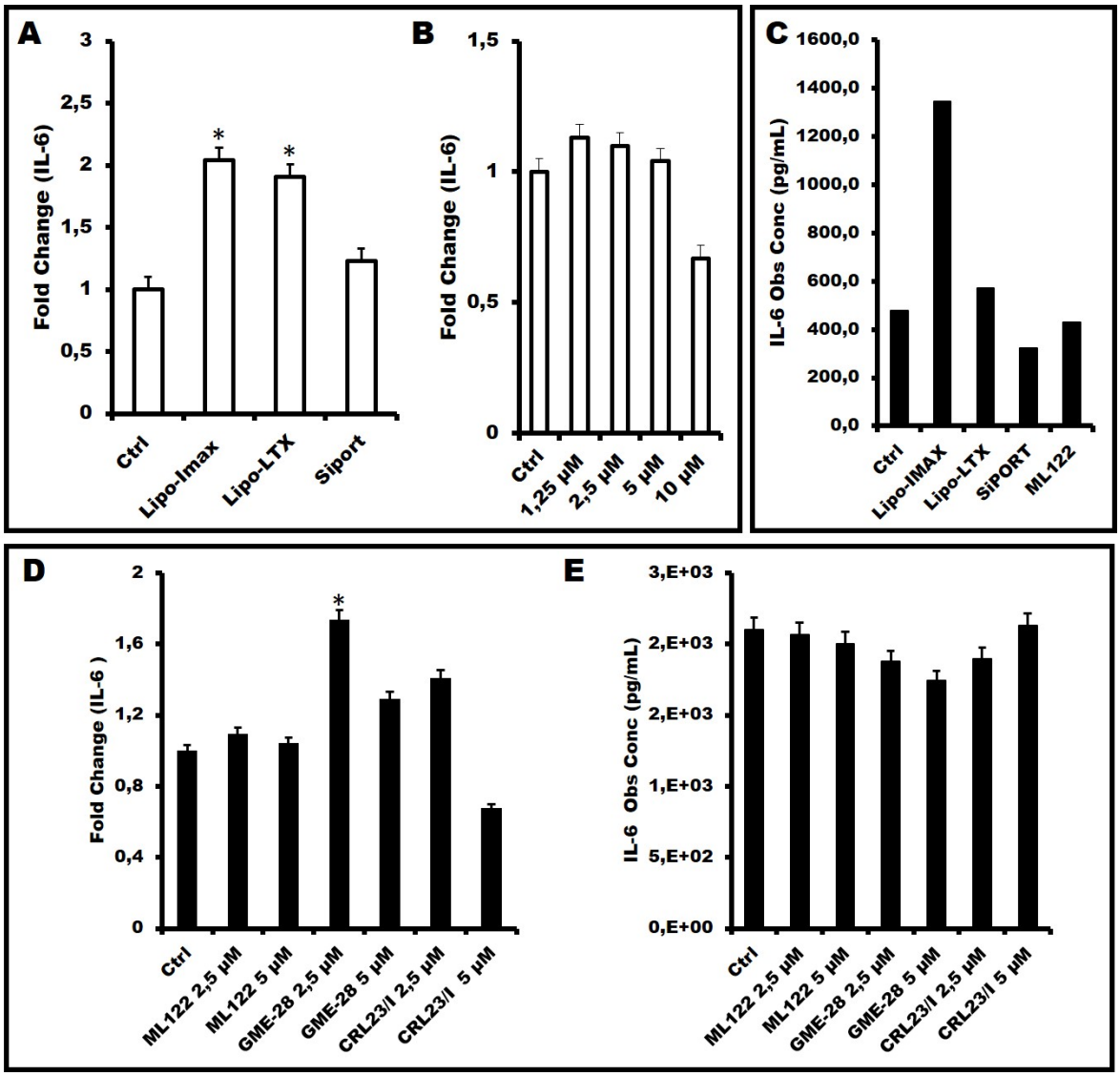

Figure 66. **Inflammatory profile evaluation in U251 cells. Panel A**: three different commercial available transfection agents were analysed. IL-6 mRNA fold change was calculated in transfected samples respect to control sample. **Panel B**: four different concentrations of ML122 were analysed for their IL-6 mRNA content. Moreover, IL-6 protein concentration was analysed by Bioplex analysis, data are expressed as pg/mL of IL-6 in supernatants isolated from transfected cells.

IL-6 mRNA fold change was calculated. In the same Figure, also data relative to IL-6 protein release, obtained by Bioplex analysis was reported. The data obtained showed that no major effects were observed on IL-6 gene expression with the exception of Lipofectamine-iMAX. To have a complete view of the inflammatory profile, a panel of pro-inflammatory cytokines were investigated through Bioplex analysis. In a first analysis, supernatants of U251 cells transfected for 48 hours with ML122 or commercial available transfection agents were characterized for a panel of 27 cytokines. A heat map of cytokines is presented in **Figure 67**. As it is clearly evident, when Lipofectamine RNA iMAX is employed a significative change in cytokines panel expression was found. Also in the case of ML122 a change in cytokines profile is shown, even to a lesser extent. In particularly, when ML122 is employed as carrier, IL-7, IL-12 and VEGF result significantly modulated.

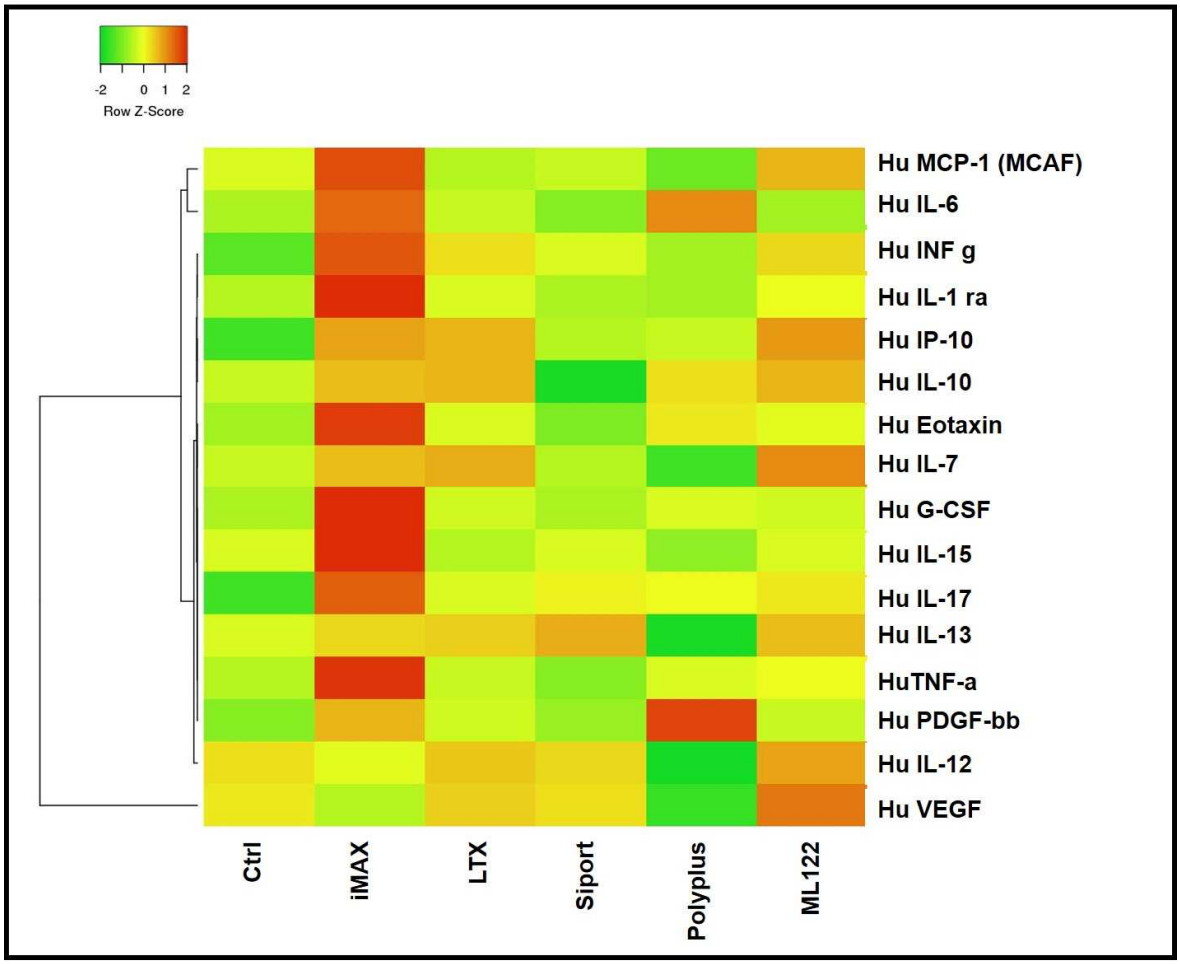

Figure 67. Analysis of a panel of 27 cytokines in transfected U251 cells. Supernatants from four different commercial available transfection agents were analysed by Bioplex analysis. The 16 cytokines expressed in supernatants are reported in the maps.

Moreover, the same panel of cytokines was also employed for the evaluation of ML122 analogs. Also in this case U251 cells were transfected with two different concentrations (2.5 and 5 µM) of ML122, GME28 or CRL23/I for 48 hours. After the treatment supernatants were collected and analysed through Bioplex analysis. Observed concentration indicated as picograms of protein for mL of supernatant, for each expressed cytokine is reported in the **Table 14**. No major induction of pro-inflammatory response was observed.

	Ctrl	ML122 2,5 µM	ML122 5 µM	GME28 2,5 µM	GME28 5 µM	CRL23/I 2,5 µM	CRL23/I 5 µM	
Hu PDGF-bb	5,33	6,08	6,08	2,3	10,55	11,28	6,08	Obs Conc
Hu IL-1b	1,79	1,63	2,07	1,52	1,9	1,14	1,85	Obs Conc
Hu IL-1ra	180	187	127	158	144	151	158	Obs Conc
Hu IL-2	5,7	12	3,6	4,75	5,33	2,23	3,79	Obs Conc
Hu IL-4	6,1	2,4	4,33	5,96	6,67	4,63	6,1	Obs Conc
Hu IL-6	2099	2067	2003	1876	1741	1898	2130	Obs Conc
Hu IL-7	22,18	24,53	20,99	37,81	42,01	26,83	24,53	Obs Conc
Hu IL-8	61367	25407	25108	15838	20161	16441	23876	Obs Conc
Hu IL-9	15,37	10,37	14,31	8,9	13,6	7,04	11,81	Obs Conc
Hu IL-10	95,62	86,67	99,58	102,49	103,81	79,58	87,72	Obs Conc
Hu IL-12 (p70)	375	365	446	380	416	358	344	Obs Conc
Hu IL-13	15,34	15,68	18,38	13,62	18,55	12,23	14,48	Obs Conc
Hu IL-15	15,68	4,85	3,2	11,6	9,79	11,8	18,31	Obs Conc
Hu IL-17	13,28	5,83	3,95	7,08	12,66	7,08	16,99	Obs Conc
Hu Eotaxin	37,86	45,57	37,86	42,95	37,86	45,47	45,47	Obs Conc
Hu FGF basic	58,81	37,77	48,31	58,81	56,79	53,69	58,81	Obs Conc
Hu G-CSF	18,24	15,26	16,26	14,76	15,76	12,23	15,76	Obs Conc
Hu GM-CSF	64,18	49,94	50,82	62,98	65,53	55,53	68,24	Obs Conc
Hu IFN-g	154	142	177	158	200	142	165	Obs Conc
Hu IP-10	97,96	90,63	105,05	97,96	105,05	86,86	90,63	Obs Conc
Hu MCP-1(MCAF)	2500	1826	1719	1834	1193	1803	2549	Obs Conc
Hu MIP-1a	1,12	1,53	1,18	1,12	1,69	1,06	1,06	Obs Conc
Hu RANTES	12,39	8,14	9,04	11,59	13,96	6,24	13,96	Obs Conc
Hu TNF-a	20,83	20,83	20	22,49	24,15	19,17	18,34	Obs Conc
Hu VEGF	7445	8051	9475	8282	8570	6754	6240	Obs Conc

Table 14: Cytokines expression in U251 cells transfected with ML122 and its analogs.

Discussion

MicroRNA are small RNA molecules of about 19-23 nucleotides in length, which do not codify for proteins. Their principal and best described function is the regulation of gene expression at post transcriptional level through mRNA target. More than 2500 miRNA sequences have been reported, and thanks to innovative techniques such as next generation sequencing, this number is going to increase. After their first introduction in 1993, miRNAs have been deeply investigated and considered important tools both in diagnostic and therapeutic field (theranostics).

The presence of cmiRNAs in plasma was firstly described by Chim and colleagues [*Chim et al., 2008*] in 2008. After this first work, which represents a milestone in circulating miRNAs research (cmiRNAs), several others studies have been published, that not only confirmed the presence of miRNA in plasma, but also in others body fluids such as saliva, urine, milk or cerebrospinal fluid. Importantly, all authors agree in saying that miRNAs are very stable in body fluids. At moment the function of cmiRNAs is still much debated, in fact while some authors claim that cmiRNAs can be considered as 'communication systems' between cells, others consider miRNAs only as 'waste products' of the cells, which enter in blood stream followed by cellular death. It is universally accepted that miRNAs are physiologically present in blood stream, but their expression profile results altered, when a change respect to physiological conditions occurred. For this reason several research group investigated miRNAs as possible markers of disease and due to heterogeneity of pathways in which miRNAs are involved, they were considered as possible biomarkers in a large variety of diseases. Moreover, the high stability of cmiRNA in body fluids, associated to the possibility of obtaining samples with non-invasive methods, makes circulating miRNAs among the most interesting novel biomarkers.

I. Circulating miRNA as tools in colorectal cancer (CRC) diagnosis: key results

IA. How much the selected protocol can influence data?

On the basis of the large number of publication about cmiRNAs available in the literature, a brief analysis is sufficient to conclude that no standard protocols are still available for plasma isolation and miRNA analysis. With respect to this consideration, it is

also clear that different factors, including plasma isolation protocol, miRNA extraction kit, miRNA reverse transcription kit and finally the chosen miRNA analysis technology can deeply affect the final results. Therefore, in order to design our experiment protocol several experiments finalized to set-up the methods were necessary.

The first important aspect that must be considered is how to obtain the starting plasma sample. Several protocols have been proposed in literature, with significative differences. While all the authors agree that blood sample needs to be processed immediately after the collection, protocols are much more heterogeneous as regard speed and time of centrifugations. For this reason we compared three different plasma isolation protocols commonly used in literature (Figure 4). The results obtained show that different employed protocols for plasma isolation affected significantly the final miRNA concentration obtained. Not surprising using low speed centrifugation (protocol A: 1200g, 10'), the loss of miRNAs content in macrovesicles was avoided, and at same time detected miRNAs levels were significative higher with respect to those obtained using protocols based on medium (protocol B 1200g, 10'; 2400g, 20') or high speed centrifugation (2000g, 20'; 16000g 10'). Considering the high difference in miRNA content between protocol A and protocol B and C, we speculated that probably protocol A is not able to ensure the complete removal of blood cells and, most of all, of platelets that at the moment of lysis release their miRNA content, affecting miRNAs quantification. By contrast, no differences were shown when protocol B and C were compared, indicating that even if high speed centrifugation is employed no loss of vesicles encapsulated miRNAs occurred. Moreover, as reported in some literature available studies, we confirmed that miRNAs are extremely stable in plasma sample. In fact after analysing the same samples after six months minimal differences were detected (Figure 5). Another important step that can affect final miRNA concentration is of course miRNA extraction from plasma. In this respect several works have been already done allowing a comparison between different miRNA extraction kit, but no data are available as regard the rate of miRNAs that are lost during extraction. Our data demonstrate that a mean loss, in the order of 10^3 occurred when miRNAs are extracted from plasma samples (Figure 2) but, very importantly, no significant differences were detected when different batches of the same kit are tested, indicating a high reproducibility as regard the extraction step.

IB. Validation of miRNA release model system looking at selected miRNAs

In the context of miRNAs analysis in CRC patients we considered three different miRNAs: miR-141-3p, miR-221-3p and miR-222-3p, which were previously shown, by several authors, to be modulated in plasma sample of CRC patients. To evaluate the effective increase of miRNAs release in presence of colorectal cancer we employed two different experimental models. Firstly, we analysed miRNAs content in three different colorectal cancer cell lines (HT-29, LoVo and Ls174T) and we compared miRNA intracellular concentration with the rate of miRNAs released in conditioned medium. Our data demonstrate that the three selected miRNAs are not only well expressed in all three cell lines, but are also released in supernatants. MiRNAs concentration in supernatants are particularly interesting. In fact, while miR-221-3p and miR-222-3p release pattern is specular to intracellular miRNAs pattern, miR-141-3p presents an expression profile in supernatants completely different from intracellular profile. This suggested us that, each miRNA presents a specific release profile, that is not completely dependent from starting miRNA intracellular concentration, but probably, may be influenced by other factors, such as miRNA sequence or modification during biogenesis. Moreover, miRNAs release is closely dependent from the employed cell lines. This is demonstrated by the fact that HT-29 cells, independently from the analysed miRNA, present the higher miRNA release ability (Figure 8). It is also important to consider that the analysed medium is supplemented with 10% of FBS, which contains bovine miRNAs. While our analysis suggests that human and bovine miR-141-3p, miR-221-3p and miR-222-3p are perfectly homologous. The amount of bovine miRNAs was found low and did not affect the conclusion drawn from the results obtained (Figure 7). We also analysed miRNAs release in an *in vivo* context, analysing plasma and tumor tissue samples isolated from nude mice xenografted with the three CRC cell lines. This model is of course very useful, because is more similar to patient condition, and takes into account possible reaction of cells and tissue surrounding tumor, reaction of the host body and blood physiological clearance mechanisms. Data obtained by analysis of cmiRNA in plasma of mouse models confirm as seen in supernatants, in fact HT-29 tumor releases the higher miRNAs rate for all the three miRNAs, confirming high release ability of HT-29 cells (Figure 11). It is also important to consider that all three human miRNAs present a sequence perfectly homologous to murine miRNAs. In this respect, healthy mice used as controls express good levels of circulating miR-141, miR-221 and miR-222. So, we hypothesize that miRNAs absolute amount in plasma derives from (a) starting miRNA amount physiologically present in blood of healthy mice, (b) a rate of human miRNA released by

tumor tissue and (c) a possible amount of murine miRNAs release as consequence of tumor presence. In order to evaluate the change of miRNA profile due to tumor presence, it is more significant to analyse relative miRNA expression respect to control mice (Figure 14). Interestingly, the presence of HT-29 tumor xenograft was able to sharply increase circulating levels of all the three miRNAs, and the fold change presents the same trend of absolute quantification. Once again, the high ability of HT-29 cells to release the three analysed miRNAs was confirmed. At same time, the presence of Ls174T tumor xenograft does not affect levels of circulating miR-141, miR-221 and miR-222, confirming supernatants data, which shown very low ability of Ls174T to release the analysed miRNA. Finally, when LoVo xenografted mice were considered only an increase in circulating miR-221 and miR-222 is detected, demonstrating how within the same cellular model miRNAs are differentially released. All together our data demonstrate that the three analysed miRNAs are released by CRC cells both in vitro and in vivo.

Which is the most efficient PCR-based technique for miRNA analysis?

The data obtained in this first set of experiments were performed using two different PCR-based techniques, droplet digital PCR (ddPCR) and absolute RTqPCR. This allowed us to compare the two techniques in order to evaluate the most suitable methods for our analysis. As it is possible to conclude comparing the data obtained with the two different techniques (Figure 8 versus Figure 10 and Figure 11 versus Figure 13), using both techniques the same trend was obtained, even if higher miRNA content values are obtained when absolute miRNA quantification is performed with RTqPCR. This is not surprising, considering that the employment of a standard curve created using known concentrations of mature synthetic miRNA controls may introduce biases, due mainly to synthetic miRNA extreme dilution, which may affect final results. Several other technical considerations must be done. First of all, ddPCR does not require standard curve to give absolute quantification, but, in this technique, absolute concentration is directly obtained applying Poisson law. Moreover, sample partitioning, performed in droplet digital PCR, creates thousands of droplets within which a single PCR reaction takes place, avoiding the need to analysed samples in duplicates or triplicates. Finally, ddPCR analysis required less amount of starting cDNA, and it is particularly useful in circulating miRNAs analysis, where the obtained RNA sample is very limited. On the basis of these considerations, ddPCR represents the first

choice in circulating miRNAs analysis, despite the cost for sample is higher with respect to RTqPCR technique.

Plasma miRNA spiked samples as a tools for validation of innovative devices (the ULTRAPLACAD project)

As previously discussed, several step are required for miRNAs quantification using PCR-based techniques. MiRNA extraction and reverse transcription are necessary for PCR-based analysis, but at the same time they are prone to introduce several biases. One of the principal innovations of project validating novel platforms for ultrasensitive detection (as the ULTRAPLACAD project) is the possibility to quantify miRNAs directly in plasma sample avoiding intermediate steps that can affect final result. One of our research goals in this respect was the creation of samples with known concentration of miRNAs in order to verify the reliability of SPR-based device. Plasma samples from CRC patients represents only the final step of the device set-up. Considering that high amount of plasma was required to develop the device, and ethical issue in requiring high amount of blood to CRC patients, the first set-up phase was performed using high amount of plasma isolated from healthy donors and opportunely additioned with known amount of mature synthetic miRNA. Our studies demonstrated that, when a naked mature miRNA is added to plasma is immediately degraded by RNAse enzymes, which are contained in plasma (Figure 15). For this reason, we developed a protocol based on the pre-treatment of plasma with RNAse inhibitor. Plasma pre-treatment, for 10 minutes at room temperature, allows the complete inhibition of RNAse providing data perfectly comparable to the situation in which synthetic miRNA is added after plasma lysis and so, when RNAse enzymes have already be inactivated by lysis solution. This protocol allows to generate high amount of plasma, spiked with known concentration of mature miRNAs, to be analysed at same time in ddPCR (Figure 16) and using ULTRAPLACAD-device (experiment undergoing) in order to verify the reliability and the efficiency of the device in direct miRNA detection. The major limit of this kind of sample is associated to the physiological presence of the investigated miRNAs in starting human plasma samples used for the spiking, and so the lowest concentration that can be detected is represented by the physiological miRNA concentration in healthy subjects plasma samples. With these considerations in mind, we can anyway conclude that spiked plasma samples, as far as concern miRNAs, are suitable for the preliminary set-up phase of characterization of devices based on novel direct detection strategies.

A panel of miRNAs is most suitable for diagnosis: implementing the list.

The final goal of our project is the analysis of plasma samples from both healthy subjects and CRC patients. As regard the miRNA analysis, we verified 32 samples from CRC patients and 9 samples from healthy subjects (Figure 18). First important point to consider is that despite several studies available in the literature demonstrated that miR-141-3p, miR-221-3p and miR-222-3p are significanly modulated in plasma of CRC patients, in our panel of patients only in few cases we detected a significant change with respect to our control samples. Following critical analysis of the available data, it was immediately clear that several methodological differences are present among those used to obtain the data by the different research groups, including employed method to obtain plasma, extraction method and miRNA detection technique. Moreover, large amounts of data were obtained by high-throughput screening methods, but were not validated by PCR-based technique. All together these data suggest us that the method of sample preparation is extremely important, especially, in circulating miRNAs analysis and can affected significantly the final data. Data available in literature can not be compared, considering high variability due to plasma isolation and extraction methods. Considering high interest of circulating miRNA as diagnostic tools, a standardization of protocols, as regard plasma biobank creation, miRNA extraction and analysis is required in order to increase reproducibility and compare data produced by different laboratories. On the other hand, we considered more carefully our panel of miRNAs, and it is clear that considering only miR-141-3p, miR-221-3p and miR-222-3p, we were unable to predict CRC is several case (25 out of 32 patients analysed). Therefore, the miRNA list to be considered for CRC diagnosis should be implemented. In conclusion, we demonstrated that miRNAs are released in the external environment by CRC cells, the amount of the release is dependent on the cells features, and moreover, within the same cellular type, the amount of released miRNAs does not depend only by the starting intracellular miRNA levels. This was confirmed also in *in vivo* models, in which several others factors interfere, such as the systemic response to the tumor presence, or blood clearance. These data confirm that cmiRNAs are useful tools for CRC diagnosis, even if several issues must be solved. The first important issue regards the reproducibility of data between laboratories. In fact our set-up data demonstrate how the protocol for sample preparation and analysis can affect final results. Moreover, we demonstrate as only a single miRNA or few miRNA (for instance miR-141, miR-221 and miR-222) are not sufficient to

make diagnostic prediction. The employment of at least 10 miRNAs is expected from our data to be more informative,

With respect to this high throughput screening analyses (such as microarray or RNAseq) are expected to be necessary, in order to identify a panel of miRNAs, which are modulated in all analysed CRC patients, while are stable in control samples. In this way it will be possible to draft a list of candidate biomarkers to be routinely used as screening tool.

II. Circulating miRNA as tools for ABT detection

In the second part of our work, we verify the possibility that cmiRNA can be employed as biomarkers of autologous blood transfusion. ABT, is an illicit practice common between athletes, employed to enhance their athletic performances. This technique consists in withdrawal of some units of blood generally, several weeks before the competition, which were then reinfused some days before the performance. Collected blood is conserved for short periods; less than 40 days at +4°C, while for long term storage cryopreservation is preferred. This practice is based on the evidence that transfusions causes an increase in haemoglobin amount, which results in an increased volume of transported oxygen and consequently in an athletic performance improvement. Despite others techniques, such as the use of erythropoietin, give better results, ABT is particularly employed because, no validated tests to detect ABT are still available. In this thesis we suggest circulating miRNAs as possible biomarkers. Is not the first time that miRNAs have been proposed as ABT markers, previously, Leuenberger and colleagues identify a small group of 5 miRNAs which levels in plasma result to be modulated immediately after blood transfusion. Respect to Leuenberger work we proposed, in our opinion, three important innovations. First of all, Leuenberger group investigated miRNAs modulation only in the first hours immediately after blood reinfusion, while our study was designed in order to verify circulating miRNA response, both in the short T6 (+3) and medium T8 (+15) term after blood reinfusion (see Figure 19 for a flow chart of the detection protocols), and furthermore, the response after blood withdrawal was verified. In the second instance, also cryopreserving storage method was taken in consideration, while Leuenberger and co-workers considered only +4°C blood storage. Starting from two considerations: (a) blood storage technique can affect the body response when blood is reinfused, (b) blood cryopreservation is more suitable for athletes,

because blood withdrawal can be performed several months before the performance, we analysed cmiRNAs profile in both athletes reinfused with +4°C stored blood and in athletes transfused with cryopreserved autologous blood.

Are miRNAs related to erythroid differentiation good candidates as ABT markers?

In the first part of the work, we started from the hypothesis that both blood withdrawal and reinfusion may cause a change in oxygen availability and consequently several parameters related to oxygen levels may be affected. In particular, several studies associated changes is oxygen levels with both erythropoiesis induction and fetal haemoglobin production [*Haase et al., 2013 and Risso et al., 2012*]. For this reason in the first phase we focused our attention in miRNAs which have been previously associated with these two pathways. The combined analysis of literature available data associated to the first preliminary data obtained by microarray analysis, allowed to identify a list of 8 miRNAs which were analysed in three pools of control subjects and in six athletes that underwent to ABT (Table 11). Between all subjects, in five of the six subjects at least one miRNA results to be modulated, while the number of modulated miRNAs is extremely variable between subjects (Table 12). Among the 8 investigated miRNAs, particularly interesting was shown to be miR-486-3p, which is upregulated in three of the six ABT trained athletes. The trend of this miRNA was also confirmed by another miRNA detection technique: ddPCR, demonstrating that data is not affected by biases due to the selected miRNA analysis method (Figure 24). In conclusion, by our preliminary data, miRNAs related to oxygen availability are modulated when ABT occurred, and may be useful as markers in anti-doping strategy. The number of analysed sample, in this preliminary phase is limited and our data must be confirmed in the others six available subjects, in which we expected similar trend. Despite the limited number of analysed samples, we considered the data obtained a proof of the principle for further analysis.

A panel of miRNAs as possible ABT biomarkers

Taking advantage from the microarray analysis, allowing quantification of all miRNAs expressed in plasma samples we performed an overall analysis to detect new miRNAs of possible interest in ABT detection. We identified 20 miRNAs which are up-

regulated in both athletes that underwent to reinfusion with both +4°C stored and cryopreserved blood, three days after blood reinfusion. At same time we considered common modulated circulating miRNAs at T3 (-25) and T8 (+15). By a first preliminary analysis, methods of blood storage seem to affect significantly the profile of modulated miRNAs. With respect to single miRNA analysis, miR-6175-3p was found to be upregulated in all six subjects at T6 (+3), while miR-6785-5p was found to be upregulated in all six subjects at T8 (+15). Unfortunately, considering their recent introduction no information are available about these two miRNAs, but of course, they need to be investigated more in deep. The difference between the two cohorts of ABT trained athletes is clear, and in our opinion will be confirmed analysing the others six subjects. Starting from the consideration that both storage methods are possible, we considered all miRNAs modulated in both cohorts of athletes, and we drafted a list of 17 miRNAs, composed by the five (or less in same cases) most modulated miRNAs at each time point. This set of miRNAs may be analysed routinely in athletes, and changes in one or more miRNAs, depending on person to person variability, may be indicative that blood withdrawal or ABT have occurred. From this point of view, a 'miRNA passport' would be useful, in which the 17 miRNAs part of the list, are analysed in 4-5 independent blood samples, taken at different time point, during the season, in order to achieve information about physiological fluctuations of selected miRNAs in each subject. Every miRNA value outside these physiological values, would be indicative of a possible illicit practice. In conclusion, we demonstrated that circulating miRNAs may be useful also as markers of changes respect to physiological condition. We identified two different list of miRNAs, one, composed by 8 miRNAs, which is based exclusively on miRNAs, that are in some way related to oxygen availability, and for which this correlation is already demonstrated in literature. An overall analysis was also performed, that considers all miRNAs expressed in plasma samples, and we identify a list of 17 miRNAs, which are stable in control subject, while are modulated in subjects that underwent ABT. Our data support the concept that miRNA analysis is important for ABT detection in sports.

III. MicroRNAs as possible therapeutic tools: application in beta thalassemia treatment

In the third part of the work we considered miRNAs as possible therapeutic tools. In fact the main function of miRNAs is the targeting of messenger RNA, resulting in regulation

of protein production. In this thesis we employed miRNA-based therapy as possible strategy for the treatment of β-thalassemia. Beta-thalassemia is a genetic disease caused by mutations within or near the β-globin gene resulting in absent synthesis of β-globin chains. The first manifestation of the pathology is anaemia, which severity depends on the type of mutation causing disease, followed by several others clinical manifestations due to the lack of β-globin chains and the consequent excess of free α-globin chains. Is now universally accepted that the co-inheritance of hereditary persistence of fetal haemoglobin phenotype and beta-thalassemia mutations ameliorate symptomatology. In fact, people which present HPFH continue to produce fetal haemoglobin also in adult age, and this phenomenon is particularly useful in beta-thalassemia patients because γ-globin chains can partially replace the lack of β-globin chains. Starting from this evidence, a new therapeutic approach based on the reactivation of fetal haemoglobin production was proposed to treat beta thalassemia. The mechanism of gamma globin gene silencing is well established and is clear that the transcription factor BCL11A is one of the principal repressor of γ-globin gene. In this context BCL11A has become a key target for different chemical or biological compounds. Another research group [*Lulli et al., 2013*] has proposed a miRNA-based approach to down-regulate BCL11A, in particular they shown that BCL11A 3'UTR is targeted by miR-486-3p. In our analysis, starting from the evidences that miR-210-3p is upregulated when fetal haemoglobin production is induced (Figure 36), we investigated possible correlation between miR-210-3p and BCL11A. Our bioinformatic analysis (Figure 37) predicted that miR-210-3p is able to bind BCL11A mRNA in the coding region (nucleotides 789-798) and the interaction was confirmed by SPR-based biomolecular interaction analysis (Figure 39). Starting from this preliminary data, we verified the effects of forced miRNAs expression in erythroid precursors cells and in cellular clones expressing BCL11A at high levels. K562-BCL11A clones were created by our research team in order to verify molecules acting on BCL11A transcript, considering that K562 cells, normally used to perform fetal haemoglobin induction experiments, expresses at very low levels BCL11A. Our data suggests that the over expression of miR-210-3p in K562-BCL11A clones, leads to a sharp decrease of BCL11A transcript and is also associated with an increase of gamma globin mRNA production, when the higher concentrations (90 and 270 nM) of premiR-210-3p are considered (Figure 40). Effects at transcriptional levels are associated to effects at post-transcriptional levels. In fact when the higher concentration of premiR-210-3p (200 nM) is transfected to cells for 72 hours a significative decrease of BCL11A protein is detected (Figure 41). Similar effects were observed in ErPCs, in this case the decrease of BCL11A

mRNA and the increase of gamma globin transcript (Figure 42) were associated with the increase of gamma globin production detected by Elisa analysis (Figure 43).

Our data suggests a direct correlation between the increase of miR-210-3p and BCL11A decrease, despite, in ErPCs, considering the high amount of proteic extracts required for western blotting analysis and low number of ErPCs obtained by isolation protocol was not possible to perform western blot analysis to verify BCL11A protein content. On the other hand, effects of miR-210-3p over expression are limited to BCL11A and γ-globin expression, in fact, no changes of others erythroid markers, such as transferrin receptor and glycophorin A were detected (Figure 43). Our data suggest that the employment of miR-210-3p mimic molecules is not sufficient to induce the activation of erythroid differentiation. At this purpose treatment with miRNA mimic molecules should be combined with other inducers of erythroid differentiation in order to fully induce HbF accumulation. Moreover, considering that miR-210-3p targets a sequence in the coding region of BCL11A, while miR-486-3p, previously validated by Lulli and colleagues, targets the 3'UTR of BCL11A transcript, a co-treatment may be considered in order to enhance the effects. All together our data demonstrate that miR-210-3p is able to target BCL11A leading to the decrease of mRNA and protein levels, starting from this evidence we also employed two PNAs, able to target BCL11A transcript in the region targeted by miR-210-3p. In fact, PNAs are much more stable respect to premiRNA molecules, and do not require transfection agents because they are already chemically modified to be easily delivered into cells. Our preliminary data demonstrate that both PNAs are able to reduce BCL11A mRNA expression, and as expected, the major reduction is obtained when the PNA perfectly complementary to miR-210-3p binding site, is employed (Figure 44). Moreover these PNAs were employed in combination with one of the most powerful fetal haemoglobin inducers: mitramycin demonstrating a good increase in benzidine-positive cells percentage when MTH is used in association with PNA, respect to MTH alone (Figure 45). The same combined treatment was also verified analysing gamma globin mRNA expression, in this case only a slight increase of gamma globin production was detected respect to cells treated with only MTH. Considering that in this case we employed the optimal MTH concentration, normally employed to obtain the best fetal haemoglobin induction, we speculate that probably differences will be more significative using sub-optimal concentrations of MTH. Only in a preliminary way, PNAs were also tested in ErPCs obtained by a beta-thalassemia patient, even in this case a decrease of BCL11A mRNA was obtained, but in this case data are very preliminary, and a deeper investigation is required, especially considering high variability in BCL11A expression levels between

beta-thalassemia patients. Despite our study is yet in a preliminary step, in particular, an analysis as regard effects of PNAs on BCL11A protein is required, the employment of PNAs binding miR-210-3p target sequence seems to be a prosing approach in BCL11A down-regulation.

IV. Delivery: Calixarene based molecules as possible miRNA-based molecules carriers

In the last part of the thesis we considered the important issue related to miRNA-based molecule delivery into cells, in fact, this kind of molecules need an appropriate delivery system to be transferred into cells. In addition, delivery molecules present another important function: they protected miRNA-based molecules from nuclease degradation. Several kinds of delivery system have been proposed in the years, starting from viral vectors, which present high efficiency, but also several issues as regard safety. On the contrary non-viral vectors, are of course much more safe, but their transfection efficiency is much lower. At moment the non-viral lipid-based vectors represent the first choice, in common laboratory practice to delivery antimiRNA and premiRNA molecules. Generally, these molecules are cationic lipids which are able to interact with negative charges present in miRNA-based molecules. Despite a large number of improvements allow to increase transfection efficiency and loading capacity, the high toxicity of this kind of molecules is still an unsolved issue. Thanks to a collaboration with Professor Sansone research group (University of Parma) we investigated a molecule, called ML122, synthesized by Professor Sansone and colleagues and previously used to DNA delivery. Starting from the hypothesis that the cup-shape of ML122, associated with positive charges present in the upper rim of the molecule may be useful for miRNA-based molecules delivery, we tested ML122 transfection efficiency in two different cell lines, the adherent U251 glioma cell line and the suspension K562, which furthermore are difficult to transfect. In a preliminary phase, we investigated ML122 transfection efficiency employing a) a mature synthetic miRNA (Figures 48 and 49) b) premiRNA molecule (Figure 50) and c) an antimiRNA molecules (Figure 53) in both cell lines with very promising results. In fact, after miRNA (Figure 49) or premiRNA (Figure 50) transfection with ML122 a dramatically increase of intracellular miRNA content was obtained. Furthermore, comparative experiments demonstrate that ML122 is very competitive with some of the most used commercial available transfection agents (Figure 50). At same way when antimiRNA molecules are transfected with ML122 a sharp decrease

of intracellular concentration of target miRNA is detected and the miRNA decrease is even better respect to decrease obtained employing one of the most competitive commercial available transfection agent (Figure 53).

Are ML122 delivered molecules biologically active?

After this preliminary set of experiment that also, allow us to set-up transfection protocol (Figures 51 and 52), we focused our attention on consequences of ML122 mediated transfection. Is important to underline that increased levels of mature miRNA resulting from premiRNA transfection using ML122 as vehicle demonstrate that, once delivered, premiRNA is not only released by the complex formed with the delivery molecule, but is also able to take part to RNA interference pathway. This in our opinion represent a first proof that miRNA-based molecules delivered by ML122 are biologically active and maintain their functions once internalized into the cells. In order to further investigate this key point we evaluate effects of delivered miRNA-based molecules on their target mRNA. Two different biological models were considered, in first instance, as previously demonstrated premiR-210-3p transfection in ErPCs, and the consequent increase of miR-210-3p intracellular levels increase is able to down-regulate BCL11A mRNA expression. PremiR-210-3p delivered by ML122 is able to produce a significative reduction of BCL11A, compared to that seen when commercial available transfection agents are employed. In the second biological model we employed an antimiRNA molecule, in this case, we start from a work performed by Brognara and colleagues [Brognara et al., 2015], which demonstrates that miR-221-3p decrease results in apoptosis induction, in different glioma cell lines. For this reason, we evaluate effects of antimiR-221-3p transfection mediated by ML122, in U251 cell lines. Our data suggest that antimiR-221-3p vehicled by ML122, is able to reduce miR-221-3p intracellular levels and results in apoptosis induction in U251 cell line, although a quite pro-apoptotic effect was detected also when ML122 was employed without antimiRNA molecule (Figure 56). Obtained data suggest that ML122 can be employed as non-viral vector to deliver miRNA-based molecules with high efficiency, in different cell lines. ML122 was shown to be very competitive with others commercial available transfection agents, and most important, we demonstrate that molecules delivered by ML122 are not only released by the complex formed with the delivery compound, but are also able to perform their biological activity. On the other hand, despite we developed a transfection protocol that require low concentration of ML122, a little pro-apoptotic effect was shown when ML122 was used with

no miRNA-based molecules, this suggest us that a more in depth study (discussed in the next chapter), to investigate ML122 toxicity is required.

Is ML122 suitable for PNA delivery?

Starting from the hypothesis that cup shape of ML122 could be useful to delivery no-charged molecules, we verify if ML122 may also deliver PNAs. Our preliminary analysis performed using PNA fluorescently labelled demonstrate a good cellular uptake when a non-functionalized PNA is delivered with ML122, even if is important to underline that our data demonstrate that PNA functionalized with polyarginine peptide (R8), presents higher transfection efficiency (Figure 57). As for miRNAs, also for PNAs was important verify, if ML122-delivered molecules are released by the transfection complex, and most important if they maintain their biological activity. Even in this case we investigated a simple biological model proposed by Brognara and co-workers: miR-221-3p decrease results in apoptosis induction in glioma cell lines, but in this case we employed a PNA targeting miR-221-3p. Apoptotic cell rate obtained when PNA against miR-221-3p was transfected using ML122, was compared to the percentage of apoptotic cells registered when a PNA with the same sequence, but functionalized with a polyarginine peptide, was employed (Figure 58). According to that previously seen for cellular uptake, PNA delivered with ML122 is able to induce apoptosis in U251 cell lines, despite the percentage of apoptotic cells, is lower respect to value registered when polyarginine functionalized PNA is employed. This does not surprise us, in fact as previously said, a lower cellular uptake is detected when PNA is delivered with ML122, and consequently lower biological effects are expected. Despite ML122 demonstrates to be less efficient than PNA functionalization with R8, an important advantage can be reached in employing ML122 as delivery system, in fact, we demonstrate that employing only a delivery molecule is possible to delivery at same time two different kinds of molecules, in our case a premiRNA and a PNA, with the same efficiency obtained when a single molecule is delivered (Figure 61). This finding is extremely important, considering that combined treatment, based on the simultaneous multi-targeting is very important in new treatment developed, and employing one delivery molecule, ML122 is possible to considerably reduce toxicity due to vehicle. Moreover, first preliminary screening of molecules with a calixarene-based structure, similar to ML122, with little chemical modifications, allows us to identify two other possible vehicles: GME28 and CRL23/I,

which needs to be investigated more in depth, in order to find molecules with similar structure, but presenting major transfection efficiency.

Evaluation of ML122 toxicity

Once evaluated efficiency of ML122 in transfection both miRNA-based molecules and PNAs, was extremely important in our opinion evaluate, toxicity of ML122 and its analogues, considering that one of the principal problems of commercial available transfection agents, is the high toxicity. In a preliminary step, we evaluate cell viability, and possible pro-apoptotic effects of ML122, in both analysed cell lines: K562 cells and U251. As seen also for commercial available transfection agents (data not shown), toxic effects, are limited when K562 cells are considered, while are more consistent when U251 cell line is considered (Figures 63a, 63b, 65a and 65b). For this reason, we speculate that probably U251 cells are much more sensitive to transfection procedure and we tested ML122-analogues: GME28 and CRL23/I only in U251 cell lines, in order to verify the worst condition. ML122 demonstrates at lower concentration very limited effects on cell viability, while sensitive reduction of viable cells was registered only when ML122 is employed at higher concentration for 72 hours. When apoptotic profile is considered, percentage of apoptotic cells is directly proportional to ML122, concentration. Is important to underline that in U251 cells, already at 2,5 μM of ML122, concentration that we consider optimal, for transfection protocol, a quite high increase of apoptotic cell percentage respect to control was detected, but it is still comparable to that see for commercial available compounds. While no significative pro-apoptotic effects were shown when K562 cells were analysed (Figure 65a). The comparison between ML122, GME28 and CRL23/I, demonstrates that despite CRL23/I and GME28 present similar or in some case a little better transfection efficiency, they have significative higher pro-apoptotic effects. Moreover, we investigated possible pro-inflammatory response followed by transfection, analysing some of the most common inflammation-involved cytokines. Our data demonstrate that, despite ML122 modulates cytokines expression profile, especially for some cytokines as IL-7 and VEGF, the effects on cytokines expression are significative less evident respect to Lipofectamine RNA iMAX, one of the best ML122 competitor, as regard transfection efficiency. All together our data suggest that ML122 does not present pro-apoptotic effects in K562, while moderate pro-apoptotic effects, especially at higher concentrations, were shown in U251 cells, which according to our past experience are very sensible to transfection agents. Both pro-apoptotic

and pro-inflammatory effects caused by transfection with ML122, are anyway comparable to effects caused by commercial available transfection agents. At same time, despite two ML122 analogous, GME-28 and CRL23/I was shown to be very competitive with ML122 as regard PNA transfection efficiency, we evaluated also their possible toxic effects, but in this case, they were shown to be significative more toxic than ML122 and for this reason no further analysis were performed for this compounds. In conclusion, we proposed ML122 as possible vehicle for both miRNA-based molecules and PNA. We demonstrate that ML122 is able to internalized into cells both kind of molecules and these, once into cells, are released by the complex with ML122, and are still biologically active. Moreover, ML122 can be employed for the simultaneous transfection of both miRNA-based molecules and PNA, with significative advantages in multi-targeting therapy. The analysis of ML122 toxicity, reveals that ML122 presents moderate pro-apoptotic effects and quite pro-inflammatory effects, that are anyway comparable to commercial available data, and can be probably reduced, with further analysis regarding transfection protocol set-up.

Conclusions

Thanks to their short sequence and their consequent multi-targets, microRNAs are involved in a large spectrum of disease. A large number of publication have been proposed since their discovery in 1993, regarding their function, and their possible applications as biomarkers or as therapeutic molecules. The results presented in this Thesis support the concept that miRNAs and miRNA-modifiers are a key tool in THERANOSTICS.

Bibliography and Sitography

Ahmed FE, James SI, Lysle DT, et al. Improved methods for extracting RNA from exfoliated human colonocytes in stool and RT-PCR analysis. Dig Dis Sci, **2004**, 49:1889–1898. *doi.org/10.1007/s10620-004-9589-9.*

Ahmed FE, Jeffries CD, Vos PW, et al. Diagnostic microRNA markers for screening sporadic human colon cancer and active ulcerative colitis in stool and tissue. Cancer Genomics Proteomics, **2009**, 6:281–295.

Aimola IA, Inuwa HM, Nok AJ, et al. Induction of foetal haemoglobin synthesis in erythroid progenitor stem cells: mediated by water-soluble components of Terminalia catappa. Cell Biochem Funct, **2014**, 32:361-367. *doi.org/10.1002/cbf.3024.*

Alhasan AH, Kim DY, Daniel WL et al. Scanometric microRNA (Scano-miR) Array Profiling of Prostate Cancer Markers Using Spherical Nucleic Acid (SNA)-Gold Nanoparticle Conjugates. Anal Chem, **2012**, 84:4153-4160. *doi.org/10.1021/ac3004055.*

Alvarez-Erviti L, Seow Y, Yin H et al. Delivery of siRNA to the mouse brain by systemic injection of targeted exosomes. Nat Biotechnol, **2011**, 29:341–345. *doi.org/10.1038/nbt.1807.*

Arrington AK, Heinrich EL, Lee W, et al. Prognostic and Predictive Roles of KRAS Mutation in Colorectal Cancer. Int J Mol Sci, **2012**, 13:12153-12168. *doi.org/10.3390/ijms131012153.*

Arroyo JD, Chevillet JR, Kroh EM et al. Argonaute2 complexes carry a population of circulating microRNAs independent of vesicles in human plasma. Proc Natl Acad Sci USA, **2011**, 108:5003–5008. *doi.org/10.1073/pnas.1019055108.*

Avitabile C, Saviano M, D'Andrea LD et al. Targeting pre-miRNA by peptide nucleic acids A new strategy to interfere in the miRNA maturation. Artif DNA PNA XNA, **2012**, 3:88-96. *doi.org/10.4161/adna.20911.*

Babar IA, Cheng CJ, Booth CJ, et al. Nanoparticle-based therapy in an in vivo microRNA-155(miR-155)-dependent mouse model of lymphoma. Proc Natl Acad Sci U S A, **2012**, 109:1695–1704. *doi.org/10.1073/pnas.1201516109.*

Bader AG, Brown D, Winkler M. The Promise of MicroRNA Replacement Therapy. Cancer Res, **2010**, 70: 7027–7030. *doi.org/10.1158/0008-5472.CAN-10-2010*

Baglio SR, Rooijers K, Koppers-Lalic D. Human bone marrow- and adipose-mesenchymal stem cells secrete exosomes enriched in distinctive miRNA and tRNA species. Stem Cell Res Ther, **2015**, 6:127. *doi.org/10.1186/s13287-015-0116-z.*

Bagnacani V, Franceschi V, Bassi M et al. Arginine clustering on calix[4]arene macrocycles for improved cell penetration and DNA delivery. Nat Commun, **2013**, 4:1721. *doi.org/10.1038/ncomms2721.*

Baker M. Digital PCR hits its stride. Nat Methods, **2012**, 9:541–544. *doi.org/10.1038/nmeth.2027.*

Baker M. MicroRNA profiling: separating signal from noise. Nat Methods, **2010**, 7:687-692. *doi 10.1038/nmeth2910-687.*

Ballehaninna UK, Chamberlain RS. Serum CA 19-9 as a Biomarker for Pancreatic Cancer A Comprehensive Review. Indian J Surg Oncol, **2011**, 2: 88–100. *doi: 10.1007/s13193-011-0042-1.*

Ballesta AM, Molina R, Filella X, et al. Carcinoembryonic antigen in staging and follow-up of patients with solid tumors. Tumour Biol, **1995**, 16:32-41. *doi.org/10.1159/000217926.*

Bamberger AM, Riethdorf L, Nollau P, et al. Dysregulated expression of CD66a (BGP, C-CAM), an adhesion molecule of the CEA family, in endometrial cancer. Am J Pathol, **1998,** 152:1401–1406.

Bartel DP MicroRNAs: genomics, biogenesis, mechanism, and function. Cell, **2004**, 116:281-297. *doi.org/10.1016/S0092-8674(04)00045-5.*

Baselga J. Why the epidermal growth factor receptor? The rationale for cancer therapy. Oncologist, **2002**, 7:2–8. *doi.org/10.1634/theoncologist.7-suppl_4-2.*

Basu S, Wickstrom E. Synthesis and characterization of a peptide nucleic acid conjugated to a D-peptide analog of insulin-like growth factor 1 for increased cellular uptake. Bioconjug Chem, *1997*, 8:481–488. *doi.org/10.1021/bc9700650.*

Ben-Neriah Y, Karin M. Inflammation meets cancer, with NF-κB as the matchmaker. Nat Immunol, **2011**, 12:715–723. *doi.org/ 10.1038/ni.2060.*

Bernhardt WM, Wiesener MS, Scigalla P, et al. Inhibition of prolyl hydroxylases increases erythropoietin production in ESRD. J Am Soc Nephrol, **2010**, 21:2151–2156. *doi.org/10.1681/ASN.2010010116.*

Bianchi E, Zini R, Salati S, et al. c-myb supports erythropoiesis through the transactivation of KLF1 and LM02 expression. Blood, **2010**, 116:99–110. *doi.org/ 10.1182/blood-2009-08-238311.*

Bianchi N, Osti F, Rutigliano C, et al. The DNA-binding drugs mithramycin and chromomycin are powerful inducers of erythroid differentiation of human K562 cells. Br J Haematol, **1999**, 104:258-265. *doi.org/10.1046/j.1365-2141.1999.01173.x.*

Bianchi N, Zuccato C, Lampronti I et al. Expression of miR-210 during erythroid differentiation and induction of gamma-globin gene expression. BMB Rep, **2009**, 42:493-499.

Binley K, Askham Z, Iqball S et al. Long-term reversal of chronic anemia using a hypoxia-regulated erythropoietin gene therapy. Blood, **2002**, 100:2406-2413. *doi.org/ 10.1182/blood-2002-02-0605.*

Biomarkers Definitions Working Group. Biomarkers and surrogate endpoints: preferred definitions and conceptual framework. Clin Pharmacol Ther, **2001**, 69:89-95. *doi.org/10.1067/mcp.2001.113989.*

Borg J, Papadopoulos P, Georgitsi M et al. Haploinsufficiency for the erythroid transcription factor KLF1 causes Hereditary Persistence of Fetal Hemoglobin. Science, **2010**, 322:1839-1842. *doi.org/10.1126/science.1165409.*

Borgatti M, Breda L, Cortesi R et al. Cationic liposomes as delivery systems for double-stranded PNA-DNA chimeras exhibiting decoy activity against NF-kappaB transcription factors. Biochem Pharmacol, **2002**, 64:609-616.

Boulad F, Wang X, Qu J, et al. Safe mobilization of CD34 cells in adults with beta thalassemia and validation of effective globin gene transfer for clinical investigation. Blood, **2014**, 123:1483e6. *doi.org/10.1182/blood-2013-06-507178.*

Boussif O, Lezoualch F, Zanta MA et al. A versatile vector for gene and oligonucleotide transfer into cells in culture and in vivo: polyethylenimine. Proc Natl Acad Sci U S A, **1995**, 92:7297-7301. *doi.org/10.1073/pnas.92.16.7297.*

Breveglieri G, Travan A, D'Aversa E et al. Postnatal and non-invasive prenatal detection of β-thalassemia mutations based on Taqman genotyping assays. PLoS One, **2017**, 12:e0172756. *doi.org/10.1371/journal.pone.0172756.*

Brognara E, Fabbri E, Aimi F et al. Peptide nucleic acids targeting miR-221 modulate p27Kip1 expression in breast cancer MDA-MB-231 cells. Int J Oncol, **2012**, 41:2119-2127. *doi.org/10.3892/ijo.2012.1632.*

Brown SD, Plumb JA, Johnston BF et al. Folding of dinuclear platinum anticancer complexes within the cavity of para-sulphonatocalix[4]arene. Inorg Chim Acta, **2012**, 393:182–186. *doi.org/10.1016/j.ica/2012.04.033.*

Brown SD, Plumb JA, Johnston BF, et al. Folding of dinuclear platinum anticancer complexes within the cavity of para-sulphonatocalix[4]arene. Inorg Chim Acta, **2012**, 393:182–186. *doi.org/10.1016/j.ica.2012.04.033.*

Brummer A, Hausser J. MicroRNA binding sites in the coding region of mRNAs: Extending the repertoire of post-transcriptional gene regulation. Bioessays, **2014,** 36:617-626. *doi.org/10.1002/bies.201300104.*

Bryzgunova OE , Tamkovich SN, Cherepanova AV, et al. Redistribution of Free- and Cell-Surface-Bound DNA in Blood of Benign and Malignant Prostate Tumor Patients. Acta Naturae, **2015**, 7:115–118.

Bushman F, Lewinski M, Ciuffi A, et al. Genome-wide analysis of retroviral DNA integration. Nat Rev Microbiol, **2005**, 3:848-358. *doi.org/10.1038/nrmicro1263.*

Bussey HJR. Familial polyposis coli: family studies, histopathology, differential diagnosis and results of treatment. Johns Hopkins University Press, **1975.** *doi.org/10.1007/978-1-4684-2442-3_11.*

Busslinger M, Moschonas N, Flavell RA. β+ thalassemia: Aberrant splicing results from a single point mutation in an intron. Cell, **1981**, 27: 289–298. *doi.org/10.1016/0092-8674(81)90412-8.*

Bustamante-Aragones A, Rodriguez de Alba M, Gonzalez-Gonzalez C, et al. Foetal sex determination in maternal blood from the seventh week of gestation and its role in diagnosing haemophilia in the foetuses of female carriers. Haemophilia, **2008**, 14:593–598. *doi.org/10.1111/j.1365-2516.2008.01670.x.*

Calin GA, Dumitru CD, Shimizu M et al. Frequent deletions and down-regulation of microRNA genes miR15 and miR16 at 13q14 in chronic lymphocytic leukemia. Proc Natl Acad Sci USA, **2002**, 99:15524–15529. *doi.org/10.1073/pnas.242606799.*

Camps C, Buffa FM, Colella S, et al. hsa-miR-210 is induced by hypoxia and is an independent prognostic factor in breast cancer. Clin Cancer Res, **2008**, 14:1340–1348. *doi.org/10.1158/1078-0432.CCR-07-1755.*

Cao A, Galanello R. Beta-thalassemia. Genetics in Medicine, **2010**, 12:61–76. *doi.org/10.1097/GIM.0b013e3181cd68e.*

Cao A, Moi P. Regulation of the Globin Genes. Pediatric Research, **2002**, 51:415–421. *doi.org/10.1203/00006450-200204000-00003.*

Casoni I, Ricci G, Ballarin E, et al. Hematological indices of erythropoietin administration in athletes. Int J Sports Med, **1993**, 14:307–311. *doi.org/10.1055/s-2007-1021183.*

Cavazzana M, Ribeil JA, Payen E, et al. Study Hgb-205: outcomes of gene therapy for hemoglobinopathies via transplantation of autologous hematopoietic stem cells transduced ex vivo with a lentiviral bA-T87Q-globin vector (LentiGlobin BB305 drug product). Blood, **2014**, 124:4797.

Cavazzana-Calvo M, Payen E, Negre O, et al. Transfusion independence and HMGA2 activation after gene therapy of human beta-thalassaemia. Nature, **2010**, 467:318e22. *doi.org/10.1038/nature09328.*

Cazzola M. A global strategy for prevention and detection of blood doping with erythropoietin and related drugs. Haematologica, **2000**, 85: 561–563.

Chang A, Kim Y, Hoehn R, et al. Cryopreserved packed red blood cells in surgical patients: past, present, and future Blood Transfus, **2017**, 15: 341-347, *doi.org/10.2450/2016.0083-16.*

Chang PY, Chen CC, Chang YS, et al. MicroRNA-223 and microRNA-92a in stool and plasma samples act as complementary biomarkers to increase colorectal cancer detection. Oncotarget, **2016**, 7:10663–10675. *doi.org/10.18632/oncotarget.7119.*

Chen LL, Carmichael GG. Altered nuclear retention of mRNA containing inverted repeats in human embryonic stem cell: functional role of nuclear noncoding RNA. Mol Cell, **2009**, 35:467-478. *doi.org/10.1016/j.molcel.2009.06.027.*

Chen Q, Xia HW, Ge XJ, et al. Serum miR-19a predicts resistance to FOLFOX chemotherapy in advanced colorectal cancer cases. Asian Pac J Cancer Prev, **2013**, 14:7421–7426.

Chen WY, Zhao XJ, Yu ZF, et al. The potential of plasma miRNAs for diagnosisand risk estimation of colorectal cancer. Int J Clin Exp Pathol, **2015**, 8:7092–7101.

Cheng H, Zhang L, Cogdell DE, et al. Circulating plasma MiR-141 is a novel biomarker for metastatic colon cancer and predicts poor prognosis. PLoS One, **2011**, 6:e17745. *doi.org/10.1371/journal.pone.0017745.*

Cherenok S, Vovk A, Muravyova I, et al. Calix [4] arene α-aminophosphonic acids: asymmetric synthesis and enantioselective inhibition of an alkaline phosphatase. Org Lett, **2006**, 8:549–552. *doi.org/10.1021/ol052469a.*

Cherenok SO, Yushchenko OA, Tanchuk VY, et al. Calix [4] arene-α-hydroxyphosphonic acids. Synthesis, stereochemistry, and inhibition of glutathione S-transferase. Arkivoc, **2012**, 4:278–298.

Chiarantini L, Cerasi A, Millo E et al. Enhanced antisense effect of modified PNAs delivered through functional PMMA microspheres. Int J Pharm, **2006**, 324:83-91. *doi.org/10.1016/j.ijpharm.2006.07.007.*

Chim SSC, Shing TKF, Hung ECW et al. Detection and characterization of placental microRNAs in maternal plasma. Clin Chem, **2008**, 54:482–490. *doi.org/10.1373/clinchem.2007.097972.*

Chiu RW, Poon LL, Lau TK, et al. Effects of blood-processing protocols on fetal and total DNA quantification in maternal plasma. Clin Chem, **2001**, 47:1607e1613.

Cho WC. MicroRNAs: Potential biomarkers for cancer diagnosis, prognosis and targets for therapy. Int J Biochem Cell Biolo, **2010**, 42:1273-1281. *doi.org/10.1016/j.biocel.2009.12.014.*

Cho WC. OncomiRs: The discovery and progress of microRNAs in cancer. Mol Cancer, **2007**, 6:60. *doi.org/10.1186/1476-4598-6-60.*

Christopher AF, Kaur RP, Kaur G. MicroRNA therapeutics: Discovering novel targets and developing specific therapy. Perspect Clin Res, **2016**, 7:68-74. *doi: 10.4103/2229-3485.179431.*

Chulmska A, Boudova L, Zamecnik M. Sessile serrated adenomas of the large bowel: clinicopathologic and immunohistochemical study including comparison with common hyperplastic polyps and adenomas. Cesk Patol, **2006**, 42:133–138.

Collins FS, Mentherall JE, Yamakawa M, et al. A point mutation in the A gamma-globin gene promoter in Greek hereditary persistence of fetal haemoglobin. Nature, **1985**, 313:325–326.

Consoli GM, Granata G, Galante E, et al. Synthesis of water-soluble nucleotide-calixarene conjugates and preliminary investigation of their in vitro DNA replication inhibitory activity. Tetrahedron, **2007**, 63:10758–10763. *doi.org/10.1002/chin.200749051.*

Cook L, Macdonald D. Management of paraproteinaemia. Postgrad Med J, **2007**, 83: 217–223. *doi.org/10.1136/pgmj.2006.054627.*

Corsten MF, Dennert R, Jochems S et al. Circulating MicroRNA-208b and MicroRNA-499 reflect myocardial damage in cardiovascular disease. Circ Cardiovasc Genet, **2010**, 3:499–506. *doi.org/10.1161/CIRCGENETICS.110.957415.*

Cowie P, Hay EA, MacKenzie A. The noncoding human genome and the future of personalized medicine. Expert Rev Mol Med, **2015**; 17:e4. *doi.org/10.1017/erm.2014.23.*

Creary LE, Ulug P, Menzel S et al. Genetic variation on chromosome 6 influences F cell levels in healthy individuals of African descent and HbF levels in sickle cell patients. PLoS One, **2009**, 4:e4218. *doi.org/10.1371/journal.pone.0004218.*

Crew E, Rahman S, Rahaman S et al. MicroRNA conjugated gold nanoparticles and cell transfection. Anal Chem, **2012**, 84:26–29. *doi.org/10.1021/ac202749p.*

D'Agata R, Breveglieri G, Zanoli LM et al. Direct detection of point mutations in nonamplified human genomic DNA. Anal Chem, **2011**, 83:8711-8717. *doi: 10.1021/ac2021932.*

Damsgaard R, Munch T, Morkeberg J, et al. Effects of blood withdrawal and reinfusion on biomarkers of erythropoiesis in humans: implications for anti-doping strategies. Haematologica, **2006**, 91:1006–1008.

Danjou F, Anni F, Galanello R. Beta-thalassemia: from genotype to phenotype. Haematologica, **2011**, 96:1573–1575. *doi.org/10.3324/haematol.2011.055962.*

David. calixarenes, royal soc chem Cambridge, **1989**, 1-2

Dean DA. Peptide nucleic acids: versatile tools for gene therapy strategies. Adv Drug Deliv Rev, **2000**, 44: 81–95. *doi.org/10.1016/S0169-409X(00)00087-9.*

Derossi D, Calvet S, Trembleau A, et al. Cell internalization of the third helix of the Antennapedia homeodomain is receptor independent. J Biol Chem, **1996**, 271:18188–18193. *doi.org/10.1074/jbc.271.30.18188.*

Di Lena M, Travaglio E, Altomare DF. New strategies for colorectal cancer screening. World J Gastroenterol, **2013**, 19:1855–1860. *doi: 10.3748/wjg.v19.i12.1855.*

Dings RP, Chen X, Hellebrekers DM, et al. Design of nonpeptidic topomimetics of antiangiogenic proteins with antitumor activities. J Natl Cancer Inst, **2006**, 98:932–936. *doi.org/10.1093/jnci/djj247.*

Dings RP, Levine JI, Brown SG, et al. Polycationic calixarene PTX013, a potent cytotoxic agent against tumors and drug resistant cancer. Invest New Drugs, **2013**, 31:1142–1150. *doi.org/10.1007/s10637-013-9932-0.*

Dong H, Lei J, Ding L, et al. MicroRNA: function, detection, and bioanalysis. Chem Rev, **2013**, 113:6207-6233. *doi.org/10.1021/cr300362f.*

Drin G, Cottin S, Blanc E, et al. Studies on the internalization mechanism of cationic cell-penetrating peptides. J Biol Chem, **2003**, 278: 31192–31201. *doi.org/10.1074/jbc.M303938200.*

Duffy MJ, Shering S, Sherry F, et al. CA 15-3: a prognostic marker in breast cancer. Int J Biol Markers, **2000**, 15:330-333.

Duursma AM, Kedde M, Schrier M et al. miR-148 targets human DNMT3b protein coding region. RNA, **2008**, 14:872-877. *doi.org/ 10.1261/rna.972008.*

Duval A, Hamelin R. Mutations at coding repeat sequences in mismatch repair-deficient human cancers: toward a new concept of target genes for instability. Cancer Res, **2002**, 62:2447–2454.

Ebert BL, Bunn HF. Regulation of the erythropoietin gene. Blood, **1999**, 94:1864–1877.

Efstratiadis A, Posakony JW, Maniatis T, et al. The structure and evolution of the human β-globin gene family. Cell, **1980**, 21:653-668. *doi.org/10.1016/0092-8674(80)90429-8.*

Ekblom B, Goldbarg AN, Gullbring B. Response to exerciseafter blood loss and reinfusion. J Appl Physiol, **1972**, 33:175–180.

Emlen W, Mannik M: Effect of DNA size and strandedness on the in vivo clearance and organ localization of DNA. Clin Exp Immunol, **1984**, 56:185-192.

Ertle JM, Heider D, Wichert M et al. A combination of α-fetoprotein and des-γ-carboxy prothrombin is superior in detection of hepatocellular carcinoma. Digestion, **2013**, 87:121-131. *doi.org/ 10.1159/000346080.*

Esteller M. Non-coding RNAs in human disease. Nat Rev Genet, **2011**, 12:861-874. *doi.org/ 10.1038/nrg3074.*

Fang H, Zhang K, Shen G et al. Cationic Shell-crosslinked Knedel-like (cSCK) Nanoparticles for Highly Efficient PNA Delivery. Mol Pharm, **2009**, 6: 615–626. *doi.org/10.1021/mp800199w.*

Fang Z, Tang J, Bai Y, et al. Plasma levels of microRNA-24, microRNA-320a, and microRNA-423-5p are potential biomarkers for colorectal carcinoma. J Exp Clin Cancer Res, **2015**, 34:86. *doi.org/10.1186/s13046-015-0198-6.*

Faruqi AF, Egholm M, Glazer PM. Peptide nucleic acid-targeted mutagenesis of a chromosomal gene in mouse cells. Proc Natl Acad Sci U S A, **1998**, 95:1398-1403. *doi.org/10.1073/pnas.95.4.1398.*

Fearon ER, Vogelstein B. A genetic model for colorectal tumorigenesis. Cell, **1990**, 61:759–767. *doi.org/10.1016/0092-8674(90)90186-I.*

Felli N, Pedini F, Romania P, et al. MicroRNA 223-dependent expression of LMO2 regulates normal erythropoiesis. Nucleic Acids Res, **2013**, 41: 4129–4143. *doi: 10.1093/nar/gkt093.*

Feng WC, Southwood CM, Bieker JJ. Analyses of beta-thalassemia mutant DNA interactions with erythroid Krüppel-like factor (EKLF), an erythroid cell-specific transcription factor. J Biol Chem, **1994**, 269:1493-1500.

Ferlay J, Parkin DM, Steliarova-Foucher E. Estimates of cancer incidence and mortality in Europe in 2008. Eur J Cancer, **2010**, 46:765–781. *doi.org/10.1016/j.ejca.2009.12.014.*

Ferracin M, Lupini L, Mangolini A, et al. Circulating Non-coding RNA as Biomarkers in Colorectal Cancer. Adv Exp Med Biol, **2016**, 937:171-181. *doi.org/10.1007/978-3-319-42059-2_9.*

Fibach E, Bianchi N, Borgatti M, et al. Mithramycin induces fetal hemoglobin production in normal and thalassemic human erythroid precursor cells. Blood, **2003**, 102:1276-1281. *doi.org/10.1182/blood-2002-10-3096.*

Filella X, Foj L. Prostate Cancer Detection and Prognosis: From Prostate Specific Antigen (PSA) to Exosomal Biomarkers. Int J Mol Sci, **2016**, 17. *doi.org/10.3390/ijms17111784.*

Filipe A, Li Q, Deveaux S, et al. Regulation of embryonic/fetal globin genes by nuclear hormone receptors: a novel perspective on hemoglobin switching. EMBO J, **1999**, 18:687–697. *doi.org/10.1093/emboj/18.3.687.*

Finotti A, Gasparello J, Breveglieri G, et al. Development and characterization of K562 cell clones expressing BCL11A-XL: Decreased hemoglobin production with fetal hemoglobin inducers and its rescue with mithramycin. Exp Hematol, **2015**, 43:1062-1071. *doi.org /10.1016/j.exphem.2015.08.011.*

Fisher ER, Sass R, Palekar A, et al. Dukes' classification revisited: findings from the National Surgical Adjuvant Breast and Bowel Projects (Protocol R-01). Cancer, **1989**, 64: 2354–2360.

Flegel WA, Wagner FF, Muller TH, et al. Rh phenotype prediction by DNA typing and its application to practice. Transfus Med, **1998**, 8:281–302. *doi.org/10.1046/j.1365-3148.1998.00173.x.*

Foley HA, Ofori-Acquah SF, Yoshimura A at al. Stat3 beta inhibits gamma-globin gene expression in erythroid cells. J Biol Chem, **2002**, 277:16211-16219.

Fragu P. Calcitonin's fantastic voyage: from hormone to marker of a genetic disorder. Gesnerus, **2007**, 64:69-92.

Gabbianelli M, Testa U, Morsilli O et al. Mechanism of human Hb switching: a possible role of the kit receptor/miR 221-222 complex. Haematologica, **2009**, 94:479-486. *doi: 10.3324/haematol.2008.002345.*

Gaglione M, Milano G, Chambery A et al. PNA-based artificial nucleases as antisense and anti-miRNAoligonucleotide agents. Mol BioSyst, **2011**, 7:2490–2499. *doi: 10.1039/c1mb05131h.*

Galanello R, OrigaR. Beta-Thalassemia. Orphanet Journal of Rare Diseases, **2010**, 5:11. *doi: 10.1186/1750-1172-5-11.*

Galindo-Murillo R, Olmedo-Romero A, Cruz-Flores E et al. Calix[n]arene-based drug carriers: a DFT study of their electronic interactions with a chemotherapeutic agent used against leukemia. Comp Theor Chem, **2014**, 1035:84–91. *doi.org/10.1016/jcomptc.2014.03.001.*

Gañán-Gómez I, Wei Y, Yang H, et al. Overexpression of miR-125a in myelodysplastic syndrome CD34+ cells modulates NF-κB activation and enhances erythroid differentiation arrest. PLoS One, **2014**, 9:e93404. *doi: 10.1371/journal.pone.0093404.*

Gao Y, Liu Y, Du L et al. Down-regulation of miR-24-3p in colorectal cancer is associated with malignant behavior. Med Oncol, **2014**, 32:362. *doi.org/10.1007/s12032-014-0362-4.*

Garcia-Carbonero R, Supko JG. Current perspectives on the clinical experience, pharmacology, and continued development of the camptothecins. Clin Cancer Res, **2002**, 8:641–661.

Garofalo M, Di Leva G, Romano G et al. miR-221&222 regulate TRAIL resistance and enhance tumorigenicity through PTEN and TIMP3 downregulation. Cancer Cell, **2009**, 16:498-509. *doi: 10.1016/j.ccr.2009.10.014.*

Geraci C, Consoli GML, Granata G, et al. First self-adjuvant multicomponent potential vaccine candidates by tethering of four or eight MUC1 antigenic immunodominant PDTRP units on a calixarene platform: synthesis and biological evaluation. Bioconjug Chem, **2013**, 24:1710–1720. *doi.org/10.1021/bc400242y.*

Ghorai A, Ghosh U. miRNA gene counts in chromosomes vary widely in a species and biogenesis of miRNA largely depends on transcription or post-transcriptional processing of coding genes. Front Genet, **2014,** 5: 100. *doi: 10.3389/fgene.2014.00100.*

Giacchetti S, Perpoint B, Zidani R, et al. Phase III multicenter randomized trial of oxaliplatin added to chronomodulated fluorouracil-leucovorin as first-line treatment of metastatic colorectal cancer. J Clin Oncol, **2000**, 18:136–147. *doi.org/10.1200/JCO.2000.18.1.136.*

Gilman JG, Huisman THJ. DNA sequence variation associated with elevated fetal Gγ globin production. Blood, **1985**, 66:783–787.

Giraldez MD, Lozano JJ, Ramirez G, et al. Circulating microRNAs as biomarkers of colorectal cancer: results from a genome-wide profiling and validation study. Clin Gastroenterol Hepatol, **2013**, 11:681–688. *doi.org/10.1016/j.cgh.2012.12.009.*

Glusker P, Recht L, Lane B. Reversible posterior leukoencephalopathy syndrome and bevacizumab. N Engl J Med, **2006**, 354:980-982.

Goel A. MicroRNAs as therapeutic targets in colitis and colitis-associated cancer: tiny players with a giant impact. Gastroenterology, **2015**, 149:859–861. *doi.org/10.1053/j.gastro.2015.08.041.*

Gold B, Cankovic M, Furtado LV, et al. Do circulating tumor cells, exosomes, and circulating tumor nucleic acids have clinical utility? A report of the association for molecular pathology. J Mol Diagn, **2015**, 17:209-224. *doi.org/ 10.1016/j.jmoldx.2015.02.001.*

Gonzalez-Redondo JM, Stoming TA, Kutlar A, et al. A C-T substitution at nt -101 in a conserved DNA sequence of the promotor region of the β-globin gene is associated with "silent" β-thalassemia. Blood, **1989**, 73:1705-1711.

Graybill RM, Bailey RC. Emerging Biosensing Approaches for microRNA Analysis. Anal Chem, **2016**, 88:431-450. *doi.org/10.1021/acs.analchem.5b04679.*

Greene FL, Stewart AK, Norton HJ. New tumor-node-metastasis staging strategy for node-positive (stage III) rectal cancer: an analysis. J Clin Oncol, **2004**, 22:1778–1784. *doi.org/10.1200/JCO.2004.07.015.*

Guibert J, Benachi A, Grebille AG et al. Kinetics of SRY gene appearance in maternal serum: detection by real time PCR in early pregnancy after assisted reproductive technique. Hum Reprod, **2003**, 18:1733–1736. *doi.org/10.1093/humrep/deg320.*

Gutsche CD, Bauer LJ. The conformational properties of calix[4]arenes, calix[6]arenes, calix[8]arenes, and oxacalixarenes. J Am Chem Soc, **1985**, 107:6052–6059. *doi.org/10.1021/ja00307a038.*

Haase VH. Regulation of erythropoiesis by hypoxia-inducible factors. Blood Rev, **2013**, 27: 41–53. *doi: 10.1016/j.blre.2012.12.003.*

Hall JG, Martin PL, Wood S et al. Unrelated umbilical cord blood transplantation for an infant with beta-thalassemia major. J Pediatr Hematol Oncol, **2004**, 26:382-385.

Hamidi Asl, Palchetti I, Hasheminejad E, et al. A rewiev on electrochemica biosensors for determination of microRNA. Talanta, **2013**, 115:74-83.

Hamilton SE, Simmons CG, Kathiriya IS, et al. Cellular delivery of peptide nucleic acids and inhibition of human telomerase. Chem Biol, **1999**, 6:343-351. *doi.org/10.1016/S1074-5521(99)80046-5.*

Han J, Lee Y, Yeom KH et al. Molecular basis for the recognition of primary microRNAs by the Drosha-DGCR8 complex. Cell, **2006**, 125:887-901. *doi.org/10.1016/j.cell.2006.03.043.*

Hanvey JC, Peffer JE, Bisi SA et al. Antisense and antigene properties of peptide nucleic acids. Science, **1992**, 258:1481-1485.

Harju-Baker S, Costa FC, Fedosyuk H, et al. Silencing of Agamma-globin gene expression during adult definitive erythropoiesis mediated by GATA-1-FOG-1-Mi2 complex binding at the -566 GATA site. Mol Cell Biol, **2008**, 28:3101-3113. *doi.org/10.1128/MCB.01858-07.*

Hassan C, Zullo A, Risio M, et al. Histologic risk factors and clinical outcome in colorectal malignant polyp: a pooled-data analysis. Dis Colon Rectum, **2005**, 48:1588–1596. *doi.org/10.1007/s10350-005-0063-3.*

Hausser J, Syed AP, Bilen B. Analysis of CDS-located miRNA target sites suggests that they can effectively inhibit translation. Genome Res, **2013**, 23:604–615. *doi.org/10.1101/gr.139758.112*

Hindson CM, Chevillet JR, Briggs HA et al. Absolute quantification by droplet digital PCR versus analog real-time PCR. Nat Methods, **2013**, 10:1003-1015. *doi.org/10.1038/nmeth.2633.*

Höck J, Gunter Meister G. The Argonaute protein family. Genome Biol, **2008**, 9: 210. *doi.org/ 10.1186/gb-2008-9-2-210.*

Holdenrieder S, Nagel D, Schalhorn A, et al. Clinical relevance of circulating nucleosomes in cancer. Ann N Y Acad Sci, **2008**, 1137:180-189. *doi.org/10.1196/annals.1448.012.*

Hsieh JS, Lin SR, Chang MY, et al. APC, K-Ras and p53 gene mutations in colorectal cancer patients: correlation to clinicopathologicfeatures and postoperative surveillance. Am Surg, **2005**, 71:336-343.

Huang X, Ding L, Bennewith K et al. Hypoxia-inducible mir-210 regulates normoxic gene expression involved in tumor initiation. Mol Cell, **2009**, 35:856–867. *doi.org/10.1016/j.molcel.2009.09.006.*

Huang Z, Huang D, Ni S, et al. Plasma microRNAs are promising novel biomarkers for early detection of colorectal cancer. Int J Cancer, **2010**, 127:118–126. *doi.org/10.1002/ijc.25007.*

Liu H, Ippolito GC, Wall JK et al. Functional studies of BCL11A: characterization of the conserved BCL11A-XL splice variant and its interaction with BCL6 in nuclear paraspeckles of germinal center B cells. Molecular Cancer, **2006**, 5:18 *doi.org/10.1186/1476-4598-5-18.*

Ho PJ, Thein SL. Gene regulation and deregulation: a β globin perspective. Blood, **2000**, 14:78-93. *doi.org/ 10.1054/blre.2000.0128.*

Hsieh JT, LuoW, SongW, et al. Tumour suppressive role of an androgen-regulated epithelial cell adhesion molecule (C-CAM) in prostate carcinomas cell revealed by sense and antisense approaches. Cancer Res, **1995**, 55:190–197.

Hulíková K, Grobárová V, Křivohlavá R, et al. Antitumor activity of N-acetyl-D-glucosamine-substituted glycoconjugates and combined therapy with keyhole limpet hemocyanin in B16F10 mouse melanoma model. Folia Microbiol, **2010**, 55:528–532. *doi: 10.1007/s12223-010-0087-5.*

Humphries RK, Ley TJ, Anagnou NP, et al. Beta 0-39 thalassemia gene: A premature termination codon causes β-mRNA deficiency without affecting cytoplasmic β-mRNA stability. Blood, **1984**, 64: 23–32.

Hunt EA, Broyles D, Head T et al. MicroRNA Detection: Current Tecnology and Research Strategies. Annu Rev Anal Chem, **2015**, 8:1-21. *doi.org/10.1146/annurev-anchem-071114-040343.*

Hurwitz HI, Fehrenbacher L, Hainsworth JD, et al. Bevacizumab in combination with fluorouracil and leucovorin: an active regimen for first-line metastatic colorectal cancer. J Clin Oncol, **2005**, 23:3502–3508. *doi.org/10.1200/JCO.2005.10.017.*

Hwang do W, Son S, Jang J, et al. A brain-targeted rabies virus glycoprotein-disulfide linked PEI nanocarrier for delivery of neurogenic microRNA. Biomaterials, **2011**, 32:4968–4975. *doi.org/10.1016/j.biomaterials.2011.03.047.*

Hyett JA, Gardener G, Stojilkovic-Mikic T, et al. Reduction in diagnostic and therapeutic interventions by non-invasive determination of fetal sex in early pregnancy. Prenat Diagn, **2005**, 25:1111–1116. *doi.org/10.1002/pd.1284.*

Imperiale TF. Noninvasive screening tests for colorectal cancer. Dig Dis, **2012**, 30:16–26. *doi.org/10.1159/000341884*

Imren S, Fabry ME, Westerman KA, et al. High-level beta-globin expression and preferred intragenic integration after lentiviral transduction of human cord blood stem cells. J Clin Invest, **2004**, 114:953-962. *doi.org/ 10.1172/JCI21838.*

Isken O, Maquat LE. Quality control of eukaryotic mRNA: Safeguarding cells from abnormal mRNA function. Genes Dev, **2007**, 21: 1833–1856. *doi.org/10.1101/gad.1566807.*

Itonaga M, Matsuzaki I, Warigaya K et al. Novel Methodology for Rapid Detection of KRAS Mutation Using PNA-LNA Mediated Loop-Mediated Isothermal Amplification. PLoS One, **2016**, 11:e0151654. *doi.org/10.1371/journal.pone.0151654.*

Jahr S, Hentze H, Englisch S, et al. DNA fragments in the blood plasma of cancer patients: quantitations and evidence for their origin from apoptotic and necrotic cells. Cancer Res, **2001**, 61:1659-1665.

Jamal-Hanjani M, Quezada SA, Larkin J, et al. Translational implications of tumor heterogeneity. Clin Cancer Res, **2015**, 21:1258-1266. *doi.org/ 10.1158/1078-0432.CCR-14-1429.*

Jelkmann W, Lundby C. Blood doping and its detection. Blood, **2011**, 118: 2395–2404. *doi.org/10.1182/blood-2011-02-303271.*

Jonker DJ, O'Callaghan CJ, Karapetis CS, et al. Cetuximab for the treatment of colorectal cancer. N Engl J Med, **2007**, 357:2040–2048. *doi.org/10.1056/NEJMoa071834.*

Jørgensen S, Baker A, Møller S et al. Robust one-day in situ hybridization protocol for detection of microRNAs in paraffin samples using LNA probes. Methods, **2010**, 52:375-381. *doi.org/10.1016/j.ymeth.2010.07.002.*

Ju J, Wang Y, Liu R, et al. Human fetal globin gene expression is regulated by LYAR. Nucleic Acids Res, **2014**, 42: 9740–9752. *doi.org/10.1093/nar/gku718.*

Juvonen E, Ikkala E, Fyhrquist F, et al. Autosomal dominant erythrocytosis caused by increased sensitivity to erythropoietin. Blood, **1991**, 78: 3066–3069.

Kadiyska T, Nossikoff A. Stool DNA methylation assays in colorectal cancer screening, World J Gastroenterol, **2015**, 21: 10057-100061 *doi.org/10.3748/wjg.v21.i35.10057.*

Kalikaki A, Politaki H, Souglakos J et al. KRAS Genotypic Changes of Circulating Tumor Cells during Treatment of Patients with Metastatic Colorectal Cancer. PLoS One, **2014**, 9: e104902. *doi.org/10.1371/journal.pone.0104902.*

Kamada R, Yoshino W, Nomura T, et al. Enhancement of transcriptional activity of mutant p53 tumor suppressor protein through stabilization of tetramer formation by calix [6] arene derivatives. Bioorg Med Chem Lett, **2010**, 20:4412–4415. *doi.org/10.1016/j.bmcl.2010.06.053.*

Kanaan Z, Roberts H, Eichenberger MR, et al. A plasma microRNA panel for detection of colorectal adenomas: a step toward more precise screening for colorectal cancer. Ann Surg, **2013**, 258:400–408. *doi.org/10.1097/SLA.0b013e3182a15bcc.*

Kang H, O'Connell JB, Maggard MA, et al. A 10-year outcomes evaluation of mucinous and signet-ring cell carcinoma of the colon and rectum. Dis Colon Rectum, **2005**, 48:1161–1168. *doi.org/10.1007/s10350-004-0932-1.*

Katapodi MC, DeFlon SL, Milliron KJ, et al. Knowledge of risk factors and modes of gene transmission among women at risk for hereditary breast and ovarian cancer syndrome. J Clin Oncol, **2011**, 29:e12017. *doi.org/10.1200/jco.2011.29.15_suppl.e12017.*

Khalil S, Fabbri E, Santangelo A et al., miRNA array screening reveals cooperative MGMT-regulation between miR-181d-5p and miR-409-3p in glioblastoma. Oncotarget, **2016**, 7: 28195–28206. *doi: 10.18632/oncotarget.8618.*

Kim ES, Lim DJ, Baek KH, et al. Thyroglobulin antibody is associated with increased cancer risk in thyroid nodules. Thyroid, **2010**, 20:885-891. *doi.org/10.1089/thy.2009.0384.*

Kinzler KW, Vogelstein B. Lessons from hereditary colorectal cancer. Cell, **1996**, 87:159–170. *doi.org/10.1016/S0092-8674(00)81333-1.*

Kolata GB, Wade N. Human gene treatment stirs new debate. Science, **1980**, 210:407. *doi.org/10.1126/science.6933693.*

Kondo Y, Hayashi K, Kawakami K, et al. KRAS mutation analysis of single circulating tumor cells from patients with metastatic colorectal cancer. BMC Cancer, **2017**, 17:311. *doi.org/10.1186/s12885-017-3305-6.*

Koppelhus U, Nielsen PE. Cellular delivery of peptide nucleic acid (PNA). Advanced Drug Delivery Reviews, **2003**, 55:267–280. *doi.org/10.1016/S0169-409X(02)00182-5.*

Koppers-Lalic D, Hackenberg M, Bijnsdorp IV et al. Nontemplated nucleotide additions distinguish the small RNA composition in cells from exosomes. Cell Rep, **2014**, 8:1649–1658. *doi.org/ 10.1016/j.celrep.2014.08.027.*

Kopreski MS, Benko FA, Borys DJ, et al. Somatic mutation screening: identification of individuals harboring K-ras mutations with the use of plasma DNA. J Natl Cancer Inst, **2000**, 92:918e923. *doi.org/10.1093/jnci/92.11.918.*

Korpal M, Kang Y. The emerging role of miR-200 family of microRNAs in epithelial-mesenchymal transition and cancer metastasis. RNA Biol, **2008**, 5: 115–119. *doi.org/10.4161/rna.5.3.6558.*

Kota J, Chivukula RR, O'Donnell KA, et al. Therapeutic microRNA delivery suppresses tumorigenesis in a murine liver cancer model. Cell, **2009**, 137-1005–1017. *doi.org/ 10.1016/j.cell.2009.04.021.*

Kouhkan F, Soleimani M, Daliri M et al. miR-451 Up-regulation, Induce Erythroid Differentiation of CD133+cells Independent of Cytokine Cocktails. Blood, **2015**, 125: 1302–1313. *doi: 10.1182/blood-2014-06-581926.*

Koury MJ, Sawyer ST, Brandt SJ. New insights into erythropoiesis. Curr Opin Hematol, **2002**, 9:93–100. *doi.org/10.1097/00062752-200203000-00002.*

Kung JYY, Colognori D, Lee JT. Long noncoding RNAs: past, present, and future. Genetics, **2013**, 193:651-669. *doi.org/10.1534/genetics.112.146704.*

Kwon MJ, Lee J, Wark AW, et al. Nanoparticle-enhanced surface plasmon resonance detection of proteins at attomolar concentrations: comparing different nanoparticle shapes and sizes. Anal Chem, **2012**, 84:1702-1707. *doi.org/10.1021/ac202957h.*

Lampronti I, Martello D, Bianchi N, et al. In vitro antiproliferative effects on human tumor cell lines of extracts from the Bangladeshi medicinal plant Aegle marmelos Correa. Phytomedicine, **2003**, 10:300-308. *doi.org/10.1078/094471103322004794.*

Lawrie CH, Gal S, Dunlop HM, et al. Detection of elevated levels of tumour-associated microRNAs in serum of patients with diffuse large B-cell lymphoma. Br J Haematol, **2008**, 141:672–675. *doi.org/10.1111/j.1365-2141.2008.07077.x.*

Lecomte T, Berger A, Zinzindohoue F, et al. Detection of free-circulating tumor-associated DNA in plasma of colorectal cancer patients and its association with prognosis. Int J Cancer **2002**, 100:542-548. *doi.org/10.1002/ijc.10526.*

Lecomte T, Ceze N, Dorval E, Laurent-Puig P. Circulating free tumor DNA and colorectal cancer. Gastroenterol Clin Biol, **2010**, 34:662-668. *doi.org/10.1016/j.gcb.2009.04.015.*

Lee ES, Oh KT, Kim D et al. Tumor pH-responsive flower-like micelles of poly(L-lactic acid)-b-poly (ethylene glycol)- b-poly (L-histidine). J Control Release, **2007**, 123:19–26. *doi.org/10.1016/j.jconrel.2007.08.006.*

Lee JM, Jung Y. Two-temperature hybridization for microarray detection of label-free microRNAs with attomole detection and superior specificity. Angew Chem Int Ed Engl, **2011**, 50:12487-12490. *doi.org/10.1002/anie.201105605.*

Lee RC, Feinbaum RL, Ambros V. The C.Elegans heterochronic gene lin-4 encodes small RNAs with antisense complementary to lin-14. Cell, **1993**, 75:843-54. *doi.org/10.1016/0092-8674(93)90529-Y.*

Lee TH, Montalvo L, Chrebtow V, et al. Quantitation of genomic DNA in plasma and serum samples: higher concentrations of genomic DNA found in serum than in plasma. Transfusion, **2001**, 41:276–282. *doi.org/10.1046/j.1537-2995.2001.41020276.x.*

Leecharoenkiat K, Lithanatudom P, Sornjai W et al. Iron dysregulation in beta-thalassemia. Asian Pac J Trop Med, **2016**, 9:1035-1043. *doi.org/10.1016/j.apjtm.2016.07.035.*

Leigh-Smith S. Blood boosting. Br J Sports Med, **2004**, 38:99–101. *doi.org/10.1136/bjsm.2003.007195.*

Leman ES, Gonzalgo ML. Prognostic features and markers for testicular cancer management. Indian J Urol, **2010**, 26:76-81. *doi.org/10.4103/0970-1591.60450.*

Leon SA, Shapiro B, Sklaroff DM, et al. Free DNA in the serum of cancer patients and the effect of therapy. Cancer Res, **1977**, 37:646–650

Leuenberger N, Barras L, Nicoli R et al. Hepcidin as a new biomarker for detecting autologous blood transfusion. Am J Hematol, **2016**, 91:467–472. *doi.org/10.1002/ajh.24313.*

Li J, Liu Y, Wang C, et al. Serum miRNA expression profile as a prognostic biomarker of stage II/III colorectal adenocarcinoma. Sci Rep, **2015**, 5:12921. *doi.org/10.1038/srep12921.*

Li Ma L, Young J, Prabhala H, et al. miR-9, a MYC/MYCN-activated microRNA, regulates E-cadherin and cancer metastasis. Nat Cell Biol, **2010**, 12: 247–256. *doi.org/10.1038/ncb2024.*

Li Y, Bai H, Zhang Z, et al. The up-regulation of miR-199b-5p in erythroid differentiation is associated with GATA-1 and NF-E2. Genes Dev, **2011**, 25: 119–124. *doi: 10.1101/gad.1998711.*

Li Y, Liu S, Sun H et al. MiR-218 Inhibits Erythroid Differentiation and Alters Iron Metabolism by Targeting ALAS2 in K562 Cells. Haematologica, **2010**, 95:1253-1260. *doi: 10.3324/haematol.2009.018259.*

Link A, Balaguer F, Shen Y, et al. Fecal MicroRNAs as novel biomarkers for colon cancer screening. Cancer Epidemiol Biomarkers Prev, **2010**, 19:1766–1774. *doi.org/10.1158/1055-9965.EPI-10-0027.*

Liu GH, Zhou ZG, Chen R, et al. Serum miR-21 and miR-92a as biomarkers in the diagnosis and prognosis of colorectal cancer. Tumour Biol, **2013**, 34:2175–2181. *doi.org/10.1007/s13277-013-0753-8.*

Liu M, Zhi Q, Wang W, et al. Up-regulation of miR-592 correlates with tumor progression and poor prognosis in patients with colorectal cancer. Biomed Pharmacother, **2015**, 69:214–220. *doi.org/10.1016/j.biopha.2014.12.001.*

Liu W, Zhou X, Xing D. Rapid and reliable microRNA detection by stacking hybridization on electrochemiluminescent chip system. Biosens Bioelectron, **2014**, 58:388-394. *doi.org/ 10.1016/j.bios.2014.02.082.*

Ljungstrom T, Knudsen H, Nielsen PE. Cellular uptake of adamantyl conjugated peptide nucleic acids. Bioconjug Chem, **1999**, 10:965–972. *doi.org/10.1021/bc990053+*.

Lo YM, Zhang J, Leung TN, et al. Rapid clearance of fetal DNA from maternal plasma. Am J Hum Genet, **1999**, 64:218-224. *doi.org/10.1086/302205.*

Loverlock JE. The haemolysis of human red blood-cells by freezing and thawing. Biochim Biophys Acta, **1953**, 10:414-426.

Lu C, Huang X, Zhang X, et al. miR-221 and miR-155 regulate human dendritic cell development, apoptosis, and IL-12 production through targeting of p27kip1, KPC1, and SOCS-1. Blood, **2011**, 117:4293-4303. *doi: 10.1182/blood-2010-12-322503.*

Lu Y, Liang H, Yu T et al. Isolation and characterization of living circulating tumor cells in patients by immunomagnetic negative enrichment coupled with flow cytometry. Cancer, **2015**, 121:3036-3045. *doi.org/10.1002/cncr.29444.*

Lu Y, Xiao J, Lin H. A single anti-microRNAantisense oligodeoxyribonucleotide (AMO) targeting multiple microRNAs offers an improved approach formicroRNA interference. Nucleic Acids Res, **2009**, 37:e24. *doi.org/10.1093/nar/gkn1053.*

Lucarelli G, Andreani M, Angelucci E. The cure of thalassemia by bone marrow transplantation. Blood, **2002**, 16:81-85. *doi.org/10.1054/blre.2002.0192.*

Lucarelli G, Isgrò A, Sodani P, et al. Hematopoietic Stem Cell Transplantation in Thalassemia and Sickle Cell Anemia. Cold Spring Harb Perspect Med, **2012**, 2: a011825. *doi.org/10.1101/cshperspect.a011825.*

Lulli V, Romania P, Morsilli O, et al. MicroRNA-486-3p Regulates γ-Globin Expression in Human Erythroid Cells by directly modulating BCL11A. PLoS One, **2013**, 8: e60436. *doi.org/10.1371/journal.pone.0060436.*

Lun FM, Chiu RW, Allen Chan KC et al. Microfluidics digital PCR reveals a higher than expected fraction of fetal DNA in maternal plasma. Clin Chem, **2008**, 54:1664–1672. *doi.org/10.1373/clinchem.2008.111385.*

Luo X, Stock C, Burwinkel B, et al. Identification and evaluation of plasma MicroRNAs for early detection of colorectal cancer. PLoS One, **2013**, 8:e62880. *doi.org/10.1371/journal.pone.0062880.*

Lv ZC, Fan YS, Chen HB, et al. Investigation of microRNA-155 as a serum diagnostic and prognostic biomarker for colorectal cancer. Tumour Biol, **2015**, 36:1619–1625. *doi.org/10.1007/s13277-014-2760-9.*

Lynch HT. Hereditary colorectal cancer. N Engl J Med, **2003**, 348:919–932. *doi.org/10.1056/NEJMra012242*.

Ma Y, She XG, Ming YZ et al. miR-24 promotes the proliferation and invasion of HCC cells by targeting SOX7. Tumor Biol, **2014**, 35:10731–10736. *doi.org/10.1007/s13277-014-2018-6.*

Macrae IJ, Li F, Zhou K et al. Structure of Dicer and mechanistic implications for RNAi. Cold Spring Harb Symp Quant Biol, **2006**, 71:73-80. *doi.org/10.1101/sqb.2006.71.042.*

Maheswaran S, Haber DA. Circulating tumor cells: a window into cancer biology and metastasis. Curr Opin Genet Dev, **2010**, 20:96–99. *doi.org/10.1016/j.gde.2009.12.002.*

Mandel JS, Bond JH, Church TR, et al. Reducing mortality from colorectal cancer by screening for fecal occult blood. N Engl J Med, **1993**, 328:1365–1371. *doi.org/10.1056/NEJM199305133281901.*

Mandel P, Metais P. Les acides nucléiques du plasma sanguin chez l'homme. C R Seances Soc Biol Fil, **1948**, 142:241–243.

Marín RM, Šulc M, Vaníček J. Searching the coding region for microRNA targets. RNA, **2013**, 9: 467–474. *doi: 10.1261/rna.035634.112.*

Marra G, Boland CR. Hereditary nonpolyposis colorectal cancer: the syndrome, the genes, and historical perspectives. J Natl Cancer Inst, **1995**, 87:1114–1125. *doi.org/10.1093/jnci/87.15.1114.*

Matsumura T, Sugimachi K, Iinuma H, et al. Exosomal microRNA in serum is a novel biomarker of recurrence in human colorectal cancer. Br J Cancer, **2015**, 113:275–281. *doi.org/10.1038/bjc.2015.201.*

McMullin MF, Percy MJ. Erythropoietin receptor and hematological disease. Am J Hematol, **1999**, 60:55–60. *doi.org/10.1002/(SICI)1096-8652(199901)60:1%3C55::AID-AJH9%3E3.0.CO;2-V.*

Melo S, Villanueva A, Moutinho C et al. The small molecule enoxacin is a cancer-specific growth inhibitor that acts by enhancing TAR RNA-binding protein 2-mediated microRNA processing. Proc. Natl Acad Sci USA, **2011**, 108:4394–4399. *doi.org/10.1073/pnas.1014720108.*

Menendez P, Padilla D, Villarejo P, et al. Prognostic implications of serum microRNA-21 in colorectal cancer. J Surg Oncol, **2013**, 108:369–373. *doi.org/10.1002/jso.23415.*

Meryman HT, Hornblower M. A simplified procedure for deglycerolizing red blood cells frozen in a high glycerol concentration. Transfusion, **1977**, 17: 438-442. *doi.org/10.1046/j.1537-2995.1977.17578014580.x.*

Metzker ML. Sequencing technologies – the next generation. Nat Rev Genet, **2010**, 11:31-46. *doi.org/10.1038/nrg2626.*

Milose JC, Filson CP, Weizer AZ, et al. Role of biochemical markers in testicular cancer: diagnosis, staging, and surveillance J Urol, **2012**, 4:1–8. *doi.org/10.2147/OAJU.S15063.*

Miotto E, Saccenti E, Lupini L et al., Quantification of circulating miRNAs by droplet digital PCR: comparison of EvaGreen- and TaqMan-based chemistries. Cancer Epidemiol Biomarkers Prev, **2014**, 23:2638-2642. *doi.org/10.1158/1055-9965.EPI-14-0503.*

Mirabelli P, Incoronato M. Usefulness of traditional serum biomarkers for management of breast cancer patients. Biomed Res Int, **2013**, 2013:685641. *doi.org/10.1155/2013/685641.*

Mircea I, Huang X. miR-210: Fine-Tuning the Hypoxic Response. Adv Exp Med Biol, **2014**, 772: 205–227. *doi.org/10.1007/978-1-4614-5915-6_10.*

Mirkin CA, Letsinger RL, Mucic RC, et al. A DNA-based method for rationally assembling nanoparticles into macroscopic materials. Nature, **1996**, 382:607-609. *doi.org/10.1038/382607a0.*

Mischiati C, Sereni A, Lampronti I, et al. Rapamycin-mediated induction of gamma-globin mRNA accumulation in human erythroid cells. Br J Haematol, **2004**, 126:612-621. *doi.org/10.1111/j.1365-2141.2004.05083.x.*

Mittal SP, Mathai J, Kulkarni AP et al. miR-320a regulates erythroid differentiation through MAR binding protein SMAR1. Cell Res, **2011**, 21:1196-1209. *doi: 10.1038/cr.2011.79.*

Møllegaard NE, Buchardt O, Egholm M, et al. Peptide nucleic acid.DNA strand displacement loops as artificial transcription promoters. Proc Natl Acad Sci USA, **1994**, 91:3892.

Moi P, Faà V, Marini MG, et al. A novel silent β-thalassemia mutation in the distal CACCC box affects the binding and responsiveness to EKLF. Br J Haematol, **2004**, 126:881-884. *doi.org/10.1111/j.1365-2141.2004.05146.x.*

Mørkeberg J, Sharpe K, Belhage B, et al. Detecting autologous blood transfusions: a comparison of three passport approaches and four blood markers. Scand J Med Sci Sports, **2011**, 21: 235–243. *doi.org/10.1111/j.1600-0838.2009.01033.x.*

Muralidharan-Chari V, Clancy JW, Sedgwick A, et al. Microvesicles: mediators of extracellular communication during cancer progression. J Cell Sci, **2010**, 123: 1603–1611. *doi.org/10.1242/jcs.064386.*

Muratovska A, Lightowlers RN, Taylor RW, et al. Targeting peptide nucleic acid (PNA) oligomers to mitochondria within cells by conjugation to lipophilic cations: implications for mitochondrial DNA replication, expression and disease. Nucleic Acids Res, **2001**, 29:1852–1863. *doi.org/10.1093/nar/29.9.1852.*

Nagrath S, Sequist LV, Maheswaran S, et al. Isolation of rare circulating tumour cells in cancer patients by microchip technology. Nature, **2007**, 450:1235-1239. *doi.org/10.1038/nature06385.*

Naldini L, Blomer U, Gallay P, et al. In vivo gene delivery and stable transduction of nondividing cells by a lentiviral vector. Science, **1996**, 272:263-267. *doi.org/10.1126/science.272.5259.263.*

Nasuhi Pur F, Dilmaghani KA. Calixplatin: novel potential anticancer agent based on the platinum complex with functionalized calixarene. J Coord Chem, **2014**, 67:440–448.

Nelson M, Ashenden M, Langshaw M, et al. Detection of homologous blood transfusion by flow cytometry: a deterrent against blood doping. Haematologica, **2002**, 87:881–882.

Nelson M, Popp H, Sharpe K,et al. Proof of homologous blood transfusion through quantification of blood group antigens. Haematologica, **2003**, 88:1284–1295.

Ng EK, Chong WW, Jin H, et al. Differential expression of microRNAs in plasma of patients with colorectal cancer: a potential marker for colorectal cancer screening. Gut, **2009**, 58:1375–1381. *doi.org/10.1136/gut.2008.167817.*

Nguyen HH, Park J , Kang S et al. Surface Plasmon Resonance: A Versatile Technique for biosensor applications. Sensors, **2015**, 15:10481-10510. *doi.org/10.3390/s150510481.*

Nielsen PE. Gene Targeting and Expression Modulation by Peptide Nucleic Acids (PNA). Curr Pharm Des, **2010**, 16:3118-3123. *doi.org/10.2174/138161210793292546.*

Nollau P, Scheller H, Kona-Horstmann M,et al. Expression of CD66a (human C-CAM) and other members of the carcinoembryonic antigen gene family of adhesion molecules in human colorectal adenomas. Cancer Res, **1997**, 57:2354–2357.

Nonaka R, Nishimura J, Kagawa Y, et al. Circulating miR-199a-3p as a novel serum biomarker for colorectal cancer. Oncol Rep, **2014**, 32:2354–2358. *doi.org/10.3892/or.2014.3515.*

O'Connell RM, Rao DS, Chaudhuri AA et al. Sustained expression of microRNA-155 in hematopoietic stem cells causes a myeloproliferative disorder. J Exp Med, **2008**, 205:585-594. *doi: 10.1084/jem.20072108.*

O'Donnell KA, Wentzel EA, Zeller KI et al. c-Myc-regulated microRNAs modulate E2F1 expression. Nature, **2005**, 435:839-843. *doi.org/10.1038/nature03677.*

Oesterling JE. Prostate specific antigen: a critical assessment of the most useful tumor marker for adenocarcinoma of the prostate. J Urol, **1991**, 145:907-923. *doi.org/10.1016/S0022-5347(17)38491-4.*

Ohno S, Takanashi M, Sudo, K, et al. Systemically Injected Exosomes Targeted to EGFR Deliver Antitumor MicroRNA to Breast Cancer Cells. Mol Ther, **2013**, 21:185–191. *doi.org/10.1038/mt.2012.180.*

Olivieri NF, Brittenham GM. Management of the thalassemias. Cold Spring Harb Perspect Med, **2013**, 3: pii: a011767. *doi.org/10.1101/cshperspect.a011767.*

Olivieri NF. The β-Thalassemias. N Engl J Med, **1999**, 341:99-109. *doi.org/10.1056/NEJM199907083410207.*

Omori A, Tanabe O, Engel JD et al. Adult stage gamma-globin silencing is mediated by a promoter direct repeat element. Mol Cell Biol, **2005**, 25:3443–3451. *doi.org/ 10.1128/MCB.25.9.3443-3451.2005.*

Orkin SH, Cheng TC, Antonarakis SE, et al. Thalassemia due to a mutation in the cleavage-polyadenylation signal of the human beta-globin gene. EMBO J, **1985**, 4: 453–456.

Osman N, O'Leary N, Mulcahy E, et al. Correlation of serum CA125 with stage, grade and survival of patients with epithelial ovarian cancer at a single centre. Ir Med J, **2008**, 101:245-247.

Overman MJ, Modak J, Kopetz S, et al. Use of research biopsies in clinical trials: are risks and benefits adequately discussed? J Clin Oncol, **2013**, 31:17-22. *doi.org/ 10.1200/JCO.2012.43.1718*.

Oving IM, Clevers HC. Molecular causes of colon cancer. Eur J Clin Invest, **2002**, 32:448–457. *doi.org/10.1046/j.1365-2362.2002.01004.x.*

Pare JM, Tahbaz N, Lopez-Orozco J et al. Hsp90 regulates the function of argonaute 2 and its recruitment to stress granules and P-bodies. Mol Biol Cell, **2009**, 20:3273–3284. *doi.org/10.1091/mbc.E09-01-0082.*

Park JE, Heo I, Tian Y et al. Dicer recognizes the 50 end of RNA for efficient and accurate processing. Nature, **2011**, 475:201–205. *doi.org/10.1038/nature10198*.

Pase L, Layton JE, Kloosterman WP et al. miR-451 regulates zebrafish erythroid maturation in vivo via its target gata2. Blood, **2009**, 113:1794-1804. *doi: 10.1182/blood-2008-05-155812.*

Peltier HJ, Latham GJ. Normalization of microRNA expression levels in quantitative RT-PCR assays: identification of suitable reference RNA targets in normal and cancerous human solid tissues. RNA, **2008**, 14:844-852. *doi.org/10.1261/rna.939908.*

Peng Y, Gao Z. Amplified detection of microRNA based on ruthenium oxide nanoparticle-initiated deposition of an insulating film. Anal Chem, **2011**, 83:820-827. *doi.org/10.1021/ac102370s*.

Perilli L, Vicentini C, Agostini M, et al. Circulating miR-182 is a biomarker of colorectal adenocarcinoma progression. Oncotarget, **2014**, 5:6611–6619. *doi.org/10.18632/oncotarget.2245.*

Piao L, Zhang M, Datta J, et al. Lipid-based nanoparticle delivery of Pre-miR-107 inhibits the tumorigenicity of head and neck squamous cell carcinoma. Mol Ther, **2012**; 20:1261–1269. *doi.org/10.1038/mt.2012.67.*

Piedbois P, Rougier P, Buyse M et al. Efficacy of intravenous continuous infusion of fluorouracil compared with bolus administration in advanced colorectal cancer. J Clin Oncol, **1998**, 16:301–308. *doi.org/10.1200/JCO.1998.16.1.301.*

Piette J, Volanti C, Vantieghem A, et al. Cell death and growth arrest in response to photodynamic therapy with membrane-bound photosensitizers. Biochem Pharmacol, **2003**, 66:1651–1659. *doi.org/10.1016/S0006-2952(03)00539-2.*

Piliarik M, Bocková M, Homola J et al. Surface plasmon resonance biosensor for parallelized detection of protein biomarkers in diluted blood plasma. Biosens Bioelectron, **2010**, 26:1656-1661. *doi.org/10.1016/j.bios.2010.08.063.*

Pottgiesser T, Schumacher YO, Funke H, et al. Gene expression in the detection of autologous blood transfusion in sports – a pilot study. Vox Sang, **2009**, 96:333–336. *doi.org/10.1111/j.1423-0410.2009.01169.x.*

Pritchard CC, Cheng HH, Tewari M. MicroRNA profiling: approaches and considerations. Nat Rev Genet., **2012**, 13:358-369. *doi.org/10.1038/nrg3198.*

Propper RD, Cooper B, Rufo RR, et al. Continuous subcutaenous administration of deferoxamine in patients with iron overload. N Engl J Med, **1977**, 297: 418–423. *doi.org/ 10.1056/NEJM197708252970804.*

Pu XX, Huang GL, Guo HQ, et al. Circulating miR-221 directly amplified from plasma is a potential diagnostic and prognostic marker of colorectal cancer and is correlated with p53 expression. J Gastroenterol Hepatol, **2010**, 25:1674–1680. *doi.org/10.1111/j.1440-1746.2010.06417.x.*

Pule GD, Mowla S, Novitzky N et al. Hydroxyurea down-regulates BCL11A, KLF-1 and MYB through miRNA-mediated actions to induce γ-globin expression: implications for new therapeutic approaches of sickle cell disease. Clin Trans Med, **2016**, 5:15. *doi.org/10.1186/s40169-016-0092-7.*

Quinn JJ, Chang HY. Unique features of long non-coding RNA biogenesis and function. Nat Rev Genet, **2015**, 17: 47-62. *doi.org/10.1038/nrg.2015.10.*

Ragusa M, Barbagallo C, Statello L, et al. Non-coding landscapes of colorectal cancer. World J Gastroenterol, **2015**, 21:11709–11739. *doi.org/10.3748/wjg.v21.i41.11709.*

Raiborg C, Stenmark H. The ESCRT machinery in endosomal sorting of ubiquitylated membrane proteins. Nature, **2009**, 458:445–452. *doi.org/10.1038/nature07961.*

Ramkissoon SH, Mainwaring LA, Sloand EM, et al. Nonisotopic detection of microRNA using digoxigenin labelled RNA probes. Mol Cell Probes, **2006**, 20:1-4. *doi.org/10.1016/j.mcp.2005.07.004.*

Raymond E, Faivre S, Woynarowski JM, et al. Oxaliplatin: mechanism of action and antineoplastic activity. Semin Oncol, **1998**, 25:4–12.

Redova M, Sana J, Slaby O. Circulating miRNAs as new blood-based biomarkers for solid cancers. Future Oncol, **2013**, 9:387–402. *doi.org/10.2217/fon.12.192.*

Richard JP, Melikov K, Vives E et al. Cell-penetrating peptides. A reevaluation of the mechanism of cellular uptake. J Biol Chem, **2003**, 278: 585–590.

Riethdorf L, Lisboa BW, Henkel U, et al. Differential expression of CD66a (BGP), a cell adhesion molecule of the carcinoembryonic antigen family, in benign, premalignant, and malignant lesions of the human mammary gland. J Histochem Cytochem, **1997**, 45:957–963. *doi.org/10.1177/002215549704500705.*

Risso A, Fabbro D, Damante G et al. Expression of fetal hemoglobin in adult humans exposed to high altitude hypoxia. Blood Cells Mol Dis, **2012**, 48:147-153. *doi: 10.1016/j.bcmd.2011.12.004.*

Robbins DH, Itzkowitz SH. The molecular and genetic basis of colon cancer. Med Clin North Am **2002**, 86:1467–1495. *doi.org/10.1016/S0025-7125(02)00084-6.*

Rodik RV, Klymchenko AS, Mely Y et al. Calixarenes and related macrocycles as gene delivery vehicles. J Incl Phenom Macrocycl Chem, **2014**, 80:189–200. *doi.org/10.1007/s10847-014-0412-8.*

Roberts DJ, Brunskill SJ, Doree C, et al. Oral deferiprone for iron chelation in people with thalassaemia. Cochrane Database Syst Rev, **2007**, CD004839. *doi.org/10.1002/14651858.CD004839.pub2.*

Rodrigue CM, Arous N, Bachir D et al. Resveratrol, a natural dietary phytoalexin, possesses similar properties to hydroxyurea towards erythroid differentiation. Br J Haematol, **2001**, 113:500-507. *doi.org/10.1046/j.1365-2141.2001.02746.x.*

Rothé F, Laes JF, Lambrechts D, et al. Plasma circulating tumor DNA as an alternative to metastatic biopsies for mutational analysis in breast cancer. Ann Oncol, **2014**, 25:1959–1965. *doi.org/10.1093/annonc/mdu288.*

Rougier P, Van Cutsem E, Bajetta E, et al. Randomised trial of irinotecan versus fluorouracil by continuous infusion after fluorouracil failure in patients with metastatic colorectal cancer. Lancet, **1998**, 352:1407–1412. *doi.org/10.1016/S0140-6736(98)03085-2.*

Ruan J, Liu X, Xiong X, et al. miR-107 promotes the erythroid differentiation of leukemia cells via the downregulation of Cacna2d1. Mol Med Rep, **2015**, 11:1334-1339. *doi: 10.3892/mmr.2014.2865.*

Rush RS, Derby PL, Smith DM, et al. Microheterogeneity of erythropoietin carbohydrate structure. Anal Chem, **1995**, 67:1442–1452. *doi.org/10.1021/ac00104a022.*

Sana J, Faltejskova P, Svoboda M et al. Novel classes of non-coding RNAs and cancer. J Transl Med, **2012**, 10:103. *doi.org/10.1186/1479-5876-10-103.*

Sankaran VG, Menne TF, Xu J, et al. Human fetal hemoglobin expression is regulated by the developmental stage-specific repressor BCL11A. Science, **2008**, 322:1839-1842. *doi.org/10.1126/science.116540.*

Sarkar D, Parkin R, Wyman S et al. Quality assessment and data analysis for microRNA expression arrays. Nucleic Acids Res, **2009**, 37:e17. *doi.org/10.1093/nar/gkn932.*

Sarko DK, McKinney CE. Exosomes: Origins and Therapeutic Potential for Neurodegenerative Disease. Front Neurosci, **2017**, 11:82. *doi.org/*10.3389/fnins.2017.00082.

Scarano S, Mascini M, Turner AP et al. Surface plasmon resonance imaging for affinity-based biosensors. Biosens Bioelectron, **2010**, 25:957-966. *doi.org/10.1016/j.bios.2009.08.039.*

Schanen BC, Li X. Transcriptional regulation of mammalian miRNA genes. *Genomics*, **2011**, 97:1–6. *doi.org/10.1016/j.ygeno.2010.10.005.*

Schetter AJ, Heegaard NHH, Harris CC. Inflammation and cancer: interweaving microRNA, free radical, cytokine and p53 pathways. Carcinogenesis, **2010**, 31:37–49. *doi.org/10.1093/carcin/bgp272*.

Shao X, He Y, Ji M, et al. Quantitative analysis of cell-free DNA in ovarian cancer. Oncol Lett, **2015**, 10:3478-3482. *doi.org/10.3892/ol.2015.3771.*

Sharma S. Tumor markers in clinical practice: General principles and guidelines. Indian J Med Paediatr Oncol, **2009**, 30:1-8. *doi.org/10.4103/0971-5851.56328.*

Simmons CG, Pitts AE, Mayfield LD et al. Synthesis and membrane permeability of PNA-peptide conjugates. Bioorg Med Chem Lett, **1997**, 3001–3006. *doi.org/10.1016/S0960-894X(97)10136-6.*

Siomi MC, Sato K, Pezic D et al. PIWI-interacting small RNAs: the vanguard of genome defence. Nat Rev Mol Cell Biol, **2011**, 12:246-258. *doi.org/10.1038/nrm3089.*

Smith KJ, James DS, Hunt WC, et al. A randomized, double-blind comparison of donor tolerance of 400 mL, 200 mL, and sham red cell donation. Transfusion, **1996**, 36:674–680. *doi.org/10.1046/j.1537-2995.1996.36896374369.x.*

Sobrero A, Guglielmi A, Grossi F, et al. Mechanism of action of fluoropyrimidines: relevance to the new developments in colorectal cancer chemotherapy. Semin Oncol, **2000**, 27:72–77.

Speights VO, Johnson MW, Stoltenberg PH, et al. Colorectal cancer: current trends in initial clinical manifestations. South Med J, **1991**, 84:575–8.

Steeg PS. Tumor metastasis: mechanistic insights and clinical challenges. Nat Med, **2006**, 12:895–904. *doi.org/10.1038/nm1469.*

Steinert G, Scholch S, Niemietz T, et al. Immune escape and survival mechanisms in circulating tumor cells of colorectal cancer. Cancer Res, **2014**, 74:1694–1704. *doi.org/10.1158/0008-5472.CAN-13-1885.*

Stryker SJ, Wolff BG, Culp CE, et al. Natural history of untreated colonic polyps. Gastroenterology, **1987**, 93:1009–1013. *doi.org/10.1016/0016-5085(87)90563-4.*

Sturgeon CM, Lai LC, Duffy MJ. Serum tumour markers: how to order and interpret them. BMJ, **2009**, 339:b3527. *doi.org/10.1136/bmj.b3527.*

Sun Z, Wang Y, Han X, et al. miR-150 inhibits terminal erythroid proliferation and differentiation. Oncotarget, **2015**, 6:43033-43047. *doi: 10.18632/oncotarget.5824.*

Sykes PJ, Neoh SH, Brisco MJ et al. Quantitation of targets for PCR by use of limiting dilution. Biotechniques, **1992**, 13:444–449.

Talbot D, Collis P, Antoniou M, et al. A dominant control region from the human beta-globin locus conferring integration site-independent gene expression. Nature, **1989**, 338:352-355. *doi.org/10.1038/338352a0.*

Thiery JP, Acloque H, Huang RY, et al. Epithelial-mesenchymal transitions in development and disease. Cell, **2009**, 139:871–890. *doi.org/10.1016/j.cell.2009.11.007.*

Thompson AA, Rasko JE, Hongeng S, et al. Initial results from the northstar study (HGB-204): a phase 1/2 study of gene therapy for b-thalassemia major via transplantation of autologous hematopoietic stem cells transduced ex vivo with a lentiviral bA-T87Q-globin vector (LentiGlobin BB305drug product). Blood, **2014**, 124:549.

Tian G, Ying XY, Luo H et al. Sequencing bias: comparison of different protocols of microRNA library construction. BMC Biotechnol, **2010**, 10:64. *doi.org/10.1186/1472-6750-10-64.*

Tian T, Zhu YL, Hu FH et al. Dynamics of exosome internalization and trafficking. J Cell Physiol, **2013**, 228:1487–1495. *doi.org/10.1002/jcp.24304.*

Tivnan A, Orr WS, Gubala V, et al. Inhibition of neuroblastoma tumor growth by targeted delivery of microRNA-34a using anti-disialoganglioside GD2 coated nanoparticles. PLOS One, **2012**, 7:e38129. *doi.org/10.1371/journal.pone.0038129.*

Toiyama Y, Hur K, Tanaka K, et al. Serum miR-200c is a novel prognostic and metastasis-predictive biomarker in patients with colorectal cancer. Ann Surg, **2014**, 259:735–743. *doi.org/10.1097/SLA.0b013e3182a6909d.*

Toiyama Y, Okugawa Y, Goel A. DNA methylation and microRNA biomarkers for noninvasive detection of gastric and colorectal cancer. Biochem Biophys Res Commun, **2014**, 455:43–57. *doi.org/10.1016/j.bbrc.2014.08.001.*

Toiyama Y, Takahashi M, Hur K, et al. Serum miR-21 as a diagnostic and prognostic biomarker in colorectal cancer. J Natl Cancer Inst, **2013**, 105:849–859. *doi.org/10.1093/jnci/djt101.*

Tonelli R, Purgato S, Camerin C et al. Anti-gene peptide nucleic acid specifically inhibits MYCN expression in human neuroblastoma cells leading to cell growth inhibition and apoptosis. Mol Cancer Ther, **2005**, 4:779-86. *doi.org/10.1158/1535-7163.MCT-04-0213.*

Tosar JP, Branas G, Laiz J et al. Electrochemical DNA hybridization sensor applied to real and complex biological samples. Biosens Bioelectron, **2010**, 26:1205-1207. *doi.org/10.1016/j.bios.2010.08.053.*

Trajkovic K, Hsu C, Chiantia S et al. Ceramide triggers budding of exosome vesicles into multivesicular endosomes. Science, **2008**, 319:1244–1247. *doi.org/10.1126/science.1153124.*

Tran HV, Piro B, Reisberg S, et al., Polymer Nanostructured by Carbon Nanotubes Application to Prostate Cancer Biomarker miR-14. Biosens Bioelectron, **2013**, 49:164-169. *doi.org/10.1016/j.bios.2013.05.007.*

Treisman R, Orkin SH, Maniatis T. Specific transcription and RNA splicing defects in five cloned β-thalassaemia genes. Nature, **1983**, 302: 591–596. *doi.org/10.1038/302591a0.*

Trush VV, Cherenok SO, Tanchuk VY, et al. Calix [4] arene methylenebisphosphonic acids as inhibitors of protein tyrosine phosphatase 1B. Bioorg Med Chem Lett, **2013**, 23:5619–5623. *doi.org/10.1016/j.bmcl.2013.08.040.*

Tsai HL, Yang IP, Huang CW, et al. Clinical signifi cance of microRNA-148a in patients with early relapse of stage II stage and III colorectal cancer after curative resection. Transl Res, **2013**, 162:258. *doi.org/10.1016/j.trsl.2013.07.009.*

Turchinovich A, Burwinkel B. Distinct AGO1 and AGO2 associated miRNA profiles in human cells and blood plasma. RNA Biol, **2012**, 9:1066–1075. *doi.org/10.4161/rna.21083.*

Turchinovich A, Weiz L, Langheinz A, et al. Characterization of extracellular circulating microRNA. Nucleic Acids Res, **2011**, 39: 7223–7233. *doi.org/10.1093/nar/gkr254.*

Vaisocherová H, Šípová H, Víšová I, et al. Rapid and sensitive detection of multiple microRNAs in cell lysate by low-fouling surface plasmon resonance biosensor. Biosens Bioelectron, **2015**, 70:226-231. *doi.org/10.1016/j.bios.2015.03.038.*

Valoczi A, Hornyik C, Varga N et al. Sensitive and specific detection of microRNAs by northern blot analysis using LNA-modified oligonucleotide probes. Nucleic Acids Res, **2004**, 32:e175. *doi:10.1093/nar/gnh17.*

Van Dijk TB, Gillemans N, Stein C, et al. Friend of Prmt1, a novel chromatin target of protein arginine methyltransferases. Mol Cell Biol, **2010**, 30:260–272. *doi.org/10.1128/MCB.00645-09.*

Vickers KC, Palmisano BT, Shoucri BM et al. MicroRNAs are transported in plasma and delivered to recipient cells by high-density lipoproteins. Nat Cell Biol, **2011**, 13:423–433. *doi.org/ 10.1038/ncb2210.*

Vikas U, Amit M, Mahavir Y, et al. Analyzing inhibition of BCL11A gene expression in K562 cells by RNAi. J BioSci Biotech, **2013**, 2: 131-136.

Villarroya-Beltri C, Gutierrez-Vazquez C, Sanchez-Cabo F et al. Sumoylated hnRNPA2B1controls the sorting of miRNAs into exosomes through binding to specific motifs. Nat Commun, **2013**, 4:2980. *doi/org./10.1038/ncomms3980.*

Viola S, Merlo S, Consoli GM, et al. Modulation of C6 glioma cell proliferation by ureido-calix [8] arenes. Pharmacology, **2010**, 86:182–188. *doi.org/10.1159/000317518.*

Vogelstein B, Fearon ER, Hamilton SR, et al. Genetic alterations during colorectal-tumor development. N Engl J Med, **1988**, 319:525–532. *doi.org/10.1056/NEJM198809013190901.*

Vona G, Sabile A, Louha M, et al. Isolation by size of epithelial tumor cells: a new method for the immunomorphological and molecular characterization of circulating tumor cells. Am J Pathol, **2000**, 156:57–63. *doi.org/10.1016/S0002-9440(10)64706-2.*

Wagner J, Riwanto M, Besler C et al. Characterization of levels and cellular transfer of circulating lipoprotein-bound microRNAs. Arterioscler Thromb Vasc Biol, **2013**, 33:1392–1400. *doi.org/ 10.1161/ATVBAHA.112.300741.*

Wahlberg K, Jiang J, Rooks H, et al. The HBS1L-MYB intergenic interval associated with elevated HbF levels shows characteristics of a distal regulatory region in erythroid cells. Blood, **2009**, 114:1254–1262. *doi.org/10.1182/blood-2009-03-210146.*

Wang F, Yu J, Yang GH et al. Regulation of erythroid differentiation by miR-376a and its targets. Iran J Basic Med Sci, **2013**, 16:756-763. *doi: 10.1038/cr.2011.79.*

Wang J, Huang SK, Zhao M, et al. Identification of a circulating microRNA signature for colorectal cancer detection. PLoS One, **2014**, 9:e87451. *doi.org/10.1371/journal.pone.0087451.*

Wang K, Zhang S, Weber J et al. Export of microRNAs and microRNA-protective protein by mammalian cells. Nucleic Acids Res, **2010**, 38:7248–7259. *doi.org/10.1093/nar/gkq601.*

Wang LG, Gu J. Serum microRNA-29a is a promising novel marker for early detection of colorectal liver metastasis. Cancer Epidemiol, **2012**, 36:e61–7. *doi.org/10.1016/j.canep.2011.05.002.*

Wang LS, Li L, Li L et al. MicroRNA-486 regulates normal erythropoiesis and enhances growth and modulates drug response in CML progenitors. Stem Cells Dev, **2012**, 21:2049-2057. *doi: 10.1089/scd.2011.0500.*

Wang Q, Huang Z, Ni S, et al. Plasma miR-601 and miR-760 are novel biomarkers for the early detection of colorectal cancer. PLoS One, **2012**, 7:e44398. *doi.org/10.1371/journal.pone.0044398.*

Wang S, Xiang J, Li Z, et al. A plasma microRNA panel for early detection of colorectal cancer. Int J Cancer, **2015**, 136:152–1361. *doi.org/10.1002/ijc.28136.*

Weber JA, Baxter DH, Zhang S et al. The microRNA spectrum in 12 body fluids. Methods, **2010**, 1741:1733–1741. *doi.org/10.1373/clinchem.2010.147405.*

Wide L, Bengtsson C, Berglund B, et al. Detection in blood and urine of recombinant erythropoietin administered to healthy men. Med Sci Sports Exer, **1995**, 27:1569–1576. *doi.org/10.1249/00005768-199511000-00015.*

Wiggins JF, Ruffino L, Kelnar K, et al. Development of a lung cancer therapeutic based on the tumor suppressor microRNA-34. Cancer Res, **2010**, 70:5923-5930. *doi.org/10.1158/0008-5472.CAN-10-0655.*

Wightman B, Ha I, Ruvkun G. Posttranscriptional regulation of the heterochronic gene lin-14 by lin-4 mediates temporal pattern formation in C. elegans. Cell, **1993**, 75:855-862. *doi.org/10.1016/0092-8674(93)90530-4.*

Wilson RC, Tambe A, Kidwell MA et al. Dicer-TRBP complex formation ensures accurate mammalian MicroRNA biogenesis. Mol Cell, **2015**, 57:397–407. *doi.org/10.1016/j.molcel.2014.11.030.*

Witkos TM, Koscianska E, Krzyzosiak WJ. Practical Aspects of microRNA Target Prediction. Curr Mol Med, **2011**, 11: 93–109. *doi: 10.2174/156652411794859250.*

Wolpin BM, Mayer RJ. Systemic Treatment of Colorectal Cancer. Gastroenterology, **2008**, 134: 1296–1310. *doi.org/10.1053/j.gastro.2008.02.098.*

Wu P, Tu Y, Qian Y, et al. DNA strand-displacement-induced fluorescence enhancement for highly sensitive and selective assay of multiple microRNA in cancer cells. Chem Commun (Camb), **2014**, 50:1012-1014. *doi.org/ 10.1039/c3cc46773b.*

Wu ZH, Wang XL, Tang HM et al. Long non-coding RNA HOTAIR is a powerful predictor of metastasis and poor prognosis and is associated with epithelial-mesenchymal transition in colon cancer. Oncol Rep, **2014**, 32:395–402. *doi.org/10.3892/or.2014.3186.*

Xi Y, Formentini A, Chien M, et al. Prognostic values of microRNAs in colorectal cancer. Biomark Insights, **2006**, 2:113–121.

Xu J, Sankaran VG, Ni M, et al. Transcriptional silencing of gamma-globin by BCL11A involves long-range interactions and cooperation with SOX6. Genes Dev, **2010**, 24:783–798. *doi.org/ 10.1101/gad.1897310.*

Xu XS, Hong X, Wang G. Induction of endogenous γ-globin gene expression with decoy oligonucleotide targeting Oct-1 transcription factor consensus sequence. J Hematol Oncol, **2009**, 2:15. *doi: 10.1186/1756-8722-2-15.*

Xua J, Bauer DE, Kerenyia MA et al. Corepressor-dependent silencing of fetal haemoglobin expression by BCL11A. Proc Natl Acad Sci U S A, **2013**, 110:6518-6523. *doi.org/10.1073/pnas.1303976110.*

Yang WJ, Li XB, Li YY, et al. Quantification of microRNA by gold nanoparticle probes. Anal Biochem, **2008**, 376:183-188. *doi.org/10.1016/j.ab.2008.02.003.*

Yao X, Kodeboyina S, Liu L, et al. Role of Stat3 and GATA-1 Interactions in γ-Globin Gene Expression. Exp Hematol, **2009**, 37: 889–900. *doi.org/10.1016/j.exphem.2009.05.004.*

Yau TO, Wu CW, Dong Y, et al. MicroRNA-221 and microRNA-18a identification in stool as potential biomarkers for the noninvasive diagnosis of colorectal carcinoma. Br J Cancer, **2014**, 111:1765–1771. *doi.org/10.1038/bjc.2014.484.*

Yin BC, Liu YQ, Ye BC. One-step, multiplexed fluorescence detection of microRNAs based on duplex-specific nuclease signal amplification. J Am Chem Soc, **2012**, 134:5064-5067. *doi.org/10.1021/ja300721s.*

Yong FL, Law CW, Wang CW. Potentiality of a triple microRNA classifier: miR-193a-3p, miR-23a and miR-338-5p for early detection of colorectal cancer. BMC Cancer, **2013**, 13:280. *doi.org/10.1186/1471-2407-13-280.*

Yoo JK, Kim J, Choi SJ et al. Discovery and characterization of novel microRNAs during endothelial differentiation of human embryonic stem cells. Stem Cells Dev, **2012**, 21:2049-2057. *doi: 10.1089/scd.2011.0500.*

Yoon JH, Abdelmohsen K, Gorospe M. Posttranscriptional gene regulation by long non-coding RNA. J Mol Biol, **2013**, 425:3723-3730.

Yu H, Gao G, Jiang L, et al. Decreased expression of miR-218 is associated with poor prognosis in patients with colorectal cancer. Int J Clin Exp Pathol, **2013**, 6:2904–2911.

Yu J, Jin L, Li W, et al. Serum miR-372 is a diagnostic and prognostic biomarker in patients with early colorectal cancer. Anticancer Agents Med Chem, **2016**, 16:424–431. *doi.org/10.2174/1871520615666150716110406.*

Yuan D, Li K, Zhu K, et al. Plasma miR-183 predicts recurrence and prognosis in patients with colorectal cancer. Cancer Biol, **2015**, 16:268–275. *doi.org/10.1080/15384047.2014.1002327.*

Zampetaki A, Kiechl S, Drozdov I et al. Plasma microRNA profiling reveals loss of endothelial miR-126 and other microRNAs in type 2 diabetes. Circ Res, **2010**, 107:810–817. *doi.org/10.1161/CIRCRESAHA.110.226357.*

Zanutto S, Pizzamiglio S, Ghilotti M, et al. Circulating miR-378 in plasma: a reliable, haemolysis-independent biomarker for colorectal cancer. Br J Cancer, **2014**, 110:1001–1007. *doi.org/10.1038/bjc.2013.819.*

Zernecke A, Bidzhekov K, Noels H et al. Delivery of microRNA-126 by apoptotic bodies induces CXCL12-dependent vascular protection. Sci Signal, **2009**, 2:ra81. *doi.org/10.1126/scisignal.2000610.*

Zhang C, Wu ZK. Molecular pharmacological basis of the YiSui ShenXu Granule in beta-thalassemia therapy. J Ethnopharmacol, **2008**, 120:437-341. *doi.org/10.1016/j.jep.2008.09.024.*

Zhang CZ, Zhang JX, Zhang AL, et al. MiR-221 and miR-222 target PUMA to induce cell survival in glioblastoma. Mol Cancer, **2010**, 9: 229. *doi: 10.1186/1476-4598-9-229.*

Zhang GJ , Chua JH, Chee RE. Label-free direct detection of MiRNAs with silicon nanowire biosensor Biosens Bioelectron, **2009**, 24:2504-2508. *doi.org/ 10.1016/j.bios.2008.12.035.*

Zhang L, Flygare J, Wong P, et al. miR-191 regulates mouse erythroblast enucleation by down-regulating Riok3 and Mxi1. Int J Mol Sci, **2015**, 16:28156-28168. *doi: 10.3390/ijms161226088.*

Zhang J, Zhang K, Bi M, et al. Circulating microRNA expressions in colorectal cancer as predictors of response to chemotherapy. Anticancer Drugs, **2014**, 25:346–352. *doi.org/10.1097/CAD.0000000000000049.*

Zhang Y, Roccaro AM, Rombaoa C, LNA-mediated anti–miR-155 silencing in low-grade B-cell lymphomas. LNA-mediated anti–miR-155 silencing in low-grade B-cell lymphomas. Blood, **2012**, 120:1678-1686. *doi.org/10.1182/blood-2012-02-410647.*

Zhang Y, Wang Z, Gemeinhart RA. Progress in MicroRNA Delivery. J Control Release, **2013**, 172: 962–974. *doi.org/10.1016/j.jconrel.2013.09.015.*

Zhou W, Zhao Q, Sutton R, et al. The role of p22 NF-E4 in human globin gene switching. J Biol Chem, **2004**, 279:26227–26232. *doi.org/10.1074/jbc.M402191200.*

Zhu Y, Wang D, Wang FA et al. comprehensive analysis of GATA-1-regulated miRNAs reveals miR-23a to be a positive modulator of erythropoiesis. Int J Biochem Cell Biol, **2013**, 45:2519-2529. *doi: 10.1016/j.biocel.2013.07.006.*

Zhu W, Su X, Gao X, et al. A label-free and PCR-free electrochemical assay for multiplexed microRNA profiles by ligase chain reaction coupling with quantum dots barcodes. Biosens Bioelectron., **2014**, 53:414-419. *doi.org/ 10.1016/j.bios.2013.10.023.*

Zilfou JT, Lowe SW. Tumor Suppressive Functions of p53. Cold Spring Harb Perspect Biol, **2009**, 1:a001883. *doi: 10.1101/cshperspect.a001883.*

Zolla L, D'Alessandro A, Rinalducci S, et al. Classic and alternative red blood cell storage strategies: seven years of "-omics" investigations. Blood Transfus, **2015**, 13: 21–31. *doi.org/10.2450/2014.0053-14.*

http://www.miRBase.org (release 21, June 2014).

http://ultraplacad.eu/

http://www.cancer.org/treatment/understandingyourdiagnosis/examsandtestdescriptions/testingbiopsyandcytologyspecimensforcancer/testing-biopsy-and-cytology-specimens-for-cancer-biopsy-types

http://www.roswellpark.org/pathology/laboratory-medicine/circulating-tumor-cells

http://www.esmo.org/Oncology-News/FDA-Approves-First-Non-invasive-DNA-Screening-Test-for-Colorectal-Cancer

http://www.wada-ama.org

http://mirtarbase.mbc.nctu.edu.tw/

http://www.cancer.org

http://www.TargetScan.com

http://www.bio-rad.com

http://www2.heatmapper.ca/expression/

http://bioinformatics.psb.ugent.be/webtools/Venn/

http://rna.tbi.univie.ac.at/cgi-bin/RNAWebSuite/RNAfold.cgi

http://groups.csail.mit.edu/pag/mirnaminer/

http://zmf.umm.uni-heidelberg.de/apps/zmf/mirwalk2/

Acknowledgments

As previously said the work presented in this thesis was possible thanks to several collaborations, I would like to say thanks to all people involved for their precious support.

I would like to say thanks to all members of ULTRAPLACAD consortium, in particular way to the coordinator of the project Professor Giuseppe Spoto (University of Catania, Department of Chemical Science) and his collaborators: PhD Maria Chiara Giuffrida and PhD Roberta D'Agata who are responsible for the quantification of miRNAs concentration in plasma samples using NESPRI technique. All data presented about miRNAs in colorectal cancer were made thanks to the close cooperation with PhD Patrizio Giacomini (Regina Elena Cancer Institute, Oncogenomics and Epigenetics Unit) and his colleagues, in particular PhD Matteo Allegretti, who recruited CRC patients and PhD Elisa Tremante who created xenografted mice.

I am also grateful to all people that take part to MARATHON project for the identification of miRNAs as possible biomarkers of ABT. In particular, to MD Fabio Mafredini (University of Ferrara, Department of Biomedical Sciences and Surgical Specialties, Section of Sport Sciences) and PhD Nicola Lamberti who designed the study, recruited athletes and performed physical tests to evaluate athletic performances. I am also grateful to MD Francesca Dalla Corte (University of Ferrara, Section of Anesthesiology) who performed all blood withdrawal and to MD Roberto Reverberi (Ferrara hospital, Department of Transfusional Immunohematology) who coordinate transfusional service. Thanks to PhD Manuela Ferracin (University of Bologna, Department of Experimental, Diagnostic and Specialty Medicine) for the technical support in performing microarray analysis.

Thanks to Professor Francesco Sansone (University of Parma, Department of Chemistry) and colleagues who synthesized ML122 and others analogues, and to Professor Roberto Corradini (University of Parma, Department of Chemistry) and co-workers who provided PNAs employed for ML122 transfections.

I am also grateful to Alessandra Romanelli research group (University of Naples Federico II, Department of Pharmacy) who synthesized PNAs targeting miR-210 sequence.

I would like to say thanks to my colleagues PhD Giulia Breveglieri (University of Ferrara, Department of Life Sciences and Biotechnologies) and PhD Giulia Montagner who performed respectively BIAcore and Bioplex analysis.

Thanks to PhD Eleonora Gallerani (University of Ferrara, Department of Life Sciences and Biotechnologies) for her, not only, technical support and to the nurses (Ferrara Hospital, Sezione di Genetica Medica) Claudia Benini, Sandra Alberti and Gianna Teodori for their precious help.